Bernd Naza

NVU-192
VOLUME 2 of 2

SELECTED ENVIRONMENTAL PLUTONIUM RESEARCH REPORTS OF THE NAEG

410191

JUNE 1978

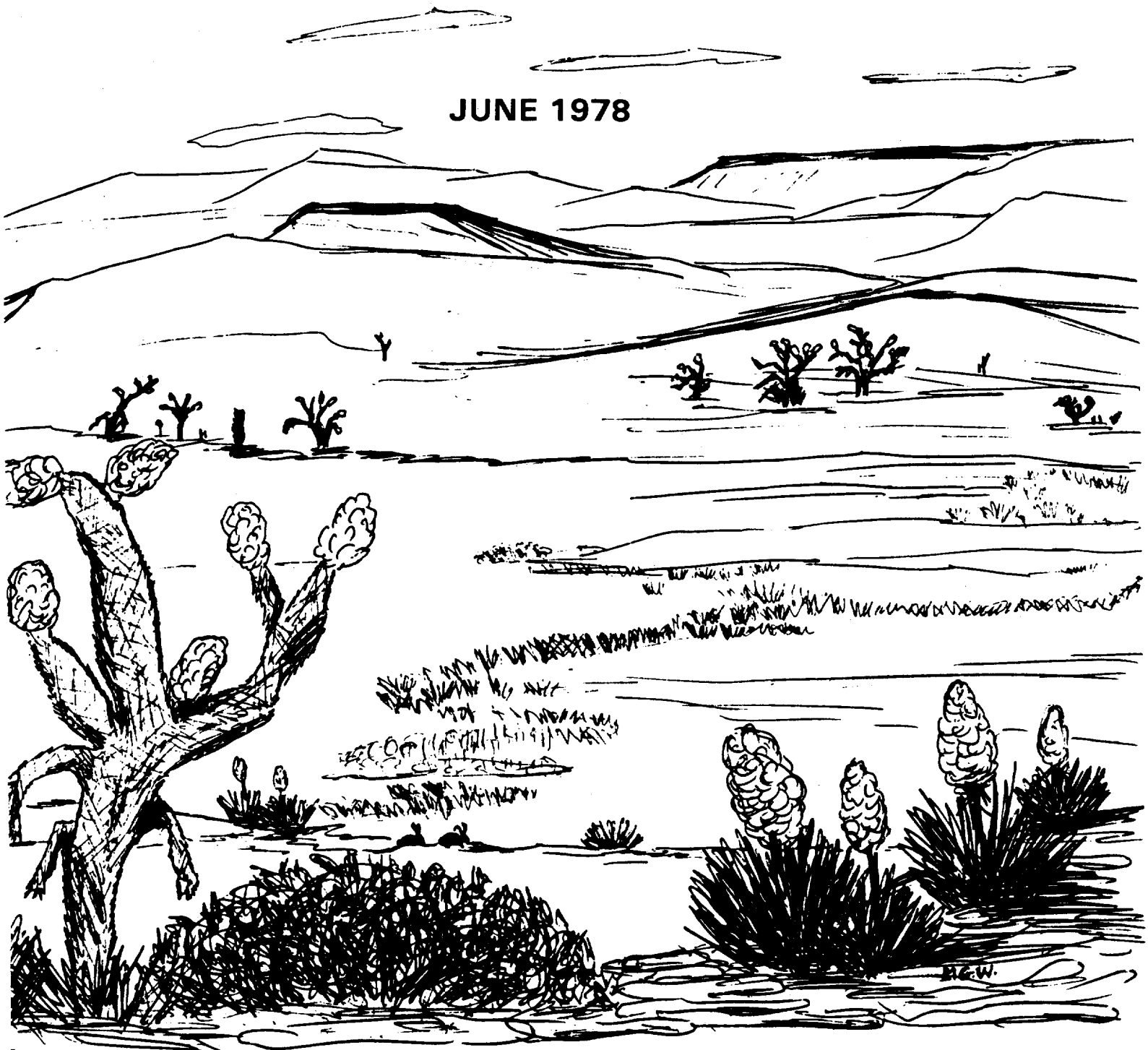

PLUTONIUM VALLEY - SPRING, 1978

NEVADA APPLIED ECOLOGY GROUP

U.S. DEPARTMENT OF ENERGY

Las Vegas, Nevada

PRINTED IN THE UNITED STATES OF AMERICA
AVAILABLE FROM:
NATIONAL TECHNICAL INFORMATION SERVICES NTIS
U.S. DEPARTMENT OF COMMERCE
5285 PORT ROYAL ROAD
SPRINGFIELD, VA. 22161
PRICE: PRINTED COPY $21.50
MICROFICHE: $3.00

NVO-192
UC-11

SELECTED ENVIRONMENTAL PLUTONIUM RESEARCH REPORTS OF THE NAEG

JUNE 1978

EDITED BY
M. G. WHITE and P. B. DUNAWAY

NEVADA APPLIED ECOLOGY GROUP
U. S. DEPARTMENT OF ENERGY
Las Vegas, Nevada

TABLE OF CONTENTS

VOLUME I

*Inside back cover.

PREFACE

PREFACE

On February 28 through March 2, 1978, the Annual Plutonium Information Conference was held in San Diego by the Nevada Applied Ecology Group. Many presentations by the NAEG research groups were summarizing reports. A few discussed progress to date on certain projects. And, the third day of the conference was set aside for contributed papers, mostly from institutions other than NAEG-contracted organizations. This publication, printed in two volumes, is of the proceedings of the conference, perhaps the best meeting ever held by the NAEG.

During the months preceding the conference, environmental research funding was curtailed for many of the NAEG projects in favor of test-directed activities at the Nevada Test Site. It is anticipated that these projects will be resumed at normal levels when additional funding is restored to the delayed aspects of the DMA-funded program.

New projects this year were reported to be in the initial phases of study, and the study plans were presented by the principal investigators. Of particular interest were the reports by Ausmus and Dodson (BCL) concerning the effects of transuranics on desert ecosystem processes; by Baker, Pillay, Rose, and Ciolkosz (Penn State) with reference to development of an approach for monitoring plant availability of transuranics in Nevada Test Site soils; and plutonium-bearing particle analysis discussed by Couch and Efurd (MCL).

Plutonium Valley in the spring (cover design) was one of the most beautiful areas at the Nevada Test Site this year. Hundreds of breathtaking wildflower species, including the purple sagebrush, profusely decorated the hills and slopes of this Area 11 location of certain NAEG environmental plutonium study sites.

At the conference, Paul Dunaway, Chairman of the Nevada Applied Ecology Group Steering Committee, read a letter from Maj. Gen. J. K. Bratton, Director, Division of Military Application, U.S. Department of Energy, Headquarters, to Nevada Applied Ecology Group management and contractor and letter of agreement personnel, congratulating them on continued outstanding contributions toward the goals of the important objectives of the environmental plutonium program at U.S. Department of Energy's Nevada Test Site. We should like to add our appreciation for the continued support of DMA and efforts of the Nevada Applied Ecology Group scientific investigators, advisory committee members, and other technical and professional people associated with the Nevada Applied Ecology Group research studies.

Certain Holmes & Narver, Inc., personnel deserve special recognition for their outstanding cooperation with the NAEG in the publication of reports and documents: Paul G. Noblitt, Henry B. Gayle, and Timothy M. Catt of Technical Support; and Ruth Preston, Murry Battle, Linda Daniels, Marlena Eckel, Camilla Harbeson, Lorine Jackson, and Shirley Smith of

the Word Processing Center. We also express special thanks to Winnie A. Howard, NAEG staff; David N. Brady, NAEG/NTS Coordinator (Reynolds Electrical & Engineering Co., Inc.); Evan M. Romney, University of California, Los Angeles, Laboratory of Nuclear Medicine; Richard O. Gilbert, Battelle Pacific Northwest Laboratories; Edward H. Essington, Los Alamos Scientific Laboratory; to Margaret Schmitt, Robert L. Hitechew, Richard H. Johnston, Robert R. Loux, John A. Koch, Robert W. Newman, Troy E. Wade, and Mahlon E. Gates (Manager), Nevada Operations Office; and to Gordon C. Facer, HQ/DMA.

Mary G. White
Scientific Program Manager
Nevada Applied Ecology Group

Paul B. Dunaway
Chairman, Steering Committee
Nevada Applied Ecology Group

STATISTICS
AND
MODELING

ON THE ESTIMATION OF SPATIAL PATTERN FOR ENVIRONMENTAL CONTAMINANTS

R. O. Gilbert

Battelle Memorial Institute, Pacific Northwest Laboratory
Richland, Washington

ABSTRACT

The estimation of the spatial pattern or geographical distribution of environmental contaminants or other spatial variables is often of interest in environmental sampling programs. One approach to this problem is to estimate the variable of interest at regular intervals on a grid covering the study site using data collected at various locations over the area. In this paper, we examine the performance of an iterative procedure for estimating the grid values. A two-phase least squares procedure is applied three times: first to the observed data, then to the residuals from the first fit, and finally to the residuals from the second fit. The three estimated grids are added together for the final grid estimates. Results are displayed as contour maps, three-dimensional surfaces, and plots of residuals.

The iterative procedure is applied to untransformed as well as log-transformed data to investigate whether fitting in terms of logarithms followed by transforming back to the original scale (the "antilog" scale) is preferable to fitting untransformed data. This evaluation is made on a data set of $^{239,240}Pu$ concentrations in surface soil samples collected by the Nevada Applied Ecology Group at the Area 13 (Project 57) "safety-shot" site on the Nevada Test Site. This data set is characterized by a very large concentration datum near ground zero with concentrations falling off rapidly with distance.

For these data, the iterative procedure reduces the standard deviation and average absolute (mean and median) size of residuals and increases the percent of the total variation explained by fits in both untransformed and antilog scales. Smaller residuals are usually obtained by fitting log-transformed data and taking antilogs rather than fitting untransformed data. Also, the iterative procedure applied to the log-transformed data appears to result in more reasonable estimates of concentration surface

at locations where samples are not collected than did fits obtained on untransformed data. Fits in either scale, but particularly in the untransformed scale, gave questionable estimates in regions of sparse data where Pu concentrations change rapidly within short distances. Plots of sample data on estimated contour maps suggest regions where more data are needed.

The two-phase grid estimation procedure used here does not give estimation variances for the grid values. Kriging is mentioned as a method that does provide such estimates. An evaluation of the applicability of Kriging to estimating spatial pattern of radionuclides in the environment is encouraged.*

INTRODUCTION

Estimating the spatial pattern or geographical distribution of environmental contaminants is often of interest in environmental sampling programs. Concentrations of the contaminant are measured at various locations and an estimate is desired of the "true" concentration "surface" for the area from which samples are collected. One approach to this problem is to use the observed data to estimate the surface at regular grid points over the study site. This estimated grid matrix can then be displayed as a three-dimensional concentration surface or as a contour map showing lines of constant concentration.

In this paper, we examine whether an iterative fitting procedure for estimating the grid matrix of concentrations would improve estimates of the true concentration surface. The iterative procedure is applied to $^{239,240}Pu$ concentrations in surface (0-5 cm) soil samples collected according to a stratified random sampling plan at the Area 13 (Project 57) "safety-shot" site on the Nevada Test Site (NTS).

This study site is one of 10 safety-shot sites on the NTS or the adjacent Tonopah Test Range currently being studied by the Nevada Applied Ecology Group (NAEG). These are sites where, during the period 1954-1963, assemblies or devices composed of plutonium and/or uranium were blown

---

*This paper was prepared for presentation at the 1976 Annual Meeting of the American Statistical Association in Boston, Massachusetts, August 23-26, 1976. This analysis of Area 13 (Project 57) $^{239,240}Pu$ data was performed prior to the kriging analyses by Delfiner and Gilbert (1978) reported elsewhere in this volume. The plutonium soil concentration data used in this latter paper is identical to that listed in Appendix A of the present paper except as noted in Appendix A and footnote 2 in Delfiner and Gilbert (1978).

apart by chemical explosives to test in part for "safety" against fission reactions. A consequence of these tests was the contamination of the immediately surrounding soil and vegetation with plutonium, americium, and/or uranium.

The Area 13 data set is characterized by a single, very large plutonium concentration obtained near ground zero (GZ, point of detonation) with surrounding concentrations falling off rapidly in all directions from GZ in an unsymmetrical pattern. Hence, the "true" concentration surface has a definite structure or pattern with relatively low levels of contamination predominating within one or two thousand feet from GZ (depending on direction). A goal of the current NAEG sampling program is to evaluate the potential hazard to man from this contamination if these areas were ever released for habitation. This evaluation has included the collection of several thousand soil, vegetation, small vertebrate, and cattle tissue samples for radiochemical analysis (White and Dunaway, 1975; Dunaway and White, 1974).

An important objective of this effort is to estimate the spatial pattern (concentration surface) of plutonium about GZ as it presently exists in surface soil (top 5 cm). Gilbert *et al.* (1975, 1976b) and Gilbert and Eberhardt (1977) have experimented with estimating the spatial pattern of plutonium in surface soil and vegetation at safety-shot sites using "nearest neighbor" and polynomial fitting routines in both original and logarithmic scales. John Tukey suggested (see discussion following the paper by Eberhardt and Gilbert, 1976) that better fits to the data might be obtained if the fitting routine was applied iteratively on residuals. For example, the residuals from the first fit would themselves be fitted and added to the initial fit of the original data. More generally, if R_{ij} is the residual between the i^{th} observation y_i ($i = 1,2,\ldots,n$) and the smoothed (fitted) value $\hat{y}_{ij}$ obtained on the j^{th} iteration ($j = 1,2,\ldots,m$), then

$$y_i = \hat{y}_{i1} + R_{i1} \qquad \text{(1st iteration)} \tag{1}$$

and

$$R_{i1} = \hat{y}_{i2} + R_{i2} \qquad \text{(2nd iteration)} \tag{2}$$

so that

$$y_i = \hat{y}_{i1} + \hat{y}_{i2} + R_{i2} \quad . \tag{3}$$

For m iterations, we may write

$$R_{im} = y_i - \sum_{j=1}^{m} \hat{y}_{ij} \quad , \tag{4}$$

where $\sum_{j=1}^{m} \hat{y}_{ij}$ is the final smoothed estimate of y_i, and R_{im} the final residual.

This iterative approach (defined explicitly below) is applied here to log-transformed data $z_i = \ell n\ y_i$ and to the untransformed concentrations y_i. Residuals at sample collection points are obtained for the fits in both scales as well as for the "antilog" scale. For this latter case, the estimates obtained in log scale are transformed back to the original scale by taking antilogarithms. The antilog residual is then the difference between the observed datum and the antilog estimate (see Table 1). Our interest in the antilog scale arises from a desire to present results in untransformed scale while taking advantage of any benefits to be had by fitting in the log scale. The log concentration surface is displayed here as a contour map in untransformed scale by drawing contours for log concentrations z such that $y = \exp(z)$, where y are contours of interest in the original scale. In this paper, contours are displayed for values of y equal to 1, 10, 100, 1,000, and 10,000 $\mu Ci/m^2$ of $^{239,240}Pu$. This is done by drawing contours for z's equal to ℓn 1, ℓn 10, ℓn 100, etc., on the estimated log concentration surface.

In this paper, we investigate whether iterating on residuals in any or all of the three scales (untransformed, log-transformed, and antilog) result in a "better" estimate of the true plutonium concentration surface than if the estimation routine were applied only once. The "best" estimated surface is considered here to be that for which the deviation between the true and estimated concentration surface at <u>all</u> locations (not just at sample points) is a minimum. Since the true surface is unknown, this investigation includes examining residuals between the observed and estimated surface at sample collection points. This analysis includes plotting and comparing residuals for each iteration, computing the mean, median, and standard deviations of residuals, and by computing the proportion of the total variation in the observed data explained by the estimated values. Further insight is gained by computing the linear

Table 1. Notation for Iterative Procedure on Untransformed, Log-Transformed, and Antilog Fits to $^{239-240}Pu$ Concentrations in Surface Soil

	Untransformed	Log	Antilog
Observed Concentration	y_i^*	$z_i = \ell n y_i$	y_i^*
Estimated Concentration at m^{th} Iteration	$\hat{y}_i = \sum_{j=1}^{m} \hat{y}_{ij}$	$\hat{z}_i = \sum_{j=1}^{m} \hat{z}_{ij}$	$\hat{y}_i = \exp(\hat{z}_i)$
Residual (R_{im})	$y_i - \hat{y}_i$	$z_i - \hat{z}_i$	$y_i - \exp(\hat{z}_i)$

*Units of $\mu Ci/m^2$. Applicable to top 5 cm of soil.

correlation coefficient between residuals and observed, and between residuals and fitted values. In addition to these analyses of residuals, the estimated surface is examined by considering the density and pattern of sample collection points relative to estimated contours, and by considering prior information available on the concentration surface of ^{241}Am in Area 13.

At the Area 13 study site, concentrations of ^{241}Am in soil are known to be correlated with $^{239,240}Pu$ concentrations (Gilbert *et al.*, 1975, p. 403). Before sampling began, information on the concentration surface of ^{241}Am was obtained from portable field instrument (FIDLER) surveys of the Project 57 site. The FIDLER was used to take readings (one foot above the soil surface) of ^{241}Am (net 60 KeV) at 400-foot intervals over the entire area and at 100-foot intervals near GZ. These readings give a general indication of the concentrations of $^{239,240}Pu$ in soil in Area 13 and were used to define the strata in Figure 1. Gilbert *et al.* (1975) estimated the correlation between FIDLER readings and $^{239,240}Pu$ concentrations to range from near zero for stratum 1 to about 0.70 for stratum 5 and 6.

METHODS

Sampling Design

Surface soil samples (0-5 cm) were collected at random locations within each stratum (Figure 1) according to a stratified random sampling plan. The number of samples allocated to the strata were determined using as a guide the optimum allocation formula for stratified random sampling (Cochran, 1963, p. 97, equation 5.20). Details of the design and allocation are given in Gilbert *et al.* (1976a). A total of 173 samples was collected, of which three were lost leaving 170 for statistical analysis. Samples were dried for 24 hours at 105° and ball-milled for five hours (Kayuha *et al.*, 1974). Ten-gram aliquots of ball-milled soil were analyzed for $^{239,240}Pu$ using wet chemistry techniques. The resulting data in units of $\mu Ci/m^2$ are listed in Appendix A along with their collection locations (Nevada Grid Coordinates).*

---

*Two observations in stratum 6 (identified by †† in Appendix A) were approximated using the average $^{239,240}Pu/^{241}Am$ ratio for the study site and estimated concentrations of ^{241}Am obtained for the two samples. Due to inappropriate amounts of tracer added to the aliquots, $^{239,240}Pu$ concentrations were not available for these two samples. All ^{241}Am concentrations were obtained using a Ge(Li) counter. The average ratio ± standard error was 9.4 ± 0.14 (from Table 18 in Gilbert *et al.*, 1975) computed from $^{239,240}Pu$ and ^{241}Am counts on the same aliquots. See †† footnote in Appendix A for further information.

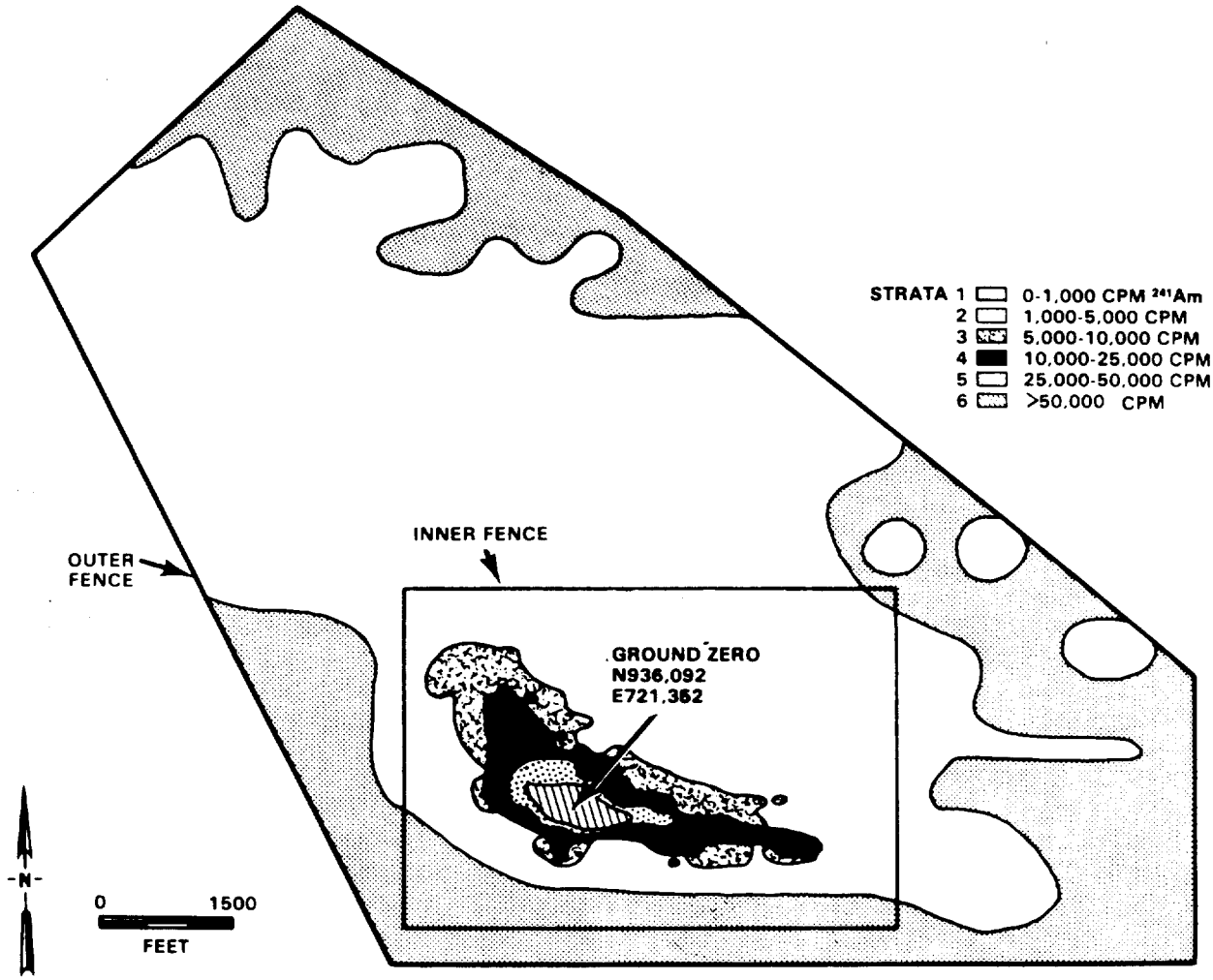

Figure 1. Strata Used in Sampling for Inventory at the Area 13 (Project 57) Site.

Estimation of Pu Concentration Surface

A two-phase estimation procedure, GRID, was used in conjunction with a nearest neighbor data search routine, NEAR (Sampson, 1975a), to estimate the plutonium concentration surface using the 170 data points obtained as described above.* This procedure was applied at each iteration as described in the next section. GRID estimated the $^{239,240}Pu$ concentration at each intersection point (grid node) of a grid laid over the study site. The grid mesh spacing was chosen to be 100 feet after trial and error computations of the concentration surface using spacings of 50 and 200 feet.** The final grid had 73 rows (east-west) and 86 columns (north-south) for a total of 6,278 grid nodes. The method used by GRID to estimate the concentration surface is described in detail in Appendix B (from Sampson, 1973).

GRID and NEAR are part of a large computer software system called SURFACE II (Sampson, 1975b) developed for the manipulation and display of spatially distributed data. This system is under continuing development by the Kansas Geological Survey. All of the contour and three-dimensional plots presented here were prepared from plots obtained on the Cal-Comp plotter using SURFACE II.

A disadvantage of GRID is that it does not yield estimation variances of the estimated grid node values. However, within the next few months, a gridding method known as Kriging is expected to become available on SURFACE II.*** Kriging yields best linear unbiased grid node estimates as well as variances of these estimates if the underlying assumptions of the method are fulfilled. The theory and practice of kriging have too many ramifications for discussion here, but the basic assumption involves second order stationarity of differences between spatial data (the "intrinsic hypothesis"). Introduction to the theory and practice of kriging are given by Huijbregts (1975) and Delfiner and Delhomme (1975). A detailed account of the underlying theory and a worked example are given by Olea (1975). Further insight into the method is given in Davis (1973), Huijbregts and Matheron (1971), Agterberg (1970), Akima (1975), and Olea (1974).

---

*The estimated plutonium contours for Area 13 (Project 57) in Gilbert *et al.* (1975) were based on 166 observations; those in Gilbert *et al.* (1976b) on 167 or 168. These earlier efforts exclused the datum 16,400 $\mu Ci/m^2$ in Appendix A, the extremely large value near GZ.

**Reducing the grid mesh size from 100 to 50 feet increases the number of grid nodes fourfold. The computing expense is similarly increased. In practice, the grid mesh size is determined in part by the desired detail in the concentration surface, the density of data points, and cost factors.

***Since this paper was originally written, kriging has become available on SURFACE II. However, we have instead used the kriging program BLUEPACK written by Dr. Pierre Delfiner (see Delfiner and Gilbert, 1978) since it offers a more general approach to the problem.

Description of Iterative Procedure

The first iteration consists of estimating the plutonium concentration surface at grid nodes using the observed $^{239,240}Pu$ data (y_i, i = 1,2,..., 170). (The subscript i will run from 1 to 170 throughout this paper.) This estimated surface is denoted as I_1 in Figure 2 and is presented in the Results section as contour and three-dimensional displays. Backward double linear interpolation between grid estimates yields the estimates of plutonium concentrations ($\hat{y}_{i1}$) at sample locations. Residuals for Iteration 1 at control (data) points were obtained by computing $R_{i1} = y_i - \hat{y}_{i1}$.

In Iteration 2, the procedure of Iteration 1 is applied to the residuals R_{i1} to obtain a new grid matrix I_2 (Figure 2). This is the estimated surface or fit to the residuals from Iteration 1. These residuals were estimated ($\hat{y}_{i2}$) at sample locations using backward double linear interpolation from the nearest grid node estimates of the residual surface. The sum $\hat{y}_{i1} + \hat{y}_{i2}$ is the new estimate of the plutonium concentration surface of sample location i. The new residual is $R_{i2} = y_i - (\hat{y}_{i1} + \hat{y}_{i2})$. At each grid node, the estimates from Iterations 1 and 2 are added together ($I_1 + I_2$; see Figure 2) to yield a new estimate of the plutonium concentration surface.

Iteration 3 consists of applying the procedure of Iteration 2 to the residuals R_{i2} to obtain a new grid matrix, I_3. $I_1 + I_2 + I_3$ is the final estimate of the concentration surface, and $R_{i3} = y_i - (\hat{y}_{i1} + \hat{y}_{i2} + \hat{y}_{i3})$ is the final residual. Conceptually, this procedure could be repeated many times until all of the "structure" in the residuals has been removed by fitting.

In this study, we have somewhat arbitrarily chosen to stop after three iterations. The question naturally arises, however, as to whether continued iteration will eventually reduce the residuals to zero so that the observed and fitted values agree exactly. This would seem to depend on the particular gridding algorithm used (GRID or kriging, e.g.), the data values themselves, and the spatial pattern and density of samples. A related question concerns whether continued iteration, while possibly resulting in progressively smaller residuals at sample collection points, might yield biased and distorted estimates of the concentration surface at other locations. As discussed below, there is some evidence of this happening for the Area 13 data after only three iterations. This is apparently related to the absence of data in certain areas near GZ. This suggests that survey design aspects of these kinds of studies need to be carefully considered.

Figure 2. Iterative Procedure

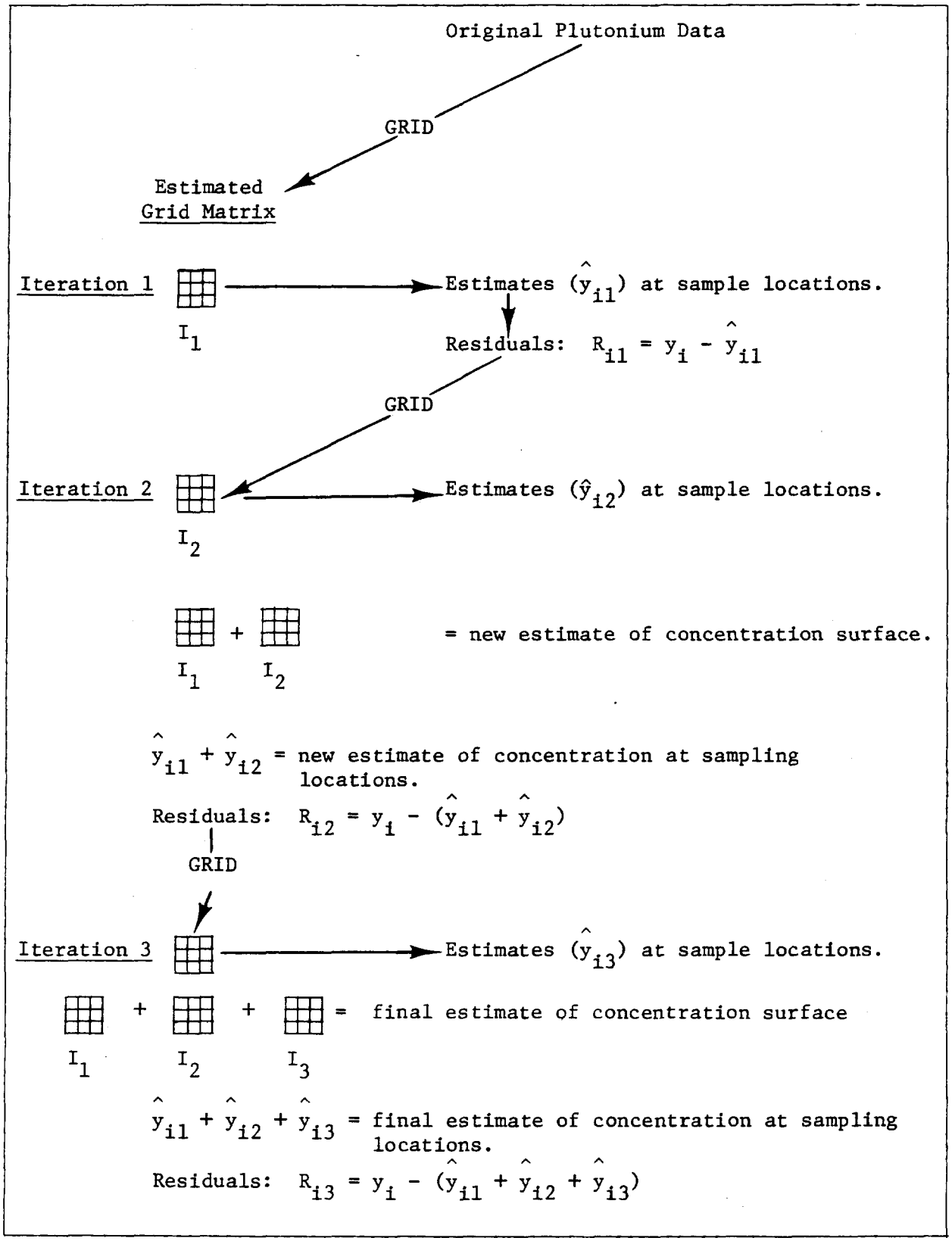

RESULTS

Concentration Surfaces (Estimated Grid Values)

Estimated $^{239,240}Pu$ concentration contours and three-dimensional plots are displayed in Figures 3 through 11 for Iterations 1, 2, and 3 for both untransformed and log-transformed data. The observed plutonium data are displayed at their collection points in Figures 3, 4, 6, and 7. Note that Figures 4 and 7 are enlargements of the GZ area in Figures 3 and 6. As expected, contours drawn from estimated grid matrices in both scales indicate greatly elevated concentrations in the GZ area. Note, however, that contours for untransformed data on Iteration 1 (Figures 3 and 4) show regions of low concentrations (< 1 $\mu Ci/m^2$) to the north, northwest, and east of GZ in regions where no data were collected. Indeed, much of the < 1 $\mu Ci/m^2$ region in Figures 3 and 4 (untransformed fits) consists of grid estimates that are negative and hence spurious. The negative concentration contours for Iteration 3 are displayed in Figure 5. These negative estimates can also be seen in the three-dimensional representation of the estimated grid node concentrations for Iteration 3 (Figure 10). The largest negative grid estimates for Iterations 1, 2, and 3 are -1435, -1666, and -1786, respectively. They occur to the south, southwest of GZ (Figure 5).

The examination of residuals in the next section indicates that the average absolute (mean, median) size of residuals for these untransformed fits decreases with each iteration. Hence, the estimated concentration surface using untransformed data is becoming distorted even though the residuals at sample locations are decreasing. This does not happen to the same extent for fits in the antilog scale. This is seen, for example, by examining Table 2, which gives the estimated grid node concentrations in the immediate GZ area for the untransformed and antilog scales. These show the changes that occur in the grid node estimates due to iterating on the residuals. In the untransformed scale grid, estimates surrounding the peak at GZ (location N936092, E721352) tend to decrease with each iteration. This effect is not as evident for the antilog scale. Note the presence of negative grid estimates in the untransformed scale and that they tend to grow larger with each iteration (also see Figures 8 and 9). The estimated antilog surface is not free from bias, however, as can be seen in Figures 6-9, where the 100 to 1,000 $\mu Ci/m^2$ region is estimated to extend several hundred feet south of GZ for both the untransformed and antilog scales. This does not agree with the ^{241}Am (FIDLER) contours for this region (Figure 1) and probably results from too few samples being collected in that area.

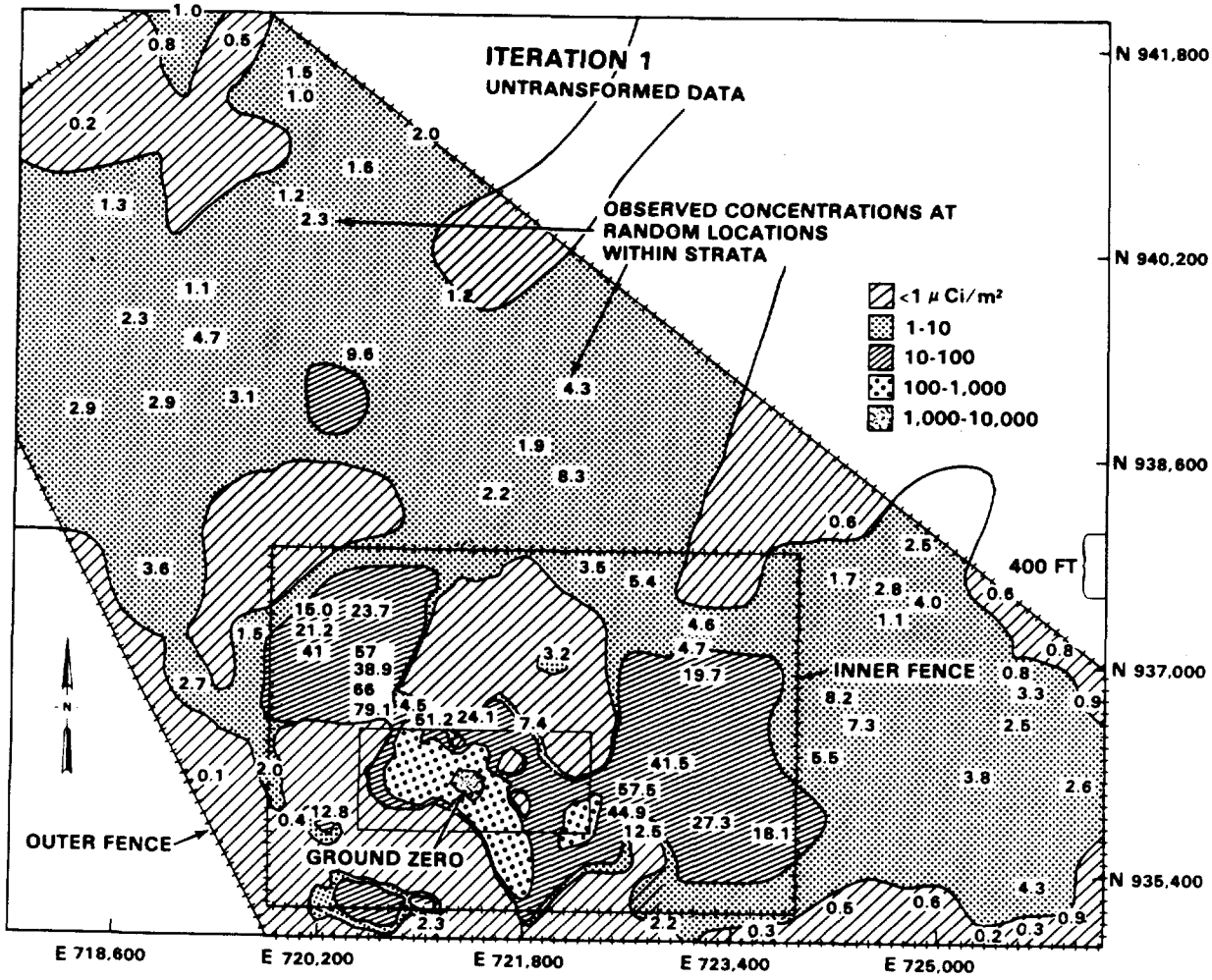

Figure 3. Estimated $^{239,240}Pu$ Concentration Contours in Surface Soil at the Area 13, Project 57 Site after 1 Iteration (Untransformed Data).

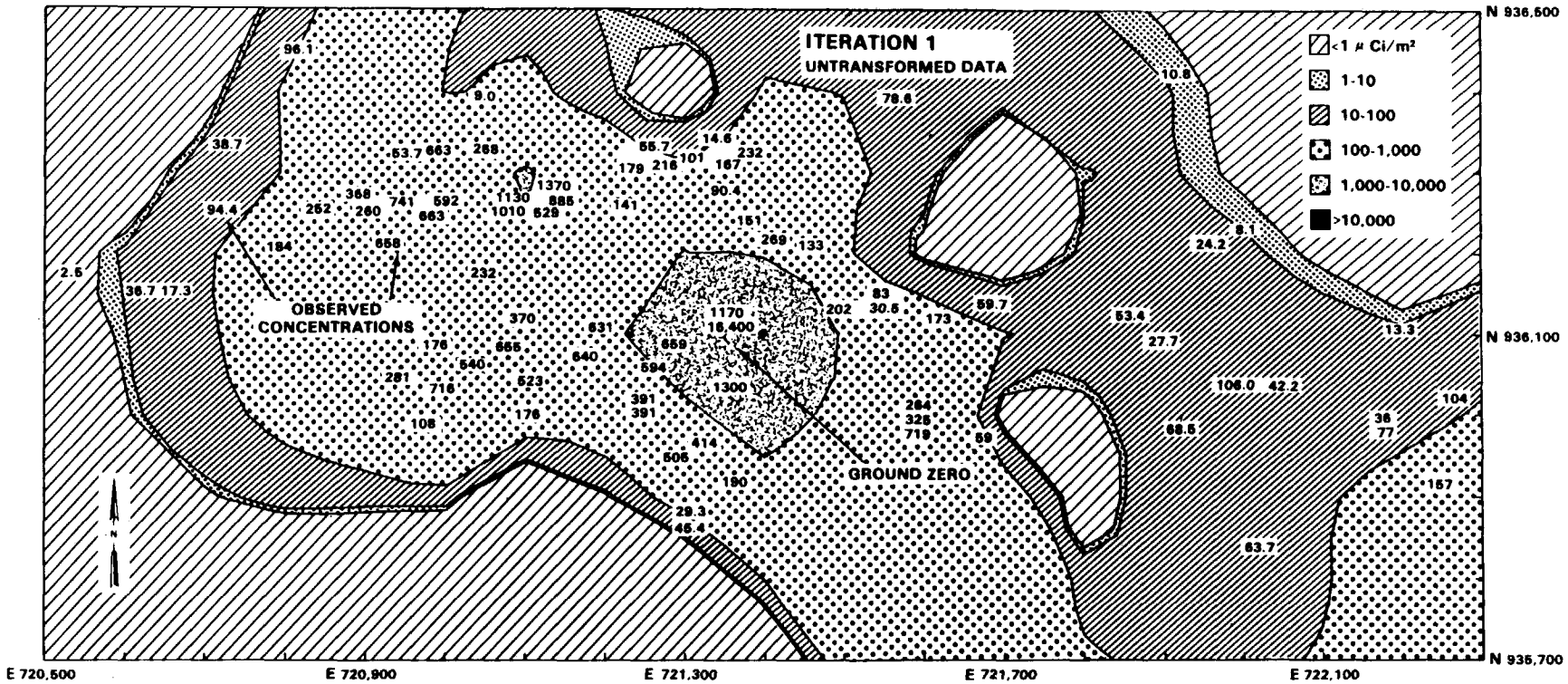

Figure 4. Estimated $^{239,240}Pu$ Concentration Contours in Surface Soil Near GZ at the Area 13, Project 57 Site After 1 Iteration (Untransformed Data).

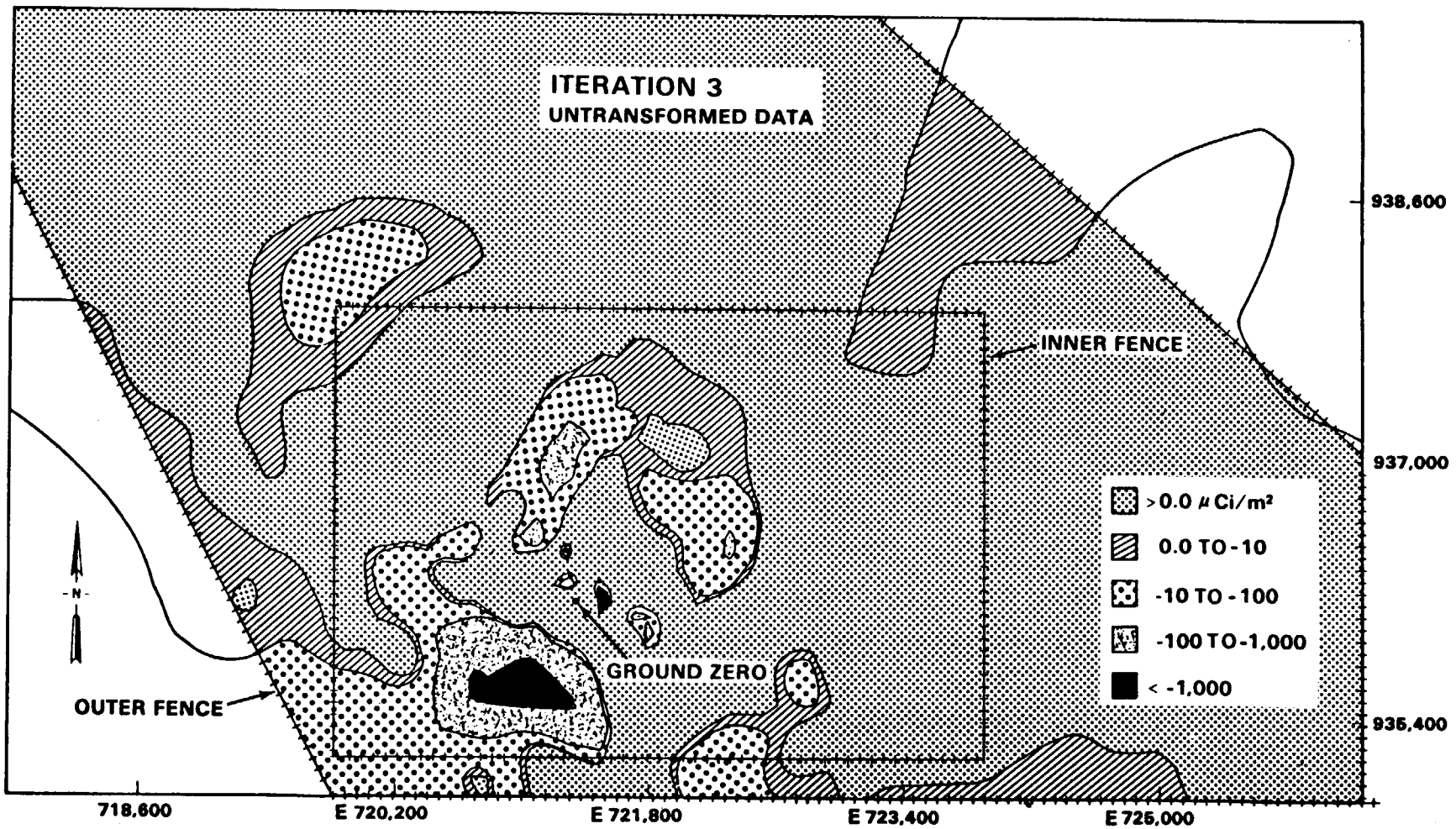

Figure 5. Estimated $^{239,240}Pu$ Concentration Contours in Surface Soil Near GZ at the Area 13, Project 57 Site After 3 Iterations (Untransformed Data).

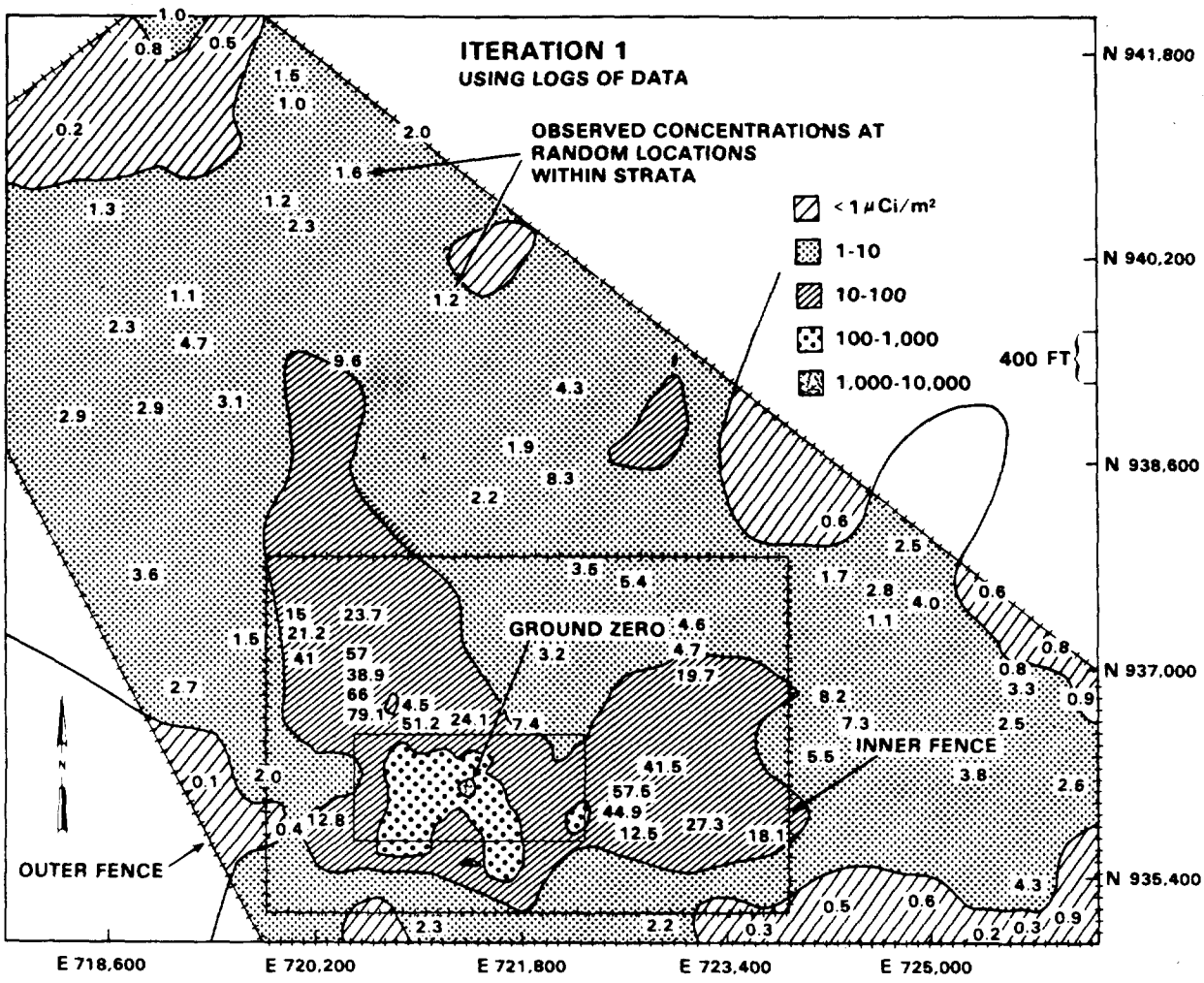

Figure 6. Estimated $^{239,240}Pu$ Concentration Contours in Surface Soil at the Area 13, Project 57 Site After 1 Iteration (Log Transformed Data).

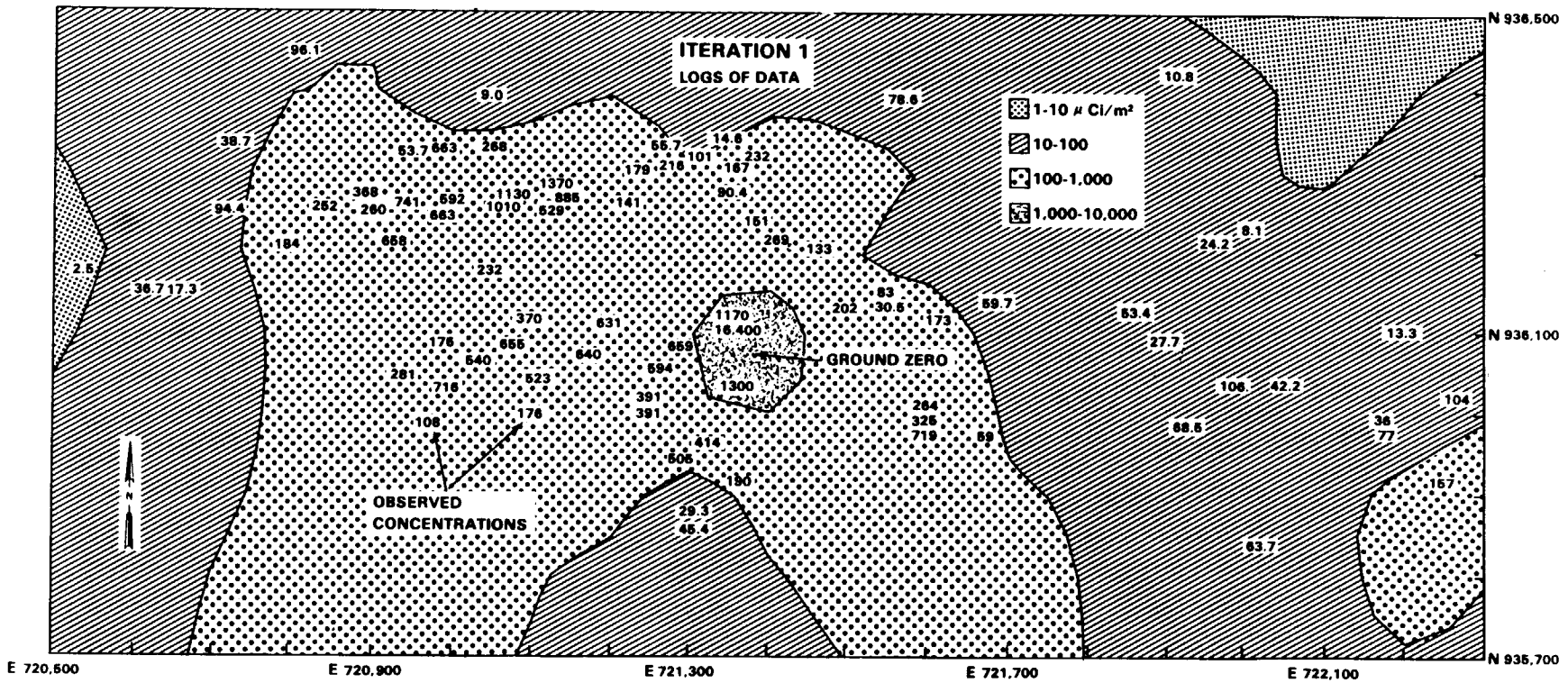

Figure 7. Estimated $^{239,240}Pu$ Concentration Contours in Surface Soil Near GZ at the Area 13, Project 57 Site After 1 Iteration (Log Transformed Data).

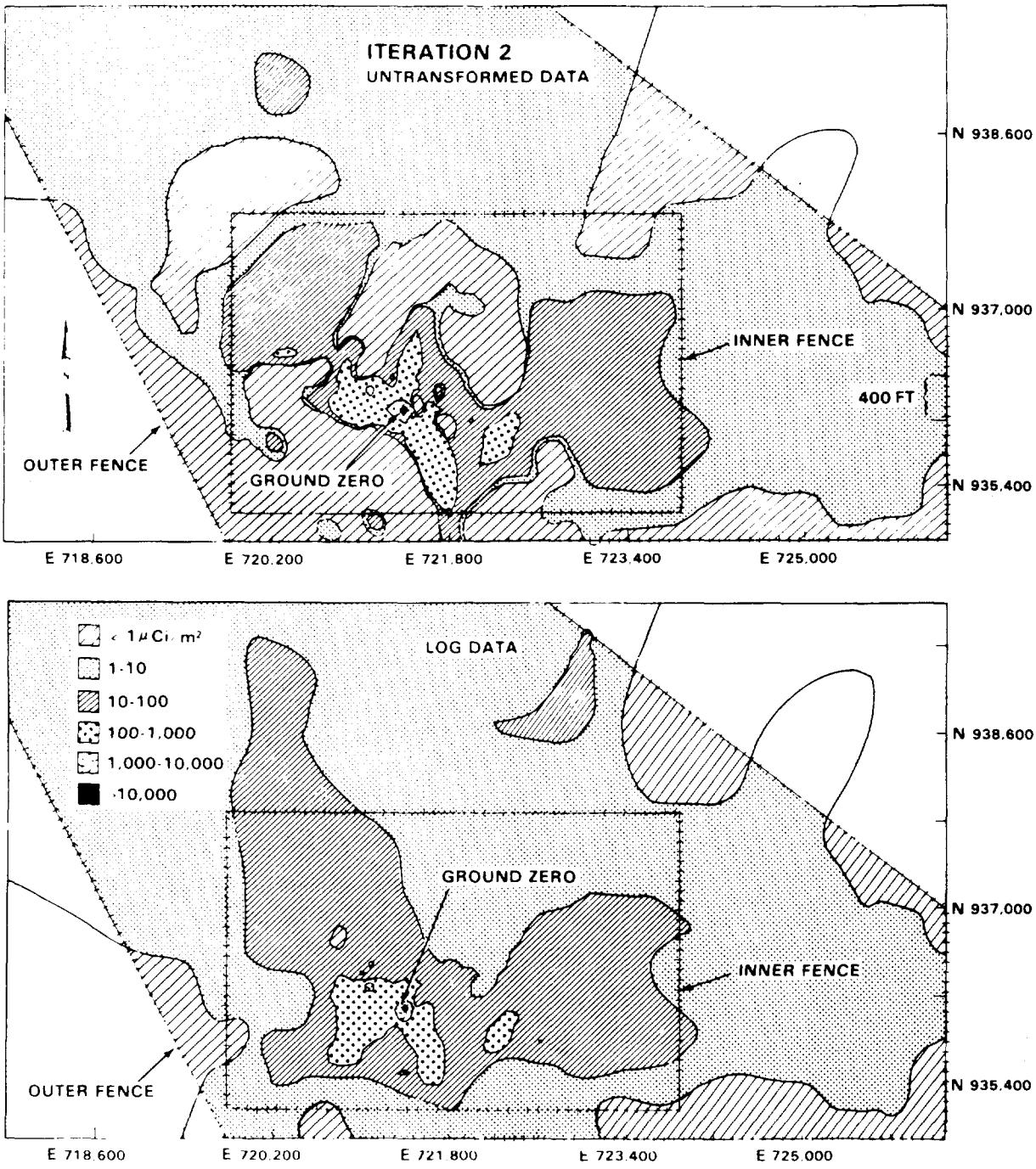

Figure 8. Estimated $^{239,240}Pu$ Concentration Contours in Surface Soil at the Area 13, Project 57 Site After 2 Iterations (Untransformed (Top) and Log Transformed (Bottom)).

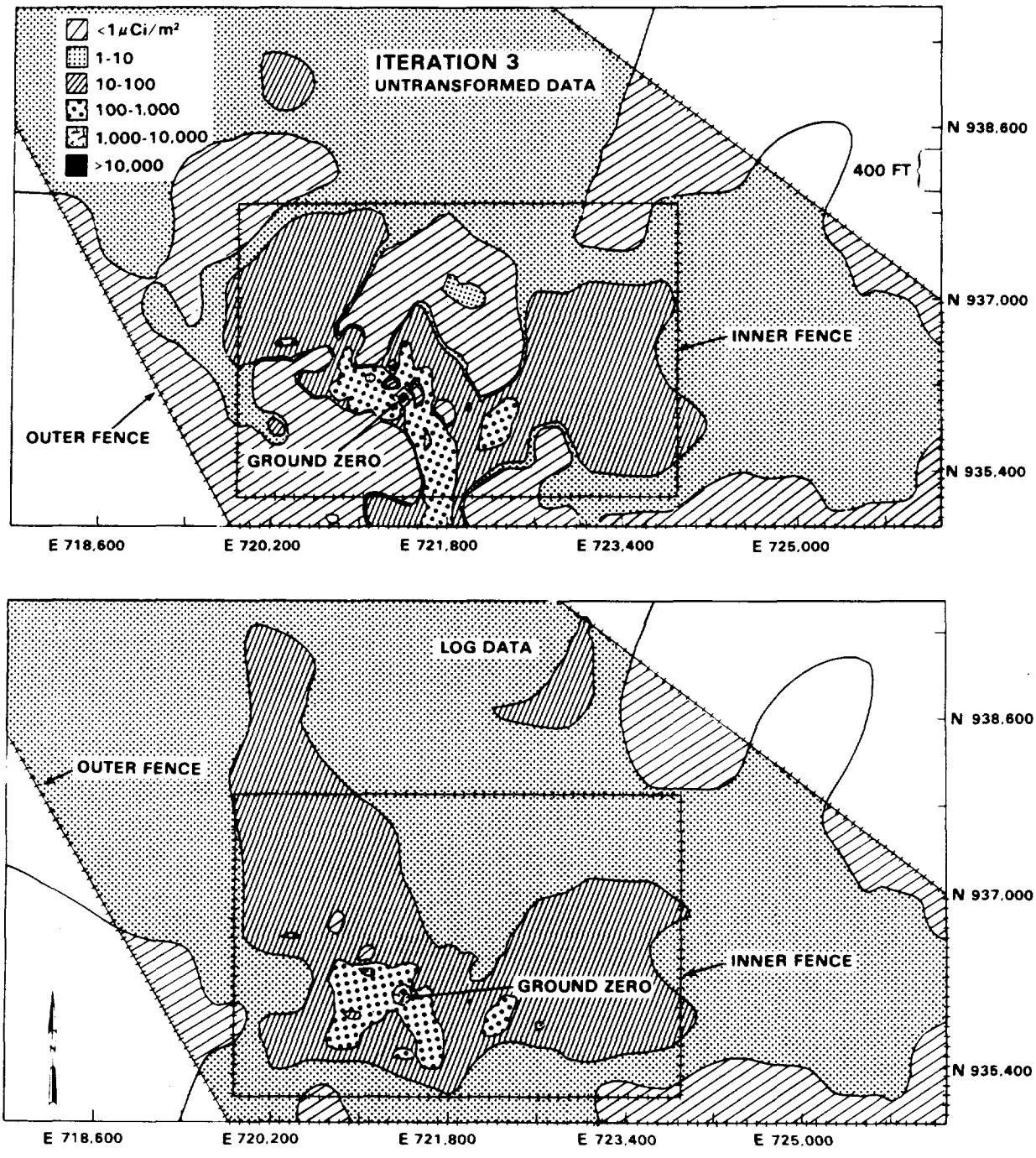

Figure 9. Estimated $^{239,240}Pu$ Concentration Contours in Surface Soil at the Area 13, Project 57 Site After 3 Iterations (Untransformed Data (Top) and Log Transformed (Bottom)).

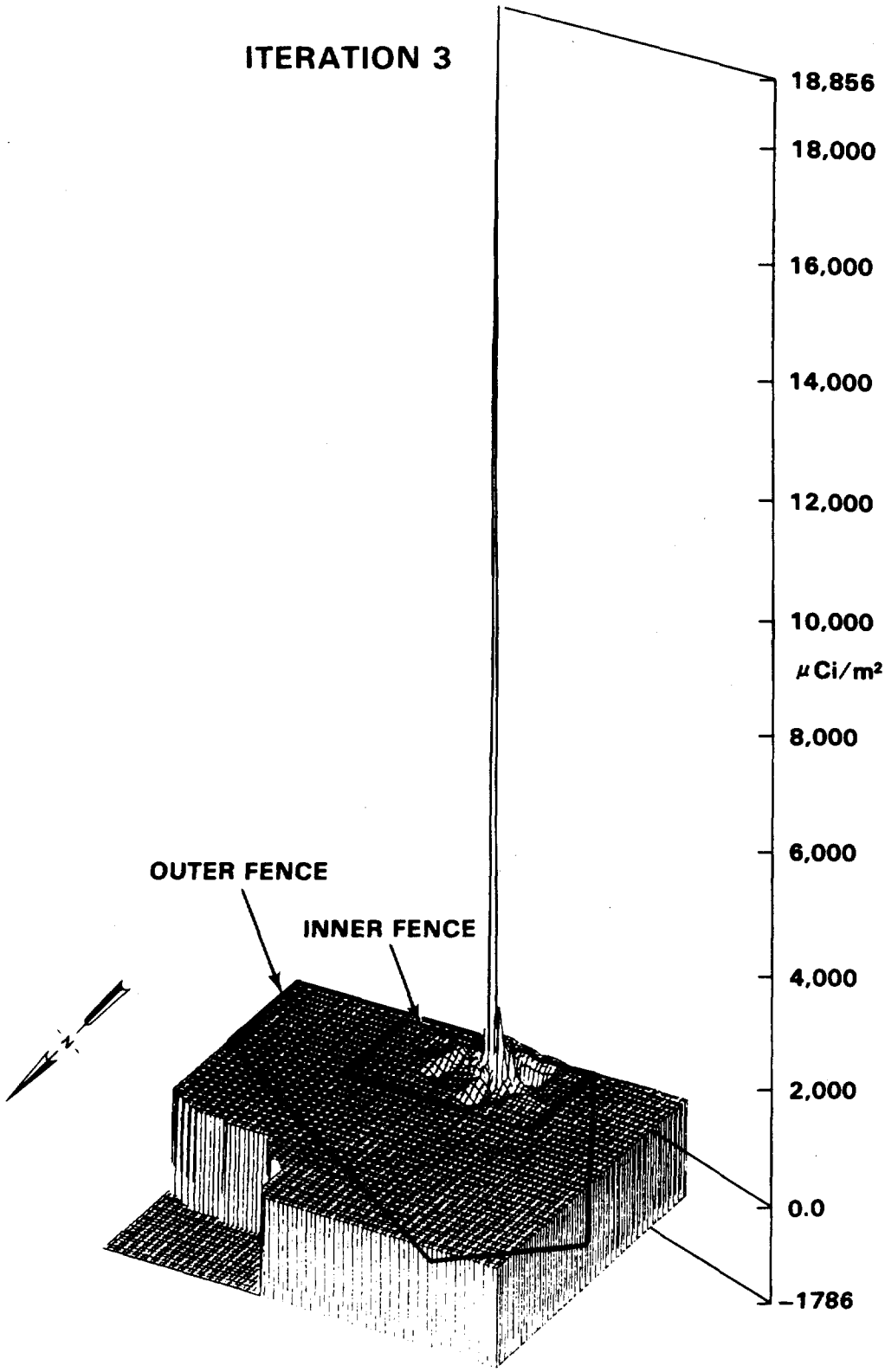

Figure 10. Estimated $^{239,240}Pu$ Concentration Surface at the Area 13, Project 57 Site After 3 Iterations (Untransformed Data).

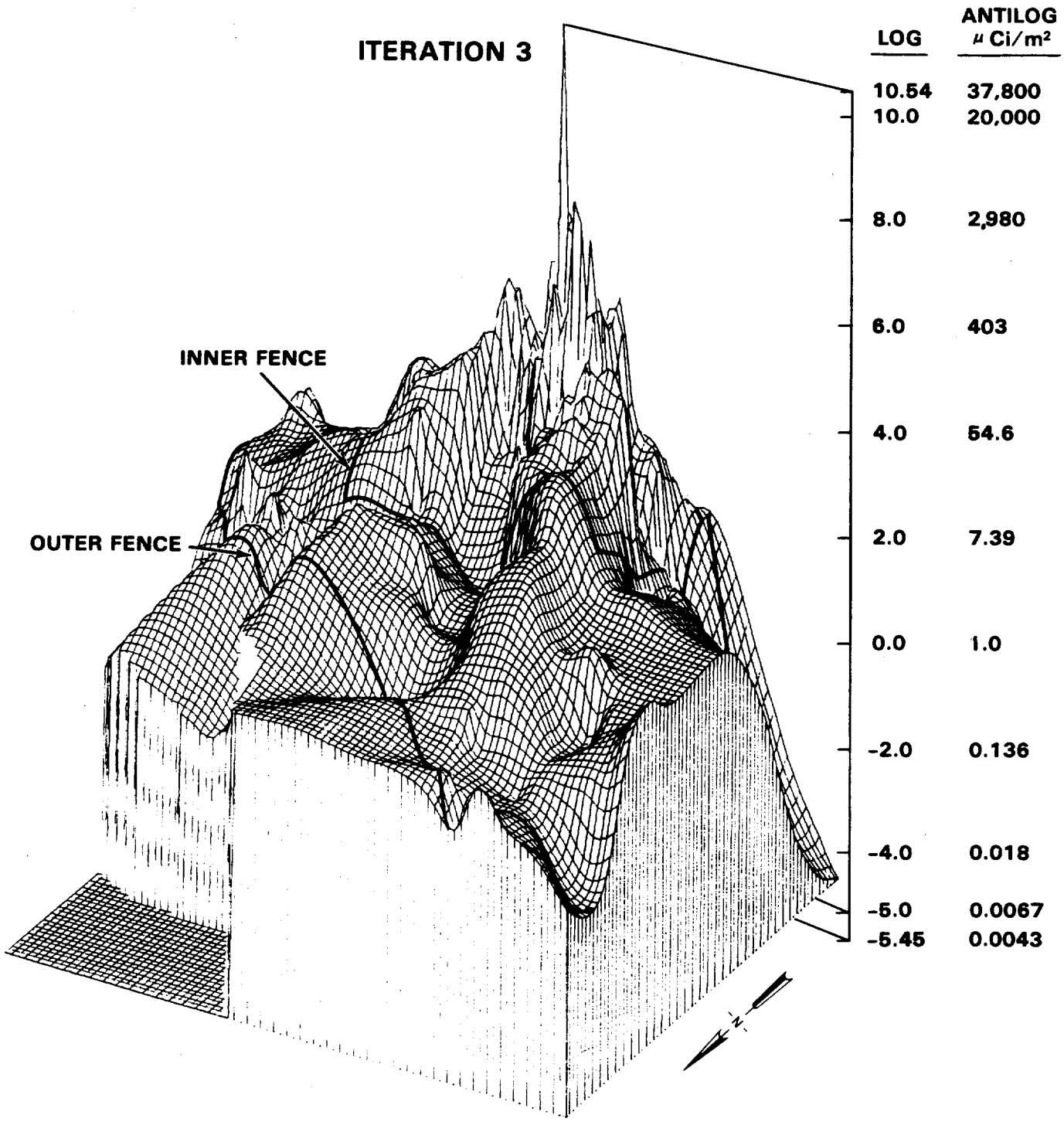

Figure 11. Estimated $^{239,240}Pu$ Logarithmic-Scale Concentration Surface at the Area 13, Project 57 Site After 3 Iterations.

Table 2. Estimated $^{239-240}Pu$ Concentrations ($\mu Ci/m^2$ per 5-cm Depth) at Grid Nodes Near GZ Using Untransformed and Log-Transformed $^{239-240}Pu$ Observations.

Iteration	Untransformed						Log Transformed*				
	E721200		E721400		E721600		E721200		E721400		E721600
	20	- 62	117	97	68	N936400	96	41	77	77	76
	252	126	223	135	34		172	108	186	129	93
	354	1045	291	115	- 13		248	251	259	105	76
1	629	2171	10340	198	199	N936100	621	963	5058	128	166
	210	664	1804	527	382		418	475	941	373	361
	- 8	175	272	660	564		173	50	167	392	301
	-434	- 156	113	508	682	N935800	62	52	82	183	278
	92	- 25	265	100	78		79	18	58	77	248
	223	100	239	109	84	N	186	114	255	125	288
	210	512	280	- 76	84		216	202	281	77	378
2	618	1787	15535	- 460	190		697	1014	18130	104	206
	135	371	1137	372	385		366	738	1438	396	53
	23	128	96	638	644		219	39	236	469	83
	-430	- 152	45	477	782		53	43	83	206	76
	88	- 81	288	65	86		69	9	43	78	76
	254	108	248	133	189		194	125	317	123	77
	39	- 304	282	- 135	236		181	137	277	63	41
3	647	1121	18856	-1019	191		717	859	37793	96	241
	217	211	67	283	375		295	937	1459	398	381
	151	140	59	785	801		290	35	311	544	298
	-382	- 111	55	632	1016		54	44	91	237	246

*Tabled values are $\exp(\hat{z}_{c,r})$, where $\hat{z}_{c,r}$ is the estimated plutonium concentration (log scale) at grid coordinate (X_c, Y_r).

The goodness-of-fit of the estimated surface to observed concentrations at sample collection points can be measured by squaring the linear correlation coefficient between the observed data and the estimated surface at the sampling locations.* This statistic (R^2, the percent of the total variation at sample locations explained by the fitted surface) is plotted in Figure 12 for each stratum, iteration, and fitting scale. The fits are very good for strata 1 and 2 for the untransformed as well as for the log and antilog fits. R^2 tends to decrease for strata near GZ particularly for the untransformed and antilog scales. The effect of iterating is to increase R^2 in all strata for all three

*Pierre Delfiner pointed out (personal communication) that R^2 will tend to be overoptimistic as a measure of goodness of fit since y_i and $\hat{y}_i$ tend to be correlated when y_i is obtained using a nearest neighbor approach.

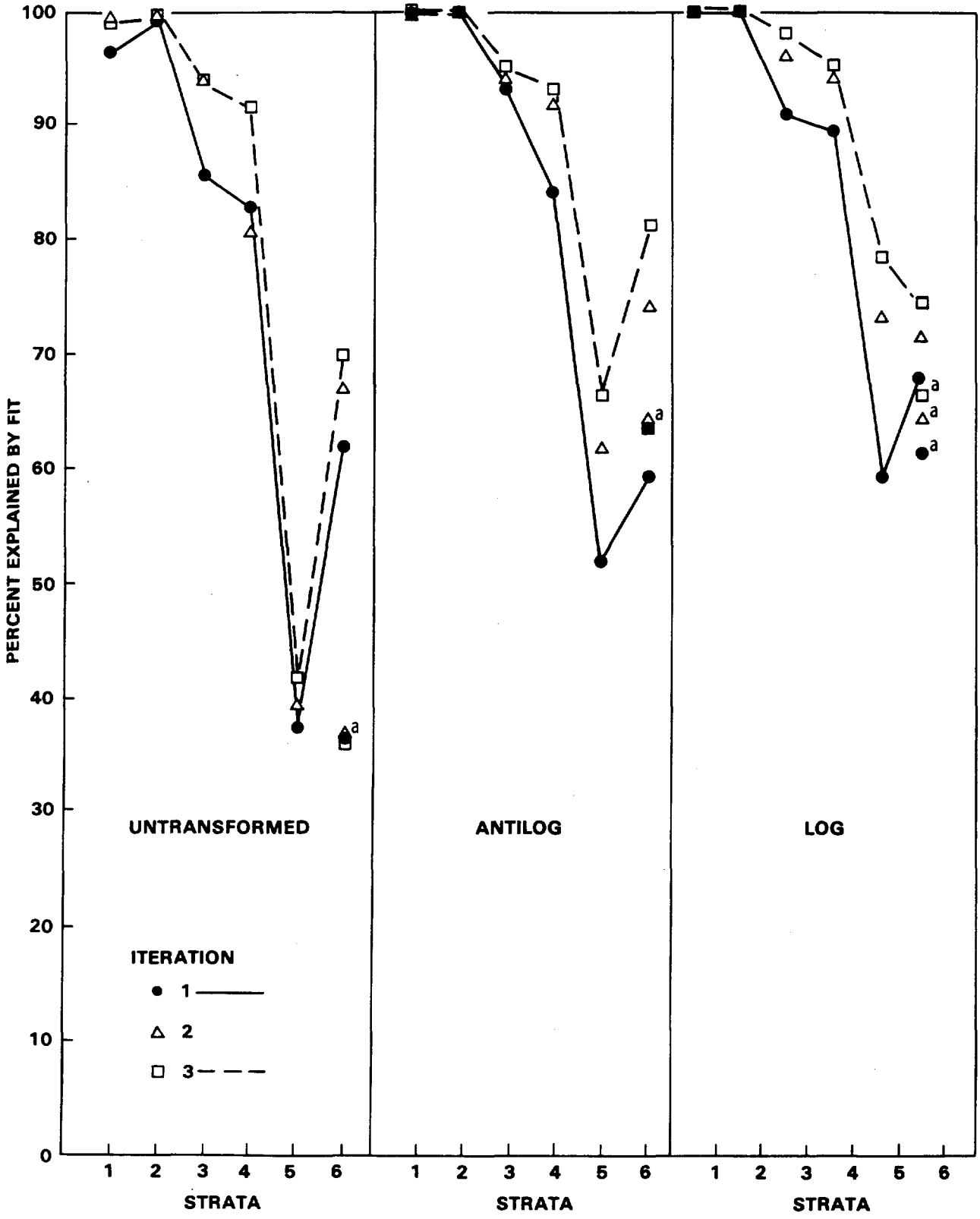

[a]Results obtained when Observation Number 28 in Stratum 6 (see Appendix A) is deleted.

Figure 12. Percent of Total Variation Explained By Fitted $^{239-240}Pu$ Concentration Surface.

data fits. Using R^2 as criterion, the antilog fits appear preferable to fits on untransformed data. In the next section, we examine residuals from the estimated surfaces in more detail.

Examination of Residuals

Residuals R_{i1}, R_{i2}, and R_{i3}, as defined by Equation 4 (also see Table 1 and Figure 2), are plotted in Figures 13-15 for the untransformed and antilog fits for strata 1, 3, and 6. Figures 16 and 17 give these results for the log scale. Several summary statistics of the residuals for all six strata are given in Table 3. These data indicate that the iterative procedure is effective in reducing the mean and median size of the absolute values of the residuals in all three scales. The smaller residuals in strata 1 tend to approach zero with only three iterations, whereas larger residuals for the more heterogeneous data in stratum 6 near GZ tend to "bounce around" and approach zero more slowly.

Figure 18 shows the percent reduction in the median of the absolute values of residuals that occur due to iterating two and three times (computed from Table 3). Percent reductions are highest in strata 1 and 2 and become smaller for the strata nearer GZ. The least reduction occurs in stratum 5 for the fit to untransformed data. The percent reduction between Iterations 2 and 3 (Figure 18) was consistently greatest for the fit on log units, followed by the antilog and untransformed data fits. Figure 18 indicates for this data set that the third iteration yielded a substantial improvement in fit over the second iteration.

The squares (R_1^2) of the linear correlation coefficients between the observed $^{239,240}Pu$ soil concentrations and the residuals from fitted surfaces are given in Figure 19. An $R_1 \simeq 1$ would indicate a linear association between residuals and observed data such that large observed values would tend to be underestimated by the estimated concentration surface, and small observations would tend to be overestimated by the concentration surface. If this occurs for strata 1 and 2, it could indicate a tendency for the estimated low-level contours to be too far out from GZ if the negative residuals occur predominately around the outer edges of the strata. This does not appear to happen, however, since Figure 19 indicates that for the untransformed data fits, R_1^2 on the first iteration is only 0.02 or 0.03 for strata 1, 2, and 3. This increases to about 0.20 for strata 4 and 5, and further increases to 0.82 percent for stratum 6. (This large R_1^2 for stratum 6 is caused by the datum 16,400 $\mu Ci/m^2$ in stratum 6 (see Appendix A) as indicated in Figure 19.) This is examined in more detail in Figures 20 and 21, where the residuals after three iterations on untransformed data are displayed on the estimated plutonium concentration contours for Iteration 3. Strata boundaries (from Figure 1) are also shown. There appears to be no obvious tendency for negative residuals to predominate around the edges of the map (Figure 21). Clusters of positive or negative residuals

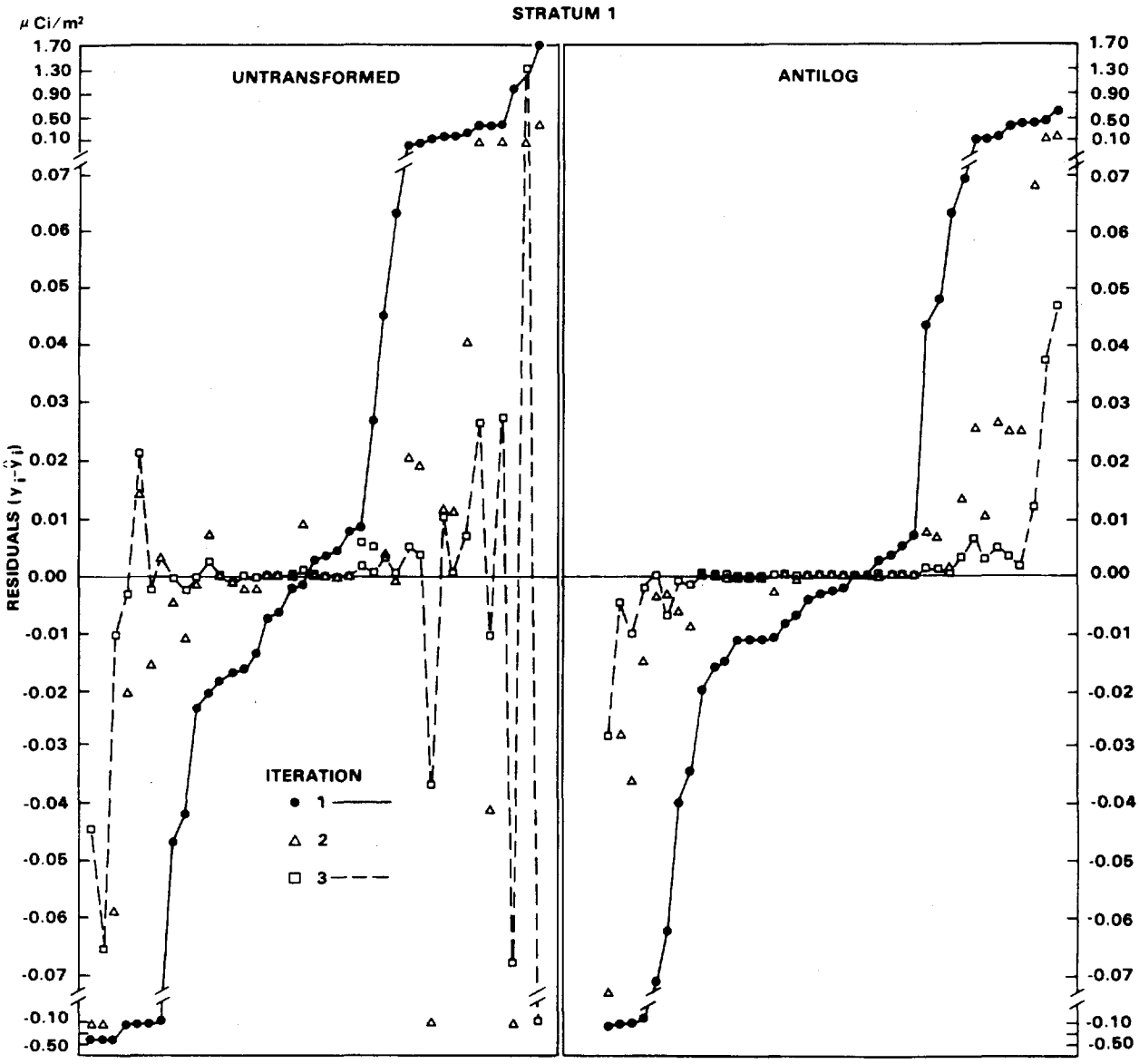

[a]To aid visual comparison, residuals for Iteration 1 are ordered in increasing value from left of plot. Residuals R_{i1} in the same relative position for the untransformed and antilog plots do not necessarily correspond to the same data point.

Figure 13. Residuals[a] From Fitted $^{239-240}Pu$ Concentration Surfaces for Stratum 1.

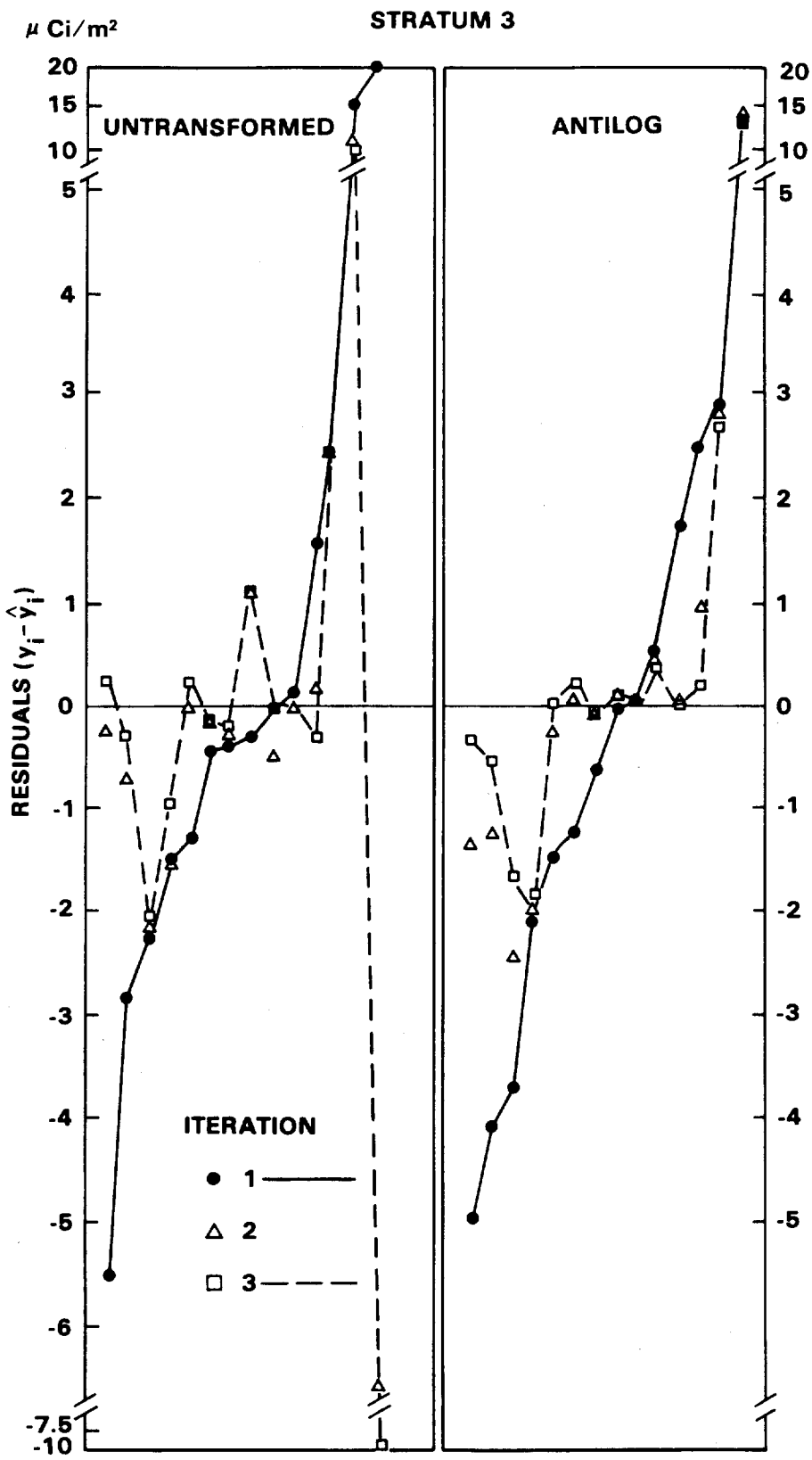

Figure 14. Residuals From Fitted $^{239-240}$Pu Concentration Surfaces for Stratum 3.

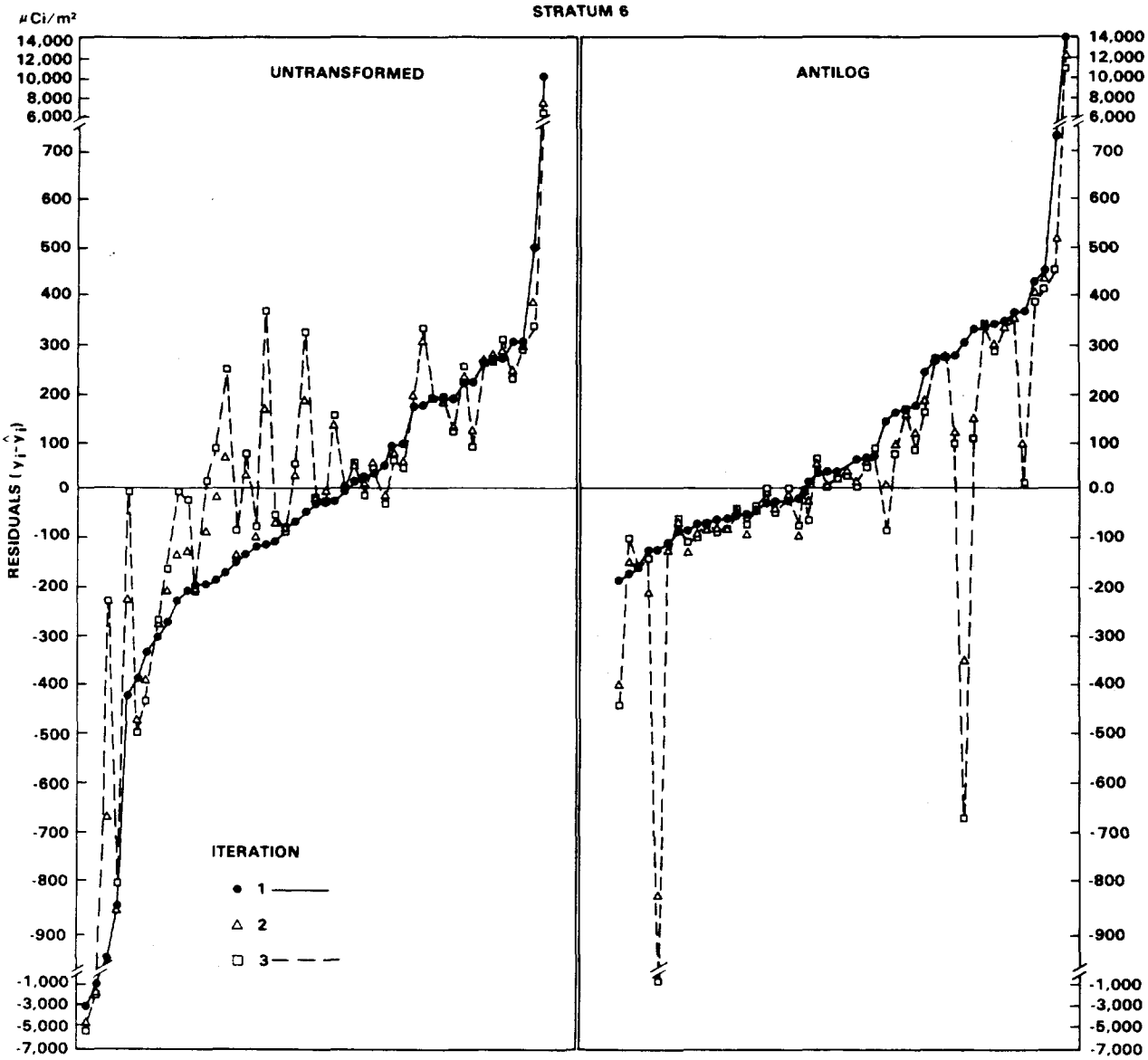

Figure 15. Residuals From Fitted $^{239-240}$Pu Concentration Surfaces for Stratum 6.

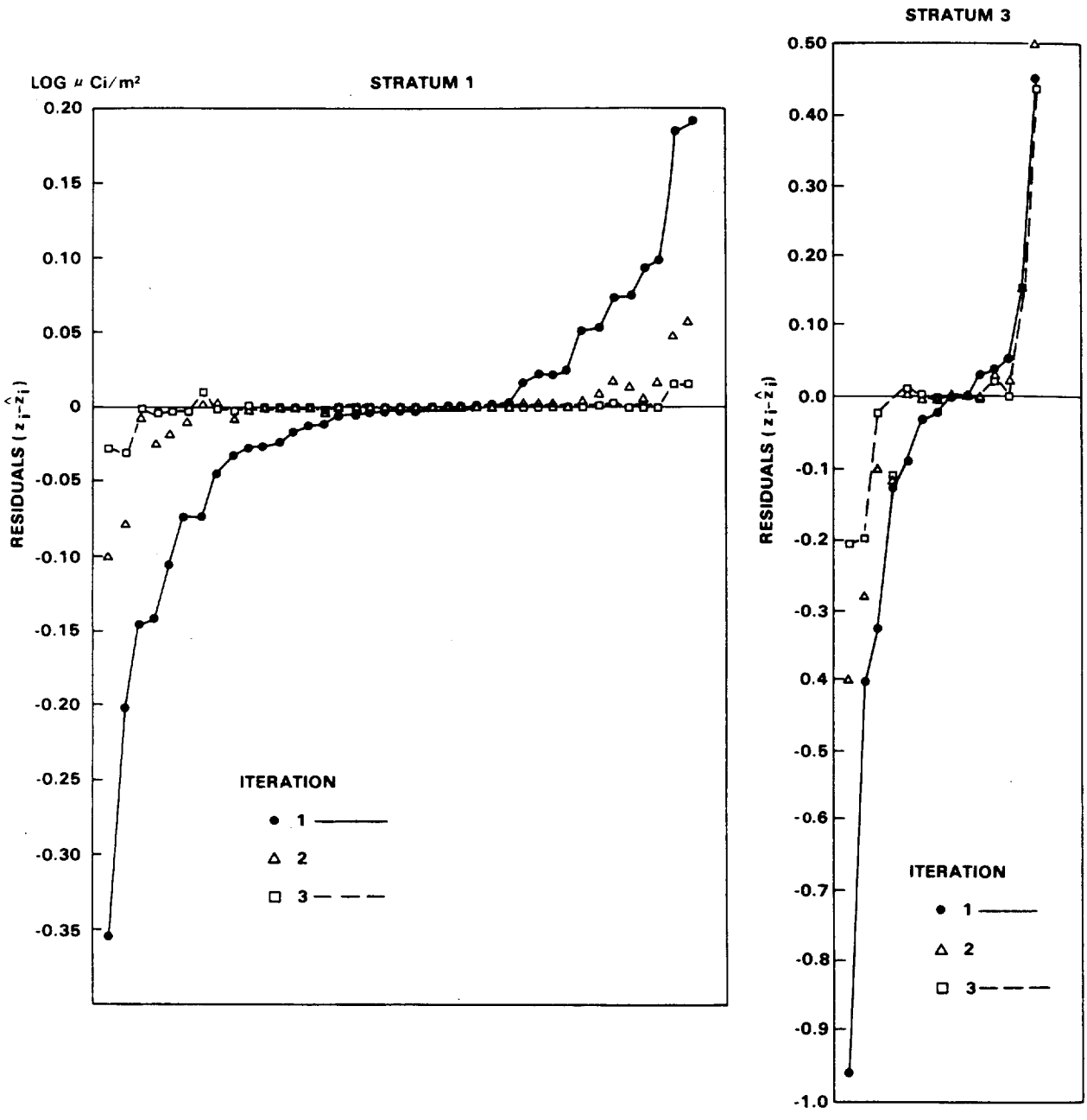

Figure 16. Residuals From Fitted Log $^{239-240}$Pu Concentration Surface For Strata 1 and 3.

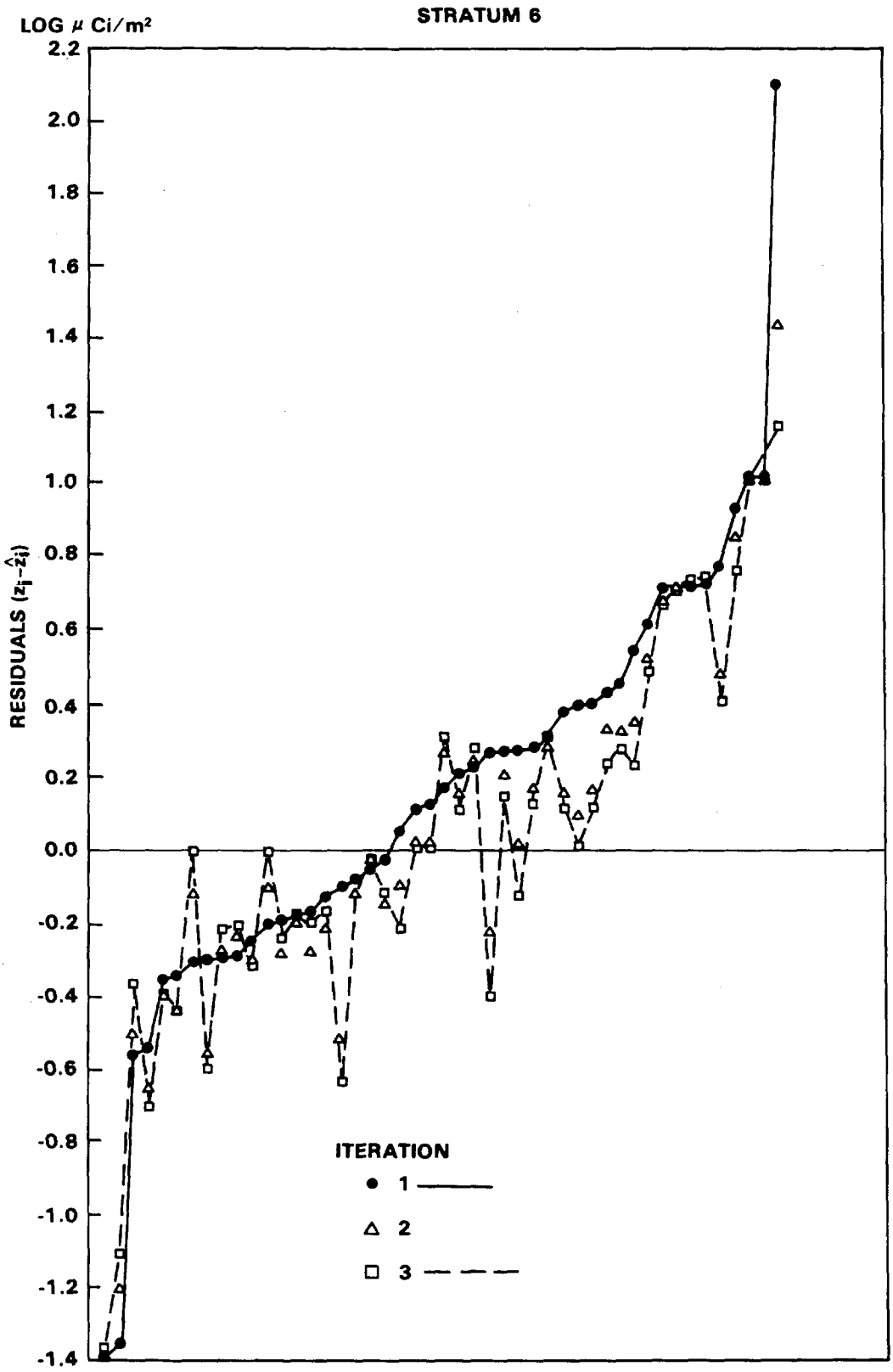

Figure 17. Residuals From Fitted Log $^{239-240}$Pu Concentration Surface For Stratum 6.

Table 3. Some Summary Statistics for Residuals from Fits to $^{239-240}Pu$ Soil Concentrations in Area 13 (Project 57), NTS.

	Iteration	Stratum 1 (n = 39)			Stratum 2 (n = 31)			Stratum 3 (n = 14)		
		Mean*	Median**	S.D.***	Mean	Median	S.D.	Mean	Median	S.D.
Untransformed	1	0.20	0.063	0.41	0.25	0.022	0.68	3.9	1.5	7.1
	2	0.056	0.0090	0.14	0.074	0.0012	0.27	2.0	0.57	4.0
	3	0.048	0.0027	0.049	0.033	0.00014	0.11	2.0	0.30	4.1
Antilog	1	0.093	0.035	0.16	0.21	0.014	0.75	2.8	1.9	4.5
	2	0.018	0.0019	0.038	0.074	0.0011	0.30	1.9	0.68	4.1
	3	0.0046	0.00060	0.011	0.030	0.00008	0.12	1.5	0.26	3.7
Log	1	0.058	0.026	0.095	0.025	0.0055	0.064	0.19	0.074	0.32
	2	0.012	0.0019	0.025	0.0072	0.00031	0.026	0.12	0.027	0.20
	3	0.0034	0.00025	0.0081	0.0029	0.00002	0.011	0.085	0.019	0.16
		Stratum 4 (n = 19)			Stratum 5 (n = 20)			Stratum 6 (n = 47)		
		Mean	Median	S.D.	Mean	Median	S.D.	Mean	Median	S.D.
Untransformed	1	12	8.9	16	50	21	75	520	185	1630
	2	10	4.8	17	45	25	74	490	164	1410
	3	7.3	4.7	11	43	24	71	460	163	1320
Antilog	1	13	10.2	17	41	24	60	470	127	2100
	2	8.5	6.9	12	32	15	53	430	100	1840
	3	6.9	4.2	10	28	13	50	400	93	1650
Log	1	0.27	0.27	0.32	0.46	0.35	0.62	0.46	0.31	0.61
	2	0.18	0.16	0.23	0.35	0.29	0.50	0.42	0.28	0.55
	3	0.15	0.12	0.21	0.29	0.18	0.45	0.39	0.28	0.52

*Mean of absolute values of residuals; Units of $\mu Ci/m^2$ to 5 cm depth.

**Median of absolute values of residuals.

***Standard deviation of residuals.

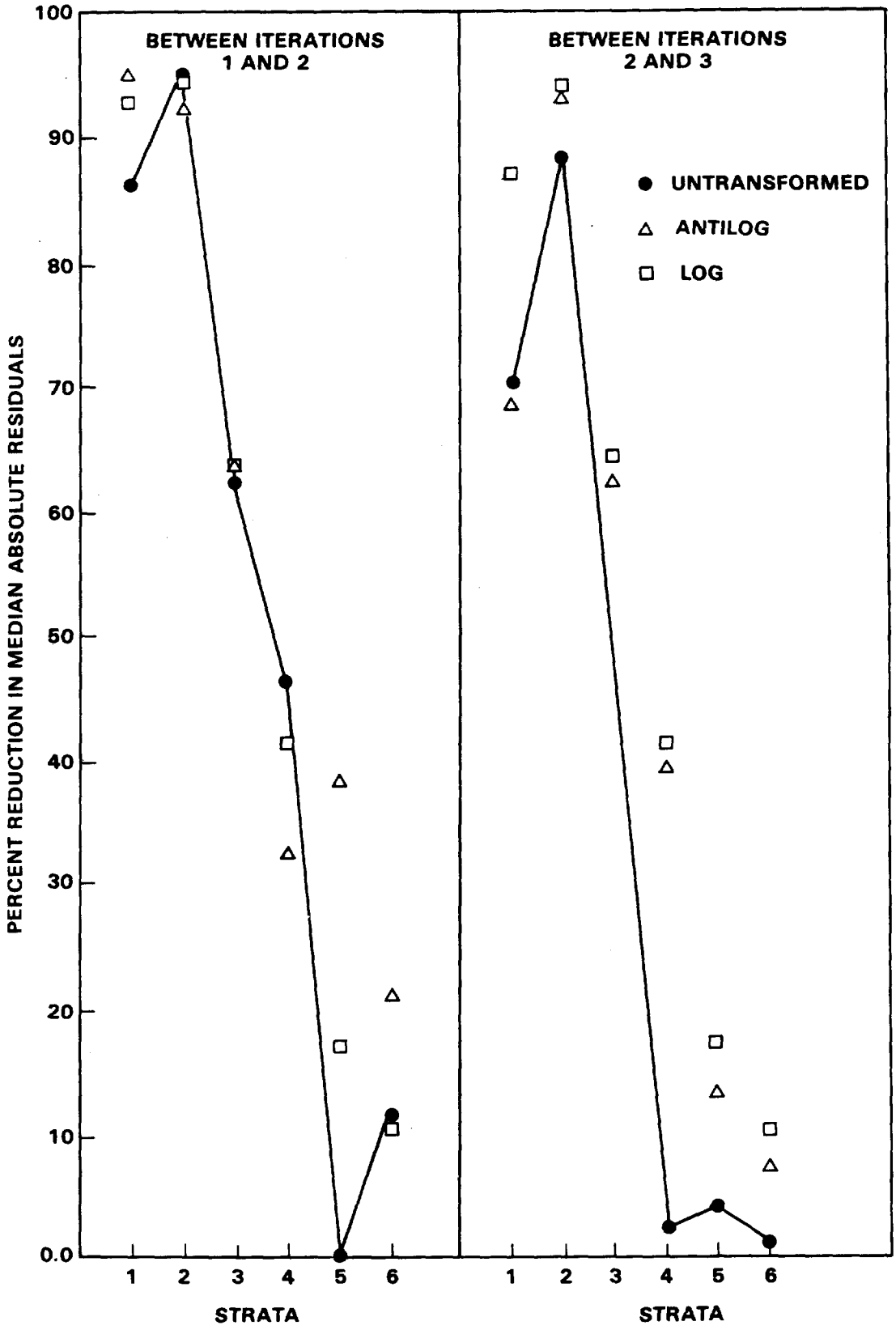

Figure 18. Percent Reductions in Median of Absolute Values of Residuals.

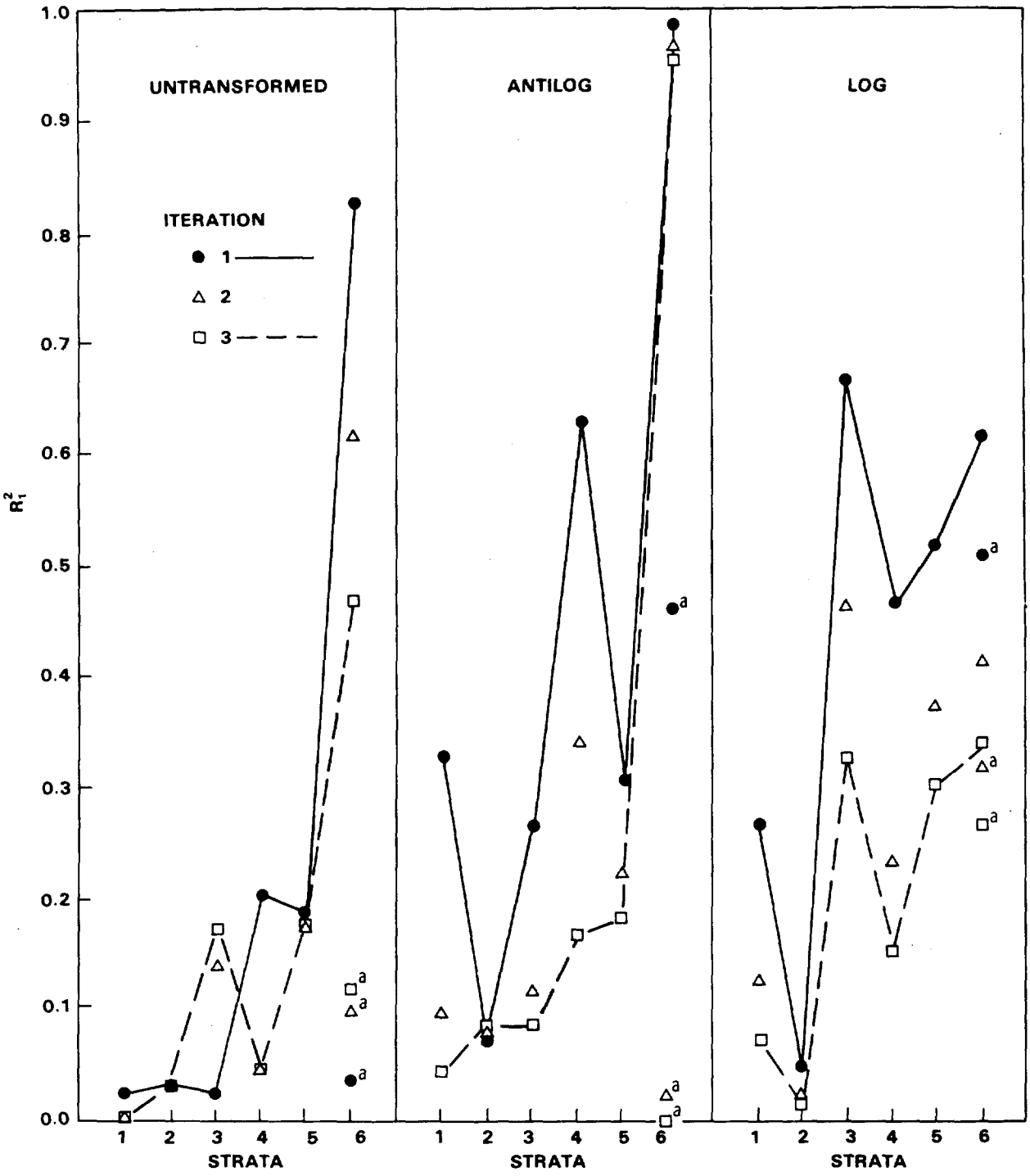

[a]Results Obtained When Observation Number 28 in Stratum 6 (see Appendix A) is Deleted.

Figure 19. Square of Correlation Coefficient (R_1^2) Between Observed $^{239-240}Pu$ Soil Concentrations and Residuals From Fitted Surfaces.

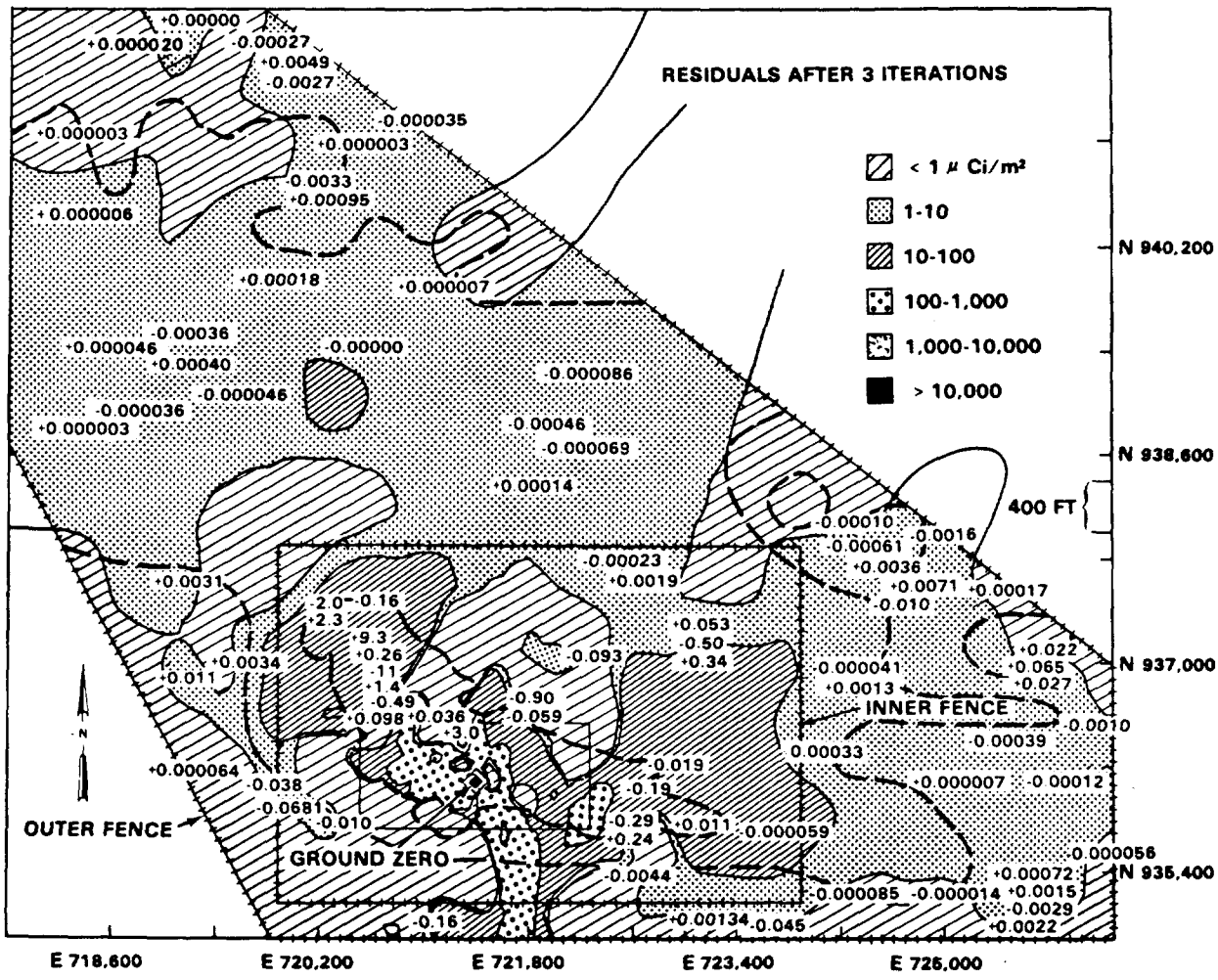

Figure 20. Estimated $^{239-240}$Pu Concentration Contours in Surface Soil at Project 57 Showing Residuals After 3 Iterations (Untransformed Data).

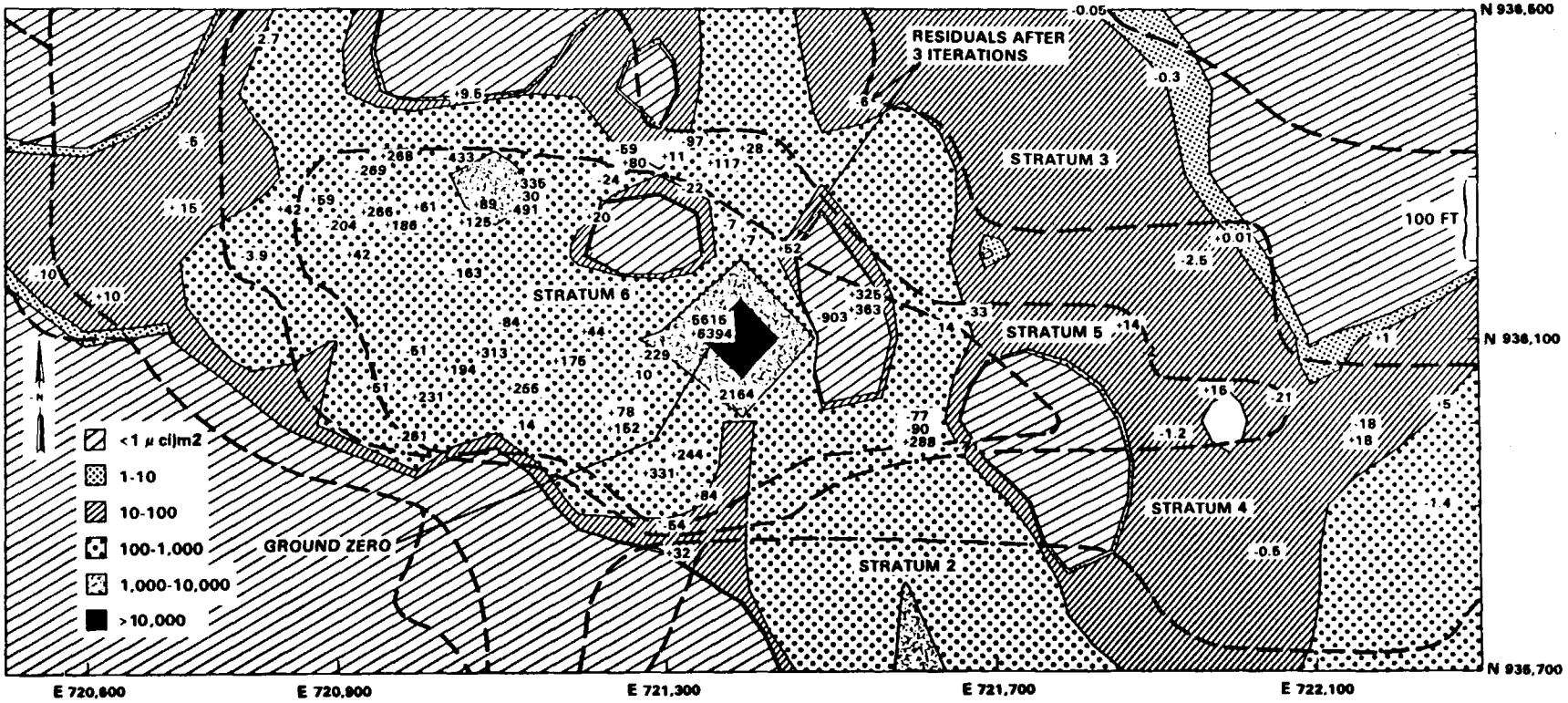

Figure 21. Estimated $^{239,240}Pu$ Concentration Contours in Surface Soil Near GZ at the Area 13, Project 57 Site Showing Residuals After 3 Iterations (Untransformed Data).

are also not in evidence, although we have not attempted any formal statistical tests to detect clustering. We have examined plots of residuals for Iteration 1 for the untransformed and antilog fits (not shown) and found no apparent clustering effects of positive and negative residuals.

Values of R_1^2 for Iteration 1 for the antilog and log fits tend to be larger than for the untransformed fits (except for stratum 6 for the log fit). Iterating tends to result in smaller values of R_1^2 for all three fits. Ideally, R_1^2 should be zero. The residuals and observed values for stratum 4 are plotted in Figure 22 for the antilog fits, Iterations 1 and 3. These illustrate the reduction in R_1^2 for that strata achieved by the iterating procedure.

We have also computed R_2^2, which is the square of the linear correlation coefficient between residuals and estimated values (Figure 23). Values of R_2^2 near 1 would indicate that large estimates ($\hat{y}_i$) tend to be less than the corresponding observed datum (y_i), and small estimates tend to be larger than the observed datum. Figure 23 indicates values of R_2^2 in the range of from near zero up to about 0.20 except for stratum 6 for the antilog scale, where R_2^2 is about 0.5. R_2^2 is reduced in most cases by iterating, and there appears to be little evidence to suggest the antilog or log fits are preferable to the fits in untransformed scale if R_2^2 is used as a criterion.

CONCLUSIONS

On the basis of results from three iterations, it appears that iterating on residuals can improve estimates of the true concentration surface for the Area 13 (Project 57) data set. If the results are interpreted in the original scale, fitting in units of logs and then transforming the estimated log-surface back to the original scale appears to be preferable to fitting in the untransformed scale. Alternately, the log fits could be left in log scale if interpretation in log units is desired. In making this conclusion, it is assumed that the estimated concentration surface of ^{241}Am obtained using FIDLER is approximately the same as the true concentration surface for $^{239,240}Pu$.

Iterating on residuals tends to yield a better fitting surface to observed concentrations at sample collection points using as a criterion the size of the average absolute (mean or median) size of residuals, the standard deviation of residuals, or the proportion of the total variability in the data explained by the fit. This is true for all three scales (untransformed, log-transformed, and log). However, estimated concentrations at grid nodes (not sample collection points) are not necessarily improved by the iteration procedure. This is particularly true for the untransformed scale, where negative grid estimates are present and become even

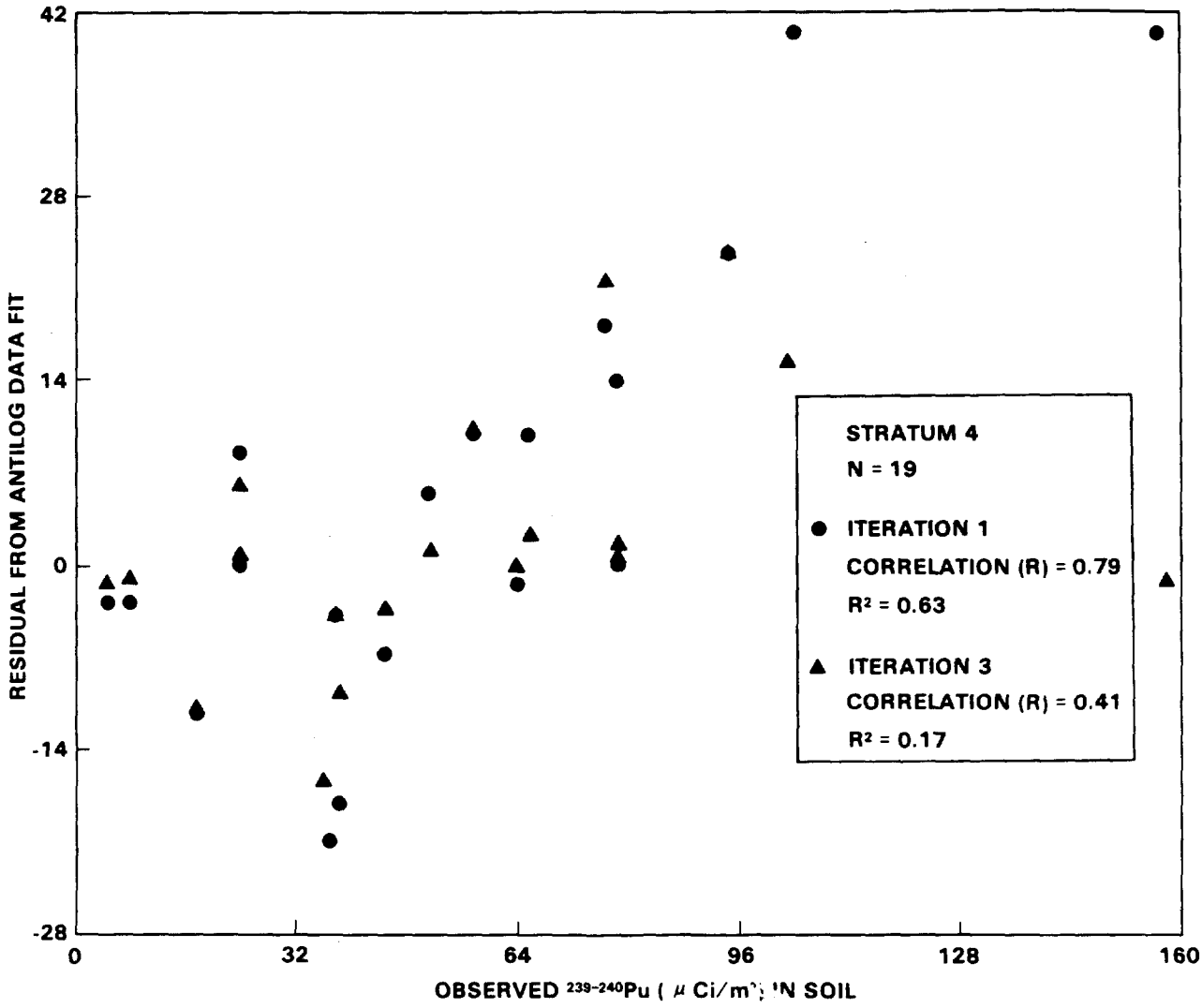

Figure 22. Plot of Observed $^{239-240}$Pu Concentrations In Soil Versus Residuals From Antilog Fit.

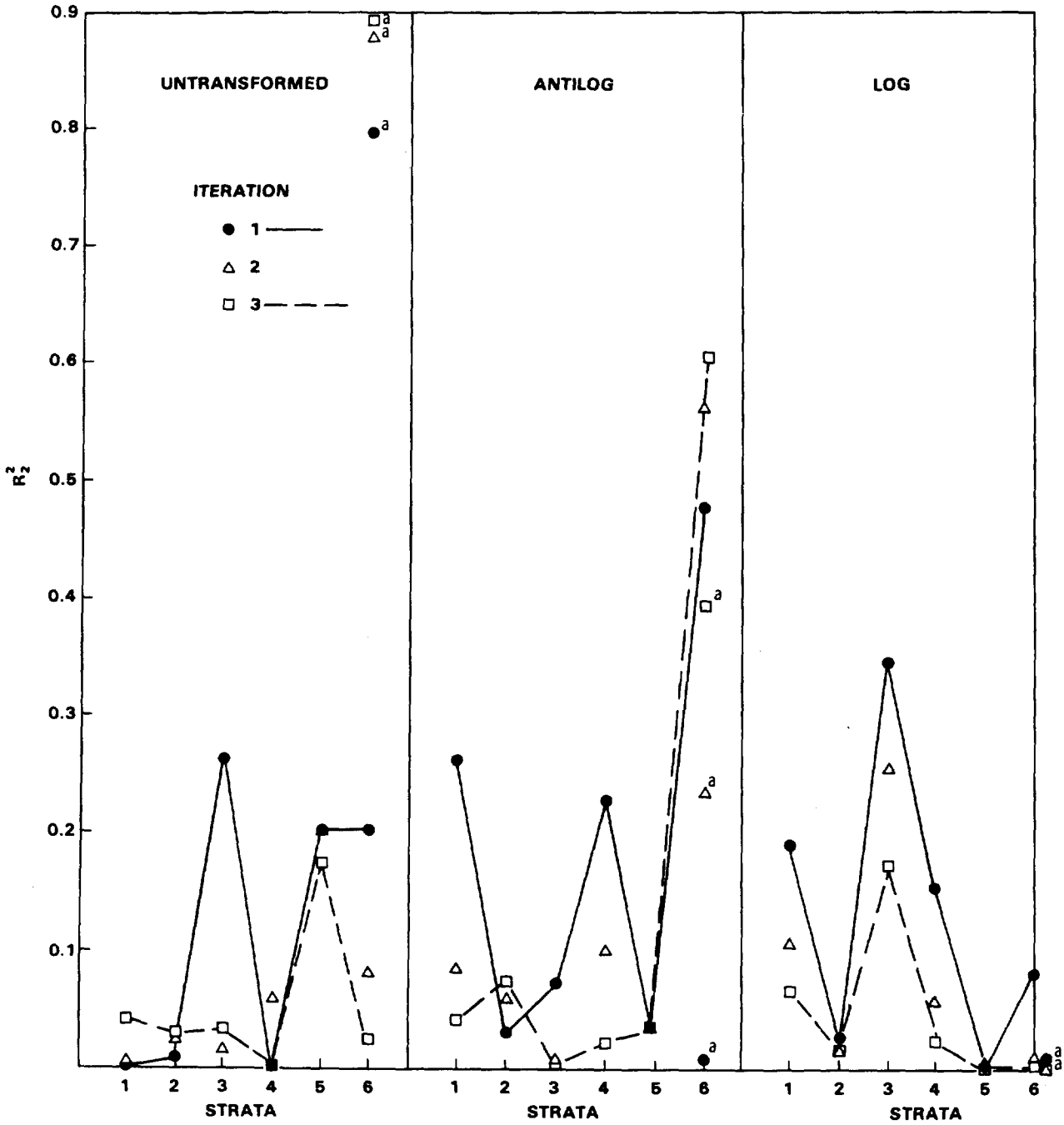

Figure 23. Square of Correlation Coefficients (R_2^2) Between Estimated $^{239-240}Pu$ Concentrations and Residuals From Fitted Surfaces.

larger after iterating. This behavior results, most likely, from the difficulty of fitting a surface to the very large concentration observed near GZ without distorting grid estimates in nearby areas.

Residuals in antilog form at sample collection points are usually smaller on the average than those from fits in the untransformed scale. Also, distortions in the antilog concentration surface due to the extreme data point near GZ appear to be minor. However, the correlation between observed data and residuals tends to be somewhat larger for the log and antilog fits than for untransformed data fits. Moreover, fitting in log scale does not, of course, eliminate fitting problems due to a lack of data in certain regions of the study site. Recall, for example, the apparently spurious contours south of GZ for both the untransformed and antilog fits due to insufficient number and placement of samples in that area (Figures 6-9).

The plotting of observed data and residuals on estimated contour maps has proved useful in subjectively evaluating the estimated surface at other than data points. Efforts should be made, however, to try kriging techniques to estimate these concentration surfaces,* since this approach yields an estimation variance for each grid node estimate. Furthermore, if the underlying assumptions of kriging are satisfied, this method yields best linear unbiased estimates of concentration at grid nodes.

ACKNOWLEDGMENTS

I wish to thank Ms. Barbara Vinson of Battelle-Northwest for her excellent assistance in writing computer programs and performing so well a variety of other computing tasks associated with this paper. Special recognition is also due Ms. Mary Lou Lomon, who did such an excellent job in typing the manuscript.

---

*See Delfiner and Gilbert (1978), this volume.

REFERENCES

1. Agterberg, F. P. 1970. "Autocorrelation Functions in Geology." *Geostatistics*. D. F. Merriam, Ed. Plenum Press, New York. pp. 113-141.

2. Akima, H. 1975. "Comments on 'Optimal Contour Mapping Using Universal Kriging' by Ricardo A. Olea." *Journal of Geophysical Research* 80:832-834.

3. Cochran, W. G. 1963. *Sampling Techniques*. Second Edition. John Wiley and Sons, New York.

4. Davis, J. C. 1973. *Statistics and Data Analysis in Geology*. John Wiley and Sons, New York.

5. Delfiner, P., and J. P. Delhomme. 1975. "Optimum Interpolation by Kriging." *In: Display and Analysis of Spatial Data*. J. C. Davis and M. J. McCullagh, Eds. John Wiley and Sons, New York. pp. 96-114.

6. Delfiner, P., and R. O. Gilbert. 1978. "Combining Two Types of Survey Data for Estimating Geographical Distribution of Plutonium in Area 13." (This report.)

7. Dunaway, P. B., and M. G. White, Eds. 1974. *The Dynamics of Plutonium in Desert Environments*. USAEC Report, NVO-142.

8. Eberhardt, L. L., and R. O. Gilbert. 1976. "Sampling the Environs for Contamination." *In: Proceedings of the First ERDA Statistical Symposium*. W. L. Nicholson and J. L. Harris, Eds. Battelle-Northwest Laboratories, BNWL-1986. pp. 187-208.

9. Gilbert, R. O., and L. L. Eberhardt. 1977. "An Initial Synthesis of Area 13 ^{239,240}Pu Data and Other Statistical Analyses." *In: Environmental Plutonium on the Nevada Test Site and Environs*. M. G. White, P. B. Dunaway, and W. A. Howard, Eds. USERDA Report, NVO-171. pp. 237-274.

10. Gilbert, R. O., L. L. Eberhardt, E. B. Fowler, E. M. Romney, E. H. Essington, and J. E. Kinnear. 1975. "Statistical Analysis of ^{239,240}Pu and ^{241}Am Contamination of Soil and Vegetation on NAEG Study Sites." *In: The Radioecology of Plutonium and Other Transuranics in Desert Environments*. M. G. White and P. B. Dunaway, Eds. USERDA Report, NVO-153. pp. 339-448.

11. Gilbert, R. O., L. L. Eberhardt, E. B. Fowler, and E. H. Essington. 1976a. "Statistical Design Aspects of Sampling Soil for Plutonium." *In: Atmosphere-Surface Exchange of Particulate and Gaseous Pollutants (1974)*. R. J. Engelman and G. A. Sehmel, Coordinators. ERDA Symposium Series 38, ERDA Technical Information Center, Oak Ridge, TN.

12. Gilbert R. O., L. L. Eberhardt, E. B. Fowler, E. H. Essington, and E. M. Romney. 1976b. "Statistical Analysis and Design of Environmental Studies for Plutonium and Other Transuranics at NAEG 'Safety-Shot' Sites." *In: Transuranium Nuclides in the Environment.* International Atomic Energy Agency, Vienna. pp. 449-460.

13. Huijbregts, C. J., and G. Matheron. 1971. "Universal Kriging (An Optimal Method for Estimating and Contouring in Trend Surface Analyses)." *In: Proceedings, 9th International Symposium on Techniques for Decision-Making in the Mineral Industry.* McGerrigle, Ed. Special Volume 12, Canadian Institute of Mining and Metallurgy. pp. 159-169.

14. Huijbregts, C. J. 1975. "Regionalized Variables and Quantitative Analysis of Spatial Data." *In: Display and Analyses of Spatial Data.* J. C. Davis and M. J. McCullagh, Eds. John Wiley and Sons, New York. pp. 38-53.

15. Kayuha, H. J., I. Aoki, and D. L. Wireman. 1974. "REECo Field Activities Sample Logistics in Support of the Nevada Applied Ecology Group." *In: The Dynamics of Plutonium in Desert Environments.* P. B. Dunaway and M. G. White, Eds. USAEC Report, NVO-142. pp. 17-19.

16. Olea, R. A. 1974. "Optimal Contour Mapping Using Universal Kriging." *Journal of Geophysical Research* 79:695-702.

17. Olea, R. A. 1975. "Optimum Mapping Techniques Using Regionalized Variable Theory." *In: Number Two, Series on Spatial Analysis.* Kansas Geological Survey.

18. Sampson, R. J. 1973. User's Manual for the SURFACE II Graphics System. Kansas Geological Survey.

19. Sampson, R. J. 1975a. "SURFACE II Graphics System." *In: Number One, Series on Spatial Analysis.* Kansas Geological Survey.

20. Sampson, R. J. 1975b. "The SURFACE II Graphics System." *In: Display and Analysis of Spatial Data.* J. C. Davis and M. J. McCullagh, Eds. John Wiley and Sons, Inc., New York.

21. White, M. G., and P. B. Dunaway, Eds. 1975. *The Radioecology of Plutonium and Other Transuranics in Desert Environments.* USERDA Report, NVO-153.

APPENDIX A. $^{239-240}Pu$ CONCENTRATIONS ($\mu Ci/m^2$) IN 10 GRAM ALIQUOTS FROM SURFACE (0-5 CM) SOIL SAMPLES COLLECTED WITHIN ^{241}Am ACTIVITY STRATA FROM AREA 13 (PROJECT 57), NEVADA TEST SITE

STRATUM 1			STRATUM 2		
NGC*			NGC		
North	East	$^{239-240}Pu$	North	East	$^{239-240}Pu$
936481	725672	2.59	938752	721675	1.96
935798	720191	12.8	936241	722779	41.50†
936127	725227	3.82	939883	721184	1.24
934929	725600	0.236	939443	718987	4.76
936737	726147	0.977	940231	719726	3.59
941589	719855	1.06	937341	723001	4.61
934961	723245	0.348	936796	724315	7.39
935259	724247	0.513	937973	724866	2.56
941730	719850	1.53	941125	718192	0.28
937086	725761	0.813	937032	723019	19.80
935090	722802	2.22	937801	722310	3.57
937056	725632	0.884	939661	718439	2.32
937759	724171	1.75	938622	722028	8.32
935093	725823	0.944	935440	722378	1.54
935325	725655	4.32	935712	723609	18.1
935847	719847	0.449	939174	722032	4.39
941866	719512	0.576	936970	724090	8.23
937729	724482	2.84	939741	718869	1.15
937015	719560	1.56	937149	722940	4.79
938065	724194	0.669	939397	720360	9.64
934915	723111	2.32	939049	719306	3.17
941183	720968	2.02	935288	724881	0.675
937674	724796	4.03	936385	723928	5.56
935022	725704	0.322	937030	722041	3.26
937601	724636	1.13	940330	717814	3.44
936104	719769	2.01	937736	722665	5.42
942096	719100	1.83	938893	718128	2.90
937602	725331	0.681	938408	721467	2.27
936922	725707	3.34	941011	720393	1.64
940689	720115	2.39	938995	718666	2.94
941899	718752	0.869	940617	718295	1.39
935060	721045	2.32			
937575	718850	3.61			
936094	719204	0.164			
936854	719122	2.76			
934910	720778	0.543			
935405	726235	0.218			
936142	726038	2.66			
940754	719962	1.25			

*Nevada Grid Coordinates (Feet)

†A new 10-gram aliquot was analyzed after the statistical analyses in this paper were completed. The new result was 28.5 $\mu Ci/m^2$. The average of 28.5 and 41.5, or 35 $\mu Ci/m^2$, was used by Delfiner and Gilbert (1978).

STRATUM 3		
NGC		
North	East	$^{239-240}Pu$
937338	720108	15.0
936007	722562	57.5
936107	722191	13.4
937004	720422	41.0
935811	722483	44.9
936499	721791	14.1
935787	722575	12.5
936148	720614	36.8
935763	723101	27.4
937331	720129	21.2
936540	721783	7.43
937375	720535	23.7
936423	721901	10.8
936173	720531	2.52

STRATUM 4		
NGC		
North	East	$^{239-240}Pu$
936230	722001	8.10
935918	722243	157.
936670	720927	51.3
936719	720771	4.59
936545	721266	24.1
936391	721556	78.7
935845	722014	63.8
935993	722168	36.1
935852	721295	45.4
937005	720581	57.0
936147	720645	17.4
936985	720585	38.9
936704	720611	79.2
936250	720714	94.4
936893	720643	66.1
936216	721950	24.2
936331	720711	38.8
935990	722172	77.0
936019	722259	104.

STRATUM 5		
North	East	$^{239-240}Pu$
936313	721304	101.
936446	720802	96.2
935986	721915	68.6
936394	721037	9.01
936332	721256	55.7
936044	720931	281.
936311	721338	167.
936038	721985	106.
935878	721296	29.4
936039	722040	42.3
936123	721849	53.4
936093	721887	27.7
936136	721674	59.7
936309	721270	216.
935974	721663	59.
936340	721330	14.7
936320	721372	232.
936254	720826	252.
936204	720784	184.
935985	720965	108.

APPENDIX B. ESTIMATING THE $^{239-240}$Pu CONCENTRATION SURFACE USING GRID

Estimating the $^{239-240}$Pu concentration surface using GRID is a two-phase procedure. In Phase 1 the slope of the surface at each data point (X_i, Y_i, y_i), $i = 1,2,\ldots,n$ is computed where X_i is the east-west coordinate, Y_i the north-south coordinate and y_i the $^{239-240}$Pu concentration at the point (X_i, Y_i). A weighted linear trend surface of the form

$$y_k = b_0 + b_1 w_{1k} X_k + b_2 w_{2k} Y_k \quad , \quad k = 1,2,\ldots,8 \tag{B1}$$

is fit by least squares to the eight nearest data points (X_k, Y_k, y_k) about each data point (X_i, Y_i, y_i), where

$$w_{1k} = \frac{X_k - X_i}{D_k} \quad , \quad w_{2k} = \frac{Y_k - Y_i}{D_k}$$

and

$$D_k = \sqrt{(X_k - X_i)^2 + (Y_k - Y_i)^2} \quad , \quad k = 1,2,\ldots,8.$$

Equation (B1) is constrained to pass through the control point (X_i, Y_i, y_i). The resulting set of coefficients (b_0, b_1, b_2) for each data point are used in Phase 2 to estimate the $^{239-240}$Pu concentration at each grid intersection point (grid node).

In Phase 2 the estimated $^{239-240}$Pu concentration $\hat{y}_{c,r}$ at each grid node (X_c, Y_r) is obtained. For the eight nearest data points about the grid node (X_c, Y_r), eight estimates of the concentration surface are obtained, each of the form

$$\hat{v}_t = b_{0t} + b_{1t} X_c + b_{2t} Y_r \quad , \quad t = 1,2,\ldots,8$$

where the eight sets of coefficients (b_{0t}, b_{1t}, b_{2t}) were obtained in Phase 1. The final estimate of the plutonium concentration at the grid node (X_c, Y_r) is then obtained as the distance weighted average

$$\hat{y}_{c,r} = \sum_{t=1}^{8} w_t \hat{v}_t \Big/ \sum_{t=1}^{8} w_t \quad , \tag{B2}$$

where

$$w_t = \left(1 - \frac{D}{1.1\, D_{max}}\right)^2 \Big/ \left(\frac{D}{1.1\, D_{max}}\right)^2 \quad . \tag{B3}$$

D is the distance to a sample data point from the grid node (X_c, Y_r), and D_{max} is the distance from (X_c, Y_r) to the most distant of the eight data points.

STRATUM 6		
NGC		
North	East	$^{239-240}Pu$
936259	721112	529.
936326	720973	663.
936261	721124	885.
936152	721541	83.0
936271	720879	368.
936057	721253	594.
935990	721597	325.
936085	721276	659.
936279	721122	1370.
936212	720923	658.
936323	720944	53.7
935945	721279	505.
936120	721610	173.
936140	721538	30.5
936263	721001	592.
936277	721341	90.4
936063	721026	540.
936327	721043	268.
935915	721350	190.
936071	721168	640.
936239	721373	151.
936177	721032	232.
936250	721068	1010.††
936216	721404	269.
936118	721091	370.
936134	721487	202.
936016	721239	391.
936108	721355	16400.††
935964	721313	414.
936107	721189	631.
936264	721080	1130.
935999	721093	176.
936085	720983	176.
936008	721589	264.
936254	720941	741.
936031	720988	716.
936303	721231	179.
936119	721341	1170.
936250	720894	260.
936035	721348	1300.
936258	721218	141.
935986	721595	719.
936041	721099	523.
936248	720973	663.
936004	721238	391.
936209	721451	133.
936082	721070	655.

††New 10-gram aliquots of these two samples were analyzed after the statistical analyses in this paper were completed. The new results were 954 and 14,300 $\mu Ci/m^2$ as compared with 1010 and 16,400 $\mu Ci/m^2$, respectively. The new results were used by Delfiner and Gilbert (1978).

COMBINING TWO TYPES OF SURVEY DATA FOR ESTIMATING GEOGRAPHICAL DISTRIBUTION OF PLUTONIUM IN AREA 13

P. Delfiner*

Centre de Geostatistique in Ecole des Mines de Paris
Fontainebleau, France

R. O. Gilbert

Battelle Memorial Institute, Pacific Northwest Laboratory
Richland, Washington

ABSTRACT

Estimates of average $^{239,240}Pu$ concentrations in surface (0-5 cm) soil lying within 100-foot by 100-foot cells are obtained for the inner fence region at the Area 13 (Project 57) safety-shot site on the Nevada Test Site. These estimates and approximate 95% confidence intervals are obtained using "kriging" in a two-stage procedure. In Stage 1, initial estimates (a "guess field") of average $^{239,240}Pu$ concentrations in 100- x 100-foot cells are obtained by (i) kriging FIDLER ^{241}Am count per minute (cpm) data to obtain average FIDLER readings in 100- x 100-foot cells, then (ii) using these initial estimates in an estimated linear regression equation relating $^{239,240}Pu$ soil concentrations and ^{241}Am FIDLER readings (both in logarithmic scale). The results of Stage 1 are given in a figure. In Stage 2, the initial estimates are "corrected" by performing kriging on the differences between observed plutonium concentrations at random locations and those predicted from the linear log Pu-log FIDLER regression. The estimated corrections and the final "corrected" arithmetic mean estimates are included in the report. Geometric mean estimates and factors for obtaining confidence intervals are listed. These factors suggest mean plutonium concentrations are estimated within, roughly, factors of 2 with approximate 95% confidence.

In general, the kriging estimates seem to be in good agreement with the observed plutonium data at most locations. Exceptions to this are

---

*Work completed under a consulting agreement B-06245-A-L with Battelle Memorial Institute, Pacific Northwest Laboratories, Richland, WA.

evident near ground zero (GZ). This probably results in part from (i) using an approximation when transforming concentration estimates from logarithmic to arithmetic scale, and (ii) ignoring any "drift" (systematic change over distance) in plutonium concentrations within 100- x 100-foot cells.

The "corrections" to the initial plutonium estimates obtained in Stage 1 are relatively small (less than factors of 2) except in areas to the south and east of GZ where the corrections increase estimated mean concentrations by factors of between 2 and 4. The corrections south of GZ are due to 4 Pu concentrations in that area that are unusually large relative to grid FIDLER readings taken previously in the vicinity. It may be desirable to take additional FIDLER readings on a finer grid in this region to confirm these Pu results. Additional soil samples may then be advisable to further refine inventory estimates. Estimates of plutonium inventory reported by Gilbert (1977) and Gilbert *et al.* (1975) are compared with those obtained here using kriging. The agreement is within 0.5, 0.3, and 0.3 curies for strata 3, 4, and 5, respectively. However, in stratum 6 (the stratum nearest GZ), the kriging estimate is less than half the inventory estimate reported by Gilbert (1977). This may be due at least in part to ignoring the "drift" that occurs within the 100- x 100-foot cells near GZ. Inventory estimates obtained using strata mean concentrations are much more sensitive to extreme concentrations than those obtained using kriging.

A number of statistical problems associated with the analysis of plutonium data for estimating spatial distribution are discussed. These include (a) transformation of skewed data, (b) interpretation of the regression coefficient relating log Pu to log FIDLER data, (c) bias of the estimated coefficient due to measurement errors in both plutonium and FIDLER data, and (d) bias problems involved in transforming estimates obtained in logarithmic scale back to arithmetic scale. The theory of kriging is briefly outlined, and the structural analysis of the Area 13 FIDLER and plutonium data (necessary for kriging) is explained and presented in some detail. A brief review of past efforts at estimating plutonium inventory and spatial distribution at Area 13 is given.

No attempt is made here to estimate average plutonium concentrations for strata 1 and 2, regions of relatively low plutonium levels. Any method (including kriging) that attempts to make use of a regression relationship between plutonium concentrations and FIDLER readings may not be applicable in these low-level areas since in these areas the correlation between these two measurements is not very strong.

The suggestion is made that kriging may be most useful in those regions of a study site that lie between the immediate GZ area and the much lower-level areas removed from GZ. Whether or not kriging is used at a particular study site must depend upon an evaluation of the additional information expected to be gained relative to the increased cost of

kriging over more conventional approaches. The necessity of careful planning of field sampling studies in order for kriging (or any statistical technique) to give reasonable estimates of inventory and spatial distribution of plutonium and other radionuclides is noted.

INTRODUCTION

The Nevada Applied Ecology Group (NAEG) has been conducting environmental transuranic studies at safety-shot sites on the Nevada Test Site (NTS) and the Tonopah Test Range (TTR) since 1971. One important objective of these studies is to estimate the total amount (inventory) and spatial distribution of ^{239,240}Pu and ^{241}Am (henceforth denoted by Pu and Am) in surface soil. Of the 10 safety-shot sites studied by the NAEG, the most intensive soil sampling program took place in Area 13 at the Project 57 site. The first estimates of Pu inventory in surface soil (0-5 cm) were given by Gilbert *et al.* (1975), with corrections to these estimates being published by Gilbert (1977). These inventory estimates were obtained using stratified random sampling, i.e., by collecting soil samples at random locations within Am activity strata (Figure 1) that had been defined on the basis of FIDLER* surveys taken on 400-foot and 100-foot grids (Figure 2) about GZ. The inventory estimate for a given stratum was obtained by multiplying the average Pu concentration ($\mu Ci/m^2$) for that stratum by the size (m^2) of the stratum.

Information on the spatial distribution of Am and Pu was available from the FIDLER Am activity strata map for Area 13 (Figure 1) since Pu and Am are correlated at this study site. The spatial distribution of Pu was also studied by estimating isopleth (contour) lines of concentration on the basis of Pu soil concentrations using a computer program "SURFACE II" (see Figures 16, 20, and 21 in Gilbert *et al.*, 1975; also see Figures 8 through 14 in Gilbert *et al.*, 1977, for the Area 5 (GMX) site). These estimated contours were unsatisfactory in several respects. They were found, for example, to be biased in the sense that estimated concentrations near GZ appeared to be too low, and those at distance from GZ were too high. Hence, we began to look for alternative methods. An iterative estimation approach on both untransformed and log-transformed data was investigated by Gilbert (1978). The iterative procedure appeared to reduce the bias in estimates of plutonium concentration contours mentioned above when calculations were done in logarithmic scale with transformation back to arithmetic scale as the last step. This work also pointed out that highly spurious estimates can result in regions of sparse data where Pu concentrations change rapidly within short distances. This iterative approach grew out of suggestions offered by Professor John Tukey at the first ERDA Statistical Symposium (Eberhardt and Gilbert, 1976).

---

*Field Instrument for the Detection of Low Energy Radiation.

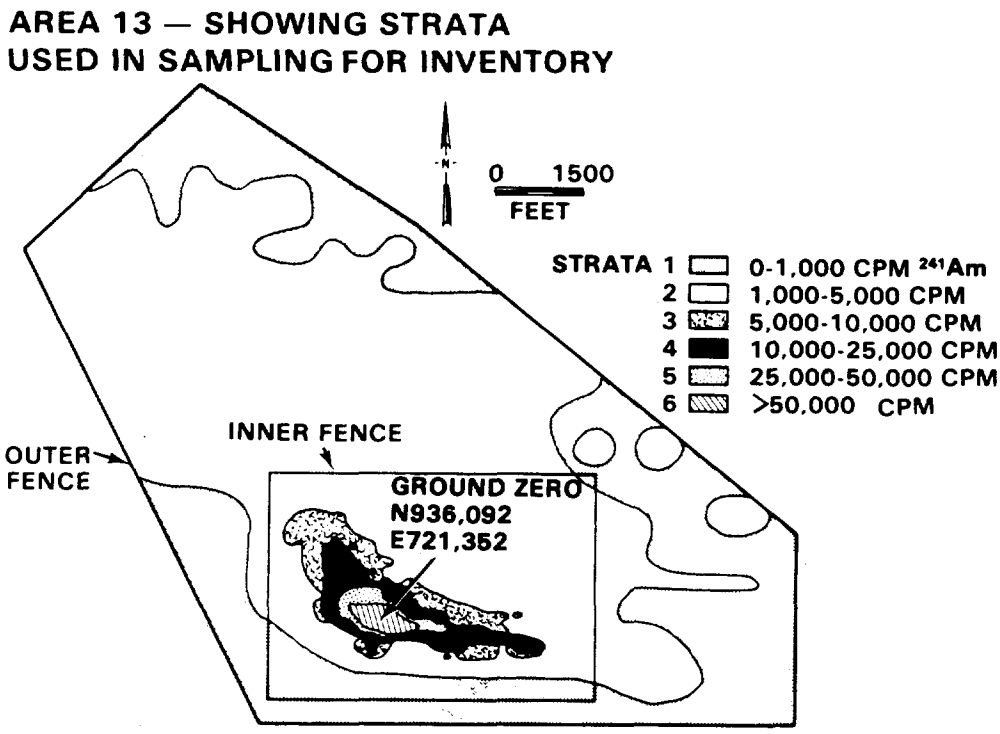

Figure 1. Area 13, Project 57--^{241}Am Activity Strata Obtained From FIDLER Grid Surveys (see Figure 2).

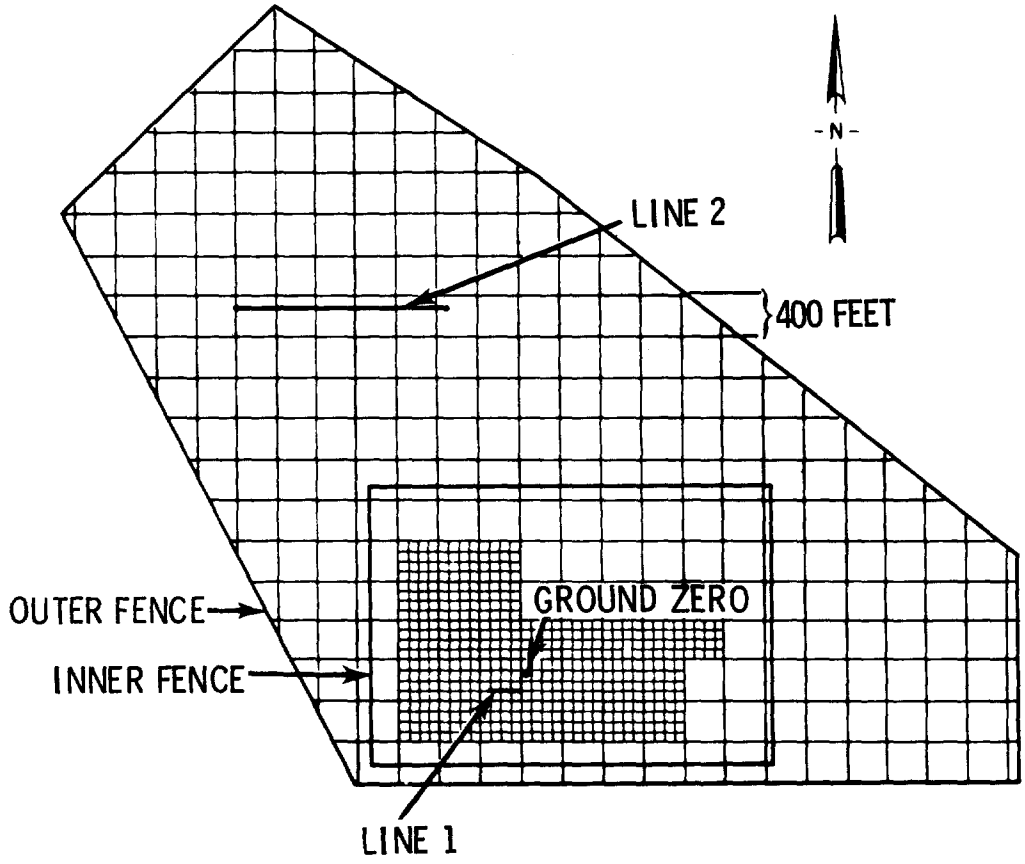

Figure 2. Area 13 Study Site Showing the 100-and 400-Foot Grid Points and Lines 1 and 2 Where FIDLER Readings Were Taken.

Our latest attempts have been directed toward an evaluation of kriging for estimating Pu concentration contours. This estimation technique involves using field data to estimate the spatial correlation structure that may exist at a given study site. This structure is then used to estimate the optimum "weights" to apply to field data points to estimate the concentration at another point. A general introduction to kriging and an account of the first attempts to use kriging for estimating Pu concentration contours at the Project 57 site was given by Barnes *et al.* (1977).

The present paper also makes use of kriging to estimate plutonium concentrations over space, but it differs from the approach used by Barnes *et al.* (1977) in that it relies primarily on the observed linear relationship (in logarithmic scale) between field FIDLER cpm readings for Am, and Pu $\mu Ci/m^2$ concentrations in 10-gram aliquots of soil. This linear relationship was first studied by Church *et al.* (1975). The Pu data are used primarily to adjust the initial estimates of average Pu concentrations obtained using the log Pu-log FIDLER regression.

The principal steps in this two-stage estimation procedure are as follows:

Stage 1

1. Estimate the linear regression relationship between Pu and FIDLER measurements using data at random locations.

2. Use the above regression equation to convert FIDLER readings into Pu concentrations.

3. Use kriging to estimate the average Pu concentration for each 100- x 100-foot cell.

Stage 2

4. Compute the differences (residuals) between observed Pu soil concentrations at random locations and those predicted from the Pu-FIDLER regression.

5. Use kriging to smooth these residuals to obtain an estimate of the average correction to apply to the estimated average Pu concentration (from step 3 above) for each cell.

The results obtained in this paper should be viewed as another step in an evolutionary process toward the evaluation of different statistical methods for handling the highly skewed and variable nature of transuranic field data. The present kriging approach is an improvement over the approaches tried by Gilbert *et al.* (1975) and Gilbert (1978) since approximate confidence intervals are obtained on cell averages. However, there is still much to be learned, particularly about the bias introduced when transforming estimates in logarithmic scale back to arithmetic scale. These and other problems are discussed in the following sections.

The Problem

The objective of this paper is to present an approach for the estimation of Pu concentration in soil at the Area 13 "safety-shot" site. We do not attempt to evaluate the Pu concentration at each "point" in space. Indeed, the variability of soil sample analyses is so large that it does not make much sense to aim at very local values. Accordingly, we will estimate average Pu concentrations over grid cells. The size of these cells may be chosen at will, in order, for example, to match the definition of safety standards given, e.g., in acres or hectares. With the present data, it is convenient to consider 100- x 100-foot cells, defined by a sampling grid covering the region surrounding GZ where Pu activity is highest.

Due to extreme skewness of the Area 13 data, our analyses are performed in logarithmic scale. It would be easiest for the statistician if he could also report results in that scale, but unfortunately, safety standards are not stated in log scale. In this paper, final results are given as both arithmetic and geometric means since it is not clear which estimate is to be preferred for comparison with safety standards. The serious bias problems encountered in transforming results from logarithmic to arithmetic scale are discussed.

The Data

In 1957, a device containing plutonium was blown apart in Area 13 by chemical explosives partly to test for "safety" against fission reactions in an accident situation involving an atomic weapon. A consequence of the test was the contamination of the immediately surrounding desert soil and vegetation with Pu and Am. The area was fenced off and the contamination has been monitored since that time. Since 1971, the Nevada Applied Ecology Group has studied the area by taking field instrument surveys and by collecting soil, vegetation, and animal tissue samples. This present study makes use of the following data accumulated in Area 13:

1. Pu concentrations (in $\mu Ci/m^2$) determined by wet chemistry on surface (top 5 cm) soil samples taken at random locations within Am activity strata (count: 174). These data are plotted in Figures 3 and 4.

2. Am concentrations in surface soil, obtained from FIDLER readings (in counts per minute (cpm)) at one foot above the surface.

   These were taken

   (a) at 145 of the above random locations and at 9 others where Pu was not measured,

   (b) in a 400-foot systematic grid over the entire area bounded by an outer fence (count: 352),

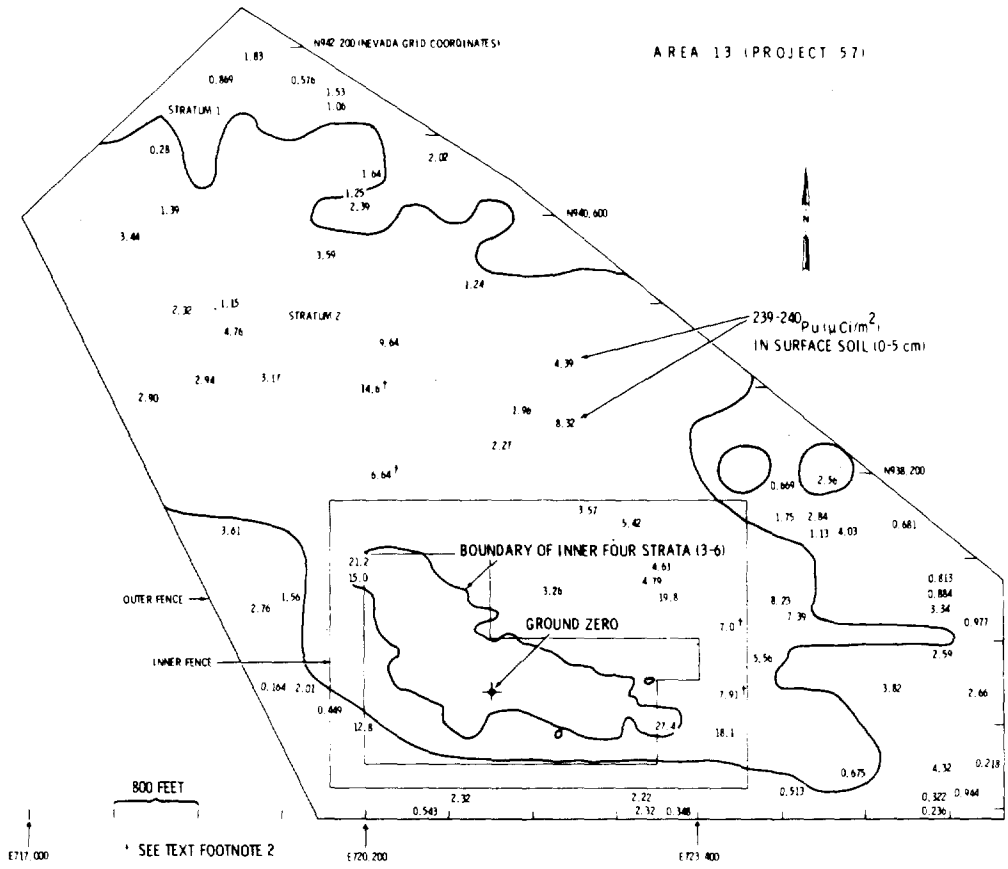

Figure 3. Observed $^{239-240}Pu$ Concentrations ($\mu Ci/m^2$) in Surface Soil (0-5 cm) Outside the 100-x 100-Foot Grid Area at the Project 57 (Area 13) Site.

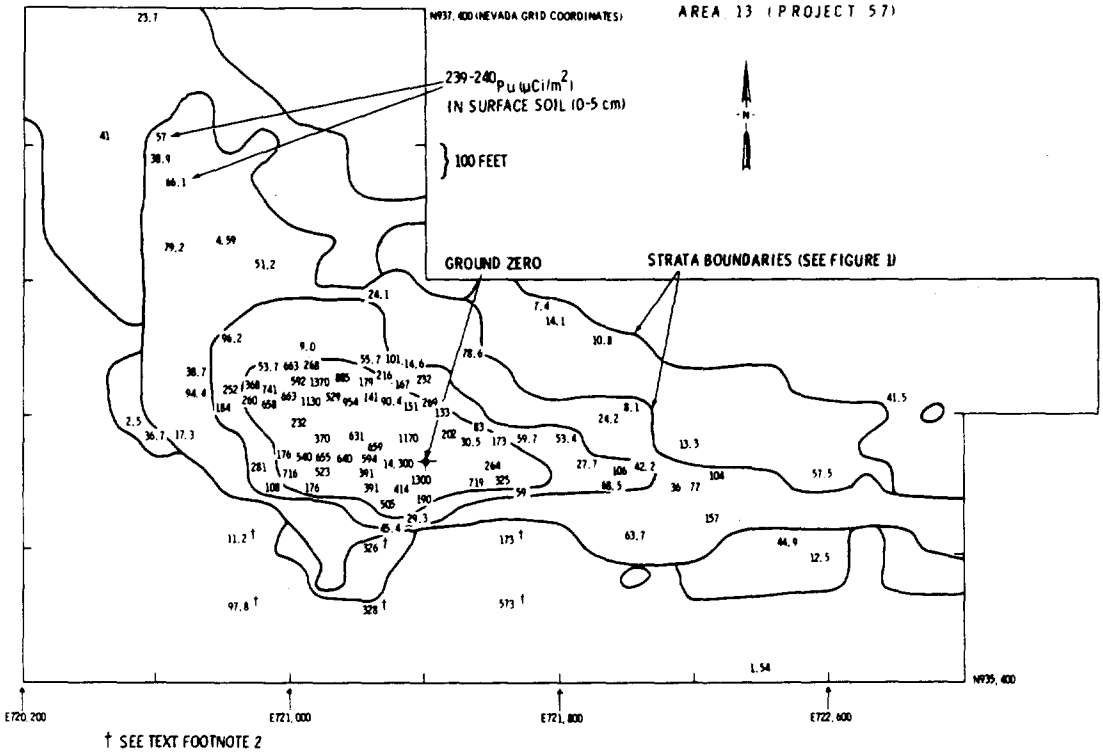

Figure 4. Observed $^{239-240}Pu$ Concentrations ($\mu Ci/m^2$) in Surface Soil (0-5 cm) Within the 100-x 100-Foot Grid Area at the Project 57 (Area 13) Site.

(c) in a 100-foot systematic grid near ground zero, within an inner fence (count: 498) (see Figure 2).

3. Two sampling lines where both Am concentrations in the soil and FIDLER readings were determined, at short intervals, for the purpose of estimating the distance--variability relationships (Figure 2). Along each line, 15 groups of 4 adjacent soil samples were collected. The spacing between groups is 20 feet in Line 1 and 150 feet in Line 2. The samples themselves are rings, 5 inches in diameter, 5 cm deep. FIDLER readings were taken both at the surface of each soil sample and at one foot above the ground. Readings were taken immediately before the soil samples were collected.

Table 1 indicates the general levels of Am activity from FIDLER readings.

Table 1. Levels of FIDLER Activity ($\log_{10}$ of FIDLER counts in 10^3 cpm units)

Data	Number of Readings	Mean	Standard Deviation	Minimum	Maximum
400 Ft. Grid	352	0.054	0.398	-1.0	1.76
100 Ft. Grid	498	0.72	0.495	-0.70	2.17
Line 1	60	0.83	0.293	0.35	1.48
Line 2	51	-0.58	0.369	-1.72	-0.07

Previous studies (Gilbert *et al.*, 1975) have established that Pu and Am concentrations are in a nearly constant ratio:

$$Pu(x) = Am(x) \times R(x) \qquad (x: \text{ location of sample}) \tag{1}$$

with $R(x) = 9.4 \pm 0.14$ ((mean Pu/mean Am) ± 1 standard deviation).

We note that FIDLER readings taken aboveground (1 foot) integrate gamma rays within a circle 1 meter in diameter about x, weighting most heavily the Am directly under the detector crystal. As a consequence, the relationship between Pu(x) and FIDLER(x) (FIDLER count above x) is expected to be more complex than in Equation 1.

Intentions

Putting Lines 1 and 2 aside, the FIDLER readings total 1,004 observations against 174 for Pu concentrations. In earlier efforts (Gilbert *et al.*, 1975; Gilbert and Eberhardt, 1974), these FIDLER data were used mainly to

define six Am activity strata (Figure 1) within which the locations of the soil samples were randomized. The idea was that a greater density of samples was needed in areas of high concentrations than in low-level areas since variability increases with mean concentration. The objective was to minimize the variance of the estimated total amount of Pu for all strata combined.

In this paper, we make a more complete use of FIDLER data on the following grounds:

1. As shown by Church *et al.* (1975), there is a good overall correlation, in log scale, between wet chemistry Pu analyses and Am FIDLER measurements at 1 foot height.

2. The cost of a FIDLER reading is roughly 50 times less than that of a Pu analysis on a soil sample.

The way in which we propose to use the FIDLER data in conjunction with the Pu analysis is borrowed from meteorologists (cf. Cressman, 1959; Chauvet *et al.*, 1976). In order to reconstruct a given field, say the constant presssure surface height (geopotential), meteorologists first construct an initial "guess field," obtained by feeding a numerical weather forecast model with yesterday's data. Then this guess field is updated to make it consistent with today's observations.

Here we will use the FIDLER readings to construct our initial guess of Pu and then use the actual Pu data to make local corrections. Clearly the proviso is that the FIDLER data carry enough information about Pu concentrations to devise a sensible initial guess. Our first task is thus to study the FIDLER-Pu relationship.

STUDY OF THE FIDLER-PLUTONIUM RELATIONSHIP

Since the data range over several orders of magnitude, it is natural to transform them into the logarithmic scale. This also has the effect of stabilizing the variance. In this paper, all logarithms are in base 10.

Gilbert *et al.* (1975) studied the correlation between untransformed Pu and FIDLER data at Area 13 and other sites where the Pu to Am ratio computed on the basis of soil samples was nearly constant. Pu-FIDLER correlations ranged from near zero in low-activity strata to about 0.95 near some GZs. Gilbert and Eberhardt (1976) concluded that except for low-activity strata, a double sampling approach (in the sense of Cochran, 1963, Chapter 12) using the Pu-FIDLER correlation (untransformed data) was feasible on grounds of reduced cost and increased precision. The correlation between Pu and FIDLER in logarithmic scale for Area 13 was found by Church *et al.* (1975) to be 0.92 for data from all activity

strata combined (n = 120). This global approach (ignoring strata) in logarithmic scale seems appropriate here, but since 145 data are now available, and for this paper to be self-contained, we redo the analysis.

The overall correlation between log(Pu) and log(FIDLER) from 145 pairs is $\rho = 0.93$. The regression equation is (see Figure 5)

$$\log(\text{Pu}) = 1.287 \log(\text{FIDLER}) + 0.096 \quad , \qquad (2)$$

(Pu in $\mu Ci/m^2$, FIDLER in 10^3 cpm). It is interesting to comment on the fact that the slope $\hat{\alpha} = 1.287$ is greater than 1. Indeed, if the gamma ray count recorded by the FIDLER is proportional to the Am concentration in a sample, and if the ratio R = Pu/Am is approximately constant, then FIDLER counts are proportional to Pu concentrations and the slope should be 1. The larger value found is explained by the difference in <u>support</u> between a soil sample analyzed for Pu--a 10-gram aliquot from the $\sim$ 700 grams of soil collected within the 5-inch-diameter sampling ring--and the much larger area integrated by a FIDLER reading. If the measurement errors effect is not overwhelming, it is to be expected that $\sigma_F^2 << \sigma_P^2$, and since ρ is near 1, the regression slope $\hat{\alpha} = \rho\sigma_P/\sigma_F$ is greater than 1.

Further evidence of this interpretation is found using the data of Lines 1 and 2. The variances of log FIDLER counts are:

	LINE 1 (60 readings)	LINE 2 (25 readings)
Contact readings	0.100	0.342
Aboveground readings	0.087	0.062

As the area integrated by aboveground measurements is larger than the surface ones, these results are in the right direction, i.e., the variance of the aboveground readings is smaller than for the surface readings.

The residual variance of the regression is 0.1313. We will not attempt to devise confidence intervals for the regression coefficients, for we believe that the basic assumptions of independence on which classical regression theory is built are violated here.

Looking carefully at the plot in Figure 5, one can distinguish two populations: one for which FIDLER > 5,000, and the other for which FIDLER < 5,000. Doing separate studies for these two subgroups, it is found that

1. <u>For FIDLER > 5,000</u>, $\hat{\rho} = 0.89$ and the regression is

$$\log(\text{Pu}) = 1.293 \log(\text{FIDLER}) + 0.092 \quad ,$$

(96 pairs) which is practically the same as that derived from the pooled samples. This circumstance is reassuring, as it is important to have a good regression where the activity is high. It is also

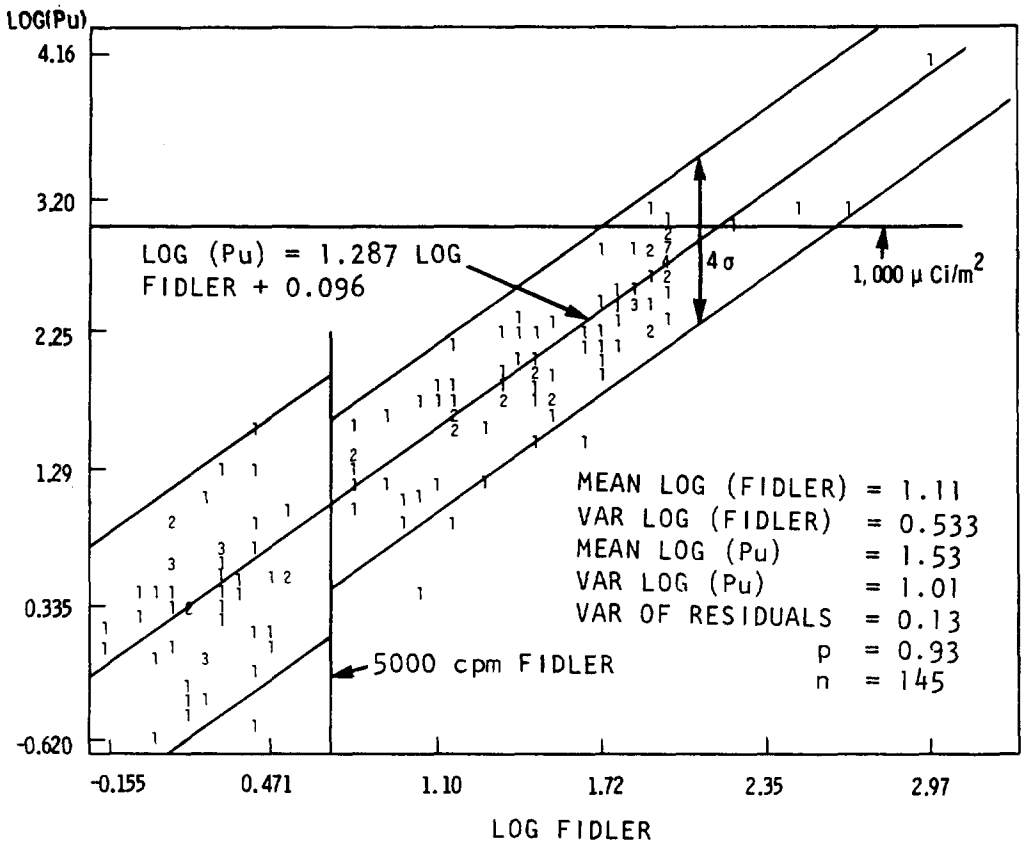

Figure 5. Regression of $Log_{10}Pu$ on $Log_{10}FIDLER$ for Area 13 Data at Random Locations.

worth noting that even at very high Pu activity levels (> 10^3 $\mu Ci/m^2$), underestimation using the regression line does not seem to be a problem.

The residual variance is 0.0834, and therefore under a Gaussian distribution of the error, the Pu concentration may be predicted within a factor of about 2 at the 68 percent confidence level, and a factor of about 4 at the 96 percent confidence level.

2. For FIDLER < 5,000, the correlation is only $\hat{\rho} = 0.22$ and the regression equation is very different from that for FIDLER > 5,000:

$$\log(Pu) = 0.6275 \log(FIDLER) + 0.2372 \quad ,$$

(49 pairs) with a residual variance of 0.2126, 2.6 times larger than for FIDLER > 5,000.

THE MODEL

Let

$$P(x) = \log Pu(x), \quad (Pu(x) \text{ in } \mu Ci/m^2)$$

and

$$F(x) = \log FIDLER(x), \quad (FIDLER(x) \text{ in } 10^3 \text{ cpm}).$$

We model P(x) and F(x) as realizations of random fields on IR^2 (two-dimensional space) of the form

$$P(x) = P_o(x) + \varepsilon(x)$$

$$F(x) = F_o(x) + \eta(x) \quad ,$$

where $P_o(x)$ and $F_o(x)$ stand for the "true" underlying fields, and $\varepsilon(x)$ and $\eta(x)$ for measurement errors, of zero means, constant variances, and uncorrelated with $P_o(x)$ and $F_o(x)$. Hence, errors are assumed multiplicative in the arithmetic scale. Constant variance and errors uncorrelated with true values do not strictly hold even in log scale, but the situation is certainly better than in the original scale. Furthermore, we can think of different error variance levels for the ranges FIDLER < 5,000 and FIDLER > 5,000.

In the light of the preceding correlation study, it is reasonable to let

$$E[P_o(x) | F_o(x)] = \alpha F_o(x) + \beta \quad . \qquad (3)$$

Note that we write Equation 3 in terms of P_o and F_o rather than P and F, while the regression analysis has been carried out with P and F data. This is done because we like to think of Equation 3 as expressing a physical relationship between the actual Pu concentration in a soil sample and the integrated gamma ray radiation. The error terms, which depend on measurement techniques, are superimposed.

The basic equation of the model we propose for Area 13 data is

$$P_o(x) = \alpha F_o(x) + \beta + T(x), \tag{4}$$

where T(x) is a random field independent of $F_o(x)$ with mean zero. The independence of T and F_o is the crucial assumption. It says that given the FIDLER reading above point x, other FIDLER readings bring no supplementary information about the Pu concentration at x.

This excludes the case of a preferential lagged influence, as it occurs for example in uranium deposits, where detectors measure gamma radiation from radium, even though the uranium has been washed away. Equation (4) also means that the integration effect of FIDLER measurements does not concern too large an area, otherwise a spot x would contribute significantly to nearby gamma ray recordings, and deconvolution would be needed.

Naturally, if the regression of P_o and F_o had not been linear, but say

$$E[P_o(x) \mid F_o(x)] = \psi[F_o(x)]$$

we would have written as well

$$P_o(x) = \psi[F_o(x)] + T(x) \quad , \quad E[T(x)] = 0 \quad ,$$

with T and F_o independent. The problem is the determination of $\psi(\cdot)$ in the presence of errors in both P and F variables. In the linear case used in this paper, it can be shown that approximately:

$$E(\hat{\alpha}) \tilde{\sim} \alpha/[1 + \sum_i \eta_i^2 / \sum_i (F_o(x_i) - \bar{F}_o)^2] \quad . \tag{5}$$

In a very tentative manner, we can evaluate the bias term in Equation 5. First, by a method explained below (under Structural Analysis) based on an analysis of the spatial variation of FIDLER data along Line 1, an order of magnitude estimate of the FIDLER error variance is found to be $E(\eta_i^2) \tilde{\sim} 10^{-3}$. Thus, using the 96 data for which FIDLER > 5,000,

$$\sum_i (F(x_i) - \bar{F})^2 = \sum_i (F_o(x_i) - \bar{F}_o)^2 + \sum_i (\eta_i - \bar{\eta})^2 = 0.191 \times 96.$$

So the denominator in Equation 5 is $1 + 0.001/(0.191 - 0.001) = 1.005$. This indicates that the bias is small enough to be ignored. For FIDLER < 5,000, the noise $E(\eta_i^2)$ is much larger and cannot be evaluated accurately. Hence, it is not possible to access the bias correction for this case.

The estimates $\hat{\alpha} = 1.287$ and $\hat{\beta} = 0.096$ will be treated in what follows as though they were true values. It is shown in the next section that β plays no role in estimating the error variance of kriging estimates.

A BRIEF OUTLINE OF KRIGING THEORY

We now relate our model to the given field procedure outlined above. As a general rule, let us denote by $F(v)$ the mean value of $F(x)$ over a volume (or area) v. We are interested in $P_o(v)$ where v is chosen here to be a 100- x 100-foot cell. As the effect of errors or microstructures averages out over an area, we have $P_o(v) = P(v)$ and $F_o(v) = F(v)$. Hence, from Equation 4,

$$P(v) = \alpha F(v) + \beta + T(v)$$

and we choose an estimator of the form

$$P^*(v) = \alpha F^*(v) + \beta + T^*(v) \quad , \tag{6}$$

where $\alpha F_o^*(v) + \beta$ is the Pu guess field and $T^*(v)$ is the block correction term. $F^*(v)$ and $T^*(v)$ can be estimated independently from $F(x)$ and $T(x)$ data, respectively. If $F^*(v)$ and $T^*(v)$ are unbiased, then so is $P^*(v)$, and by the independence of T and F, the mean squared errors (MSE) just add up:

$$E[P^*(v) - P(v)]^2 = \alpha^2 E[F^*(v) - F(v)]^2 + E[T^*(v) - T(v)]^2 \quad .$$

The MSE is a minimum when both terms on the right-hand side are a minimum. The estimation procedure can indeed be decomposed into two independent phases.

Specifically, $F^*(v)$ and $T^*(v)$ may be constructed by the kriging method (Matheron, 1963, 1965, 1969, 1971, 1973; Delfiner and Delhomme, 1973; Delfiner, 1973). A brief outline of the theory of kriging (which gives minimum mean square error unbiased estimates) is given below. For further details, the reader is referred to the references.

Suppose we want to estimate the mean value over v, say $Z(v)$, of a given variable Z. The kriging estimator $Z^*(v)$ is a moving average predictor

$$Z^*(v) = \sum_{i=1}^{N} \lambda_i \, Z(x_i) \quad ,$$

where the weights λ_i are chosen so as to achieve

$$E[Z^*(v) - Z(v)] = 0 \qquad \text{(unbiasedness)}$$

$$E[Z^*(v) - Z(v)]^2 \quad \text{is a minimum.} \qquad \text{(minimum MSE)} \tag{7}$$

The actual equations to which Equation 7 leads depends on the assumptions that have to be made on Z. There are basically two situations, according to whether or not the mean of Z(x) can be considered constant.

In the simplest case, the variable Z(x) fluctuates about a constant value m, and it is natural to let $E[Z(x)] = m$ for all x. In the scope of second-order stationary random functions, one could furthermore assume that Z(x) has a stationary covariance

$$E[Z(x) - m]\,[Z(x + h) - m] = C(h)$$

depending on the vector h only. Then Equation 7 could be made explicit in terms of C(h), leading to Wiener-Hopf type equations. But in practice, this approach has two drawbacks. One is that m is unknown and has to be replaced by an estimate; the other, noted for example by Matérn (1960, p. 51), is that when the data are available over a restricted region, the covariance is in fact defined up to a constant. For these reasons, it is preferable to consider <u>increments</u> $Z(X + h) - Z(x)$ which filter out the unknown mean m, and work with the <u>variogram</u>

$$\gamma(h) = \frac{1}{2} E[Z(x + h) - Z(x)]^2 \ .$$

The assumption that the increments are stationary to the second order--called the "intrinsic hypothesis"--is less restrictive than the classical stationarity assumptions on the process itself. And it has proven to be very effective. Equation 7 then leads to the linear system:

$$\sum_j \lambda_j \gamma(x_i - x_j) + \mu = \bar{\gamma}(x_i, v) \quad , \quad i = 1,2,\ldots,N$$

$$\sum_i \lambda_i = 1 \ , \qquad \text{SIMPLE KRIGING SYSTEM} \tag{8}$$

Where μ stands for a Lagrange parameter and

$$\bar{\gamma}(x_i, v) = \frac{1}{v} \int_v \gamma(x_i - x)\,dx$$

is the average value of the variogram, when x_i is the origin and the end point x sweeps throughout v.

A more complicated situation is when Z(x) shows some systematic behavior, as is the case with Pu or Am concentrations that tend to decline with increasing distance from ground zero. Then it is more sensible to model Z(x) as the sum $Z(x) = m(x) + Y(x)$ of a smooth deterministic function

m(x) called the drift, and a fluctuation term Y(x) of mean zero with a variogram $\gamma(h)$ called the underlying variogram. The drift function m(x) varies slowly and can be modeled, at least locally, as

$$m(x) = \sum_{\ell=0}^{k} b_\ell \, f^\ell(x) \quad ,$$

where the $f^\ell(\cdot)$ stand for known basic functions--monomials in practice--and the b_ℓ are unknown coefficients. Under this model

$$E[Z(v)] = \sum_\ell b_\ell \frac{1}{v} \int_v f^\ell(x)dx = \sum_\ell b_\ell f^\ell(v)$$

and

$$E[Z^*(v)] = \sum_i \lambda_i E[Z(x_i)] = \sum_i \lambda_i \sum_\ell b_\ell f^\ell(x_i), \text{ so that}$$

$$E[Z^*(v) - Z(v)] = \sum_\ell b_\ell [\sum_i \lambda_i f^\ell(x_i) - f^\ell(v)].$$

If we want the bias to be zero whatever the true unknown b_ℓ (universal unbiasedness), we have to impose the conditions

$$\sum_i \lambda_i f^\ell(x_i) = f^\ell(v), \qquad \ell = 0,\ldots,k \quad .$$

Minimizing $E[\sum_i \lambda_i Z(x_i) - Z(v)]^2$ subject to the unbiasedness conditions leads to the Universal Kriging system with k + 1 lagrange parameters μ_ℓ:

$$\begin{aligned} &\sum_j \lambda_j \gamma(x_i - x_j) + \sum_\ell \mu_\ell f^\ell(x_i) = \bar{\gamma}(x_i, v), && i = 1,\ldots,N \\ &\sum_i \lambda_i f^\ell(x_i) = f^\ell(v), && \ell = 0,\ldots,k \end{aligned} \qquad \begin{matrix} \text{UNIVERSAL KRIGING} \\ \text{SYSTEM} \end{matrix} \qquad (9)$$

Naturally, Equation 8 is a special case of Equation 9, provided $f^0(x) \equiv 1$. At its minimum, the MSE (kriging variance) is

$$\sigma_K^2 = E[Z^*(v) - Z(v)]^2 = \sum_i \lambda_i \bar{\gamma}(x_i, v) + \sum_\ell \mu_\ell f^\ell(v)$$

and provides a measure of the error of estimation.

The inference of the variogram $\gamma(h)$ in the presence of a drift poses a serious problem. Indeed, the "raw" variogram

$$\hat{\gamma}(h) = \frac{1}{2N_h} \sum_i [Z(x_i + h) - Z(x_i)]^2$$

(N_h = number of pairs, h apart) is biased upward by the quantity

$(1/2N_h) \sum_i [m(x_i + h) - m(x_i)]^2$, while the variogram of residuals, computed after removal of an estimated drift, is biased downward. This inference problem may be approached by another method that cannot be presented here (see Matheron, 1973; Delfiner, 1975). It will suffice to say that this method allows automatic identification of the optimum local drift and variogram models within a prespecified class. This task can be performed by BLUEPACK (see Delfiner *et al.*, 1976) a kriging program package, now available in Las Vegas on the computer at the Nevada Operations Office of the U.S. Department of Energy.

STRUCTURAL ANALYSES

In order to apply the kriging procedure, we need to specify the structural parameters: type of drift, if any, and variogram model. Since our goal is to estimate Pu concentrations in cells defined by the 100-foot FIDLER grid, it is preferable to consider only the data located in that area (to guard against heterogeneities).

The F(x) Field

As noted above, the field of FIDLER counts is certainly not stationary, even in the log scale. The automatic structure identification module of BLUEPACK found that the best local model for the 100-foot grid F(x) data is:

1. a linear drift (i.e, in IR^2: $m(x,y) = b_0 + b_1x = b_2y$)
2. a linear variogram, with a "nugget effect" (a discontinuity at the origin), i.e.

$$\gamma(0) = 0$$

$$\gamma(h) = 0.0127 + 1.53 \times 10^{-4}|h| \quad . \quad (|h| > 0, \text{ in feet}) \qquad (10)$$

As an indication of what is meant by "local," the program outputs a rough estimate of the maximum radius of the circular moving neighborhood within which the model is valid: here 270 feet. Also, the selected model is cross-validated by reestimation of known values as if they were unknown.

Another way of checking the above variogram model is to plot it together with the raw directional variograms (Figure 6). At first glance, it may

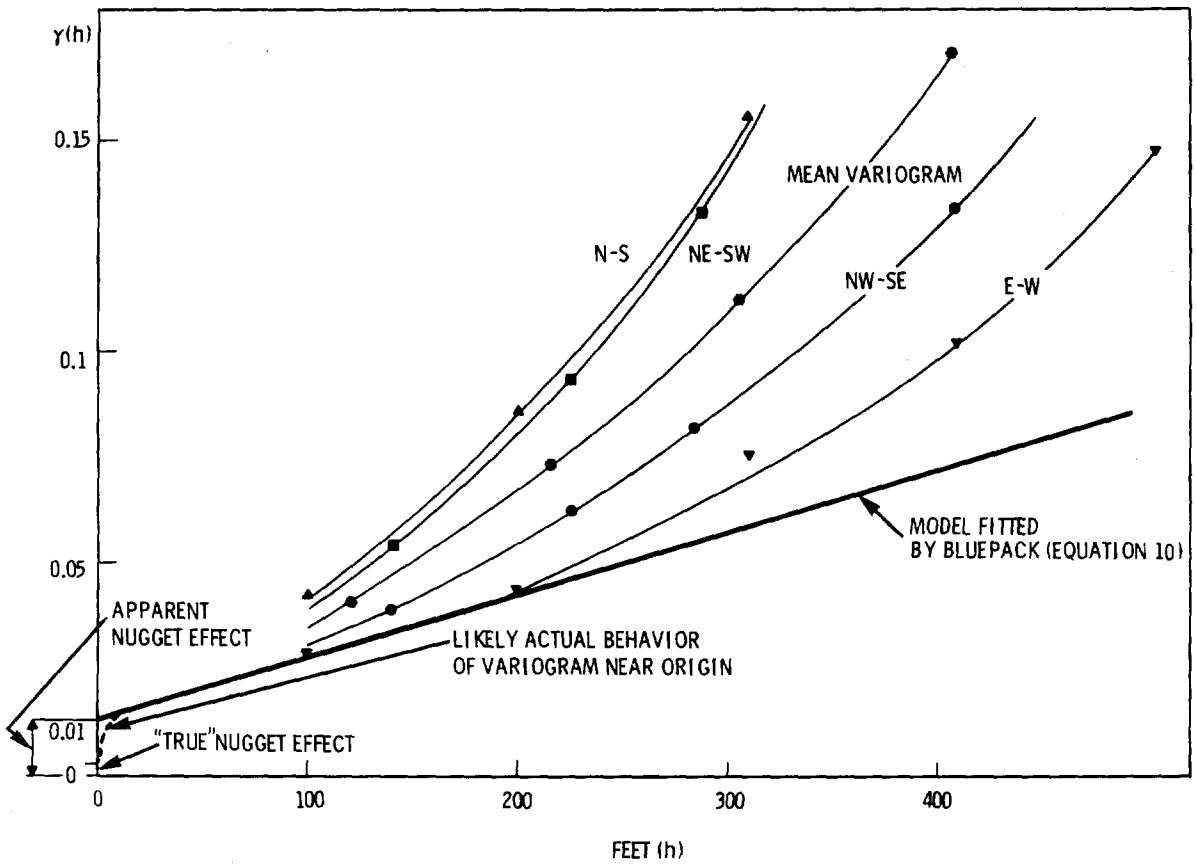

Figure 6. Raw and Fitted Variograms of Log_{10}FIDLER Data Collected on 100 Foot Grid.

seem that the agreement is very poor since all raw variograms lie above the fitted model. One should remember, however, that the presence of a drift results in an upward bias in the raw variograms. It is only at short distances, perhaps, that the raw variograms may coincide with the underlying ones. This coincidence indeed happens here: the raw variogram in the east-west direction becomes tangent to the fitted model at distances less than 200 feet. Therefore, the agreement is actually very good, especially since the model resulted from an automatic identification procedure based on quite a different approach than that used to calculate the raw variograms. There is no theorem that says there must be some direction for which the drift effect is not felt, at least at short distances, but it often occurs in practice.

It is of interest to comment on the nugget effect of 0.0127 found here. Typically, it can originate from

1. measurement errors

2. microstructures at a scale much smaller than that at which the observations are made (as occurs with golden nuggets in gold mines, where the ore grade varies discontinuously from inside to outside nuggets).

But the interpretation of the nugget effect is more complex for the FIDLER data. Basically, the value $C_o = 0.0127$ results from extrapolations to the origin of a variogram computed at a 100-foot scale. This is clearly shown in Figure 6. Yet, if the phenomenon is analyzed at a much finer scale, it emerges that the discontinuity of the variogram at the origin is only apparent. The "true" variogram probably resembles the dashed curve in Figure 6, decreasing steeply to zero, with a small nugget effect left to account for measurement errors. Such conjecture is based on the variogram computed from Line 1 FIDLER data (Table 2). This table clearly indicates that the $F_o(x)$ field is continuous, as can be expected since two close FIDLER readings integrate radiation from a large common area. A nugget effect still shows, but of the order of 10^{-3} (rather than 10^{-2} as found above), corresponding to a counting error $\sigma/\text{count} \tilde{\sim} 7$ percent.

Table 2. Variogram of Line 1 and Line 2 FIDLER Data (1 Foot Aboveground)

Line	Lag Number	Number of Pairs	Distance (Inches)	Variogram (x 10^{-3})
1	1	45	5	1.116
	2	30	10	1.455
	3	15	15	2.818
	48	224	240	20.07

Table 2. Variogram of Line 1 and Line 2 FIDLER Date (1 Foot Aboveground) (Continued)

Line	Lag Number	Number of Pairs	Distance (Inches)	Variogram ($\times 10^3$)
	1	34	5	58.37
	2	22	10	56.78
2	3	10	15	55.91
	360	161	1800	124.1

It does not seem possible though, to use these results from Line 1 to model the short distance behavior of the variogram over all the area covered by the 100-foot grid, since the counting error depends on the level of activity. At very low levels along Line 2, we get pure noise (Table 2), signifying no correlation structure.

A question at this point is: "Are the 1-foot and the 100-foot scale analyses consistent?" The answer is yes. Seen from a 100-foot grid, the details of the 1-foot scale structures merely appear as noise. The value $C_o = 0.0127$, which may be called the "apparent nugget effect," is the variance of that noise. Since we are working at a 100-foot scale, we do not need a precise modeling of microstructures and can instead use a simplified macroscopic model with a discontinuity of magnitude C_o.

The T(x) Field

We do not have direct access to T(x), the true correction term, and what we analyze are the estimated residuals from the regression:

$$\hat{T}(x_i) = P(x_i) - \alpha F(x_i) - \beta = T(x_i) + [\varepsilon(x_i) - \alpha n(x_i)]. \qquad (11)$$

Figure 7 shows the raw variograms of these residuals computed separately for FIDLER > 5,000 and FIDLER < 5,000. The variograms of the differences $\{\log Am(x) - \alpha_A F(x) - \beta_A\}$ on Lines 1 and 2 data are also plotted for comparison (α_A and β_A regression coefficients were calculated using pooled Lines 1 and 2 data). Since the Pu to Am ratio is approximately constant in the log scale, these differences should be comparable to values of T(x).

Each of these variograms stabilizes at a certain level, called the "sill," indicating a stationary behavior of T(x). This was to be expected since the drift effect is already accounted for by the guess field $\alpha F(x) + \beta$. The value at the sill is equal to the overall variance of the

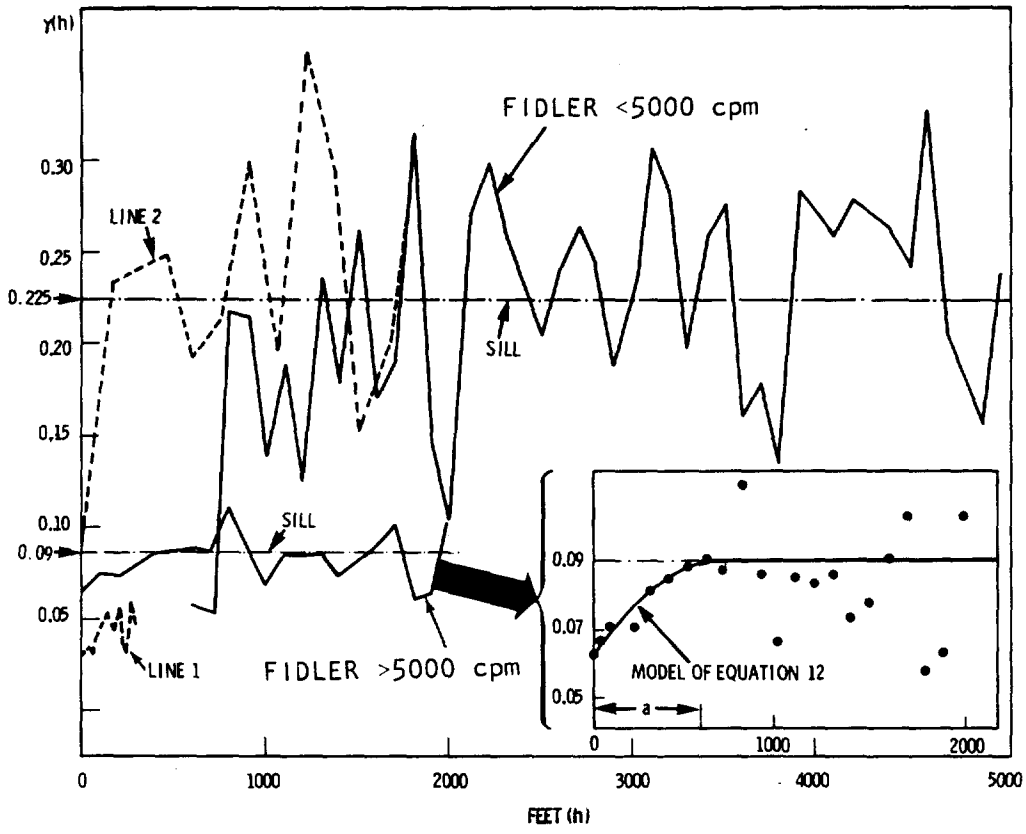

Figure 7. Variograms of the Residuals from Regressions of $Log_{10}Pu$ on $Log_{10}FIDLER$ (FIDLER < 5000 and FIDLER > 5000) and of $Log_{10}Am$ on $Log_{10}FIDLER$ (Lines 1 and 2).

variable, and thus here to the residual variance of the Pu-FIDLER regression; hence the difference between FIDLER > 5,000 and FIDLER < 5,000 sills.

An enlargement of the variogram for FIDLER > 5,000 is also shown in Figure 7. We can fit it to a spherical model with a range "a" of 600 feet (the distance at which correlations vanish):

$$\gamma(0) = 0$$

$$\gamma(h) = 0.065 + 0.025\,[3/2\,(h/600) - 1/2\,(h/600)^3] \qquad (12)$$

$$0 < |h| \leq 600 \text{ feet}$$

$$\gamma(h) = 0.09 \qquad |h| \leq 600 \text{ feet}$$

The "apparent nugget effect" of 0.065 is the sum of the FIDLER data nugget effect $\alpha^2\sigma_F^2 = (1.287)^2 \times 0.0127 = 0.02$ and the Pu data nugget effect, which by Pu variogram extrapolation is found to be 0.045 (variogram not shown here). Thus T(x)--the true value--has no nugget effect of its own and its variogram is simply the spherical model with a sill at 0.025. Though blurred by noise, T(x) does show a structure up to a distance of 600 feet and it is worth exploiting it.

The variogram of $\hat{T}(x)$ is not well determined when FIDLER < 5,000, especially at short distances, as a consequence of much sparser sampling (number of pairs typically less than 15). For simplicity, we will assume that the variogram in this case is the same as above, except for an upward shift of 0.135 = 0.225 - 0.09 (Figure 7). It is convenient to think of this shift as due to a nonsystematic uncertainty of variance 0.135, attached to correction terms when FIDLER < 5,000. Then, all data may be processed by BLUEPACK in the same manner: the uncertainty variance is just added to the appropriate diagonal terms of the kriging system matrix.

COMING BACK TO ARITHMETIC SCALE

We now have all the elements to carry out the estimation of $P_o(v)$--or equivalently P(v), since these are equal--that is, of the mean concentration in the log scale. How can we come back to the arithmetic scale?

An Estimate of the Geometric Mean

One way is to simply use the inverse transform $10^{P^*(v)}$ to estimate the geometric mean $10^{P(v)}$. By the unbiasedness property of kriging, we know that the error $P^*(v) - P(v)$ has mean zero. If moreover this error has a symmetric distribution, then

$$\text{Prob}\left\{P^*(v) - P(v) > 0\right\} = 1/2 = \text{Prob}\left\{10^{P^*(v)} > 10^{P(v)}\right\}.$$

So for the symmetric case, $10^{P^*(v)}$ is a median unbiased estimator of the geometric mean concentration $10^{P(v)}$. If in a cell v the point values $P(x) = \log Pu(x)$ are symmetrically distributed about their mean $P(v)$, then $10^{P(v)}$ is also the median concentration in that cell.

Under Gaussian theory, it is easy to set a 95 percent confidence interval for the geometric mean:

$$10^{P^*(v)}/10^{2\sigma_K} < 10^{P(v)} < 10^{P^*(v)} \times 10^{2\sigma_K}, \qquad (13)$$

where $\sigma_K^2 = E[P^*(v) - P(v)]^2$ is the kriging variance.

An Estimate of the Arithmetic Mean

Things are much more complicated if we insist that we want an unbiased estimator of the mean concentration Pu(v) and a confidence interval for it. The difficulty remains even if we adopt the (questionable) assumption that point concentrations Pu(x) are lognormal; this for two reasons:

1. We are dealing with a nonstationary phenomenon so that the distribution changes with location.

2. We are dealing with mean block values, and theory shows that these cannot be lognormal if the point values are lognormal.

So we will have to resort to approximations. We believe these are at least as acceptable as the lognormal model itself.

Let us first derive an exact expression. If $P(x) = \log Pu(x)$ is Gaussian with mean m(x) and variance Var P(x), (Var P(x) = constant), then

$$E[Pu(x)] = 10^{m(x) + M \text{ Var } P(x)/2},$$

where the constant $M = \ln 10 = 2.3026$ is introduced by the fact that we use logarithms in base 10. Now,

$$E[Pu(v)] = \frac{1}{v}\int_v E[Pu(x)]dx = \overline{10^m} \times 10^{M \text{ Var } P(x)/2},$$

where the upper bar denotes averaging over a cell v. On the other hand,

$$E[10^{P^*(v)}] = 10^{m(v) + M \text{ Var } P^*(v)/2}.$$

(As usual, m(v) denotes the average of m(x) over v.) An unbiased estimator of Pu(v) is therefore:

$$P_u^*(v) = 10^{P^*(v)} + (M/2)\ [\text{Var } P(x) - \text{Var } P^*(v)] \times \left[\overline{10^m}/10^{m(v)}\right] \quad .$$

Var P(x) - Var P^*(v) in fact depends on the variogram only:

$$\text{Var } P(x) - \text{Var } P^*(v) = \sum_i \sum_j \lambda_i \lambda_j \gamma(x_i - x_j) = \sigma_K^2 - 2 \sum_\ell \mu_\ell f^\ell(v),$$

where the λ's and the μ's are the solutions to the kriging system (Equation 9). Bringing pieces together, we get the final correct formula

$$P_u^*(v) = 10^{P^*(v)} + M[\sigma_K^2/2 - \sum_\ell \mu_\ell f^\ell(v)] \times \left[\overline{10^m}/10^{m(v)}\right] \quad . \qquad (14)$$

The first approximation we use is to set $\overline{10^m}/10^{m(v)} = 1$, i.e., we neglect the variation of the drift m(x) within a cell v. By the convexity of the exponential function 10^x, we have $\overline{10^m}/10^{m(v)} > 1$. However, if m(x) varies slowly enough at the scale of v, this corrective term should be close to 1. Let us look at orders of magnitude. For a linear drift in IR^2: $m(x,y) = b_0 + b_1 x + b_2 y$, and averaging over a square of side L yields:

$$\overline{10^m}/10^{m(v)} = 10^{(b_1 + b_2)L/2}\ (1 - 10^{-b_1 L})\ (1 - 10^{-b_2 L})/M^2\ b_1 b_2 L^2.$$

With a maximum $b_1 L = b_2 L$ of 0.5--corresponding to a three-fold variation of m(x) within 100 feet--we find that

$$\overline{10^m}/10^{m(v)} = 1.115 \quad .$$

With $b_1 L = b_2 L = 0.3$--two-fold variation within 100 feet--the ratio is 1.048. So our results may be biased downward, especially near GZ where the gradient is high. But in any case, *the bias should not exceed* 10 percent unless more than three-fold variation of m(x) occurs within 100 feet.

The second approximation is introduced in order to relate the arithmetic mean concentration Pu(v) to the logarithmic mean concentration P(v). Under the assumption that the cell v is small enough--say, to ensure $\gamma(L\sqrt{2}) < 0.5$--it may be shown that, to the first order:

$$Pu(v) = 10^{P(v) + M\,\bar{\gamma}(v,v)/2} \quad .$$

Naturally in this formula, γ refers to the variogram of *the logarithmic* concentrations P(x). A confidence interval for Pu(v) is then simply obtained by multiplying the bounds of Equation 13 by the factor $10^{M\bar{\gamma}(v,v)/2}$. This factor may be calculated using charts of $\bar{\gamma}(v,v)$, which have been computed for the common variogram models (e.g., see Matheron, 1971). However, a simple exact formula is available in the case of a linear variogram $\gamma(h) \quad \bar{\omega}|h|$, when v is a square of side L:

$$\bar{\gamma}(v,v) = 0.5214\ \bar{\omega}\ L.$$

It may also be applied to spherical variograms as long as L is small compared with the range, since then the variogram is practically linear.

Applying this formula to our fitted variogram models, we get:

$$\bar{\gamma}(v,v) = (1.287)^2 \times 0.5214 \times 1.53 \times 10^{4} \times 100 + 0.5214 \times (3/2) \times (0.025/600) \times 100 = 0.016$$

and the multiplicative factor is 1.04.

RESULTS

The figures that follow show the different steps of the estimation (all concentration results are in $\mu Ci/m^2$):

Figure 8 shows contours of Pu values derived from the 100-foot FIDLER grid data through straight regression (no kriging) using Equation 2 followed by taking antilogarithms. Blanks within the 100-foot grid indicate missing values. We note that the FIDLER stratum boundaries of 50,000, 25,000, 10,000, and 5,000 counts per minute (Figure 1) become Pu concentrations of 192, 79, 24, and 9.9 $\mu Ci/m^2$, respectively, using Equation 2.

Figure 9 shows contours of the mean 100- x 100-foot cell Pu concentrations estimated by kriging using Equation 9 on the basis of FIDLER data, i.e.,

$$\left[10^{\alpha F^*(v) + \beta}\right] \times \left[10^{M\alpha^2[\sigma^2_{FK}/2 - \sum_{\ell}\mu_\ell f^\ell(v)]}\right], \qquad (15)$$

where σ^2_{FK} is the kriging variance for the FIDLER data for a given cell. In this estimation, all FIDLER data were used including those at random locations and the 400-foot grid (useful in the edges). The bias correction factor, i.e.,

$$10^{M\alpha^2[\sigma^2_{FK}/2 - \sum_{\ell}\mu_\ell f^\ell(v)]},$$

arises from Equation 14 applied to the guess-field $(10^{\alpha F^*(v) + \beta})$, neglecting the $10^m/10^{m(v)}$ term. The bias correction factor ranges between 1.05 and 1.07. Note the general similarity between Figures 8 and 9. The principal difference is that the kriging contours are "smoother" in appearance.

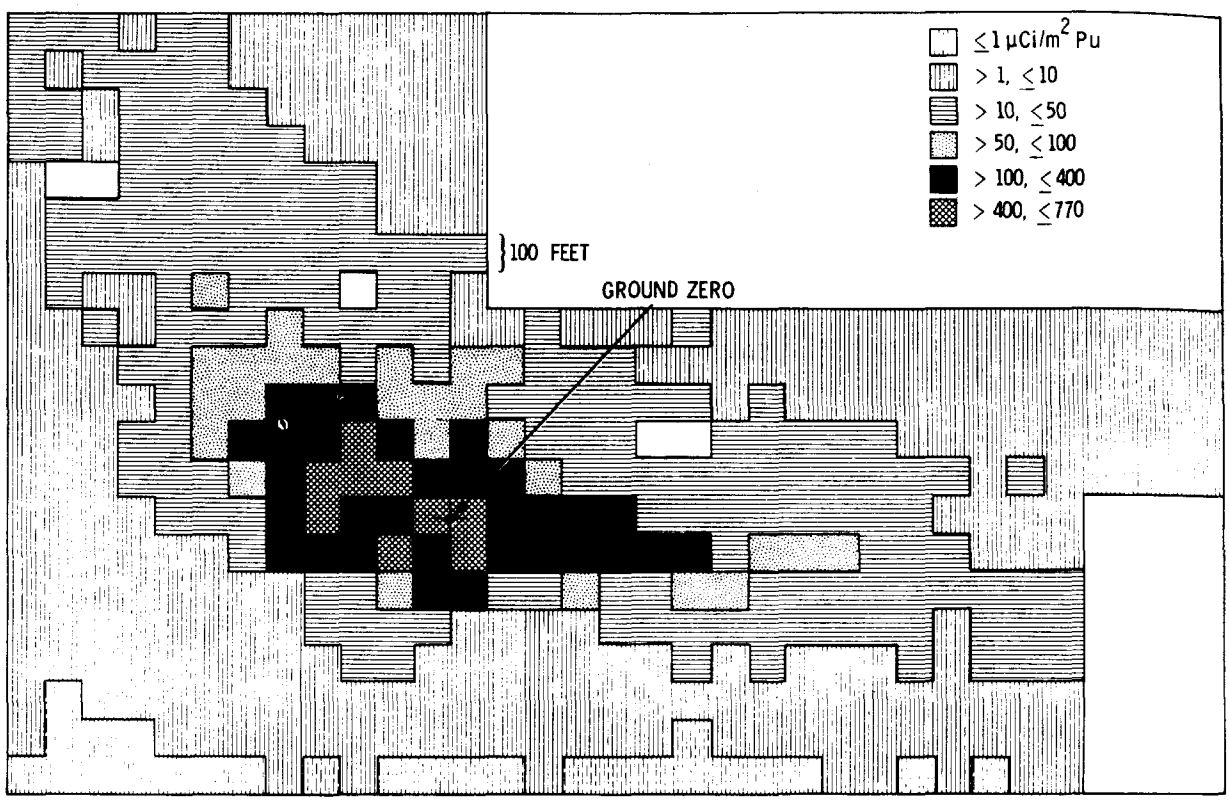

Figure 8. Contours of Estimated Pu Concentrations at Grid Points Using Equation 2 With No Kriging.

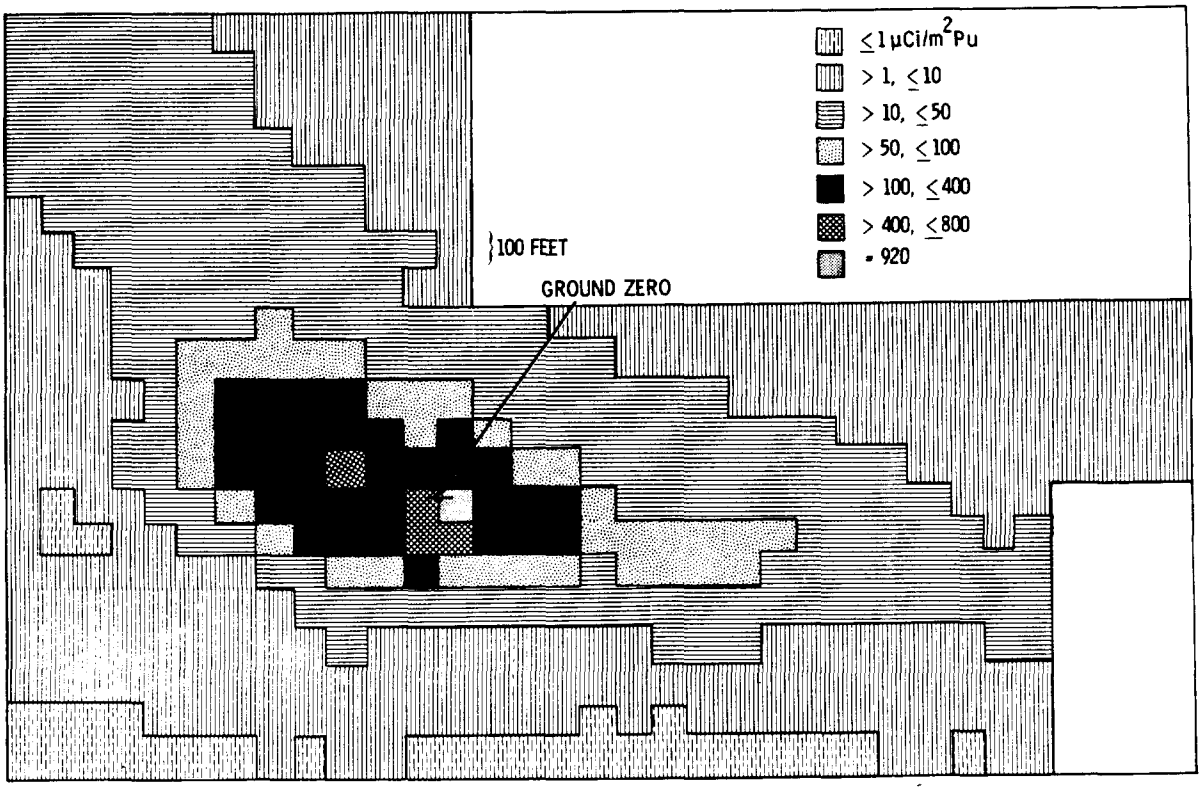

Figure 9. Contours of Estimated Mean Block Pu Concentrations Using Equation 9 Based on FIDLER Data and Ignoring the Block Correction Term $T^*(v)$.

Figure 10 shows contours of the mean block correction term computed as

$$\left[10^{T^*(v)}\right] \times \left[10^{M[\sigma^2_{TK}/2 - \sum_{\ell} \mu_\ell f^\ell(v)]}\right] , \qquad (16)$$

where σ^2_{TK} is the kriging variance for a given block for the residuals $T^*(x)$. Formula 16 was calculated by kriging using Equation 8 on the basis of the 145 residuals $\hat{T}(x_i)$ (see Equation 11). The bias correction factor is between 1.01 and 1.04. We note that the mean block correction term is greater than a factor of two only to the south and east of GZ where it ranges between 2 and 4. The increase south of GZ is caused by soil Pu concentrations that were higher than would be expected on the basis of FIDLER readings on the 100- x 100-foot grid in the general vicinity**. $T^*(v)$ should be greater than 1 when measured Pu is higher than expected from FIDLER, and less than 1 when Pu is less.

Figure 11 shows contours of the product of Formulas 15 and 16. These estimates are those obtained using the entire two-stage estimation procedure. Note from Formula 15 that we are ignoring the drift m(x) within 100- x 100-foot cells as discussed in the previous section.

Figure 12 gives the numerical estimates shown in contour form in Figure 11. The FIDLER strata boundaries in Figure 1 are superimposed on the two-stage kriging results in Figure 12 for comparison purposes. The reader may wish to draw on Figure 12 a contour line connecting cell averages of 9.9 $\mu Ci/m^2$, the Pu concentration corresponding to the 5,000 cpm FIDLER line using Equation 2 (see discussion under Figure 8 above). You will find that the total land area enclosed by this line is larger than the area enclosed by the 5,000 cpm FIDLER line drawn in Figure 12. The increase occurs mostly to the south and east of GZ, and this results from the rather large positive block correction terms in those regions (see discussion above concerning Figure 10).

**In 1976 six new soil samples were collected south of GZ, 2 north of GZ, and 2 east of GZ. Their locations and Pu concentrations ($\mu Ci/m^2$) are given in Figures 3 and 4. Four of the samples south of GZ (Pu concentrations of 11.2, 173, 326, and 97.8 $\mu Ci/m^2$) were used in the kriging computations. FIDLER values (taken from the 100-foot-grid readings) used for these Pu concentrations are 2,300, 4,300, 5,300, and 2,400 cpm, respectively. The data collected at the remaining 2 locations within the 100- x 100-foot-grid area (south of GZ) were inadvertently left out of the analysis. If these two concentrations (328 and 573 $\mu Ci/m^2$) had been included, the kriging estimates would have been larger in that area. The four new observations north and east of GZ were not used since they were collected outside the 100- x 100-foot-grid area.

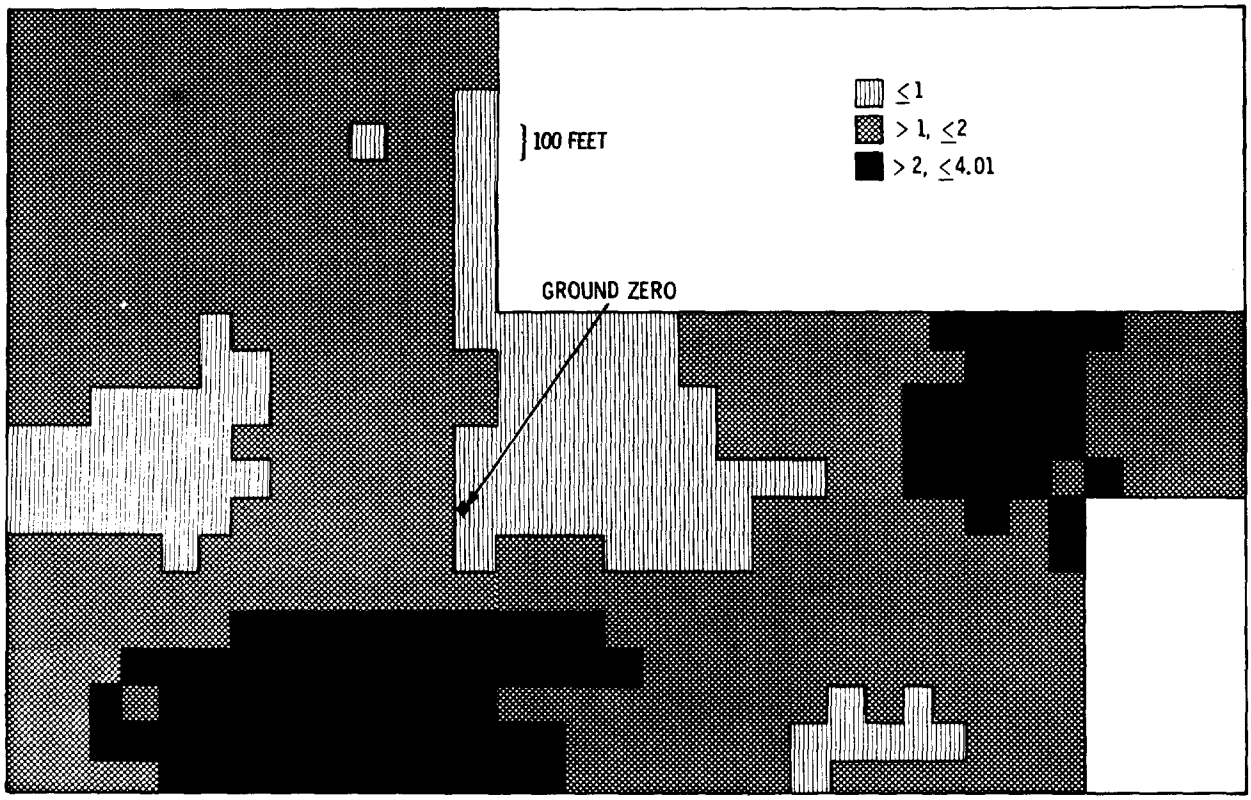

Figure 10. Contours of the Estimated Mean Block Correction Term $T^{*}(v)$ Based on Equation 8 and Computed Using Formula 16.

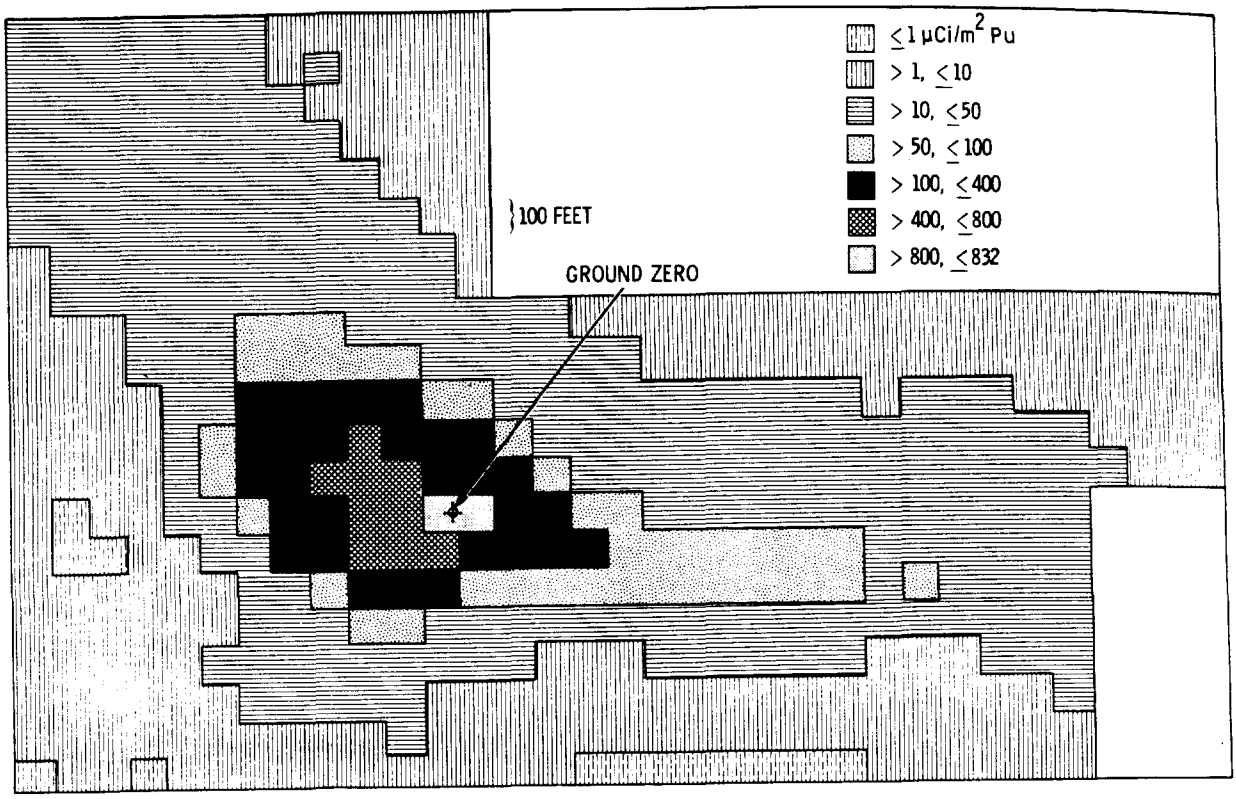

Figure 11. Contours of Estimated Mean Block Pu Concentrations ($\mu Ci/m^2$) Using Equation 14 Ignoring $\overline{10^m}/10^{m(v)}$, or Equivalently the Product of Formulae 15 and 16.

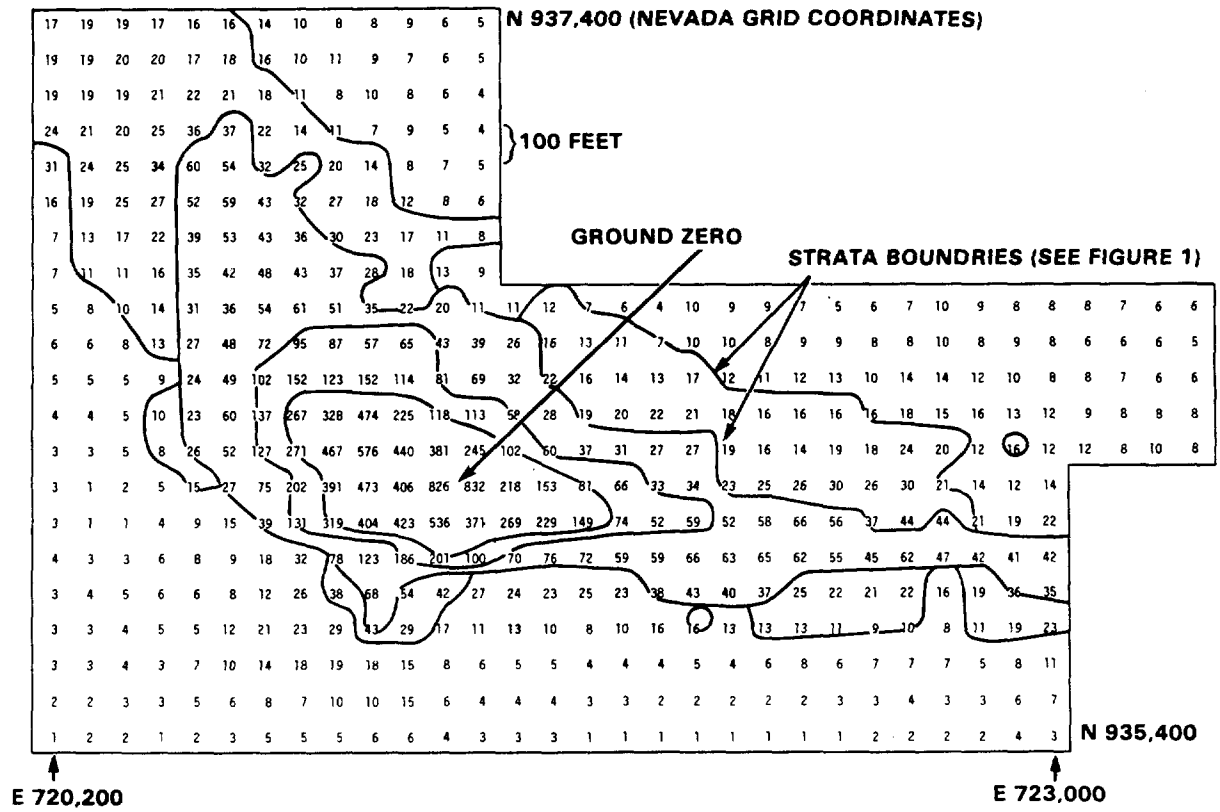

Figure 12. Estimate Arithmetic Mean Block Pu Concentrations ($\mu Ci/m^2$) Using Equation 14 Ignoring $\overline{10^m}/10^{m(v)}$, or Equivalently, The Product of Formulae 15 and 16.

Hence, the two-stage kriging results place the 9.9 $\mu Ci/m^2$ line further from GZ than do the straight regression estimates (no kriging) given in Figure 8. Study of Figures 8 and 9 suggests the 1st stage kriging estimates (Figure 9) are in close agreement in this regard with the regression results (Figure 8). This is not surprising since the 1st stage results are based solely on FIDLER data. In regions near GZ where more data is available, the inner two Pu contour lines of 192 and 79 $\mu Ci/m^2$ (corresponding to 50,000 and 25,000 cpm using Equation 2) are in about the same locations for both the 1st and 2nd stage kriging results.

Figure 13 shows contours of estimates $10^{P^*(v)}$, i.e., of

$$10^{\alpha F^*(v) + \beta + T^*(v)} \quad , \tag{17}$$

where $10^{P^*(v)}$ estimates the geometric mean $10^{P(v)}$. These contours are most similar to those obtained for the two-stage results. The two differ by factors less than 1.2 (see Figure 14).

Figure 14 shows contours of the overall bias correction factor, i.e.,

$$\left[10^{M\alpha^2[\sigma^2_{FK}/2 - \sum_\ell \mu_\ell f^\ell(v)]}\right] \times \left[10^{M[\sigma^2_{TK}/2 - \sum_\ell \mu_\ell f^\ell(v)]}\right] \quad , \tag{18}$$

as it results from Equation 14, neglecting $\overline{10^m}/10^{m(v)}$. Hence Figures 11 and 12 are the product of Formulae 17 and 18. Formula 18 is the product of the bias correction factors for FIDLER regression (stage 1) and $T^*(v)$ (stage 2).

Figure 15 shows $10^{2\delta}K$ for use in Formulae 13. To get a 95 percent confidence interval for the geometric mean $10^{P(v)}$, it suffices to divide and multiply Formula 17 by $10^{2\delta}K$. Up to a multiplication by 1.04, this interval is also valid for the mean Pu concentrations Pu(v) in Figure 12.

Our final (two-stage) estimates (Figures 11 and 12) seem to be in good agreement with the observed Pu data at most locations (see Figures 3 and 4). However, reservations must be made in the region of very high levels of activity in stratum 6 near GZ where estimates appear to be too low. This may result from the log-transformation which has the effect of downweighting large Pu concentrations. The estimates for the two cells adjacent to GZ are 826 and 832 $\mu Ci/m^2$, while soil sample values of 1,170, 1,300, and 14,300 $\mu Ci/m^2$ were observed in that general area (Figure 4). Very high concentrations probably do exist in the immediate vicinity of GZ, but it is not clear to what extent local highs may be "extended" to larger areas. Note, for example, that such highs are

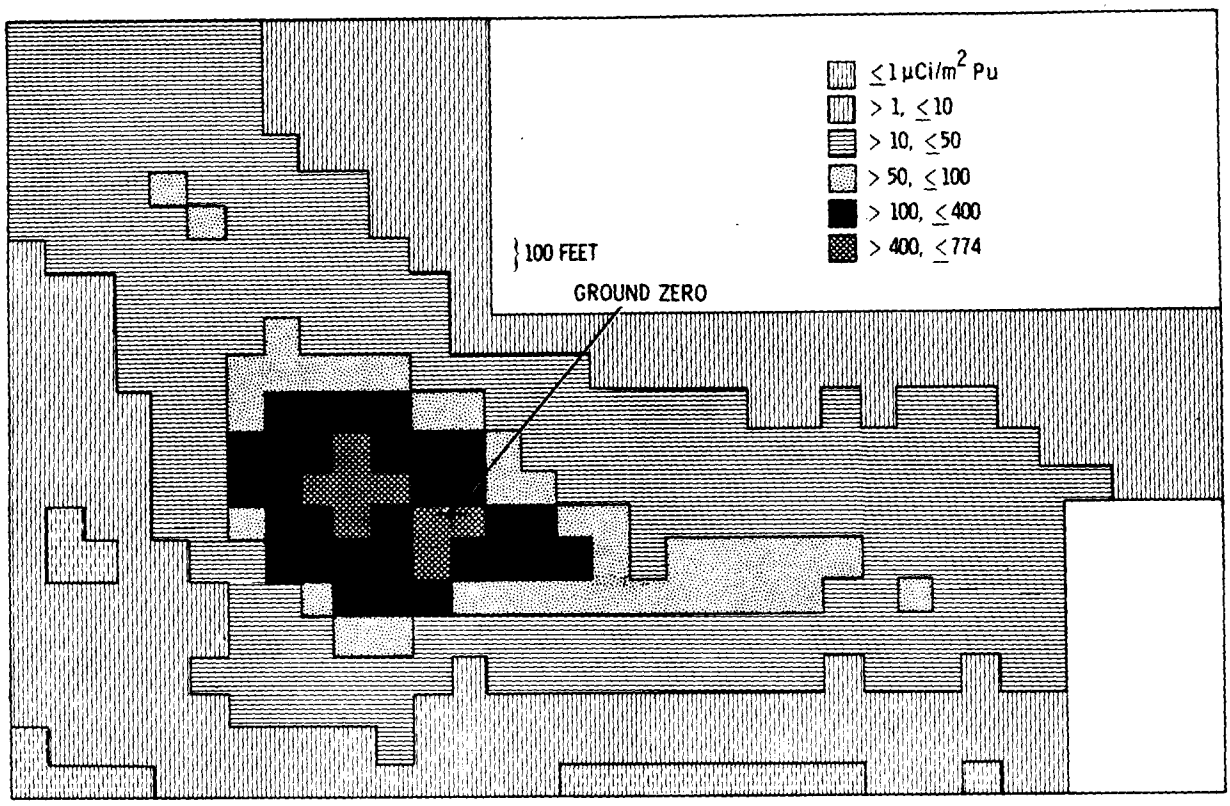

Figure 13. Estimated Geometric Mean Block Pu Concentrations $10^{P^*(v)}$ Using Equation 17.

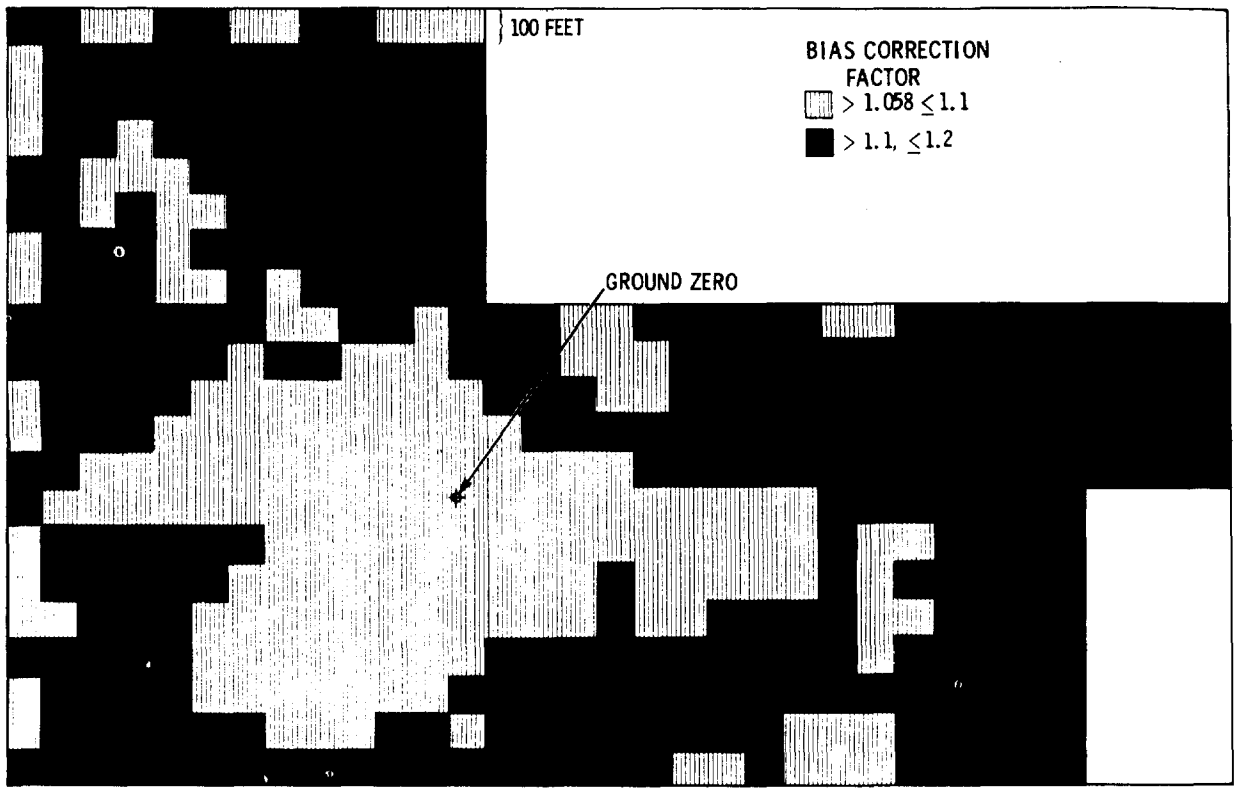

Figure 14. Estimated Total Bias Correction Factor for $P^{*}(v)$ Using Formula 18.

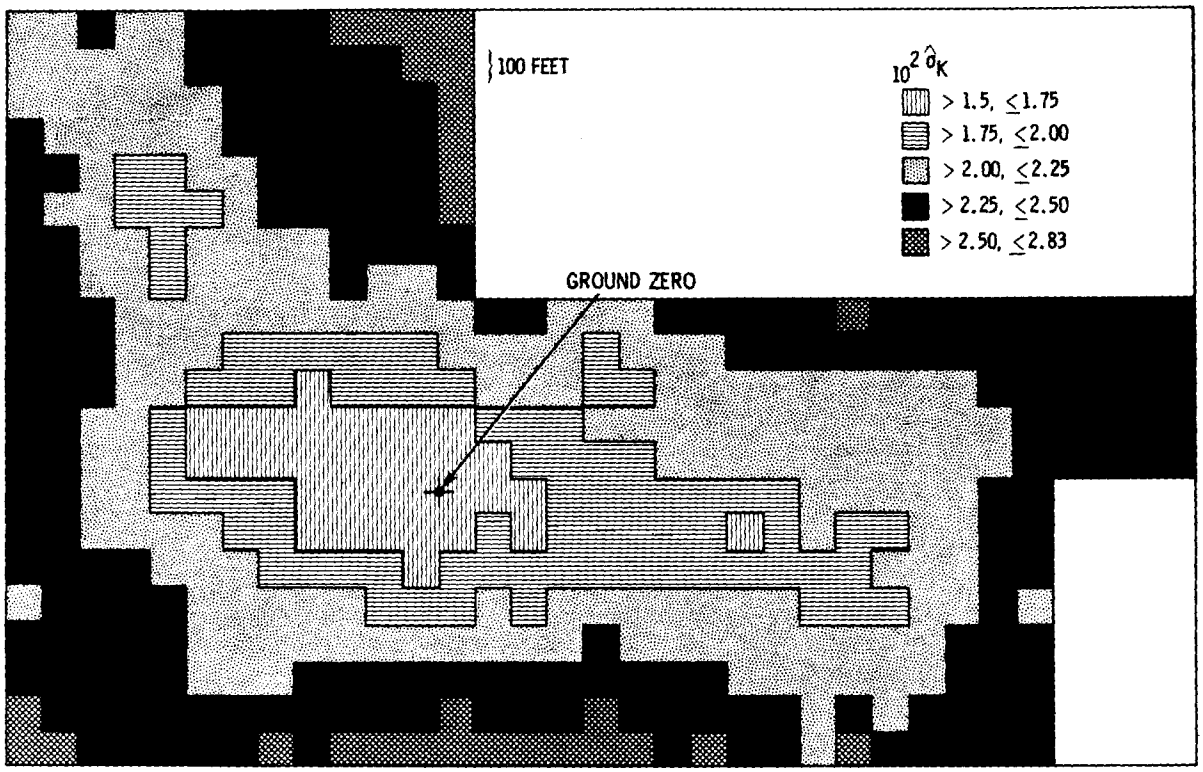

Figure 15. Contours of the Factor $10^{2\hat{\sigma}_K}$ for Obtaining an Approximate 95 Percent Confidence Interval for the Average Geometric Mean Concentration $10^{P(v)}$.

already missed by the 100-foot FIDLER grid which estimates 422 and 770 $\mu Ci/m^2$ (Figure 8 for the two cells adjacent to GZ. Perhaps there should be a specific correction factor $10^m/10^{m(v)}$ to account for a steep decline in Pu concentration within 100 feet or less of GZ. Perhaps the lognormal model itself is not quite adequate at very high levels. Only a custom-made sampling experiment could help solve that question.

The kriging estimates, approximately 400 feet south of GZ, are also somewhat lower than observed concentrations (Figure 4). However, some of these data were not used in the analysis (see Footnote 2), so that a certain amount of underestimation is expected.

The correction (Formula 16) to the guess field is relatively small in areas of high activity near GZ and gets large only in areas of low activity (Figure 10). The relatively large correction south of GZ appears to be caused by the several Pu concentrations that were higher in that area than expected on the basis of prior FIDLER readings. The sparseness of data east of GZ may be related to the rather large correction in that area. In general, however, it may be said that most of the information about the geographical distribution of the Pu is already contained in the FIDLER data. The main role of Pu analysis is to calibrate the regression (Equation 2).

In general, the confidence interval factors in Figure 15 suggest we are able to estimate arithmetic mean Pu concentrations over 100- x 100-foot cells within, roughly, a factor of 2 with approximate 95 percent confidence.

INVENTORY

In Table 3, Part A, we compare estimates of Pu inventory (total amounts in the top 5 cm of soil) reported by Gilbert (1977) for Area 13 with those obtained using the kriging results given here in Figure 12. We recall that Gilbert (1977) used stratified random sampling, where the inventory estimate for a given stratum was obtained by multiplying the average Pu concentration ($\mu Ci/m^2$) for that stratum by the size (m^2) of the stratum.

The kriging estimate of Pu inventory for a given stratum was obtained by estimating the inventory for each 100- x 100-foot cell and summing these for all cells within the stratum. The estimated inventory for a given cell was computed by multiplying the average (kriging) Pu concentration ($\mu Ci/m^2$) by the size of the cell (929 m^2). For cells that overlapped into adjoining strata, the area of the cell lying within the stratum of interest was approximated by "eyeball."

Table 3. Estimates of $^{239,240}Pu$ Inventory in Surface Soil (0-5 cm) in Area 13 (Project 57) Using Two-Stage Kriging and Average $^{239,240}Pu$ Concentrations for Strata.

Part	Strata	Size of Strata (m^2)	Number of Samples (n)	Number of 100- x 100-Ft. Cells* (ν)	Estimated Inventory (Curies)					
					Using Kriging			Using Strata Means		
					$\hat{I}$	SE	100(SE/$\hat{I}$)	$\hat{I}$	SE†	100(SE/$\hat{I}$)
A										
(2 Cells Near GZ Not Deleted)	3	108,000	14	116	2.0	0.37	18%	2.5	0.46	18%
	4	74,000	18	80	3.7	0.61	16%	4.0	0.64	16%
	5	19,000	20	20	2.3	0.37	16%	2.0	0.36	18%
	6	24,000	47	26	8.5	0.91	11%	19**	7.2	39%
	Total	225,000	99	242	16.5	1.2	7%	27	7.2	27%
B										
(2 Cells Near GZ Deleted)	6	22,140	44	24	7.0	0.77	11%	9.9	1.0	10%
	Total	223,140	96	240	15	1.1	7.4%	18	1.3	7.1%

*One cell equals 929 m^2.

**This estimate is one curie less than reported by Gilbert (1977). This results from the analysis of a new 10g aliquot from three stored library samples collected in stratum 6. These new Pu values were also used in obtaining the kriging results.

†Obtained using standard stratified random sampling theory. Note that the relatively low value of 1.3 in Part B versus 7.2 in Part A does not necessarily imply the estimate of inventory in Part B is closer to the true inventory than that in Part A. The deletion of the three high Pu concentrations have simply reduced the estimated standard deviation in stratum 6 from 2,043 to 300 $\mu Ci/m^2$.

The standard error (SE) for the total (strata 3-6) kriging inventory estimate in Table 3 is a "ball-park" estimate obtained as the square root of the approximate expression:

$$\text{Var}(\hat{I}-I) \simeq s^2 M^2 \sum_i \hat{I}_i^2/n_i + \alpha^2(\sigma_E^2 M^2 \sum_i \hat{I}_i^2/\nu_i) \quad . \qquad (19)$$

This was derived using stratified random sampling theory with a constant variance of $s^2 = 0.09$ per stratum (sill of the sperical variogram of residuals; Figure 7). Other parameters in Equation 19 are: $\alpha = 1.287$, the slope of the regression between log Pu and log FIDLER (see Equation 2); $\sigma_E^2 = 0.00373$ is the extension variance of the center of a grid cell to the cell for a linear variogram; and $M = \ell n\ 10 = 2.3026$. I_i, n_i, and ν_i are the estimated inventory, number of Pu concentrations, and number of 100- x 100-foot cells, respectively, for the i^{th} strata. The expression in parentheses in the second term of Equation 19 is the contribution to the total variance due to the FIDLER. The first term is the contribution due to the "block correction term" $T^*(v)$. Using the values of s^2, M, α, and σ_E^2 given above, Equation 19 becomes:

$$\text{Var}(\hat{I}-I) \simeq 0.4769 \sum_i \hat{I}_i^2/n_i + (1.287)^2(0.0198) \sum_i \hat{I}_i^2/u_i \quad .$$

Hence, the contribution to total variance due to the FIDLER is negligible compared to that contributed by $T^*(v)$.

From Table 3, Part A, we see that for strata 3, 4, and 5, the kriging and strata mean inventory estimates differ by only 0.5, 0.3, and 0.3 curies, respectively. However, for stratum 6, the innermost strata surrounding GZ (see Figure 1), the kriging estimate of inventory is slightly less than half that obtained using strata means (8.5 versus 19 curies). There is little doubt that the kriging estimate for this stratum is too low since one of our approximations was to ignore the term $10^m/10^{m(v)}$, which is always greater than 1. We have noted above that our results may be biased downward, especially near GZ where the drift m(x,y) may change by several orders of magnitude within short distances. More FIDLER readings near GZ are required before the change in drift near GZ can be estimated with much assurance.

We should not necessarily assume, however, that the 20 curies estimated by Gilbert (1977) or the 19 curies given in Table 3 are closer to the true inventory than the kriging estimate. As discussed by Gilbert and Essington (1977), the estimate of 20 curies has a large standard deviation (8.2 curies) that results from the highly skewed distribution of Pu data obtained for stratum 6. These authors illustrate, using a hypothetical example, the extreme instability of inventory estimates using the estimated stratum mean when sampling from a highly skewed distribution. If more precise estimates of inventory are needed for stratum 6, a reasonable approach might be to take FIDLER readings on a much finer grid and

use the kriging approach discussed here, making specific corrections using the factor $10^{m}/10^{m(v)}$. The magnitude of this factor could, hopefully, be estimated from the finer grid FIDLER readings.

In Table 3, Part B, we have recomputed Pu inventory estimates for stratum 6 and the total for strata 3 through 6 after deleting from consideration the two 100- x 100-foot cells adjacent to GZ. Recall that these had kriging estimates of 826 and 832 $\mu Ci/m^2$ and that they contained the three highest observed Pu concentrations in stratum 6 (1,170, 1,300, and 14,300 $\mu Ci/m^2$). Both kriging and stratified random sampling estimates of inventory were recomputed. The two inventory estimates for stratum 6 now differ by 2.9 curies rather than by the 10.5 curies when these two cells were not ignored (Part A, Table 3). The stratified random estimate for strata 3 through 6 drops by 9 curies, whereas, the kriging estimate drops by only 1.5 curies. Hence, the inventory estimates obtained by strata mean concentrations are much more sensitive to extreme values than those obtained using kriging. This is partly due to a different weighting scheme and also to the use of logarithms in the kriging procedure.

The results in Table 3 suggest that inventory estimates obtained using two stage kriging or arithmetic average Pu concentrations for strata may tend to be similar in magnitude for study sites where extreme trends (drift) or variability in Pu concentrations do not occur over the region for which estimates are required.

DISCUSSION

The kriging approach used here may be particularly applicable for those regions that lie between the immediate GZ area and the relatively low-level areas at distance from GZ. The tremendous variability present close to GZ makes questionable, perhaps, the application of any "smoothing" or weighted average procedure in that region, i.e., concentrations may be simply too chaotic to model. At distances far from GZ where relatively low levels of Pu are evident, the kriging approach has not been adequately studied to allow us definite conclusions as to its applicability. However, we have seen in this report that Pu concentrations are not as well predicted from the FIDLER when FIDLER readings drop below 5,000 cpm (Figure 5). We have also noted (Table 2) that along Line 2, which is in an area where FIDLER counts are < 5,000 cpm, there appears to be no correlation structure even for adjacent FIDLER readings, i.e., the variogram is a horizontal line with a large nugget effect. In other words, along Line 2, we have pure "noise." In the absence of a correlation structure, there appears to be little advantage to using kriging.

For situations where it appears kriging can be applied, the investigator should consider carefully whether the benefits to be gained from kriging are worth the extra time and expense of performing the necessary structural analysis and kriging of the data. The average Pu concentrations and confidence limits over 100- x 100-foot cells are clearly more informative and useful than the stratum averages reported by Gilbert *et al.* (1975). They would be particularly useful in a cleanup situation where the cell averages might be used to indicate those portions of the study site requiring remedial action. Furthermore, if the mathematical assumptions underlying kriging are not unreasonable at a given site, then theory tells us that the estimates obtained using kriging are "best" in that they are unbiased and have minimum variance of all linear estimators we might try (see Barnes *et al.*, 1977, for other advantages to kriging).

An initial cost of kriging involves training a statistician in the theory of kriging (so that inappropriate applications are avoided) and writing or acquiring the necessary computer programs. The availability of the kriging program BLUEPACK on the Nevada Operations Office computer is a tremendous help in that regard. However, as with any computer program, BLUEPACK can be used inappropriately. Hence, a person experienced in the use of BLUEPACK and familiar with field and laboratory procedures is essential if a serious attempt at kriging is anticipated.

It is also clear that the use of kriging cannot overcome a lack of data. It is important to design a field sampling program so that enough information over the entire study site is available for estimating spatial pattern. Hence, the design of the sampling plan is an important step in any environmental sampling effort.

ACKNOWLEDGMENTS

We would like to thank Madaline Barnes of the Desert Research Institute, Las Vegas, and Pam Doctor and Lee Eberhardt of Battelle-Northwest Laboratories for the stimulating discussions we have had about kriging and its potential for application to transuranic field studies. Special thanks are also extended to Mary Lou Lemon of Battelle-Northwest for her excellent work in typing the manuscript. The figures were very ably drawn by the Graphics Section, Communications Department of Battelle-Northwest. The support of Mary G. White of the NAEG in our efforts at evaluating the potential of kriging for transuranic studies is also gratefully acknowledged.

REFERENCES

1. Barnes, M. G., P. Delfiner, and R. O. Gilbert. 1977. "A New Statistical Tool, Kriging, and Some Applications." *In: Transuranics in Desert Ecosystems.* M. G. White, P. B. Dunaway, and D. L. Wireman (Eds.). USDOE Report, NVO-181.

2. Chauvet, P., J. Pailleux, and J. P. Chilès. 1976. "Analyse Objective des champs météorologiques par cokrigeage." *La Météorologie, Sciences et Techniques,* 6 Série, No. 4, 37-54.

3. Church, B. W., E. S. Medling, and D. N. Brady. 1975. "A Different Look at Area 13 FIDLER Survey Data." *In: The Radioecology of Plutonium and Other Transuranics in Desert Environments.* M. G. White and P. B. Dunaway (Eds.). USERDA Report, NVO-153. pp. 231-235.

4. Cochran, W. G. 1963. *Sampling Techniques.* 2nd Ed., New York, John Wiley & Sons.

5. Cressman, G. P. 1959. "An Operational Objective Analysis System." *Monthly Weather Review.* 87 (No. 10).

6. Delfiner, P. 1973. "Analyse du géopotential et du vent géostrophique par Krigeage Universel." *Revue de la Météorologie* 25:1-57.

7. Delfiner, P. 1975. "Linear Estimation of Nonstationary Spatial Phenomena." *In: Advanced Geostatistics in the Mining Industry.* M. Guarascio, M. David, and C. Huijbregts (Eds.). NATO A.S.I., Rome 1975, Dordrecht-Holland, D. Reidel Publishing Company. pp. 49-68.

8. Delfiner, P., and J. P. Delhomme. 1973. "Optimum Interpolation by Kriging." *In: Display and Analysis of Spatial Data.* J. C. Davis and M. J. McCullogh (Eds.). New York, John Wiley & Sons. pp. 96-114.

9. Delfiner, P., J. P. Delhomme, and J. P. Chilès. 1976. "'BLUEPACK' User's Manual." Ecole Nationale Superieure des Mines de Paris, Fontainebleau, France.

10. Eberhardt, L. L., and R. O. Gilbert. 1976. "Sampling the Environs for Contamination." *In: Proceedings of the First ERDA Statistical Symposium.* W. L. Nicholson and J. L. Harris (Eds.). Battelle, Pacific Northwest Laboratories, Richland, WA. BNWL-1986. pp. 187-208.

11. Gilbert, R. O. 1976. "On the Estimation of Spatial Pattern for Environmental Contaminants." This volume. Also published by Battelle, Pacific Northwest Laboratories, Richland, WA. BNWL-SA-5771, 1976.

12. Gilbert, R. O. 1977. "Revised Total Amounts of ^{239,240}Pu in Surface Soils at Safety-Shot Sites." *In: Transuranics in Desert Ecosystems.* M. G. White, P. B. Dunaway, and D. L. Wireman (Eds.). USDOE Report, NVO-181.

13. Gilbert, R. O., and L. L. Eberhardt. 1974. "Statistical Analysis of Pu in Soil at the Nevada Test Site--Some Results." *In: The Dynamics of Plutonium in Desert Environments.* P. B. Dunaway and M. G. White (Eds.). USAEC Report, NVO-142. pp. 43-50.

14. Gilbert, R. O., and L. L. Eberhardt. 1976. "An Evaluation of Double Sampling for Estimating Plutonium Inventory in Surface Soil." *In: Radioecology and Energy Resources.* C. E. Cushing (Ed.). Dowden, Hutchinson and Ross, Inc., Stroudsburg, Pennsylvania. pp. 157-163.

15. Gilbert, R. O., L. L. Eberhardt, E. B. Fowler, E. M. Romney, E. H. Essington, and J. E. Kinnear. 1975. "Statistical Analysis of ^{239,240}Pu and ^{241}Am Contamination of Soil and Vegetation on NAEG Study Sites." *In: The Radioecology of Plutonium and Other Transuranics in Desert Environments.* M. G. White and P. B. Dunaway (Eds.). USERDA Report, NVO-153. pp. 339-448.

16. Gilbert, R. O., and E. H. Essington. 1977. "Estimating Total ^{239,240}Pu in Blow-Sand Mounds of Two Safety-Shot Sites." *In: Transuranics in Desert Ecosystems.* M. G. White, P. B. Dunaway, and D. L. Wireman (Eds.). USDOE Report, NVO-181.

17. Gilbert, R. O., L. L. Eberhardt, and D. D. Smith. 1977. "An Initial Synthesis of Area 13 ^{239}Pu Data and Other Statistical Analyses." *In: Environmental Plutonium on the Nevada Test Site and Environs.* M. G. White, P. B. Dunaway, and W. A. Howard (Eds.). USERDA Report, NVO-171. pp. 237-274.

18. Matérn, B. 1960. "Spatial Variation." *Meddelanden Fran Statens* skogsforskningsinstitut, Band 49, No. 5.

19. Matheron, G. 1963. "Traité de Géostatistique Appliquée-Tome II: Le Krigeage." Editions Technip, Paris.

20. Matheron, G. 1965. "Les Variables Régionalisées et leur Estimation." Masson et Cic, Paris.

21. Matheron, G. 1969. "Le Krigeage Universel." Fasc. No. 1, Cahiers du C.M.M., Fontainebleau, France.

22. Matheron, G. 1971. "The Theory of Regionalized Variables and Its Applications." Fasc. No. 5, Cahier du C.M.M., Fontainebleau, France.

23. Matheron, G. 1973. "The Intrinsic Random Functions and Their Applications." *Advances in Applied Probability* 5:439-468.

TWO STUDIES IN VARIABILITY FOR SOIL CONCENTRATIONS: WITH ALIQUOT SIZE AND WITH DISTANCE

P. G. Doctor and R. O. Gilbert

Battelle Memorial Institute, Pacific Northwest Laboratory
Richland, Washington

ABSTRACT

Two sources of variability encountered in radionuclide field studies include within-sample (between aliquot) variability and variability in concentrations over distance in the field. This paper describes the results of two studies conducted by the Nevada Applied Ecology Group (NAEG) to investigate these sources of variability on the Nevada Test Site (NTS).

The first study reported here investigates the variability in ^{241}Am concentrations in <10-mesh, ball-milled soil aliquots of size 1, 10, 25, 50, and 100 g drawn from a single, large composite sample collected at Nuclear Site (NS)-201 in a region where the average ^{241}Am concentration is about 1.9 nCi/g dry soil in the surface 5 cm. The standard deviation (s) between aliquots withdrawn from this field sample was found to decline from a high of 1.52 nCi/g for the 1-g size to 0.17 nCi/g for 100-g aliquots. The coefficients of variation also declined from 79% to 9% for these aliquot sizes. These results imply that many more 1-g aliquots are required to estimate the true mean concentration of an individual soil sample with specified precision than is required for, say, 100-g aliquots.

The estimated median and geometric mean concentrations were found to increase with increasing aliquot size. This results from an observed decrease in skewness of the underlying distribution of aliquot concentrations as aliquot weight increases. However, the arithmetic mean concentration did not systematically increase with aliquot size, a result

expected from theoretical arguments. The relative stability of the arithmetic mean for different aliquot sizes implies it is preferred to the geometric mean and the median when comparing results from studies that have used different aliquot sizes.

A linear relationship between logarithms of s and aliquot weight (w) at this sampling location is suggested by the data. This equation was used to obtain expressions for determining aliquot weight and number of aliquots per sample for ^{241}Am and $^{239,240}Pu$ analyses as a function of analysis costs and the desired standard error of the sample mean. An approach used by Cochran (1977) is suggested as a way of obtaining optimum numbers of field samples and number of aliquots per field sample for minimizing either total cost or the variance of the mean computed over all field samples. Additional studies are required to determine the degree to which these results are applicable to other sampling locations on NTS and to other study sites where different sources of contamination and environmental factors are present.

The purpose of the variability with distance study was to obtain data useful for estimating the variogram (correlation structure) between ^{241}Am concentrations at various distances. This information is needed in our continuing evaluation of kriging, an optimal procedure (under certain conditions) for estimating spatial distribution of contaminants. This study was conducted along two sampling transects at the Area 13 (Project 57) Site on NTS. Line 1 was near ground zero (GZ) and cut across several activity strata. Line 2 was 3,600 ft north of GZ where activity levels are relatively low (in the pCi/g range). Both 70-g soil aliquots and FIDLER readings at the soil surface and at 1-ft height were taken to measure ^{241}Am. These measurements were taken in clusters of four adjacent locations, each cluster separated by 20 ft in Line 1 and 150 ft in Line 2. One hundred adjacent FIDLER readings were also taken near Lines 1 and 2. The data are plotted and the experimental (estimated) variograms computed and displayed for all cases. Some basic concepts of kriging are discussed.

For the relatively high ^{241}Am concentrations along Line 1 (nCi/g range), there appears to be a definite correlation between observations as a function of distance for both soil Ge(Li) analyses on 70-g aliquots and for FIDLER readings. This is evident from the experimental variograms. This does not appear to be the case for the lower levels (pCi/g range) along Line 2. This suggests that kriging may not be advantageous at these low levels for the data collection methods used here (soil and FIDLER). Its use in these low-level areas would seem to depend on using measurement techniques that integrate over a larger region. Additional analyses of the Line 1 and 2 data are given by Delfiner and Gilbert (1978).

INTRODUCTION

The purpose of this paper is to report the results of two field sampling studies into the nature of the variability in Am soil concentrations at NTS. The first study examines the relationship of aliquot size to observed Am soil concentration. The second investigates the pattern of Am variability as a function of the distance between samples in the field.

The variability with aliquot size study is important in part because the basic data in field studies are concentrations. Knowledge of the effect of aliquot size on observed concentration and variability is needed to assess the appropriateness of ascribing the observed aliquot concentration to the entire sample. One of the recommendations made at the EPA Workshop (1976) on Soil Collection and Analytical Techniques held in April 1974 was to conduct aliquot studies such as the one discussed here. The variability with distance study was designed to provide information on the interrelationship of Am concentrations over space at the Project 57 (Area 13) site on NTS. This type of information is needed for a statistical method called kriging to estimate the spatial distribution of radionuclide concentrations. Additional motivation for these two variability studies is given below. Throughout this paper, ^{239,240}Pu and ^{241}Am are referred to as Pu and Am, respectively.

VARIABILITY WITH ALIQUOT SIZE STUDY

MOTIVATION

Soil samples collected in the field are typically too large to permit the entire sample to be analyzed for transuranics by wet chemistry techniques. Standard NAEG procedures involve drying the entire sample followed by ball-milling for several hours. Typically one or more 10-g aliquots are withdrawn from the ball-milled sample and analyzed for Pu and Am. The resulting average aliquot concentration (expressed on a per gram basis) is then used as an estimate of the true concentration of the field sample that would be obtained if the entire field sample could be analyzed.

Am and Pu in environmental samples are often known or assumed to be in particle form, in which case variability between aliquots is inevitable due to random differences in the number and size of particles in different aliquots. This randomness will exist even though ball-milling has been conducted. Incomplete ball-milling or mixing may, of course, contribute additional variability. Presumably, a complete dissolution of the entire sample into liquid form would result in truly homogeneous aliquots.

As the number of transuranic particles in the field sample increases and/or volume of individual particles decreases, the aliquots become more homogeneous. This in turn will result in a reduction in aliquot to aliquot variability. Equation 4 of Grant and Pelton (1973) is a mathematical representation of this phenomenon.

Aliquot size can also have an effect on the computed geometric mean and median of aliquot concentrations. Michels (1977) points out in the context of sampling air for particulates that the geometric mean concentration of a scarce contaminant will tend to increase with volume of aliquot if aliquot concentrations are lognormally distributed. His Figure 1 gives for the lognormal case the ratio of geometric means to be expected as a function of geometric standard deviation and the ratio of aliquot volumes. We are concerned here with the weight of soil aliquots rather than the volume of air passed through an air filter, but our results discussed below show this same effect. Aitchison and Brown (1969) give a comprehensive discussion of the lognormal distribution.

It is important to note that on the average, the arithmetic mean should not increase with aliquot size. This is, the mathematical expected value of $\bar{x}$ is always the true mean concentration of the sample, regardless of aliquot size or the underlying distribution. As a consequence, estimates of transuranic inventory that are computed using $\bar{x}$ will not systematically change with aliquot size. Clearly, arithmetic means from different studies are more directly comparable than geometric means.

We note that the variability studied here is between aliquots from a single location in the field. Taking larger size aliquots will reduce this within-sample variability, but it will not reduce the between-sample variability, i.e., the variability between soil samples collected at different locations. If between-sample variability is substantially greater than within-sample variability (resulting perhaps from a strong trend in concentration level with distance from ground zero), then use of larger aliquot sizes would not materially reduce the variance of a sample mean computed from all sampled locations.

A study of the type discussed here, conducted before routine sampling starts, can give information on within-sample variability. This information, when combined with data on the variability between locations in the field, can be used to devise sampling plans for achieving a specified level of precision in concentration estimates or estimates of inventory. Cochran's (1977) approach to this problem is discussed in this paper. Wallace and Romney (1977) point out the problems of taking very small aliquots of soil for cleanup purposes when precise and accurate estimates of very low concentration levels may be required. The implications are that relatively large aliquots or many smaller aliquots will be required.

SAMPLING AND SOIL PREPARATION METHODS

This section is a summary of the complete field sampling and soil preparation protocol given in Appendix A.

Twenty-four adjacent standard NAEG surface soil samples (5-in. diameter ring to a depth of 5 cm) were collected on a 6 by 4 grid (see diagram, Appendix A) approximately 150 ft north of GZ at NS-201. Each sample was dried, ball-milled, and sieved through a 10-mesh screen. The <10-mesh fractions from all samples were composited (pooled) and mixed by kneading for approximately 10 minutes.

The aliquoting procedure for the <10-mesh fraction proceeded as follows: the entire mixed sample was divided into four quarters, each quarter divided into fifths, and each fifth placed in a separate bottle. This gives a total of 20 bottles. One aliquot each 1, 10, 25, 50, and 100 g was taken from each bottle for a total of 100 aliquots. The order in which the different size aliquots were taken was systematically varied according to a "latin-square" design (Federer, 1963, Chapter 6) as described in Table A1 in Appendix A. This was done to mitigate any confounding of concentration for a particular aliquot size with the order in which that size aliquot was drawn from the bottle. Each aliquot was Ge(Li) counted for Am by REECo* personnel at Mercury, Nevada. Counting times were 1,000 minutes or until the counting error (2σ level) was <10%. Actual counting errors were about 7%. Special samples were also collected in the vicinity of NS-201 for the purpose of calibrating the Ge(Li) counting system for the different size aliquots. Details are given in Appendix A.

The >10-mesh fraction was handled similarly to the <10-mesh fraction except that only 10 ten-gram aliquots were analyzed for comparison with ten-gram aliquots of the <10-mesh soil. The average Am concentration for the >10-mesh aliquots were 0.00748 ± 0.00213 nCi/g ($\bar{x}$ ± standard error). This mean is about three orders of magnitude less than the mean obtained for the <10-mesh soil (see next section).

RESULTS

The Am concentrations in nCi/g for the five aliquot sizes are given in Table 1 in the form of "stem-and-leaf" displays. Figure 1 is a plot of the data that also gives the median, arithmetic mean ($\bar{x}$), geometric mean (GM), standard deviation (s), standard error (SE), and coefficient of variation (c) of the 20 aliquots for each aliquot size. In Figure 1, the two outer solid lines delineate the ranges of the observed data and should not be construed as confidence limits. The center line connects the arithmetic mean for each aliquot size. The stars locate the medians and the parentheses denote the mid 50% (interquartile range) of each data set.

It is clear that the variability between aliquots is highest for the 1-g size and decreases as the aliquot size increases. The data are skewed

---

*Reynolds Electrical and Engineering Co.

Table 1. Stem-and-Leaf Displays of ^{241}Am [Ge(Li)] Concentrations (nCi/g in Soil Aliquots of Different Sizes From a Composited Soil Sample Collected 150 ft North of Ground Zero at Nuclear Site-201, Nevada Test Site

1 Gram		10 Gram		25 Gram		50 Gram		100 Gram	
Stem	Leaf	Stem	Leaf	Stem	Leaf	Stem	Leaf	Stem	Leaf
8.1									
8.0	0								
7.9									
3.8									
3.7									
3.6									
3.5		3.5		3.5					
3.4		3.4	3	3.4	0				
3.3		3.3		3.3					
3.2		3.2		3.2					
3.1		3.1		3.1					
3.0		3.0		3.0					
2.9		2.9		2.9					
2.8	0	2.8		2.8					
2.7		2.7		2.7					
2.6	9	2.6	3	2.6	8				
2.5		2.5		2.5		2.5			
2.4		2.4		2.4	0 6	2.4	6	2.4	
2.3	0	2.3		2.3		2.3		2.3	0
2.2		2.2		2.2	0	2.2		2.2	4
2.1	3	2.1		2.1	9	2.1		2.1	1 3
2.0		2.0	0 7	2.0		2.0	0 1 2 3	2.0	0 6
1.9		1.9	3 5	1.9		1.9	0 4	1.9	0 1 5 6 9
1.8	6	1.8	3 6	1.8		1.8	6 7 9	1.8	0 1 3
1.7	1 1 3	1.7	3 7	1.7	1 5	1.7	0 1 2 3 7	1.7	0 2 4 5 8 9
1.6		1.6	6 7 9	1.6	1	1.6	3 7 8 9	1.6	
1.5	4 7	1.5	0 4	1.5	1 2 2 4 8	1.5	5	1.5	
1.4	5	1.4	1 6 7 9	1.4	4	1.4		1.4	
1.3		1.3	6	1.3	3 3 6	1.3		1.3	
1.2	2 2 7	1.2		1.2	3 7	1.2		1.2	
1.1	0 7	1.1		1.1		1.1		1.1	
1.0	1 4 5	1.0		1.0		1.0		1.0	

(Example of how to read: the row 1.3|3 3 6 in the 25 gram column represents three concentrations whose third digits are 3, 3, and 6; i.e., the three concentrations are 1.33, 1.33, and 1.36.)

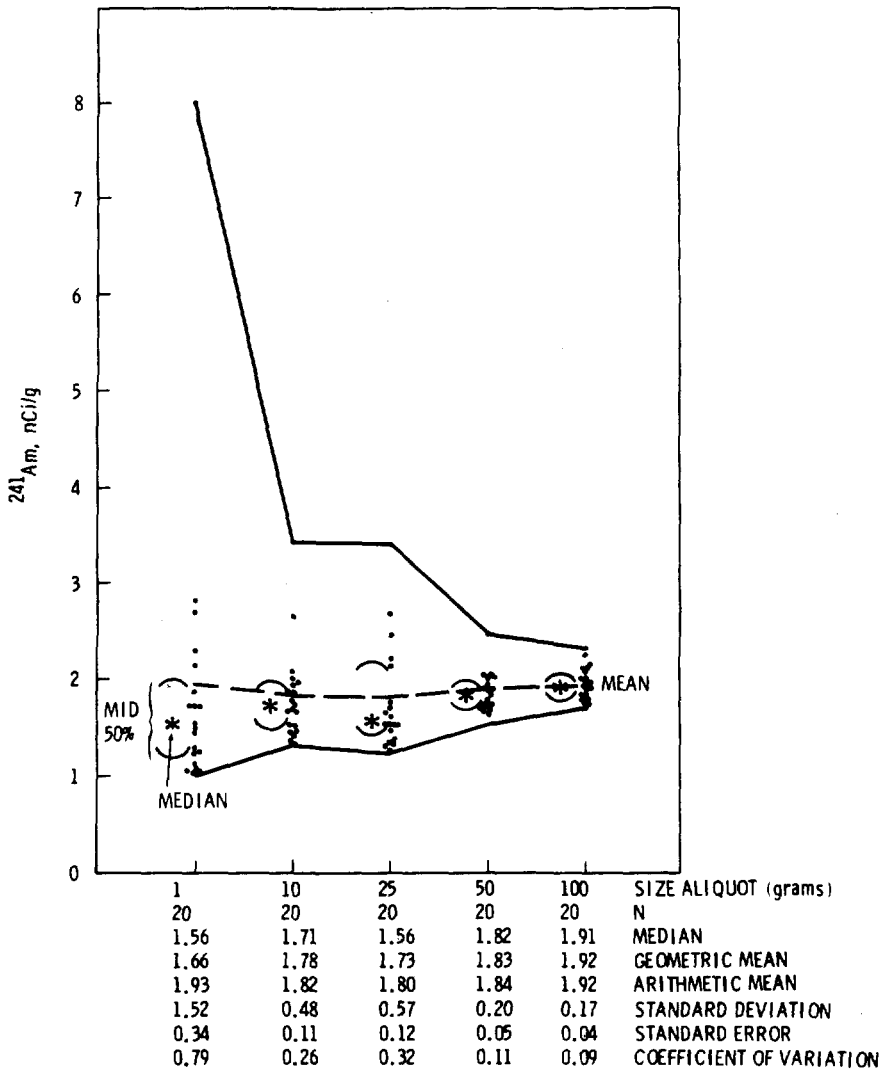

1	10	25	50	100	SIZE ALIQUOT (grams)
20	20	20	20	20	N
1.56	1.71	1.56	1.82	1.91	MEDIAN
1.66	1.78	1.73	1.83	1.92	GEOMETRIC MEAN
1.93	1.82	1.80	1.84	1.92	ARITHMETIC MEAN
1.52	0.48	0.57	0.20	0.17	STANDARD DEVIATION
0.34	0.11	0.12	0.05	0.04	STANDARD ERROR
0.79	0.26	0.32	0.11	0.09	COEFFICIENT OF VARIATION

Figure 1. ^{241}Am Concentrations in Soil Aliquots of Different Sizes from Nuclear Site-201.

toward high concentrations for all sizes, but the skewness decreases as aliquot size increases. The standard deviation decreases from 1.52 for the 1-g size to only 0.17 for 100-g aliquots. The coefficient of variation ($s/\bar{x}$) similarly decreases from 0.79 to 0.09. The arithmetic mean remains relatively constant over all aliquot sizes, but both the median and geometric mean tend to increase with increasing aliquot size. For both the 50- and to 100-g sizes, the median, arithmetic mean, and geometric mean are almost identical.

One way of comparing results for the five aliquot sizes is to consider the question: "How many aliquots of size less than 100 g would be required to achieve the same precision (standard error) in the mean $\bar{x}$ for a field sample as was achieved using 100-g aliquots?" The SE for 100-g aliquots was 0.04 nCi/g (Figure 1). If we solve the equation $SE = s/\sqrt{n}$ for n we obtain $n = (s/SE)^2$. By using SE = 0.04 and the estimate of s obtained for a smaller aliquot size, we may use this equation to estimate the number of smaller aliquots required to achieve a SE of 0.04. Results are given in Table 2. As expected, the smaller size aliquots require substantially more aliquots than the 100-g size to achieve the desired SE. For example, an estimated 31 fifty-g aliquots and a phenomenal 1,444 one-g aliquots are required to achieve the precision obtained using only 20 aliquots of 100-g size. This illustrates the point that stringent requirements on sampling precision require either a great many small aliquots or relatively large aliquots. This same conclusion was reached by Wallace and Romney (1977) based on Pu particle size distribution arguments.

Table 2. Number of Aliquots of Size Less Than 100 g Required to Achieve the Same Precision (SE) in the Estimated Mean of the Field Sample as Obtained Using 20 Aliquots of 100-g Size

Aliquot Size (g)	100	50	25	10	1
Standard Error†	0.04	0.05	0.12	0.11	0.34
Standard Deviation(s)†	0.179	0.224	0.537	0.492	1.52
$n = (s/0.04)^2$	20	32	181	152	1,444
Ratio of Sample Sizes $(\frac{n}{20})$	1	1.6	9	7.6	72.2

†Units of nCi/g.

VARIABILITY AND THE NUMBER OF ALIQUOTS PER FIELD SAMPLE

We noted above that between-aliquot variability is an important parameter in designing environmental transuranic studies to meet precision requirements. For example, one may want to estimate the number of aliquots, n, per field sample needed to be (1-α)% confident that the estimated mean concentration $\bar{x}$ of the individual sample is within, say, d% of the true mean m of that sample. An estimate of n can be obtained from the equation

$$n = (Z_{\alpha/2}\ c/d)^2 \qquad (1)$$

(Snedecor and Cochran, 1967, page 516), where $Z_{\alpha/2}$ is the standard normal deviate corresponding to α% (two-tailed) confidence, c is the known or estimated coefficient of variation in percent $[100(s/\bar{x})]$,

and d is the percent deviation of $\bar{x}$ from m, the true mean. That is, $d = 100(\bar{x} - m)/\bar{x}$.

Table 3 gives values of n computed using Equation (1) for $\alpha = 0.01$ and 0.05 (i.e., 99 and 95% confidence*), d = 10, 25, and 50% and the c's actually obtained for the five aliquot sizes. These results assume the estimated mean $\bar{x}$ to be normally distributed. This should be approximately true (Snedecor and Cochran, 1967, page 51), particularly for the larger aliquot sizes, even though the individual aliquot concentrations are clearly not normal.

Table 3 indicates the prohibitively large number of aliquots of 1-g size required to estimate the soil sample mean even with only 50% accuracy. Clearly, the average of 1 or 2 one-g aliquots per sample would give a very crude estimate of the true mean concentration for each field sample. On the other hand, if study objectives require an accuracy of 10% with 95 or 99% confidence for each sample, then only 4 to 6 aliquots of 100-g size would appear to be sufficient.

Table 3. Number of Aliquots Required to Be 1-α Percent Confident That the Estimated Arithmetic Mean of a Field Sample is Within d% of the True Mean for Aliquot Sizes of 1, 10, 25, 50, and 100 g

Aliquot Size	Coefficient of Variation	Percent Accuracy (d)					
		50%		25%		10%	
		α = 5%	1%	5%	1%	5%	1%
1 g	0.79	10	17	39	66	240	413
10 g	0.27	2	2	5	8	28	49
25 g	0.30	2	2	6	10	35	60
50 g	0.12	1	1	1	2	6	10
100 g	0.09	1	1	1	1	4	6

Please note that we are considering here only the number of aliquots per field sample. Optimum numbers of field samples are discussed at the end of the next section.

CHOOSING THE NUMBER AND SIZE OF ALIQUOTS

A number of references discuss and/or derive theoretical mathematical expressions that, under certain simplifying assumptions, relate variables such as aliquot size and the volume and density of contaminate particles

*$Z_{\alpha/2}$ for $\alpha = 0.01$ and 0.05 is 2.57 and 1.96, respectively.

to the standard deviation or coefficient of variation to be expected between aliquots. A summary of this information is given by Grant and Pelton (1973), whose reference list gives an introduction to the literature. A simple mathematical expression relating aliquot size to aliquot variability would be a very useful tool for estimating the appropriate aliquot size to achieve a specified or required precision. In addition, if a cost equation were available to relate cost per analysis to aliquot size, this could be used in conjunction with the above aliquot size variability equation to estimate the number and size of aliquots for specified costs and desired precision in the mean of a field sample.

In this section we begin by using the information from Figure 1 to estimate the relationship between aliquot size and variability for the particular location sampled at NS-201. This is then combined with a simple cost function to obtain estimates of the number and size of aliquots needed to achieve a desired precision for the mean Am concentration in a sample. Approximate results are also obtained for Pu by using the Pu/Am ratio believed to be appropriate for NS-201.

Also discussed is a procedure given by Cochran (1977, pp. 280-283) for estimating the optimum number of field samples and aliquots per field sample when suitable information on costs as well as between sample and within sample variable is available.

Results for Am

Consider Figure 2 which is a log-log plot of the observed standard deviations s (from Figure 1) versus the corresponding aliquot sizes w to which these values of s apply. The correlation between log s and log w is 0.96, and the estimated linear regression is

$$\widehat{\log s} = 0.20 - 0.46 \log w. \qquad (2)$$

Taking antilogarithms on both sides of Equation (2) gives

$$s = 1.58\, w^{-0.46}. \qquad (3)$$

We note that the theoretical equation given by Grant and Pelton (their Equation 4) can be expressed as

$$\log s = 0.5 \log f - 0.5 \log w, \qquad (4)$$

where f is a multiplicative function of the density, volume, and concentration of the particulate species of interest, and w is the aliquot weight. It is perhaps noteworthy that the last term of Equations 2 and 4 above are nearly identical.

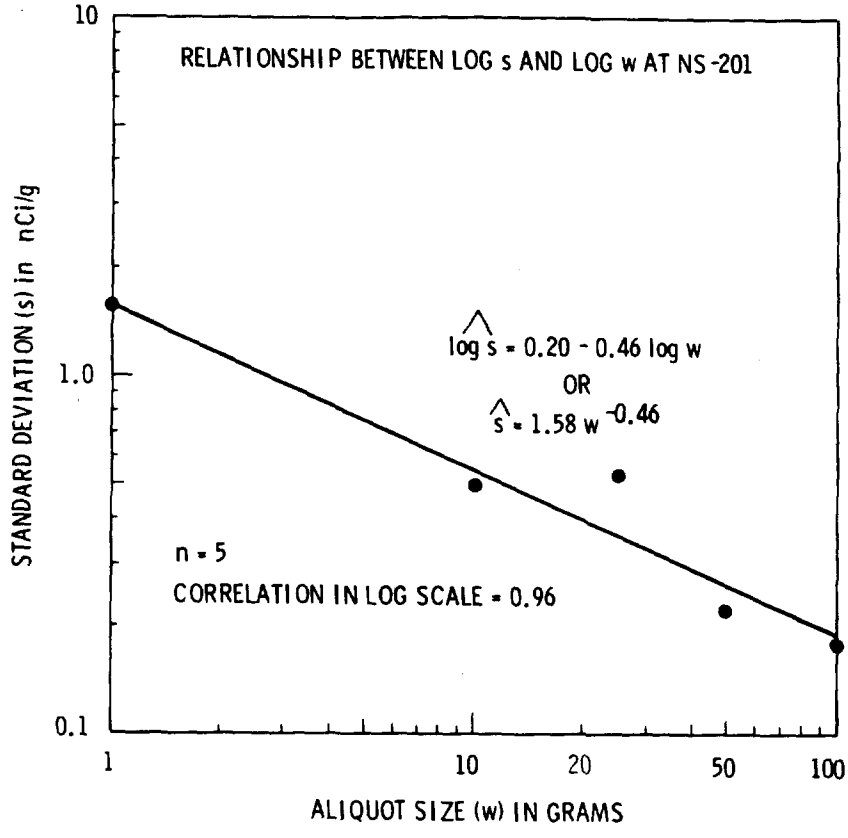

Figure 2. Estimated Relationship Between Log s and Log w for the Composite Soil Sample Collected Approximately 150 ft North of GZ at NS-201.

Suppose we want to estimate the mean Am concentration of a field sample by withdrawing n independent aliquots of a given size w. The variance V_A of the resulting $\bar{x}$ is s^2/n. Hence, using Equation (3) we obtain

$$V_A = 2.5/nw^{0.92}. \quad (5)$$

Now, consider the cost of counting an aliquot of soil for Am on a Ge(Li) system. Let us assume that a counting laboratory will charge the same rate, of, say, K dollars per aliquot, for any aliquot size that can be counted without special counting procedures. Thus, we assume that the total Am Ge(Li) analysis cost (C) for n aliquots from a field sample does not depend on w. That is, C = nK or

$$n = C/K . \quad (6)$$

Substituting Equation (6) in Equation (5) yields

$$w = (2.5\ K/CV_A)^{1.09} . \qquad (7)$$

Hence, for a specified ratio of costs K/C and a given (desired) precision (V_A) of $\bar{x}$, Equation (7) may be solved to yield the required aliquot size w. The number n of aliquots of size w is easily obtained from Equation (6). Note that this approach does not take into account the need to decide on the number of field samples to collect. This is discussed in a later section.

To illustrate the use of Equation 7, suppose K = \$25 per aliquot, C = \$150, and V_A = 0.01. Then Equations (6) and (7) give n = 6 and w = 58.3 ≃ 60 g. Alternatively, if we can afford only one aliquot per sample, i.e., suppose K = C = \$25, then w = 410.9 ≃ 400 g. This illustrates that as the number of aliquots (n) decreases, the aliquot size (w) must increase if the precision level V_A is held constant. To see this, we note from Equation (7) that $w = (2.5/nV_A)^{1.09}$ Also, for a given (desired) precision V_A, the total analysis cost per sample (C) will be minimized when n = 1, in which case $w = (2.5/s^2)^{1.09}$. Conversely, if costs C and K are fixed, then V_A will be minimized by using the largest possible aliquot size. This can be seen by expressing Equation (5) as

$$V_A = 2.5\ K/Cw^{0.92}. \qquad (8)$$

Figure 3 gives values of V_A for w between 1 and 100 g using Equation (8) for the two cost situations of C = K and C/K = 4, i.e., for n = 1 and 4, respectively. For either situation, V_A decreases very rapidly for w between 1 and 25.

Results for Pu

Now we consider determining aliquot size and number of aliquots for Pu analyses. The average (median) Pu to Am ration at NS-201 was estimated by Gilbert *et al.* (1977) to be 11.2. By considering 11.2 to be free of error, we obtain Var(Pu) ≃ $(11.2)^2$ Var(Am). Taking the square root of both sides of this equation yields s(Pu) ≃ 11.2 s(Am), where s( ) denotes the standard deviation of the quantity in parentheses. Multiplying Equation (3) by 11.2 gives

$$s(Pu) \simeq 17.7\ w^{-0.46}. \qquad (9)$$

Hence, the variance of the mean Pu concentration (V_p) based on n aliquots of size w is approximately

$$V_p \simeq [s(Pu)]^2/n \simeq 313/nw^{0.92}. \qquad (10)$$

To simplify results below, we use the theoretical value of -0.50 obtained by Grant and Pelton (1973) rather than the -0.46 in Equation 9. This gives

$$V_p \simeq 313/nw . \qquad (11)$$

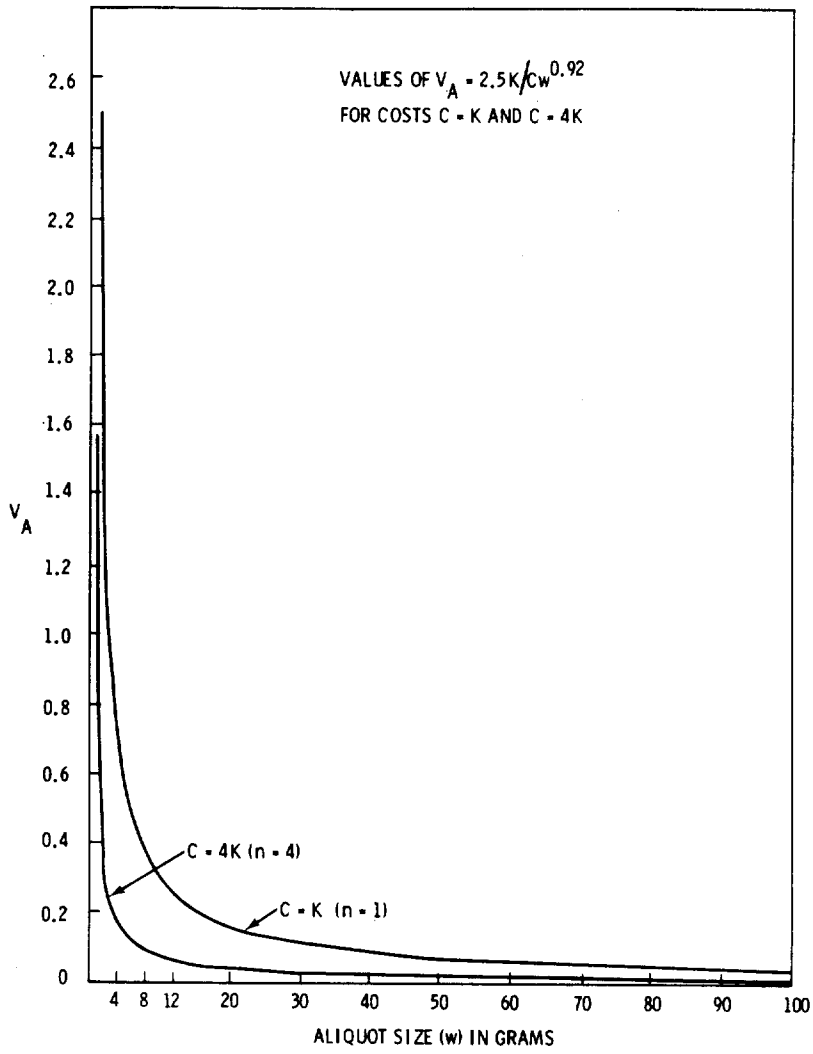

Figure 3. Estimated Values of the Variance of Average Am Ge(Li) Scans as a Function of Aliquot Size for a Composite Soil Sample Collected Approximately 150 ft North of GZ at NS-201.

The cost equation relating the cost in dollars for Pu wet chemistry analysis of n aliquots of size w is assumed here to be given by

$$C = n(83 + 1.8\ w). \qquad (12)$$

This gives a range in cost per aliquot of from \$85 to \$263 for aliquots between 1 and 100 g. Solving Equation 12 for n gives

$$n = C/(83 + 1.8\ w). \tag{13}$$

Hence, using Equation 11,

$$V_{\bar{p}} \simeq \frac{26000}{Cw} + \frac{563}{C}\ . \tag{14}$$

From Equation 14 we find that

$$w \simeq 26000/V_{\bar{p}}C - 563). \tag{15}$$

Hence, if both $V_{\bar{p}}$ and C are specified, where $V_{\bar{p}}C > 563$, Equation 15 may be solved for w. This may then be substituted in Equation 13 to obtain n.

As an example, suppose our budget allows \$200 per field sample for Pu analysis and we require $V_{\bar{p}}$, the variance of $\bar{x}$, to be no more than 100. Then $V_{\bar{p}}C = 20{,}000$ and Equation 15 gives $w = 1.4$. Using this value for w in Equation (13) we find $n = 2.3$. Hence, for C = \$200 and $V_{\bar{p}} = 100$ we should analyze two aliquots, each weighing 2 g. Equation 12 indicates this would cost \$173 per sample.

We note from Equation 14 that $V_{\bar{p}}$ will attain its minimum value of 563/C when w is infinitely large. $V_{\bar{p}}$ can be made as close to its minimum value as desired by choosing w sufficiently large. Figure 4 is a plot of $V_{\bar{p}}$ computed using Equation 14 for C = \$100 and \$200. The curves for $V_{\bar{p}}$ drop off rapidly for w between 1 and 10 g then decrease more gradually for w greater than about 10. For each value of w, the corresponding n may be computed using Equation 13.

It is clear from Figures 3 and 4 that there is little to be gained by using aliquots larger than about, say, 20 g. However, further studies should be conducted under a variety of contamination levels, sources, and environmental factors to determine the generality of our results. It is likely, for example, that the regression relationship (log s versus log w, Equation 2) is site specific, and of course, Equation 2 is based on only five data points.

In Appendix B we derive general analogs of Equations 7, 8, 14, and 15. These may be used to estimate w and n for variability and cost functions of the form $s = aw^{-b}$ and $C = n(\alpha + \beta w)$, i.e., for any values of a, b, α, and β that may be applicable in a given situation.

Optimum Allocation of Numbers of Field Samples and Aliquots

The above sections do not address directly how to determine the optimum number of field samples in relation to the number of aliquots per field sample. An approach to this problem is given by Cochran (1977, pp. 280-283).

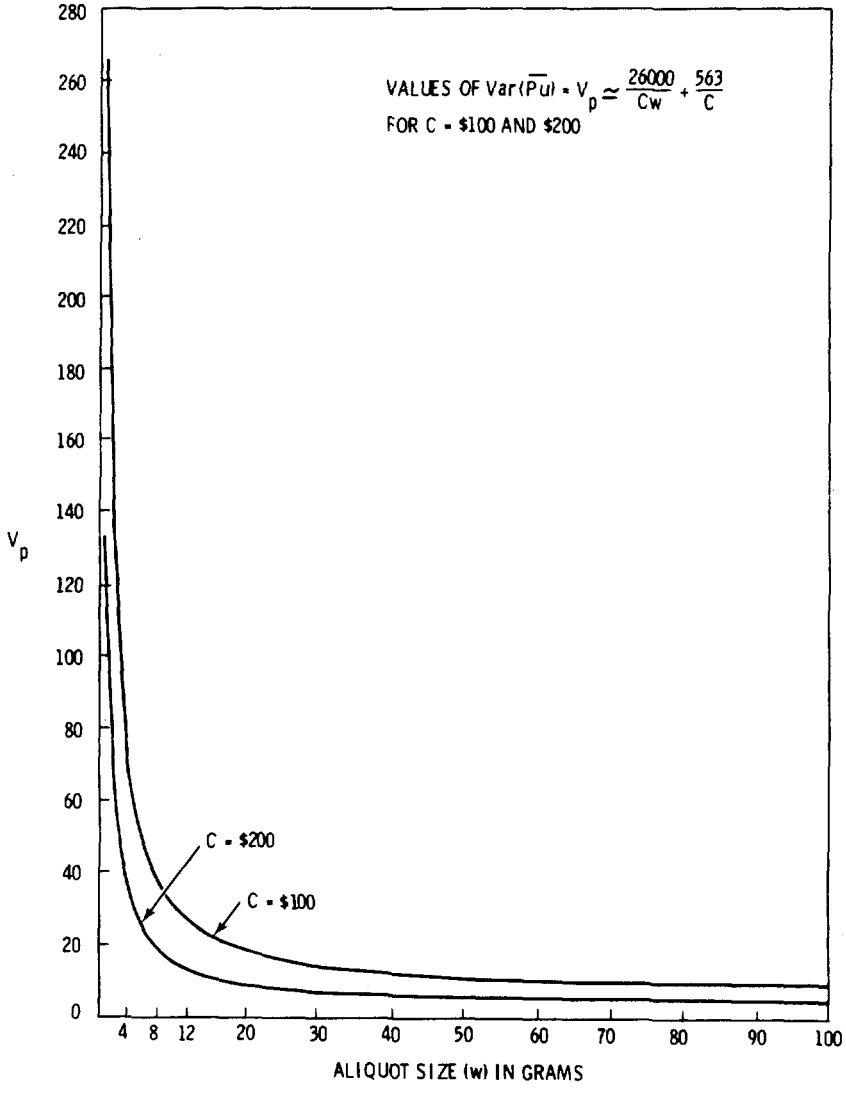

Figure 4. Approximate Values of the Variance of Average Pu Concentrations as a Function of Aliquot Size for a Composite Soil Sample Collected Approximately 150 ft North of GZ at NS-201.

Suppose the purpose of the study is to estimate the average Am concentration over a defined area by randomly choosing n' soil samples from the area and analyzing n aliquots randomly drawn from each soil sample. Under the assumption of a simple cost function, Cochran finds the optimum number of aliquots per field sample to be given by the equation (in our notation)

$$n_{opt} = \sqrt{\frac{s^2}{s_1^2} \cdot \frac{c_1}{K}} \ ,$$

where s_1^2 is the variance between different sampling locations in the field, s^2 is the variance between aliquots from the same field sample, c_1 is the sampling cost per field sample, and K is the cost per aliquot. From Equation 3 we suppose $s^2 = 2.5\ w^{-0.92}$. Hence,

$$n_{opt} = \sqrt{\frac{2.5}{s_1^2\ w^{0.92}} \cdot \frac{c_1}{K}}$$

Consequently, if we know the ratio of costs c_1/K and have an estimate of s_1^2 from previous studies, then the above equation for n_{opt} may be solved for different values of w. It's clear that n_{opt} decreases as aliquot weight increases. Once n_{opt} has been chosen, the optimum value of n' (number of different field samples) may be obtained by solving Cochran's cost equation (if the total study budget is considered fixed) or the appropriate variance equation (if the study must be designed to achieve a specified precision of the mean over all sample locations). The cost equation is given by Cochran (1977) on page 280. His Equation 10.15 (p. 278) gives the approximate variance equation.

If interest centers on estimating the average Pu concentration for the sampled area, then, making use of Equation 9 we find that for NS-201

$$n_{opt} \simeq \sqrt{\frac{313}{s_1^2\ w} \cdot \frac{c_1}{83 + 1.8\ w}} \ .$$

Specifying s_1^2 and c_1 will allow us to choose an appropriate n by examining the solution of n_{opt} for different values of w. Note that s_1^2 is now the variance of Pu concentrations between field sample locations. As was the case for Am discussed above, n' may be obtained by solving Cochran's cost or variance equation depending on whether cost or the variance of the overall area mean has been preassigned.

EFFECTS OF CHANGING ALIQUOT SIZE ON MEDIANS AND GEOMETRIC MEANS

We have seen from Figure 1 that the median and geometric mean Am concentrations tend to increase with increasing aliquot size. Based on arguments by Michels (1977), we believe that this is not due to chance.

Michels considers a hypothetical, large environmental air sample that has some true average arithemtic mean (expected value) concentration. He supposes that this sample is subsampled using aliquots of different volumes V_1 and V_2, where $V_2 > V_1$. If the concentrations resulting from the use of both aliquot sizes are lognormally distributed, Michels shows that the ratio of the true geometric means for aliquot volumes V_2 and V_1 is

$$\frac{GM_2}{GM_1} = \frac{\exp\ [\pm 0.5\sigma^2/V_1]}{\exp\ [0.5(\sigma^2/(V_2/V_1)]}\ , \qquad (16)$$

where σ^2 is the true variance of the logarithms for aliquots of volume V_1. Note that this ratio is necessarily greater than 1. Michels makes the point that this ratio can be substantially greater than 1 when σ is greater than 2 or 3 and V_2/V_1 is greater than 5. He also makes use of the Poisson distribution to give guidance on assessing the number of Pu particles that must be present for Equation 16 to be near 1.

In Table 4 we have computed the ratio of Am geometric means for the five aliquot sizes (data from Figure 1). In all but one case the ratio is greater than 1. The largest ratio is 1.157 for $GM_{100\ g}/GM_{1\ g}$, i.e., GM_{100g} is about 16% larger than GM_{1g}. Essentially the same results are obtained using the sample medians rather than geometric means. Since the arithmetic mean is not systematically biased in this way by aliquot size, it is the preferred estimate of central tendency for comparing "average" results from studies that have used different aliquot sizes.

Table 4. Ratio of Observed Geometric Means of Am for Aliquots of Different Sizes Using Data From Figure 1

Aliquot Size (g)	1	10	25	50
10	1.072			
25	1.042	0.972		
50	1.102	1.028	1.058	
100	1.157	1.079	1.110	1.049

Michels restricts his discussion to the lognormal distribution. However, the phenomenon of increasing medians and geometric means with increasing aliquot size is also applicable for other skewed distributions. The essential ingredients are that the distribution for each aliquot size be unimodal and skewed toward high values. Also, this skewness must decrease with increasing aliquot size. The geometric mean (or median) is always less than the true mean (expected value) of a distribution that is skewed to the right. As the aliquot sizes increases and the distribution of aliquot concentrations becomes less skewed (more symmetric), the true geometric mean and median must approach in value the true mean of the distribution. This occurs since the mean and median are identical in value for a completely symmetric distribution.

The effect of skewness on geometric means and medians is illustrated in Figure 5 where we have plotted the density functions of lognormal distributions with parameters μ and σ as estimated from the experimental

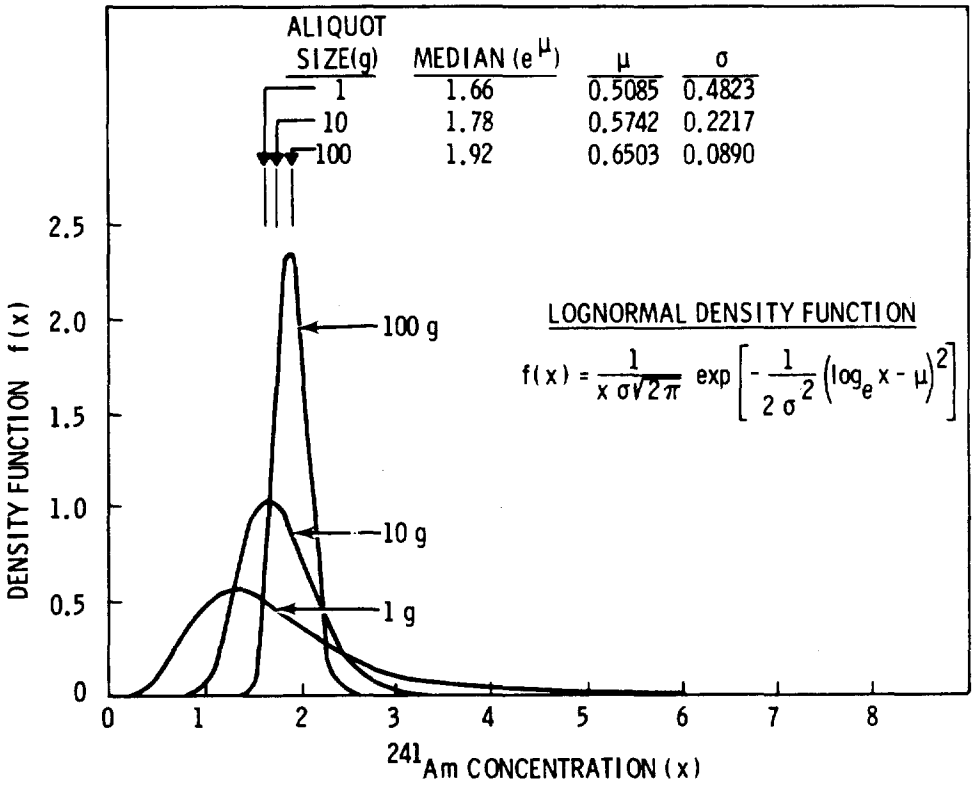

Figure 5. Density Functions of 1, 10, and 100 g Aliquots Assuming the Observed Data (Figure 1) are Lognormally Distributed with Parameters μ and σ as Estimated from the Data.

results* for aliquot sizes of 1, 10, and 100 g. The median and mean of a lognormal distribution are given by $\exp(\mu)$ and $\exp(\mu + \sigma^2/2)$, respectively. We see from Figure 5 that the estimates of μ increase while those of σ decrease as aliquot size increases. Hence, as $\hat{\mu}$ increases from 0.5085 to 0.6503, the median necessarily increases from 1.66 to 1.92. However, the mean remains relatively constant at 1.87, 1.82, and 1.92 for 1-, 10-, and 100-g aliquots, respectively, due to the decrease in $\hat{\sigma}$ for the larger aliquot sizes. Indeed, as σ approaches zero the lognormal distribution approaches the symmetric normal distribution for which the mean and median are identical. The above remarks for the

*μ and σ are estimated as the mean and standard deviation of the $\log_e$- transformed data.

median also apply to the geometric mean since for the lognormal distribution the estimated geometric mean is identical to the estimated median, i.e., $\exp(\hat{\mu})$.

CONCLUSIONS FOR ALIQUOT SIZE STUDY

The variability with aliquot size study illustrates a number of features that should be considered at the design stages of an environmental study. The choice of aliquot size has been shown in this study to influence aliquot to aliquot variability as well as the expected value of the median and geometric mean. Between-aliquot variability was quite drastically reduced by using 100-g rather than 1- or 10-g aliquots. This implies a larger number of 1-g aliquots are required to estimate the true concentration of each field sample with specified accuracy and precision than would be the case if 25-, 50-, or 100-g aliquots were used.

The shape of the distribution of aliquot concentrations, as determined by μ and σ, was observed to depend on aliquot size. This change in μ and σ is responsible for changes in the median and geometric mean with aliquot size. Aliquot size did not, however, have a systematic effect on the arithmetic mean. The rationale for these conclusions are illustrated for the lognormal distribution.

The relative stability $\exp(\mu + \sigma^2/2)$ suggests the arithmetic mean is preferred over the geometric mean and median for comparing studies that have used different aliquot sizes or other sampling techniques that tend to change the underlying skewed distribution shape of the data.

A linear regression between the logarithms of aliquot standard deviation and aliquot size was found to fit the data. This was combined with cost functions to obtain an expression for the variance of the mean concentration as a function of analysis cost (or equivalently, the number of aliquots) and aliquot size. This variance expression decreases rapidly as aliquot size increases from 1 to 10 g. The rate of decline is much slower for aliquot sizes greater than 10 g.

The question of determining the optimum number of field samples and number of aliquots per field sample is also discussed. A method by Cochran (1977) was cited that takes into account costs of collecting samples and analyzing aliquots.

VARIABILITY WITH DISTANCE STUDY

MOTIVATION AND BASIC CONCEPTS

The purpose of this study was to obtain data that would be useful in determining the variogram (correlation structure) for Am concentrations

at various distances. This type of information is needed in our evaluation of kriging as a technique for estimating Pu and Am spatial distribution and inventory in soil in NTS. Delfiner and Gilbert (1978) use kriging to estimate average Pu concentrations and inventory in soil for unit areas of size 100- x 100-ft at the Area 13 (Project 57) site on NTS. Barnes *et al.* (1977) discuss some basic concepts of kriging and illustrate the technique using Area 13 data.

An advantage of kriging over other moving average methods is that it gives the "proper" weight to spatial observations to estimate a concentration at a nonsampled location (see Figure 6). "Proper" has to be qualified; it means optimum if the correlation structure (called the variograms) of the data is known with some assurance.

The variogram is the basis of kriging. It expresses the variability of the difference of two observations as a function of their distance from each other. Referring to Figure 6, let the concentration at each dot be given by a random variable Z(x), where x represents the location of the point and Z(x) the concentrations at point x. When there are no trends or "drift" in concentrations over distance, the experimental (estimated variogram) is computed using

$$\hat{\gamma}(h) = \frac{1}{2N_h} \sum_{i=1}^{N_h} \pm Z(x + h) - Z(x)1^2 , \qquad (17)$$

where h is the distance between two points and N_h is the number of pairs of observations that are distance h apart. At each distance h, $\hat{\gamma}(h)$ is the average squared difference between two observations. Therefore, $\hat{\gamma}(h)$ is a measure of variability between two observations as a function of their distance h from each other.

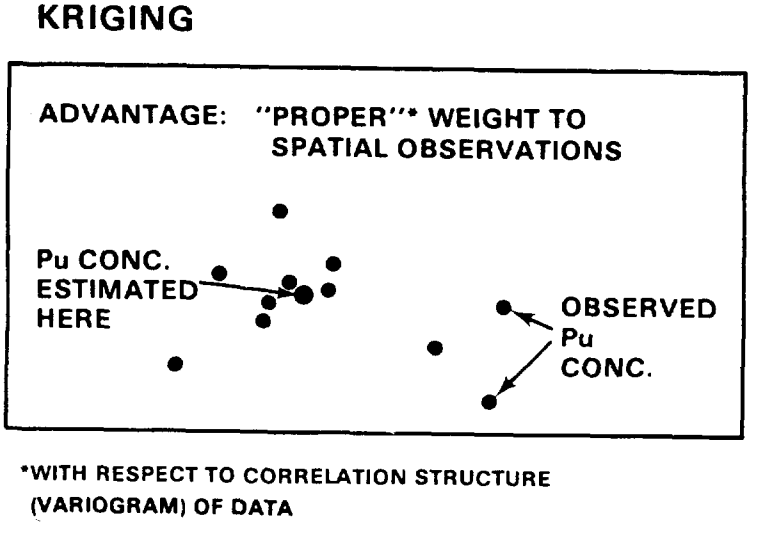

Figure 6. Estimation of Concentration at a Nonsampled Location Using Kriging.

Some possible theoretical variograms are shown in Figure 7 (from Barnes *et al.*, 1977). The horizontal axis represents distance h and the vertical axis the value of the variogram $\gamma(h)$. The variogram in Figure 7(a) is zero at h=0, increases, and then levels off. The point where it levels off, denoted h_0, is the range; its interpretation is, that after distance h_0, the concentrations are no longer related (correlated). The value $\gamma(h_0)$ is called the "sill" and is the variance of the (independent) variables greater than distance h_0 apart. Figure 7(b) represents a variogram that increases proportional to the distance. This implies that the observations Z(x) and Z(x + h) are related no matter how large the distance h. This is hardly realistic in practice. Figure 7(c) illustrates a type of variogram that appears to be common in radionuclide field studies; $\gamma(h)$ is discontinuous at 0. A variogram must be 0 at h=0 since Z(x) - Z(x) = 0. But Figure 7(c) shows a case where no matter how close two points become, there is still some variability left. The discontinuity of the variogram at h=0 is called the "nugget effect."

Finally, Figure 7(d) represents a flat variogram, or pure nugget, meaning the variables appear to be independent regardless of their proximity. As we shall see, variograms of the soil and FIDLER data collected here exhibit some of the features of types a, c, and d.

STUDY DESIGN AND RESULTS

The data in this study were taken along two transects, one near GZ and the other 3,600 ft north of GZ at the Area 13 site. The approximate location of the two lines is given in Figure 8. Note that Line 1 (near GZ) crosses several activity level strata, while Line 2 is contained in one of the lowest-level Am strata. The data consists of both surface soil samples analyzed for Am by Ge(Li) counting and FIDLER Am readings in counts per minute. For Line 1, three sets of FIDLER readings and four adjacent ring samples (5-in. diameter and 5-cm deep) were taken every 20 ft. For Line 2, the interval was every 150 ft. There were a total of 15 such clusters of data for each line, spanning about 280 and 2,100 ft for Lines 1 and 2, respectively.

The three sets of FIDLER measurements consisted of (1) readings with the instrument placed directly on the ring, (2) readings made with the instrument held 1 ft above the ring, and (3) readings taken at the center of the four samples at 1-ft height. Two 70-g aliquots per ring sample were counted using REECo's Ge(Li) system, giving a total of 120 soil concentrations per line.

At a later time, 100 adjacent FIDLER readings, both surface and 1-ft height, were taken at 5-in. intervals 10 ft south of both lines. The purpose was to obtain information on the changes in activity occurring on a scale of less than 40 ft. The complete field sampling and laboratory protocol for this study is given in Appendix C.

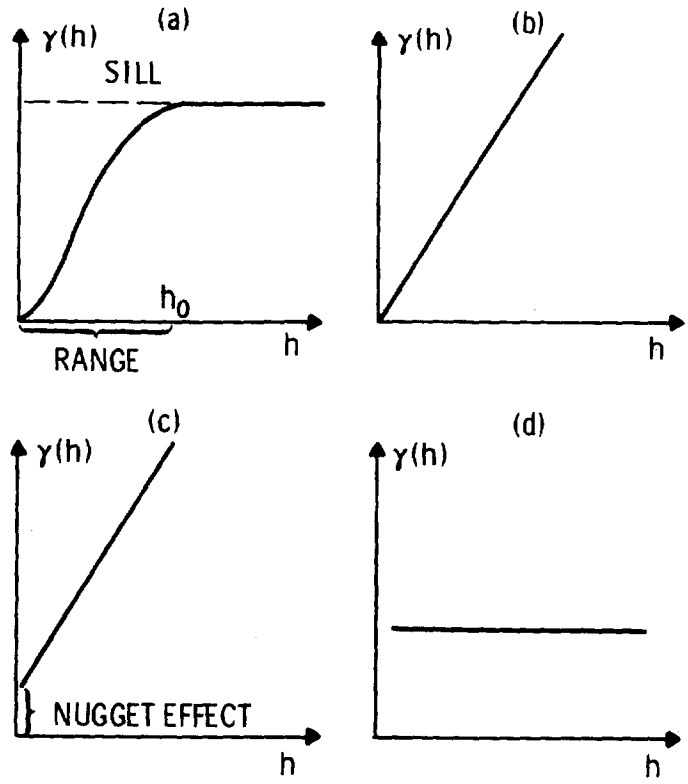

Figure 7. Theoretical Variograms.

AREA 13 — PROJECT 57

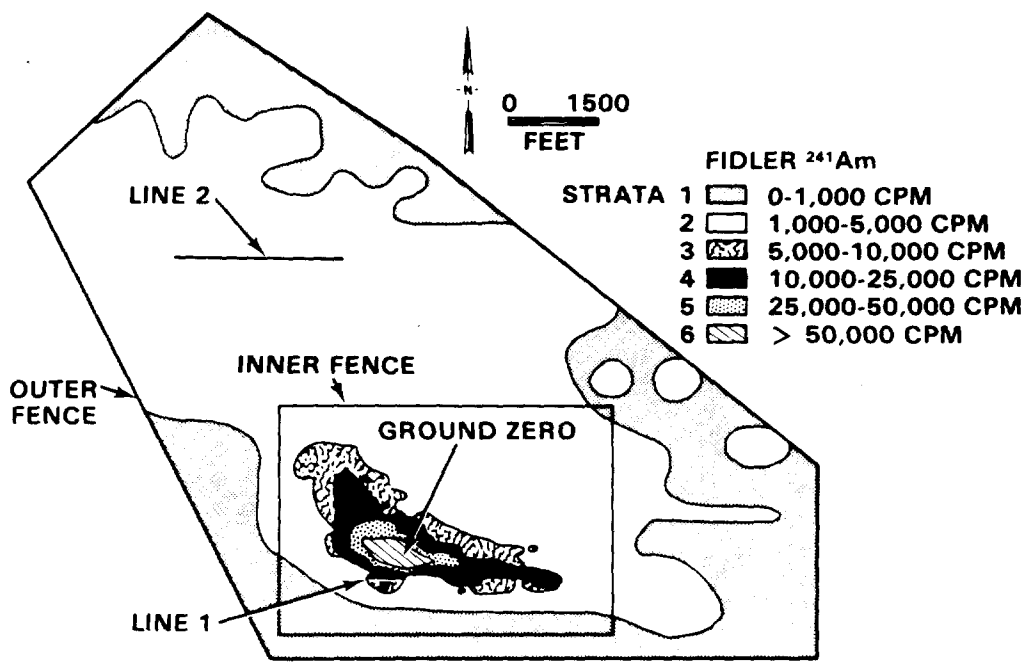

Figure 8. Locations of Lines 1 and 2.

Results for Line 1

The soil concentrations for Line 1 are given in Figure 9. The horizontal axis is distance along the line in feet and the vertical axis is Am concentrations (nCi/g dry soil). The mean of the two aliquots at each location is also plotted. The means in each cluster are connected by bold lines to give a better visual presentation of the variability with distance within a cluster. The ends of the vertical bars are the observed concentration for the two aliquots.

The concentration peak that occurs at about 140 ft corresponds to Line 1 crossing a higher activity level stratum. The clusters with the highest concentrations have the most variability, both among the four samples in a cluster and between the aliquots. The clusters past 220 ft tend to be reasonably constant. The greatest proportion (82%) of the total variance of these Am data is due to differences between clusters. Variation between adjacent samples within clusters accounts for 15%. The remaining variability (3% of the total) is accounted for by variability between the 70-g aliquots within each soil sample.

The estimated variogram for Line 1 soil samples, as computed using Equation 17, is given in Figure 10. Notice the peak at 120 ft. This occurs because of the peak in the data at that distance in Figure 9. This variogram is a biased estimate of the true underlying variogram that should be used for kriging purposes. This bias results from the strong trend (called "drift" in the kriging literature) in concentrations along the line evidenced by the peak kriging literature) in concentrations along the line evidenced by the peak at 140 ft. We have noted above that Equation 17 should not be used under these circumstances. Methods are available (Delfiner, 1975) for obtaining variograms that are free from the effects of drift. Delfiner and Gilbert (1978) discuss in greater detail the estimation of the variogram in the presence of a drift. Kriging could use unbiased estimates of the variogram to estimate average Am concentrations at unsampled locations along the line or over unit areas where the same correleation structure applied.

The net FIDLER readings for Line 1, both surface and 1-ft height, are given in Figure 11. The data plotted represent the mean of two readings. The solid line connects the means within a cluster for the 1-ft readings, while the dashed line connects the surface readings. The star is the 1-ft reading at the center of the cluster.

The 1-ft and center readings are generally higher than the surface readings, which is expected since the instrument held at 1-ft height receives input from a larger area (Tinney, 1968). Comparing Figures 9 and 11, soil concentrations and FIDLER readings show the same pattern of variability within clusters with a peak at 140 ft.

The estimated variograms for the FIDLER readings are given in Figure 12; the solid-line and dashed-line curves are the 1-ft height and surface

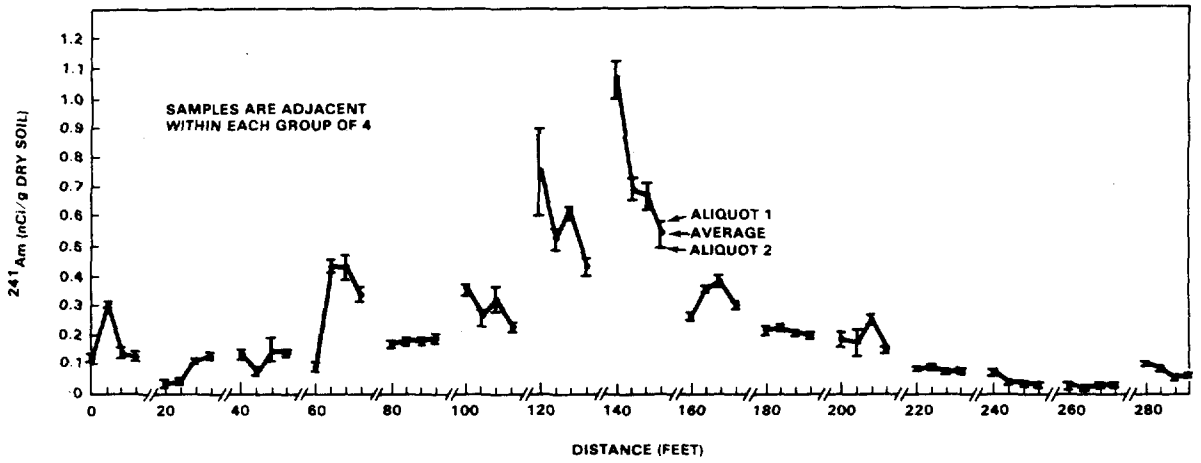

Figure 9. Concentrations of ^{241}Am (nCi/g dry) in 70-g Aliquots of Soil Along Line 1 in Area 13, Project 57.

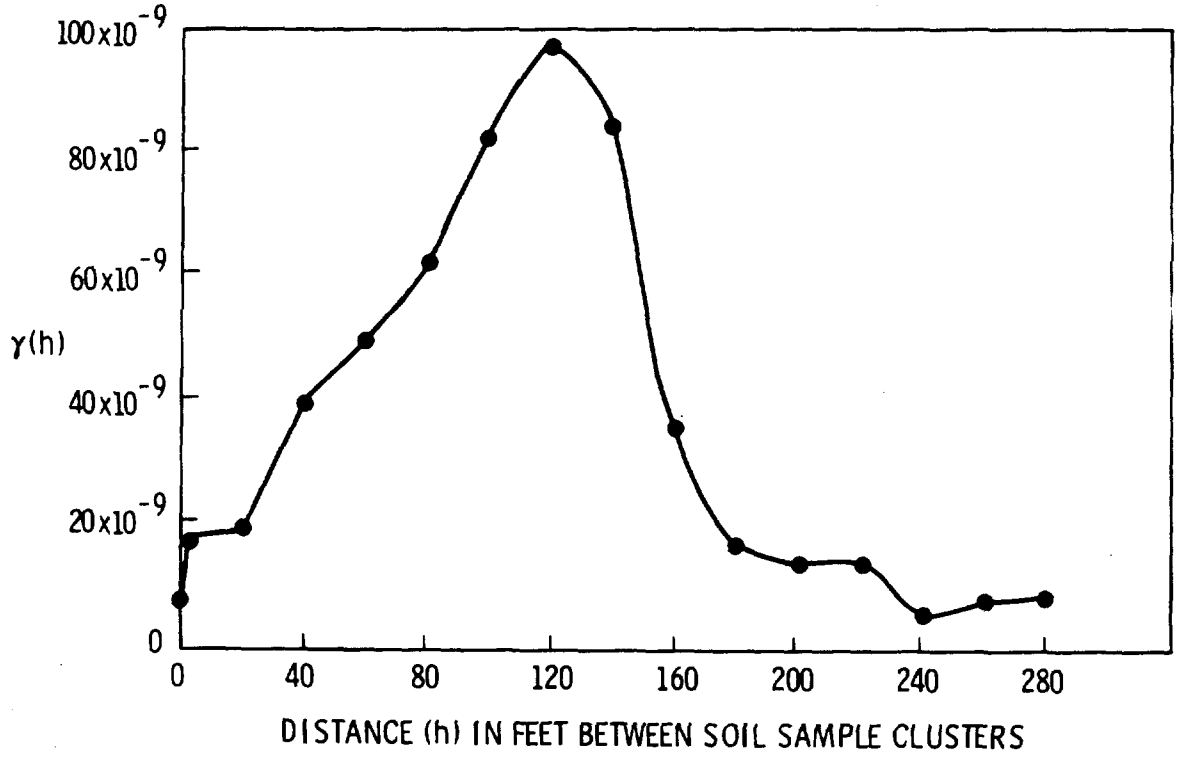

Figure 10. Estimated Raw Variogram of Line 1 ^{241}Am Concentrations.

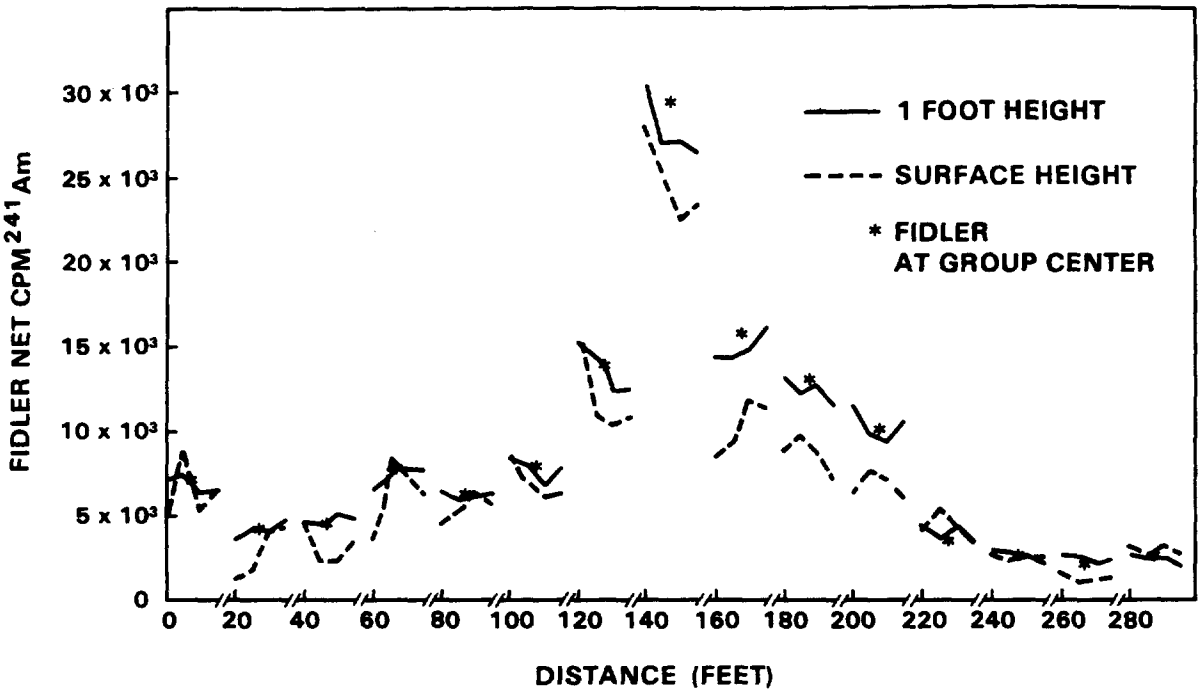

Figure 11. FIDLER Net CPM ^{241}Am Readings on Line 1 in Area 13, Project 57.

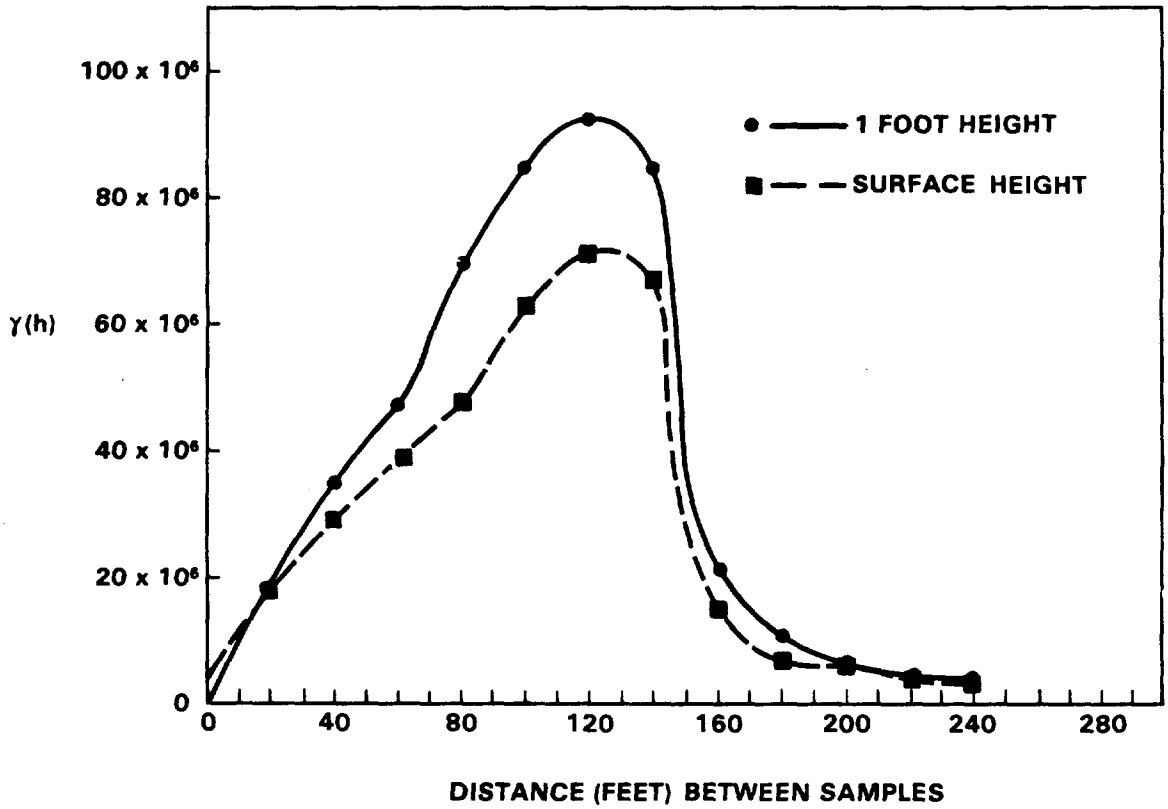

Figure 12. Estimated Raw Variograms or Line 1 FIDLER Data.

height variograms, respectively. These variograms, computed using Equation 17, follow the same pattern as the soil variogram (Figure 10) with a peak at about 140 ft. They are biased estimates of the true underlying variograms due to the presence of "drift." The two FIDLER variograms diverge as the trend in concentrations becomes strong, with the 1-ft readings showing more variability.

Since the spacing of the clusters for Line 1 was 20 ft, there is no information on the relationship between concentrations 20 in. to 20 ft apart. The 100 adjacent FIDLER readings taken 10 ft south of the lines cover 500 in. or 42 ft. This corresponds to the distance covered by the first two clusters from the original sampling plan. These readings are given in Figure 13, where each point plotted is the mean of two readings. The lower line connects the surface height readings and the upper line the 1-ft height readings. The two lines tend to follow each other, with 1-ft readings being almost always higher and smoother because the instrument is integrating over a larger soil surface.

The estimated variograms for the two sets of FIDLER readings along Line 1 are given in Figure 14. Consistent with the observed FIDLER readings, the 1-ft height variogram is lower and smoother than that of the surface readings. The 1-ft height variogram increases until the distance between readings is about 350 in. or 29 ft and then decreases. The number of data pairs for estimating the variogram at distances greater than 29 ft are relatively few, so these points have relatively poor precision. These data suggest there is a correlation structure among FIDLER readings at short distances.

The experimental variograms in Figure 14 were also computed using Equation 17. These variograms are probably not badly biased since the FIDLER data plotted in Figure 13 do not show evidence of strong systematic "drift" over the 42-ft distance. Notice that the "nugget effect" is greater for the surface than the 1-ft height, a reflection of the smaller variability between adjacent readings at the 1-ft height.

Results for Line 2

The soil concentration data for Line 2 are given in Figure 15. Note that these concentrations are in the pCi/g range, as opposed to the nCi/g range for Line 1. In comparison to Line 1 Am data, the variability between clusters along Line 2 accounts for a much smaller proportion of the total variance; 55 rather than 82%. The variability between adjacent samples and that between aliquots within samples account for 25 and 21%, respectively, of the total variability along Line 2. This contrasts with 15 and 3% for Line 1. Along Line 2, there is almost as much variability between aliquots as there is between adjacent samples. We note that this type of information can be used to estimate the optimum allocation of sampling effort for estimating average concentrations, i.e., for determining the optimum number of clusters, samples within clusters, and aliquots per sample for estimating the mean concentration

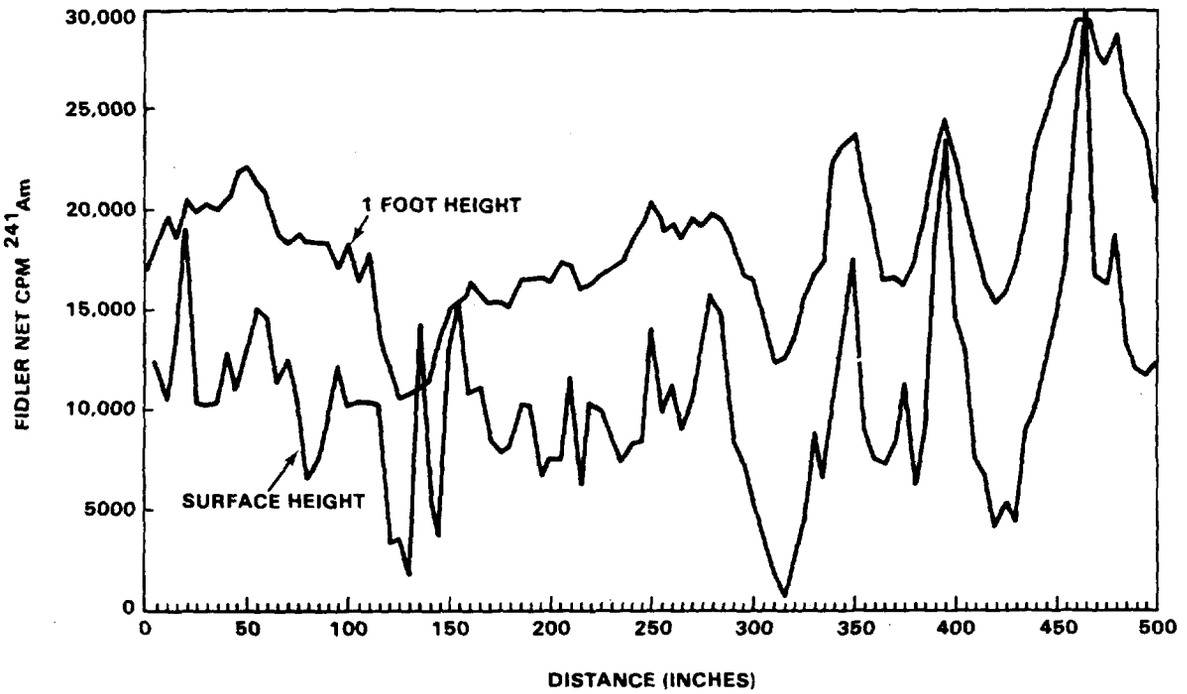

Figure 13. FIDLER Net CPM ^{241}Am (Average of Two Readings) at 5-in. Intervals Along Line 1 in Area 13, Project 57.

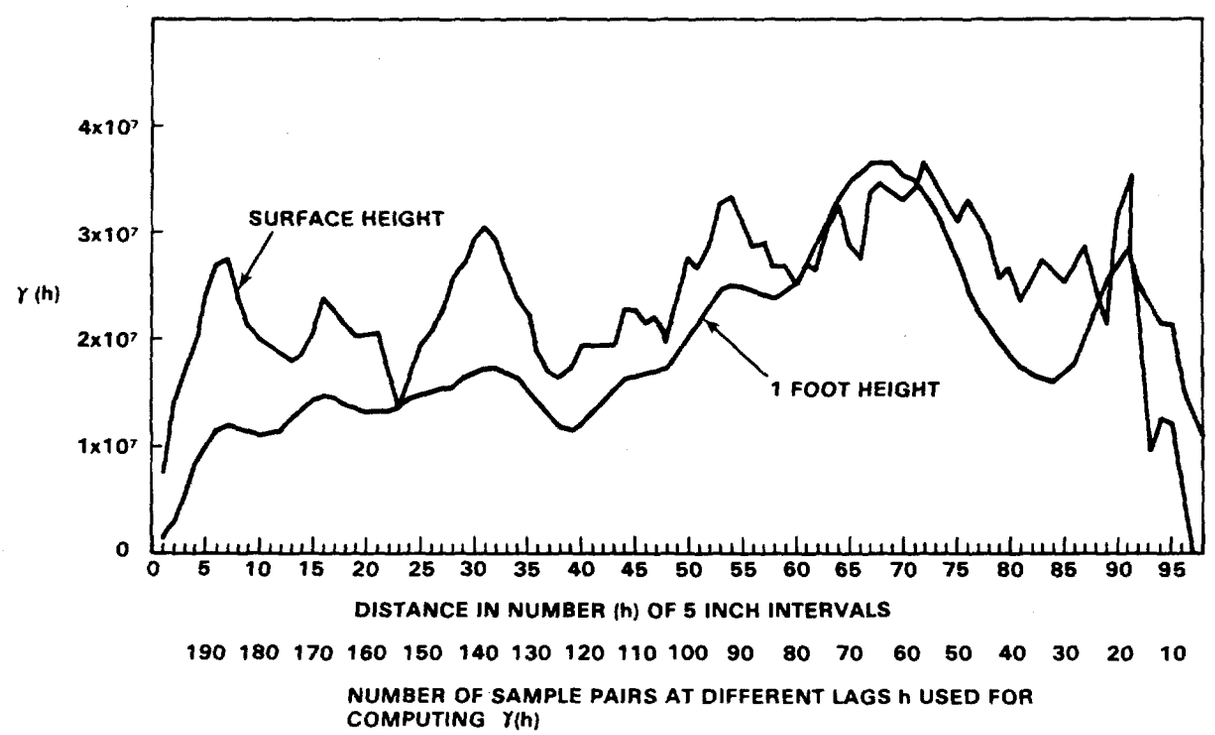

Figure 14. Variogram of Adjacent FIDLER Net CPM Am Readings Along Line 1 in Area 13, Project 57.

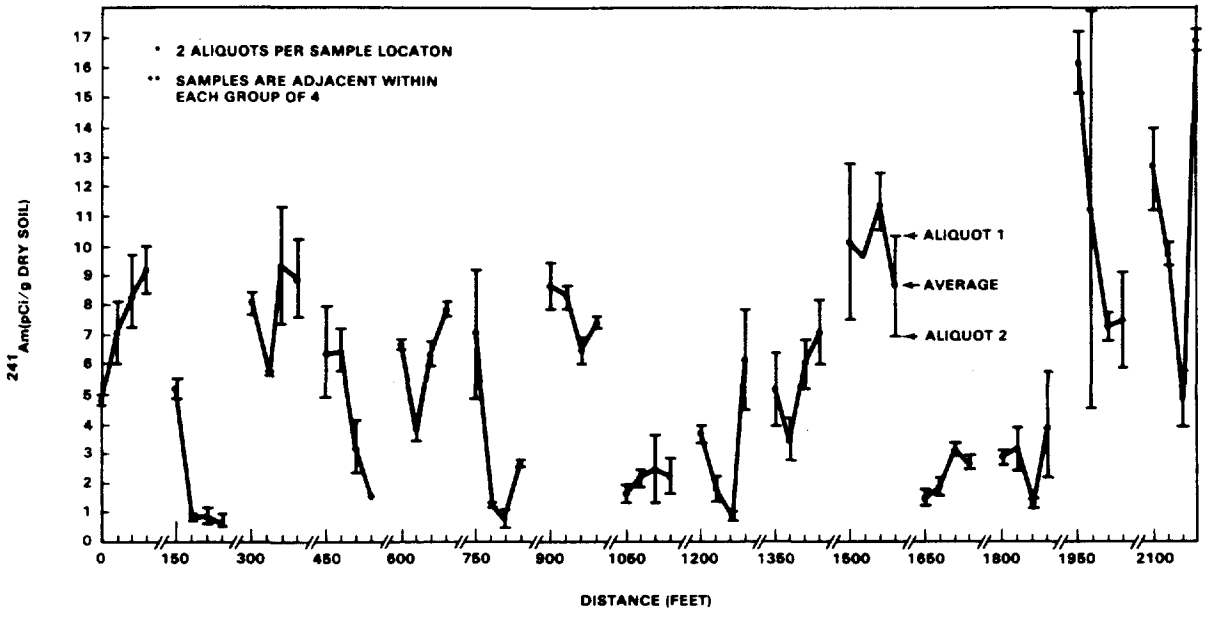

Figure 15. Average* Concentrations of ^{241}Am (pCi/g dry) in 70 g Aliquots of Soil Along Line 2** in Area 13, Project 57.

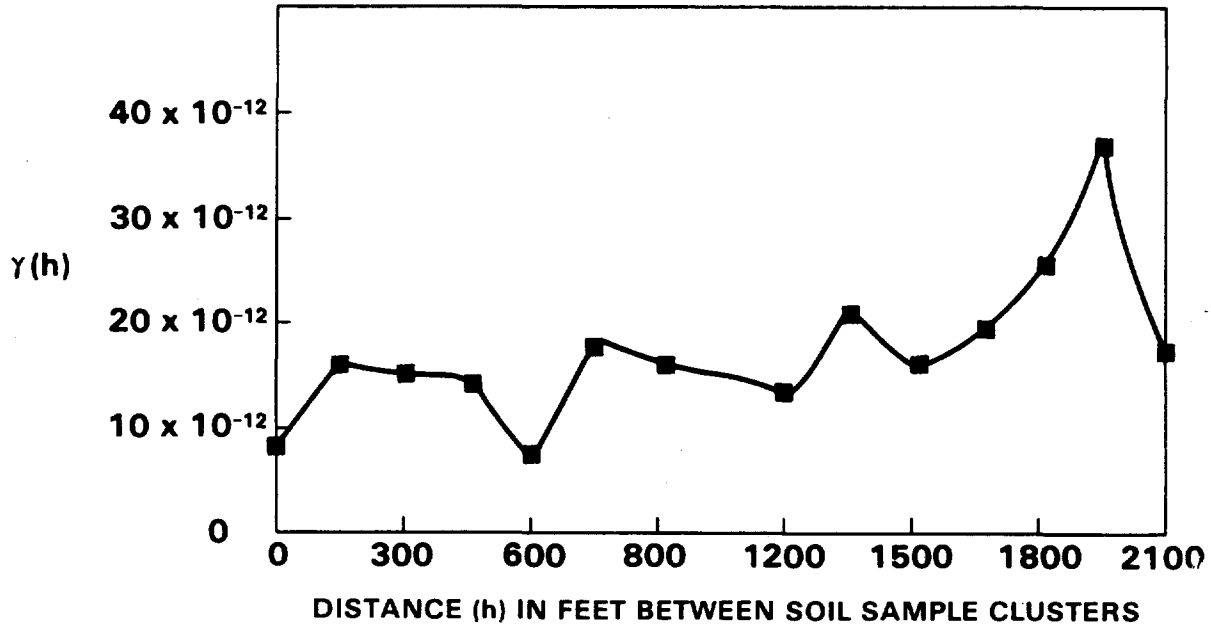

Figure 16. Estimated Raw Variogram of Line 2 ^{241}Am Concentrations.

with greatest precision (smallest variance). This optimum allocation would be different for Line 1 and Line 2. This allocation could be estimated using the general approach given by Cochran (1977) as discussed above for the aliquot study.

The variogram for the soil data of Line 2 is given in Figure 16. The values for $\hat{\gamma}(h)$ for 5-, 10-, and 15-inch spacings are 6.4×10^{-12}, 8.9×10^{-12}, and 7.5×10^{-12}, respectively. These data are about half the value observed for 150 ft (see Figure 16), which suggest the real increase in $\gamma(h)$ between 15 inches and 150 ft. However, no data are available to assess the form of the curve between those points. The form of the $\hat{\gamma}(h)$ curve beyond 150 ft suggests little if any correlation between Am concentrations spaced greater than 150 ft.

The FIDLER readings corresponding to the soil samples for Line 2 are given in Figure 17. The same absence of pattern seen in the soil data is seen here. Note that a high percentage of the surface readings are at background levels.

The estimated variograms for both sets of FIDLER readings are given in Figure 18. With the possible exception of a within-cluster (spacings less than 15 inches) structure at the 1-ft height, the readings appear to be uncorrelated.

The 100 adjacent FIDLER readings were taken 10 ft south of Line 2, for a distance of 42 ft, which corresponds to only the first cluster of observations from the original sampling plan. The readings are given in Figure 19. The 1-ft height readings are uniformly higher than the surface reading; but unlike the Line 1 adjacent FIDLER data, the 1-ft height readings are slightly more variable than the surface readings. This is evident by examining the variograms for the adjacent FIDLER readings in Figure 20. The variograms are essentially flat, with the 1-ft height variogram being slightly above the surface height variogram. This latter point indicates slightly greater variability for the 1-ft data. The flatness of these variograms suggest there is no correlation structure between FIDLER readings along Line 2 no matter how close the readings are taken. This is probably a function of the Am activity being at near background levels.

CONCLUSION FOR VARIABILITY WITH DISTANCE STUDY

For relatively high Am concentrations (nCi/g range), there appears to be a correlation between observations as a function of distance for FIDLER readings and possibly for the soil Ge(Li) analyses. For lower levels (pCi/g range), this does not appear to be the case. This suggests that in these low-level (pCi/g) areas, kriging may not be feasible using soil or FIDLER data as collected here since kriging depends on the existence of a correlation structure. However, for higher activity level areas within the inner fence in Area 13, Delfiner and Gilbert (1978) successfully use kriging on both FIDLER and soil data to estimate spatial distribution and inventory of Pu in soil.

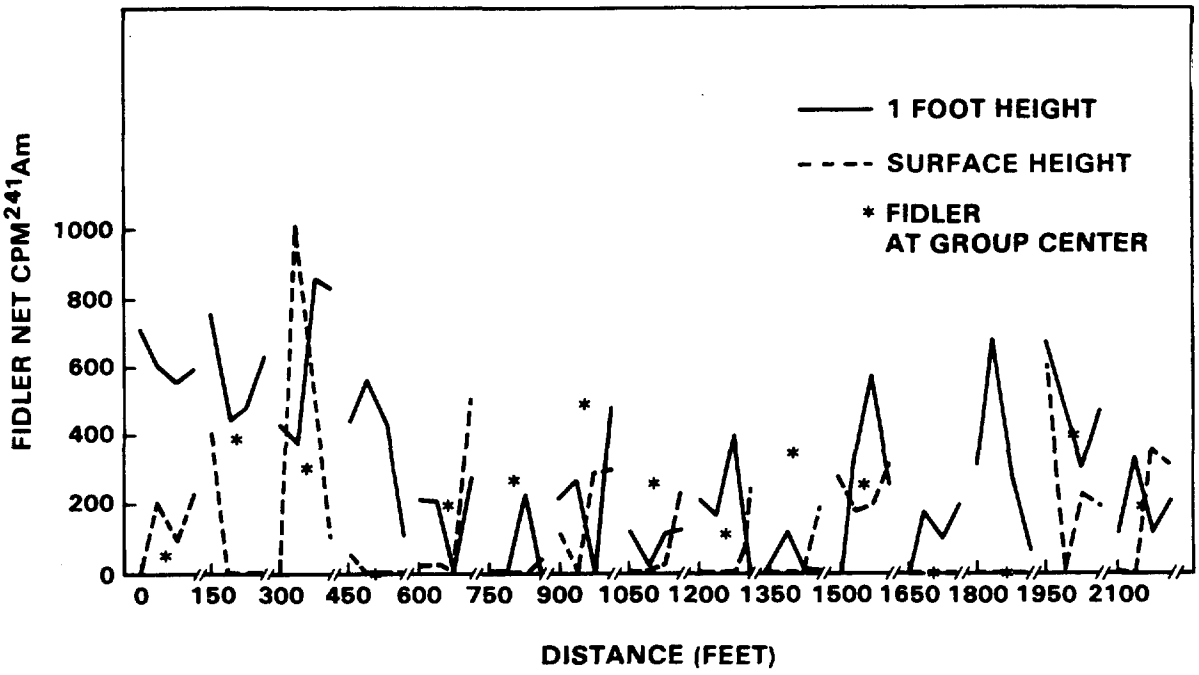

Figure 17. FIDLER Net CPM ^{241}Am Readings on Line 2 in Area 13, Project 57.

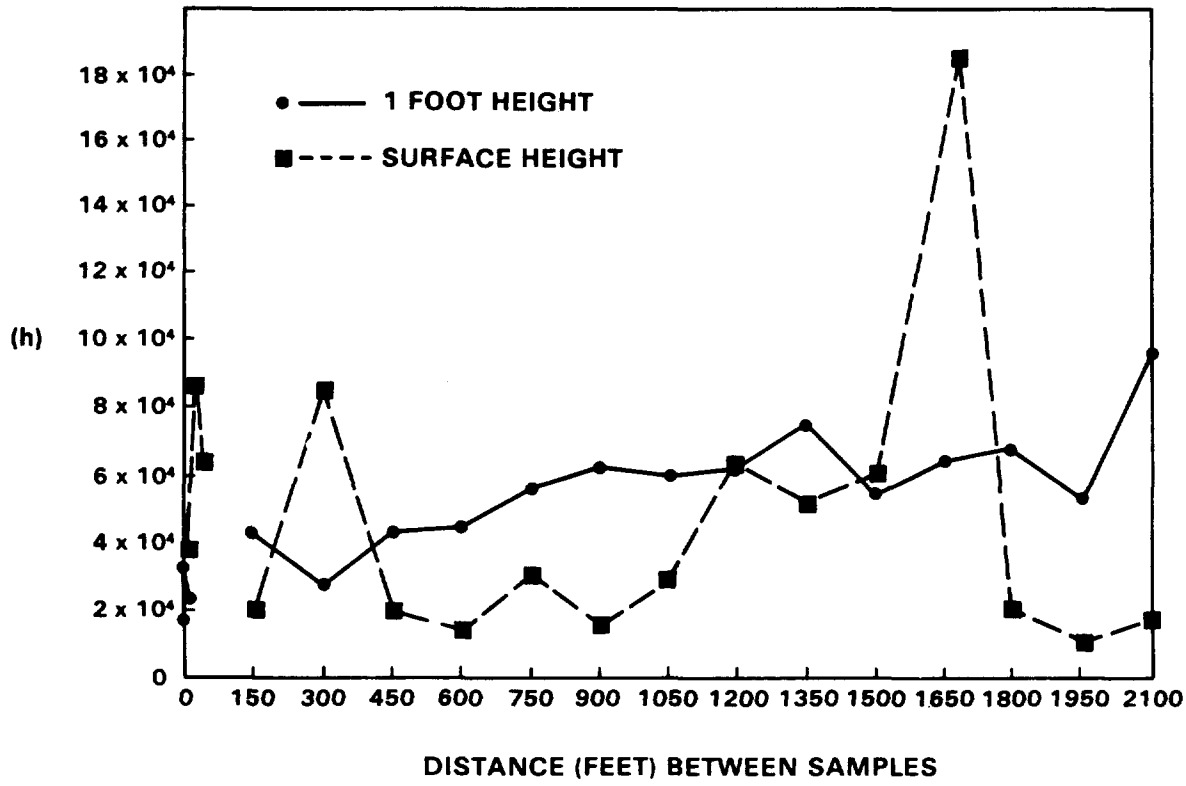

Figure 18. Estimated Raw Variograms of Line 2 FIDLER Data.

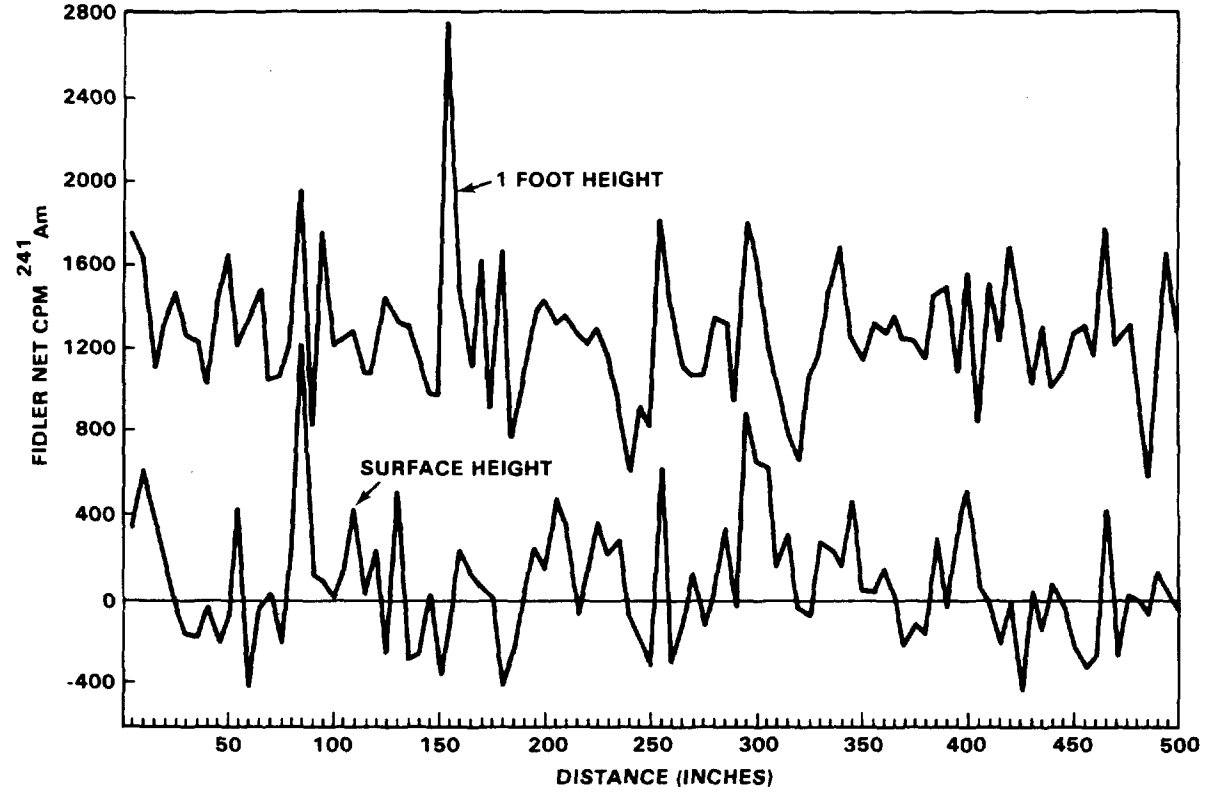

Figure 19. FIDLER Net CPM ^{241}Am (Average of Two Readings) at 5-in. Intervals Along Line 2 in Area 13, Project 57.

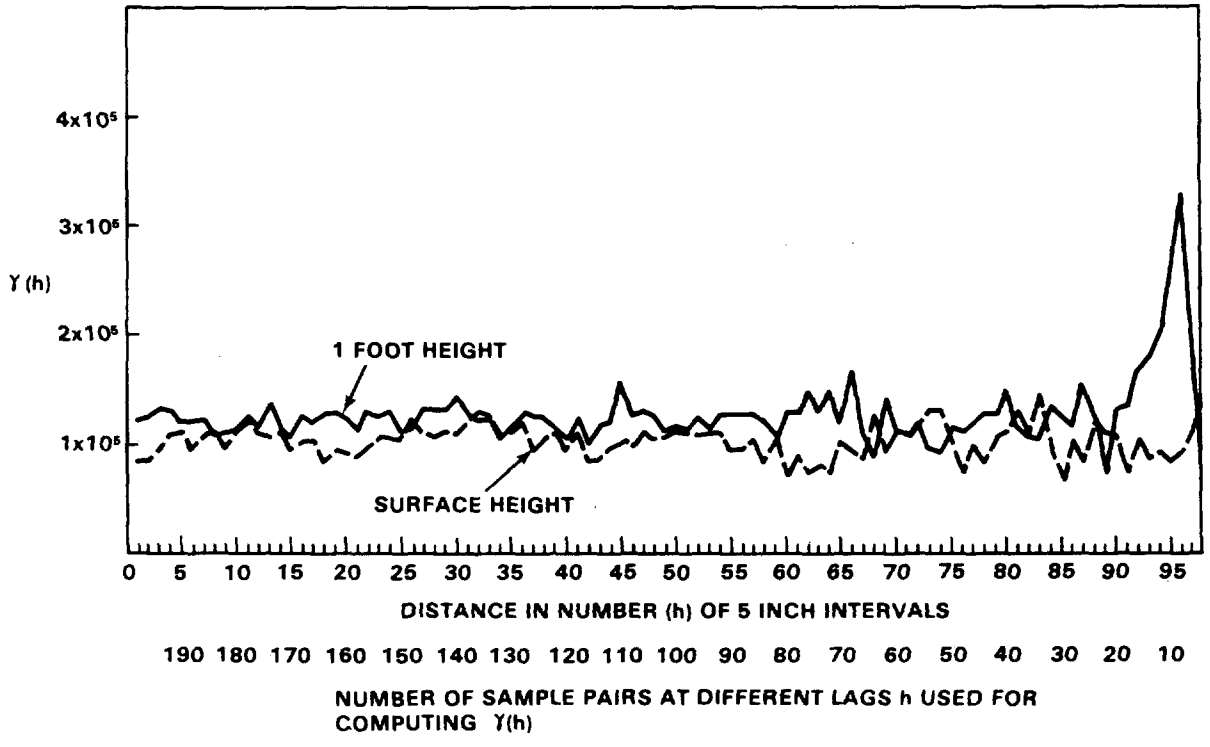

Figure 20. Variogram of Adjacent FIDLER Net CPM ^{241}Am Readings Along Line 2 in Area 13, Project 57.

The Am data suggest that the optimum number of clusters, samples within clusters, and aliquots per sample for estimating average concentrations will be different for areas near GZ, where concentration levels change rapidly as opposed to lower-level regions such as along Line 2.

ACKNOWLEDGMENTS

We would like to thank Ed Essington for his helpful suggestions concerning the design of these two studies. We also greatly appreciate the very competent performance of the REECo field sampling crews and members of the REECo counting laboratory. Special thanks also go to B. B. Vinson for her assistance in data reduction and analysis. Finally, we acknowledge Mary White for her support and interest in these studies.

REFERENCES

1. Aitchison, J., and J. A. C. Brown. 1969. *The Lognormal Distribution*. Cambridge University Press.

2. Barnes, M., P. Delfiner, and R. O. Gilbert. 1977. "A New Statistical Tool, Kriging, and Some Applications to Area 13 Data." *In: Transuranics in Desert Ecosystems*. M. G. White, P. B. Dunaway, and D. L. Wireman (Eds.). USDOE Report, NVO-181. pp. 431-445.

3. Cochran, W. H. 1977. *Sampling Techniques*. 3rd Edition. John Wiley and Sons, New York.

4. Delfiner, P. 1975. "Linear Estimation of Nonstationary Spatial Phenomena." *In: Advanced Geostatistics in the Mining Industry*. M. Guarascio, M. David, and C. Huijbregts (Eds.). NATO A.S.I., Rome, 1975, Dordrecht-Holland, D. Reidel Publishing Company. pp. 49-68.

5. Delfiner, P., and R. O. Gilbert. 1978. "Combining Two Types of Survey Data for Estimating Geographical Distribution of Plutonium in Area 13." This report.

6. EPA Workshop. 1976. "Evaluation of Sample Collection and Analytical Techniques for Environmental Plutonium." USEPA, Office of Radiation Programs, Las Vegas. ORP/LV-76-5.

7. Federer, W. T. 1963. *Experimental Statistics, Theory and Application*. MacMillan Company, New York.

8. Grant, C. L., and P. A. Pelton. 1973. "Role of Homogeneity in Powder Sampling." *In: Sampling Standards and Homogeneity*. AOTM Special Technical Publication 540. American Society for Testing and Materials, Philadelphia. pp. 16-29.

9. Gilbert, R. O., E. H. Essington, D. N. Brady, P. G. Doctor, and L. L. Eberhardt. 1977. "Statistical Activities During 1976 and the Design and Initial Analysis of Nuclear Site Studies." *In: Transuranics in Desert Ecosystems*. M. G. White, P. B. Dunaway, and D. L. Wireman (Eds.). USDOE Report, NVO-181. pp. 331-366.

10. Michels, D. E. 1977. "Sample Size Effect on Geometric Average Concentrations for Log-Normally Distributed Contaminants." *Environmental Science and Technology* 11(3):300-302.

11. Snedecor, G. W., and W. G. Cochran. 1967. *Statistical Methods.* Iowa State University Press, Ames, Iowa.

12. Tinney, J. F. 1968. "Calibration of X-Ray Sensitive Plutonium Detector." *In: Hazards Control Progress Report* No. 31 (May-August). Lawrence Livermore Laboratory, University of California, Livermore, California. TID-4500, UCRL-50007-68-2.

13. Wallace, A., and E. M. Romney. 1977. "The Particle Size Problem in the Assay of Plutonium in Field Soil Samples." *In: Transuranics in Desert Ecosystems.* M. G. White, P. B. Dunaway, and D. L. Wireman (Eds.). USDOE Report, NVO-181. pp. 41-52.

APPENDIX A

PROTOCOL FOR A SPECIAL STUDY AT NUCLEAR SITE 201 TO ESTIMATE THE RELATIONSHIP BETWEEN ^{241}Am CONCENTRATIONS AND THE SIZE OF SOIL ALIQUOT

Prepared by

R. O. Gilbert and E. H. Essington

April 14, 1977

1. At a distance of 150 ft along the established transect[1] from ground zero (GZ) at Nuclear Site 201 collect 24 surface soil samples, 6 samples along each of 4 east-west lines. The 4 lines and the 6 samples in each line should be as close together as possible (see diagram below). However, samples should be taken with care to avoid disturbances of sampling locations. One approach would be to lay a board over lines 2, 3, and 4 while collecting the 6 samples on Line 1. Then move the board to expose Line 2, etc. The samples are to consist of the standard NAEG surface ring sample (12.7 cm diameter to a depth of 5 cm). Large rocks (>1 in. in diameter) may be removed and discarded from the sample after placing any soil attached to the rock in with the soil sample. Discarded rocks should be returned to the hole left by the samples. If 150 ft from GZ is a very rocky area, move along transect until a less rocky area is found. Do not go beyond 200 ft. Samples may be taken as close as 100 ft from GZ if necessary. Record location where samples were collected as well as general terrain features of the sampled area.

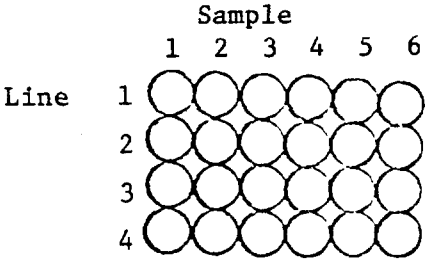

[1] A line 1000 ft from ground zero at an azimuth of 326° and thence for an additional 500 ft at azimuth of 331°.

2. Repeat the above procedure at a distance of 1050 ft from GZ along the transect.[2] If rocky or graded area is encountered, samples can be collected elsewhere along transect between 1000 and 1100 ft. Be careful not to locate sampling point on a graded road or berm.

3. Dry the 48 samples according to established NAEG procedures.

4. Ball mill each of the 48 samples for 5 hr.

5. Screen each ball-milled sample collected at 150 ft through a 10-mesh screen. Weigh each fraction, then combine the <10-mesh fractions of each of the 24 samples in a plastic bag; mix by kneading until the material is thoroughly mixed (at least 10 minutes).

6. Place the >10-mesh soil collected at 150 ft in a separate plastic bag and mix by kneading for 10 minutes. Set aside until Step 12 below.

7. Spread out the <10-mesh soil in the shape of a circle on a clean plastic sheet. Divide the soil into 4 approximately equal quarters using a clean straight edge.

8. For each quarter do the following:

   a) Transfer the soil to a clean plastic sheet and spread out uniformly into the shape of a circle.

   b) Divide soil into 5 approximately equal pie-shaped parts using a straight edge.

   c) Transfer each part into a separate plastic bottle.

   d) Record dry weight of soil in each bottle.

   e) Assign library numbers to each bottle.

9. Number the 20 bottles from 1 to 20; numbers 1 - 5 for quarter 1, 6 - 10 for quarter 2, 11 - 15 for quarter 3, and 16 - 20 for quarter 4.

10. Five aliquots, one each of 1-g, 10-g, 25-g, 50-g, and 100-g size, are to be taken from each of the 20 plastic bottles. Look up the order in which the different size aliquots are to be taken from the bottles by referring to the attached "Schedule for Taking Aliquots." Use the same size scoop (about 5 g) for all aliquot sizes. For example, the 100-g aliquot will require about 20 scoops using a scoop holding 5 g. Rotate the bottle of soil (corner to corner) about 5 seconds before each sample (aliquot) is taken. The soil must not be poured out to obtain aliquots. Assign aliquot numbers to the 100 aliquots. Record the dry weight of each aliquot. Store soil remaining in bottles in the soils library.

---

[2]These samples were stored but have not been analyzed as of October 1978.

11. Do not process the 24 ball-milled samples collected at 1050 ft. Store the 24 samples in soils library for possible future use.

12. (From Step 6 above). Spread >10-mesh soil (collected at 150 ft) in the shape of a circle on a clean plastic sheet. Divide soil into 10 approximately equal pie-shaped parts using a clean straight edge. Place each part in a plastic bottle, record dry weight, and assign library numbers. Rotate each bottle corner to corner for 5 sec. Take a 10-g aliquot from each bottle using plastic spoon. Assign aliquot numbers. Store the soil remaining in the 10 bottles in soils library.

13. Count each of the 110 aliquots (100 are <10-mesh and 10 are >10-mesh) for ^{241}Am using Ge(Li) for 1000 minutes or until the percent count error (2σ) is 10% or less, whichever time is less. Save samples in their present bottles for possible recounts or further analysis.

14. At a location well outside the radiation fallout pattern of NS-201 yet within the same general soil type, collect 12 soil samples in the same manner as was done in Step 1 above. These samples will be used to provide radiation counter calibration. Dry and ball mill these samples as in Steps 3 and 4 above used for radioactive samples. Sieve samples (no weights required) through a 10-mesh screen combining the <10-mesh fraction as one and the >10-mesh as another. Mix each fraction separately by kneading for 10 minutes. Withdraw aliquots of appropriate size from the <10-mesh soil fraction and dose with standard solution used to calibrate for gamma spectra as per discussion with Derek Engstrom. Prepare dosed standards in same configuration (same bottle size and style) as that to be used in counting samples. It is suggested that not less than 5 such standard aliquots of each size (1 g, 10 g, 25 g, 50 g, and 100 g) be prepared and used for estimating the calibration curves.

15. Ten gram samples of the >10-mesh material collected in Step 14 above are to be prepared as standards also as in Step 14 above. Since the sample will probably contain a wide range of soil particle sizes, a large number of such standards should be prepared, perhaps 10.

16. A report giving the following information should be distributed to Ms. Mary White (NAEG), Richard O. Gilbert (Battelle-Northwest), E. H. Essington (LASL), and to any other individuals designated by Ms. White:

    a) ^{241}Am concentrations (activity per gram dry weight), associated aliquot numbers, aliquot weights, and bottle numbers (1 through 20).

    b) percent counting error (2σ)

    c) Dry weight (grams) of <10-and >10-mesh soil fractions before the samples were combined. Dry weights of soil in plastic bottles.

d) Short description of terrain features where samples were collected.

e) Feet from GZ where closest soil sample of each set was collected.

f) Short description of soil mixing (kneading operation) and aliquoting operations; e.g., length of time kneading was done or any special problems that arose that might effect thoroughness of mixing or uniformity of aliquots.

SCHEDULE FOR TAKING ALIQUOTS

Table A1 below gives the order in which the five aliquots are to be taken from each of the 20 plastic bottles of <10-mesh soil collected at 150 ft from GZ along the transect at Nuclear Site 201. The letters in the table correspond to aliquot sizes as follows:

Letter	Aliquot Weight
A	1 g
B	10 g
C	25 g
D	50 g
E	100 g

Table A1. Order for Removing Aliquots from Bottles

Quarter	1	2	3	4
Bottle No.	1 2 3 4 5	6 7 8 9 10	11 12 13 14 15	16 17 18 19 20
Order 1	E C D B A	E D A B C	C D B A E	B A E C D
2	A B E C D	A E D C B	D A E B C	A E C D B
3	B E A D C	C B E A D	B C D E A	D B A E C
4	C D B A E	D C B E A	E B A C D	C D B A E
5	D A C E B	B A C D E	A E C D B	E C D B A

Example: Bottle number 13 in quarter 3 will have aliquots taken in the following order:

1st 10 g
2nd 100 g
3rd 50 g
4th 1 g
5th 25 g

APPENDIX B

GENERALIZED EQUATIONS FOR ESTIMATING ALIQUOT WEIGHT AND NUMBER OF ALIQUOTS PER SAMPLE

Results for Am

Suppose that the relationship between the standard deviation (s) for Am Ge(Li) counts and aliquot weight (w) in grams is

$$s = aw^{-b} . \tag{B1}$$

In addition, assume the total cost C for Ge(Li) counting n aliquots of any size w is

$$C = nK , \tag{B2}$$

where K is the cost per aliquot. Since the variance of the estimated mean Am concentration is $V_A = s^2/n$, we see from Equation A1 and A2 that

$$V_A = a^2/nw^{2b} = a^2K/Cw^{2b} . \tag{B3}$$

This can be solved for w to give

$$w = (a^2/V_A n)^{\frac{1}{2b}} = (a^2K/CV_A)^{\frac{1}{2b}} . \tag{B4}$$

Hence, for fixed counting costs C and K, and a desired precision V_A of $\bar{x}$ we can estimate both the number (n) and weight (w) of aliquots that are required by solving Equations A2 and A4. This assumes, of course, that we have previously obtained data that give reliable estimates of a and b in Equation B1.

For a specified precision V_A the cost C will be minimized by taking n = 1. In that case, Equation A4 gives

$$w = (a^2/V_A)^{\frac{1}{2b}} . \tag{B5}$$

Conversely, if C and K are fixed (equivalent to fixing n) then V_A will be minimized by using the largest possible aliquot size w up to the limit where the flat rate of K dollars per aliquot no longer applies. This can be seen from Equation B3.

Results for Pu

Let R be the true Pu to Am ratio, i.e., Pu = R x Am. Therefore, s(Pu) = R s(Am). Using Equation B1 for s(Am) we obtain

$$s(Pu) \simeq R\, a w^{-b} \quad . \tag{B7}$$

Hence,

$$V_p = [s(Pu)]^2/n \simeq R^2 a^2/n w^{2b} \quad . \tag{B8}$$

Suppose the following linear cost equation is applicable:

$$C = n(\alpha + \beta w) \quad , \tag{B9}$$

where $\alpha + \beta w$ is the Pu analysis cost for a single aliquot of size w (in grams). α and β are parameters to be determined on the basis of cost information from the analytical laboratory. Then

$$n = C/(\alpha + \beta w)$$

and

$$V_p \simeq R^2 a^2 (\alpha + \beta w)/C w^{2b} \quad . \tag{B10}$$

If b = 0.5 as suggested by our Am data and by theoretical considerations (Grant and Pelton, 1973, p. 20), then

$$V_p \simeq \frac{R^2 a^2 \alpha}{Cw} + \frac{R^2 a^2 \beta}{C} \quad . \tag{B11}$$

Solving Equation (B10) for w gives

$$w \simeq R^2 a^2 \alpha/(CV_p - R^2 a^2 \beta) \quad , \tag{B12}$$

where CV_p must be greater than $R^2 a^2 \beta$.

Hence if estimates of R and a are available from the analysis of prior samples, if cost parameters α, β, and C are specified, and the desired precision of the mean Pu concentration per sample (V_p) is agreed upon, then Equation (B12) may be solved to obtain the aliquot size w. An estimate of n may be obtained from Equation (B9). If Pu analyses are available that relate s(Pu) to w, then this functional form should be used for s(Pu) in Equation (B8). This would eliminate the need for using Equation B7 in B8.

APPENDIX C

PROTOCOL FOR ^{241}Am VARIABILITY-WITH-DISTANCE STUDY

Prepared by

R. O. Gilbert and E. H. Essington

August 10, 1976

INTRODUCTION

The objective of this study is to obtain data that will be useful in determining the correlation structure between Pu concentrations collected at various distances. This information is necessary in order to determine whether Universal Kriging will be a useful technique for estimating Pu contours in soil.

Two series of surface (0-5 cm) soil samples are to be collected along two straight lines in Area 13, Project 57 using the standard NAEG 5-in.-diameter ring. Sixty samples are to be collected on each line for a total of 120 samples. Two aliquots from each sample are to be analyzed for ^{241}Am using the Ge(Li) system at REECo for a total of 240 analyses. FIDLER readings are to be taken along the line as indicated below.

PROCEDURE

1. The spacing and location of surface (0-5 cm) soil samples along Line 1 is as follows:

   Collect 15 groups of 4 adjacent samples along a line beginning at Nevada Grid Coordinate N935900, E721100 and proceeding due east along the line N935900. Separate the first sample in each group of 4 by 20 ft. That is, collect the first sample in the first group at location N935900, E721100, the first sample in the second group 20 ft due east at location N935900, E721120,..., the first sample in the last (15th) group at location N935900, E721380.

2. The spacing and location of surface (0-5 cm) soil samples along Line 2 is as follows:

   Collect 15 groups of 4 adjacent samples along a line beginning at location N939700, E718600 and proceeding due east along the

the line N939700. The spacing between the first sample in each group of four samples in Line 2 is 150 ft. That is, the first sample in the first group of four samples is at N939700, E718600, the first sample in the second group of four is at N939700, E718750,..., the first sample in the last (15th) group of four is at location N939700, E720700.

3. The four samples within each group in Lines 1 and 2 are collected so that the sampling rings are adjacent (butt up against each other).

4. Assign stake numbers 1 through 60 to the sample locations in Line 1 starting with 1 at the west end of the line (N935900, E721100) and progressing due east along the line to number 60.

5. Assign stake numbers 61 through 120 to the sample locations in Line 2 starting with 61 at the west end of the line (N939700, E718600) and progressing due east along the line to number 120.

6. The spacings and locations of samples for Lines 1 and 2 are illustrated below:

Line 1

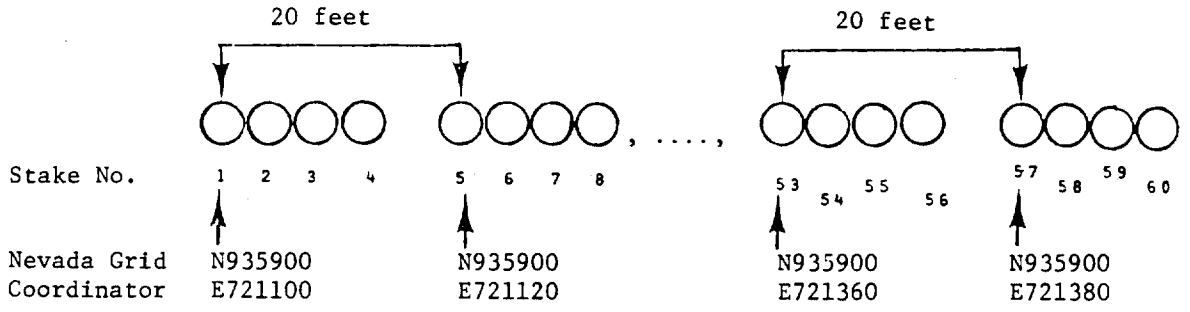

Line 2

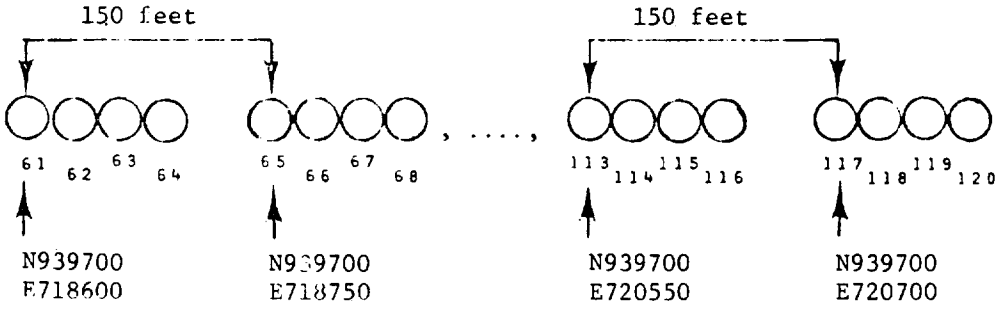

Group of 4 Adjacent Samples

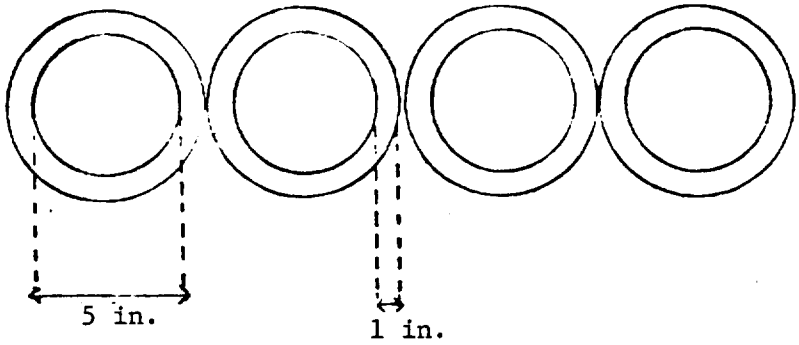

7. The samples are to be taken along the sampling lines indicated above unless two or more of the groups of four samples in the line happens to fall on a man-made disturbance (such as down a road) or a disturbance caused by grazing cattle (e.g., down a path leading to a watering trough). In such cases the following lines are to be substituted for the original lines given above.

Original Line	Substitute Line
N935900	N936025
N939700	N939800

If only one or two groups of four along the line are in these disturbed areas then follow the procedure in item 15 below.

8. Before inserting the 4 sampling rings take FIDLER readings 1 ft above each of the 4 sampling points and at the center of the 4 sampling points - a total of 5 FIDLER readings per station. Insert 4 sampling rings and take 4 FIDLER readings at the surface of the sampling point - a total of 4 additional FIDLER readings per station. FIDLER readings are to be taken at all 30 stations.

9. The FIDLER used in number 7 above should be equipped with an integrater rather than a rate meter.

10. If soil sample locations are under or adjacent to shrubs that will influence FIDLER readings and/or interfere with the subsequent collection of soil, these shrubs or vegetation are to be cut away at ground level and removed from the immediate area before FIDLER readings are taken. The soil to be sampled must not be disturbed in the process of removing vegetation.

11. The 5-in.-diameter soil-sampling ring should be pushed flush into the soil to a uniform depth of 5 cm on all sides of the ring. Hence, if a sample falls on the sloping surface of a blow-sand mound the ring should follow the slope of the mound (not be placed horizontal to level ground).

12. Care should be taken to prevent cross contamination between adjacent samples (within groups) before and during the process of taking FIDLER readings and collecting the soil samples.

13. Record whether each soil sample is taken from:

    a) desert pavement
    b) blow sand mound
    c) wash area
    d) rodent mound
    e) other (describe)

14. Sample should always be collected unless prevented by a physical obstruction (concrete pad, lumber, old animal pens, etc.).

15. If a sample cannot be collected due to a physical obstruction then skip that group of four samples and add an additional group of four at the eastern end of the line, maintaining the appropriate spacing (20 or 150 ft for Lines 1 or 2, respectively.

16. Record the weights of the soil samples:

    a) Dry weight before ball-milling
    b) Weight of the total ball-milled fraction

17. Dry and ball-mill samples according to established NAEG procedures. Do not sieve.

18. Assign unique library numbers to each of the 120 samples.

19. Take two 70-g aliquots from each ball-milled sample. Assign unique aliquot numbers to all 240 aliquots.

20. Store remaining ball-milled soil from each sample. Label with library number and aliquot number.

21. Count for ^{241}Am (GeLi) on each aliquot. Counting time should be sufficient to attain a 2% counting error (100 x 1σ/count = 2.0) or up to 1000 minutes, whichever occurs first.

23. Design a data sheet to be used in the field and in the lab that provides space for all pertinent field parameters and laboratory sample preparation parameters. Any other information deemed important or pertinent to the study should be recorded perhaps as remarks. The following information should be recorded on the data sheet and in a peripheral data base:

Output Data Categories

Data Element	: Soil
Study Name	: Distance-Variability Samples
Study Site	: Area 13, Project 57, NTS
Study Period	: Summer, 1976
Line Number	: 1 or 2
Stake Number	: 1 through 120
Library Number	:
Aliquot Number	:
Aliquot Weights	: 70 grams
Sample Weights	: Record weights indicated in item 2 above.
Nevada Grid Coordinates (NGC)	: a) Assign NGC of the first sample in each group of 4 to all 4 samples in the group and to the net 60 KeV FIDLER readings for group.
FIDLER	: Net 60 KeV ^{241}Am counts per minute for each FIDLER reading.
GeLi Results	: ^{241}Am (GeLi) in nCi/gram dry of ball-milled soil.
Percent Counting Error	: See item 21 above.
Comments	: Record information indicated in item 13 above.

24. Report the information in the "Output Date Categories" defined in item 23 above to M. G. White, R. O. Gilbert, BNW, and to those individuals specified by Ms. White.

STATISTICAL DESIGN AND ANALYSIS FOR NAEG STUDIES:

CURRENT STATUS AND A REVIEW OF PAST EFFORTS

R. O. Gilbert and L. L. Eberhardt

Battelle, Pacific Northwest Laboratories
Richland, Washington

ABSTRACT

In this paper, we summarize our statistical design and analysis activities for the NAEG since 1971 and report on the current status of our work. The statistical analyses completed during Calendar Year 1977 are discussed and recommendations are made for future cleanup and other studies (see the SUMMARY). A list of references on statistical topics we have studied for the NAEG is also provided and our past synthesis efforts are briefly reviewed.

Some specific items discussed in this paper are: (1) a historical review of the design and analysis of field data for estimating Pu spatial distribution and inventory at safety-shot and nuclear test sites on the Nevada Test Site (NTS) and Tonopah Test Range (TTR), (2) maps giving the latest information on spatial pattern of $^{239,240}Pu$, ^{241}Am, and ^{137}Cs soil concentrations and beta plus gamma GM instrument readings at Nuclear Site (NS)-201, (3) a grid map showing where additional soil samples at NS-201 have been obtained, (4) a grid map for a possible new field FIDLER and soil survey of the Clean Slate 2 site on the TTR to investigate the need for possible cleanup or remedial action at that site, and (5) a grid map showing sampling plans for NS-200 on NTS.

INTRODUCTION

Statistical design and analysis have played an important role in NAEG environmental transuranic studies on NTS and TTR since the first studies began in 1971. In this paper, we give a historical review of our involvement as statisticians in these studies up to the present time. This review includes a discussion of our activities since the last NAEG Pu Information Conference in March, 1977. We also take this opportunity

to suggest areas of research and statistical analysis that the NAEG might consider for future use.

Most of our attention over the years has been directed toward soil and vegetation studies, with special emphasis on soil. We have had little if any direct involvement in the design of small mammal, cattle grazing, or resuspension studies. Probably our greatest effort has been in the design and analysis of studies for estimating the inventory (total amount) and spatial distribution of $^{239,240}Pu$ in surface (0-5 cm) soil at safety-shot and nuclear test sites. The design and analysis of blow-sand mound studies has also been a major effort. In addition, we have contributed to the development of plans for possible cleanup efforts at the Clean Slate 2 site on TTR and to efforts at synthesizing soil, vegetation, small mammal, and cattle data at the Area 13 (Project 57) site. Our experience in the design and analysis of studies at safety-shot sites stimulated us to try new field designs and methods of statistical analysis at nuclear test sites. In our NAEG publications, we have also pointed out the effect that different statistical treatment of the same data can have on estimates of inventory and ratios of plutonium to americium or vegetation to soil concentrations. Through the years, we have developed a close working relationship with other NAEG scientists, particularly Ed Essington at the Los Alamos Scientific Laboratory. Ed's contributions are particularly evident in the field sampling protocols developed for the blow-sand mound and nuclear site studies.

ESTIMATING PLUTONIUM INVENTORY AT SAFETY-SHOT SITES

Historical Account

One of the first NAEG objectives presented to us in 1971 was to estimate the inventory (total amount) of Pu in soil at safety-shot sites. (Throughout this paper, $^{239,240}Pu$ and ^{241}Am will be denoted by Pu and Am). The first data available for designing such studies was a limited amount of FIDLER,* Pu, and Am data from the GMX site in Area 5. These data were used by Eberhardt and Gilbert (1972) to investigate the feasibility of using the FIDLER and/or Ge(Li) Am data in conjunction with Pu analyses to estimate inventory. It was suggested that since Am and Pu soil concentrations were highly correlated at GMX, the cost of obtaining Pu inventory estimates there would be reduced by relying primarily on Am (Ge(Li)) analyses on soil samples. The available FIDLER data also suggested that they could be a basis for dividing the GMX site into several Am activity strata within which soil samples could be chosen at random according to a stratified random sampling plan. Such a plan

---

*Field Instrument for the Detection of Low Energy Radiation

would have the benefits of increasing the precision of inventory estimates over what would likely result if stratification were not done.

The first two safety-shot sites to be studied intensively by the NAEG were Area 13 (Project 57) and Area 5 (GMX) in that order. Based on the results in Eberhardt and Gilbert (1972), the decision was made to use stratified random sampling as the basic approach to estimating Pu inventory. This was a conservative approach in the sense that we would not be relying on the correlation between Am and Pu concentrations to estimate Pu inventory, i.e., Pu inventory would be estimated by obtaining wet chemistry Pu determinations on all soil samples collected. Ge(Li) scans for Am on soil samples (same aliquots as used for Pu determinations) would be done on all samples primarily (i) to estimate Pu to Am ratios, (ii) to relate Am concentrations in soil to those in other ecosystem components like vegetation and small mammals, and (iii) to evaluate more fully the feasibility of using Am to help estimate Pu inventory.

An extensive number of FIDLER readings at 1-foot height were taken on grid systems to estimate the spatial distribution of Am. This information was used to divide the area into activity strata within which soil samples were collected at random locations. Before each surface soil sample* was collected at 1-foot height, net FIDLER reading was taken over the sampling location. These FIDLER-Pu data were used to evaluate the correlation between FIDLER count per minute readings and Pu wet chemistry concentrations on 10-gram soil aliquots removed from the soil samples. The details of the design of these studies are given in Gilbert and Eberhardt (1974), Gilbert *et al.* (1975), and Gilbert *et al.* (1976a). Once the studies at Project 57 and GMX were under way, FIDLER surveys began at Clean Slates 1, 2, 3, and Double Tracks on TTR, and in Area 11 (Plutonium Valley) on NTS for the purpose of establishing strata. The same basic design used at the Area 13 (Project 57) and GMX sites (stratified random sampling relying on Pu wet chemistry analyses) was used at these new study areas.

The first estimates of inventory to be published appeared in Gilbert and Eberhardt (1974) for Area 13. Estimates and their standard errors were given for individual activity strata as well as for the total area (sum of the six strata areas). A year later, estimates of Pu inventory were published (Gilbert *et al.*, 1975) for all 10 safety-shot sites except A Site in Area 11 where data were not then available. The inventory estimates for the four TTR sites and Sites B, C, D, CD overlap, and ABCD overlap in Area 11 were preliminary since only 40 percent of the samples collected had been chemically analyzed and reported up to that time. Estimates of $^{239,240}Pu$ and total uranium inventory in vegetation are given in Romney *et al.*, 1977.

---

*5-inch-diameter ring to a depth of 5 cm.

A problem arose in that most of the remaining sample aliquots from TTR and Area 11 sites that had been shipped to the analytical laboratories for analysis were of <100-mesh soil, i.e., these aliquots were of soil that had passed through a 100-mesh screen after ball-milling. But the results reported in Gilbert *et al.* (1975) were for aliquots of only ball-milled soil, i.e., for which no sieving was done. The question arose as to whether results on <100-mesh and unsieved soil are really comparable, i.e., do these two soil fractions contain (on the average) different levels of Pu concentration? Gilbert and Eberhardt (1976a) examined the available data and concluded that <100-mesh soil aliquots in relatively high activity soils tended to have higher concentrations than unsieved aliquots, but that the effect tended to be less pronounced for low-level samples. It was decided to circumvent the problem by preparing new unsieved aliquots from stored ball-milled library samples to replace the <100-mesh aliquots previously shipped to the analytical laboratories. The Pu and Am (Ge(Li)) results on these new unsieved aliquots were reported to us in May of 1977. However, our attention to other NAEG studies (primarily the blow-sand mound studies) and reduced levels of support since October, 1977, have prevented the statistical analyses of these data. This is most unfortunate since the major expense of chemical analysis has been completed.

Additional information also exists from 188 soil and 173 vegetation samples collected at new locations from all 10 safety-shot sites to "fill in the gaps" left by the original random selection process. We requested that these new samples be collected so that improved estimates of Pu spatial distribution (discussed below) and inventory could be obtained. The Pu and Am concentrations on unsieved 10-gram aliquots of these samples were also reported in the summer of 1977. These data have been placed on computer cards in preparation for statistical treatment, but the actual analyses have not begun due to budget restrictions. These new location data and the data on unsieved aliquots discussed in the previous paragraph have been entered into the NAEG data bank by Reynolds Electrical & Engineering Co. (REECo) personnel.

In the spring of 1977, we discovered that some estimates of Pu inventory for safety-shot sites reported in Gilbert *et al.* (1975) were in error due to inaccurate planimetering of the Am activity maps (Figures 4-14, Gilbert *et al.*, 1975). Subsequently, the size of all strata was recomputed by dividing each stratum into small squares and counting the number of squares falling within the stratum. These new stratum sizes were then used to recompute Pu inventory estimates which are reported by Gilbert (1977b). The corrected total estimated inventory for the 10 sites is about 146 curies as compared to a total of about 155 curies originally reported by Gilbert *et al.* (1975).

Effect of Estimation Technique on Inventory Estimates

Before turning to our work on estimating Pu concentration contours, it is important that we mention the considerably different estimates of Pu inventory that can be obtained depending on whether the "average" Pu concentration for a stratum is estimated by the arithmetic mean or some statistic that is less affected by unusually high concentration samples such as the geometric mean or median. Gilbert *et al.* (1977a) illustrate the problems involved with the Pu data from stratum 6 (near ground zero) in Area 13. If the geometric mean is used in place of the arithmetic mean, the estimate of Pu inventory in surface soil at Area 13 drops from the 46 curies reported by Gilbert (1977b) to roughly 24 curies. This difference occurs because the statistical distribution of the observed Pu concentrations for each stratum is highly skewed (a few concentrations much higher than the bulk of the data). Which estimate is more nearly correct? The answer to this is not known with assurance.

Some insight may be gained by examining the most recent estimates of Pu inventory as reported by Delfiner and Gilbert (1978) for strata 3 through 6 of Area 13. These were obtained using kriging techniques making use of a linear relationship between FIDLER and Pu measurements (each in logarithmic scale). The inventory estimate for strata 3 through 6 combined is about 17 curies compared with the 28.6 curies reported by Gilbert (1977b) for these strata. Delfiner and Gilbert note, however, that their estimates are probably biased low due to ignoring changes in mean concentration levels over distances less than 100 feet when transforming inventory results computed in logarithmic scale back to arithmetic scale. Also, the method used to make this transformation is based on the assumption that the Pu data are lognormally distributed, which may not be the case, particularly near ground zero in stratum 6. These authors suggest that taking a large number of FIDLER readings on a fine mesh grid may be a viable option for obtaining more reliable inventory estimates, at least in relatively high activity strata where the linear log FIDLER-log Pu relationship appears to be well established.

ESTIMATING SPATIAL DISTRIBUTION OF PLUTONIUM AT SAFETY-SHOT SITES

Initial Efforts

The first estimates of the spatial distribution of Pu at safety-shot sites appeared in Gilbert and Eberhardt (1974). They gave three-dimensional plots of FIDLER Am count per minute data collected on 100- and 400-foot grids over the Area 13 (Project 57) study site. Three-dimensional plots of actual Pu concentrations over space were also shown. Additional information was published by Gilbert *et al.* (1975) in the form of FIDLER Am activity strata for nine safety-shot sites, and estimated Pu contours for Area 13 and the GMX site in Area 5.

The FIDLER activity strata are probably the best estimates presently available on the spatial distribution of Pu at safety-shot sites. Am and Pu in soil samples are known to be highly correlated at safety-shot sites so that Pu can be predicted fairly well from Ge(Li) Am analyses. The FIDLER is certainly a less precise predictor of Pu concentrations in 10-gram soil aliquots than are Ge(Li) scans on these soil samples in the laboratory. However, the correlation is sufficiently strong between FIDLER field readings and Pu 10-gram soil aliquot concentrations that the general pattern of surface soil Pu contamination at safety-shot sites is believed to be well estimated by FIDLER surveys. It is also true, however, that more extensive FIDLER surveys may be desirable in some or all safety-shot areas since the FIDLER strata maps are based on readings taken no closer than 25 feet, and in many cases, the spacing is 100 feet or more (see Gilbert *et al.*, 1975, pages 343-345, for details on grid spacing).

Using Kriging

The Pu contours given in Gilbert *et al.* (1975) were estimated using a computer program called "SURFACE II" developed by the Kansas Geological Survey. This program was applied to the Pu concentrations of 10-gram soil aliquots taken from surface (0-5 cm) soil samples at random locations. SURFACE II was also used to obtain Pu concentration contours for vegetation at these locations. These initial contours were exploratory in nature and were believed to be biased in several respects. Later attempts at obtaining contours with less bias were made by Gilbert (1976b; also this publication), who used iterative techniques in conjunction with SURFACE II; and by Barnes *et al.* (1977) and Delfiner and Gilbert (1978). These latter two papers make use of kriging techniques. The kriging approach has definite advantages over previous methods. One of these is that estimates of precision are available on estimated Pu inventories for unit blocks of land. The reader is referred to these papers for details. We note that Dr. Delfiner is presently on a consulting contract with Battelle, Pacific Northwest Laboratories, to work on the application of kriging to environmental Pu studies.

We have noted above that soil and vegetation Pu and Am data at new locations at safety-shot sites became available in 1977. These new data, in conjunction with the analysis of new unsieved soil samples from TTR and Area 11, total to over 500 new data points. We hope to analyze these data using kriging methods to estimate the spatial distribution and inventory of Pu at these sites if additional funding becomes available.

To assist in the evaluation of kriging techniques for estimating spatial distribution and inventory, a special study was conducted along two transect lines at the Area 13 site during 1976-77 to investigate the spatial correlation structure of Am soil concentrations as well as FIDLER readings. Presumably, FIDLER readings and soil concentrations in

close proximity are not completely independent. The degree of dependence with distance between samples is required information for kriging. The design and results of this study are discussed by Doctor and Gilbert (1978).

Our capability for using kriging techniques was greatly enhanced in 1977 by arranging to access the BLUEPACK kriging program available on the Nevada Operations Office computer in Las Vegas via a high-speed computer terminal operated by Boeing Computer Services in Richland, Washington. This will allow us to handle efficiently the rather large amounts of data commonly required for kriging. Thus far, our major use of BLUEPACK has been by Dr. Delfiner in the analysis of the Area 13 (Project 57) data (Delfiner and Gilbert, 1978).

ESTIMATING PLUTONIUM INVENTORY AND SPATIAL DISTRIBUTION AT NUCLEAR SITES

Design Aspects

We have used the experience gained at safety-shot sites to try new sampling designs at nuclear test sites for estimating Pu inventory and spatial distribution. Perhaps a fundamental change in our approach is to design field sampling plans for the primary purpose of estimating spatial distribution as opposed to inventory. If a field sampling plan allows for the efficient estimation of spatial distribution, then inventory estimates can also be estimated from the data. However, the reverse is not necessarily true. That is, a sampling plan for inventory may not be efficient for estimating spatial distribution.

The basic field design approach is set out in sampling protocols developed during 1977 by NAEG scientists for nuclear site studies. These are discussed by Essington (1978). A basic design change from safety-shot sites is to no longer insist that sample locations be chosen at random. Instead, field instrument readings (beta + gamma, alpha, and FIDLER) as well as soil and vegetation samples are collected on systematic grids over the study site. Sampling is done in two phases. During Phase 1, the grid spacing is rather wide (usually 400 feet). Data at these locations are augmented by instrument readings every 20 feet taken along eight radials at 45° intervals commencing at ground zero and continuing out as far as 2,000 feet. This grid and transect information is used to design Phase 2 sampling where soil, vegetation, and/or instrument measurements suitable to the particular features of the study site in question are obtained. Phase 2 designs are expected to use grids of different mesh sizes, the finer grid spacing being used near ground zero areas or in other regions where concentration levels appear to change rapidly on the basis of information gathered during Phase 1. The grid data should be suitable for estimating both Pu spatial distribution and inventory

using kriging or other methods. The general protocol for Phase 1 sampling is given by Essington (1978). He also gives the Phase 2 protocol developed for NS-201 discussed in the next section.

Results at Nuclear Site-201

At the NAEG Pu Information Conference held in March, 1977, we presented the design and analysis work accomplished during 1976 at NS-201 (Gilbert *et al.*, 1977b). This included the analysis of preliminary soil samples at 315 grid locations. These data were used to estimate the spatial patterns of ^{137}Cs and Am over the study site. The ratios of Am to ^{137}Cs concentrations were quite variable (from less than 1 to over 50) over the study site. Pu to Am ratios did not appear to change with location, the median ratio being 11.2 with 95% confidence limits of 8.3 and 14.1. Some preliminary analyses on metal fragments, profile samples, rocks, and soil fractions were also given.

A portion of the preliminary grid results were not available in March 1977. These were 68 grid locations near ground zero chosen to better define spatial pattern in that region. (These locations are shown in Figure 9 in Gilbert *et al.*, 1977b.) Data for these 68 locations are now available and are given here in Figures 1, 2, and 3. These figures show hand-drawn (by REECo personnel) contours of Am, ^{137}Cs, and beta + gamma instrument readings, respectively.* Figures 1 and 2 may be used in conjunction with Figures 10 and 11 in Gilbert *et al.* (1977b) for a more complete picture of concentration patterns at NS-201. The beta + gamma readings were taken to help evaluate how useful they might be in the study of nuclear sites. It's clear that they do show some patterns of interest near ground zero. However, at further distances the instruments are not sufficiently sensitive to be very useful.

As mentioned above, Figure 13 in Gilbert *et al.* (1977b) shows Pu to Am ratios obtained at various locations at NS-201. These locations were along the main fallout pattern and were the only samples for which Pu analyses had been done. Hence, there was a lack of Pu information in what were expected to be low concentration areas. As a consequence, aliquots from a number of the stored library soil grid samples collected on the 200-foot grid, but away from the main fallout pattern, were analyzed for Pu. These data became available to us in August, 1977. The Pu concentrations of all presently available Pu results for 0-5 cm surface samples are shown in Figure 4. These include locations where Pu to Am ratios were given by Gilbert *et al.* (1977b, Figure 13), and the

---

*Sampling locations are at the grid line intersections in Figures 1, 2, 3, 4, 6, and 7. In Figure 5, the sampling points are at the location of the dots.

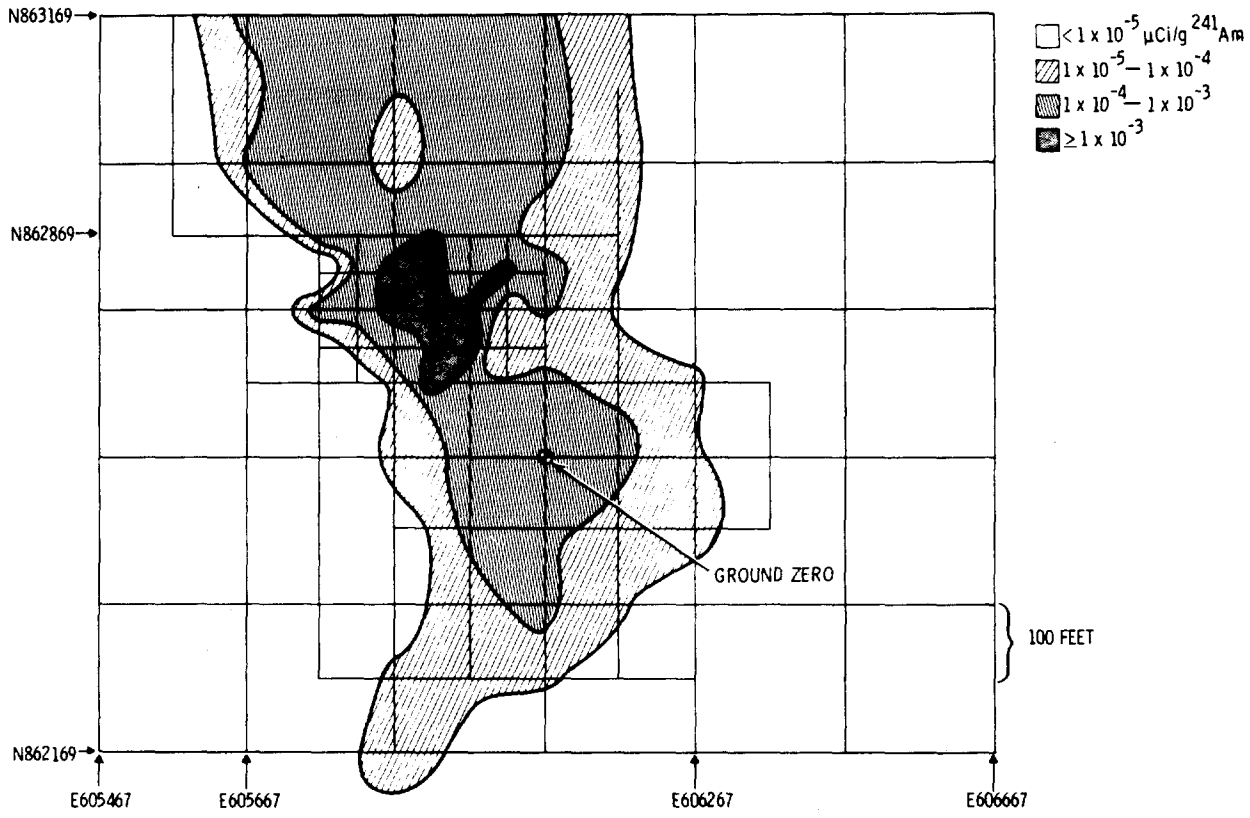

Figure 1. Hand Drawn Concentration Contours of ^{241}Am Near Ground Zero at Nuclear Site-201.

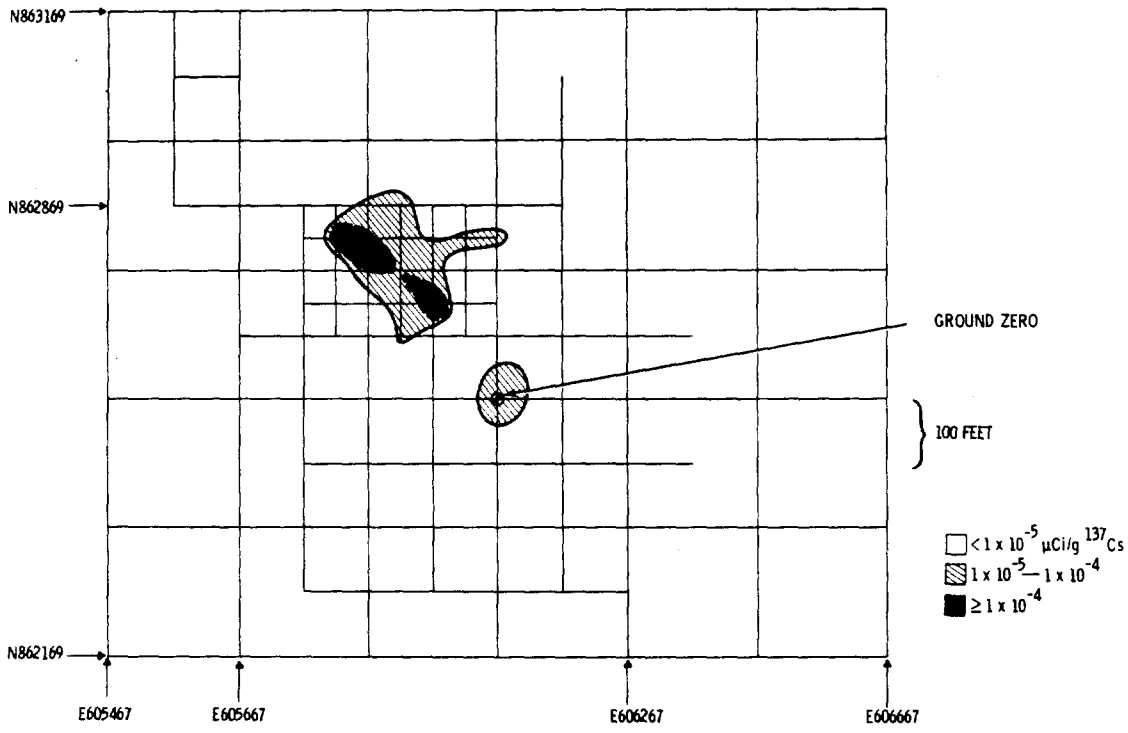

Figure 2. Hand Drawn Concentration Contours of ^{137}Cs Near Ground Zero at Nuclear Site-201.

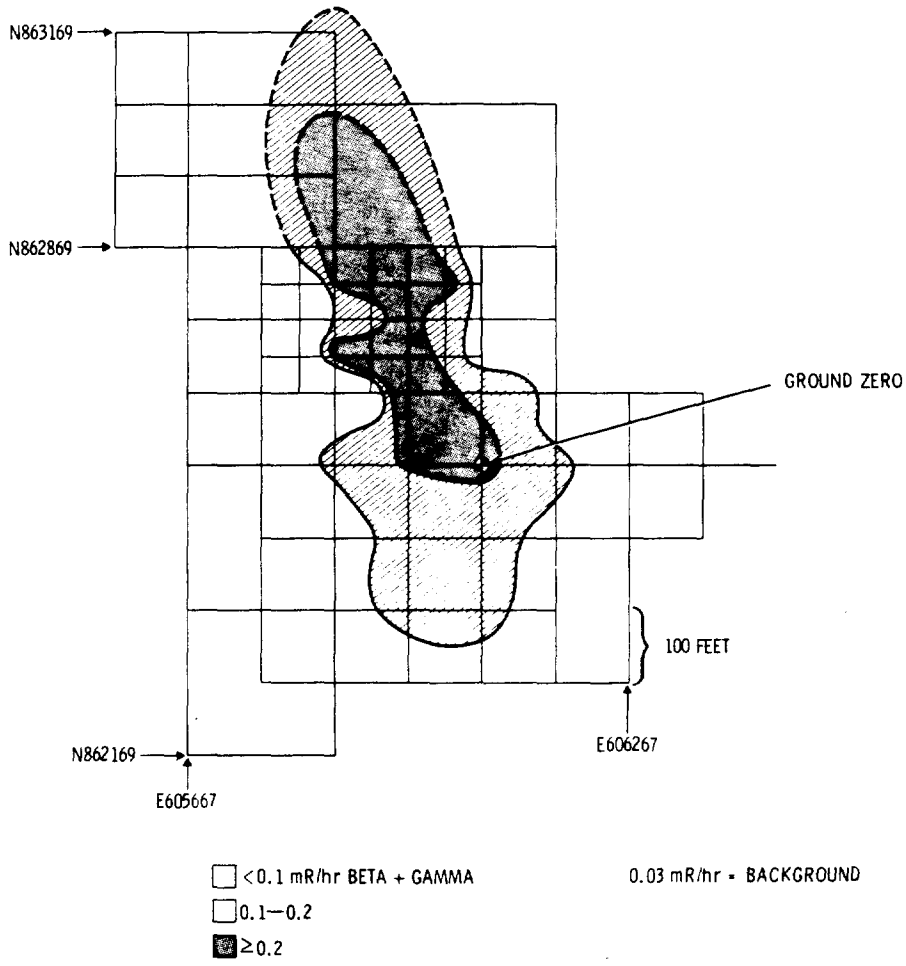

Figure 3. Contact Pancake GM Tube Beta Plus Gamma Readings Near Ground Zero at Nuclear Site-201.

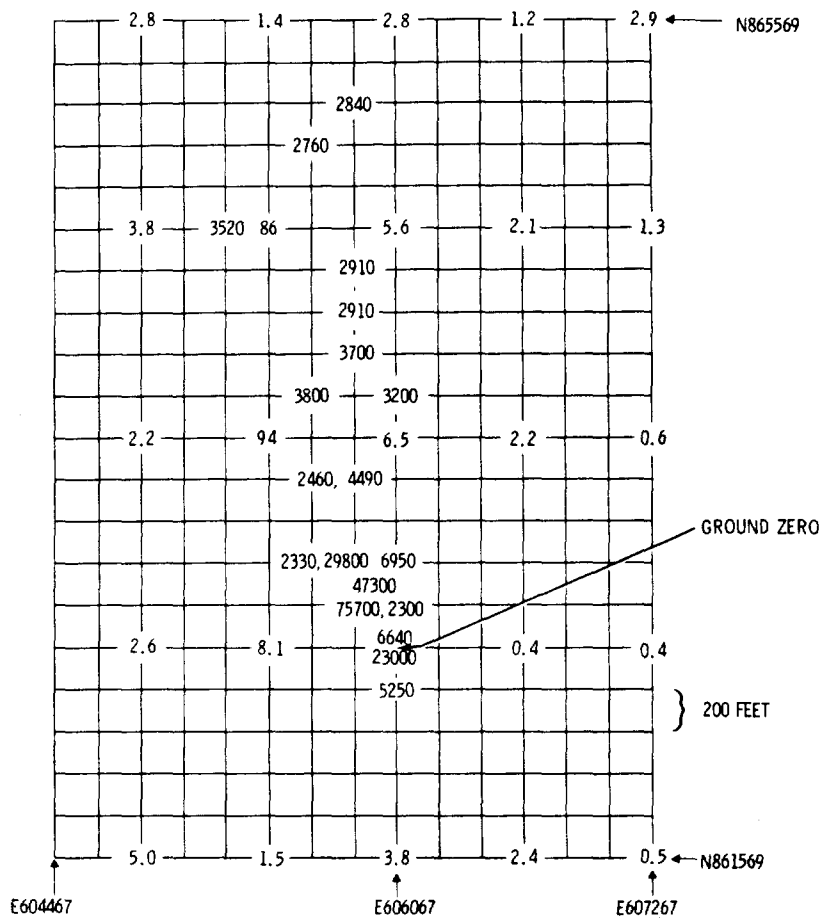

Figure 4. $^{239-240}$Pu Concentrations (pCi/g) in Surface (0-5 cm) Soil at Nuclear Site-201 (Concentrations are for < 2 mm soil; No ball-milling was done).

new Pu results from the stored library samples.* It is clear that Pu concentrations on the periphery of the 200-foot grid (to the south, east, and west) are in the picocurie per gram range. A series of five soil samples were also collected along an east-west line 4,000 feet north of the ground zero at NS-201. Table 1 gives the ^{137}Cs, Am, and estimated (see footnote in Table 1) Pu results for these samples. The data in Figure 4 and Table 1 suggest additional samples may be required further north along the fallout pattern if the extent of this pattern needs to be accurately known.

New Studies at Nuclear Sites-200, 201, and 202

Preliminary results available in the fall of 1976 at NS-201 resulted in the design of a more intensive soil sampling program at this site (discussed briefly by Gilbert *et al.*, 1977b). This new effort resulted in the collection of 320 additional soil samples at the grid points indicated in Figure 5. It is our understanding that these soil samples have not been shipped to analytical laboratories for Pu and other radionuclide analyses. If these analyses are completed in the future, the data could be used to estimate Pu spatial distribution and inventory using kriging and/or more conventional techniques. The preliminary grid data may also be useful in this effort. These early samples were selected to avoid rocky areas. Whether this tends to bias their concentrations relative to the later results collected on the grid in Figure 5 will need to be evaluated.

The new sampling effort at NS-201 also included additional samples of vegetation, metal fragments, and soil profiles (for both inventory and particle-size analysis purposes). In addition, samples from the large debris mound at ground zero were collected and quality assurance soil samples prepared. Results from these samples are not available at this time.

During 1977, we also began design work at NS-200 for estimating spatial distribution and inventory. By June, 1977, the Phase I grid design depicted in Figure 6 had been finalized and was available for implementation when resources became available. The location of Phase 1 sampling grids at NS's-201 and 202 are also shown in Figure 6 since they are in close proximity to NS-200. Phase 1 sampling plans for these two nuclear sites are given by Essington (1978). It's possible the fallout pattern of NS-200 overlaps that of NS-202. Hence, the narrow band between these two sites may also require sampling at some future date. The data from these three sites may indicate that the entire region should be considered as a single unit rather than three separate studies.

---

*Not included are 5 Pu concentrations for 0-2.5 cm soil samples collected at 0, 100, 300, 400, and 500 feet from ground zero along a transect. See Figures 7 and 9 in Gilbert *et al.* (1977b) for these results.

Table 1. Ge(Li) Results (pCi/g) on Soil Samples Collected on an East-West Line 4,000 Feet North of Ground Zero at Nuclear Site-201

Nevada Grid Coordinates*	^{137}Cs	^{241}Am	$^{239,240}Pu$***
E 607267	0.323 ± 55.3	N.D.	---
E 606667	1.01 ± 24.2	3.72 ± 39.1	42
E 606067	---	---	---
E 605467	2.21 ± 17.7	11.6 ± 18.3	130
E 604867	0.439 ± 48.4	---	---

*The north coordinate for all locations is N 866569.

**± % error (2σ).

***Based on an assumed median Pu to Am ratio of 11.2 estimated for NS-201 Gilbert *et al.*, 1977b).

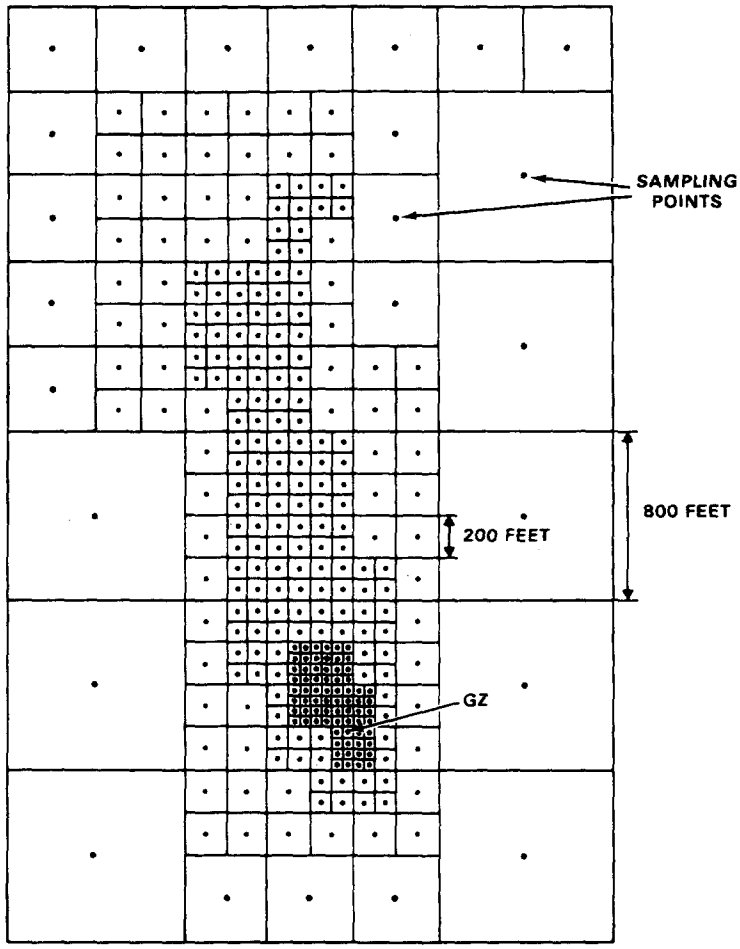

Figure 5. New Soil Sampling Grid at Nuclear Site-201, NTS, For Obtaining Estimates of $^{239-240}Pu$ Inventory and Distribution.

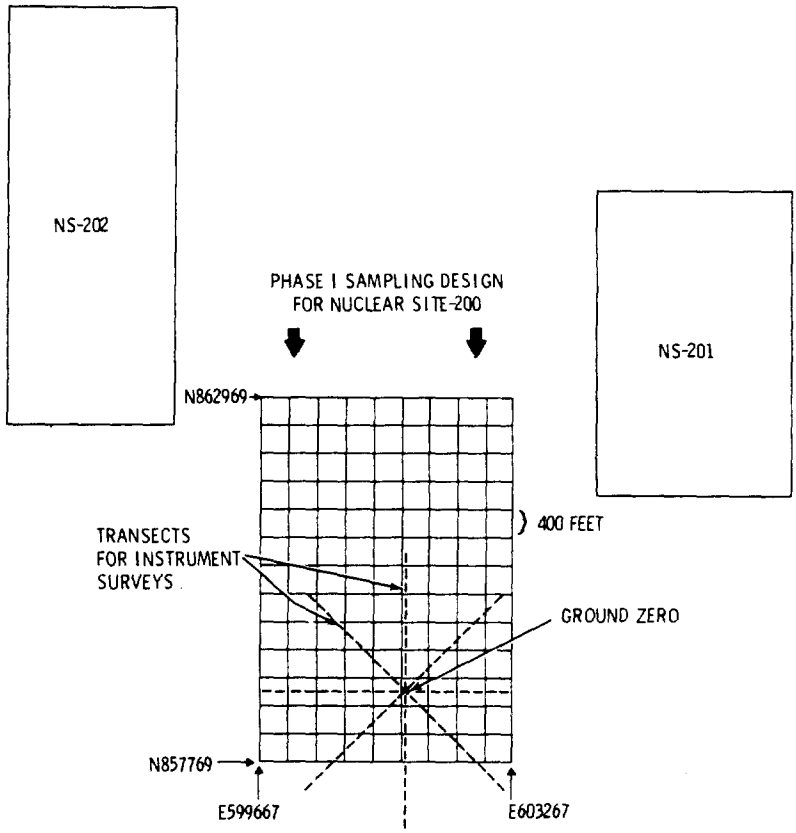

Figure 6. Phase 1 Sampling Grid Design for Nuclear Site-200 and the Location of Nuclear Sites-201 and 202 Grid Boundaries.

NSs-219 and 221 are also currently under study by the NAEG. Some preliminary information on these sites was given by Gilbert *et al.* (1977b). Phase 1 sampling was conducted at these sites during 1977. Dave Brady of REECo is the principal investigator at Ns's-219 and 221. Phase 1 results are discussed by Brady *et al.* (1978) and Essington (1978).

VARIABILITY WITH ALIQUOT SIZE STUDY AT NUCLEAR SITE-201

A special study at NS-201 was also conducted during 1977 to help evaluate the relationship between Am (Ge(Li)) concentrations in soil aliquots of different sizes (1, 10, 25, 50, and 100 grams). Twenty-four adjacent surface soil samples (5-inch diameter, 5-cm deep) were pooled together and mixed. All aliquots were withdrawn from the combined sample. The 24 samples were collected 150 feet from ground zero along a line transect (see Figure 9 in Gilbert *et al.*, 1977b, for the location of the transect). The Am activity at that location was about 1.9 nCi/g. Details concerning the statistical design and analyses of this study are given by Doctor and Gilbert (1978). This study was motivated in part by Wallace and Romney (1977a), who discuss the large variability expected in soil samples that have Pu concentrations at the low levels suggested for cleanup.

In general, these data indicate a linear relationship between aliquot variability (standard deviation) and aliquot size (both in logarithmic scale) over the range of aliquot sizes studied (standard deviation decreasing with aliquot size). A number of questions are raised by these results. Does this relationship also hold for Pu variability? Will this relationship be different in areas of higher or lower concentration? Will similar results prevail at safety-shot sites where larger particles of Pu may be present? We recommend that future studies be conducted at nuclear sites and safety-shot sites to evaluate these and other questions.

BLOW-SAND MOUND STUDIES

Initial Efforts

The original soil sampling for estimating surface (0-5 cm) inventory at safety-shot sites was not designed to study the amount or distribution of Pu within blow-sand mounds separately from desert pavement areas. It is true, however, that mounds were sampled, since soil sample locations were chosen at random within strata. However, the number sampled was

not sufficient to accurately estimate Pu inventory separately for mounds. Also, no information was obtained on amounts of Pu below 5 cm in mounds. Profiles to 25-cm depth were taken, but only in desert pavement areas.

In October, 1974, a mound study (now given the title Mound Study 1) was conducted near ground zero at C Site in Area 11 on NTS. Profile samples (each with ten 2.5-cm depth increments) in ten blow-sand mounds and ten adjacent desert pavement locations were collected and analyzed for Am using REECo's Ge(Li) system. These data were taken to obtain information on the distribution of Am with depth in mounds versus that in desert pavement. The results of this study have been discussed by Gilbert *et al.* (1975), Brady (1976), and Essington *et al.* (1977). This study indicated that for each 2.5-cm depth increment from the surface of the blow-sand and desert pavement profiles, the average Am concentration was higher in the blow-sand mound. Also, the depth at which Am occurred was less in desert pavement than in blow-sand mounds; and mound profiles had a smaller fraction of the total Am in the top 2.5 or 5 cm than did desert pavement profiles.

Mound Study 2

On the basis of these results, it was decided to initiate a larger-scale mound study (Mound Study (MS)-2) at two safety-shot sites: the Project 57 site in Area 13 and the Clean Slate 3 site on TTR. Information on the motivation, design, and protocol development of MS-2 is given by White and Dunaway (1976, pp. 33-122). Design aspects and results of statistical analyses of the resulting data are given by Essington *et al.* (1977) and Gilbert and Essington (1977).

The primary objective of MS-2 was to estimate the total amount (inventory) of Pu in blow-sand mounds at the two chosen study sites. This was accomplished by sampling entire mounds (actually "mound tops" and "mound bottoms" were collected separately) except for "diffuse" mounds at Clean Slate 3. These mounds were too large to collect in total. Desert pavement samples adjacent to the sampled mounds were also collected for comparison purposes. FIDLER readings over mounds and desert pavement were also taken.

A major finding of MS-2 was that roughly 60 to 65 percent of the total (mound top + mound bottom) mound inventory was estimated to be in mound bottoms even though Pu concentrations on a per gram dry weight basis were roughly twice as large in mound tops as in mound bottoms. At Clean Slate 3, about 70 percent of the total surface inventory (mound + desert pavement down to the 5-cm depth datum) was estimated to be in desert pavement areas. In Area 13, the percentage was about 85 percent. The FIDLER readings over mounds tended to be higher than those taken over adjacent desert pavement. This was also the case for soil concentrations when expressed on a per gram basis. Some data on the change in the Pu to Am ratio in soil over time is also presented by Essington *et al.* (1977) and Gilbert and Essington (1977).

Another interesting finding from MS-2 was that the estimate of Pu mound + desert pavement inventory at Area 13 was somewhat lower than the 46 + 9 curies reported by Gilbert (1977b) for just surface soil at Area 13. ("Surface soil" excluded the interior of mounds below 5-cm depth. This portion of the mound was included, however, in MS-2.) Gilbert and Essington (1977) discuss the possibility that the differences in estimates are due to sampling variability arising from the skewed nature of Pu soil concentrations, particularly near ground zero.

Much of our analyses of these mound data were accomplished during 1977 after the March, 1977, NAEG Pu Information Conference. The statistical analyses of these data are now essentially complete. While inventory estimates meet certain DOE requirements, we feel that particle-size studies at different depths of mounds would provide urgently needed information on potential hazards to man from inhalation or ingestion of Pu particles, if future mound studies are performed.

CLEANUP STUDIES

Initial Efforts

Sampling studies dealing with possible cleanup efforts at NTS and/or TTR study sites have been under discussion by NAEG scientists for several years. Wallace and Romney (1975) presented cleanup procedures and experience gained at a number of locations and gave an extensive reference list. A companion reference is that of Rhoads (1976), who gives a position paper on treatment of certain Pu-contaminated areas on NTS. Gilbert and Eberhardt (1976b) mention some planning needs for cleanup experiments, and Wallace and Romney (1977b) discuss what is known thus far on initial land reclamation procedures following a possible Pu-cleanup activity at TTR. Some possible approaches to the statistical analyses of data for deciding whether some type of cleanup or other remedial action is required at a particular site are considered by Gilbert and Eberhardt (1977) and Gilbert* (1977a). The design of sampling plans for cleanup purposes is discussed briefly by Eberhardt and Gilbert (1972).

Wide-ranging discussions on the design of cleanup treatment and trial experiments were conducted at NAEG meetings in Boulder City, Nevada, in March, 1975, and at Battelle-Northwest Laboratories in Richland, Washington, in October, 1975. The design of cleanup sampling plans was discussed

---

*Work funded by Division of Biomedical and Environmental Research, Department of Energy.

in separate letters to Paul Dunaway (NAEG) by R. O. Gilbert and E. B. Fowler in December of 1975, and there were undoubtedly other NAEG scientists considering various aspects of possible future cleanup activities.

Future Studies

During 1977, we prepared a protocol to take additional FIDLER, soil, and vegetation samples at the Clean Slate 2 site on TTR in anticipation of a possible remedial action or cleanup effort at that site. Aerial surveys by EG&G, Las Vegas, in February, 1977, indicated some additional sampling to refine estimates of Am surface contamination at this site. The field sampling design completed in October, 1977, is given in Figure 7. This design is an outgrowth of a preliminary plan sent to the NAEG in April, 1977. The sampling objectives are (i) to refine estimates of spatial patterns and inventory of Pu and Am, (ii) to evaluate whether a cattle grazing study might be conducted, and (iii) to collect information suitable to better define the area that might require remedial or cleanup action according to recently proposed EPA guidelines.* Soil samples to 1-, 2.5-, and 5-cm depths would be collected using 5-inch-diameter rings in the configuration shown in Figure 8. Surface FIDLER readings would be taken over each sampling ring and at 1-foot height over the cluster of three. The 1-cm samples would be sieved to 2-mm size and both fractions analyzed. The 1-cm samples on 2-mm size fractions are included since the proposed EPA guidelines call for this type of sample. At 23 grid locations, both 10- and 50-gram aliquots of soil would be analyzed for Pu (wet chemistry) and Am (Ge(Li) or wet chemistry). The 50-gram aliquots are included to help evaluate the variability of these larger aliquots relative to the standard 10-g NAEG aliquot size used up to the present time. This is motivated by results of the special aliquot size study discussed by Doctor and Gilbert (1978) that indicates substantial reduction in variability between aliquots from the same sample if 50-gram rather than 1- or 10-gram aliquots are used.

There are a number of other sampling questions that need to be studied in anticipation of possible cleanup efforts. There is a need, e.g., to determine under what conditions and levels of contamination FIDLER field data could be used in such studies. A great many FIDLER readings taken at a height of 1 foot were obtained at safety-shot sites (Gilbert and Eberhardt, 1974, and Gilbert *et al.*, 1975) that could be examined in greater detail. Information on FIDLER readings taken at the soil surface as well as at 1-foot height were taken as part of the "variability with distance" study conducted in Area 13 (see Doctor and Gilbert, 1978). More information of this type will be generated in the Clean Slate 2

---

*Proposed Guidance on Dose Limits for Persons Exposed to Transuranium Elements in the General Environment," FEDERAL REGISTER NOTICE, November 1977. U.S. Environmental Protection Agency, Office of Radiation Programs, Washington, D.C. 20460.

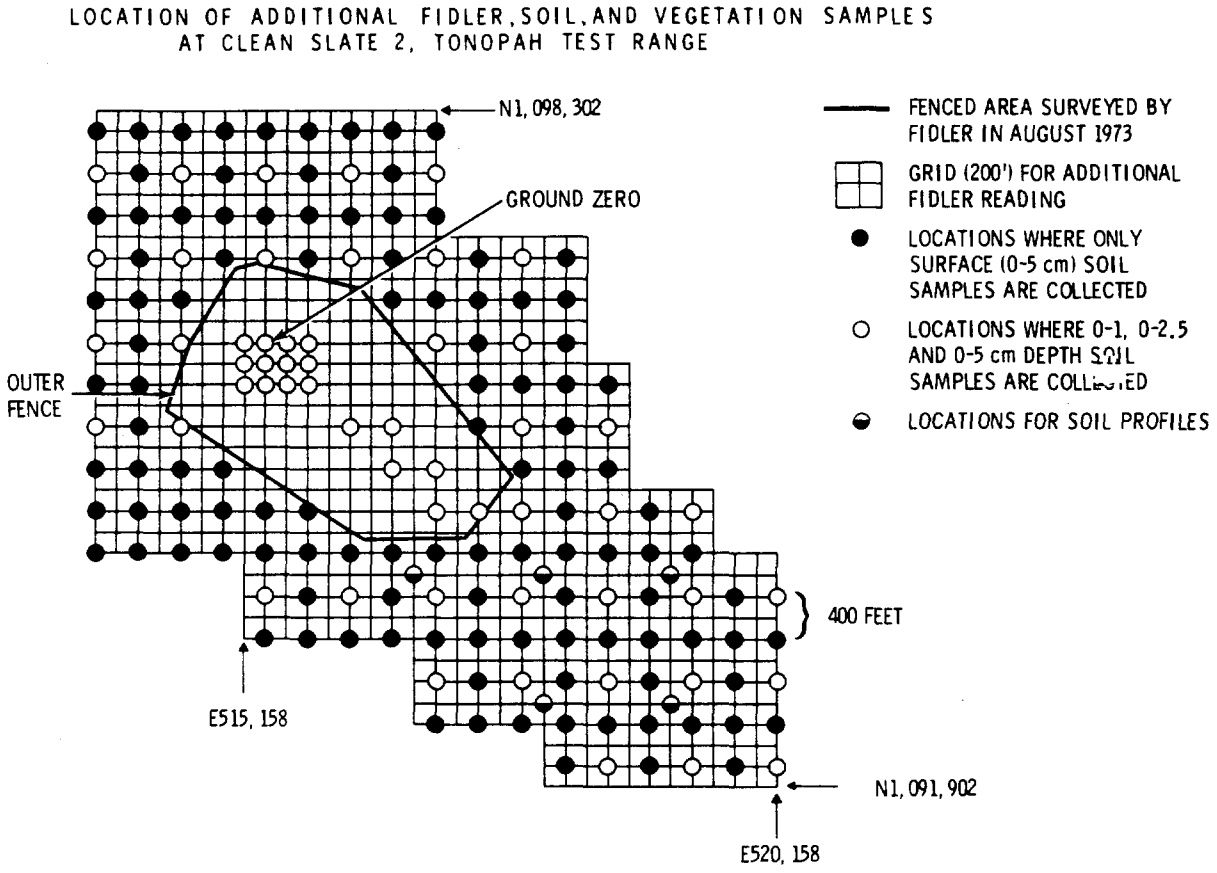

Figure 7. Sampling Design for Possible Future Studies at Clean Slate 2, TTR.

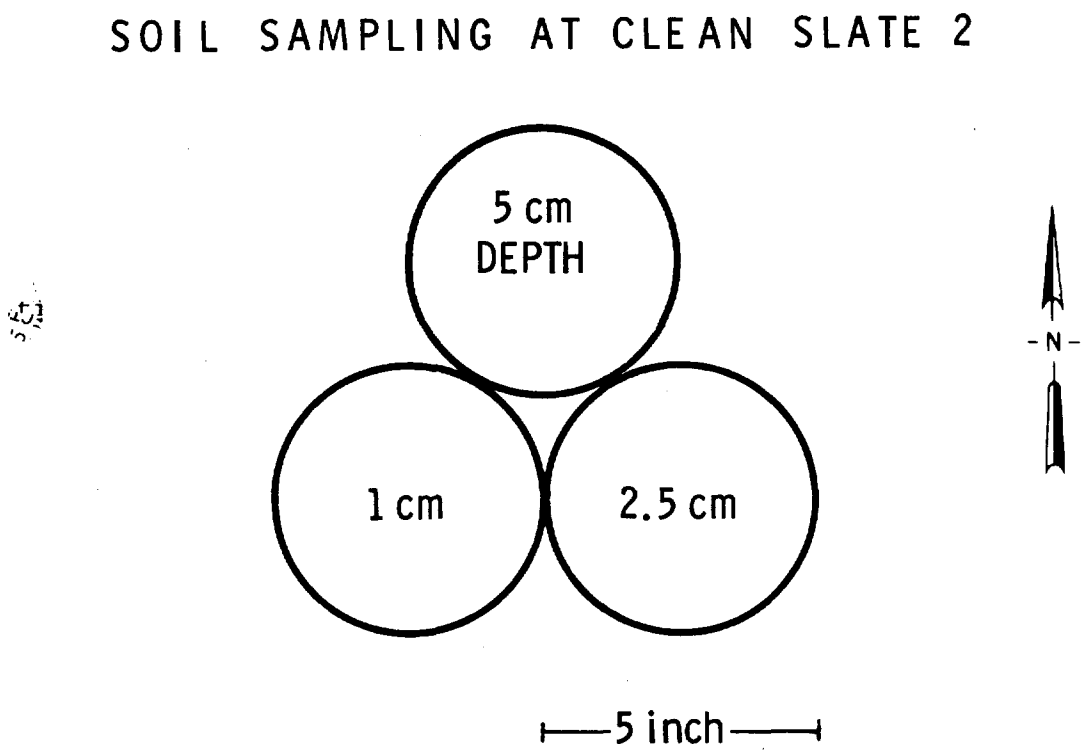

Figure 8. Proposed Arrangement of Soil Sampling Rings at Selected Locations at Clean Slate 2 (see Figure 7) to Investigate Pu and Am Concentration with Depth.

study discussed above. Special studies using the FIDLER at other heights would be desirable. An important source of information is Tinney (1968), who discusses the calibration of the FIDLER instrument at 1-foot height. Also, a great deal of experience is presently being gathered on mobile field detectors in connection with the Enewetak Atoll cleanup effort (Ms. Madaline Barnes, Desert Research Institute, Las Vegas, should be contacted for statistical details). These data should be carefully studied.

SYNTHESIS

Our principal contribution to the synthesis of soil, vegetation, small mammal, and cattle Pu concentration data appeared in Gilbert *et al.* (1977a). Data for these sample types collected at the Project 57 site in Area 13 were plotted on a single graph as an aid to understanding the total data picture. Hypothetical Pu concentrations in tissues of a standard man assumed to live in and obtain most of his food from the area was also computed and plotted. These hypothetical values were obtained using the Pu transport and dose estimation model of Martin and Bloom (1976). Our synthesis efforts during 1977 involved relating estimates of Pu inventory in blow-sand mounds to previous Pu inventory estimates in surface soil (Gilbert and Essington, 1977). There is clearly a need for more extensive synthesis efforts in the future. Considerably more small mammal data is available now at several safety-shot sites than was the case in 1976. More cattle data from Area 13 are also available. How this synthesis effort should be organized is open to question. One approach would be to have one or two individual investigators be responsible for synthesizing certain available data and to assist in making recommendations regarding the design and coordination of future synthesis efforts.

OTHER ACTIVITIES

In Table 2, we list a number of statistical topics not discussed above that we have studied for the NAEG during the period 1971-1977. All references except numbers 16 and 18 were funded wholly or in part by the NAEG. This list does not include papers on these topics by other NAEG scientists that have appeared in NAEG publications or under NAEG sponsorship.

Table 2. Some References Dealing With Topics Not Discussed Elsewhere in This Paper

Topic	Reference Number*
Counting Statistics	15
Coefficient of Variation	7, 8, 19, 20, 24
Compositing	7, 8, 18
Data Summarization (Methods)	27
Estimation of Ratios (Pu/Am, Veg./Soil)	5, 8, 19, 21, 24, 31, 32, 33, 34
Field Design Guidelines	22
Frequency Distributions	4, 7, 14, 19
Interlaboratory Comparisons	8, 19, 20, 24
Microplot Study (Area 13)	8, 19, 24, 31
Models	7, 9, 27, 29
NAEG Data Bank (Philosophy)	13
Soil Profiles	10, 11, 12, 19, 20, 24, 26, 28

*Numbers correspond to reference numbers in the reference list of this paper.

SUMMARY

In this paper, we have attempted to review the extent of our statistical design and analysis activities for the NAEG since 1971. This review includes our activities during Calendar Year 1977 with regard to Mound Study 2, nuclear site studies, and planning for possible future cleanup efforts at Clean Slate 2. We have also pointed out the current status of these projects for future planning purposes. We wish to note again the following:

1. Pu and Am concentrations on over 500 new soil and vegetation samples from safety-shot sites are essentially ready for statistical analysis to update estimates of Pu spatial pattern and inventory. These data are in the NAEG data bank and also on computer cards at Battelle-Northwest.

2. Three hundred twenty soil samples have been collected at the grid intersections in Figure 5 at NS-201, but have not been shipped to analytical laboratories for radionuclide analyses. If these data are obtained, they would be useful for estimating spatial pattern and inventory of radionuclides at NS-201.

3. Plans are ready for Phase 1 sampling to begin at several nuclear sites including NS-200 discussed in this paper and NS's-202 and 203 as discussed by Essington (1978).

4. Design plans for additional studies at Clean Slate 2 in anticipation of a possible cleanup effort at that site have been submitted to the NAEG. Samples of the type specified in recent EPA guidelines should be collected for evaluation of their applicability to NTS and TTR sites.

5. Statistical analyses for the estimation of Pu inventory in blow-sand mounds at Area 13 and Clean Slate 3 are completed (Gilbert and Essington, 1977). Particle size and spatial distribution aspects of Pu and Am are suggested as future blow-sand mound studies.

6. FIDLER and other mobile field detectors should continue to be evaluated for their applicability to field studies. Special studies aimed at calibrating more closely these instrument readings to Pu concentrations in field samples are encouraged.

7. A comprehensive synthesis of NAEG data needs attention. A definition of "synthesis" is needed before such an effort begins.

ACKNOWLEDGMENTS

We wish to thank Paul Dunaway, Mary White, Don Wireman, and Winnie Howard of the NAEG administrative staff, who have supported and encouraged our work over the past years. Our work could not have been accomplished without their personal goodwill, patience, and sustaining friendship.

REFERENCES

1. Barnes, M. G., P. Delfiner, and R. O. Gilbert. 1977. "A New Statistical Tool, Kriging, and Some Applications to Area 13 Data." *In: Transuranics in Desert Ecosystems*. M. G. White, P. B. Dunaway, and D. L. Wireman (Eds.). USDOE Report, NVO-181. pp. 431-445.

2. Brady, D. N. 1976. "Results of Preliminary Study of Soil Mound and Desert Pavement Vertical Profile Pairs in Area 11, NTS." *In: Nevada Applied Ecology Group Procedures Handbook for Environmental Transuranics*. M. G. White and P. B. Dunaway (Eds.). USERDA Report, NVO-166. pp. 53-58.

3. Brady, D. N., L. M. Rakow, and C. E. Rosenberry, Jr. 1978. "On-Site REECo Support Activities for 1977." (This report.)

4. Delfiner, P., and R. O. Gilbert. 1978. "Combining Two Types of Survey Data for Estimating Geographical Distribution of Plutonium in Area 13." (This report.)

5. Doctor, P. G., and R. O. Gilbert. 1977. "Ratio Estimation Techniques in the Analysis of Environmental Radionuclide Data." *In: Transuranics in Natural Environments*. M. G. White and P. B. Dunaway (Eds.). USERDA Report, NVO-178. pp. 601-620.

6. Doctor, P. G., and R. O. Gilbert. 1978. "Two Studies in Variability for Soil Concentrations: With Aliquot Size and With Distance." (This report.)

7. Eberhardt, L. L. 1976. "Sampling for Radionuclides and Other Trace Substances." *In: Radioecology and Energy Resources*. C. E. Cushing, Jr. (Ed.). Dowden, Hutchinson, and Ross, Inc., Stroudsburg, PA. pp. 199-208.

8. Eberhardt, L. L., and R. O. Gilbert. 1972. "Statistical Analysis of Soil Plutonium Studies, Nevada Test Site." Battelle Pacific Northwest Laboratories, Richland, WA. BNWL-B-217.

9. Eberhardt, L. L., and R. O. Gilbert. 1974. "General Statistical Considerations in Environmental Plutonium Studies." *In: The Dynamics of Plutonium in Desert Environments*. P. B. Dunaway and M. G. White (Eds.). USAEC Report, NVO-142. pp. 43-49.

10. Essington, E. H. 1978. "Soil Radioactivity Distribution Studies for the Nevada Applied Ecology Group." (This report.)

11. Essington, E. H., E. B. Fowler, R. O. Gilbert, and L. L. Eberhardt. 1976. "Plutonium, Americium, and Uranium Concentrations in Nevada Test Site Soil Profiles." *In: Transuranium Nuclides in the Environment.* International Atomic Energy Agency, Vienna. pp. 157-174.

12. Essington, E. H., R. O. Gilbert, D. L. Wireman, D. N. Brady, and E. B. Fowler. 1977. "Plutonium, Americium, and Uranium in Blow-Sand Mounds of Safety-Shot Sites at the Nevada Test Site and Tonopah Test Range." *In: Transuranics in Desert Ecosystems.* M. G. White, P. B. Dunaway, and D. L. Wireman (Eds.). USDOE Report, NVO-181. pp. 81-146.

13. Gilbert, R. O. 1976a. "Philosophy and Mechanics of Synthesizing Data From Different Data Bases." *In: Nevada Applied Ecology Group Procedures Handbook for Environmental Transuranics.* M. G. White and P. B. Dunaway (Eds.). USERDA Report, NVO-166. pp. 471-476.

14. Gilbert, R. O. 1976b. "On the Estimation of Spatial Pattern for Environmental Contaminants." Battelle Pacific Northwest Laboratories, Richland, WA. BNWL-SA-5771. (Also appears in this report.)

15. Gilbert, R. O. 1976c. "Recommendations Concerning the Computation and Reporting of Counting Statistics for the NAEG". *In: Nevada Applied Ecology Group Procedures Handbook for Environmental Transuranics.* M. G. White and P. B. Dunaway (Eds.). (Also published by Battelle Pacific Northwest Laboratories, Richland, WA, 1974, BNWL-B-368). USERDA Report, NVO-166. pp. 405-470.

16. Gilbert, R. O. 1977a. "TRAN-STAT (Statistics for Environmental Transuranic Studies)." Battelle Pacific Northwest Laboratories, Richland, WA. November, Number 2, PNL-SA-6696.

17. Gilbert, R. O. 1977b. "Revised Total Amounts of $^{239,240}Pu$ in Surface Soil at Safety-Shot Sites." *In: Transuranics in Desert Ecosystems.* M. G. White, P. B. Dunaway, and D. L. Wireman (Eds.). USDOE Report, NVO-181. pp. 423-429.

18. Gilbert, R. O. 1978. "TRAN-STAT (Statistics for Environmental Transuranic Studies)." Battelle Pacific Northwest Laboratories, Richland, WA. February, Number 3, PNL-SA-6697.

19. Gilbert, R. O., and L. L. Eberhardt. 1974. "Statistical Analysis of Pu in Soil at the Nevada Test Site--Some Results." *In: The Dynamics of Plutonium in Desert Environments.* P. B. Dunaway and M. G. White (Eds.). USAEC Report, NVO-142. pp. 51-90.

20. Gilbert, R. O., and L. L. Eberhardt. 1976a. "Statistical Analysis of 'A Site' Data and Interlaboratory Comparisons for the Nevada Applied Ecology Group." *In: Studies of Environmental Plutonium and Other Transuranics in Desert Ecosystems.* M. G. White and P. B. Dunaway (Eds.). USERDA Report, NVO-159. pp. 117-154.

21. Gilbert, R. O., and L. L. Eberhardt. 1976b. "Some Statistical Design and Analysis Aspects for Nevada Applied Ecology Group Studies." *In: Studies of Environmental Plutonium and Other Transuranics in Desert Ecosystems*. M. G. White and P. B. Dunaway (Eds.). USERDA Report, NVO-159. pp. 101-116.

22. Gilbert, R. O., and L. L. Eberhardt. 1977. "Some Design Aspects of Transuranic Field Studies." *In: Transuranics in Natural Environments*. M. G. White and P. B. Dunaway (Eds.). USERDA Report, NVO-178. pp. 575-592.

23. Gilbert, R. O., and E. H. Essington. 1977. "Estimating Total $^{239,240}Pu$ in Blow-Sand Mounds of Two Safety-Shot Sites." *In: Transuranics in Desert Ecosystems*. M. G. White, P. B. Dunaway, and D. L. Wireman (Eds.). USDOE Report, NVO-181. pp. 367-445.

24. Gilbert, R. O., L. L. Eberhardt, E. B. Fowler, E. M. Romney, E. H. Essington, and J. E. Kinnear. 1975. "Statistical Analysis of $^{239,240}Pu$ and ^{241}Am Contamination of Soil and Vegetation on NAEG Study Sites." *In: The Radioecology of Plutonium and Other Transuranics in Desert Environments*. M. G. White and P. B. Dunaway (Eds.). USERDA Report, NVO-153. pp. 339-448.

25. Gilbert, R. O., L. L. Eberhardt, E. B. Fowler, and E. H. Essington. 1976a. "Statistical Design Aspects of Sampling Soil for Plutonium." *In: Atmosphere-Surface Exchange of Particulate and Gaseous Pollutants (1974)*. R. J. Engelmann and G. A. Sehmel (Eds.). USERDA, Technical Information Center, Oak Ridge, TN. ERDA Symposium Series 38. pp. 689-708.

26. Gilbert, R. O., L. L. Eberhardt, E. B. Fowler, E. M. Romney, and E. H. Essington. 1976b. "Statistical Analysis and Design of Environmental Studies for Plutonium and Other Transuranics at NAEG 'Safety-Shot' Sites." *In: Transuranium Nuclides in the Environment*. IAEA-SM-199/67. IAEA, Vienna. pp. 449-460.

27. Gilbert, R. O., L. L. Eberhardt, and D. D. Smith. 1977a. "An Initial Synthesis of Area 13 ^{239}Pu Data and Other Statistical Analyses." *In: Environmental Plutonium on the Nevada Test Site and Environs*. M. G. White, P. B. Dunaway, and W. A. Howard (Eds.). USERDA Report, NVO-171. pp. 237-274.

28. Gilbert, R. O., E. H. Essington, D. N. Brady, P. G. Doctor, and L. L. Eberhardt. 1977b. "Statistical Activities During 1976 and the Design and Initial Analysis of Nuclear Site Studies." *In: Transuranics in Desert Ecosystems*. M. G. White, P. B. Dunaway, and D. L. Wireman (Eds.). USDOE Report, NVO-181. pp. 331-422.

29. Martin, W. E., and S. G. Bloom. 1976. "Plutonium Transport and Dose Estimation Model." *In: Transuranium Nuclides in the Environment*. IAEA-SM-199/78. IAEA, Vienna. pp. 385-400.

30. Rhoads, W. A. 1976. "A Wise Resolution of the Pu-Contaminated Lands Problem in Certain Parts of NTS May Be to Isolate and Maintain Them Without Further Disturbances: A Position Paper." *In: Studies of Environmental Plutonium and Other Transuranics in Desert Ecosystems*. M. G. White and P. B. Dunaway (Eds.). USERDA Report, NVO-159. pp. 165-180.

31. Romney, E. M., A. Wallace, R. O. Gilbert, S. A. Bamberg, J. D. Childress, J. E. Kinnear, and T. L. Ackerman. 1974. "Some Ecological Attributes and Plutonium Contents of Perennial Vegetation in Area 13." *In: The Dynamics of Plutonium in Desert Environments*. P. B. Dunaway and M. G. White (Eds.). USAEC Report, NVO-142. pp. 91-106.

32. Romney, E. M., A. Wallace, R. O. Gilbert, and J. E. Kinnear. 1975. "^{239,240}Pu and ^{241}Am Contamination of Vegetation in Aged Plutonium Fallout Areas." *In: The Radioecology of Plutonium and Other Transuranics in Desert Environments*. M. G. White and P. B. Dunaway (Eds.). USERDA Report, NVO-153. pp. 43-88.

33. Romney, E. M., A. Wallace, R. O. Gilbert, and J. E. Kinnear. 1976. ^{239,240}Pu and ^{241}Am Contamination of Vegetation in Aged Fall-Out Areas." *In: Transuranium Nuclides in the Environment*. International Atomic Energy Agency, Vienna. pp. 479-492.

34. Romney, E. M., R. O. Gilbert, A. Wallace, and J. E. Kinnear. 1977. "Estimated Inventory of Plutonium and Uranium Radionuclides for Vegetation in Aged Fallout Areas." *In: Environmental Plutonium on the Nevada Test Site and Environs*. M. G. White, P. B. Dunaway, and W. A. Howard (Eds.). USERDA Report, NVO-171. pp. 35-52.

35. Tinney, J. F. 1968. "Calibration of an X-Ray Sensitive Plutonium Detector". *In: Hazards Control Progress Report No. 31* (May-August). Lawrence Radiation Laboratory, University of California, Livermore, CA. TID-4500, UCRL-50007-68-2.

36. Wallace, A., and E. M. Romney. 1975. "Feasibility and Alternate Procedures for Decontamination and Post-Treatment Management of Pu-Contaminated Areas in Nevada." *In: The Radioecology of Plutonium and Other Transuranics in Desert Environments*. M. G. White and P. B. Dunaway (Eds.). USERDA Report, NVO-153. pp. 251-338.

37. Wallace, A., and E. M. Romney. 1977a. "The Particle Size Problem in the Assay of Plutonium in Field Soil Samples." *In: Transuranics in Desert Ecosystems*. M. G. White, P. B. Dunaway, and D. L. Wireman (Eds.). USDOE Report, NVO-181. pp. 41-52.

38. Wallace, A., and E. M. Romney. 1977b. "Initial Land Reclamation Procedures Related to Possible Pu-Cleanup Activities at the Tonopah Test Range." *In: Environmental Plutonium on the Nevada Test Site and Environs*. M. G. White, P. B. Dunaway, and W. A. Howard (Eds.). USERDA Report, NVO-171. pp. 65-78.

39. White, M. G., and P. B. Dunaway (Eds.). 1976. *Nevada Applied Ecology Group Procedures Handbook for Environmental Transuranics*. USERDA Report, NVO-166. pp. 33-122.

SIMULATION OF PLUTONIUM INGESTION BY GRAZING CATTLE

W. E. Martin and S. G. Bloom

Battelle's Columbus Laboratories
Columbus, Ohio

ABSTRACT

A simple model of plutonium ingestion by cattle grazing a uniformly contaminated pasture is $I_{Pu} = I_v C_v + I_s C_s$ where I_{Pu} is the plutonium ingestion rate (pCi/day), I_v and I_s are vegetation and soil ingestion rates (g/day), C_v and C_s are plutonium concentrations (pCi/g) in vegetation and soil. In a ground zero area such as the inner compound of Area 13 (NTS), where the spatial distribution of plutonium is nonuniform and highly variable, the simple ingestion model seems to require a stochastic interpretation.

This paper provides evidence for assuming that the five factors of the ingestion model are lognormally distributed. Estimates of the geometric means and standard deviations of the four factors on the right side of the model equation were used to generate synthetic random samples of I_v, I_s, C_v, and C_s. The means of these synthetic samples were then used to obtain iterative solutions of the model equation in which the factors on the right were varied randomly and independently within the limits specified by the synthetic geometric means and standard deviation. The resulting synthetic composite random sample of I_{Pu} (n = 500 days) indicated an average plutonium ingestion rate, for a hypothetical 410-kg cow grazing the inner compound of Area 13, of 557 ± 526 nCi/day. Subsamples (n = 100 days) ranged from 486 ± 330 to 629 ± 526 nCi/day. This result compares favorably with previous estimates: 565 nCi/day based on fistulated steer rumen contents (Smith *et al.*, 1976), 620 nCi/g based on an assumed diet of winterfat and shadscale (Gilbert *et al.*, 1977), and 585 nCi/day based on general theoretical considerations (Martin and Bloom, 1977).

The conclusions to be drawn from these simulation studies are: (1) that the grazing, soil, and plant studies conducted in Area 13 were apparently well designed; (2) that a repetition of the study would probably yield results similar to those already obtained; (3) that given an adequate sampling design, reasonably accurate estimates of plutonium ingestion rates by grazing cattle can be obtained in spite of the extreme variability of the contributing factors; and (4) that given site-specific

input parameters, the simulation model provides estimates of I_{Pu} which are as accurate as those obtained from long-term grazing studies relying on fistulated steers.

INTRODUCTION

Studies of large grazing animals in plutonium-contaminated areas of the Nevada Test Site have been somewhat restricted by the fact that most such areas are relatively small and unable to support more than one or a few animals for any appreciable period of time. Area 13* was chosen for the EPA grazing study because it is larger ($\sim$ 402 hectares) than most plutonium-contaminated areas at NTS and because the vegetation available to grazing animals is better than average. One cow was kept in the inner compound of Area 13 for 177 days. On 14 separate occasions, four fistulated steers were pastured for three days in the same enclosure (see the article by D. D. Smith in this publication). Based on plutonium concentrations in the vegetation (semisolid) and fluid portions of the rumen contents of the fistulated steers, Smith *et al.* (1976) estimated that the cow's total plutonium intake during 177 days of grazing the inner compound was 100 μCi, which amounts to an average plutonium ingestion rate of about 565 nCi/day.

According to Gilbert *et al.* (1977), the average total weight of material removed from the rumens of the fistulated steers was about 30 kg and the average vegetation ingestion rate was about 6 kg/day (dry weight). Using this estimated ingestion rate, an assumed diet of 64 percent shadscale (*Atriplex canescens*) and 36 percent winterfat (*Eurotia lanata*), and the plutonium concentrations for shadscale and winterfat reported by Romney *et al.* (1975), Gilbert *et al.* (1977) estimated the cow's average plutonium ingestion rate as 620 nCi/day. The hypothetical diet was a composite in which the fraction contributed by each sampling stratum was proportional to the area of the stratum. Neither Smith *et al.* (1976) nor Gilbert *et al.* (1977) considered soil ingestion as a separate component of plutonium ingestion. Martin and Bloom (1977), considering both vegetation and soil ingestion, provided a third estimate of 585 nCi/day based on general theoretical considerations of factors which apply to NTS as a whole but are not site-specific for the inner compound of Area 13.

---

*Maps of Area 13, showing fences and sampling strata, appear elsewhere in this publication. See the article by Delfiner and Gilbert in this report.

Considering the extreme variability of plutonium concentrations in vegetation and soil samples taken from Area 13 by other members of the NAEG and the inherent uncertainties involved in estimating vegetation and soil ingestion rates, the writers of this article felt it would be worthwhile to reexamine the available vegetation and soil data and the theoretical basis for estimating plutonium ingestion rates for herbivores. This led to the development of a quasistochastic model for simulating the ingestion of plutonium by a hypothetical cow or a hypothetical herd of cattle grazing the inner compound of Area 13, unhampered by the real-world restrictions imposed by limited space and vegetation. By means of a simulation model, the area in question can be hypothetically stocked with as many cows as might be desired and for as long a period of time as might be deemed appropriate. Based on well-defined assumptions and making full use of available data, a simulation model based on strictly defined random processes should provide a fair estimate of the mean plutonium ingestion rate as well as an idea of the range of mean values and error terms that might be expected from hypothetical experiments conducted with or without the restrictions imposed on real-world experiments.

THE MODEL

In previous studies (Martin and Bloom, 1976 and 1977), it was assumed that cattle grazing a plutonium-contaminated desert range would ingest both vegetation and soil and that the total plutonium ingestion rate could be expressed by

$$I_{Pu} = I_v C_v + I_s C_s \qquad (1)$$

where, I_{Pu} is the plutonium ingestion rate, pCi/day,
I_v is the vegetation ingestion rate, g/day (dry weight),
C_v is the plutonium concentration, pCi/g, in vegetation,
I_s is the soil ingestion rate, g/day,
and C_s is the plutonium concentration, pCi/g, in soil.

Cattle are assumed to graze randomly within the fenced area (95.5 ha) of the inner compound. What this assumption means, in effect, is that if the area of the inner compound were divided into a grid of very small squares all the same size, each subdivision would have an equal probability of contributing to the intake of vegetation and soil. Individual animals may exhibit a preference for one subarea compared to another or for one plant species compared to another. A whole herd of animals may exhibit seasonal preferences with respect to subdivisions of the fenced area or with respect to plant species, and similar unspecified but nonrandom behavior patterns may apply to the ingestion of soil. The point of the "random-grazing-assumption" is that during the course of a year, the total vegetation and soil consumption by a herd of grazing

cattle would be expected to comprise a composite random sample of the vegetation and soils present in the compound, and the contribution of each sampling stratum to the herd's composite diet of vegetation and soil would be proportional to the area of the sampling stratum divided by the total area of the compound.

In subsequent sections of this report, the means and standard deviations of I_v, C_v, I_s, and C_s will be estimated. These estimates of population parameters, μ and σ, and a random number generator described in Appendix I will be used to generate synthetic composite random samples of I_{Pu} which are iterative solutions of Equation 1 for which each of the four factors on the right side of the equation is an independent random variable specified by its estimated mean and standard deviation. The means and standard deviations of these synthetic samples will provide the basis for generating synthetic composite random samples of I_{Pu}. Comparing these simulation results with the previous estimates of I_{Pu}, described in the Introduction, should provide a rough idea of the probable accuracy of I_{Pu} estimation in general.

Vegetation Ingestion Rate

The fistulated steer data mentioned in the introduction and discussed elsewhere in this volume (see the article by D. D. Smith) provide the best empirical basis for estimating rates of vegetation ingestion by cattle grazing the inner compound of Area 13. At this writing, however, the only data at hand are the concentrations (nCi/kg) of plutonium in the vegetation and fluid components of rumen contents. Data concerning the weights of these components, the body weights of the fistulated steers, and the fraction of daily intake represented by a 24-hour rumen sample are also required for estimating I_{Pu}. While simulation studies based on fistulated steer data will be deferred until the complete data set is available for examination, it is worth noting here that the plutonium concentrations published in Appendices III and IV of Smith's paper (this volume) appear to be lognormally distributed and that this is quite in line with expectations based on examination of other data sets concerning the distribution of plutonium in Area 13.

For simulation purposes, estimates of vegetation ingestion rates are based on a theoretical model formulated as follows:

$$I_v = 163.5\ W^{0.73}/4.5\ D \qquad (2)$$

where I_v is the vegetation ingestion rate, g/day,
$163.5\ W^{0.73}$ is the digestible energy, kcal/day, required for maintenance of an adult cow (Siegmund, ed., 1967),
W is the total live body weight, kg, of the cow,
4.5 kcal/g is the caloric value of most plant materials (Golley, 1961),
and D is the digestibility (dimensionless) of ingested vegetation.

To generate synthetic random samples of I_v based on Equation 2, body weight (W) and digestibility (D) were assumed to vary normally with means and standard deviations of 410 ± 82 kg and 0.48 ± 0.12, respectively. Random variation of body weight simulates variations in apparent metabolic weight and appetite while random variation of digestibility simulates variations in quality of vegetation ingested. The mean body weight was chosen to match that of the 409-kg cow left in the inner compound for 177 days. A mean digestibility of 0.48 was chosen to match the Gilbert *et al.* (1977) estimate of $I_v \approx 6$ kg/day (dry weight). When D is held constant and W is allowed to vary normally, synthetic samples of I_v based on Equation 2 had means close to 6,000 g/day and exhibited apparently normal distributions. When both W and D were varied normally, as indicated above, synthetic samples of I_v based on Equation 2 exhibited lognormal distributions. A histogram of one such synthetic sample is shown in Figure 1.* The arithmetic mean of this sample (n = 100) was 6,760 ± 2,439 g/day. The median, indicated by exp ($\overline{xg}$), was 6,400 g/day. Both of these values are higher than the value obtained (6,006 g/day) by substituting the assumed means of W and D in Equation 2.

Soil Ingestion Rate

Cattle are known to ingest quantities of soil and a variety of other nonfood items such as flagging material, rope, and rubber boots. In some regions, cattle occasionally ingest so much soil that their gastrointestinal tracts are blocked and massive doses of castor oil are required to relieve the situation. In earlier modeling studies (Martin and Bloom, 1976 and 1977), soil ingestion rates were conservatively assumed to be as much as 2,000 g/day, a quantity which would probably result in the problem mentioned above.

The only site-specific soil ingestion data presently available were provided by Smith (1977), who reported the weights of soil recovered from the rumen and reticula of three cows which had been grazing the outer compound of Area 13 just prior to sacrifice in January, 1976. The quantities reported were 8.5 g, 57.3 g, and 278 g. As Smith aptly observed, "These data suggest that the total amount of soil ingested is much less than 2 kg per day and that a reasonable estimate would be between 0.25 and 0.5 kg."

The arithmetic mean and standard deviation of 8.5, 57.3, and 278 are 115 ± 144 g/day. Since the coefficient of variation (144/115) is greater than 1, a lognormal distribution is assumed. (Note also that the numbers

---

*All the histograms, Figures 1-8, have been normalized and the "normality" of distribution has been "confirmed" by chi square tests comparing observed cell counts with frequencies expected for a normal distribution.

approximate a logarithmic sequence to the base 2.) The mean and standard deviation of ln 8.5, ln 57.3, and ln 278 are 3.9387 ± 1.7464. To estimate the magnitude of a "reasonable estimate" based on these three measurements, the log mean and standard deviation were used to generate a synthetic sample (n = 500) of I_s. The individual values based on ln I_s = 3.9387 ± 1.7464 ranged from 2 g/day to 3,575 g/day; the overall mean (n = 500) was 213 ± 609 g/day.

Plutonium Concentrations in Vegetation and Soil

The concentrations of plutonium (pCi/g) in vegetation and soil samples collected from Area 13 are listed in Tables 1 and 2. The areas of sampling strata are given in Table 3. The arithmetic (normal) and geometric (lognormal) estimates of population parameters for each sampling stratum are given in Table 4.

The raw data of Tables 1 and 2 and their natural logarithms were used to construct normalized histograms in which the cell width on the horizontal axis is determined by $z = (x-\bar{x}g)/sg$, where x is the limit between two cells, $\bar{x}g$ is the mean, and sg is the standard deviation of the sample set. The vertical height of the cell is the number of variates (frequency of observations) that fall in the cell interval divided by the total number of variates (n) in the sample. To facilitate comparison, a normal curve, i.e., $\phi(z) = (s(2\Pi)^{1/2})^{-1} \exp(-1/2\ z^2)$, was sketched on the same coordinates.

The histogram (not shown) for $C_v(1,2)$, the concentrations (Table 1) of plutonium in vegetation samples from strata 1 and 2, was sharply skewed to the right, suggesting a lognormal distribution, while the histogram of ln $C_v(1,2)$ was sharply skewed to the left, suggesting a truncated lognormal distribution. Maps of Area 13 sampling strata (see the article by Delfiner, and Gilbert, this volume) show that parts of strata 1 and 2 extend beyond the fenced area and were not sampled. In other words, the apparently truncated distribution curve appears to be a true reflection of the actual situation.

The histogram of ln $C_v(1\text{-}5)$, Figure 2, is not perfectly symmetrical, but the observed cell counts (5, 17, 35, 21, 17, 9) are close to the counts expected for a normal curve (5.3, 16.5, 29, 29, 16.5, 5.3). A chi square test, comparing the observed and expected cell counts, indicated χ^2 = 3.1547 and $P(\chi^2) = 0.3239$. As $P(x^2) \geq 0.95$ is required for rejection of the null hypothesis, the test provides no basis for rejecting the hypothesis that the observed frequency distribution is lognormal. The same procedure was followed in constructing and testing all the histograms shown in Figures 1 through 8. In no case did the chi square test indicate that rejection of the null hypothesis was required.

Based on the results displayed in Figures 2, 3, 4, and 5, it was assumed that C_v and C_s are lognormally distributed in each of the six sampling strata of the inner compound. The population parameters for each sampling stratum ($\bar{x}g$ and sg) are given in Table 4.

Table 1. Vegetation: pCi (Pu 239-240)/g (Dry Weight) in Vegetation Samples From the Six Sampling Strata of Area 13 (NTS)

Stratum 1 (n = 36)	Stratum 2 (n = 25)	Stratum 3 (n = 15)	Stratum 4 (n = 18)	Stratum 5 (n = 10)	Stratum 6 (n = 37)
9.48 (0)*	2.64 (0)	3.53 (1)	1.81 (2)	1.21 (2)	3.34 (2)
1.28 (1)	5.82 (0)	4.37 (0)	3.19 (1)	7.13 (1)	1.11 (3)
1.64 (0)	4.97 (0)	1.54 (1)	6.57 (1)	2.99 (2)	5.75 (2)
7.21 (-1)	8.92 (0)	9.69 (0)	2.91 (1)	1.38 (2)	2.42 (3)
5.90 (0)	9.40 (-1)	1.67 (0)	6.21 (1)	8.90 (2)	1.03 (4)
7.80 (0)	1.90 (1)	1.02 (1)	2.52 (1)	1.13 (2)	3.97 (2)
1.40 (0)	2.25 (0)	1.95 (1)	1.96 (1)	4.42 (2)	5.63 (1)
1.89 (0)	2.20 (0)	1.01 (1)	3.29 (1)	2.75 (2)	1.20 (3)
6.88 (0)	7.76 (0)	5.84 (0)	4.36 (1)	1.31 (2)	3.93 (2)
6.17 (0)	1.31 (1)	1.66 (1)	7.37 (1)	3.08 (2)	7.45 (2)
5.53 (0)	7.41 (0)	6.02 (0)	7.58 (1)		1.13 (3)
6.85 (0)	5.81 (0)	1.29 (1)	3.51 (2)		2.30 (2)
7.52 (-1)		2.39 (0)	8.80 (1)		2.13 (3)
1.78 (0)			3.96 (1)		7.98 (2)
6.46 (0)			8.14 (1)		2.18 (2)
1.49 (0)			1.55 (1)		8.52 (3)
3.24 (0)			8.60 (1)		5.37 (2)
2.67 (0)			4.03 (1)		2.68 (3)
1.98 (0)			7.31 (1)		2.25 (2)
3.78 (0)			6.68 (1)		6.88 (2)
9.24 (-1)			1.27 (2)		1.97 (3)
7.39 (0)			7.83 (1)		1.09 (3)
5.50 (-1)					8.38 (2)
7.88 (0)					3.21 (2)
					9.14 (2)

*Numbers in parentheses are exponents of ten.

Table 2. Soil: pCi (Pu 239-240)/g (Dry Weight) in Soil Samples From the Six Sampling Strata of Area 13 (NTS)

Stratum 1 (n = 39)		Stratum 2 (n = 31)		Stratum 3 (n = 14)		Stratum 4 (n = 19)		Stratum 5 (n = 20)		Stratum 6 (n = 47)	
5.09 (1)*	1.65 (1)	3.02 (1)	1.01 (1)	2.71 (2)	4.18 (2)	1.40 (2)	3.38 (2)	2.14 (3)	8.17 (3)	4.36 (3)	
3.05 (2)	4.42 (1)	7.29 (2)	1.15 (2)	9.85 (2)	1.27 (3)	2.78 (3)	6.34 (3)	2.15 (3)	9.38 (3)	5.84 (3)	
7.59 (1)	5.61 (1)	2.14 (1)	6.55 (1)	2.01 (2)	1.04 (3)	1.08 (3)	5.91 (3)	1.21 (3)	1.28 (4)	2.66 (5)**	
4.48 (0)	2.85 (0)	8.85 (1)	5.35 (1)	6.15 (2)	5.37 (2)	8.48 (1)	4.22 (3)	1.89 (2)	1.71 (3)	6.78 (3)	
1.76 (1)	5.23 (1)	5.21 (1)	1.17 (2)	7.64 (2)	9.21 (2)	1.46 (3)	2.29 (3)	8.91 (2)	7.89 (3)	8.74 (3)	
1.69 (1)	9.71 (0)	6.63 (1)	6.49 (1)	2.29 (2)	1.36 (3)			5.58 (3)	8.90 (3)	1.82 (4)	
5.41 (0)	5.97 (0)	1.45 (2)	3.39 (1)	1.87 (2)	3.98 (2)			3.82 (3)	6.73 (3)	3.05 (3)	
8.38 (0)	4.50 (1)	3.55 (1)	2.71 (1)	7.25 (2)	8.56 (2)			2.09 (3)	1.03 (4)	3.41 (3)	
2.77 (1)	1.96 (1)	4.23 (0)	5.51 (1)	4.26 (2)	1.72 (3)			5.92 (2)	2.13 (4)	5.62 (3)	
1.54 (1)		3.30 (2)	2.27 (1)	4.48 (2)	1.77 (3)			9.57 (2)	1.13 (4)	1.12 (4)	
3.51 (1)		6.35 (1)		1.17 (2)	1.40 (3)			1.24 (3)	1.96 (3)	1.10 (4)	
1.56 (1)		4.57 (1)		4.44 (2)	4.47 (2)			7.03 (2)	7.60 (3)	2.53 (3)	
3.11 (1)		1.38 (2)		1.86 (2)	7.75 (2)			1.35 (3)	4.39 (3)	2.10 (4)	
2.04 (1)		3.16 (1)		4.28 (1)	1.36 (3)			4.11 (3)	3.10 (3)	3.65 (3)	
7.30 (1)		2.99 (2)			1.69 (3)			1.46 (3)	1.13 (4)	2.00 (4)	
8.38 (0)		7.25 (1)							2.42 (3)	1.94 (3)	
9.91 (0)		1.39 (2)							3.57 (3)	1.43 (4)	
4.64 (1)		1.90 (1)							1.49 (4)	7.86 (3)	
2.72 (1)		7.94 (1)							4.81 (3)	9.22 (3)	
1.11 (1)		1.49 (2)							5.61 (3)	5.90 (3)	
3.78 (1)		5.68 (1)								2.64 (3)	
3.08 (1)										1.02 (4	
6.47 (1)											
4.94 (0)											
1.66 (1)											
5.39 (1)											
2.84 (1)											
1.09 (1)											
5.84 (1)											
3.84 (1)											

*Numbers in parentheses are exponents of ten.

**Inclusion of this value increases the mean soil concentration of Stratum 6 by approximately 70 percent. It was not included in the histogram (Figure 5).

Table 3. Areas (m^2) of Sampling Strata of Area 13 (NTS)

Strata	Area 13 (m^2)	%	Inner Compound (m^2)	%
1	1,245,000	30.993	120,000	12.565
2	2,547,000	63.406	610,000	63.874
3	108,000	2.689	108,000	11.309
4	74,000	1.842	74,000	7.749
5	19,000	0.473	19,000	1.990
6	24,000	0.597	24,000	2.513
Σ	4,017,000	100.000	955,000	100.000

Table 4. Arithmetic and Geometric Means ($\bar{x}$) and Standard Deviations (s) of Plutonium (239-240) Concentrations (pCi/g) in Vegetation and Soil Samples From Area 13 (NTS)*

Parameter	n	Arithmetic		Geometric		
		$\bar{x}$	s	$\bar{x}g$	sg	a***
Cv (1)**	36	5.37	4.05	1.35993	0.88180	5.75
Cv (2)	25	13.01	10.20	2.27398	0.82398	13.65
Cv (3)	15	172.73	214.26	4.61398	1.02060	169.83
Cv (4)	18	76.66	74.25	4.06855	0.72314	74.25
Cv (5)	10	278.83	244.63	5.35224	0.76283	211.08
Cv (6)	37	1230.01	2111.29	6.38724	1.13624	1133.15
Cs (1)	39	35.97	48.73	3.11794	0.96197	35.90
Cs (2)	31	101.95	139.18	4.10400	1.02727	102.68
Cs (3)	14	402.91	279.52	5.72206	0.84979	435.40
Cs (4)	19	1055.09	669.76	6.68777	0.88452	1186.73
Cs (5)	20	2379.00	1930.84	7.40404	0.96084	2606.09
Cs (6)	47	13,320.85	38,021.93	8.77720	0.98218	10,504.23

*The raw data are listed in Tables 1 and 2.

**The numbers in parentheses refer to the sampling strata of Tables 1, 2, and 3.

***a = exp ($\bar{x}_g = 0.5\ s_g^2$), used as an estimator of $\bar{x}$.

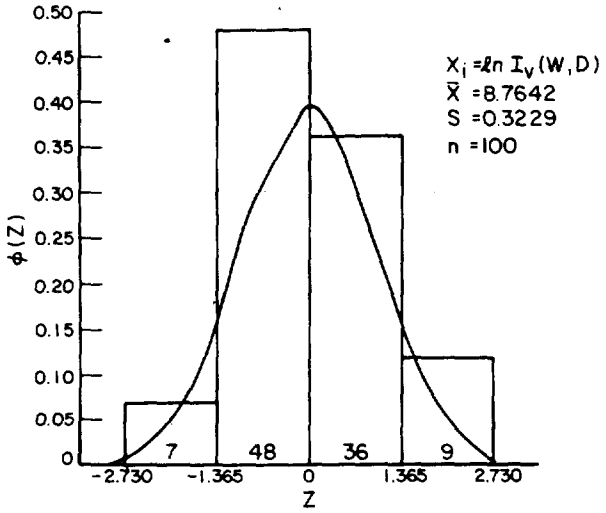

FIGURE 1. LOGNORMAL DISTRIBUTION OF VEGETATION INGESTION RATES (g/day) FOR GRAZING CATTLE
Synthetic Sample Based on Equation 2, W=410±82 kg, and D=0.48±0.12 (dimensionless).

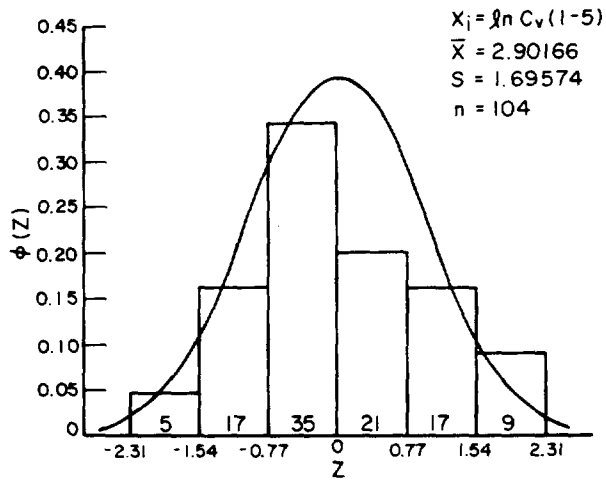

FIGURE 2. LOGNORMAL DISTRIBUTION OF PLUTONIUM (239-240) CONCENTRATIONS (p Ci/g) IN VEGETATION SAMPLES FROM AREA 13 (NTS), STRATA 1-5

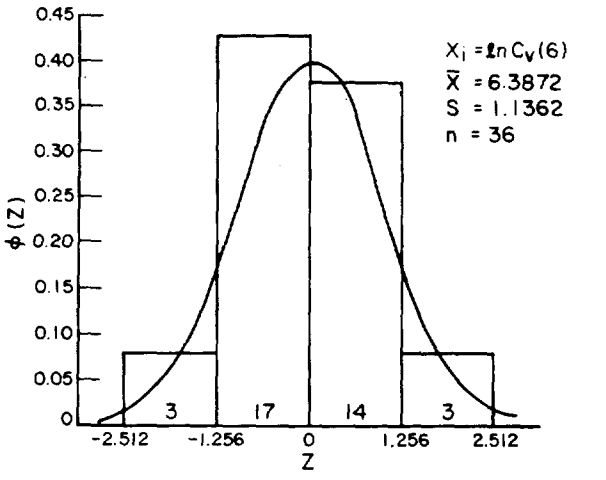

FIGURE 3. LOGNORMAL DISTRIBUTION OF PLUTONIUM (239-240) CONCENTRATIONS (p Ci/g) IN VEGETATION SAMPLES FROM AREA 13 (NTS), STRATUM 6.

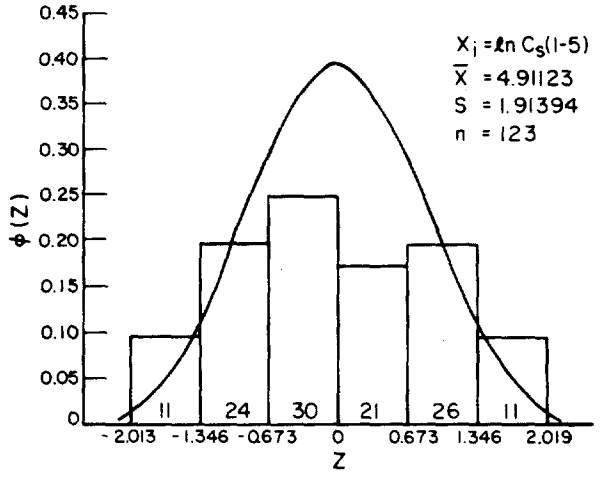

FIGURE 4. LOGNORMAL DISTRIBUTION OF PLUTONIUM (239-240) CONCENTRATIONS (pCi/g) IN SOIL SAMPLES FROM AREA 13 (NTS), STRATA 1-5

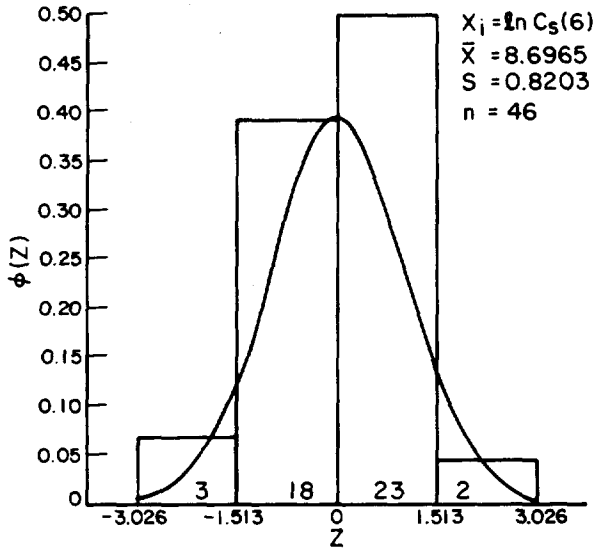

FIGURE 5. LOGNORMAL DISTRIBUTION OF PLUTONIUM (239-240) CONCENTRATIONS (pCi/g) IN SOIL SAMPLES FROM AREA 13 (NTS), STRATUM 6

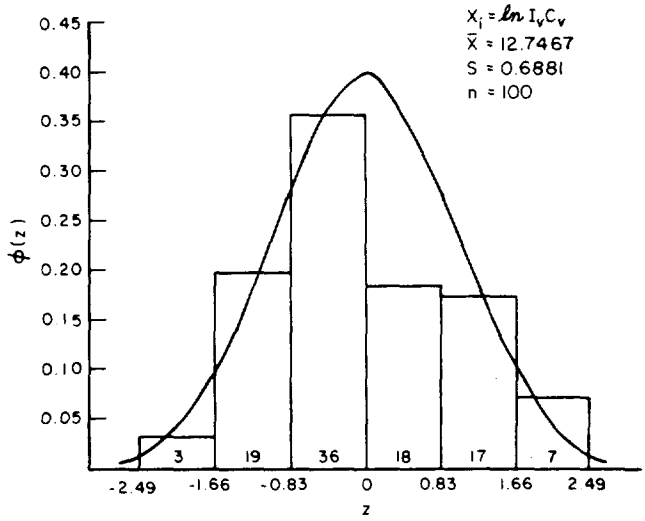

FIGURE 6 LOGNORMAL DISTRIBUTION OF PLUTONIUM UPTAKE FROM VEGETATION BY GRAZING CATTLE

(Synthetic Composite Random Sample)

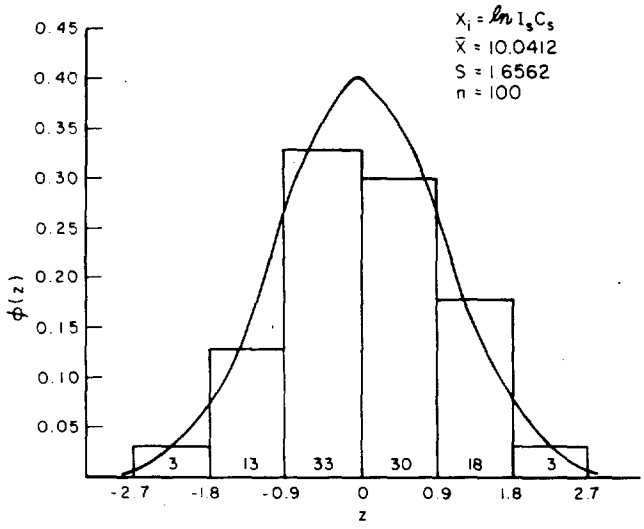

FIGURE 7. LOGNORMAL DISTRIBUTION OF PLUTONIUM UPTAKE FROM SOIL BY GRAZING CATTLE

(Synthetic Composite Random Sample)

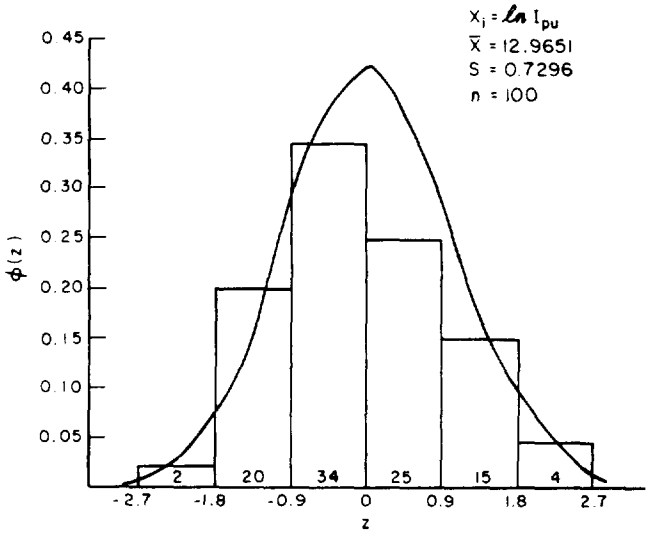

FIGURE 8. LOGNORMAL DISTRIBUTION OF TOTAL PLUTONIUM UPTAKE (VEGETATION AND SOIL) BY GRAZING CATTLE

(Synthetic Composite Random Sample)

Basis for Lognormal Distribution

Normal distributions are assumed to result from additive processes, while lognormal distributions are usually attributed to multiplicative processes. In the case of vegetation ingestion rates (I_V), a normal distribution was apparently converted to a lognormal distribution by introduction of a normally varying reciprocal factor. Soil ingestion rates were assumed to be lognormally distributed because the three data points available (8.5, 57.3, and 278 g) approximate the power sequence (8, 64, 256, i.e., 2^3, 2^6, 2^8) and because the coefficient of variation ($s/\bar{x}$ = 144/112) is greater than 1. Then it was demonstrated that the frequency distributions of plutonium concentrations in vegetation and soil samples from Area 13 (Tables 1 and 2) are also well described by assuming that they are lognormally distributed.

An examination of the area data in Table 3 and the corrected plutonium inventory data published by Gilbert (1977) shows that the spatial distribution of plutonium in surface soils (0-5 cm depth) of Area 13 exhibits a logarithmic pattern and that this pattern probably accounts for the more or less lognormal distributions of plutonium concentrations in vegetation and soil samples. The log-log relationship which describes the spatial pattern of plutonium distribution has the general form $y = ax^b$, the linear form of which is

$$\ln y = \ln a + b \ln x \qquad (3)$$

where y = the cumulative amount of plutonium, ΣPu, in the surface soils of sampling strata 6 through 1 in Area 13 (in curies),

x = the cumulative area, ΣA, of sampling strata 6 through 1 (in hectares),

a is the y-intercept of the regression line,

and b is the slope of the regression line.

The amount of plutonium in the surface soil of stratum j, (Pu)j, was calculated as follows:

$$(Pu)j = \bar{C}_{sj} M_s A_J 10^{-8}$$

where (Pu)j is the amount (curies) of plutonium in the surface soil of stratum j,

$\bar{C}_{sj}$ is the mean concentration (pCi/g) of Pu in the surface soil of stratum j,

M_s is the weight of soil (0-5 cm depth) in g/m^2 (this is the bulk density soil sample. The mean bulk density was 1.13 ± 0.03 g/cm^3; so the average value of M_s is about 56,500 g/m^2.),

A_j is the area (hectares) of stratum j,

and $10^{-8} = 10^{-12}$ Ci/pCi x 10^{4} m^2/ha.

Both the input data and the results of the regression analysis based on Equation 4 are shown in Figure 9. The log-log regression equation, $\hat{y} = ax^b$ fits the cumulative inventory, ΣPu, estimates quite well, as shown by the graph and a correlation coefficient of r = 0.9999. A similar relationship would be expected for the regression of soil concentrations on distance from ground zero, but this regression line would, of course, have a negative slope. In other words, the results shown in Figure 9 provide a basis for expecting that the frequency distributions of plutonium concentrations in randomly selected soil samples will be more or less lognormally distributed. As soil is the source of plutonium in vegetation samples, the same reasoning should apply to plutonium concentrations in vegetation samples.

Composite Means of C_v and C_s

As mentioned earlier, it is assumed that cattle grazing the inner compound at random would (in time) consume a composite sample of vegetation and soil, taking from each stratum an amount of vegetation and soil proportional to the area of the stratum enclosed by the fence. This notion of composite sampling, or composite grazing if you prefer, is formulated as follows:

$$C_k = \sum_{1}^{6} \exp (\ln C_j + \ln f_j), \quad j = 1,2, \ldots 6. \qquad (5)$$

where C_k is the average concentration of plutonium (pCi/g) in 1 day's intake of vegetation or soil,

ln C_j is a normally distributed random number specified by the estimated population parameters ($\mu = \bar{x}g$ and $\sigma = sg$) listed for stratum j in Table 4,

and fj is the area of stratum j divided by the total area of the inner compound, given as percentages, in Table 3.

Applying the procedure indicated by Equation 5 to the arithmetic means listed in Table 4 yields $\bar{C}_v$ = 71 pCi/g and C_s = 579 pCi/g. These values are used below to estimate I_{Pu}.

Estimates of I_{Pu} Based on Parameter Means

The empirical and theoretical estimates made thus far can be used to estimate the value of I_{Pu}. For example,

$$I_{Pu} = (6,115 \times 71) + (236 \times 579) = 570,809 \text{ pCi/day} \qquad (6)$$

where $6,115 = I_v = 163.5(410)^{0.73}/(4.5 \times 0.48)$, Equation 1,

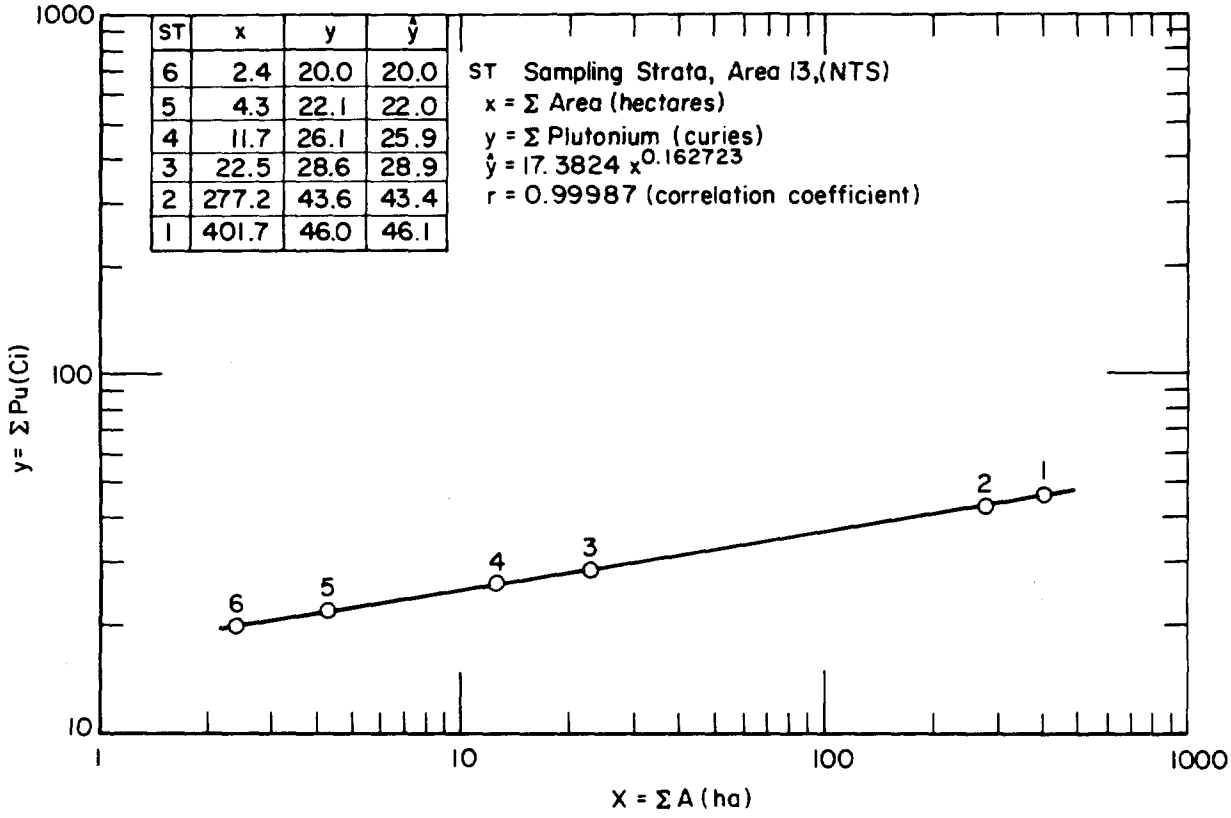

FIGURE 9. PLUTONIUM INVENTORY AS A FUNCTION OF AREA, BOTH CUMULATIVE, IN AREA 13 (NEVADA TEST SITE). RAW DATA (x AND y) FROM GILBERT (1977)

$71 = \bar{C}_v = [(5.37 \times 0.12565) + \ldots + (1230.01 \times 0.02513)]$; (Equation 6, the arithmetic strata means in Table 4 and the percentage area values in Table 3),

$236 = I_s = \exp [3.9387 + 0.5(1.7464)^2]$,

and $579 = \bar{C}_s = [(35.97 \times 0.12565) + \ldots + (7827.83 \times 0.02513)]$ based on Equation 6, the arithmetic strata means of Table 4 and the percentage area values of Table 3.

The mean value of I_{Pu} indicated by Equation 6, i.e., 571 nCi/day, is about 1 percent more than Smith's empirical estimate, 565 nCi/day, based on the rumen contents of fistulated steers. (See the article by D. D. Smith in this volume.) It could be concluded at this point that Smith's estimate has been resoundingly confirmed by an independent estimate based on (1) a theoretical model of I_v correctly adjusted to site-specific conditions, (2) an uncertain estimate of I_s based on but three site-specific data points, and (3) estimates of mean plutonium concentrations in composite random samples of vegetation and soil, $\bar{C}_v$ and $\bar{C}_s$, based on the means and relative areas (Tables 3 and 4) of the sampling strata. It could also be concluded that the excellent agreement between the two almost independent estimates of I_{Pu} confirms the validity of the random grazing assumption in spite of the clear evidence, provided by the fistulated steers (D. D. Smith, this volume), of marked seasonal preferences for different plant species.

The Problem of Estimating Digestibility

While these conclusions are probably valid, there is at least one "Catch 22" which must be reconsidered. The principal adjustment of I_v model, Equation 2, was to set $\bar{D} = 0.48 \pm 0.12$. The mean of D (digestibility) was selected to make it possible for a 410-kg cow to obtain sufficient food energy (kcal) to meet its digestible energy requirement on a daily ration of about 6 kg of vegetation. The actual value of $\bar{D}$ for Area 13 vegetation is not known. The large standard deviation was assumed to simulate variation of forage quality. If the mean were 0.36 as suggested by one study of desert vegetation digestibility (McKell, 1975), the daily ration required for maintenance of a 410-kg cow would be over 8 kg of vegetation and the corresponding estimate of I_{Pu}, Equation 4, would be 713 nCi/day instead of 571 nCi/day, an increase of 25 percent. Therefore, practical application of the I_v model to other sites requires development of a dependable method of estimating the mean and standard deviation of D for a given area based perhaps on the species composition and biomass of its vegetation.

Simulation of Random Grazing

Another question of more than passing interest is whether or not the results of vegetation, soil, and grazing studies conducted in Area 13 are reproducible. It would be impractical and expensive to actually repeat vegetation and soil studies conducted in Area 13 and also time

consuming to repeat the grazing and fistulated steer studies. It might be desirable, however, to conduct similar studies in other areas or to apply the results of the Area 13 studies to other contaminated sites at NTS or elsewhere. Considering the variability of the data obtained from Area 13 and expecting similar variability in another study area, how accurately can the means and standard deviations be estimated on the basis of a reasonable number of samples? Can reasonably accurate estimates of I_{Pu} be obtained from model of I_v, an estimate of I_s, and measurements of C_v and C_s without having to carry out expensive grazing studies?

To obtain preliminary answers to these and similar questions, a series of simulation studies was carried out as follows: Equation 1 was used to generate five synthetic samples (n = 100) of the vegetation ingestion rate, I_v, based on $\bar{W} = 410 \pm 82$ kg and $\bar{D} = 0.48 \pm 0.12$. These results were used as estimates of the true means (μ) and standard deviations (σ). The data, given in Table 5, show little variation and good agreement between the arithmetic and the geometric estimates of means. Five synthetic samples of I_s were based on the previously explained assumption that $\ln I_s = 3.93866 \pm 1.74636$. The results given in Table 6 show estimates (n = 100) ranging from about 150 to about 250 g/day, somewhat below the "reasonable" range (250 to 500 g/day) suggested by Smith (1977).

Synthetic samples of C_v and C_s, Tables 7 and 8, were generated by means of Equation 3, the lognormal parameters given in Table 4, and the values of fj indicated in Table 3. The synthetic samples of C_v indicate an overall mean of 70 pCi/day (n = 500) versus 71 pCi/day expected. The means of subsamples (n = 100) ranged from 67 to 73 pCi/day. Synthetic samples of C_s, Table 8, exhibit similar properties; but the overall mean, 540 pCi/g, was about 7 percent less than the expected value, 579 pCi/g.

The final step in the simulation study was to generate synthetic samples of I_{Pu} based on Equation 1 and the lognormal distribution parameters obtained from the synthetic samples just discussed and summarized in Tables 5, 6, 7, and 8. The specific values of ($\bar{x}g \pm sg = \mu \pm \sigma$) were the following:

Table 5: $\bar{x}g(\ln I_v) = 8.72942 \pm 0.31988$

Table 7: $\bar{x}g(\ln C_v) = 4.05989 \pm 0.57563$

Table 6: $\bar{x}g(\ln I_s) = 3.87002 \pm 1.77244$

Table 8: $\bar{x}g(\ln C_s) = 6.10021 \pm 0.59454$.

The pocket calculator program used to generate the synthetic samples of I_{Pu}, summarized in Table 9, is described in Appendix I.

The simulation estimate of I_{Pu}, 557 nCi/day (Table 9), is about 2.5 percent less than the estimate, 571 nCi/day, based on the arithmetic

Table 5. Synthetic Samples of I_v (Vegetation Ingestion Rate, g/day) Based on Equation 2, $\bar{W}$ = 410 ± 82 kg and $\bar{D}$ = 0.48 ± 0.12

n	$\bar{x}$	s	$\bar{x}_g$	sg	a
100	6,799	3,080	8.75623	0.34727	6,745
100	6,444	2,374	8.71785	0.31581	6,424
100	6,402	2,105	8.71921	0.29630	6,394
100	6,076	1,720	8.67395	0.27178	6,069
100	7,035	3,634	8.77784	0.36002	6,923
500	6,551	2,673	8.72942*	0.31988*	6,507

Table 6. Synthetic Samples of I_s (Soil Ingestion Rate, g/day) Based on $\bar{x}_g + s_g$ = 3.93866 ± 1.74636

n	$\bar{x}$	s	$\bar{x}_g$	sg	a
100	154.52	386.22	3.63200	1.75301	175.65
100	196.85	365.26	4.14994	1.60010	288.17
100	240.93	679.54	3.65995	1.99416	283.80
100	254.66	935.83	3.96075	1.74550	240.84
100	220.31	489.19	3.94745	1.74668	238.15
500	213.45	609.83	3.87002*	1.77244*	230.62

Table 7. Synthetic Samples of C_v (Plutonium Concentration in Vegetation, pCi/g) Based on Equation 5, the $\bar{x}_g$ ± sg Estimates (Six Strata) Given in Table 4, and the Percentage Area Values in Table 3

n	$\bar{x}$	s	$\bar{x}_g$	sg	a
100	73.01	56.06	4.09335	0.59813	71.68
100	66.92	45.27	4.02999	0.56679	66.06
100	74.27	92.95	4.05485	0.62049	69.92
100	66.84	45.87	4.04902	0.52475	65.81
100	69.86	49.48	4.07225	0.56338	68.78
500	70.18	60.64	4.05898*	0.57563*	68.41

Table 8. Synthetic Samples of C_s (Plutonium Concentration in Soil, pCi/g) Based on Equation 5, the $\bar{x}g \pm sg$ Estimates (Six Strata) Given in Table 4, and the Percentage Area Values in Table 3

n	$\bar{x}$	s	$\bar{x}g$	sg	a
100	580.48	485.42	6.15474	0.62008	570.77
100	509.84	397.92	6.03412	0.60753	502.03
100	571.36	592.16	6.16829	0.58335	565.91
100	519.76	285.73	6.05470	0.59552	508.78
100	517.03	243.60	6.08922	0.56465	517.31
500	539.69	420.86	6.10021*	0.59454*	532.16

Table 9. Synthetic Samples of I_{Pu} (Plutonium Ingestion Rate, pCi/day) Based on Equation 1, the Synthetic Estimates of $\bar{x}g \pm sg$ Marked * in Tables 5-8, and the Calculator Program Described in Appendix I

n	$\bar{x}$	s	$\bar{x}g$	sg	a
100	634,697	508,027	13.11080	0.71491	638,161
100	522,627	387,306	12.94687	0.66083	521,893
100	486,297	329,585	12.88630	0.67368	495,450
100	511,803	373,380	12.90408	0.68562	508,450
100	628,809	890,343	13.02459	0.96747	724,032
500	556,847	525,621	12.97453	0.74936	570,089

means of the lognormal distributions used to generate the synthetic samples (Equation 6) but only about 1.5 percent less than the estimate, 565 nCi/g, based on the fistulated steer data (Smith, this volume).

DISCUSSION

The results described above indicate that the simulation model, Equation 1, does a fair job of duplicating the results of the fistulated steer study (D. D. Smith, this volume). Considering the large error term indicated by simulation, 557 ± 526 nCi/day, the differences among various estimates of I_{Pu} are negligible; but both the arithmetic (557 nCi/day) and the geometric (571 pCi/day) estimates based on simulation are closer to the estimate of I_{Pu} based on fistulated steer data (565 nCi/day, Smith *et al.*, 1976) than were previous independent estimates based on theory (585 nCi/day, Martin and Bloom, 1977) or assumed dietary composition (620 nCi/day, Gilbert *et al.*, 1977).

When an earlier but quite similar version of this paper was presented at the San Diego meeting of NAEG, two questions were raised which merit consideration here. One had to do with the "apparently inevitable outcome" of the simulation "given the manner in which it was carried out." The second was an expression of skepticism concerning the evidence cited for assuming that all factors of the simulation model, Equation 1, are lognormally distributed. These questions are discussed below.

Except for the parameter D in Equation 2, which was adjusted to meet the apparent requirement that a 410-kg cow should be able to obtain enough digestible energy for maintenance on a daily ration of about 6 kg of vegetation, the simulation model and the fistulated steer study were independent. Because of the "adjustment" of D, a critical parameter, the two estimates of I_{Pu} have been characterized as "almost independent." The only development required to make them truly independent is an independent and site-specific method of estimating D, the digestibility of vegetation available to grazing animals.

If the simulation model yields estimates of I_{Pu} which are essentially the same as estimates based on the rumen contents of fistulated steers allowed to graze a fenced area (and it does), this outcome can be characterized as "inevitable" if, and only if, the model correctly simulates the grazing process. This means that the assumption incorporated in the model design and the input data used to implement the simulation must be essentially correct. The principal assumptions incorporated in the simulation model are (1) that grazing is a random process which, given sufficient time, results in the ingestion of a composite random sample of vegetation and soil and (2) that the factors of the simulation model, Equation 1, can be represented as independent random variables having lognormal distributions. The best evidence that these assumptions and

the input data are correct is the demonstration that the model does, in fact, yield estimates of I_{Pu} which are quite close to the best estimate available.

The evidence, Figures 1 through 9, in support of the lognormal hypothesis is fairly persuasive but it may not meet the requirements for rigorous mathematical proof. The best data available for testing the lognormal hypothesis are the plutonium concentrations in vegetation and soil samples from Area 13, Tables 1 and 2. Sampling within strata was random, but the maximum number of samples from a given stratum is 47, too few to provide an accurate measure of the true frequency distribution. Strata 1 and 2 were sampled only in part, i.e., no samples were collected in the parts of these strata located outside the fenced portion of Area 13. In other words, the sampling design is adequate and efficient for inventory purposes but leaves much to be desired if one's statistical objective is to determine the shape of a frequency distribution curve. A better approach for this purpose would be to collect between 100 and 200 non-stratified random samples from strata 3, 4, 5, and 6 which are completely enclosed by the inner fence. In spite of these "faults" in the sampling design, the histograms do show that the logarithms of the sample values in Tables 1 and 2 are symmetrically distributed around their means and that the actual distributions, whatever they may be, can be represented as lognormal.

An alternative to the lognormal hypothesis is simply to use the arithmetic means of I_v, C_v, I_s, and C_s to generate synthetic samples of I_{Pu}. The only objective to this procedure is that the coefficients of variation ($s/\bar{x}$) are so large, for some inputs, that normal variation would be expected to include a predictable percentage of negative values which, of course, have no meaning with respect to the factors of Equation 1. To determine whether the occurrence of negative values in synthetic samples affects the overall results of the simulation model and, at the same time, whether or not the usefulness of the simulation model depends on the assumption of lognormal distributions, it was decided to repeat the simulation study using arithmetic means and standard deviations instead of the means and standard deviations of logarithms.

New estimates of $\bar{x} \pm s$ were calculated for I_v and I_s. The procedure for generating the synthetic samples upon which the new estimates were based was the same as used to obtain the estimates listed in Tables 5 and 7, except that the total sample size was increased from n = 500 to n = 1,000. The synthetic means and standard deviations thus obtained were $I_v = 6{,}526 \pm 2{,}396$ g/day and $I_s = 227.3 \pm 669.5$ g/day. (N.B. The mean and standard deviations of ln 8.5 g, ln 57.3 g, and ln 278 g, i.e., 3.93866 ± 1.74636, were used to estimate the synthetic values given above for I_s because the arithmetic mean and standard deviation of these three samples, 115 ± 144 g, would indicate an average soil ingestion rate much lower than the 250 to 500 g/day suggested, as a "reasonable estimate," by Smith (1977). With only three site-specific samples to go on, it is difficult to defend any estimate of I_s. The estimate given above is judged to be the best available at present.)

The procedure followed in generating new synthetic composite samples (n = 1,000) of C_v and C_s were based on the arithmetic means and standard deviations listed in Table 4 and the stratum areas given in Table 3. No logarithms were involved. The synthetic means and standard deviations thus obtained (n = 1,000) were $\bar{C}_v$ = 70.38 ± 62.32 pCi/g and $\bar{C}_s$ = 580.9 ± 931.9 pCi/g. About 15 percent of the synthetic samples of C_v and approximately 35 percent of the synthetic samples of C_s were negative values. The expected means, based on the arithmetic means given in Table 4 for six strata, the area data given in Table 3, and the procedure implied by Equation 5 were $\bar{C}_v$ = 71 pCi/g and $\bar{C}_s$ = 579 pCi/g.

The calculator program, described in Appendix I, was modified to operate on the synthetic means and standard deviations ($\bar{x}$ ± s), discussed above, and was used to generate synthetic samples of I_{Pu} as indicated by Equation 1. The results of this simulation, based on estimates of arithmetic means and standard deviations, are shown in Table 10.

Table 10. Synthetic Samples of I_{PU} (pCi/day Based on Equation 1 and the Following Estimates of Arithmetic Means and Standard Deviations: I_v = 6,526 ± 2,396 g/day, C_v = 70.38 ± 62.32 pCi/g, I_s = 227 ± 670 g/day C_s = 581 ± 932 pCi/g

n	x	s	n	$\bar{x}$	s
100	743,668	909,937	100	594,596	851,972
100	701,631	995,215	100	754,221	1,028,018
100	546,061	893,357	100	487,977	791,335
100	483,138	922,872	100	521,907	910,771
100	403,493	880,953	100	524,160	1,045,871
500	575,598	921,336	500	576,572	930,832
			1,000	576,085	926,096

The overall estimate, I_{Pu} = 576 nCi/day (n = 1000), is about 3.5 percent higher than the overall estimate shown in Table 9 (557 nCi/day, n = 500) and approximately 2 percent higher than the estimate (565 nCi/day) based on the rumen contents of fistulated steers. The number of negative values in the total synthetic sample (n = 1,000) was 217, a frequency of 21.7 percent. The expected frequency for a normal distribution based on μ = 576 and σ = 926 is about 26.7 percent. The coefficients of variation indicated by the estimates shown in Table 9, based on the lognormal hypothesis, are generally smaller than those indicated by the estimates shown in Table 10, which are based (except for I_s) on assumed normal distributions. From these results and comparisons, it is obvious that the simulation model does not depend on the lognormal hypothesis.

Simulations based on arithmetic means and standard deviation *and* simulations based on the means and standard deviations of logarithms both result in estimates of I_{Pu} which are quite close to the best empirical estimates available, i.e, the estimate based on the rumen contents of fistulated steers (Smith, this volume).

The good agreement between these almost independent estimates of I_{Pu} tends to confirm the usefulness of the simulation model, Equations 1 and 2, and the basic assumption that grazing can be represented as a random process. It does not, however, confirm the structure of the model. It could be, for example, the the soil ingestion rate is actually much lower than indicated, by this study, on the basis of but three samples. Indeed, the soil, or sediment, recovered from the gastrointestinal tracts of cattle may have been ingested not as soil *per se* but rather in the form of dust deposited loosely on vegetation. As the digestibility of the vegetation consumed by grazing cattle in Area 13 is unknown, it is theoretically possible, as pointed out earlier, that the daily intake of vegetation could be closer to 8 kg than to 6 kg. If that were the case, most of the observed plutonium ingestion, 565 nCi/day, might be due to vegetation intake (i.e., 8 kg/day x 70 pCi/g = 560 nCi/day), leaving only a small amount that might be due to soil ingestion.

The model can, of course, be applied to other contaminated areas at or near the Nevada Test Site, but the results of such applications will remain uncertain until methods are devised for estimating (a) the digestibility of vegetation available to grazing cattle in a given area and (b) the soil ingestion rate. The soil ingestion rate is difficult to measure directly, but it seems probable that some sort of estimate could be made by sampling the sediment (soil) content of fecal materials. As estimates of I_{Pu}, based on the simulation model, are obviously less expensive and less time-consuming than grazing studies conducted by means of fistulated steers, efforts to implement the model via independent field studies could prove to be quite rewarding.

REFERENCES

1. Delfiner, P., and R. O. Gilbert. 1978. "Combining Two Types of Survey Data for Estimating Geographical Distribution of Pu in Area 13." (This report.)

2. Gilbert, R. O. 1977. "Revised Total Amounts of ^{239,240}Pu in Surface Soil at Safety-Shot Sites." BNWL-SA-6448. (NVO-181.)

3. Gilbert, R. O., L. L. Eberhardt, and D. D. Smith. 1977. "An Initial Synthesis of Area 13 ^{239}Pu Data and Other Statistical Analysis." *In: Environmental Plutonium on the Nevada Test Site and Environs.* M. G. White, P. B. Dunaway, and W. A. Howard (Eds.). NVO-171. pp. 237-274.

4. Golley, F. B. 1961. "Energy Values of Ecological Materials." *Ecology* 42(3):581-584.

5. Martin, W. E., and S. G. Bloom. 1976. "Plutonium Transport and Dose Estimation Model." *In: Transuranium Nuclides in the Environment.* STI/PUB/410. IAEA, Vienna. pp. 385-398.

6. Martin, W. E., and S. G. Bloom. 1977. "Nevada Applied Ecology Group Model for Estimating Plutonium Transport and Dose to Man." *In: Transuranics in Natural Environments.* M. G. White and P. B. Dunaway (Eds.). NVO-178. pp. 621-706.

7. McKell, C. M. 1975. "Shrubs: A Neglected Resource of Arid Lands." *Science* 187:803-809.

8. Romney, E. M., A. Wallace, R. O. Gilbert, and J. E. Kinnear. 1975. "^{239,240}Pu and ^{241}Am Contamination of Vegetation in Aged Plutonium Fallout Areas." *In: The Radioecology of Plutonium and Other Transuranics in Desert Environments.* M. G. White and P. B. Dunaway (Eds.). NVO-153. pp. 43-88.

9. Siegmund, O. H. (Ed.). 1967. *The Merck Veterinary Manual.* Third edition. Merck and Company, Inc.

10. Smith, D. D. 1977. "Grazing Studies on a Contaminated Range on the Nevada Test Site." *In: Environmental Plutonium on the Nevada Test Site and Environs.* M. G. White, P. B. Dunaway, and W. A. Howard (Eds.). NVO-171. pp. 139-149.

11. Smith, D. D. 1978. "Area 13 Grazing Studies--Additional Data." (This report.)

12. Smith, D. D., J. Barth, and R. G. Patzer. 1976. "Grazing Studies on a Plutonium-Contaminated Range of the Nevada Test Site." *In: Transuranium Nuclides in the Environment*. STI/PUB/410. IAEA, Vienna. pp. 325-336.

APPENDIX I

MODEL FOR SIMULATION OF PLUTONIUM INGESTION BY GRAZING CATTLE

Purpose of Program

The purpose of this pocket calculator (Texas Instrument Model 59) program is to simulate the ingestion of plutonium by cattle grazing randomly in a fenced area where the vegetation and soils contain known concentrations of plutonium. The simulation model equation is

$$I_{Pu} = I_v C_v + I_s C_s \qquad (1)$$

where I_{Pu} is the plutonium ingestion rate, pCi/day,
I_v is the vegetation ingestion rate, g/day,
I_s is the soil ingestion rate, g/day,
C_v is the plutonium concentration in vegetation, pCi/g,
and C_s is the plutonium concentration in soil, pCi/g.

Input Data

The required input data are the means and standard deviations ($\bar{x}g \pm sg$) of $\ln(I_v)$, $\ln(C_v)$, $\ln(I_s)$, and $\ln(C_s)$. To generate synthetic samples of I_{Pu}, Equation 1 is solved repeatedly by substituting random values, based on the input data, for the factors on the right side of the equation. Input data for C_v, I_s, and C_s may be estimated directly on the basis of samples collected from the specific reference site. For this model, the estimated mean and standard deviation of $\ln(I_v)$ are obtained from synthetic samples based on

$$\ln(I_v) = \ln(163.5\ W^{0.73}/4.5\ D) \qquad (2)$$

where $163.5\ W^{0.73}$ is the digestible energy (kcal/day) required for maintenance (no weight gain or loss) of adult cattle,
W is the total live body weight (kg) of the animal,
4.5 kcal/g is the average calorie content of vegetation,
and D is the digestibility (dimensionless) of the vegetation ingested.

To generate synthetic samples of I_v, the site-specific estimates of the arithmetic means and standard deviations of W and D are required. The values for W can be obtained from direct measurements of a reference herd. The values for D might be obtained from studies of the nutritional values of composite vegetation samples from the reference site. Vegetation and soil, of course, may be sampled directly at the reference site. The most difficult parameter to estimate may be I_s, the soil ingestion rate. It seems probable, however, that some sort of estimate could be obtained by sampling the soil content of fecal materials.

Random Number Generator

The key part of the program for generating synthetic samples of I_{Pu} (and of the similar program, not shown, for generating synthetic samples of I_V) is the random number generator which consists of two subroutines, "DMS" and "D." Subroutine "DMS" generates uniformly distributed random numbers on the interval (0,1). It operates as follows: First a "seed" number x_o, $0 \leq x_o \leq 199{,}017$, is stored in register 9. The seed is substituted in Equation 3, which generates a new seed, i.e.,

$$X_{i+1} = [(24{,}298x_i + 99{,}991) \bmod 199{,}017] \quad . \qquad (3)$$

The operations indicated by "mod 199,017" are (see program steps 019-039) as follows: First, $p = 24{,}298x_i + 99{,}991$ is divided by 199,017. Then the decimal portion of p is multiplied by 199,017, and the new seed, X_{i+1} is stored in register 9. Then (see program steps 040-053) the new seed is divided by 199,017 and multiplied by 10^5. Finally, the integral portion of this intermediate result is divided by 10^5. The result is u_i, a uniformly distributed random number on the interval (0,1).

Subroutine "D" generates normally distributed random numbers, having the means and standard deviations specified by the input data, by calling subroutine "DMS" for two uniformly distributed random numbers, u_1 and u_2, which are substituted in Equation 4, which follows:

$$x = \sqrt{-2 \ln u_1} \cos(2\pi u_2)\sigma + \mu \qquad (4)$$

where μ is the population mean estimated by $\bar{x}_g$,
and σ is the standard deviation estimated by s_g.

Lognormal Versus Normal Distributions

Note that the program is designed to operate on the means and standard deviations of the logarithms of lognormally distributed variables, but it can be modified to operate on the arithmetic means and standard deviations of the same variables. There is, however, one caveat: If the arithmetic standard deviations are large compared to their means, some of the synthetic sample values may be negative. If this happens, attempting to calculate the mean and standard deviation of the logarithms of the synthetic samples will result in an error condition as the logarithms of negative numbers are imaginary.

Table A-1. User Instructions

Step	Procedure	Enter	Press	Display
1	Partition memory	9	OP, 17	239.89
2	Enter program (keyboard or magnetic card)	0	(Card)	1
3	STORE INPUT DATA			
3a	k = sets of n = 50 synthetic samples	k	STO, 08	k
3b	Seed: $0 \geq$ Seed $\geq$ 199,017	Seed	STO, 09	Seed
3c	$\bar{x}_g$ = mean of logarithms	$\bar{x}_g(I_v)$	STO, 16	$\bar{x}_g(I_v)$
3d	s_g = standard deviation of logarithms	$s_g(I_v)$	STO, 17	$s_g(I_v)$
3e	I_v = vegetation ingestion rate	$\bar{x}_g(C_v)$	STO, 18	etc.
3f	C_v = concentration in vegetation	$s_g(C_v)$	STO, 19	
3g	I_s = soil ingestion rate	$\bar{x}_g(I_s)$	STO, 20	
3h	C_s = concentration in soil	$s_g(I_s)$	STO, 21	
3i	See Equation 1	$\bar{x}_g(C_s)$	STO, 22	
3j		$s_g(C_s)$	STO, 23	
4	START AUTOMATIC EXECUTION AND PRINT		E	x_1
	The program prints a list of 50(1) synthetic values (x_i) of I_{Pu}(2). It then prints the number of synthetic values (n), the arithmetic mean ($\bar{x}$), and standard deviation (s) of the sample, the mean of the natural logarithms of synthetic values ($\bar{x}_g$), the standard deviation (s_g) of the log mean, and a = exp ($\bar{x}_g + 0.5\ s_g^2$), an estimator of the arithmetic mean. This procedure is repeated k times.(3)			x_2 etc. x_{50} n $\bar{x}$ s s_g a
	Running time is about k x 30 min.			Repeat

(1) Lable B can be modified to decrease the sample size or to increase it to a maximum of n = 76.

(2) If the list of individual values is not desired, substitute NOP for PRT at location 152.

(3) To operate the program without the printer, store 1 in register 08 and substitute R/S for PRT instructions at locations 162, 166, 169, 200, 204 and 215. Values of x_i or $\ln(x_i)$ can be recalled from storage registers 30-79 inclusive.

Table A-2. Storage Register Contents and Functions for Grazing Simulation Program

(Stopped at Step 154)

Contents	Reg.	Function
36.	00	ST* and RC*
6,094,286.863	01	Σx
1.4491997E13	02	Σx^2
6.	03	n
15.	04	Σy } Ignore
55.	05	Σy^2 } Ignore
13,553,352.61	06	Σxy } Ignore
44.	07	DSZ n
10.	08	DSZ k
25,015.81995	09	Current "seed"
199,017.	10	mod, see Equation 3
0.46105	11	u_i, see Steps 060, 061
6.10021	12	Current μ
0.59454	13	Current σ
12.71927495	14	$\ln(I_V C_V)$
10.21117646	15	$\ln(I_S C_S)$
8.72942	16	$\bar{x}_g$ } I_V
0.31988	17	s_g } I_V
4.05989	18	$\bar{x}_g$ } C_V
0.57563	19	s_g } C_V
3.87002	20	$\bar{x}_g$ } I_S
1.77244	21	s_g } I_S
6.10021	22	$\bar{x}_g$ } C_S
0.59454	23	s_g } C_S
0.	24	Available for additional data storage
0.	25	
0.	26	
0.	27	
0.	28	
0.	29	
360,098.0444	30	x_1 } Synthetic random samples of I_{Pu} (pCi/day) based on Equation 1
541,620.8125	31	x_2 } Synthetic random samples of I_{Pu} (pCi/day) based on Equation 1
360,8417.309	32	x_3 } Synthetic random samples of I_{Pu} (pCi/day) based on Equation 1
903,037.6651	33	x_4 } Synthetic random samples of I_{Pu} (pCi/day) based on Equation 1
319,780.9743	34	x_5 } Synthetic random samples of I_{Pu} (pCi/day) based on Equation 1
361,332.0582	35	x_6 } Synthetic random samples of I_{Pu} (pCi/day) based on Equation 1
0.	36	etc. ↓ } Synthetic random samples of I_{Pu} (pCi/day) based on Equation 1
0.	37	} Synthetic random samples of I_{Pu} (pCi/day) based on Equation 1
0.	38	} Synthetic random samples of I_{Pu} (pCi/day) based on Equation 1
0.	39	} Synthetic random samples of I_{Pu} (pCi/day) based on Equation 1

Table A-3. Grazing Simulation Program for Programmable Pocket Calculator (Texas Instrument Model 59)

(LOC = Location in Memory; CD = Code (Keyboard Coordinates)

LOC	CD	KEY	LOC	CD	KEY	LOC	CD	KEY	LOC	CD	KEY	LOC	CD	KEY
000	76	LBL	050	05	5	100	13	13	150	58	FIX	200	99	PRT
001	88	DMS	051	22	INV	101	14	D	151	00	00	201	53	(
002	53	(	052	28	LOG	102	42	STO	152	99	PRT	202	22	INV
003	53	(	053	54	)	103	14	14	153	78	Σ+	203	79	$\bar{x}$
004	02	2	054	92	RTN	104	43	RCL	154	69	OP	204	99	PRT
005	04	4	055	76	LBL	105	18	18	155	20	20	205	33	x^2
006	02	2	056	14	D	106	42	STO	156	97	DSZ	206	55	÷
007	09	9	057	70	RAD	107	12	12	157	07	07	207	02	2
008	08	8	058	71	SBR	108	43	RCL	158	11	A	208	85	+
009	65	x	059	88	DMS	109	19	19	159	98	ADV	209	79	$\bar{x}$
010	43	RCL	060	42	STO	110	42	STO	160	43	RCL	210	54	)
011	09	09	061	11	11	111	13	13	161	03	03	211	22	INV
012	85	+	062	71	SBR	112	14	D	162	99	PRT	212	23	LNX
013	09	9	063	88	DMS	113	44	SUM	163	58	FIX	213	58	FIX
014	09	9	064	53	(	114	14	14	164	02	02	214	00	00
015	09	9	065	53	(	115	43	RCL	165	79	$\bar{x}$	215	99	PRT
016	09	9	066	24	CE	116	20	20	166	99	PRT	216	98	ADV
017	01	1	067	65	x	117	42	STO	167	22	INV	217	98	ADV
018	54	)	068	02	2	118	12	12	168	79	$\bar{x}$	218	92	RTN
019	55	÷	069	65	x	119	43	RCL	169	99	PRT	219	76	LBL
020	01	1	070	89	π	120	21	21	170	92	RTN	220	15	E
021	09	9	071	54	)	121	42	STO	171	76	LBL	221	12	B
022	09	9	072	39	COS	122	13	13	172	12	B	222	11	A
023	00	0	073	65	x	123	14	D	173	03	3	223	12	B
024	01	1	074	53	(	124	42	STO	174	00	0	224	13	C
025	07	7	075	43	RCL	125	15	15	175	42	STO	225	97	DSZ
026	42	STO	076	11	11	126	43	RCL	176	00	00	226	08	08
027	10	10	077	23	LNX	127	22	22	177	05	5	227	15	E
028	54	)	078	65	x	128	42	STO	178	00	0	228	01	1
029	53	(	079	02	2	129	12	12	179	42	STO	229	07	7
030	53	(	080	94	+/-	130	43	RCL	180	07	07	230	03	3
031	53	(	081	54	)	131	23	23	181	36	PGM	231	01	1
032	22	INV	082	34	$\sqrt{x}$	132	42	STO	182	01	01	232	01	1
033	59	INT	083	65	x	133	13	13	183	71	SBR	233	06	6
034	65	x	084	43	RCL	134	14	D	184	25	CLR	234	69	OP
035	43	RCL	085	13	13	135	44	SUM	185	92	RTN	235	02	02
036	10	10	086	85	+	136	15	15	186	76	LBL	236	69	OP
037	54	)	087	43	RCL	137	53	(	187	13	C	237	05	05
038	42	STO	088	12	12	138	43	RCL	188	73	RC*	238	92	RTN
039	09	09	089	54	)	139	14	14	189	00	00	239	00	0
040	55	÷	090	92	RTN	140	22	INV	190	23	LNX			
041	43	RCL	091	76	LBL	141	23	LNX	191	78	Σ+			
042	10	10	092	11	A	142	85	+	192	69	OP	LABELS		
043	65	x	093	43	RCL	143	43	RCL	193	20	20	000	88	DMS
044	05	5	094	16	16	144	15	15	194	97	DSZ	056	41	D
045	22	INV	095	42	STO	145	22	INV	195	07	07	092	11	A
046	28	LOG	096	12	12	146	23	LNX	196	10	C	172	12	B
047	54	)	097	43	RCL	147	54	)	197	58	FIX	187	13	C
048	59	INT	098	17	17	148	72	ST*	198	05	05	220	15	E
049	55	÷	099	42	STO	149	00	00	199	79	$\bar{x}$			

THE EFFECT OF VARIATIONS IN SOURCE TERM AND PARAMETER VALUES ON ESTIMATES OF RADIATION DOSE TO MAN

S. G. Bloom and W. E. Martin

Battelle Columbus Laboratories
Columbus, Ohio

ABSTRACT

Models had been previously developed to characterize the general behavior of plutonium in a typical ecosystem at the Nevada Test Site (NTS) and to provide a basis for estimating the radiation dose from ^{239}Pu that might be received by a hypothetical man who resides in and obtains most of his food from this ecosystem. The source term and parameters in these models are subject to wide variations due to uncertainties in sampling, measuring, and interpreting plutonium levels in laboratory experiments and in the environment. Regardless of the extent of these variations, previous exercises with the models indicate that inhalation is far more significant than ingestion as a pathway for transporting ^{239}Pu to man and that the lung and bone are the critical organs for radiation dose estimates. These features are used to develop simpler forms of the models which are then used to examine the effects of variations in the source term and parameters.

The most significant effects are due to variations in average soil concentration, mass loading factor for air, and the parameters of the lung model used for radiation dose estimates. Average soil concentration can range over several orders of magnitude and radiation dose estimates are directly proportional to this source term. The mass loading factor can also have a wide range of values to which the dose rate to lungs is directly proportional for all practical purposes. The parameters in the lung model are a function of particle size and those chemical and physical factors which determine the translocation class. The effects of particle size are significant but the translocation class has a much greater effect. Particle size within the respirable range can cause a factor of 6 variation in dose rate to lungs but translocation class can cause a factor of 600 to 700 variation. The variation in the rate for bone is not so large with particle size causing less than a factor of 4 variation and translocation class causing less than a factor of 60 variation.

None of the variations examined are surprising except, perhaps, for the large range that occurs due to variations in the parameters of the lung model. However, the biggest variations are due to translocation class, and it is generally acknowledged the plutonium-bearing particles at NTS fall into the year translocation class.

INTRODUCTION

In previous publications (Martin and Bloom, 1976; 1977), we presented models that attempt to characterize the general behavior of plutonium in a typical ecosystem at the NTS. The purpose of these models was to estimate the transport and accumulation of plutonium in the ecosystem and to provide a basis for estimating the radiation dose from ^{239}Pu that might be received by a hypothetical man who resides in and obtains most of his food from this ecosystem. The major transport pathways considered in these models are shown in Figure 1. The large square represents an arbitrary boundary of a contaminated area. Boxes represent the principal ecosystem components of interest and arrows represent net transport via the pathways indicated. Arrows which cross the arbitrary boundary represent net transport out of the system.

The plutonium concentration in the soil is the principal factor forcing the transport system in Figure 1. The soil contamination resulted from nuclear safety tests carried out from 1954 through 1963. Other inputs to the system (e.g., fallout) are insignificant compared with existing levels. Air is contaminated by resuspension of plutonium-bearing soil particles. Vegetation is contaminated internally by root uptake from soil and externally by deposition of resuspended particles. Plutonium input to herbivores is due to ingestion of soil and vegetation and to inhalation. Plutonium could reach man by inhalation of contaminated air, by accidental ingestion of contaminated soil, and by ingestion of milk or meat (skeletal muscle or internal organs) from animals raised in the contaminated area. Drinking water for herbivores and man is assumed to come from deep wells or from sources outside the contaminated area and to contribute nothing to plutonium intakes by herbivores or by man.

One of the major applications of the models developed on the bases of Figure 1 is to estimate whether and to what extent environmental decontamination might be required to limit or reduce potential health hazards to man from the plutonium at NTS. In previous publications (Martin and Bloom, 1976; 1977), we concluded that the principal exposure pathway for ^{239}Pu to man is via inhalation and the critical organs in terms of radiation dose are lungs and bone. It was estimated that inhalation accounts for 100 percent of the plutonium that reaches the lungs and 95 percent of the plutonium that reaches bone, liver, and kidney. Table 1 (Martin and Bloom, 1977) indicates that ingestion could be significant at ratios of ingestion to inhalation in excess of 400. However, the

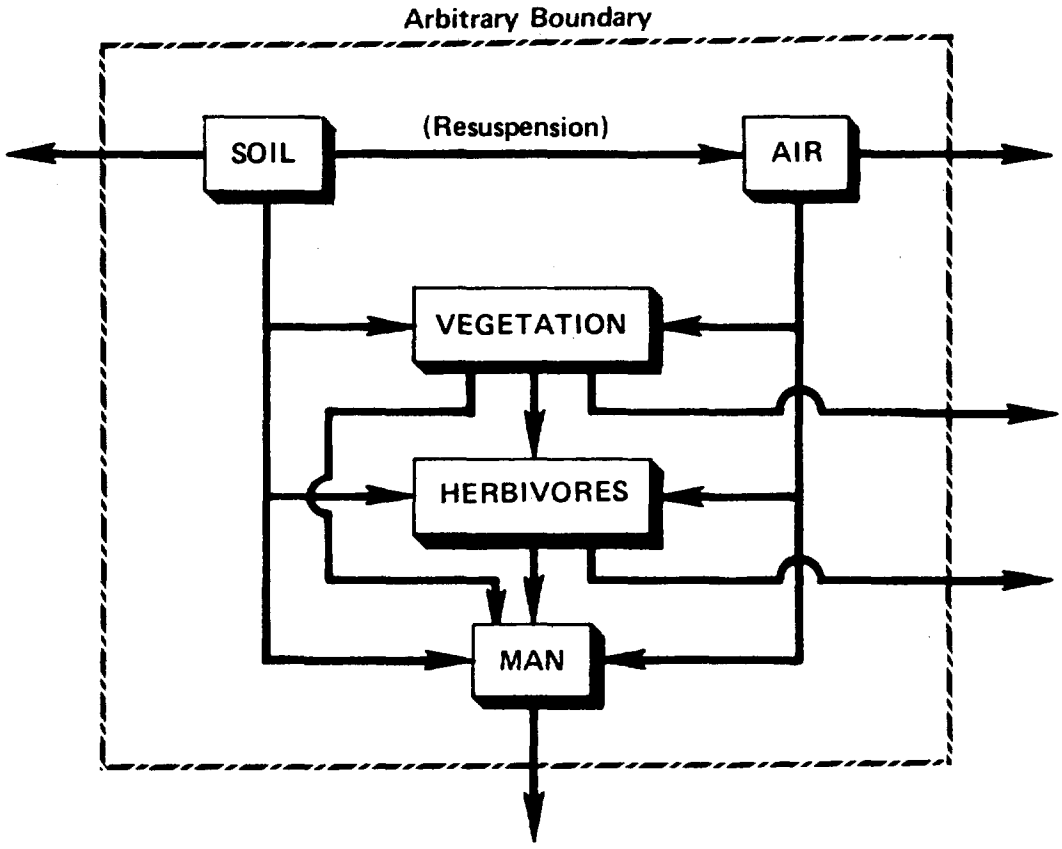

FIGURE 1. PRINCIPAL PATHWAYS OF PLUTONIUM TRANSPORT TO MAN

estimated ratio at NTS is only about 100. The designation of lungs and bone as critical organs was based on radiation dose calculations which showed these two organs receiving the highest dose, after 70 years, of all organs for which radiation dose criteria have been established by the International Commission on Radiological Protection (ICRP). The calculated dose to lymph nodes was higher but ICRP has not established dose criteria for lymph nodes. The results of these dose calculations are shown in Figure 2 (Martin and Bloom, 1977).

Table 1. Fractions of ^{239}Pu in Bone, Liver, or Kidney Due to Chronic Ingestion and Inhalation for a Period of 50 Years [(a)]

Ingestion/Inhalation	Fraction Due to Ingestion	Fraction Due to Inhalation
1	0.0005	0.9995
10	0.0053	0.9947
100[(b)]	0.0506	0.9494
200	0.0964	0.9036
400	0.1758	0.8242
1000	0.3478	0.6522

(a) Estimated burdens based on *ICRP Publications 2 and 19.*
(b) Estimated ratio at the Nevada Test Site.

The previous calculations are subject to considerable uncertainty due to variations in source term and parameters in the models. These variations result from uncertainties in sampling, measuring, and interpreting plutonium levels in laboratory experiments and in the environment. A detailed analysis of the effects of all these variations would be a prohibitively large task. Fortunately, this is not necessary since it has been shown that the most significant effects of these variations are directed toward the inhalation pathway and the radiation dose to lungs and bone. This report examines these parts of the model by developing simplified equations that are valid for periods of exposure greater than about 19 years and exploring the effects of these variations on this simpler model.

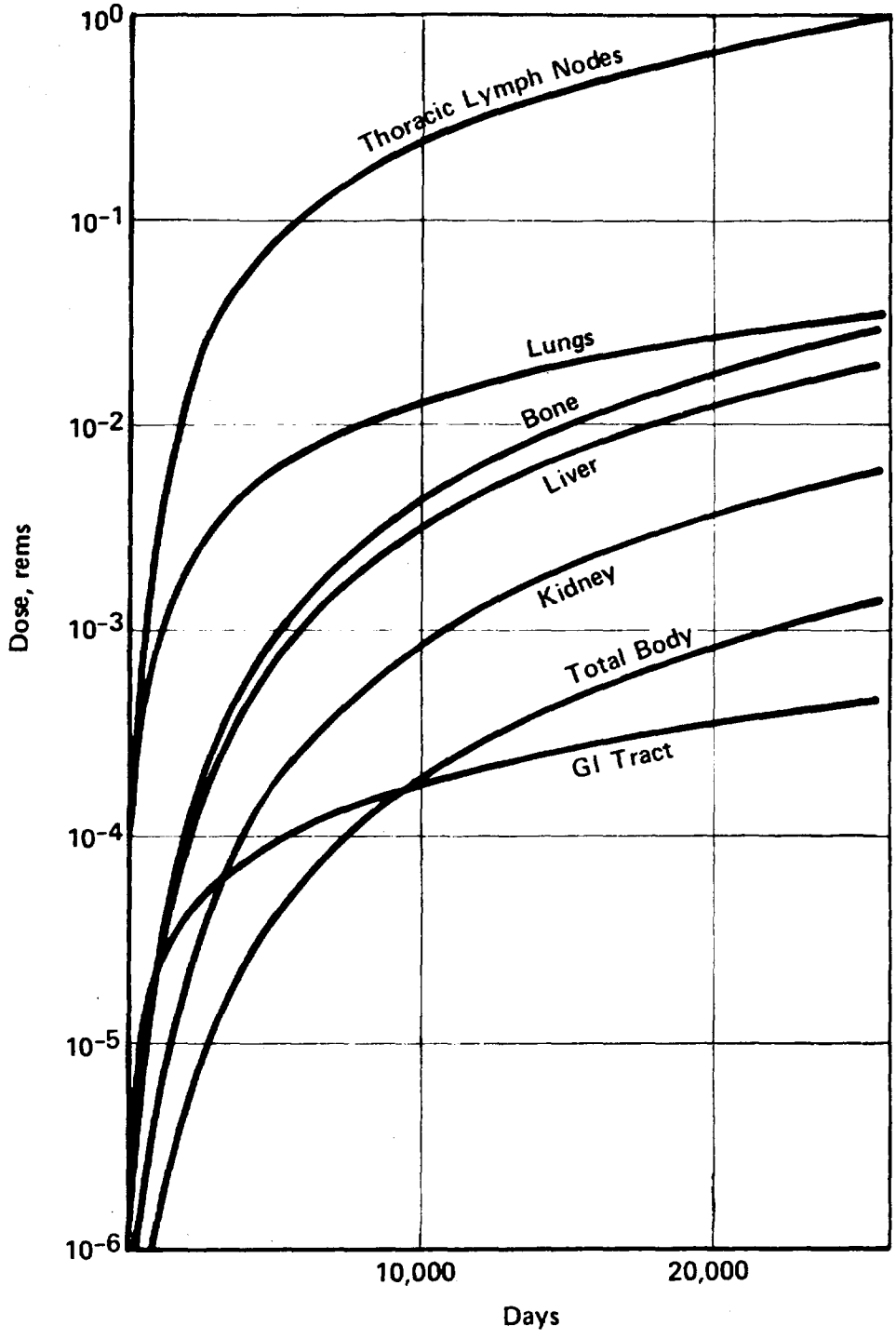

FIGURE 2. PREDICTED CUMULATIVE DOSES DUE TO ^{239}Pu IN DIFFERENT ORGANS OF STANDARD MAN

SIMPLIFIED MODEL

The radiation dose model for the lungs was developed by the ICRP Task Group on Lung Dynamics (Morrow *et al.*, 1966) and modified in a subsequent report (ICRP 19, 1972). This model is also used to estimate the rate of transfer of inhaled and ingested plutonium to blood and from blood to bone. Figure 3 shows the detailed structure of the lung model including all the compartments and transport pathways. The pulmonary region is used for calculations of radiation dose to the lungs. Bone is not shown in Figure 3 but involves a simple transfer from blood similar to the other transfers indicated in Figure 3. The mechanism and parameters for the transfer from blood to bone and the retention by bone are based on an earlier model presented by the ICRP Committee II (ICRP 2, 1959) and subsequently modified in ICRP 19 (1972).

On the basis of Figure 3, the equations for the transport and accumulation of ^{239}Pu in the lung model are:

$$r_{GIT} = \lambda_b y_{NPb} + \lambda_d y_{TBd} + \lambda_f y_{Pf} + \lambda_g y_{Pg} + H_m \quad (1)$$

$$r_B = \lambda_a y_{NPa} + \lambda_c y_{TBc} + \lambda_e y_{TBe} + \lambda_i y_{LMi} + f_j r_{GIT} \quad (2)$$

$$dy_{NPa}/dt = f_a D_3 A_m - (\lambda_A + \lambda_a) y_{NPa} \quad (3)$$

$$dy_{NPb}/dt = f_b D_3 A_m - (\lambda_A + \lambda_b) y_{NPb} \quad (4)$$

$$y_{NP} = y_{NPa} + y_{NPb} \quad (5)$$

$$dy_{TBc}/dt = f_c D_4 A_m - (\lambda_A + \lambda_c) y_{TBc} \quad (6)$$

$$dy_{TBd}/dt = f_d D_4 A_m - (\lambda_A + \lambda_d) y_{TBd} \quad (7)$$

$$y_{TBfg} = (\lambda_f y_{pf} + \lambda_g y_{Pg}) T_{TBfg} \quad (8)$$

$$y_{TB} = y_{TBc} + y_{TBd} + y_{TBfg} \quad (9)$$

$$dy_{Pe}/dt = f_e D_5 A_m - (\lambda_A + \lambda_e) y_{Pe} \quad (10)$$

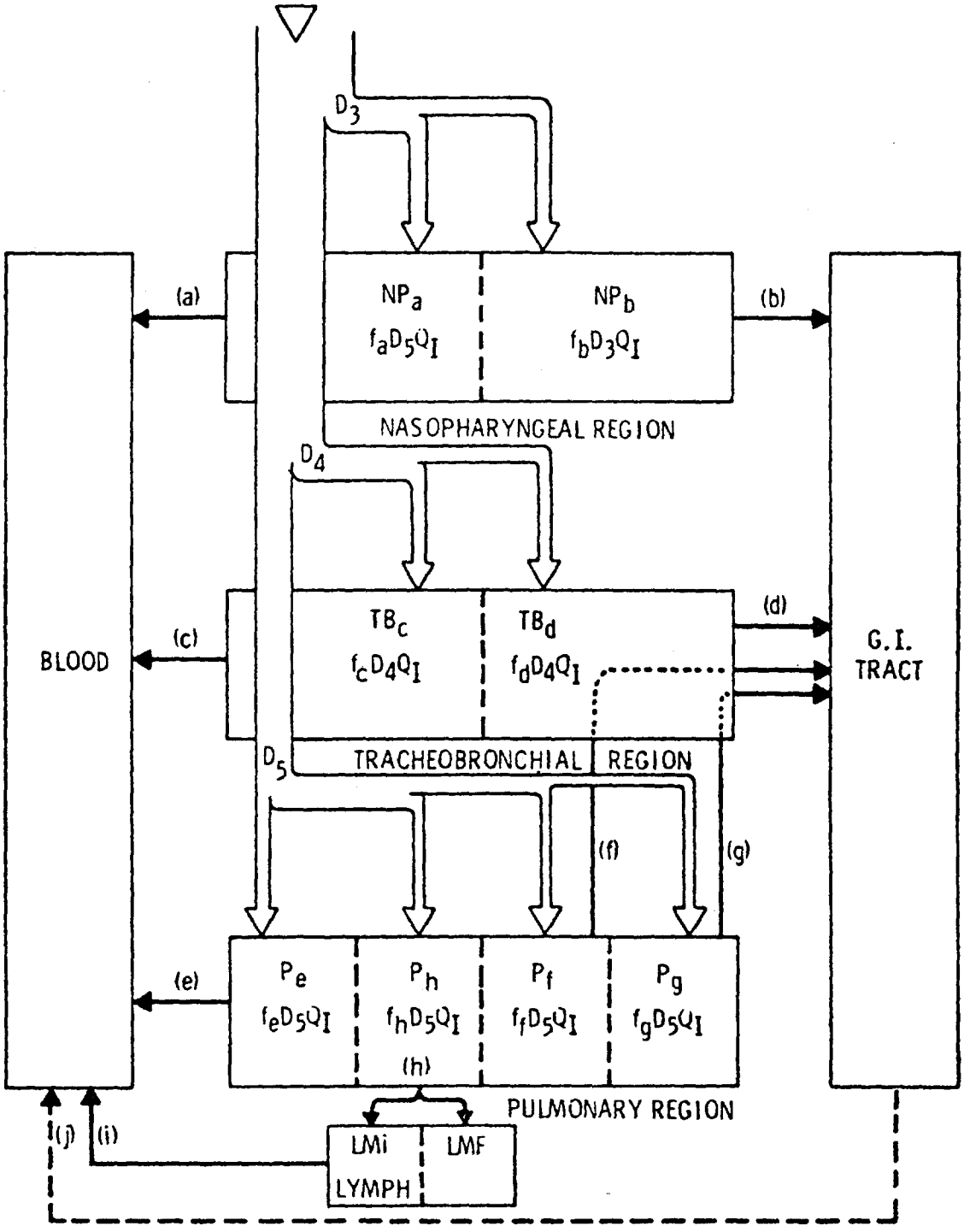

FIGURE 3. SCHEMATIC DIAGRAM OF THE TASK GROUP LUNG MODEL
From Houston *et al.*, 1975

$$dy_{Pf}/dt = f_f D_5 A_m - (\lambda_A + \lambda_f) y_{Pf} \quad (11)$$

$$dy_{Pg}/dt = f_g D_5 A_m - (\lambda_A + \lambda_g) y_{Pg} \quad (12)$$

$$dy_{Ph}/dt = f_h D_5 A_m - (\lambda_A + \lambda_h) y_{Ph} \quad (13)$$

$$y_P = y_{Pe} + y_{Pf} + y_{Pg} + y_{Ph} \quad (14)$$

$$dy_{LMi}/dt = f_i \lambda_h y_{Ph} \quad (\lambda_A + \lambda_i) y_{LMi} \quad (15)$$

$$dy_{LMF}/dt = (1 - f_i) \lambda_h y_{Ph} - \lambda_A y_{LMF} \quad (16)$$

$$y_{LM} = y_{LMi} + y_{LMF} \quad (17)$$

$$dy_B/dt = f_{BBN} r_B - (\lambda_A + \lambda_B) y_B \quad (18)$$

where

r_B, r_{GIT} are the rates that plutonium reaches the blood and gastrointestinal tract (GIT), respectively (μCi/day),

λ is the biological elimination rate constant where the subscripts refer to the compartments listed in Figure 3 and Table 2, except B refers to bone and λ_A is the radiological decay rate for ^{239}Pu (day^{-1}),

$\lambda = \ln(2)/T_k^b$ where T_k^b are the biological half-times listed in Table 2 (days),

y is the plutonium burden where the subscripts refer to the compartments listed in Figure 3 and Table 2 except B refers to bone (μCi),

t is time (days),

D_3, D_4, D_5 are the fractions of inhaled material that are deposited in the nasopharyngeal, tracheobronchial, and pulmonary regions, respectively, of the respiratory tract (see Figure 3 and Table 2),

A_m, H_m are the plutonium inhalation and ingestion rates, respectively (μCi/day),

Table 2. Task Group Lung Model Parameter Values [a]

Fraction of Inhaled Particles Deposited in the Respiratory System Versus Particle Diameter [b]

Particle Size AMAD [c] Micrometers	Fraction of Inhaled Quantity Retained		
	Nasopharyngeal Region, D_3	Tracheobronchial Region, D_4	Pulmonary Region, D_5
0.05	0.001	0.08	0.59
0.1	0.008	0.08	0.50
0.3	0.063	0.08	0.36
0.5	0.13	0.08	0.31
1.0	0.29	0.08	0.23
2.0	0.50	0.08	0.17
5.0	0.77	0.08	0.11

Clearance Parameter Values [d]

Compartment	k	Translocation Class [e]					
		D		W		Y	
		T_k^b [f]	f_k [g]	T_k^b	f_k	T_k^b	f_k
NP	a	0.01	0.50	0.01	0.10	0.01	0.01
	b	0.01	0.50	0.40	0.90	0.40	0.99
TB	c	0.01	0.95	0.01	0.50	0.01	0.01
	d	0.20	0.05	0.20	0.50	0.20	0.99
P	e	0.50	0.80	50	0.15	500	0.05
	f	n.a.	n.a.	1	0.40	1	0.40
	g	n.a.	n.a.	50	0.40	500	0.40
	h	0.50	0.20	50	0.05	500	0.15
L	i	0.50	1.00	50	1.00	1000	0.90

(a) Source: U.S. Nuclear Regulatory Commission (1976).
(b) Estimated from data of Task Group on Lung Dynamics (Morrow, 1966).
(c) AMAD is activity mean aerodynamic diameter.
(d) As amended by ICRP Publication 19 (1972).
(e) D, W, Y = Days, Weeks, Years.
(f) T_k^b = Biological Half-Time (days) for pathway k (see Figure 3).
(g) f_k = Fraction cleared by pathway k (see Figure 3).

f is the fraction of plutonium transferred from one location to another within the body where the subscripts refer to the compartments and the pathways listed in Figure 3 and Table 2 except BBN is the fraction from blood to bone,

T_{TBFg} is the residence time of material following pathways f and g in the tracheobronchial region (days).

Values of most of the parameters in the above equations are given in Table 2 (U.S. Nuclear Regulatory Commission, 1976). T_{TBfg} is assumed to be one hour of 1/24-day (Snyder, 1967; Kotrappa, 1968; 1969) while f is usually 0.003 percent (ICRP 2, 1959; ICRP 19, 1972). The parameter values for bone are $f_{BBN} = 0.45$ and $T_B^b = 100$ years (ICRP 19, 1972). The radiological decay rate for ^{239}Pu is 7.786×10^{-8} $(days)^{-1}$.

The radiation dose rate to any of the compartments shown in Figure 3 or any other organ of the body is given by

$$dD/dt = E\ y/m \qquad (19)$$

where

D is the dose to the compartment (rems),
E = 51.2159 ε, is a dose rate factor (g rem)/μCi day)),
ε is the effective energy absorbed in the compartment per disintegration of radionuclide (MeV/dis),
y is the plutonium burden in the compartment (μCi),
m is the mass of the compartment (g).

Only the dose rate to lungs (pulmonary region) and bone is of interest. The usual values of the parameters in Equation (19) for these two compartments are $\varepsilon_P = 53$, $\varepsilon_B = 270$, and $m_B = 7000$ as given by the ICRP (ICRP 2, 1959) and $m_P = 500$ as given by Snyder (1967) and Kotrappa (1968; 1969).

The biological half-time values (T_k^b) in Table 2 range from less than one day to 1,000 days which corresponds to a minimum λ value of about 6.9×10^{-4} $(days)^{-1}$. These λ values are much larger than the radiological decay rate for ^{239}Pu ($\lambda_A = 7.786 \times 10^{-8}$ $days^{-1}$) which can be neglected by comparison in Equations (1) through (17). The λ_B value for bone is small enough that λ_A will have a very slight effect on Equation (18).

Another consequence of the half-time values listed in Table 2 is the time it takes the compartments to reach the equilibrium burden of ^{239}Pu resulting from a constant inhalation or ingestion rate. The time to reach about 99 percent of the equilibrium burden is about seven times the biological half-time. For the compartments of the lung model, the maximum half-time is 1,000 days (LMi) and the equilibrium time is no longer than about 7,000 days (about 19 years). Figure 4 shows the ^{239}Pu organ burdens predicted previously (Martin and Bloom, 1976; 1977) and it can be seen that the pulmonary region (lung in Figure 4) and compartment

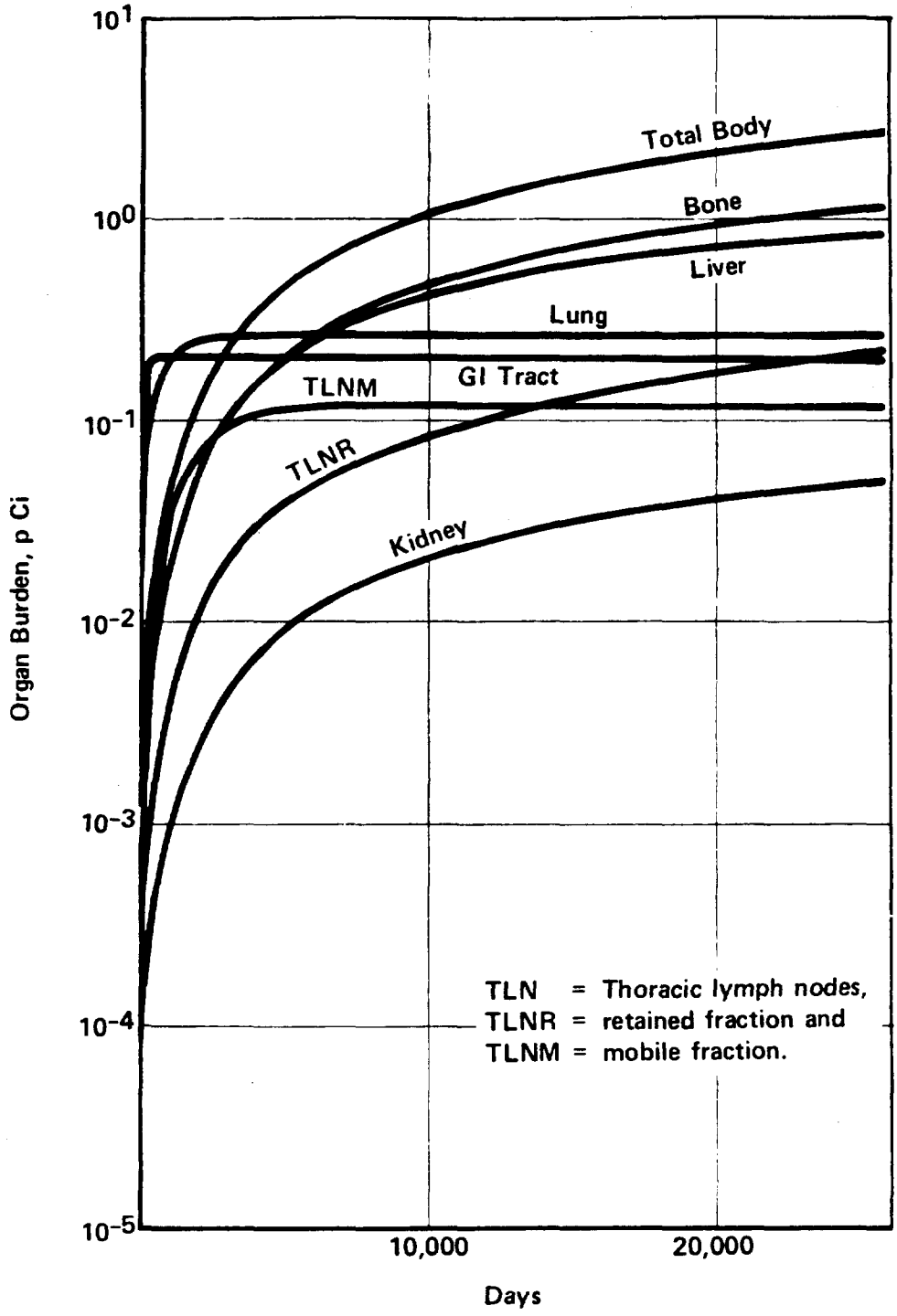

FIGURE 4. PREDICTED ORGAN BURDENS OF ^{239}Pu IN DIFFERENT ORGANS OF STANDARD MAN

LMi of the lymph (TLNM in Figure 4) reaches equilibrium values by about 7,000 days. However, the bone burden is still increasing after 20,000 days since the time for bone to reach equilibrium is on the order of 700 years (255,500 days).

When a compartment is in equilibrium, the time derivative of the burden is zero (dy/dt = 0) and the equilibrium burdens of the lung compartments can be calculated from the algebraic system of equations formed by setting all the time derivatives to zero in Equations (1) through (17). The compartments of the pulmonary region are the most significant for computing the radiation dose to the lungs. Since λ_A is so small in comparison to the other λ values, it can be set to zero in Equations (1) through (18) and the equilibrium ^{239}Pu burden of the pulmonary region is:

$$y_P = A_m D_5 \left(f_e/\lambda_e + f_f/\lambda_f + f_g/\lambda_g + f_h/\lambda_h\right). \quad (20)$$

The equilibrium rate that ^{239}Pu reaches the blood is:

$$r_B = A_m((f_a + f_b f_j) D_3 + (f_c + f_d f_j) D_4 + (f_e + f_f f_j + f_g f_j + f_h f_i) D_5) + f_j H_m. \quad (21)$$

The ^{239}Pu burden in bone is never in equilibrium during the time period of interest (less than 70 years) but its burden after 20 years can be easily calculated since r_B is at equilibrium and the solution to Equation (18) for constant r_B is:

$$y_B = [f_{BBN}\, r_B/\lambda_B]\, [1.0 - \exp(-\lambda_B t)]. \quad (22)$$

Equations (19) through (22), along with expressions for estimating the inhalation and ingestion of ^{239}Pu, form the simplified model used to examine the effects of variations in source term and parameter values. The model previously used to estimate inhalation of ^{239}Pu (Martin and Bloom, 1976; 1977) is already simple in form and is:

$$A_m = B_m L_a C_s \quad (23)$$

where

B_m is man's inhalation rate (about 20 m^3/day).

L_a is the mass loading factor for soil in the air (about 100 $\mu g/m^3$),

C_s is the average concentration of ^{239}Pu in the soil of a contaminated area ($\mu Ci/g$).

The model previously used to estimate ingestion is considerably more complicated but, as indicated in Table 1, ingestion of ^{239}Pu is not nearly as significant as inhalation. Therefore, the only variation

examined with respect to ingestion was the ingestion to inhalation ratio (H_m/A_m). The ingestion model takes the form (Martin and Bloom, 1976; 1977):

$$H_m = C_s \Sigma I_i D_i \quad (24)$$

where

I_i is the ingestion rate for substance i (g/day)

D_i is the discrimination factor which is the ratio of concentration of ^{239}Pu in substance i to the concentration of ^{239}Pu in soil.

The principal item to note from Equation (24) is that H_m is directly proportional to C_s, but varies with respect to the composition of the diet.

ANALYSIS OF THE EFFECTS OF VARIATIONS

The simplified model given by Equations (19) through (24) allows us to examine the effects of variations in the significant parameters in a relatively easy manner. The parameters subject to the most variation are (a) the average soil concentration (C_s), (b) the mass loading factor (L_a), (c) the various fractions and biological half-times involved in the lung model (Equations (20) and (21)), (d) the ingestion to inhalation ratio (H_m/A_m), and (e) the biological elimination rate for bone ($\lambda_B = \ln(2)/T_B^b$) and fraction from blood to bone. Statistical summaries of soil inventory data by Gilbert *et al.* (1975) show large variations of soil concentration within a particular area. This variation is compounded by uncertainties as to the proper size and boundaries to assign to the ecosystem model. The mass loading factor is also quite variable and depends on wind velocities and frequencies as well as the size of soil particles and whether the soil has been mechanically disturbed (e.g., plowed). The various fractions and half-times in the lung model are subject to considerable uncertainty because we are generally ignorant of the particle size which affects the initial deposition fractions (D_3, D_4, and D_5) as well as the chemical and physical form of the plutonium (which affects the translocation class). The ingestion to inhalation ratio is uncertain because of the potential variation in the parameters of the ecosystem model that predicts ingestion as well as uncertainties in L_a and C_s. The biological elimination rate (or half-time) of bone and the fraction from blood to bone can be significant because bone does not reach equilibrium within the time period of interest (50-70 years) and because a range of values has been proposed for these two parameters (ICRP 19, 1972).

The effects of variations in the average soil concentration (C_s) are easily seen from the equations. Both A_m and H_m are directly proportional to C_s and, therefore, the ^{239}Pu burdens and the corresponding radiation dose rates for lungs and bone are also directly proportional to C_s. This relationship was recognized in previous studies (Martin and Bloom, 1976; 1977) and was used to normalize all calculations to 1 pCi/g soil and to determine an acceptable soil concentration at NTS. Since C_s can have values which range over several orders of magnitude, the estimated radiation dose rates to lungs and bone can also range over several orders of magnitude.

The nominal value of the mass loading factor used previously (Martin and Bloom, 1976; 1977) is 100 $\mu g/m^3$. Measured air concentrations of ^{239}Pu at NTS are in good agreement with predictions based on this value (Anspaugh *et al.*, 1975). However, this parameter can also range over several orders of magnitude and the inhalation rate (A_m) is directly proportional to L_a. Variations in L_a can also affect H_m but the effects may be smaller and less obvious. Also, since inhalation is far more significant than ingestion in transporting ^{239}Pu to bone and is the exclusive mechanism for transport to lungs, the range of variation in dose rate to the lungs is directly proportional to the range in L_a values, and the rate to bone is also directly proportional for all practical purposes.

It is much more difficult to visualize from the equations the effects of variations in the fractions and half-times involved in the lung model as well as the ingestion to inhalation ratio. Table 3 shows the equilibrium lung burden of ^{239}Pu due to a chronic inhalation of 1 pCi/day as a function of particle size and translocation class. The dose rate to lungs is directly proportional to the burden. These data are plotted in Figure 5. The data show that the burden decreases with increasing particle size, within the range of respirable particle sizes. For a given translocation class, the maximum variation is about a factor of five to six. There is a much larger variation from one translocation class to another with the year class (insoluble, immobile particles) being about 600 to 700 times greater than the corresponding particles in the day class (soluble, mobile particles).

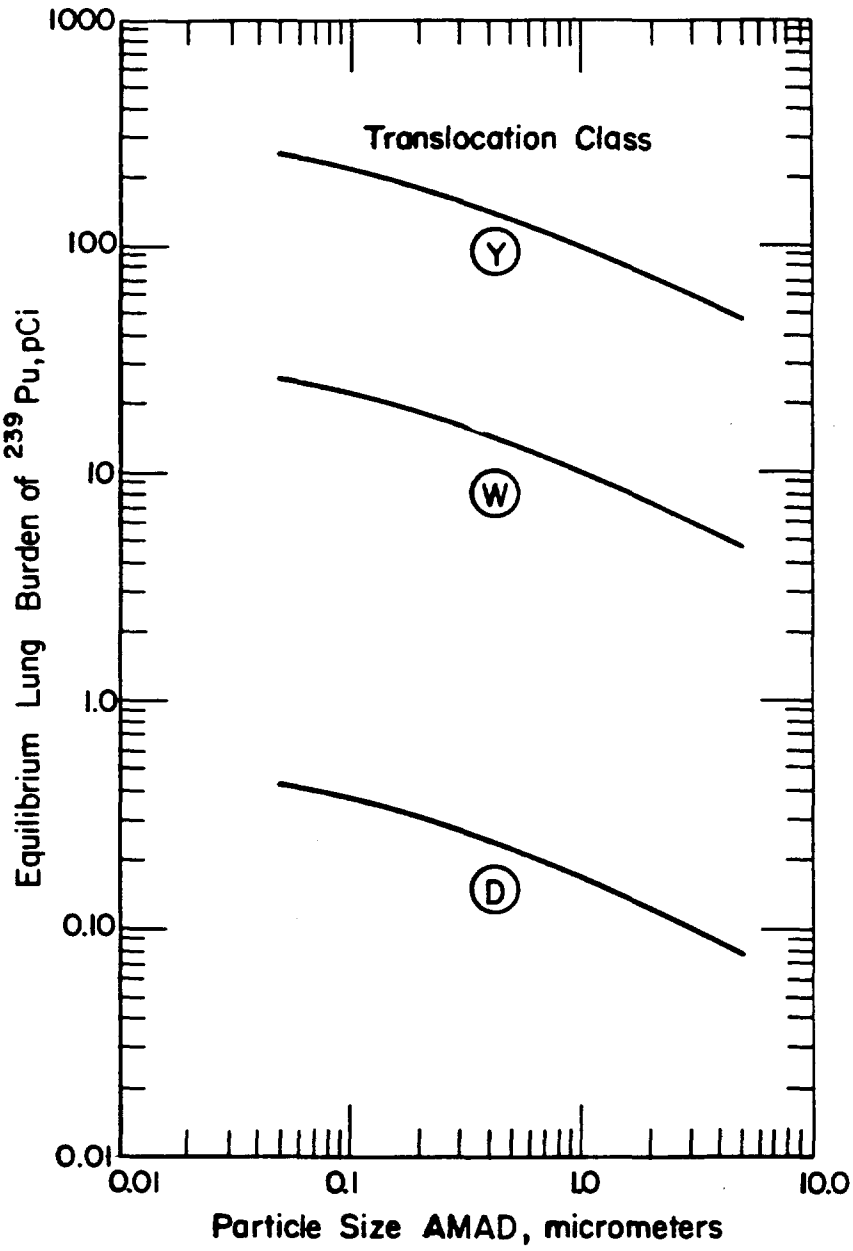

FIGURE 5. EQUILIBRIUM LUNG BURDEN OF ^{239}Pu DUE TO CHRONIC INHALATION OF 1 pCi/DAY

Table 3. Equilibrium Lung Burden of ^{239}Pu Due to Chronic Inhalation of 1 pCi/day

Particle Size AMAD[a] Micrometers	Translocation Class[b]		
	D	W	Y
0.05	4.26E-1[c]	2.59E1	2.56E2
0.10	3.61E-1	2.19E1	2.17E2
0.30	2.60E-1	1.58E1	1.56E2
0.50	2.24E-1	1.36E1	1.34E2
1.00	1.66E-1	1.01E1	9.97E1
2.00	1.23E-1	7.46E0	7.37E1
5.00	7.93E-2	4.82E0	4.77E1

(a) AMAD is activity mean aerodynamic diameter.

(b) D.W.Y. = Days, Weeks, Years.

(c) Values are ^{239}Pu burdens in the pulmonary region of the lung. Numbers following E are exponents of 10.

Parameter variations in the lung model are even more difficult to visualize when their effect is on the rate of ^{239}Pu transport to blood (from where it goes to bone). Table 4 shows the effects of particle size, translocation class, fraction of ^{239}Pu in the gastrointestinal tract (GIT) which reaches blood, and ingestion to inhalation ratio (Hm/Am). Some of these data are plotted in Figures 6, 7, and 8. In these figures, the fraction from GIT to blood is assumed to be 0.001 for Class D, 3.0E-5 for Class W, and 1.0E-6 for Class Y. As with the lung burden, the variation from one translocation class to another is greater than the variation with particle size. The variations with particle size show a minimum value between 0.5 and 1.0 micrometers for day and week classes while the year class values decrease with increasing particle size. The maximum variation with particle size is less than a factor of 2 for day and week classes, but it is as much as a factor of 3 to 4 for the year class. The variation with translocation class for a given particle size is about a factor of 6 for the smaller particles at the lower Hm/Am values and all values of the fraction from GIT to blood (f_j). For larger particles, the variation with translocation class can be greater than a factor of 50. It should be noted that an f_j of 3.0E-5 is recommended by ICRP (ICRP 19, 1972), but they report experimental values ranging from 1.0E-6 to 0.001.

The effects of variations in the biological half-time (T_B^b) for bone and the fraction from blood to bone (f_{BBN}) are shown in Table 5 and Figure 9. The ^{239}Pu is directly proportional to f_{BBN} (Equation (22)). The recommended value is 0.45 (ICRP 19, 1972) but values as high as 0.8 had been

Table 4. Rate at Which ^{239}Pu Reaches the Blood Divided by the Inhalation Rate (r_B/A_m)

Particle Size AMAD Micrometers[b]	Translocation Class (a)								
	D			W			Y		
	Fraction from GIT to Blood								
	1.0E-3	3.0E-5	1.0E-6	1.0E-3	3.0E-5	1.0E-6	1.0E-3	3.0E-5	1.0E-6
					Hm/Am = 0.0[c]				
0.05	0.667	0.667	0.667	0.159	0.158	0.158	0.111	0.110	0.110
0.10	0.580	0.580	0.580	0.141	0.141	0.141	0.094	0.093	0.093
0.30	0.468	0.468	0.468	0.119	0.118	0.118	0/068	0.068	0.068
0.50	0.451	0.451	0.451	0.115	0.115	0.115	0.060	0.059	0.059
1.00	0.451	0.451	0.451	0.115	0.115	0.115	0.047	0.046	0.046
2.00	0.496	0.496	0.496	0.125	0.124	0.124	0.038	0.037	0.037
5.00	0.571	0.571	0.571	0.140	0.139	0.139	0.030	0.029	0.029
					Hm/Am = 1.0				
0.05	0.668	0.667	0.667	0.160	0.158	0.158	0.112	0.110	0.110
0.10	0.581	0.580	0.580	0.142	0.141	0.141	0.095	0.093	0.093
0.30	0.469	0.468	0.468	0.120	0.118	0.118	0.069	0.068	0.068
0.50	0.452	0.451	0.451	0.116	0.115	0.115	0.061	0.059	0.059
1.00	0.452	0.451	0.451	0.116	0.115	0.115	0.048	0.046	0.046
2.00	0.497	0.496	0.496	0.126	0.124	0.124	0.039	0.037	0.037
5.00	0.572	0.571	0.571	0.141	0.139	0.139	0.031	0.029	0.029
					Hm/Am = 10.0				
0.05	0.677	0.667	0.667	0.169	0.158	0.158	0.121	0.110	0.110
0.10	0.590	0.580	0.580	0.151	0.141	0.141	0.104	0.094	0.093
0.30	0.478	0.468	0.468	0.129	0.119	0.118	0.078	0.068	0.068
0.50	0.461	0.451	0.451	0.125	0.115	0.115	0.070	0.060	0.059
1.00	0.461	0.451	0.451	0.125	0.115	0.115	0.057	0.047	0.046
2.00	0.506	0.496	0.496	0.135	0.124	0.124	0.048	0.038	0.037
5.00	0.581	0.571	0.571	0.150	0.139	0.139	0.040	0.029	0.029
					Hm/Am + 100.0				
0.05	0.767	0.670	0.667	0.259	0.161	0.158	0.211	0.113	0.110
0.10	0.680	0.583	0.580	0.241	0.144	0.141	0.194	0.096	0.093
0.30	0.568	0.471	0.468	0.219	0.121	0.118	0.168	0.071	0.068
0.50	0.551	0.454	0.451	0.215	0.118	0.115	0.160	0.062	0.060
1.00	0.551	0.454	0.451	0.215	0.118	0.115	0.147	0.049	0.046
2.00	0.596	0.499	0.496	0.225	0.127	0.124	0.138	0.040	0.037
5.00	0.671	0.574	0.571	0.240	0.142	0.139	0.130	0.032	0.029
					Hm/Am = 1000.0				
0.05	1.667	0.697	0.668	1.159	0.188	0.159	1.111	0.140	0.111
0.10	1.580	0.610	0.581	1.141	0.171	0.142	1.094	0.123	0.094
0.30	1.468	0.498	0.469	1.119	0.148	0.119	1.069	0.098	0.069
0.50	1.451	0.481	0.452	1.115	0.145	0.116	1.060	0.089	0.060
1.00	1.451	0.481	0.452	1.115	0.145	0.116	1.047	0.076	0.047
2.00	1.496	0.526	0.497	1.125	0.154	0.125	1.038	0.067	0.038
5.00	1.571	0.601	0.572	1.140	0.169	0.140	1.030	0.059	0.030

(a) D.W.Y. = Days, Weeks, Years.

(b) AMAD is activity mean aerodymanic diameter.

(c) For Hm = 0, values are also fractions of inhaled ^{239}Pu which reach the blood.

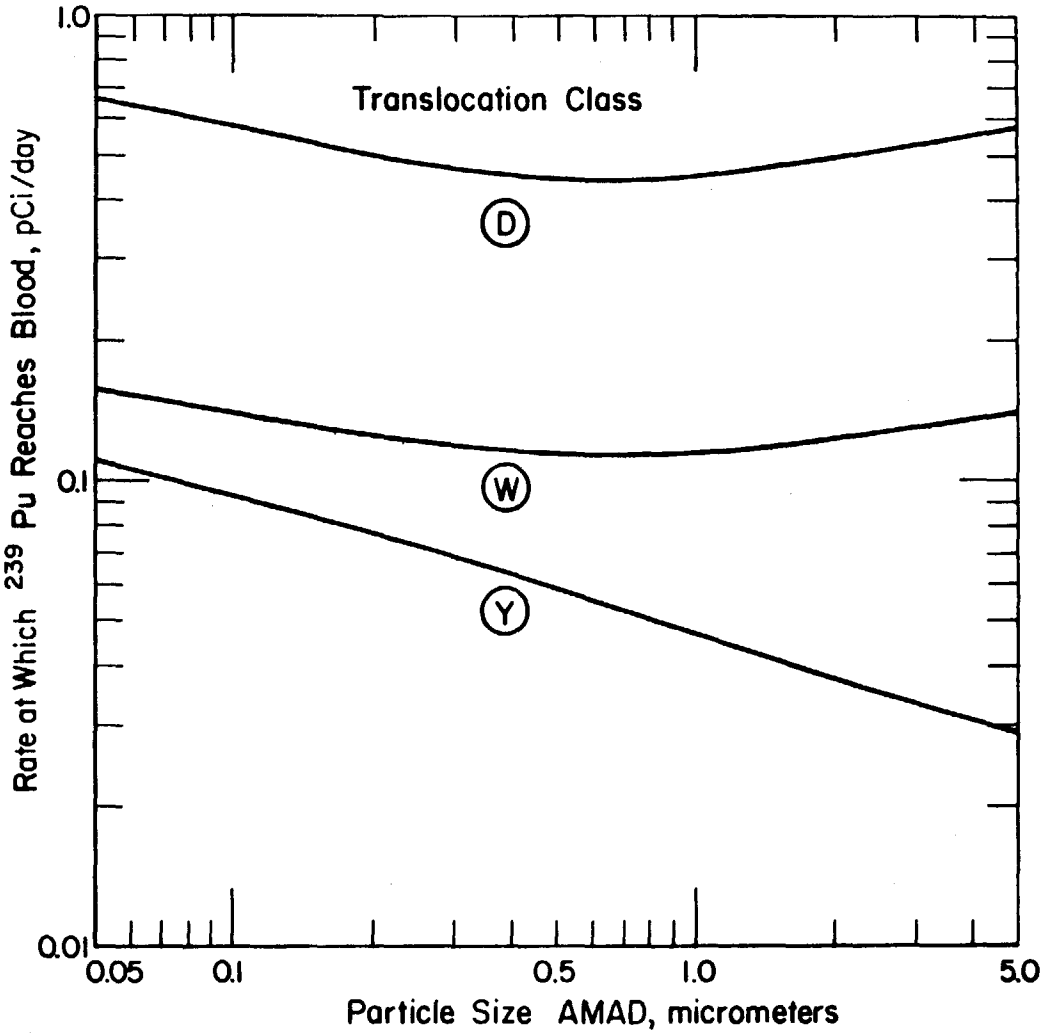

FIGURE 6. RATE AT WHICH ^{239}Pu REACHES BLOOD FROM INHALING 1 pCi/DAY (Hm/Am = 0)

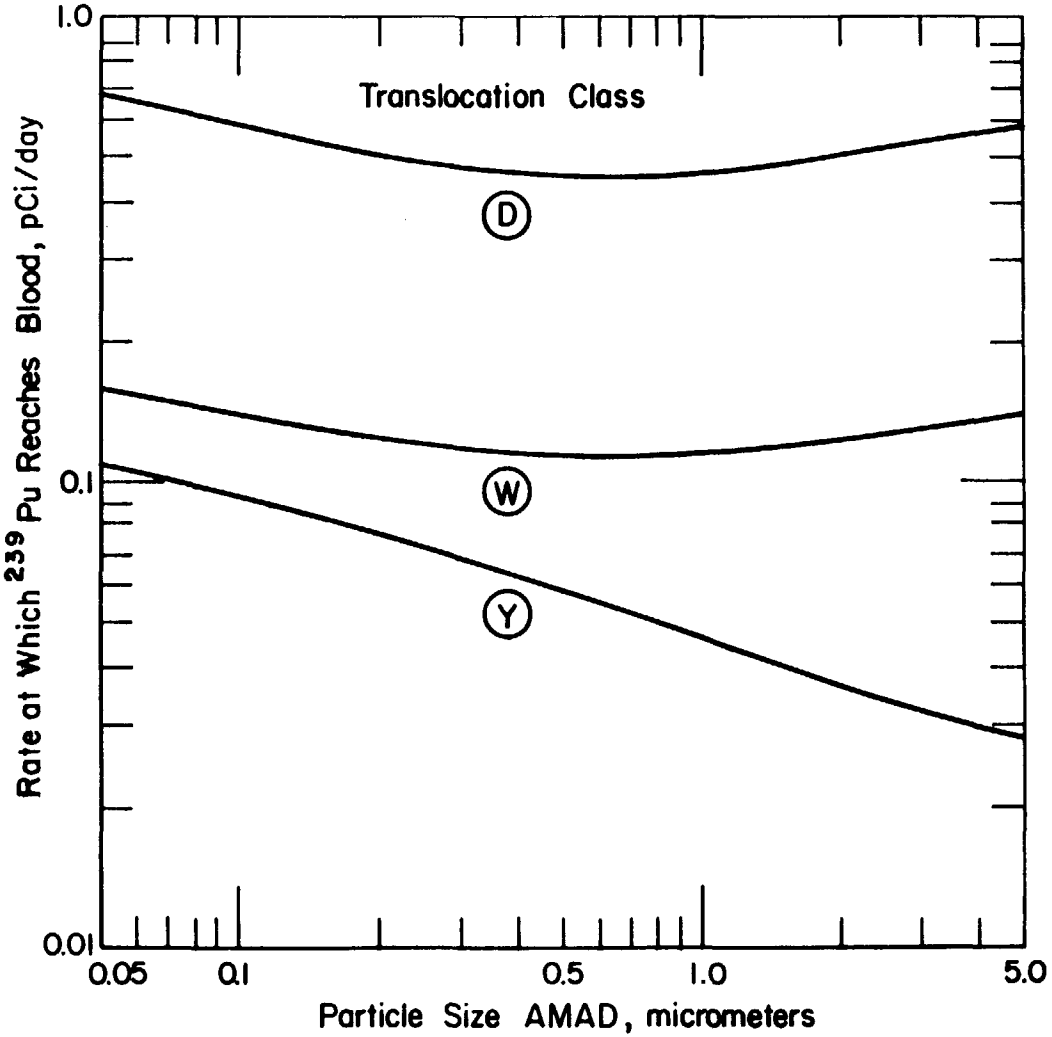

FIGURE 7. RATE AT WHICH ^{239}Pu REACHES BLOOD FROM INHALING 1 pCi/DAY AND INGESTING 10 pCi/DAY (Hm/AM = 10)

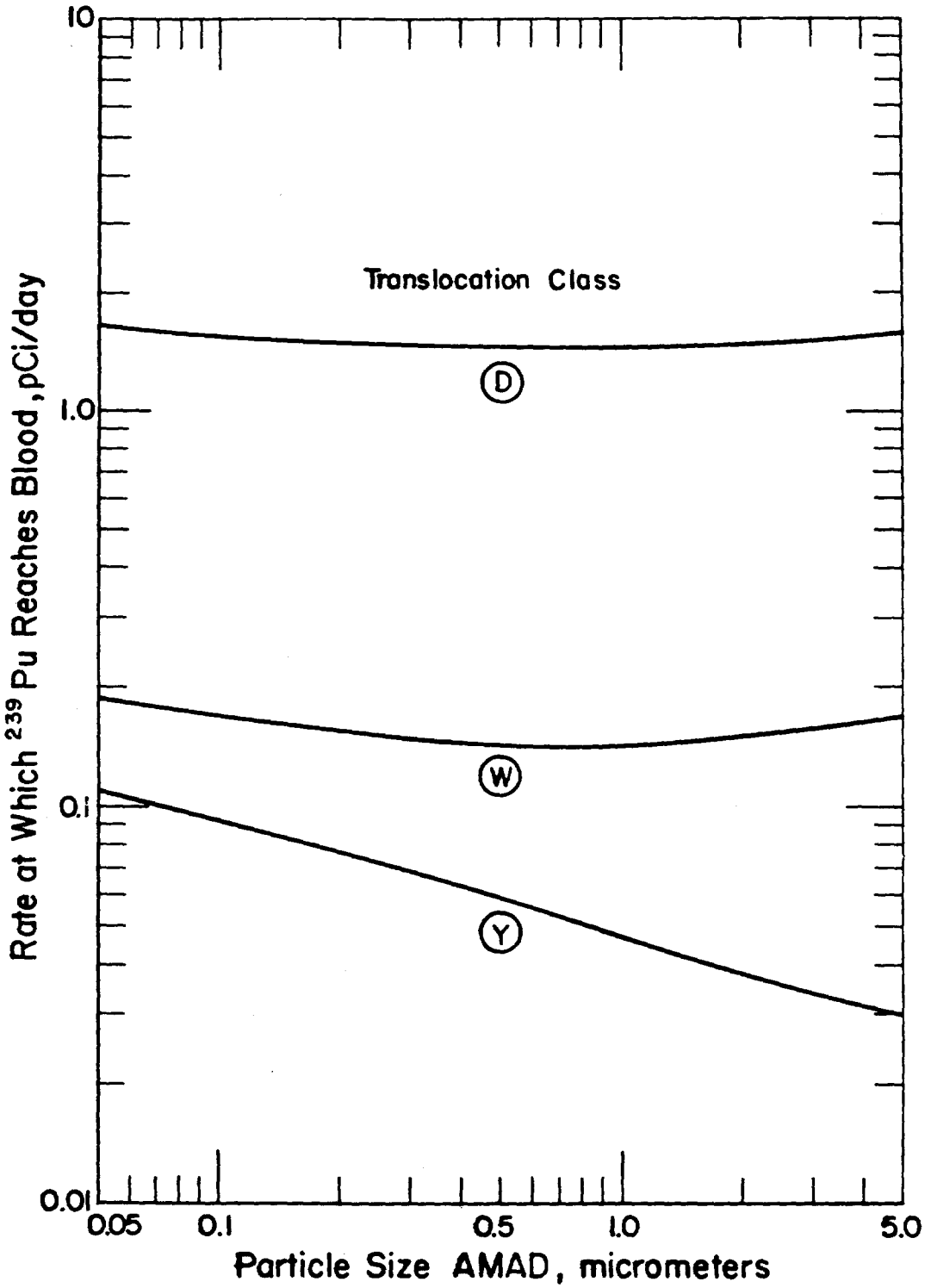

FIGURE 8. RATE AT WHICH ^{239}Pu REACHES BLOOD FROM INHALING 1pCi/DAY AND INGESTING 1000 pCi/DAY (Hm/Am = 1000)

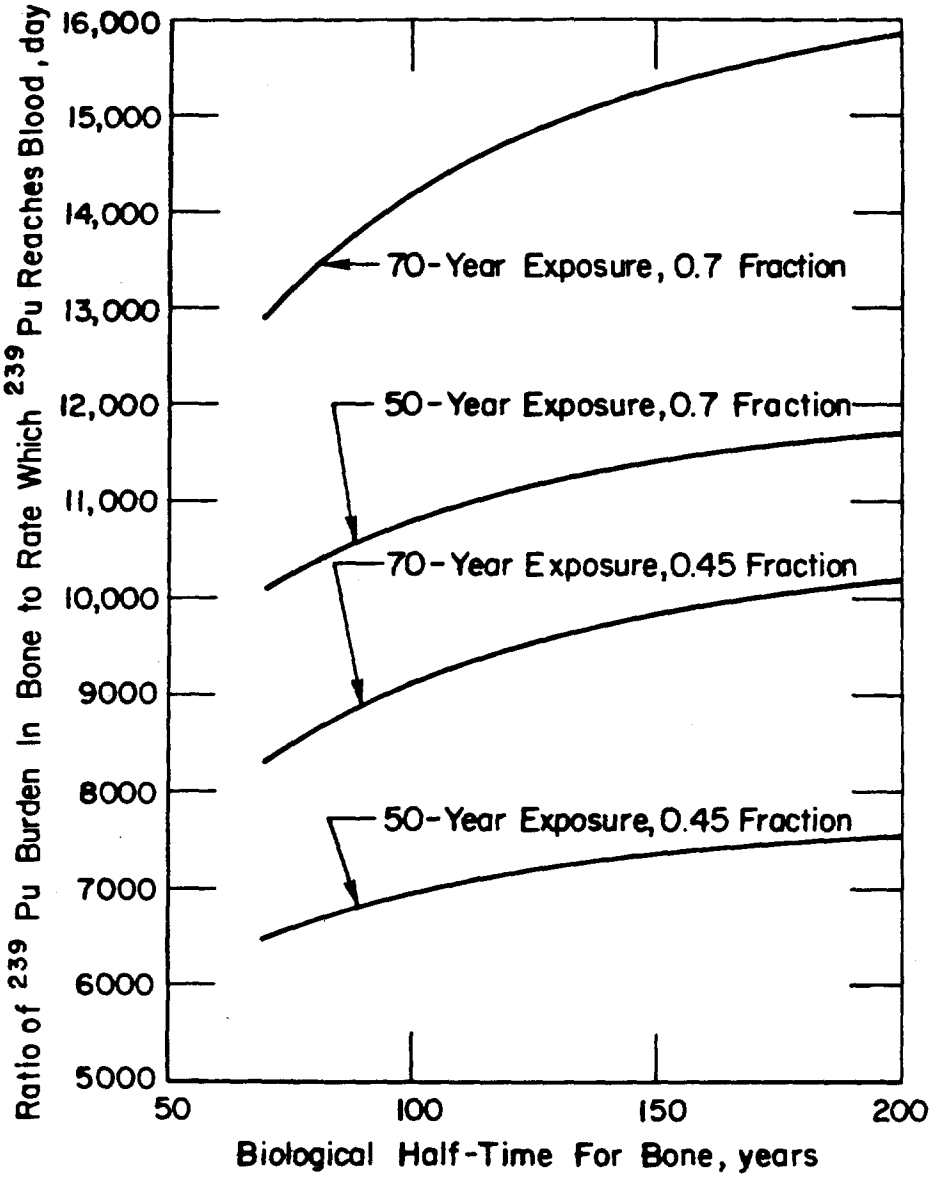

FIGURE 9. EFFECT OF BIOLOGICAL HALF TIME AND FRACTION FROM BLOOD TO BONE

recommended earlier (ICRP 2, 1959). The effects of variations in T_B^b or exposure period are much smaller, for the range of parameter values of interest, being less than a factor of 2.

Table 5. Ratio of ^{239}Pu Burden in Bone to Rate Which ^{239}Pu Reaches Blood (y_B/r_B) [a]

Fraction From Blood to Bone (f_{BBN})	Biological Half-Time for Bone (T_B^b), Years				
	70	100	130	160	200
			50-Year Exposure		
0.45	6477[a]	6940	7209	7384	7540
0.5	7197	7712	8010	8204	8378
0.6	8636	9254	9612	9845	10054
0.7	10076	10796	11214	11486	11729
0.8	11515	12339	12816	13127	13405
			70-Year Exposure		
0.45	8294	9110	9596	9918	10209
0.5	9215	10122	10662	11020	11343
0.6	11058	12146	12794	13224	13612
0.7	12901	14170	14927	15428	15881
0.8	14744	16195	17059	17632	18150

(a) Units of ratio are day.

CONCLUSIONS

The results of this analysis are not surprising. Soil concentration is the most significant source term and is subject to a great deal of variation. The parameter for relating the soil concentration to the concentration in air is also very significant and also subject to wide variations. It is, perhaps, surprising to see the variation in estimated dose rates that could result from uncertainties in the size and chemical/physical properties of plutonium-bearing particles. However, dose variations due to particle size are much less than those due to variations in soil concentration and mass loading factor, and it is generally assumed that the plutonium-bearing particles at NTS are of such a chemical and physical nature that they are always in the year translocation class.

REFERENCES

1. Anspaugh, L. R., J. H. Shinn, P. L. Phelps, and N. C. Kennedy. 1975. "Resuspension and Redistribution of Plutonium in Soils." *Health Physics* 29:571-582.

2. Gilbert, R. O., L. L. Eberhardt, E. B. Fowler, E. M. Romney, E. H. Essington, and J. E. Kinnear. 1975. "Statistical Analysis of $^{239,240}Pu$ and ^{241}Am Contamination of Soil and Vegetation on NAEG Study Sites." *In: The Radioecology of Plutonium and Other Transuranics in Desert Environments.* M. G. White and P. B. Dunaway (Eds.). ERDA Report, NVO-153. pp. 339-448.

3. Houston, J. R., D. L. Strenge, and E. C. Watson. 1975. "DACRIN--A Computer Program for Calculating Organ Dose From Acute or Chronic Radionuclide Inhalation." Battelle Pacific Northwest Laboratories (Dec. 1974; Reissued Aug. 1975). BNWL-B-389.

4. International Commission of Radiological Protection. 1959. "Recommendations Report of Committee II on Permissible Dose for Internal Radiation." ICRP Publ. 2. Pergamon Press, New York.

5. International Commission of Radiological Protection. 1972. "The Metabolism of Compounds of Plutonium and Other Actinides." ICRP Publ. 19. Pergamon Press, New York.

6. Kotrappa, P. 1968. "Dose to Respiratory Tract From Continuous Inhalation of Radioactive Aerosol." University of Rochester. Department of Radiation Biology and Biophysics. USAEC Report, UR-49-964.

7. Kotrappa, P. 1969. "Calculation of the Burden and Dose to the Respiratory Tract From Continuous Inhalation of a Radioactive Aerosol." *Health Physics* 17(3):429-432.

8. Martin, W. E., and S. G. Bloom. 1976. "Plutonium Transport and Dose Estimation Model." *In: Transuranium Nuclides in the Environment.* IAEA, Vienna. IAEA-SM-199/78.

9. Martin, W. E., and S. G. Bloom. 1977. "Nevada Applied Ecology Group Model for Estimating Plutonium Transport and Dose to Man." *In: Transuranics in Natural Environments.* M. G. White and P. B. Dunaway (Eds.). ERDA Report, NVO-178. pp. 621-706.

10. Morrow, P. E., D. V. Bates, B. R. Fish, T. F. Hatch, and T. T. Mercer. 1966. "Deposition and Retention Models for Internal Dosimetry of the Human Respiratory Tract." *Health Physics* 12:173-207.

11. Snyder, W. S. 1967. "The Use of the Lung Model for Estimation of Dose." *In: Proceedings of the 12th Annual Bio-Assay and Analytical Chemistry Meeting.* C. M. West, Comp. USAEC Report. CONF-661018.

12. U.S. Nuclear Regulatory Commission. 1976. "Calculated Doses From Inhaled Transuranium Radionuclides and Potential Risk Equivalence to Whole-Body Radiation." Internal Working Paper. Office of Nuclear Regulatory Research. Division of Safeguards, Fuel Cycle and Environmental Research, NR-SFE-001 (IAEA-SM-199/114).

PLUTONIUM-BEARING PARTICLE STUDIES

ISOLATION OF PLUTONIUM-BEARING PARTICLES FROM THE TEST SITE

M. W. Nathans and E. Francisco

LFE Environmental Analysis Laboratories
Richmond, California

ABSTRACT

One hundred plutonium-bearing particles have been isolated from surface-soil samples obtained from two locations each around five shot sites. These particles are analyzed by other laboratories by means of an electron microprobe, an ion microprobe, a scanning electron microscope, and by mass spectrometry. In this paper, the method of isolation is discussed and some observations with regard to the particles isolated are presented.

INTRODUCTION

The isolation of 100 plutonium-bearing fallout particles from the Nevada Test Site was undertaken by our laboratory last summer at the request of M. G. White, of ERDA's Nevada Operations Office. The purpose of this particle isolation project is to provide W. Efurd, of McClellan Central Laboratory of the U.S. Air Force, and L. Dietz, of Knolls Atomic Power Laboratory, with individual particles for analysis by scanning electron microscopy, mass spectrometry, electron microprobe analysis, and ion microprobe analysis. At the completion of the project, each of the two laboratories will have analyzed 50 particles. The results of the analyses will be reported by the two laboratories independently.

Soil samples were received from five different sites, two samples from each site, for a total of 10 samples. The two samples from each site were such that one sample was obtained from a location about 100 feet from Ground Zero on the hot line, and the other sample from a location about 500 feet from Ground Zero on the hot line. Special samples were obtained by REECo personnel by careful scooping up of about 1 centimeter of topsoil.

At the time of the Conference, 86 particles had been isolated. Of these, 50 had been sent to McClellan Central Laboratory and 36 to Knolls Atomic Power Laboratory. The project was completed a short time later with the transmittal of the remaining 14 particles to KAPL.

METHODS

The methodology was discussed briefly in a previous paper (Nathans and Soinski, 1977). The sequential scheme employed is shown in Figure 1. After receipt of the samples, the -300 mesh fraction was separated by dry sieving in order to remove the particles that are not appropriate for alpha autoradiography because of their size. A density separation was performed on the small-size fraction with a liquid of density 2.96 g/cm^3 (1,1,2,2-tetrabromoethane). The heavy fraction was used for the isolation of particles, because this fraction generally contains the greater part of the plutonium activity. This step introduces a bias in favor of particles that consist primarily of device debris. However, in most of the samples, the plutonium concentrations were expected and also found to be low, so that this concentration step was designed to reduce the time necessary to find the required number of particles. Furthermore, a similar bias would have been introduced anyway, because, for the techniques used to locate particles of interest, unreasonably long exposure times would have been required to find plutonium-bearing particles that consist primarily of soil components (have densities significantly less than 2.96 g/cm^3).

The heavy fractions were transferred to microscope slides, fixed with a drop or so of collodion in amyl acetate, and subjected to alpha autoradiography (Nathans *et al.*, 1976) ("hollow-star technique"). Exposure times varied from 7 days to 1 hour. The detection limit for a 7-day exposure is about 5×10^7 atoms of ^{239}Pu in a single particle, or a $^{239}PuO_2$-equivalent diameter of 0.15 μm. This detection limit was deemed adequate for the purposes of the project. Moreover, longer exposure times would have increased the difficulties associated with the location and isolation of the particles.

After scanning the slides and marking of the areas where particles of interest were located, the isolation of the particles was accomplished in two or three repetitive steps. A small section of the collodion containing the particle of interest, but also other particles, was removed from the sample slide, and transferred to a clean microscope slide. A drop of collodion in amyl acetate was added, dissolving the collodion holding the particles. The particles were spread with a pick, and the collodion was allowed to dry. The slide was then subjected to a repeat alpha autoradiography procedure. Usually the particle of interest was readily identifiable and sufficiently far away from neighboring particles to allow isolation. If not, the procedure was repeated. The particle was then transferred to the sample mount. Autoradiography was

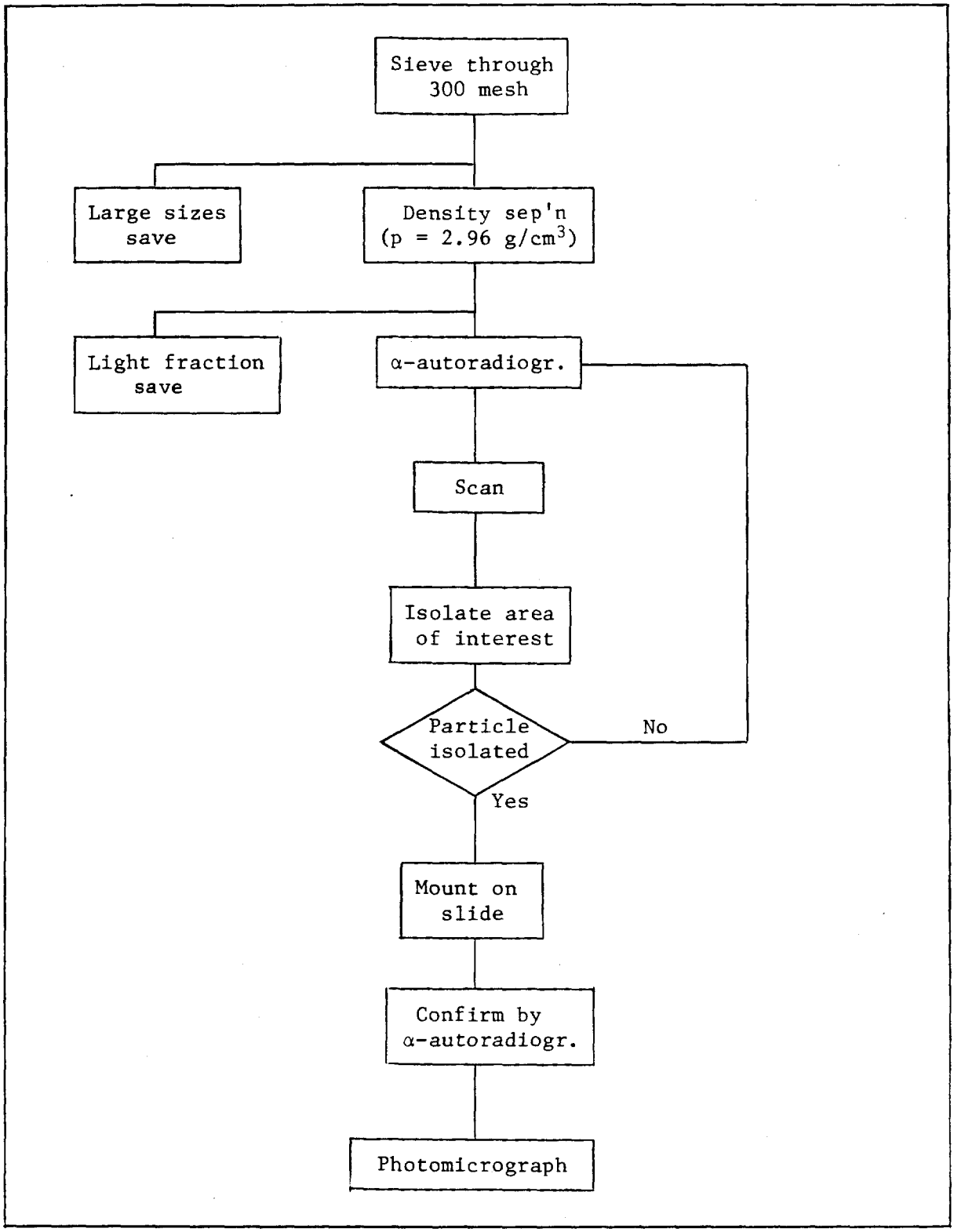

Figure 1. Schematic of Particle Isolation Procedure

then done once more, to confirm that the intended particle had indeed been mounted. Photomicrographs were prepared of each particle for the record, but also to accompany the mounts for recognition by analysts.

OBSERVATIONS AND RESULTS

When the alpha emitter is contained in a small particle of a few millimicrons diameter or less, the tracks in the nuclear emulsion are radially oriented and appear to have emanated from a well-defined central point or very small area. However, when the alpha emitter is randomly distributed over the surface or throughout the volume of the particle, the orientation of the tracks is more random, although the general appearance of a star is maintained. Therefore, if one observes the track star generated by a large particle, or in a small particle attached to or incorporated in the large particle, one can determine the manner in which the alpha-emitter is incorporated into the observed particle. The application of these inferences to our observations on the isolated particles yields the result that, with the exception of the particles isolated from samples 16910 and 16911 and a few particles from samples 17153 and 17154, the plutonium is present in small particles attached to large ones, presumably soil.

Generally, there was little difference between the particles from the two locations near a given detonation point. The exception was the pair of samples 16910 and 16911. The particles in 16910 contained a large amount of plutonium compared to the particles in samples from other slides, and were easily recognized and isolated. Only one such particle was isolated from sample 16911. A number of other particles with plutonium were initially located on the slides, but these particles could not be isolated. They may have been very small particles attached to large particles, becoming separated from the host particles during manipulation, or they were very fragile and broke up when attempts were made to isolate them. Selected isolated particles are shown in Figure 2.

The results of our measurements are listed in Table 1. The plutonium concentrations in the particles have been calculated as though the plutonium is distributed homogeneously throughout these particles. This fiction may have some validity if one wants to consider inhalation hazards, but is useless if one wants to search for size dependence of the concentration. Such a search was made with the data from sample 16910 but no correlation was found, although the particles from this sample were probably homogeneous. It has been our experience, however, that the variability of fission product and heavy element concentrations in particles of any given size generally extends over one or more orders of magnitude, so that 9 or 10 particles are not sufficient to establish the presence or absence of a concentration-particle size with any degree of confidence.

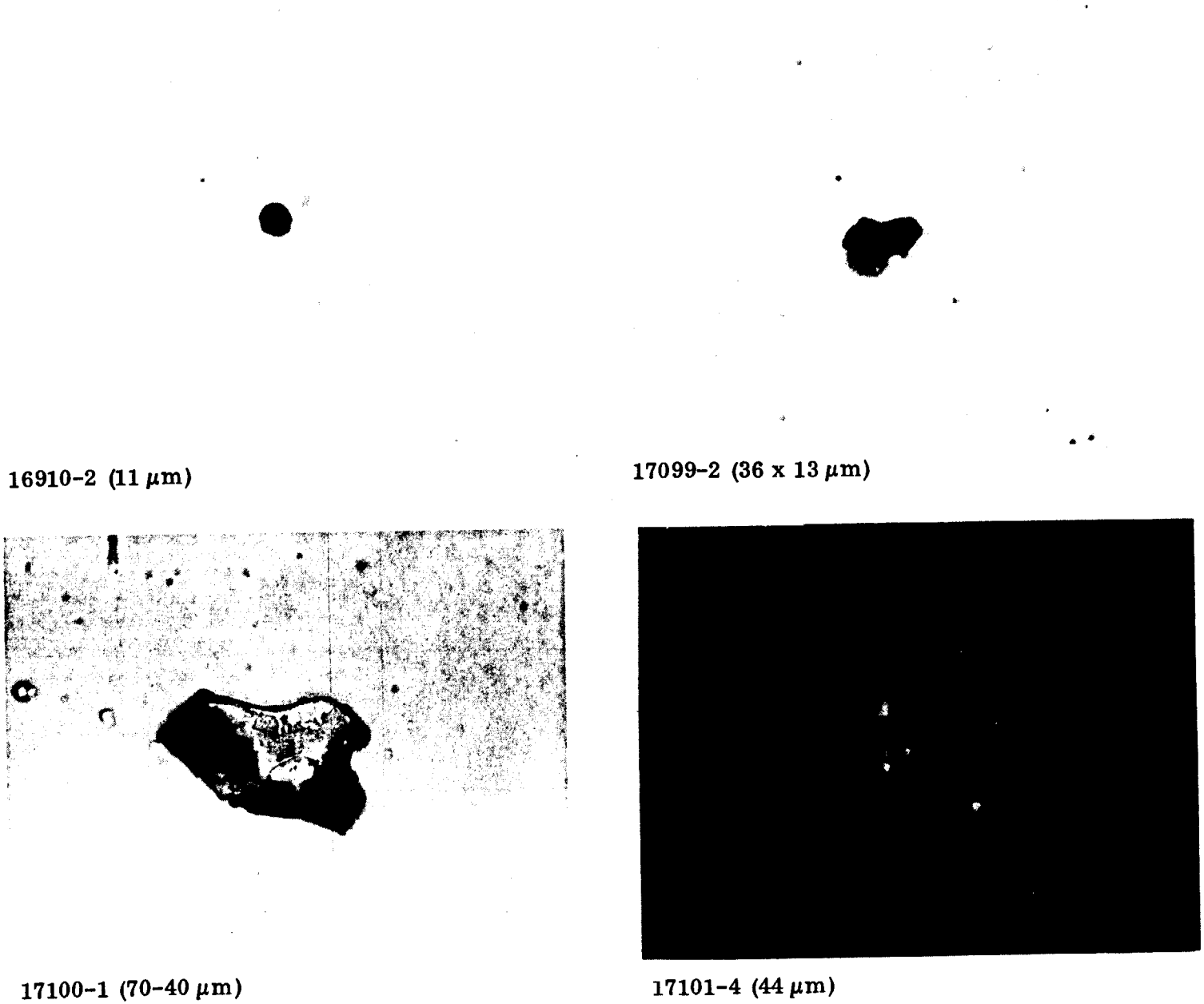

16910-2 (11 μm)

17099-2 (36 x 13 μm)

17100-1 (70-40 μm)

17101-4 (44 μm)

Figure 2. Photomicrographs of Some Typical Particles

Table 1. Characteristics of Isolated Particles

Particle No.	Size (μm)	dpm	^{239}Pu (atoms)	^{239}Pu (atoms/μm^3)
16910-01	9	24	4.4×10^{11}	1.2×10^{9}
-02	11	97	1.3×10^{13}	1.8×10^{10}
-03	*	82	1.5×10^{12}	
-04	20	2.1	3.9×10^{10}	9.3×10^{6}
-05	6	9.6	1.8×10^{11}	1.6×10^{9}
-06	4	7.8	1.4×10^{11}	4.3×10^{9}
-07	5	30	5.5×10^{11}	8.4×10^{9}
-08	6	38	7.0×10^{11}	6.2×10^{9}
-09	5	0.55	1.0×10^{10}	1.6×10^{8}
-10	6	0.48	8.9×10^{9}	7.8×10^{7}
-11	14	98	1.8×10^{12}	8.4×10^{8}
-12	4	12	2.2×10^{11}	4.3×10^{9}
-13	6	26	4.8×10^{11}	2.8×10^{9}
-14	5.5	3.1	5.7×10^{10}	4.3×10^{8}
16911-01	2	1.19	2.2×10^{10}	3.5×10^{9}
-02	2.5	0.21	3.9×10^{9}	2.0×10^{8}
-03	1	0.028	5.2×10^{8}	6.6×10^{8}
-04	2	0.039	7.2×10^{8}	1.1×10^{8}
-05	4.5	0.62	1.1×10^{10}	1.5×10^{8}
-06	2	0.033	6.1×10^{8}	9.7×10^{7}
16924-01	70	0.057	1.1×10^{9}	5.9×10^{3}
-02	48	0.012	2.2×10^{8}	3.8×10^{3}
-03	30	0.019	3.5×10^{8}	2.5×10^{4}
-04	40	0.047	8.7×10^{8}	2.6×10^{4}
-05	30	0.038	7.0×10^{8}	4.9×10^{4}
-06	50	0.017	3.1×10^{8}	4.8×10^{3}
-07	44	0.048	8.9×10^{8}	2.0×10^{4}
-08	40	0.0085	1.6×10^{8}	4.7×10^{3}

*Highly irregular.

Table 1. Characteristics of Isolated Particles (Continued)

Particle No.	Size (μm)	dpm	^{239}Pu (atoms)	^{239}Pu (atoms/μm^3)
16924-09	34	0.010	1.8×10^8	8.9×10^3
-10	54	0.048	8.9×10^8	1.1×10^4
-11	68 x 40	0.056	1.0×10^9	8.9×10^3
-12	58	0.027	5.0×10^8	3.3×10^3
-13	30	0.027	5.0×10^8	2.4×10^4
-14	48	0.014	2.6×10^8	3.1×10^3
16925-01	64 x 30	0.12	2.2×10^9	5.0×10^4
-02	15	0.065	1.2×10^9	6.8×10^5
-03	32	0.0065	1.2×10^8	7.0×10^3
-04	25	440	8.1×10^{12}	1.0×10^9
-05	12	144	2.6×10^{12}	2.9×10^9
-06	52 x 36	0.0065	1.2×10^8	1.9×10^3
-07	80 x 36	0.0054	1.0×10^8	6.3×10^2
-08	1	0.061	1.1×10^9	1.4×10^9
17099-01	60 x 44	0.16	3.0×10^9	4.2×10^4
-02	36 x 13	0.0087	1.6×10^8	3.0×10^4
-03	50 x 40	0.048	8.9×10^8	9.5×10^3
-04	44	0.0048	8.9×10^7	2.0×10^3
-05	10	0.012	2.2×10^8	4.2×10^5
-06	45	0.081	1.5×10^9	3.1×10^4
-07	26	0.0058	1.1×10^8	8.0×10^3
-08	60 x 60	0.0048	8.8×10^7	5.2×10^2
17100-01	70 x 40	0.13	2.4×10^9	3.1×10^4
-02	65	0.089	1.6×10^9	1.1×10^4
-03	14	0.011	2.0×10^8	1.4×10^5
-04	40	0.0087	1.6×10^8	4.8×10^3
-05	30	0.0077	1.4×10^8	1.0×10^4

Table 1. Characteristics of Isolated Particles (Continued)

Particle No.	Size (μm)	dpm	^{239}Pu (atoms)	^{239}Pu (atoms/μm^3)
17100-06	25	0.0048	8.9×10^7	1.1×10^4
-07	44	0.0087	1.6×10^8	3.6×10^3
-08	50	0.0097	1.8×10^8	2.7×10^3
-09	60	0.075	1.7×10^9	1.5×10^4
-10	56	0.045	8.3×10^8	9.0×10^3
17101-01	30 x 10	0.016	3.0×10^8	1.1×10^5
-02	40	0.056	1.0×10^9	3.1×10^4
-03	40	0.30	5.6×10^9	1.7×10^5
-04	44	0.50	9.3×10^9	2.1×10^5
-05	24	0.0077	1.4×10^8	2.0×10^4
-06	20	0.014	2.6×10^8	6.2×10^4
-07	16	0.0097	2.0×10^8	9.1×10^4
-08	27	0.068	1.3×10^9	1.2×10^5
-09	16	0.014	2.6×10^8	1.2×10^5
-10	25	0.041	7.6×10^8	9.2×10^4
17102-01	36	0.0067	1.3×10^8	3.5×10^3
-02	80	0.012	2.3×10^8	5.7×10^2
-03	15	0.0083	1.6×10^8	6.0×10^4
-04	30 x 50	0.0046	8.7×10^7	1.9×10^3
-05	18	0.0028	5.3×10^7	1.2×10^4
-06	35	0.0045	8.3×10^7	2.5×10^3
-07	43 x 29	0.0090	1.7×10^8	4.9×10^3
17153-01	23	0.016	3.0×10^8	4.6×10^4
-02	50	0.011	2.0×10^8	3.1×10^3
-03	20	0.068	1.3×10^9	3.0×10^5
-04	16	0.027	5.0×10^8	2.3×10^5
-05	8	0.043	8.0×10^8	3.0×10^6

Table 1. Characteristics of Isolated Particles (Continued)

Particle No.	Size (μm)	dpm	^{239}Pu (atoms)	^{239}Pu (atoms/μm^3)
17153-06	25	0.054	1.0×10^{9}	1.2×10^{5}
-07	42	0.0077	1.4×10^{8}	3.7×10^{3}
-08	14	34	6.3×10^{11}	4.4×10^{8}
-09	14	0.035	6.4×10^{8}	4.5×10^{5}
-10	8	0.0077	1.4×10^{8}	5.3×10^{5}
-11	12	0.14	2.6×10^{9}	1.9×10^{6}
-12	58	0.018	3.3×10^{8}	2.2×10^{3}
-13	*	2.3	4.2×10^{10}	
-14	2.5	0.27	5.0×10^{9}	4.1×10^{8}
17154-01	2	0.020	3.8×10^{8}	9.1×10^{7}
-02	1	0.17	3.2×10^{9}	6.1×10^{9}
-03	17	0.027	5.1×10^{8}	1.3×10^{5}
-04	45	0.047	8.9×10^{8}	1.9×10^{4}
-05	5	0.013	2.4×10^{8}	2.4×10^{6}
-06	1.5	0.040	7.7×10^{8}	2.9×10^{8}
-07	16	0.053	1.0×10^{9}	3.1×10^{5}
-08	12	0.47	9.0×10^{8}	6.6×10^{5}
-09	2	0.040	7.7×10^{8}	1.2×10^{8}

* Highly irregular.

ACKNOWLEDGMENTS

The authors want to acknowledge the support of D. Wireman, of REECo, for arranging to have the samples taken and shipped to our laboratory. They further want to acknowledge the advice of R. J. Reinhart and the help with scanning the slides by M. Datzman, both of LFE Environmental. They are also grateful for the support and encouragement of M. G. White, of NV.

REFERENCES

1. Nathans, M. W., R. Reinhart, and W. D. Holland. 1976. "Methods of Analysis Useful in the Study of Alpha-Emitting and Fissionable-Material Containing Particles." *In: Atmosphere-Surface Exchange of Particulate and Gaseous Pollutants*. Proc. Symposium held at Richland, Washington, 1974. R. J. Engelmann and G. A. Sehmel (Eds.). pp. 661-674.

2. Nathans, M. W., and A. J. Soinski. 1977. "Methodology for Identification and Isolation of Fallout Particles." *In: Transuranics in Desert Ecosystems*. M. G. White, P. B. Dunaway, and D. L. Wireman (Eds.). USDOE Report, NVO-181. pp. 159-172.

CHARACTERISTICS OF RADIOACTIVE PARTICLES IN CLOSE-IN FALLOUT

M. W. Nathans

LFE Environmental Analysis Laboratories
Richmond, California

ABSTRACT

The author is in the process of systematizing available data on a number of properties of fallout particulates from cratering events and from surface and near-surface bursts in order to provide a better understanding of the properties of the radioactive soil at the Test Sites. In this paper, the results of the work through January, 1978, are presented. Included are the results of observations on shape and color, and some of the systematics of radionuclide concentration in its dependence on the particle size over a size range extending from about 1 μm to more than 1 mm. Plutonium data are very scarce, and the behavior of plutonium is inferred from the behavior of gross radioactivity.

For a better understanding of the fallout characteristics of particles from different types of bursts, a general discussion of relevant phenomenology precedes the presentation and discussion of the data.

INTRODUCTION

The characterization of fallout particles containing transuranic elements and present in the soil of the Nevada Test Site is important to the achievement of the objectives of the Nevada Applied Ecology Group (NAEG). The first step was the preparation of a document containing an overview of the available data on the physical, chemical, and radiochemical properties of fallout particulates, and of the methods by which these data had been obtained (Nathans, 1976a). The essential contents of this document were presented at the Gatlinburg meeting in October, 1976 (Nathans and Leventhal, 1977). Among the conclusions reached were that many of the available data remained uncorrelated, and that they did not provide

much direct information about transuranic elements. Thus, the present work was undertaken to correct certain of these deficiencies, and provide further information.

This paper is a progress report of what has been accomplished to date, primarily with material published before the early sixties. Consequently, most cratering shots have not as yet been considered in detail. The properties to be reported here are density, color, and specific activity. The first two properties are rather nonspecific and are dealt with rather briefly. The specific activity, however, is dealt with in some detail. Its general behavior as a function of particle size will be sketched, though not all relevant data have as yet been incorporated. Completion of the project is planned within the next three months.

PHENOMENOLOGY

As a first step towards our attempt to bring some order to the mass of data on radioactive fallout particles, we are presenting here a brief review of those early processes which are relevant to the generation of cloud particles.

We focus first on the distinction between worldwide fallout, intermediate fallout, and close-in or local fallout and their relationship to various kinds of tests. The different types of fallout mentioned are qualitatively distinguished by their distance of occurrence from the location of the test. Local fallout is present in the immediate environment of the shot point, such as within the boundaries of the Nevada Test Site. Intermediate fallout is found beyond the region of occurrence of local fallout, perhaps for several hundred miles or more. Worldwide fallout occurs beyond the region of intermediate fallout. The occurrence and the relative magnitude of these different kinds of fallout depend on the particle sizes present in the cloud and on the altitude at which the cloud stabilizes, as the main mechanism for the appearance of fallout on the surface of the earth is gravitational settling through the atmosphere. Thus, the mean particle size of the fallout decreases with increasing distance from the shot point. This is not necessarily true anymore for worldwide fallout because the particle sizes are sufficiently small for these particles to remain suspended, and to be carried to the surface by moving air parcels and surface-air exchange mechanisms other than deposition by simple gravitational settling.

For bursts occurring at the surface of soil or rock and above, the mean size of the cloud particles generally decreases with increasing height of burst, scaled to some reference yield such as 1 kiloton or 1 megaton. Thus, a surface burst will yield considerable local fallout, whereas a free-air burst yields virtually no local fallout. Tower bursts are intermediate between surface and airbursts; balloon shots approach free-air bursts with regard to deposition of fallout.

Detonations below the surface follow a different phenomenology. When the depth of burial is quite small, the cloud characteristics are very similar to those of a surface burst. For greater depths of burial, the time sequence of different steps leading to local fallout becomes more and more dominant as a factor determining the nature and properties of the fallout, with complete containment (no fallout) occurring at a depth of burial which depends on the device yield and, to some extent, on the properties of the overburden.

In order to provide a general understanding of the properties of local fallout, it is advantageous to discuss subsurface explosions and surface and near-surface explosions separately. A brief discussion of the phenomenology of the former is found also in Teller *et al.* (1968).

During the early stages of a contained nuclear explosion, a cavity is formed containing vaporized device debris and host rock materials. The cavity wall is lined with molten rock. While the vapor cools and condenses into droplets, the molten material begins to collect at the bottom by flowing down the wall or falling from the upper portions. After a period of time, from a few seconds to a few hours, the cavity collapses and leaves a column of brecciated (loose) material behind the chimney. Most of the fused material remains in the lower portion of what once was the cavity, but some fragments of fused rock are interdispersed with the rubble. The radioactivity is mostly concentrated in the once-molten rock. However, radionuclides that are present in the vapor state when the cavity collapses may be found throughout the rubble as well as their daughter products. Thus, the detailed distribution of radionuclides between fused rock and rubble is dependent on the time-history of the cavity and its contents.

When structural weaknesses are present in the overburden, such as an improperly stemmed emplacement hole, failure may occur with venting as a result. Since, *inter alia*, the cavity contents must travel a long distance to reach the surface, the vented material is highly enriched in volatile species, rare gases being a major component. Fused cavity material would essentially be absent in the fallout (and "throwout"), so that any radioactivity present (mostly $^{89,90}Sr$ and ^{137}Cs, and some shorter-lived species) is in the form of surface coatings on some of the particulate matter. Thus, the fallout is highly depleted in refractory species such as ^{95}Zr and rare earths, as well as in transuranic elements.

Complete containment (except for venting as described above) occurs when the shock wave from the detonation has degraded to a weak seismic wave upon reaching the surface. When the depth of burial is such that the initial shock is still strong when it reaches the surface, the shock wave splits into a surface wave and a reflected dilatational or rarefaction wave while the surface moves upward. As the tension wave moves deeper, the tension increases until the tensile strength of the rock is exceeded. The result is spallation of the rock into the air. When the rarefaction wave subsequently reaches the expanding cavity, a second upward acceleration phase provides additional momentum to the overburden.

The result is the formation of a crater with a considerable amount of close-in fallout and throwout.

Since in cratering the cavity never stabilizes, a significant amount of fused rock will be present in the fallout, as well as species that are volatile, primarily present as a surface coating on many of the particles formed during the fracturing and spallation of the overburden. The fraction of activity, including transuranics, released to the fallout field depends on the yield and the depth of burial (scaled to 1 kiloton). The optimum emplacement depth of the device for producing the largest crater is approximately that depth for which spallation and gas acceleration contribute about equally to crater formation. This depth is not necessarily the depth at which the maximum amount of radioactivity appears in the fallout, however. When the emplacement of the device is at shallow depth so that the cavity or even the fireball breaks through the surface, the characteristics of a surface burst are approached. However, fallout from a surface burst and from bursts above the surface is better understood by an approach starting with a consideration of free-air bursts. For a more extensive discussion of free-air bursts, see Glasstone (1962).

A free-air burst is defined as a burst in which the fireball does not interact with the land or water surface beneath it. Here, we limit the definition to include only those bursts occurring at an altitude such that no surface materials enter the fireball before it has cooled to at least the solidification temperature of the vaporized species resulting from the chemical interaction of the device materials with the air.

As the fireball increases in size and cools, the vapors condense and form a cloud of solid particles of device debris. Thus, the solid contents of the cloud consist almost entirely of highly radioactive device debris in the form of small, generally smooth, round particles having an approximately lognormal size distribution with a geometric mean (median) diameter of about 0.14 μm and a geometric standard deviation of about 2.1 (Nathans, 1976a). The radionuclide concentrations more or less follow the radial distribution theory of Freiling in the particle size range above several micrometers; that is, the concentrations have a particle size dependence as $(\text{diameter})^{-m}$, where m lies between 0 and -1, depending upon the volatility of the radionuclide species condensing in the fireball. However, in the particle size range below a few micrometers, the radionuclide concentrations increase quite sharply with decreasing particle size (Nathans, 1971). Because of the small size of the particles that are formed, a free-air burst leaves virtually no local fallout.

Usually, as the cloud rises, some of the particles are left behind to form a "stem." There is some evidence that the mean size of the particles in this "stem" is a little larger than that of the particles in the main cloud (Nathans, 1971). In addition, the cloud rise causes the appearance of a strong updraft in its wake with inflowing winds ("afterwinds").

When the height of burst is lowered, as is the case with balloon shots and with many tower shots, these afterwinds are strong enough at the surface to entrain loose dust and carry it aloft. A visible stem is formed which trails the cloud and which is practically free from radioactivity. Eventually, however, the top of this stem will merge with the lower portions of the cloud. Most of the stem will rapidly fall back to the surface, because the entrained particles are too large to remain aloft for a long time. It follows, further, that the incorporation of radionuclides in balloon shots is quite similar to that in airburst particles, and that the same is true for many of the tower shots. In the latter case, however, portions of the tower are also incorporated in the particles as though the tower, or at least the upper part of it, were part of the device.

At still lower heights of bursts (as in many tower shots) no trailing of the stem is observable, and more and more of the stem mixes with the debris cloud. Some of the stem particulates form a substrate to which still hot debris particles become attached, and onto which some of the more volatile species become attached. Thus, the debris cloud becomes more diluted with inert and slightly radioactive particles as the detonation point gets closer to the surface and the mean particle size increases. At some rather low height of burst, soil particulates reach the fireball before cooling is complete and some of the particulates become partially or totally fused. The effect is that the mean particle size increases further and that more particles incorporate radionuclides, either within their volume or on their surface.

Fusion of the soil as a direct result of the interaction of the fireball with the surface does not occur until the height of burst is quite low. This is because as the result of shock wave reflection at the surface, the lower boundary of the fireball does not touch the surface until the detonation point is at a scaled height of perhaps 25 feet per $(\text{kiloton})^{1/3}$. At lower heights of bursts, the events may be considered surface shots.

In surface shots, a large amount of soil debris enters the cooling fireball at an early time. Thus, much soil becomes completely fused, or partially fused. As a result, the radioactivity is distributed over a wider range of particle sizes, although particles resembling airburst particulates in size as well as shape are still found in abundance in the range below a few micrometers. In addition, fused ejecta particles are also found. These particles may be quite large, well over 1 mm, and often possess typical teardrop shapes. They may be presumed to have originated from the molten lining of the incipient crater.

How these observations relate to the specific fallout characteristics, particularly size distribution and radioactivity behavior, will become clearer in the following sections.

SHAPE AND COLOR

Particles of many shapes and colors have been identified. Descriptive details vary with the investigators and are qualitative only. Table 1 summarizes the findings for balloon, tower, ground surface, and underground shots at the Nevada Test Site. Most of the radioactivity is associated with glassy, fused material, particularly with rounds. Some more detail with regard to color is provided in Table 2, which shows the color distribution of round particles from various types of shots from the Plumbbob and Teapot series. Additional data of this type from other shots and series are available, but these data would not add anything material and therefore have been omitted.

The data show that there is no clear height-of-burst dependence of the color distribution, as expected. In general, the particles from tower shots are darker than those from air or balloon shots, probably as a result of the large amounts of iron and/or soil present. The color distribution of the particles from the one underground (cratering) shot mentioned is similar to that of the tower shots, although the sample renders this conclusion unclear.

DENSITY OF RADIOACTIVE PARTICLES

The particles for which density data have been found are mostly larger than 100 μm, and were selected on the basis of their radioactivity content. Their representativeness may be questioned.

The data are tabulated in Table 3. Whereas the density of airburst particles is mostly in the 3-4 g/cm^3 range, the densities measured on particles from near-surface, surface, and subsurface bursts are smaller, rarely exceeding 3.0 g/cm^3. Often the densities are even less than the density of the "host rock," sometimes significantly so. Even for the balloon shot, a type closest to an airburst, the particle densities are not especially high. This is apparently caused by vesiculation. Vesiculation is probably also the cause of the large variability of the densities. It is further noted that the great majority of particles were larger than 100 μm.

We have arranged the table in such a way as to facilitate the detection of regularities, if any exist: by type of shot, by substrate, by scaled height of burst. There is no apparent dependence of the measured densities on the scaled height of burst in tower shots over coral or over alluvium, nor in surface bursts on coral. Particles from tower shots over alluvium appear to have somewhat lower densities than those from tower shots over coral. This is commensurate with the lower density of

Table 1. Shapes and Color

Type of Shot	Shape	Color and Characteristics
Balloon	1. Spherical	Black specks, glassy, transparent. Many bubbles on surface, melted. Cream opaque, semitransparent, melted, slightly bubbly surface, grey-green inside, olive green, interior bubbles and black specky material, transparent perfect sphere, mottled amber, clear in spots, perfect sphere.
	2. Cylindrical	Opaque yellow-brown, melted bubbly surface projections. White opaque, melted bubbly surface projections. Cream opaque, melted bubbly surface projections. Clear transparent, hollow or tubelike.
	3. Beanlike	Cream opaque, glassy smooth surface with cracks, melted surface. Mottled amber with clean spots, melted bubbly surface projections.
	4. Disc with jagged edges	Opaque rose-grey, rough disc shape, melted bubbly surface.
	5. Rough ellipsoidal	Sandy semitransparent, melted bubbly surface, unmelted interior containing black specks. White opaque, melted bubbly surface, green-black interior. Amber opaque, melted bubbly surface.
	6. Angular	White semitransparent, quartz-like, jagged edges, smooth melted surface. Sandy opaque, melted bubbly projections. Cream sandy, no indications of melted surface. Cream-brown opaque, melted bubbly surface. Rose opaque, slightly melted. Amber and milk colored, broken particles, air bubbles inside. Yellow opaque.

Table 1. Shapes and Color (Cont.)

Type of Shot	Shape	Color and Characteristics
	7. Ellipsoidal	White opaque, melted bubbly projections, green-black interior. Amber opaque, melted bubbly projections.
	8. Teardrop irregulars	
Tower	1. Spheres	Smooth perfect glassy spheres as individual particles adhering to soil grains. Sometimes clusters of spheres of transparent material. Black glassy spheres, often magnetic. They appear to have solidified in air. *Spheroids, oval in shape,* opaque. Spheroidal, dull black, cracked, veined with white crystalline material.
	2. Irregulars	White irregulars in shape, appearance of coral sand grains. Rare. Black irregulars. Grey irregulars. Yellow irregulars.
	3. Needles	Orange needles.
	4. Flakes	Yellow-orange flakes.
Ground Surface	1. Spherical or spheroidal	Shape depends upon soil type and device characteristics. All particles composed of transparent and colorless glass. Most of glass contains fragments of mineral grains and air bubbles. Large percentage of particles highly vesicular. Small percentage dumbbell-shaped, pear-shaped, and various modifications of these.
	2. Irregular	Many particles were flaky. None of the particles hollow. White opaque irregular porous particles. Sometimes these particles are

Table 1. Shapes and Color (Cont.)

Type of Shot	Shape	Color and Characteristics
		fused. Milky, translucent, crystalline. Grey, ashlike, irregular, porous. Pink, porous, opaque. Black, fused, irregular. In operation Redwing (Zuni, etc.), opaque, corals, translucent corals. Yellow and white spheres.

NOTE:

1. The fallout particles collected following low-yield surface shot in Nevada consisted of glass derived from melting of silicate minerals of soil. The fallout particles were transparent spheres of yellow-green color, irregular opaque grains brown in color which did not differ in appearance from unaltered mineral grains of original soil.

2. Fused particles are most important from standpoint of activity. Common feature is that at least one side of every particle is clear, glassy material with green tints. The fused material contained gas bubbles. The particles which contained no activity but contributed most weight are yellow, opaque, oblate spheroid and white opaque.

3. Particles from underground shots were irregular in shape and opaque in appearance. Particles appear to be fused earth with adhering small metallic points and imbedded black specks. (1-4)% of particles are glassy spheres (transparent, either colorless or blue-green amber). Occasionally one finds black pitch appearance.

   Few glassy particles exhibit teardrop shapes. Most radioactive particles are irregular shaped, white to grey, translucent to opaque.

Table 2. Color Distribution Among Round Particles

Shot Type	Shot No.	Scaled Height of Burst[1] (ft)	Color Distribution					
			White	Light Yellow	Yellow	Gold	Brown	Black
Air	1	707[2]	1	2	13	27	14	2
	2	501	2	4	25	13	9	3
Balloon	3	562	1	5	51	74	27	1
	4	510	4	13	15	9	10	6
	5	234	7	4	8	13	34	8
	6	230	5	2	5	10	7	1
	7	211	22	4	2	0	1	0
Tower	8	250	0	1	1	3	37	68
	9	224	0	0	1	0	4	16
	10	206[3]	2	1	0	5	70	179
	11	196	0	0	0	1	0	7
	12	165	0	1	0	0	10	2
	13	164[4]	0	1	5	11	74	88
	14	158[4]	0	1	4	1	14	76
	15	142[3]	2	4	16	30	49	80
	16	142[3]	7	2	27	31	51	89
Under-ground	17	60	0	1	1	2	5	0

[1] (height of burst)/(yield in kilotons)$^{1/3}$

[2] Composite of 2 samples

[3] Composite of 4 samples

[4] Composite of 3 samples

Table 3. Particle Densities*

Type of Shot	Operation	Scaled Height of Burst (ft)[1]	Density (g/cm^3) Low	High	Average	Remarks
Balloon	Plumbbob	210	2.05 1.5	2.55 2.25	2.19 1.84	Regular spheres Irregular particles
Tower	Sandstone[2]	55 60 76	1.8 1.8 1.8	2.8 2.8 2.8	2.4 2.4 2.4	
Tower	Greenhouse[2]	84	2.55	3.24	2.91	Sample collected at 26,000 ft. alt.
Tower	Upshot-Knothole	84	1.38	2.56		Large variation due to varying number of air bubbles in particles
Tower	Tumbler-Snapper	120 135	1.7 2.0	3.2 2.4	2.2 2.2	
Tower	Plumbbob	195	1.95 1.25	3.17 2.75	2.72 2.25	Regular spheres Irregular spheres
Tower	Teapot	225			1.28 2.23	420-500 μm 500-840 μm
Surface	Ivy[2]	(3)	2.41	2.49		Many porous particles
Surface	Castle[2]	0.3	2.24	2.45	2.36	

[1] (height of burst)/(yield in kilotons)$^{1/3}$

[2] Coral shots

[3] Surface, 10 MT

*See DASA-1251, Vol, III, pp. 474-500.

Table 3. Particle Densities* (Cont.)

Type of Shot	Operation	Scaled Height of Burst (ft)[1]	Density (g/cm^3) Low	High	Average	Remarks
Surface	Redwing[2]	0.6			2.53	Yellow spheres
					2.33	White spheres
					2.46	Mean for all shots
Surface	Redwing[2]	5.0			2.69	
Surface	Buster-Jangle	2.3	2.55	2.98	2.66	
Underground	Buster-Jangle	-16	2.37	2.78	2.60	Black spheres, 105-125 μm, 8,000 ft. from GZ
			1.72	2.80	2.32	Pale green to black, vesicular 300-420 μm, 8,000 ft. from GZ
					< 2.95	

the alluvial soil. However, this relationship between particle density and soil density does not seem to hold for surface bursts. The particles from the balloon shots have an anomalously low density, presumably as a result of vesiculation. The densities of the particles from the underground shot appear to increase as they become smaller. This is consistent with an expected decrease in vesiculation with decreasing particle size.

We conclude that for large particles ($d > 100$ μm), the density is about 2.4 g/cm^3, but that each shot generated particles with considerably lower and higher densities.

THE PARTICLE SIZE DEPENDENCE OF THE CONCENTRATION OF TRANSURANICS

Introduction

The extent of the data has been discussed in a previous paper. It was found that until the early sixties, mostly gross activity measurements in fallout samples were made. Sometimes these samples were size-fractionated by means of sieving. At other times, fused particles were isolated and their radioactivity measured. Measurements of the concentrations of individual radionuclides were rarely made in size-separated samples or in individual particles. The principal characteristics of all these measurements were that they were made rather shortly after each test and that they covered the largest particles of our interest in the fallout field.

Primarily as a result of the pioneering work of Russell (1965) and of Heft and Steele (1968), more detailed work on both fallout and cloud samples was performed. The investigations covered not only the debris from tests conducted during the sixties, but also samples from earlier tests in the Pacific and at the Nevada Test Site. Only cloud samples above about 200 μm, and in some cases less, could not be considered. We did not find cases where an attempt was made to isolate individual particles for measurement of these radionuclide concentrations. In this particular report, we will discuss only events that occurred in the very early sixties and before.

The concern for potential health hazards from radioactive particles at the Test Site requires us to look into the activity of individual particles, and the problem is: Can we infer the concentrations of transuranics, or at least the particle-size-dependence of these concentrations, from the type of data that are available, particularly from beta and gamma measurements? This problem is attached in the next subsection.

Plutonium Behavior

Plutonium in debris from nuclear devices is the result of neutron capture by ^{238}U, is derived from plutonium present in the fuel, or is derived from both. In the first case, the dependence of the plutonium concentration on the particle size is determined by the behavior of uranium (^{239}U has a half-life of about 23 minutes). Therefore, we must discuss both uranium and plutonium behavior in order to enlighten ourselves with regard to the particulate properties of the contamination at NTS. We refer to the statements made and conclusions reached by Russell (1966) on the basis of work by himself (Russell, 1965) and others, such as Freiling (1961a, 1961b, 1963), Freiling and Rainey (1963), Freiling *et al.* (1964a), Stevenson (1957), Lane (1964), and Miskel and Bonner (1964). The data used had been obtained almost exclusively by the radiochemical analysis of cloud and fallout samples without detailed size separation.

The order of increasing refractivity (or decreasing volatility) has been established to be approximately as follows:

^{137}Cs, ^{89}Sr, ^{136}Cs, ^{115}Cd, $\underline{^{237}U}$, ^{111}Ag, ^{90}Sr, ^{131}I, ^{132}Te, $\underline{^{237}U}$,

^{140}Ba, ^{141}Ce, ^{91}Y, ^{99}Mo, ^{147}Nd, ^{239}Pu, ^{143}Pr, ^{144}Ce, ^{153}Sm,

^{156}Eu, ^{161}Tb, ^{95}Zr, ^{97}Zr, $\underline{^{237}U}$

Differences in the rankings between airbursts, tower bursts, and surface bursts are small. The behavior of ^{91}Y and the following nuclides is essentially refractory. Thus, ^{239}Pu (when present *ab initio*) behaves refractorily in about the same manner as ^{147}Nd or the latter's daughter, ^{147}Pm. The behavior of ^{239}U, the ^{239}Pu precursor, is, of course, the same as that of ^{237}U (formed by an (n,2n) reaction of ^{238}U). This nuclide, ^{237}U, is listed more than once in the volatility rankings, because its behavior appears to be dependent on the substrate over which or in which the shot is fired. The data and correlations examined by Russell (1966) have indicated that uranium behaves like a refractory element in coral surface and water surface bursts. For bursts on silicate, for which at the time of Russell's analysis, only data from low-yield (< 1.7 kt) shots were available, uranium behaves more volatile than ^{95}Zr. In Jangle S and Jangle U, the behavior was less volatile than ^{140}Ba, ^{111}Ag, ^{115}Cd, and ^{89}Sr. In Johnie Boy (Clark *et al.*, 1963) and in Small Boy (Freiling *et al.*, 1964b), the volatile character of uranium is similar to that of ^{140}Ba.

From these observations, it would appear, then, that at the Nevada Test Site, the plutonium behavior as a function of the particles can be expected to be like a nuclide of intermediate volatility such as ^{140}Ba, when the plutonium is exclusively present as an induced activity; like a refractory nuclide such as ^{147}Nd (or ^{147}Pm) when the plutonium was

originally present in the device as the fuel, and little is formed by neutron capture by uranium; and like a nuclide of volatility intermediate between ^{140}Ba and ^{147}Nd, if both induced and original plutonium are present.

We will investigate this matter further in the following subsection using data obtained from size-separated samples. We also determine to what extent plutonium behavior can be inferred from gross-activity behavior.

Relation of Pu Behavior to Gross Activity Behavior

The principle of our investigation is the following: Data on uranium, plutonium, and fission product concentrations in size-separated samples exist. These data relate the radionuclide concentrations to the particle size. Because of the age and nature of the samples, the fission products measured are usually limited to ^{90}Sr and ^{147}Pm (^{147}Nd-daughter), although in some samples, other fission products can also be determined. The fission product ^{147}Pm is a refractory nuclide. Such refractory nuclides are by far the most significant contributors to the gross beta and gross gamma activities. If the particle-size-dependence of plutonium is approximately the same as the particle-size-dependence of promethium (or other refractory species), such particle-size-dependence can then be inferred from the particle-size-dependence of the gross activities.

The contribution of refractory nuclides to the total fission-product activity can be derived from the work of Bolles and Ballou (1956). In Table 4, we have shown the contributions of various groups of fission products to total activity at various times after a test. No distinction is made between different fuels. At about the time that the gross activity measurements were made (certainly less than a year after each test), the refractory nuclides contributed between 60% and 85% to the total fission-product activity, exclusive of the rare gases and the halogens. In addition, some fraction of the alkaline earths and noble metals was not incorporated in the fallout because of their own volatility or that of their precursors during fallout formation. Of the alkaline earths (Sr, Ba), perhaps the major portion is missing. If it is assumed that only 50% of the alkaline earths and noble metals were present in the fallout samples, only about 75% of the total fission product activity was represented in the fallout at 25 days and about 90% after 1 year. Therefore, the refractory fission products constituted from 80% to 95% of the fission product activity in the fallout during the time that measurements were made. Since the data are most often reported as the activity at 25 days after the test, the lower percentage figure would apply more generally.

In order to obtain a comparison of the distribution of plutonium with that of refractory nuclides over different particle sizes, it is sufficient if the relative concentrations in size-separated fractions of cloud and fallout samples are known, even though particles of all kinds are usually present in the samples. In our analysis, it is assumed that

Table 4. Contribution of Element Groups to Fission Product Activity

Time after test: / Element Group	Percent Contribution			
	25 d	1 yr.	10 yrs.	20 yrs.
Rare earths*	50	63	42	30
Alkaline earths	17	5.7	39	46
Noble metals	10.6	5.7	0	0
Nb, Zr*	10.0	23	0	0
Rare gases**	5.3	0.4	2.7	2.0
Halogens**	4.8	0	0	0
Oxygenated anions	1.6	0	0	0
Alkali metals	∿ 0	1.5	17	21

*Refractory

**Not condensable

the dependence of the concentration or activity ratio, R, of plutonium to a refractory nuclide, such as ^{147}Pm or ^{144}Ce, on the particle diameter, has the form:

$$R = ad^m \qquad (a)$$

where a and m are constants, and d is the median (geometric mean) diameter of the size fraction.

The justification of our assumption, above, is derived from the radial distribution theory of Freiling (1961a). According to this theory, most radionuclides are volume-distributed, surface-distributed, or distributed with a concentration gradient in the particles, so that the radionuclide content of the particles is described by:

$$A = bd^n \qquad (b)$$

where A is the activity of the nuclide, or the number of atoms in a particle, d is the particle diameter, and b and n are constants. The value of n lies usually between 2 and 3. Consequently, the ratio of the activities of two nuclides, i and j, has the following particle size dependence:

$$(A_i/A_j) = R_{i,j} = (b_i/b_j)d^{n_i - n_j} = ad^m \qquad (c)$$

We admit that for surface and subsurface bursts, these relationships are too simplistic, and the description (b) is not valid for the entire size range of radioactive particles, which may extend from less than 0.1 μm to 1 mm or above. No other resource can be had, however.

Twelve sets of data from the events have thus been analyzed. These events include one subsurface shot in alluvium at shallow depth, seven shots on or above coral, and three shots above alluvium. The scaled heights of burst ranged from -21 feet to almost 400 feet, yields ranged from about 1 kiloton to more than 10 megatons. Lower limits of the particle size ranges varied from less than 0.1 μm to about 12 μm, upper limits ranged from 1 μm to almost 1 mm. The smaller ranges were associated with the greater scaled heights of burst.

The data were correlated statistically by least-squares regression in the log-log plane. Values for the exponent, m, were thus obtained as slopes of the log R-log d correlation. The significance of the correlations were tested by means of the correlation coefficient. The hypothesis that $m \neq 0$ was tested by means of the t-test. The results are shown in Table 5.

It is expected that the $^{239}Pu/^{147}Pm$ and $^{239}Pu/^{147}Pm$ ratios are independent of the particle size, if plutonium behaves like a refractory species. In that case, therefore, the expectation is that $m = 0$. If plutonium is more volatile than the rare earths, its concentration decreases more rapidly with increasing particle size, and $m < 0$. If plutonium behaves in a more refractory fashion than the rare earths, $m > 0$.

Table 5. Relation Between $^{239}Pu/^{147}Pm$ and Particle Size

Test No.	Scaled Height of Burst (ft.)	Substrate	Particle Size Range		Number of Points	Exponent		Correlation Coefficient	Significance Level
			Lower Limit (μm)	Lower Limit (μm)		Value	Standard Deviation		
1	-21	Alluvium	3.4	850	14	-0.39	0.22	0.451	0.91
1*	-21		0.62	120	13	-0.32	0.20	0.440	0.88
2	0.3	Coral	0.76	68	12	0.073	0.032	0.579	0.96
3	0.6	Coral	0.54	91	13	0.29	0.15	0.506	0.92
4(a)	2.7	Coral	0.58	100	13	0.30	0.49	0.397	< 0.90
4(b)	2.7		1.0	54	14	0.50	0.20	0.589	0.98
5	5	Coral	0.49	33	9	-0.081	0.036	-0.646	0.95
6*	42	Coral	0.34	16	11	0.14	0.20	0.214	<<0.90
7*	100	Coral	12	5.2	9	0.19	0.27	0.260	<<0.90
8*	198	Alluvium	0.25	0.98	4	0.25	0.097	0.845	0.93
9*	229	Alluvium	0.082	9.7	7	0.17	0.12	0.536	< 0.90
10**	362	Alluvium	0.10	10.5	8	-0.17	0.17	0.379	<<0.90

*Yield range: 0.5 kt-15 Mt

The correlation coefficients show significance of the correlations at the 95% level (or higher) for three sets of data: Shots 2, 4 (Set b), and 5. However, for these, m is significantly different from zero only for Shots 2 and 4 (Set b), and of these, $m < 0.1$ for Shot 2. The correlation in Shot 4 (Set b) is not duplicated in Set "a" from this shot.

The correlation coefficients are significant at the 90% level for Shots 1 (239/147), 3, and 8. The value of m is significantly different from zero only for Shot 3, although we see 88% significance levels for Shot 1.

It is our conclusion that these results confirm the qualitative statement made by Russell (1966): Plutonium, and by inference uranium, behaves like a refractory nuclide in shots on or over coral. The behavior is not entirely clear in the shot detonated at shallow depth (Johnie Boy). The apparent behavior of plutonium is a little less refractory than that of the rare earths, as evidenced by the calculated negative slope of the correlation. The significance of the slope has not been established definitely. The remaining three shots over alluvium all had scaled heights of burst of about 200 feet or more and approached free-air bursts. In all of these, the apparent plutonium behavior was about the same as the behavior of the ^{144}Ce, which is refractory.

It would appear, then, that no large errors are made when it is assumed that the plutonium and refractory fission products are distributed similarly, and that, therefore, plutonium behavior may be inferred from gross beta or gross gamma measurements. Any errors caused by this inference would be such that the plutonium concentrations would be overestimated in fallout samples if such estimates are made on the basis of cloud-sample analyses.

REVIEW OF RADIOACTIVITY DATA

Airbursts

The objectives of this work do not relate to free-air bursts. Yet a capsule overview of radionuclide behavior in such shots is appropriate, not only because airbursts comprise the limiting case of height-of-burst phenomena, but also because radionuclide behavior in all or most balloon shots resembles radionuclide behavior in airbursts. Some of the work in this country has been published (Benson and Leventhal, 1965; Nathans, 1971), but most of it remains as yet unpublished (primarily work by Hicks, Stevenson, Nathans and Benson, and Nathans).

The specific beta and gamma activities of particles larger than about 2 or 3 μm of medium- and high-yield shots is usually independent or only very slightly dependent on the particle size. Figure 1, where the points represent grouped data, shows an example. Regression analysis

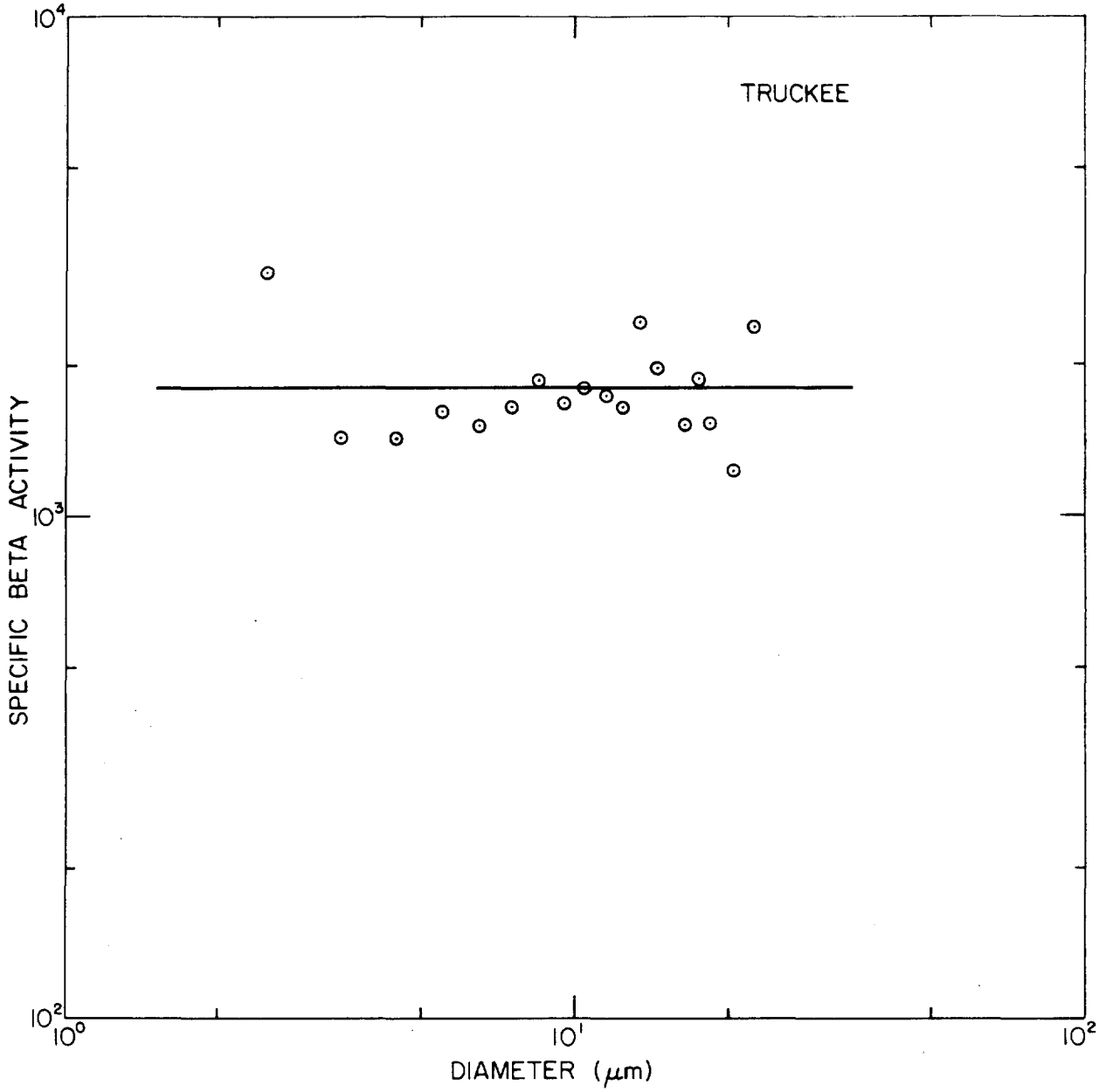

Figure 1. Specific Beta Activity of Particles from an Intermediate-Yield Airburst.

showed that the slope of the line is not significantly different from zero.

For a few low-yield airbursts, data have been obtained for single or grouped particles as small as 0.3 μm. These submicrometer particles had been located on slide preparations of the debris by photoreversal of the autoradiographic image, transferred to an appropriate substrate, and measured in an electron microscope. Activity measurements were made on groups of particles of approximately the same size. Size separation of debris by sequential centrifugation extended the size range downward even further, but also magnified the uncertainties of the measurements.

Examples of gross activity behavior are shown in Figures 2 and 3. In Figure 2, the specific activity is essentially constant above about 2 μm, then increases towards smaller particles sizes. The data from the size fractions appear to fit the single-particle data rather well, but our experience has shown that such data may have uncertainties as large as an order of magnitude or even more. This is evident, for example, from Figure 3, where the size-fraction data are a factor of about 6 lower than the single-particle data. In general, plots like these indicate that below a few micrometers, the specific activity curve begins to rise, and that this rise may become very dramatic below a few tenths of a micrometer.

A word of caution is in order. The curves should not be blindly extrapolated below 0.04 or 0.05 μm. Doing so would result in more radioactivity than was actually generated by the shot. In reality, there is a minimum particle size, probably of the order of 0.01 μm, but the presence of a maximum in the specific activity-size curve also cannot be discounted.

Evidence not adduced here suggests that the transition between constancy and increase of specific activity occurs at smaller particle sizes as the explosion yield increases.

Individual radionuclides for which data have been obtained behave similar to the gross activities, as expected. However, the behavior above about 3 μm is dictated by the relative volatilities and, therefore, the specific abundance of a particular radionuclide is not necessarily constant in this size range. Uranium and plutonium data are few and far between, but these elements may also be expected to behave in accordance with our general observations.

Balloon and Low-Altitude Airbursts

Data for this type of shot are rather scarce. We have analyzed data from King (Ivy series, high-yield device detonated at a scaled height of burst under 200 feet over coral, soil, and seawater) and from Lassen, Priscilla, and Wilson (Plumbbob series, devices with yields under 100 kt suspended from tethered balloons over alluvium with scaled heights of burst above 200 feet).

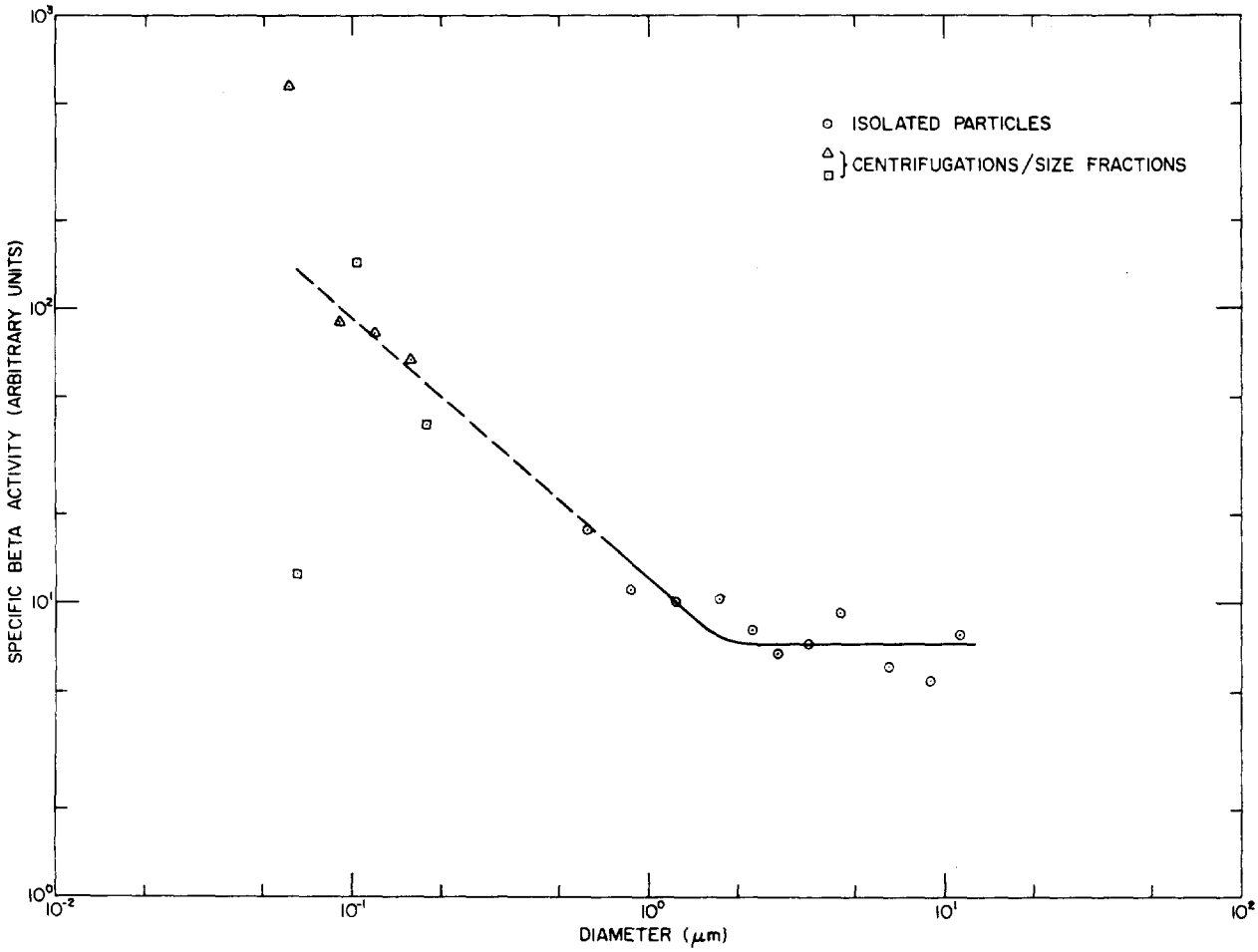

Figure 2. Specific Beta Activity of Particles from a Low-Yield Airburst.

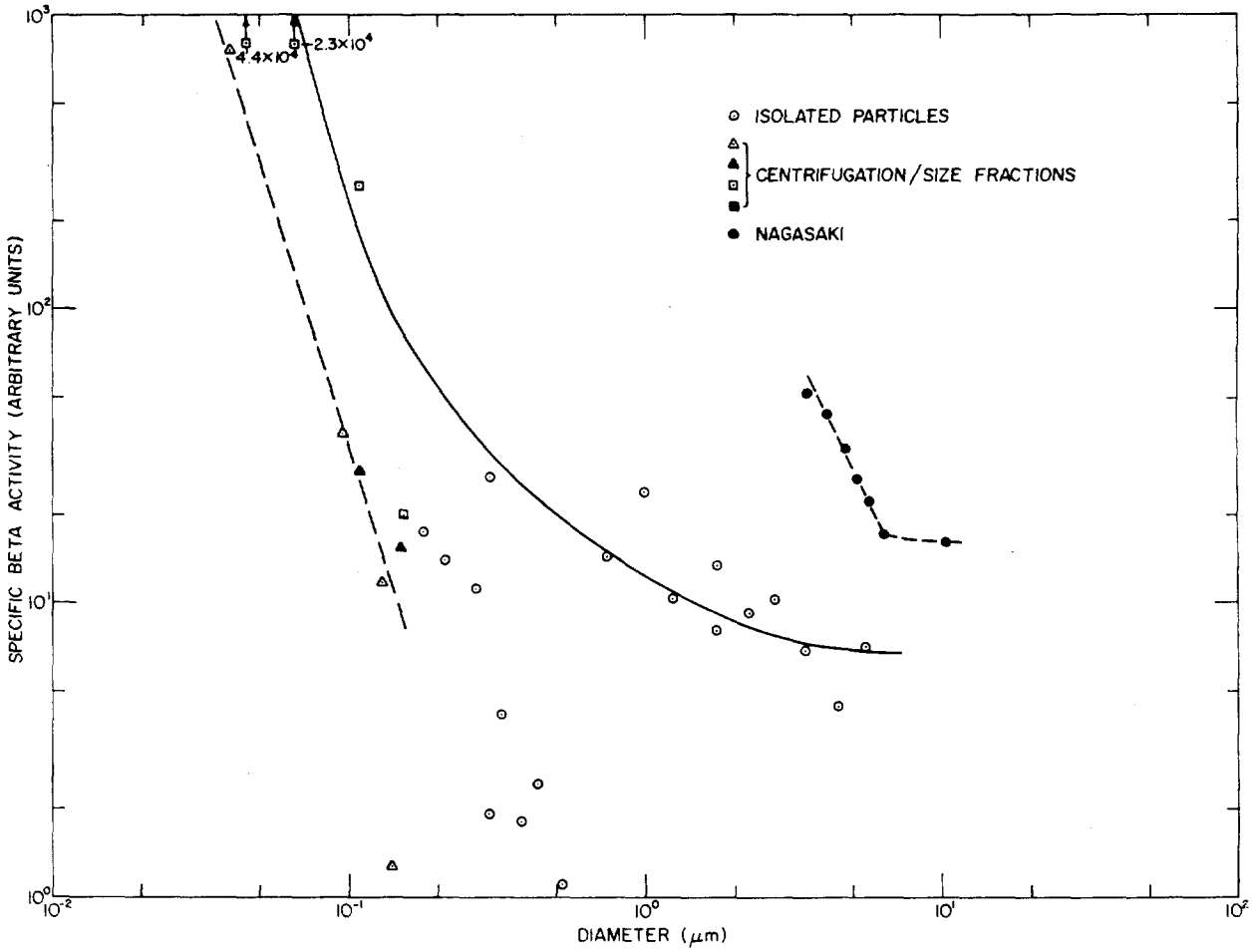

Figure 3. Specific Beta Activity of Particles from a Second Low-Yield Airburst.

Many of the data were read from plots, others were available in tabular form. The particles were placed in size bins, and the specific activities were averaged. Hence in the plots that follow, each point may represent from 2 to 20 particles.

Data from King are plotted in Figure 4. Only particles smaller than 5 μm appear to have been measured. The large rate of increase of specific activity with decreasing particle size is evident.

Data from Lassen are shown in Figure 5. They do not lend themselves readily to interpretation. This may be the result of the fact that this shot had an anomalously low yield.

Data from Priscilla found so far were only for "fallout" particles between 500 and 3,000 μm and were gamma activities at 14 days. Since particles that large are not representative of balloon shots or airbursts, we suspect that radioactivities induced in the soil were measured.

Data from Wilson are based on unpublished work by Nathans done during the early seventies. Cloud samples were subjected to a size separation by combined gravitational settling and sequential centrifugation, and the specific abundance of a number of nuclides was determined in the size fractions. In addition, the fraction of fused particles was determined by microscopy. By dividing the values of this fraction into the radionuclide specific abundances in the size fractions, the average specific abundances in the fused particles which contain most of the radioactivity are obtained.

The results for plutonium are shown in Figure 6. The size range extended from 0.08 μm to 10 μm. No increase below a few micrometers is evident. The data below 1 μm are somewhat tenuous, however, because of the large uncertainties associated with them.

Tower Shots

Gross activity data have been analyzed from three Greenhouse shots, four Tumbler-Snapper shots, one Upshot-Knothole shot, and two Plumbbob shots. The scaled heights of burst varied from 30 feet to 200 feet, the yields from 5 kt to 40 kt. The particles covered the range from about 1 μm to about 1 cm, although the size ranges for individual shots were much more limited. Plutonium data were analyzed for one shot from the Upshot-Knothole series.

The gross activity data are plotted in Figures 7 through 9. Figure 7 is a composite plot showing the general behavior of the specific activity with size. Figures 8 and 9 show the specific activity of Tumbler-Snapper particles below 50 μm (T-S6) or below 25 μm (T-S5, 7, 8). These Tumbler-Snapper data have been plotted separately so as not to crowd any more points into Figure 7. The straight lines drawn in Figure 8 are least-squares regression lines, as are the lines drawn through the various sets of points below 20 μm in Figure 7. The slopes of these lines vary

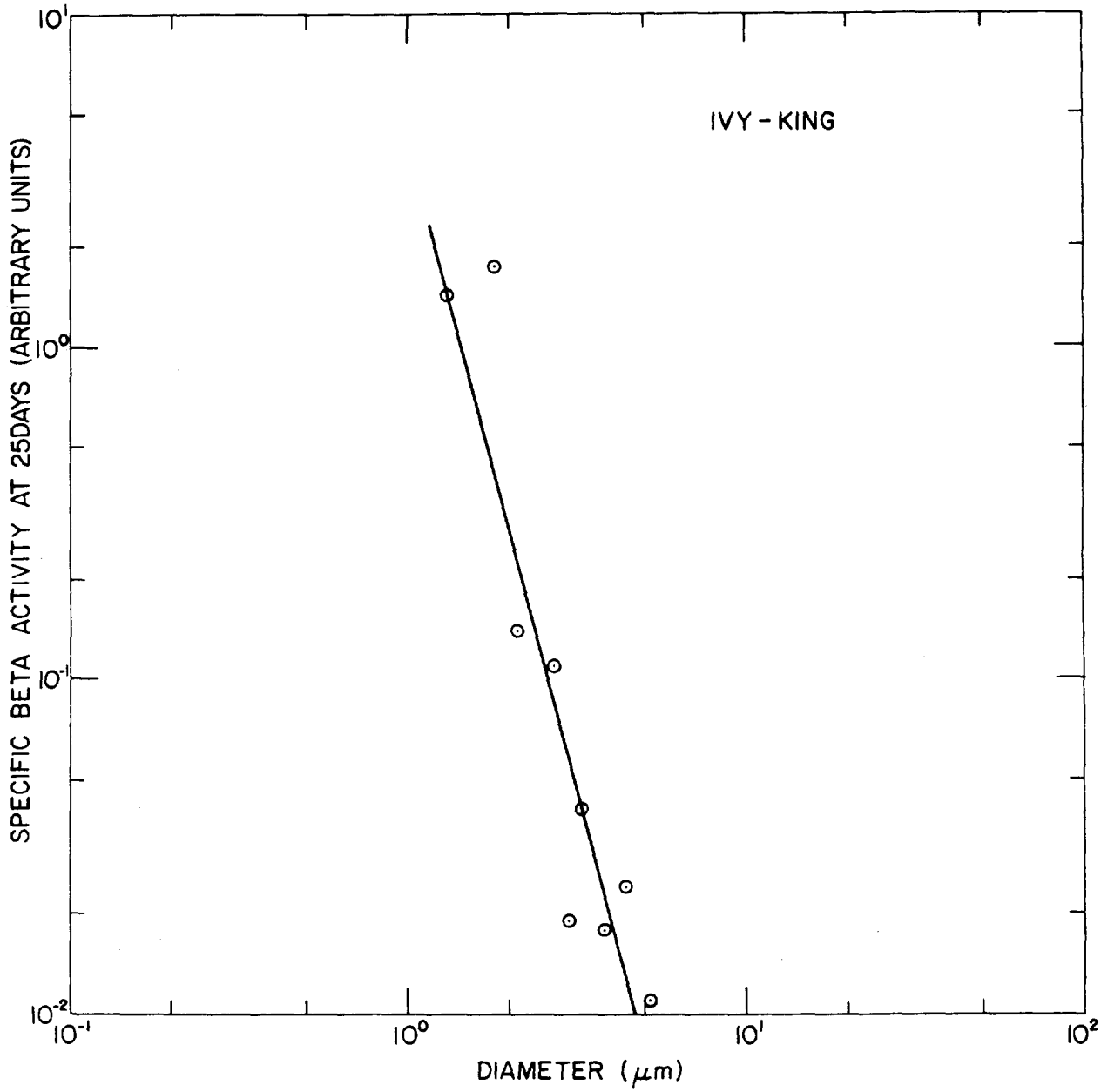

Figure 4. Specific Beta Activity of Particles from a Low-Altitude Airburst.

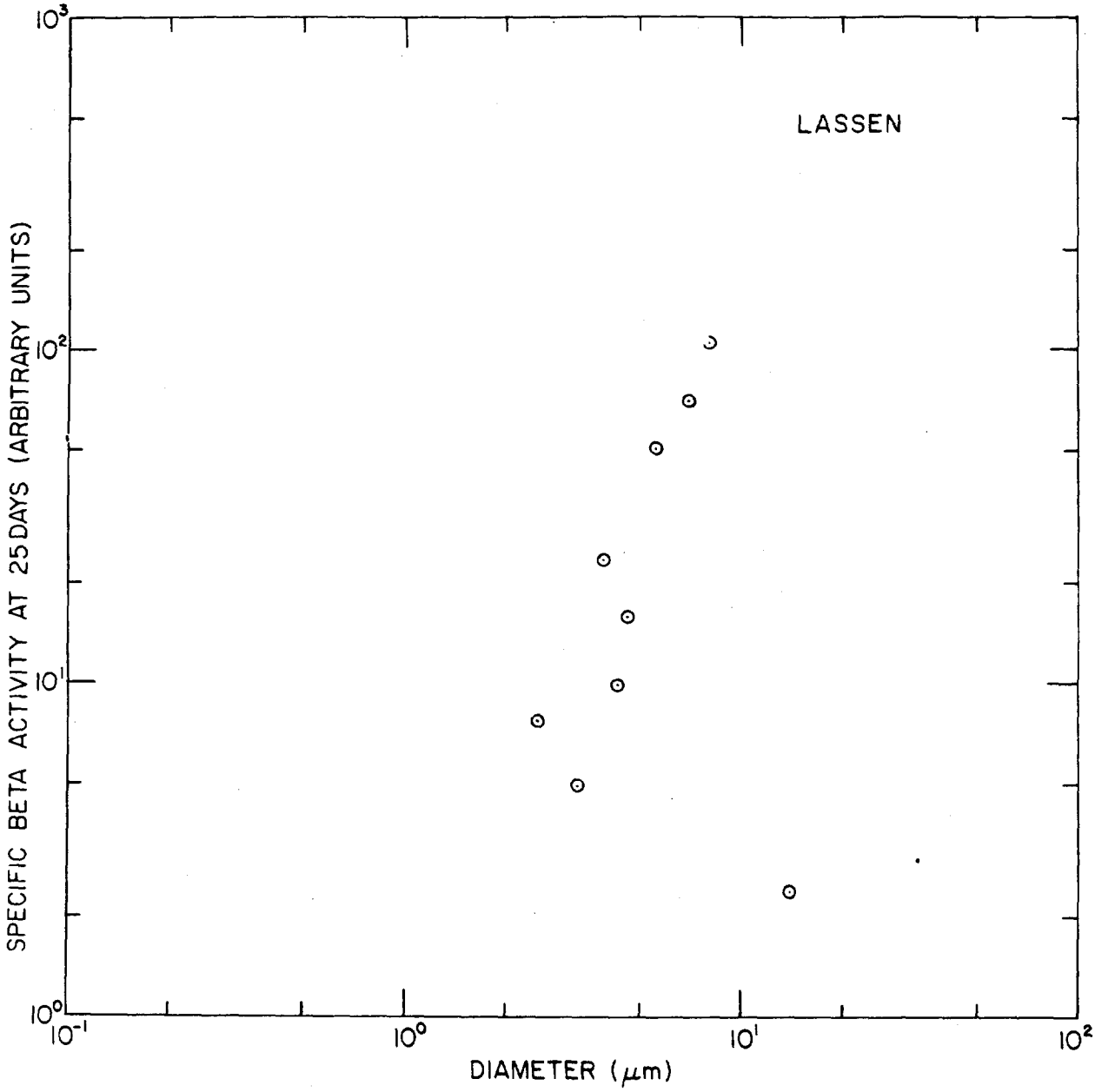

Figure 5. Specific Activity of Some Particles of a Very Low-Yield Balloon Shot.

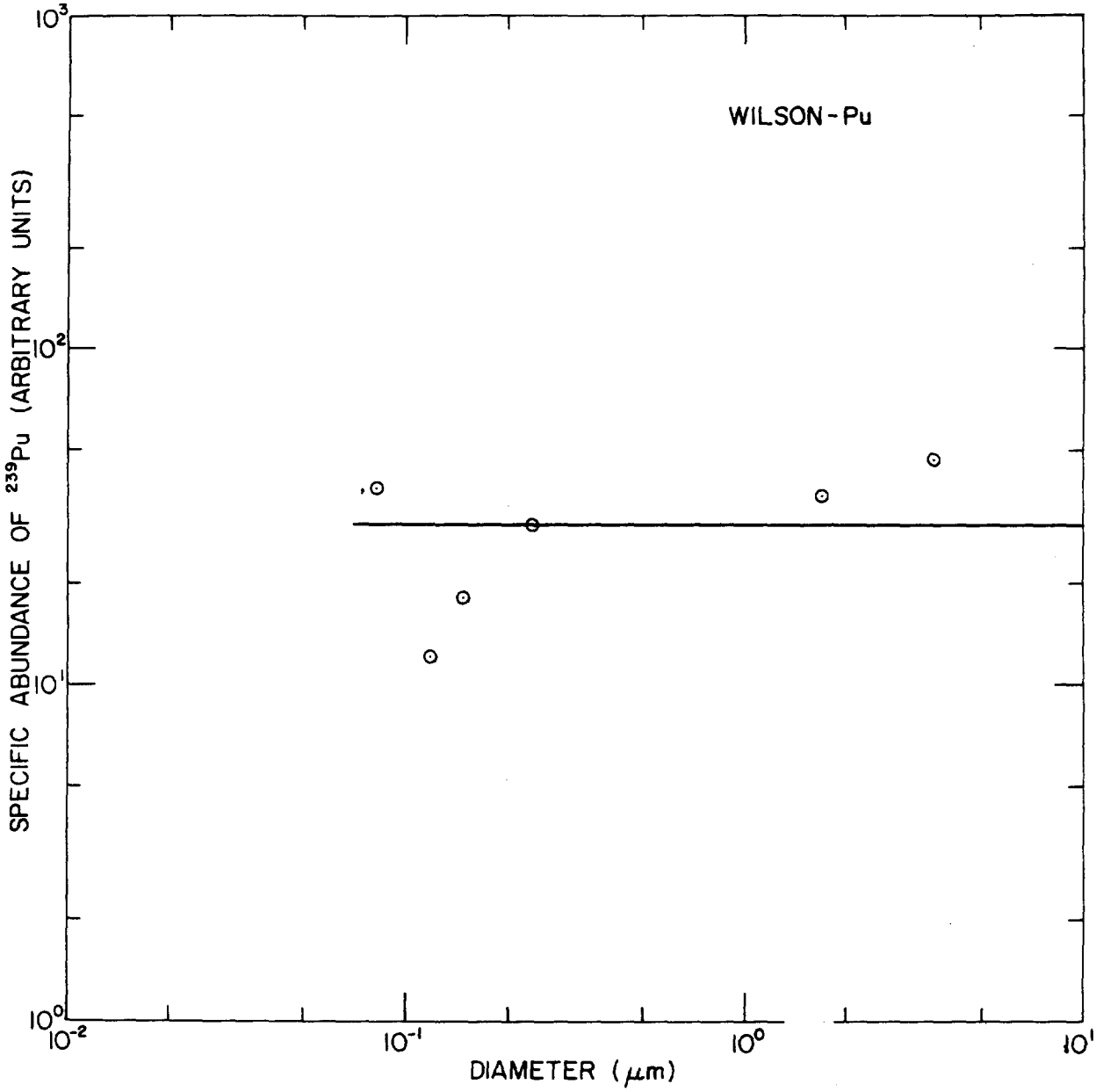

Figure 6. Specific Abundance of ^{239}Pu of Particles from a Balloon Shot.

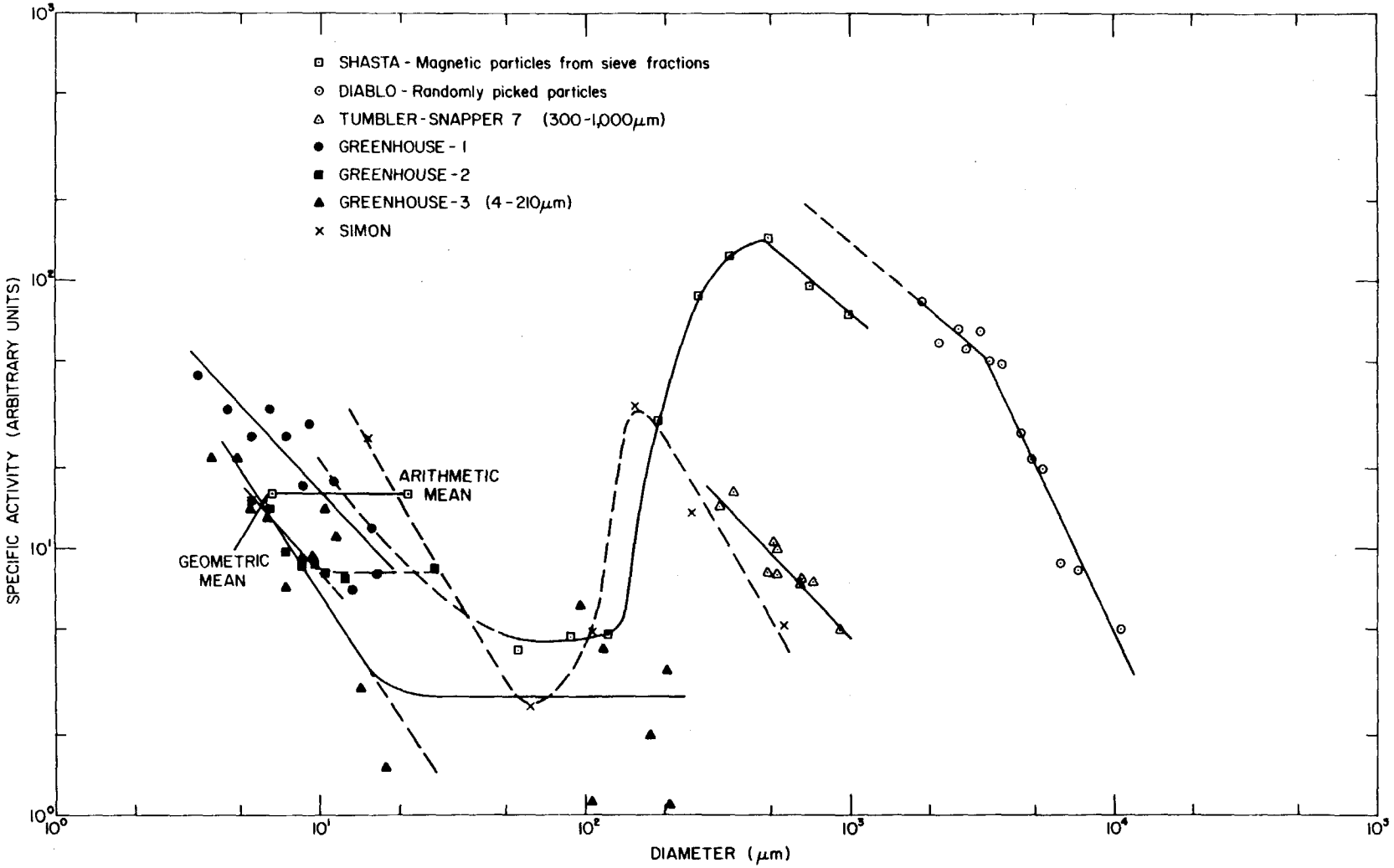

Figure 7. Specific Beta Activity of Particles from Several Tower Shots over a Large Size Interval.

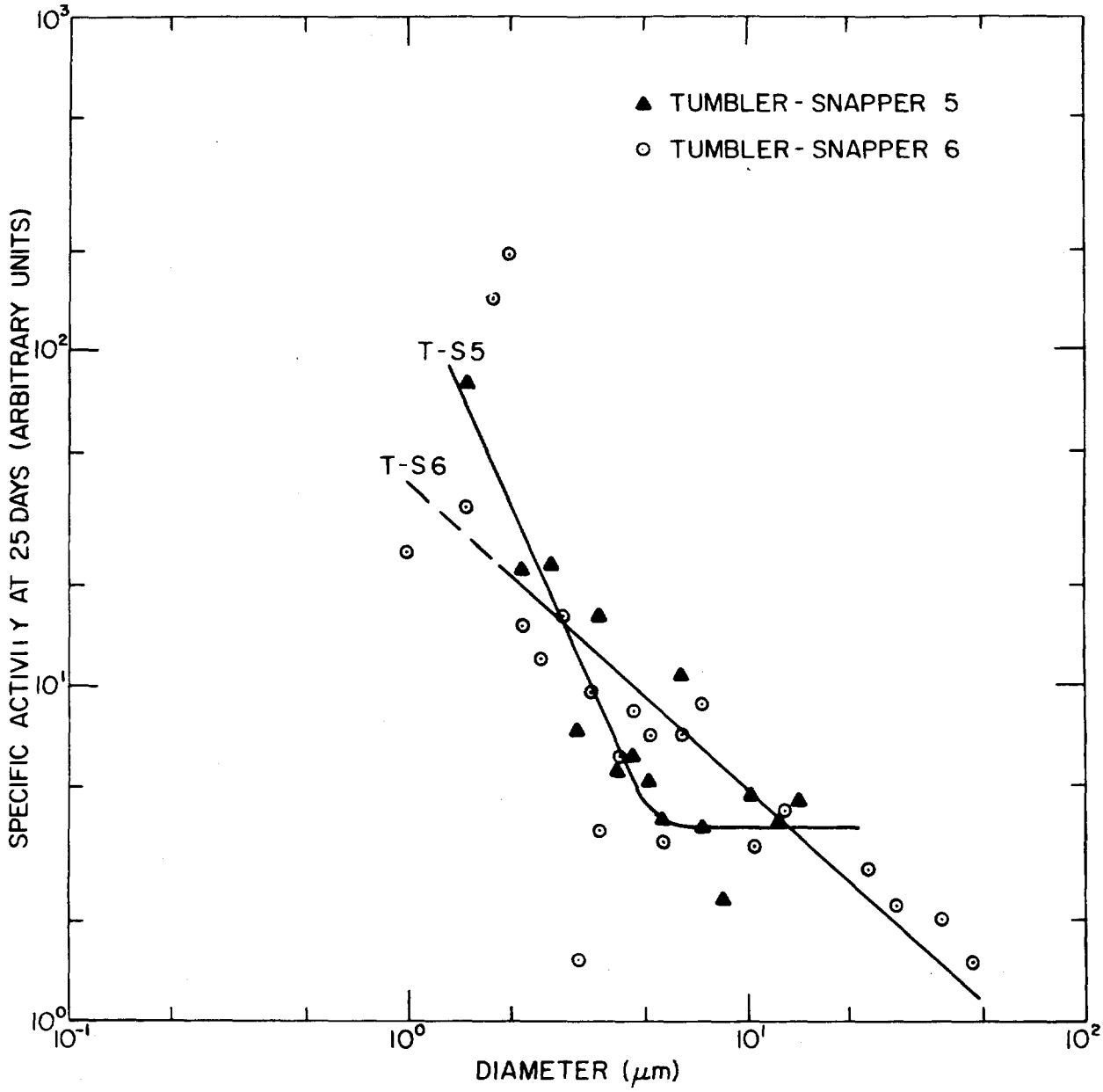

Figure 8. Specific Beta Activity of Particles from Tower Shots Tumbler-Snapper 5 and 6.

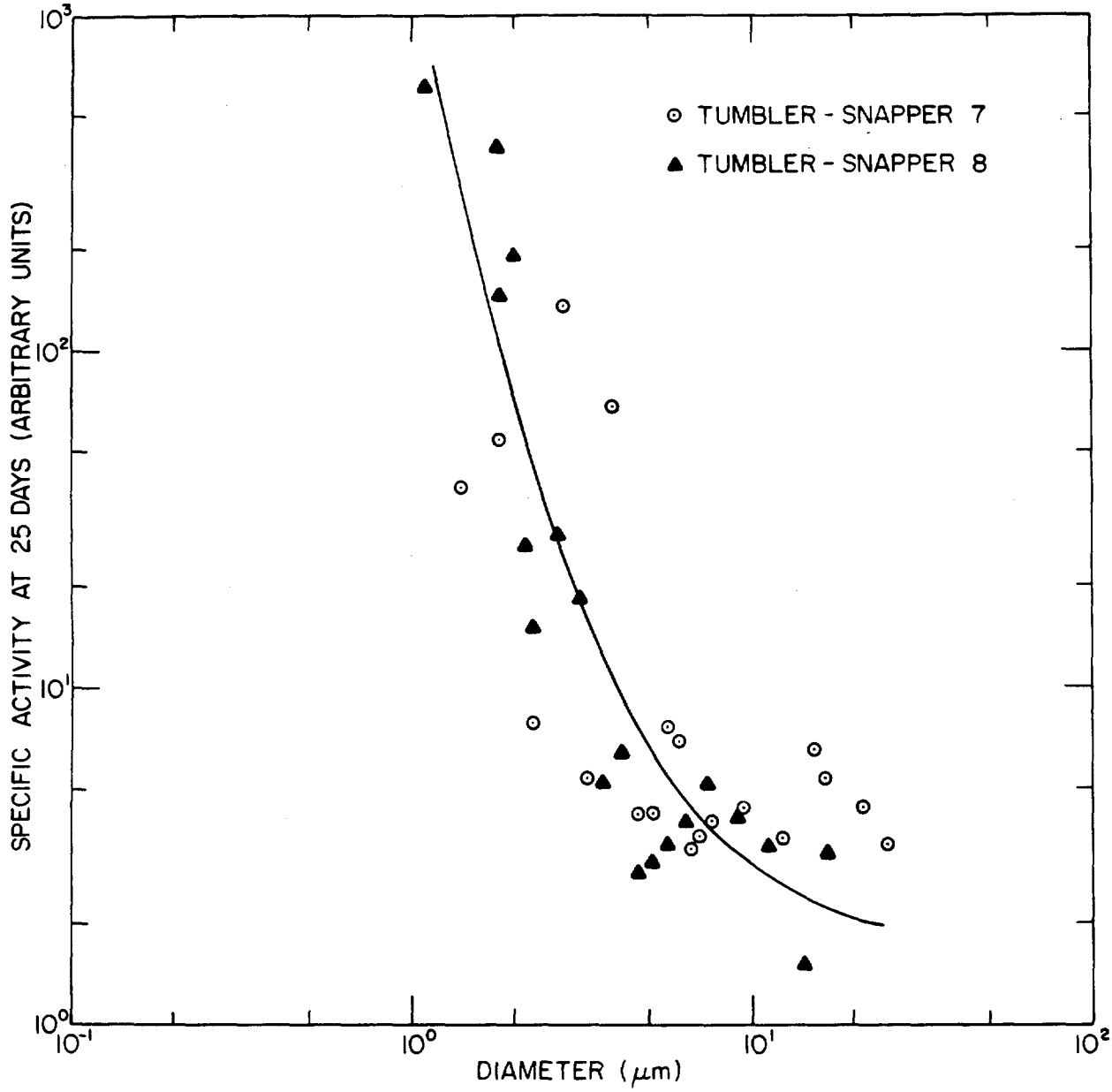

Figure 9. Specific Beta Activity of Particles from Tower Shots Tumbler-Snapper 7 and 8.

from about -1 to about -2. The differences among the Tumbler-Snapper lines are probably artifactitious, however, because the yields and scaled heights of burst of all four shots were quite similar. In particular, the two points at 1.0 and 1.5 μm for Tumbler-Snapper 6 appear anomalous, in which case the points from all four shots probably fall on the same correlation line within the precision of the measurements. That is, the points below 5 μm may be correlated by a single line with a slope of about -2.

The significant observation is that a general rule appears to obtain for the particle size dependence of the specific activity.

Starting at about 1 μm and moving towards larger particle sizes, the specific activity of particles from tower shots decreases with a slope which may vary from about -1 to about -2. At a particle size of about 5 to 20 μm, the specific activity becomes independent of the particle size, then begins to increase at about 150 to 250 μm. A maximum is reached at a size of several hundred micrometers, after which the specific activity decreases continuously to the largest particles for which activity data have been obtained.

Plutonium data have been obtained by Nathans (unpublished) for two shots from the Redwing series. Figure 10 shows the data. The major difference between the two shots was the scaled heights of burst, which was much greater for Shot 2 than for Shot 1, which actually began to approach a surface burst.

CONCLUSION

The major trends in the particle size dependence of specific activities has been rather well established for above-surface shots. Further work on this subject will deal with surface and subsurface bursts.

In addition to the particle properties discussed in this paper, a review will be conducted of principal-constituent concentrations and activity translocation in soil. It is expected that this work will be completed in about three to four months, and that a report can be presented at a later meeting.

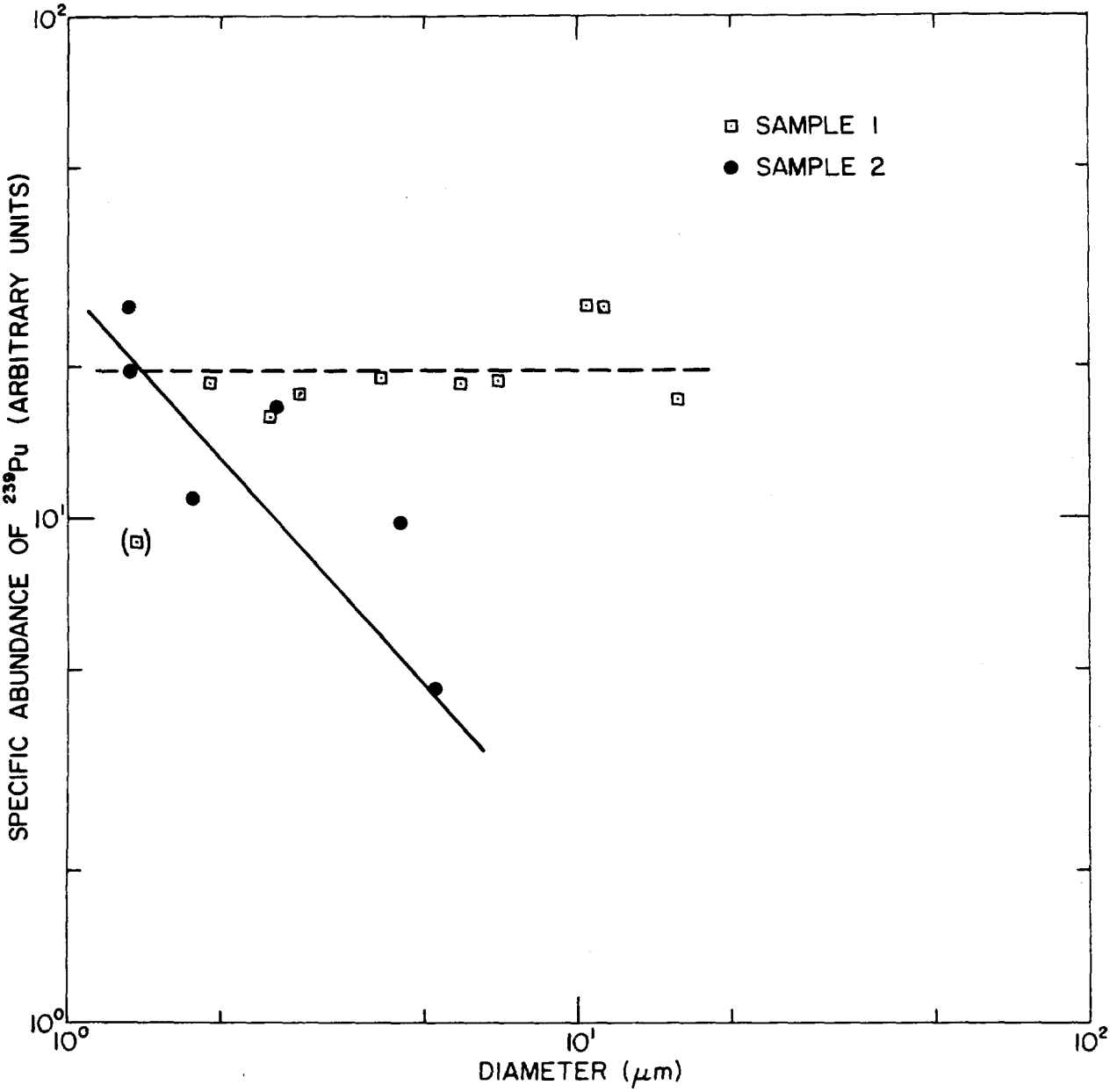

Figure 10. Specific Abundance of ^{239}Pu in Particles from Two Tower Shots in Coral.

REFERENCES

1. Benson, P. A., and L. Leventhal. 1965. "Radiochemical Fractionation Characteristics of Single Particle From High-Yield Airbursts." *In: Conf. Radioactive Fallout From Nuclear Weapons Tests.* USAEC. Report USAEC CONF-765.

2. Bolles, R. C., and N. E. Ballou. 1956. Calculated Activities and Abundances of U-235 Fission Products. U.S. Naval Radiological Defense Lab Report. USNRDL-TR-456.

3. Clark, D. E., F. K. Kawahara, and W. C. Cobbin. 1963. Unpublished report.

4. Freiling, E. C. 1961a. "Fractionation I, High-Yield Surface Burst Correlations." U.S. Naval Radiological Defense Lab Report. USNRDL-TR-385; *Science* 133:1991.

5. Freiling, E. C. 1961b. "Radionuclide Fractionation of Bomb Debris." *Science* 133:3469.

6. Freiling, E. C. 1963. "Fractionation III, Estimation of Degree of Fractionation and Radionuclide Partition for Nuclear Debris." U.S. Naval Radiological Defense Lab Report. USNRDL-TR-680; *Science* 139:1058.

7. Freiling, E. C., and S. C. Rainey. 1963. "Fractionation II, On Defining the Surface Density of Contamination." U.S. Naval Radiological Defense Lab Report. USNRDL-TR-631.

8. Freiling, E. C., G. R. Crocker, and C. E. Adams. 1964a. "Nuclear Debris Formation Reviews and Lectures." U.S. Naval Radiological Defense Lab Report. No. 151. USNRDL, December 21, 1964.

9. Freiling, E. C., L. R. Bunney, and F. K. Kawahara. 1964b. "Physicochemical and Radiochemical Analysis." Operation SUN BEAM, Shot Small Boy, Dept. of Defense Report. POR 2216.

10. Glasstone, S. (Ed.). 1962. *The Effects of Nuclear Weapons.* Ch. 2. G.P.O., Washington, D.C.

11. Heft, R. E., and W. A. Steele. 1968. "Procedures for the Systematic Separation and Analysis of Radioactive Particles From Nuclear Detonations." UCLRL Report. UCRL-50428.

12. Lane, W. B. 1964. "Some Radiochemical and Physical Measurements of Debris From an Underground Nuclear Detonation." Project Sedan. U.S. Naval Radiological Defense Lab Report. USNRDL PNE-229F.

13. Miskel, J. A., and N. A. Bonner. 1964. "Distribution of the Radioactivity From a Nuclear Crater Experiment, Project Danny Boy." Report WT-1817.

14. Nathans, M. W. 1971. "The Determination of the Homogeneity of Nuclear Clouds From Airbursts, Part I." Final Report USAEC Contract No. AT(04-3)-682, Mod. 4. Also unpublished data.

15. Nathans, M. W. 1976a. "Brief Survey of Particle Work Relevant to the Test Sites." Final Report USERDA Contract No. E(26-1)-657, Mod. 2. September 27, 1976.

16. Nathans, M. W. 1976b. Unpublished report.

17. Nathans, M. W., and L. Leventhal. 1977. "Brief Survey of Particle Work Relevant to the Test Sites." *In: Transuranics in Natural Environments.* M. G. White and P. B. Dunaway, Eds. USERDA Report, NVO-178.

18. Russell, I. J. 1965. "Radioisotope Fractionation and Particle Size Characteristics of a Low-Yield Surface Nuclear Detonation, Operation SUN BEAM, Shot Johnie Boy." Dept. of Defense Report. POR 2291.

19. Russell, I. J. 1966. Unpublished report.

20. Stevenson, P. C. 1957. Unpublished report.

21. Teller, E., W. K. Talley, G. H. Higgins, and G. W. Johnson. 1968. *The Constructive Uses of Nuclear Explosives.* Ch. 4. McGraw-Hill, New York, New York.

CONTRIBUTED PAPERS

PRECONCENTRATION OF PLUTONIUM RADIONUCLIDES FROM NATURAL WATERS

K. M. Wong, V. E. Noshkin, and T. A. Jokela

Lawrence Livermore Laboratory
Livermore, California

ABSTRACT

A large-volume water sampler using manganese dioxide impregnated cartridges for the *in situ* separation of plutonium in seawater and groundwater was studied. Plutonium concentrations obtained by this technique are compared with a radiochemical coprecipitation method. Consistent results were obtained between the two methods for water samples from the Pacific Ocean and Enewetak lagoon. Different results were noted from samples collected in the Enewetak reef and groundwater stations.

We were able to demonstrate, using this preconcentration technique and the coprecipitation method, that the physical-chemical characteristics of Pu in Enewetak reef and groundwater are different from the lagoon and open ocean.

INTRODUCTION

Accurate measurements of plutonium in the marine environment require very large samples due to the extremely low concentration of Pu which originates mainly from worldwide fallout. For example, measurement of a surface seawater sample with a $^{239,240}Pu$ concentration of 2×10^{-16} Ci/liter, a typical surface seawater concentration in the 30-40° N latitude (Noshkin *et al.*, 1978), would require 100 liters of sample and 1 week of counting time to obtain a one sigma counting error of 10% (assuming 80% chemical recovery and 30% counting efficiency). Even larger samples would be needed to determine ^{238}Pu concentration.

The Battelle Large Volume Water Sampler (Silker *et al.*, 1971), BLVWS, has been used for concentrating *in situ* plutonium from natural water (Emery *et al.*, 1974; Schell and Watters, 1975), but the interpretation of the quantitites collected by the BLVWS is not without problems (Noshkin

et al., 1974; Nevissi and Schell, 1975; 1976). Other procedures have been developed for the radiochemical separation of transuranic elements from natural waters (Lai and Goya, 1967; Miyake and Sugimura, 1968; Wong, 1971; Hodge and Gurney, 1975; Livingston *et al.*, 1975; Scott and Reynolds, 1975). Most of these procedures are not adaptable to sample large volumes of water for Pu analysis from remote environments.

For our analytical requirements, a large-volume water sample using MnO_2 Impregnated Cartridge Extraction, MICE, was developed (Wong *et al.*, 1978) to preconcentrate low-level plutonium and other radionuclides from fresh and saltwaters. Preconcentration of Pu by the MICE procedure is similar in principle to collection using the BLVWS. The MICE sampler is considerably less expensive to build; it is more efficient for preconcentration of plutonium from seawater; it is easily adaptable for field operation; and the subsequent plutonium analysis of the MnO_2 cartridges is much easier than the Al_2O_3 beds used in the BLVWS.

The purpose of this report is to discuss the results obtained by the MICE sampler in field operations for the preconcentration of plutonium from marine and groundwaters.

SAMPLE COLLECTION AND ANALYSIS

A schematic of the MICE sampler is shown in Figure 1. Water is pumped through a 1 μm prefilter cartridge at a flow rate of 4-8 liter/m to isolate Pu associated with particulate materials. The filtrate is passed through two (or more) MnO_2 impregnated cartridges connected in series to separate the exchangeable plutonium. The cartridges are then dry ashed and each cartridge is analyzed separately for plutonium by standard radiochemical techniques. The detailed procedure has been reported by Wong *et al.* (1978).

The collection efficiency, E, can be calculated from the activity determined in each of the two cartridges in series using the equation:

$$E = 1-B/A \qquad (1)$$

Where, A = Plutonium absorbed on the first MnO_2 cartridge (pCi)
B = Plutonium absorbed on the second MnO_2 cartridge (pCi)

If the sample volume, V, is measured in m^3, the plutonium concentration in the filtrate in pCi/m^3 may be calculated by the relationship:

$$pCi/m^3 = A^2/(A-B)V \qquad (2)$$

The derivation of the collection efficiency is based on the assumption that the adsorption efficiency for any plutonium chemical species in the

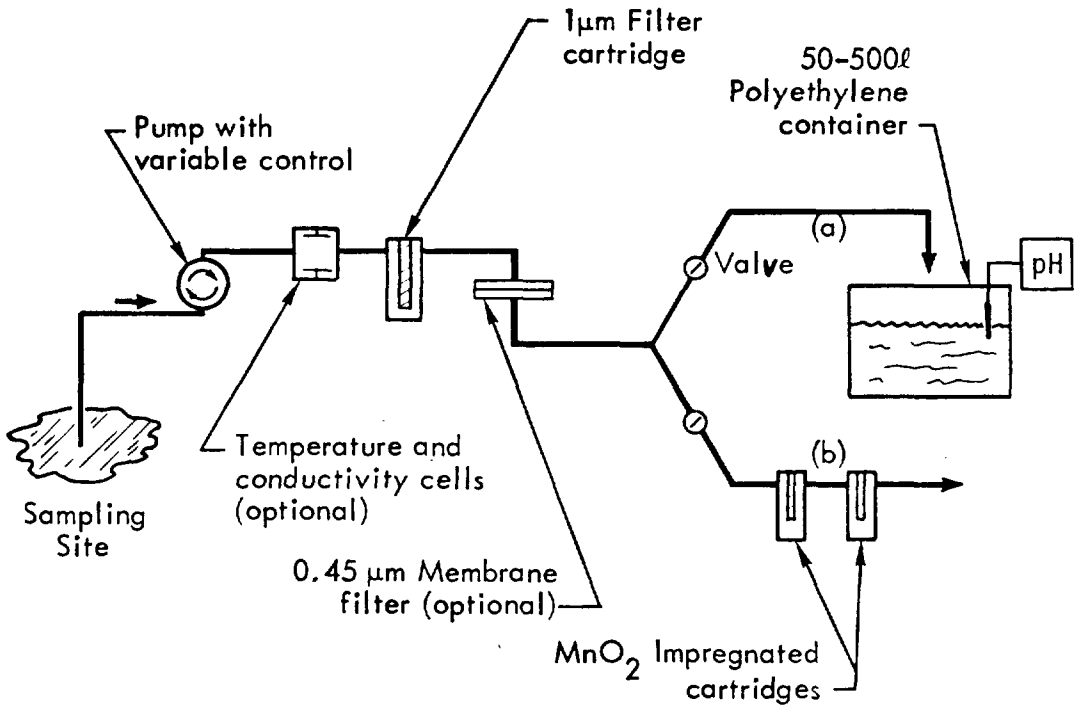

Schematic for the collection of water samples for (a) MnO_2 coprecipitation or (b) direct adsorption of plutonium on MnO_2-impregnated cartridges.

Figure 1.

water sample is the same for each MnO_2 cartridge. We found this to be true for ^{242}Pu tracer Pu (III), Pu (IV) and Pu (VI) tested in the laboratory. Collection efficiency is reproducible if the MnO_2 cartridges are prepared just prior to use so that any physical damage to the MnO_2 surface is minimized. Temperature ranges between 10-30° C. and pH variations between 7-9 seem to have no significant effect on the efficiency.

The MICE procedure has been used to preconcentrate plutonium from water contaminated by different sources. Fallout plutonium has been separated from surface Pacific Ocean water south of the Farallon Islands, west of San Francisco (37° N 123° W) and near the Marshall Islands (10° N 165° E). Plutonium remobilized to solution from the solid phases of the environment has been concentrated from Enewetak Atoll lagoon, reef, and groundwater.

To verify the accuracy of the calculated collection efficiency using Equation 1, representative aliquots of 50-200 liters of filtered water from each station were collected and analyzed separately for plutonium by standard radiochemical coprecipitation methods.

RESULTS AND DISCUSSION

The four types of environmental water samples collected for this study are listed in Tables 1 and 2 along with the sample volumes processed with the MICE technique. Also tabulated for each sample are the $^{239,240}Pu$ concentrations associated with the material removed by the 1 μm prefilter (PF), the activity adsorbed on each MnO_2 cartridge (A,B), the plutonium concentration in the filtrate determined from Equation 2, the aliquot concentration determined by the radiochemical coprecipitation method (RC), and the collection efficiency of the MnO_2 cartridges.

The first point of interest in Table 1 is the good agreement of the $^{239,240}Pu$ concentration in the filtrate determined by the MICE and radiochemical method for both the ocean and lagoon samples. Only one (sample E-11) out of twelve samples from these two areas shows a deviation greater than the counting error. The plutonium concentration of the filtrate determined by the MICE was calculated by Equation 2 using the measured collection efficiency from each sample. The Pu collection efficiency computed from Equation 1 for the lagoon and open ocean waters (Table 1) varied from 48 to 95% and average 72 ± 13%. These differences may be related to sample flow rates, matrices or cartridge loading characteristics, but at this time it is unclear which mechanism is responsible. This variation is noted even in samples collected sequentially from the same area as shown by sample E-1. The result clearly shows that a mean computed collection efficiency would not be adequate for correcting the loss of plutonium in the preconcentration step;

Table 1. $^{239,240}Pu$ Concentration and MICE Collection Efficiency of Ocean and Enewetak Lagoon Water, fCi/liter (σ%) (a)

Sample Station		Date	Volume	$^{239,240}Pu$ on Cartridge			$^{239,240}Pu$ in Filtrate		% Collection Efficiency (S.D.) (a)		
			(liter)	PF	A	B	MICE	RC	$(1-^{B}/A)$	$(^{A}/RC)$	(Δ)
								(b)	(c)	(d)	(e)
Ocean	F1	Jan 77	1275	0.030(12)	0.115(13)	0.036(13)	0.167(18)	0.140(24)	69(12)	82(25)	13
37°N 123°W	F2		545	0.058(7)	0.113(6)	0.023(18)	0.142(19)	0.142(19)	80(15)	80(21)	0
	F2A		410	0.046(23)	0.131(6)	0.028(15)	0.167(15)	0.154(19)	79(13)	85(21)	6
10°N 165°E	01		681	0.046(15)	0.216(6)	0.069(10)	0.317(12)	0.33(45)	68(8)	65(26)	-3
Lagoon	E4	Apr 76	681	--	1.66(4)	0.44(8)	2.28(9)	2.34(7)	73(7)	71(8)	-3
Enewetak	E8		1003	1.66(8)	10.5(4)	3.20(3)	15.0(5)	16.0(6)	69(3)	66(5)	-3
110°N 162°E	E9		1048	2.0(15)	6.60(3)	3.20(3)	12.8(4)	13.1(6)	52(2)	50(4)	-2
	E10		1003	14.3(5)	21.3(3)	1.17(3)	22.5(4)	25.8(4)	95(4)	83(5)	-8
	E11		1003	5.6(3)	9.83(1)	2.80(1)	13.7(2)	18.5(3)	71(1)	53(2)	-18
	E12		1052	1.6(3)	16.7(6)	2.61(3)	19.8(7)	18.2(6)	84(6)	92(8)	8
	E1	Nov 77	1103	71(4)	34.0(4)	8.9(5)	46(6)	40(3)	74(4)	85(6)	11
	E1		2250	21(4)	20.0(4)	10.5(5)	42(6)	40(3)	48(3)	50(3)	2
								Average	72(13)	72(15)	

(a) The value in parentheses is the 1 sigma counting error expressed as percent in the concentration measurement (σ%). Actual deviation (S.D.) is shown for the collection efficiency.

(b) Aliquot determined by radiochemical analysis.

(c) Calculated collection efficiency of MICE samples using Equation 1.

(d) Measured collection efficiency of MICE samples calculated from the first MnO_2 cartridge (A) and the plutonium concentration in the filtrate determined by radiochemistry (RC).

(e) $\Delta = (d) - (c)$

Table 2. $^{239,240}Pu$ Concentration and MICE Collection Efficiency of Reef and Groundwater Well at Enewetak Atoll, fCi/liter (± σ%) (a)

Sample Station		Date	Volume	$^{239,240}Pu$ on Cartridge			$^{239,240}Pu$ in Filtrate		% Collection Efficiency (S.D.) (a)		
			(liter)	PF	A	B	MICE	RC	$(1-^{B}/A)$	$(^{A}/RC)$	(Δ)
								(b)	(c)	(d)	(e)
Windward Reef	C1	May 77	244	100(3)	11.3(3)	2.61(6)	14.7(7)	84(3)	77(5)	13(1)	-64
Enewetak	C3		295	182(3)	7.70(3)	1.88(5)	10.2(6)	83(4)	57(3)	9(1)	-48
Atoll	C4		238	152(4)	6.45(3)	5.23(4)	34(5)	71(3)	19(1)	9(1)	-10
Groundwater	W1	May 77	309	4800(3)	63.3(1)	10.2(3)	76(3)	110(2)	84(3)	58(3)	-26
Enewetak	W5		842	1.78(3)	0.20(7)	0.020(18)	0.22(19)	0.71(2)	90(17)	28(6)	-62
Atoll	W6		435	80.0(3)	0.67(5)	0.110(7)	0.80(9)	4.8(7)	84(8)	14(2)	-60
	W7		795	0.17(8)	0.030(19)	0.027(21)	0.44(28)	1.3(10)	10(3)	2(1)	-8

(a) . . . (e) See Table 1.

instead, the calculated collection efficiency determined by Equation 1 for each sample should be used.

Comparing the Pu results in Table 2 for the reef and groundwater, however, we find large discrepancies in the concentration determined by the MICE and radiochemical methods. This becomes even more apparent if we compare the calculated efficiency of the MICE samples and the measured efficiency using the radiochemical data.

The other notable difference in Table 1 and Table 2 is the range of activity in the 1 μm prefilters. In the ocean and lagoon samples, the particulate Pu ranges between 8 and 64% (average 26 ± 16%) of the total sample concentration. The concentration range of particulate Pu for the reef and groundwater was 12 to 98% of the total sample activity with an average of 67 ± 28%. The higher calculated collection efficiency for the reef and groundwater samples could be caused by microparticulates penetrating the prefilter and being sorbed on the first MnO_2 cartridge. If this were the case, then, the measured collection efficiency (value of A/RC in Table 2) should also be higher than the lagoon samples. But this is not the case. Plutonium associated with microparticulate or colloidal materials, if present in the reef and groundwater, is not preconcentrated significantly by the first MnO_2 cartridge.

In the seven reef and groundwater samples, an average of only 33% of the plutonium measured by radiochemistry was accounted for by the MICE procedure. This may be an indication that the reef and groundwater contain plutonium in chemical forms that are not readily exchangeable with the MnO_2 cartridge.

An attempt was made to further characterize the Pu in the reef water by passing aliquots of filtered samples through the four types of ion exchange resins listed in Table 3.

The cation exchange resin, AG-50, retained 28% of the plutonium; the two anion exchange resins, AG-1 and AG-21K, adsorbed 23-28%; and the Chelex-100 adsorbed essentially 100% of the total filterable amount determined on a separate aliquot by radiochemistry. We also estimated the plutonium associated with the organic materials in the water by incorporating a charcoal cartridge in line with the MICE samples. In one sample, 4% of the plutonium activity in the filtrate was found in the charcoal when it was placed ahead of the MnO_2 cartridges and 3% was adsorbed when the charcoal cartridge was placed behind the MnO_2 filters.

This small but distinctly organically bound fraction of Pu was not adsorbed by the MnO_2 cartridges.

The high adsorption shown by the chelating resin, Chelex-100, suggests that the major fraction of plutonium in the filtrate is chemically reactive. The high Chelex-100 value also indicates that inorganic species different from that found in the lagoon, perhaps strongly complexed, are the probable form of plutonium in the reef water.

Table 3. Adsorption of Plutonium From Enewetak Reef Seawater by Different Ion Exchange Resins (a)

Resin (b)	Type	^{239,240}Pu, fCi/liter (±σ %) on resin column	% Adsorbed
AG-50-4x, 100-200 mesh	Cation	23(14)	28
AG-21K, 100-200 mesh	Anion	18(11)	23
AG-1-4x, 100-200 mesh	Anion	23(9)	28
Chelex-100, 50-100 mesh	Chelating	81(7)	103

(a) Reef seawater filtered through 1 μm cartridge. Average ^{239,240}Pu in filtered sample was 79 ± 7 fCi/liter.

(b) Column dimension was 5.0 cm dia x 25 cm length.

In conclusion, we have demonstrated with simple equipment that plutonium radionuclides can be preconcentrated in the field using MnO_2 impregnated cartridges from large-volume water samples. Using both the MnO_2 cartridges and radiochemical techniques, we have shown that various inert and complexed chemical forms of plutonium exist in Enewetak reef and groundwater compared to the highly exchangeable species in the lagoon water and open-ocean water. Plutonium remobilized to solution by active processes at Enewetak appears initially to be relatively inert and highly complexed, and in a relatively short period of time, natural interactions convert this plutonium to a more exchangeable form when it enters the lagoon. The adsorption characteristics of lagoon Pu appear to be similar to fallout Pu in the open-ocean water.

ACKNOWLEDGMENTS

Work performed under the auspices of the U.S. Department of Energy by the Lawrence Livermore Laboratory under Contract Number W-7405-ENG-48. References to a company or product name does not imply approval or recommendation of the product by the University of California or the U.S. Department of Energy to the exclusion of others that may be suitable.

REFERENCES

1. Emery, R. M., D. C. Klopfer, and W. C. Weimer. 1974. "The Ecological Behavior of Plutonium and Americium in a Freshwater Ecosystem--Phase I." Battelle Pacific Northwest Labs. BNWL-1867.

2. Hodge, V. F., and M. E. Gurney. 1975. "Semi-Quantitative Determination of Uranium, Plutonium, and Americium in Sea Water." *Anal. Chem.* 47:1866-1868.

3. Lai, M. G., and H. A. Goya. 1967. "Plutonium Analysis of Seawater by Ion Exchange With Chelex-100." USNRDL-TR-67-73.

4. Livingston, H. D., V. T. Bowen, and D. R. Mann. 1975. "Analytical Procedures for Transuranic Elements in Sea Water and Marine Sediments." *In: Advances in Chemistry.* Series 147, Am. Chem. Soc. pp. 124-138.

5. Miyake, Y., and Y. Sugimura. 1968. "Plutonium Content in the Western North Pacific Waters." *Meteorology and Geophysics* 19:481-485.

6. Nevissi, A., and W. R. Schell. 1975. "Distribution of Plutonium and Americium in Bikini Atoll Lagoon." *Health Physics* 28:539-547.

7. Nevissi, A., and W. R. Schell. 1976. "Efficiency of Large Volume Water Samples for Some Radionuclides in Salt and Fresh Water." *In: Radioecology and Energy Resources.* C. E. Cushing, Jr. (Ed.). pp. 277-282.

8. Noshkin, V. E., K. M. Wong, R. J. Eagle, and C. Gatrousis. 1974. "Transuranics at Pacific Atolls, 1. Concentrations in the Waters at Enewetak and Bikini." UCRL-51612. pp. 18-20.

9. Noshkin, V. E., K. M. Wong, T. A. Jokela, R. J. Eagle, and J. Brunk. 1978. "Radionuclides in the Marine Environment Near the Farallon Islands." UCRL-52381.

10. Schell, W. R., and R. L. Walters. 1975. "Plutonium in Aqueous Systems." *Health Physics* 29:589-597.

11. Scott, T. G., and R. L. Reynolds. 1975. "Determination of Plutonium in Environmental Samples, Part II. Procedures." *Radiochem. Radioanal. Letters* 23:275-281.

12. Silker W. B., R. W. Perkins, and H. C. Rieck. 1971. "A Sampler for Concentrating Radionuclides From Natural Water." *Ocean Eng.* 2:49-55.

13. Wong, K. M. 1971. "Radiochemical Determination of Plutonium in Sea Water, Sediments, and Marine Organisms." *Anal. Chem. Acta* 56:355-364.

14. Wong, K. M., G. S. Brown, and V. E. Noshkin. 1978. "A Rapid Plutonium Separation in Large Volumes of Fresh and Saline Water by Manganese Dioxide Precipitation." *J. Radioanal. Chem.* (In press).

ALPHA-SENSITIVE CELLULOSE NITRATE TRACK DETECTORS: APPLICATIONS TO THE STUDY OF ENVIRONMENTAL CONTAMINATION

R. W. Buddemeier

University of Hawaii, Honolulu

A. H. Biermann and C. Gatrousis

Lawrence Livermore Laboratory--Livermore, CA

ABSTRACT

Kodak LR-115 Type II cellulose nitrate alpha track detection film was evaluated for its utility in environmental plutonium studies. It was found that with fast and simple etching and reading techniques, the film "detects" 60 to 90% of the incident alpha particles with energy less than 4 MeV; both precision and efficiency may be increased by careful control of procedures. When applied to previously analyzed soil samples from Enewetak Atoll, it was found that ball-milled and gross soil samples were both highly heterogeneous in Pu distribution, with most activity concentrated in discrete particles of various types and sizes. For a one-day exposure to soil or a similar "solid" surface, detection sensitivity (5 x background) is approximately 50 pCi/g of total alpha activity and increases linearly with increased exposure time. Track detection films of this type provide a rapid and inexpensive means of obtaining quantitative estimates of environmental sample activity, and have unique utility for methods evaluation and the investigation of activity distribution as a function of phase, particle size, or organ in a heterogeneous sample.

INTRODUCTION

Applications of solid-state track detectors in a wide variety of fields have expanded dramatically during the last two decades; a comprehensive review of the field as of mid-1973 is given by Fleischer *et al.* (1975). Although successful alpha-sensitive films (usually of cellulose nitrate or cellulose acetate) have found widespread application only during the present decade, their utility is by now well established.

Kienzler and Polig (1975) and Polig (1975a, b) have reported on the use of alpha autoradiography in biological studies. Film determinations of natural alpha activity have been used in uranium exploration (Gingerich, 1975) and geochronology (Fisher, 1977). Bhatt and Singh (1974) have suggested film use for plutonium contamination measurements, Center and Ruddy (1976) have applied the method to characterization of alpha-radioactive aerosols, and Levy *et al.* (1977) have used it to study the history of uptake of Pu by a coral in Bikini lagoon.

Alpha autoradiography has many advantages: it is nondestructive; it yields information about the spatial distribution of activity within a sample; and for many applications, it is faster, simpler, and less expensive than conventional radioanalytical techniques. Its failure to achieve wider application has probably resulted from the fact that, until recently, commercial detectors and standard methods were not available, requiring investigators to develop their own films and validate technique on a step-by-step basis. However, Eastman Kodak now markets two alpha-sensitive cellulose nitrate films (CA 80-15, 100 μm thick, and LR-115, with a sensitive layer thickness ranging from 6 to 13 μm depending on type and batch), and a substantial literature on their use and characteristics has developed (for example, Costa-Ribeiro and Labão, 1975; Qaqish and Besant, 1976; Spurný and Turek, 1976; Levy *et al.*, 1977; Eastman Kodak, no date).

The purpose of the study reported on here was to investigate the utility of Kodak LR-115, Type II for rapid quantitative or semiquantitative activity measurements and studies of activity distribution in biogeochemical samples and environments contaminated with plutonium.

MATERIALS AND METHODS

Most of the work reported here was done with batch I.76.I of Kodak LR-115, Type II film. This film has a dark red cellulose nitrate layer 13 μm thick deposited on a plastic backing. The recommended development procedure (Eastman Kodak, no date) is to etch in 2.5 N NaOH solution at 60° C. for 90 minutes. Under these conditions, damage tracks resulting from alpha particles with energies less than 4 MeV are expected to etch completely through the cellulose nitrate layer, leaving holes on the order of a few μm to a few tens of μm which may readily be observed, counted, and measured with transmitted light.

Activity sources and samples used included commercial ^{241}Am standard planchets, Pu-electroplated planchets which had been accurately counted by alpha spectrometry at Lawrence Livermore Laboratory, and soils, sediments, and other samples from the Pu/Am-contaminated environments of Enewetak and Bikini atolls.

Exposure conditions studied included direct film-source contact as well as the use of Mylar energy degraders ranging in thickness from 6.35 μm (.00025") to 25.6 μm. Studies of etching technique included variation of the time and temperature of etch, agitation of the NaOH bath, and methods of rinsing the etched film. Procedures were deliberately kept as simple as possible, and the etch bath for most of the work consisted of a beaker of NaOH solution inside a stirred water jacket on a hot plate, with temperature monitored every 15-20 minutes. Etch temperatures reported are a linear average over a smoothly interpolated plot of temperature versus time for each etch.

For measuring and mapping track density, a variety of methods were tried. Microscopic observation using transmitted light, both with and without a green filter, was used at magnifications ranging from 70x to 400x. For area determinations, both the field of the microscope and transparent gridded mounting slides were employed. Films were also scanned on a Quantimet image analysis system, consisting of an automated stage microscope, a video system, and an image analyzing computer. This instrument automatically measures hole sizes and locations as well as counting total tracks.

RESULTS

1. General exposure techniques: The film may be cut to desired shapes or sizes and mounted on slides or other holders. Drafting tape is useful for noncritical mounting, as it comes away clearly and does not leave a residue which might poison the etch bath. Code numbers and area boundaries (e.g., sample, standard, blank) may be scribed directly into the emulsion with a scalpel point. Parafilm is convenient for shielding portions of the film while other areas are exposed.

2. Etching techniques: It was found, in agreement with Costa-Ribeiro and Labão (1975), that if the NaOH bath was not stirred (in accordance with Kodak recommendations), an excessively rapid and uneven etch resulted. After an initial trial series, the etch bath was mechanically stirred for all samples. It was also found that the bulk-etched surface material did not uniformly rinse off the film when it was dipped in or sprayed with distilled water at the end of the etching process. In order to eliminate the mottled appearance caused by incomplete clearing of the etched surface, film pieces were placed in an ultrasonic cleaner for approximately three minutes. This resulted in a very uniform rinse.

3. Film reading: The Kodak-recommended procedure of enlarging the etched film 7x and counting the black points (hole images) with a magnifying glass is useful in producing a large, visible map for

viewing overall activity distribution, but it is tedious and imprecise for quantifying hole counts and sizes. Microscopic examination of the film with transmitted green light causes the holes which have completely etched through the red film to appear as brilliant spots of light, readily visible at magnifications of 70-125x. Incompletely etched tracks are also visible, but in the interests of speed and simplicity, it was decided to count only those which had etched completely through. If this is done, there is little advantage to be gained from higher magnification. Films were also scanned with the Quantimet analysis system. Although it is no faster than manual counting and requires access to sophisticated instrumentation, this technique permits acquisition and storage in computer-compatible form of quantitative distribution and track dimension information. Agreement between manual and automated counting techniques could be brought to within about 5% if careful attention were paid to setting analyzer detection thresholds to agree with the microscopist's track acceptance criteria; without such effort, differences of about 15% were typical. Representative data are presented in Table 1 and discussed below.

4. Standard source exposures: Table 1 summarizes the results obtained from exposures of films under various conditions to a Pu-plated planchet with 616 dpm $^{239,240}Pu$ and 314 dpm ^{238}Pu in an active plated area with a diameter of 1.8 cm. All films had both an area exposed to the source (normally through a 12.8 μm Mylar energy degrader, although exposures with no degrader and with 1.8 cm of air were also made) and a similar area reserved for blank determination. All completely etched tracks in an area 500-600 mm^2 containing the exposed portion were counted, and a similar count was made in an equivalent blank area. This total count approach was taken to avoid problems with nonuniformity of source distribution; counts made by microscope are coded "M," while those obtained from the image analyzer system are coded "IA." Figures 1-3 are image analyzer plots of the distributions of track diameters (or the diameter of a sphere of equivalent projected area for asymmetric tracks) for representative samples. Figure 1 is the blank of film XXX, Figure 2 is for source exposure XXIX (see Table 1), where Eα ranged from 0 to 3.7 MeV, and Figure 3 is for source exposure XXXV, with an Eα range of 2.05 to 3.70 MeV.

5. Environmental sample exposures: Samples of previously analyzed soils and sediments were used to investigate film sensitivities and exposure techniques for environmental samples. Table 2 gives the results obtained from relatively long exposure of the films to dried but otherwise unprocessed sediments from Bravo Crater in Bikini Atoll lagoon. The film pieces, mounted on slides, were gently covered with sediment (either in direct contact or with an intervening Mylar energy degrader), left for three weeks, and then rinsed off and etched. Portions of each film were selected at random, measured, and the tracks counted. For one measurement, a gridded slide was used and the tracks in each square millimeter

Table 1. Plutonium Source Exposures of LR-115/II

Sample	Degrader	Etch Time (min.)	Etch Temp. (°C)	Blank (Tracks/mm^2)	Net Sample Tracks	Incident* Alphas	Efficiency (%)	Method**
X	.0005" Mylar	92	59.7 ± 0.6	0.22	2461	3180	77	M
XIV	.0005" Mylar	90	∿ 60.0	0.04	2162	3180	68	M
XVIII	.0005" Mylar	90	∿ 60.0	0.12	2349	3180	74	M
(XVIII)	.0005" Mylar	90	∿ 60.0	***	2689	3180	85	IA
XXIX	.0005" Mylar	90	59.8 ± 0.4	0.43	2880	3180	91	IA
XXX	.0005" Mylar	90	60.2 ± 0.9	0.69	2317	3500	66	IA
XXXIII	.0005" Mylar	90	61.7 ± 0.4	0.93	1944	3180	61	IA
XXXIV	none	90	60.1 ± 0.4	0.20	133	1.4×10^5	<0.1	IA
XXXV	1.8 cm air	90	60.1 ± 0.4	0.13	5143	****		IA
XXXVIII	.0005" Mylar	90	57.0 ± 0.4	0.03	1264	3500	36	IA

NOTES:

*Incident alphas calculated from source strength, exposure time, and geometric factors.

**M = visual count by microscope; IA = automatic scanning image analysis.

***Not determined; visually measured background used to calculate net tracks.

****Not calculated because of exposure area uncertainty. See Figure 3.

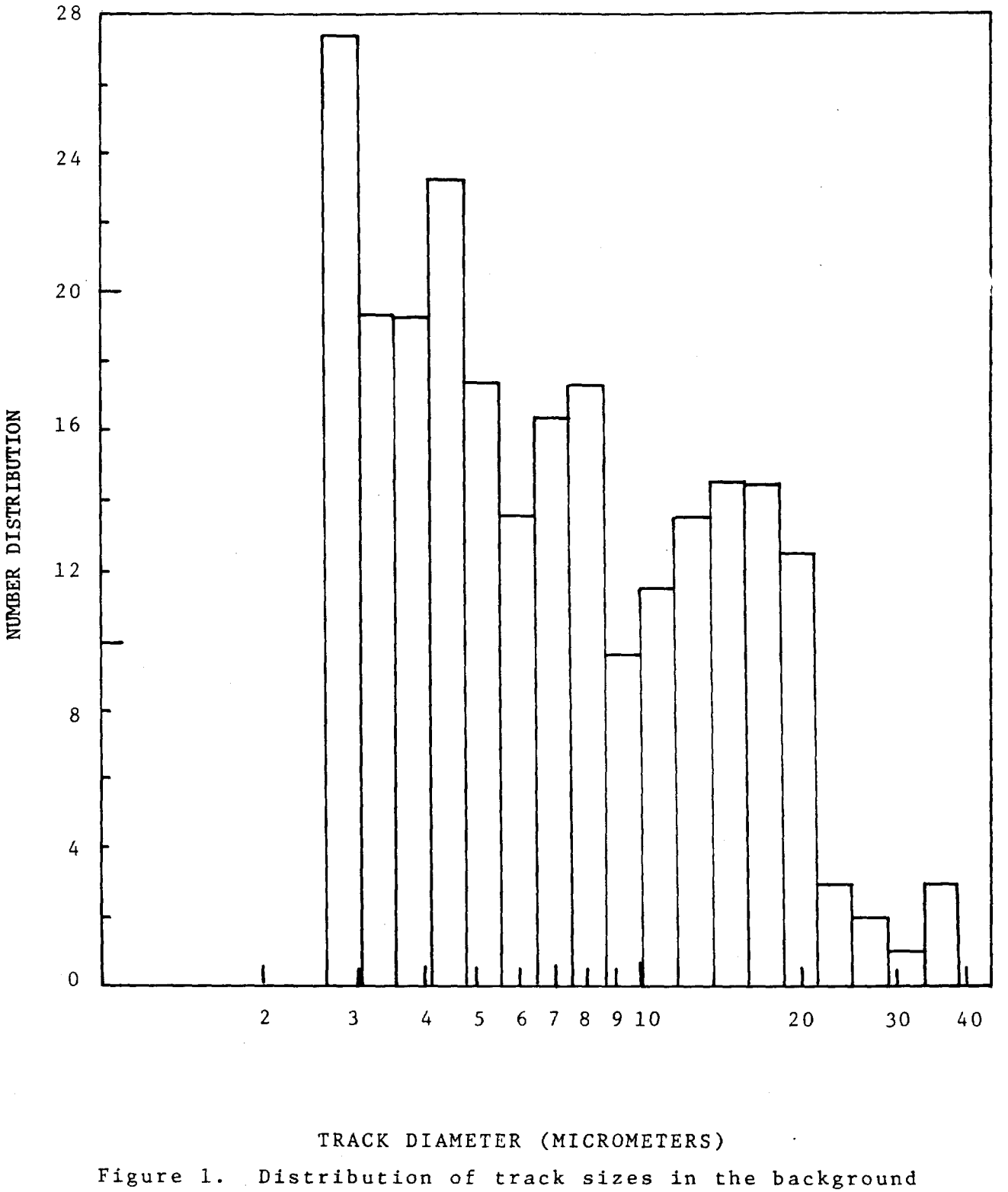

Figure 1. Distribution of track sizes in the background portion of film XXX.

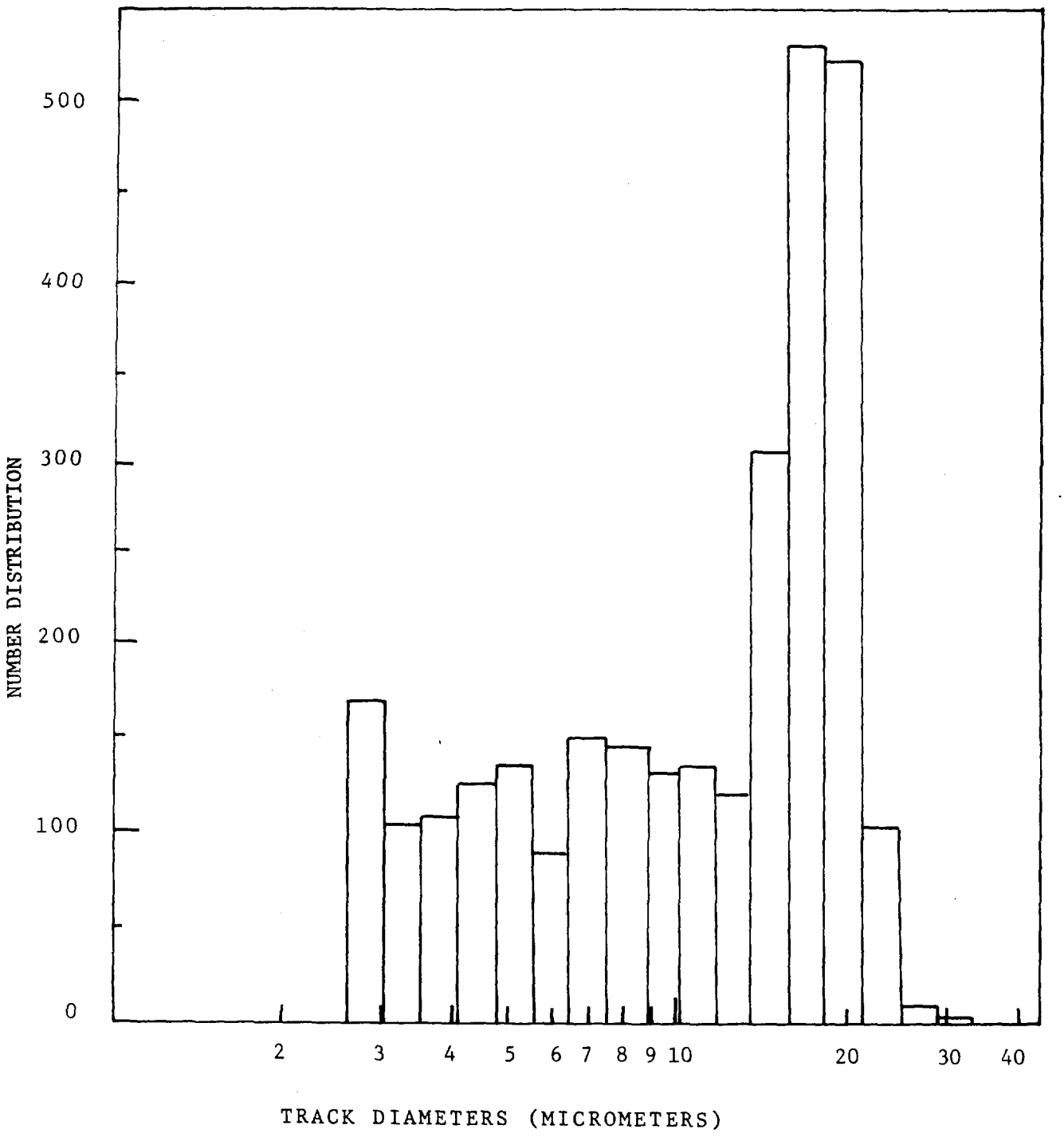

Figure 2. Distribution of track sizes in the exposed portion of film XXIX.

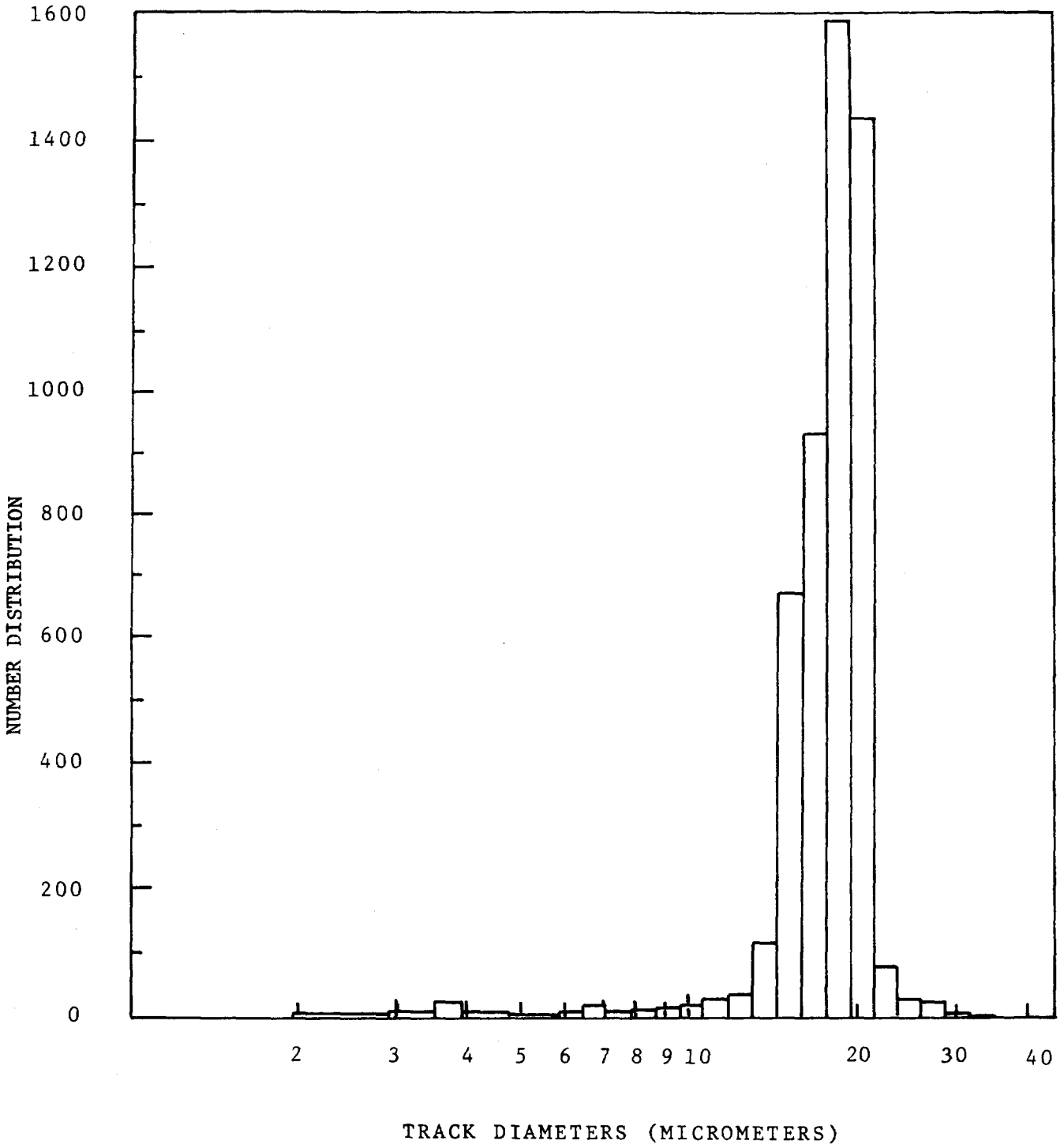

Figure 3. Distribution of track sizes in the exposed portion of film XXXV.

Table 2. Bravo Crater (Bikini) Sediment Exposures

Film	Bulk* Activity (pCi/g)	Degrader	Blank (mm^{-2})	Exposure Time (Hrs.)	Tracks/mm^2	Net R** (± %S)	Sensitivity*** X 10^4
XXII	∿ 120	none	∿ 0.11	522	739/23	32.02	5.11
					827/23	35.85	5.72
XXII	∿ 120	.00025" Mylar	0.11	525	788/23	34.15	5.42
					828/23	35.89	5.70
					741/18	41.06	6.51
						±14%	±0.91
XXI	∿ 120	.0005" Mylar	∿ 0.11	525	377/23	16.28	2.58
					372/23	16.06	2.55

NOTES:

*Activity estimated as 45 pCi/g ^{241}Am, 71 pCi/g $^{239,240}Pu$, and 4 pCi/g ^{238}Pu based on analyses of adjacent samples (V. Noshkin, pers. comm.).

**R = tracks/mm^2; S = standard deviation, expressed as % of R, calculated for the average R from tracks/mm^2 values for individual square millimeters.

***Tracks per mm^2 per pCi/g per hour of exposure (x 10^4).

were recorded; for this, both an average track density per mm^2 and a standard deviation (expressed as percent of track density/mm^2) were calculated. Finally, a sensitivity factor (tracks mm^{-2} $(pCi/g)^{-1}$ hr^{-1}) was calculated for each exposure, based on the estimated bulk activity of the sample. The tracks produced by this sample showed an extremely uniform distribution, with no evidence of particulate clusters. Table 3 gives the results of short-term exposures to soil samples from Runit I., Enewetak Atoll; these samples were selected from among those analyzed for the 1972 Enewetak radiological survey (U.S. Atomic Energy Commission, 1973) on the basis of their known high Pu concentrations. Sample A is 70-5205-24A, Sample B is 74-5221-24A, and Sample C is 76-5223-24A; all samples had been ball-milled to a powder as part of the original analytical procedures. Exposures were carried out as with the Bravo Crater sediment, except that portions of the film were shielded for blank measurement and for subsequent exposure to a commercial ^{241}Am standard to provide for efficiency comparisons between exposures. Track counts were recorded for each square mm observed in order to calculate both average track density and its percent standard deviation for each exposure. These samples were found to be extremely heterogeneous, with most of the activity concentrated in particles represented by track clusters of various sizes (0.01 to 0.5 mm diameter); this feature is reflected in the high and erratic standard deviations calculated for the sample R values. The sensitivities, based on the published bulk Pu activities of the samples, were calculated as above and then normalized to the lowest observed standard track density value in the set.

DISCUSSION

Qaqish and Besant (1976) have demonstrated that, with careful optimization and control of procedures, both LR-115 and CA 80-15 have detection efficiencies of 98-99%, a linear dependence of etch rate on temperature, and track diameter, which is a function of particle energy. They conclude that it is possible to control combined etching, track identification, and statistical uncertainties at the 1% level. The level of effort required to achieve this, however, tends to negate the track detector's inherent advantages of speed, simplicity, and economy. This study, by contrast, has attempted to address the question of how easily the commercially available cellulose nitrate films may be made to yield useful results.

The studies of standard source exposures (see Table 1) show that, with the techniques adopted, efficiencies range from 66 to 91% of the incident alphas for etching conditions close to the manufacturer's recommendations. The blank values and the efficiencies both drop as temperature is reduced

Table 3. Enewetak (Runit I.) Soil Sample Exposures

Film	Bulk Activity (pCi/g)	Degrader	Blank (mm^{-2})	Exposure Time (Hrs.)	Gross Track/mm^2	Net R* (± %S)	Normalized** Sensitivity
A-1 STD		2.2 cm air	0.10	0.17	562/20	28.00 ± 24%	
A-1 SAM	730	none	0.10	4.30	312/60	5.10 ± 577%	14.8×10^{-4}
A-2 STD		2.2 cm air	0.40	0.17	521/20	25.65 ± 25%	
A-2 SAM	730	.00025" Mylar	0.40	4.30	114/80	1.03 ± 358%	3.26×10^{-4}
A-3 STD		2.2 cm air	0.20	0.17	570/20	28.30 ± 19%	
A-3 SAM	730	.0005" Mylar	0.20	5.97	98/80	1.03 ± 519%	2.13×10^{-4}
B-1 STD		2.2 cm air	0.40	0.17	560/20	27.60 ± 19%	
B-1 SAM	840	none	0.40	4.30	111/50	1.82 ± 68%	4.66×10^{-4}
B-2 STD		2.2 cm air	0.30	0.17	535/20	26.45 ± 17%	
B-2 SAM	840	.00025" Mylar	0.30	6.00	98/50	1.66 ± 136%	3.17×10^{-4}
B-3 STD		2.2 cm air	0.15	0.17	583/20	29.00 ± 22%	
B-3 SAM	840	.0005" Mylar	0.15	4.30	100/40	2.35 ± 84%	5.72×10^{-4}
C-1 STD		2.2 cm air	0.20	0.17	1086/40	26.95 ± 20%	
C-1 SAM	840	none	0.20	4.30	641/153	3.99 ± 360%	10.38×10^{-4}
C-2 STD		2.2 cm air	0.25	0.17	515/20	25.50 ± 21%	
C-2 SAM	840	.00025" Mylar	0.25	4.30	111/30	3.45 ± 260%	9.55×10^{-4}
C-3 STD		2.2 cm air	0.45	0.17	599/20	29.50 ± 18%	
C-3 SAM	840	.00025" Mylar	0.45	6.03	106/40	2.20 ± 78%	3.75×10^{-2}

NOTES:

*See Table 2 for definition.

**Tracks/mm^2/(pCi/g)/hr, normalized to R std. = 25.50.

(for constant etching time); blank values, but not necessarily efficiencies, tend to rise with increasing temperature. These results are consistent with the observations of Qaqish and Besant (1976) and Costa-Ribeiro and Labão (1975). The observed variations among generally comparable exposures are probably due to etch bath temperature fluctuations, the relatively uncontrolled introduction of two new operations (etch bath stirring and ultrasonic rinse), and failure to achieve sample-to-sample consistency in setting the track acceptance thresholds for the image analyzer. Better control over all of these parameters can be achieved without prohibitive cost or effort; however, the practice of treating each piece of film as an individual "counter" with separate but equivalent sample, standard, and background areas reduces the number of assumptions required to quantify the film data.

The sediment sample exposures (Table 2) show good agreement between repeat counts, and indicate that a value of about 5×10^{-4} tracks/mm^{-2} $(pCi/g)^{-1}$ hr^{-1} is a good estimate of film sensitivity to reasonably homogeneous solid sample alpha activity. Although 0.5 mil (12.8 μm) Mylar is an optimal energy degrader for surface-plated Pu activity, the self-absorption in a three-dimensional sample reduces or eliminates the need for additional energy degraders. There appears to be little difference between direct contact sensitivity and sensitivity with 0.25 mil (6.4 μm) Mylar interposed, so it should be possible to use such a film when it is desirable to contain the sample or to protect the film from direct physical or chemical interaction with the sample.

The Enewetak soil samples were intended as a test of the potential of short exposure studies of contaminated environments using the combined sample-standard-background approach to single film analysis. However, the extreme heterogeneity of the samples frustrated a rigorous comparison. The following points may nonetheless be made on the basis of Table 3: (a) the track densities for the standard exposures on the different films were in satisfactory agreement; (b) blanks were reasonably consistent, although apparently somewhat higher than the value of about .06 mm^{-2} suggested by Eastman Kodak; (c) the calculated sensitivities were generally comparable in magnitude to the values obtained in Table 2, although the sample heterogeneity makes it doubtful that the published bulk activity values can be directly applied to this type of calculation; and (d) the relative standard deviation provides a crude but useful measure of sample homogeneity.

The effectiveness of sample homogenization procedures (e.g., ball-milling), the distribution of environmental activity in relation to subcomponents of a sample, and the implications of inhomogeneous activity distribution in terms of sampling and analytical design and procedures are all subjects which have received less than adequate attention, due in large part to the lack of an appropriate research method. Alpha autoradiography permits addressing these subjects on a variety of levels. The standard deviation of the average track density is one useful index, as is subjective visual observation. However, use of image analyzing systems will permit a much more powerful approach to the question of partitioning

activity between various classes of particles and "dispersed" phases. Since there are distinct differences in track diameter distributions between background tracks and samples with different Eα distributions (see Figures 1-3), one can envision a combination of track position and size analyses which could be used to characterize particle size, activity, and depth within sample. If the sample surface is solid (e.g., resin-bedded soil) and the film properly indexed, it would then be possible to locate and retrieve for direct investigation selected "hot spots" (Levy *et al.*, 1977).

SUMMARY AND CONCLUSIONS

Commercial cellulose nitrate track detectors have some disadvantages: they cannot discriminate well between alpha particles from different nuclides; they require some form of optical readout; and fairly demanding procedures must be followed to maximize sensitivity and reproducibility. However, their advantages are even more persuasive: they provide unique information on spatial distribution of activity; they are adaptable to the study of small and/or inhomogeneous samples (the volume of sample actually sensed by the film for any of the environmental samples in this study was less than 0.1 cm^3, or a few hundred mg); and, for applications where semiquantitative determinations are adequate, they are fast, cheap, and simple when compared to radiochemical methods.

Specifically, the following areas of application appear able to profit from immediate use of alpha track detectors:

1. Analysis of amounts and distributions of activity in small samples such as aerosol filters, specific soil or sediment size fractions or phases, and biological subsamples (e.g., specific organs);

2. Screening of samples from a contaminated environment in order to design the most efficient survey and to target a limited number of critical samples for radiochemical analysis;

3. Research into the statistical basis for sampling environments and analyzing samples with inhomogeneous activity distributions.

ACKNOWLEDGMENTS

Much of the work described was done while the senior author held a summer research appointment at Lawrence Livermore Laboratory, but additional work was carried out at the University of Hawaii under DOE Contract EY-76-S-08-641. We gratefully acknowledge the assistance of all those at LLL and U. of H. who gave willingly of their time and advice. The assistance of Mr. Barry Fankhauser is especially appreciated.

REFERENCES

1. Bhatt, R. C., and D. Singh. 1974. "Cellulose Acetate Damage Track Detector for Plutonium Contamination Measurements." *Health Physics* 27:219-220.

2. Center, B., and F. H. Ruddy. 1976. "Detection and Characterization of Aerosols Containing Transuranic Elements With the Nuclear Track Technique." *Analytical Chem.* 48:2135-2139.

3. Costa-Ribeiro, C., and N. Labão. 1975. "Testing of the LR-115 Kodak-Pathé Red-Dyed Cellulose Nitrate for Alpha Particle Detection." *Health Physics* 28:162-166.

4. Eastman Kodak Co. (No date.) "Instructions for the Use of CA80-15 Film and LR-115 Film, Type I and Type II."

5. Fisher, D. E. 1977. "Deep-Sea Sedimentation Rates Determined by Alpha and Fission-Track Counting." *Trans. Am. Geophys. Union* 58:421.

6. Fleischer, R. L., P. B. Price, and R. M. Walker. 1975. *Nuclear Tracks in Solids.* University of California Press, Berkeley.

7. Gingerich, J. E. 1975. "Results From a New Uranium Exploration Method." *Trans. Soc. Min. Eng. AIME* 258:61-64.

8. Kienzler, B., and E. Polig. 1975. "Microphotometry as a Tool for Automatic Scanning of Solid State Nuclear Track Detectors." *Radiation and Environmental Biophysics* 12:77-80.

9. Levy, Y., D. S. Miller, G. M. Friedman, and V. E. Noshkin. 1977. "The Distribution of Alpha Emitters in the Coral *Favites Virens*, Bikini Lagoon." *In:* Proceedings, Third International Coral Reef Symposium, University of Miami. pp. 549-553.

10. Polig, E. 1975a. "α-Microdosimetry in Bone Sections by Means of Dielectric Track Detectors and Electronic Image Analysis." *International Journal of Applied Radiation and Isotopes* 26:471-479.

11. Polig, E. 1975b. "Automatic Determination of High α-Track Densities in Polymer Detectors." *International Journal of Applied Radiation and Isotopes* 26:519-525.

12. Qaqish, A. Y., and C. B. Besant. 1976. "Detection Efficiency and Range Determination of Alpha Particles in Cellulose Nitrate." *Nuclear Instruments and Methods* 138:493-505.

13. Spurný, F., and K. Turek. 1976. "To the Alpha Particle Detection by the Kodak LR-115 Solid State Track Detector." *Czechoslovak Journal of Physics*, Sect. B., 26:235-238.

14. U.S. Atomic Energy Commission. 1973. *Enewetak Radiological Survey*. U.S. AEC Nevada Operations Office, Las Vegas, Nevada. Report NVO-140.

ESTIMATION OF EXPECTED VALUES OF ENVIRONMENTAL POLLUTANTS WITH LOGNORMAL AND GAMMA DISTRIBUTIONS

G. C. White

Los Alamos Scientific Laboratory
Los Alamos, New Mexico

ABSTRACT

Concentrations of environmental pollutants tend to follow positively skewed frequency distributions. Two such density functions are the gamma and lognormal. Minimum-variance unbiased estimators of the expected value for both densities are available. The small-sample statistical properties of each of these estimators were compared for its own distribution, as well as the other distribution to check the robustness of the estimator. Results indicated that the arithmetic mean provides an unbiased estimator when the underlying density function of the sample is either lognormal or gamma, and that the achieved coverage of the confidence interval is greater than 75 percent for coefficients of variation less than two. Further, Monte Carlo simulations were conducted to study the robustness of the above estimators by simulating a lognormal or gamma distribution with the expected value of a particular observation selected from a uniform distribution before the lognormal or gamma observation is generated. Again, the arithmetic mean provides an unbiased estimate of expected value, and the achieved coverage of the confidence interval is greater than 75 percent for coefficients of variation less than two.

INTRODUCTION

The concentrations of environmental pollutants have been suggested to follow positively skewed frequency distributions by numerous researchers. In particular, Pinder and Smith (1975) investigated the goodness of fit of the lognormal, Weibull, exponential, and normal distributions to radiocesium concentrations in soil and biota. They found that the lognormal distribution fit the majority of the data sets. Giesy and Weiner (1977) found that the lognormal also tended to fit the concentrations of trace metals in fish better than the Weibull, exponential, or

normal distributions. Ellett and Brownell (1964) suggest the gamma distribution may be preferred to the lognormal distribution. Eberhardt and Gilbert (1975) made an extensive study of how to distinguish these two distributions and concluded that this is difficult for less than 200 observations. Extensive Monte Carlo simulations were done to reach this conclusion. Forsythe *et al.* (1975) compared the fit of the gamma and lognormal distributions for the concentration of DDT in earthworms and concluded that both fit the data equally well. Figure 1 shows the similarity of the lognormal and gamma probability density functions for a variety of coefficients of variation and expected value equal 1.

Given that both these distributions appear to explain contaminant data equally well, I want to explore the implication of selecting one of these two distributions in estimating the expected value of concentration. Some investigators (Eberhardt and Gilbert, 1973) have suggested using the median of the observed data to measure central tendency when a portion of the samples are below detection limits. I believe that the median may be quite useful for answering some questions, but that usually the expected value is the desired measure. This paper presents the results of Monte Carlo simulations studies of estimating the expected value (EX) for these two distributions.

Link and Koch (1975) explored the bias which may result when the lognormal estimator of expected value is used for distributions other than lognormal. They found that a large negative bias (up to 97%) may result when the distribution of the logarithmically transformed variable is heavier tailed than the normal distribution. However, no bias was found when the logarithmically transformed variable has less tail area than the normal distribution. They did not consider lognormal estimation with gamma distributed data.

ESTIMATORS

First the estimation of EX for the lognormal distribution will be considered. The density function is given by Aitchison and Brown (1976):

$$f(x) = \frac{1}{\sigma_y \times \sqrt{2\pi}} \exp\left[-\frac{1}{2\sigma_y^2} (\ln x - \mu_y)^2 \right] dx$$

$$(x > 0;\ \sigma_y > 0,\ -\infty < \mu_y < \infty) ,$$

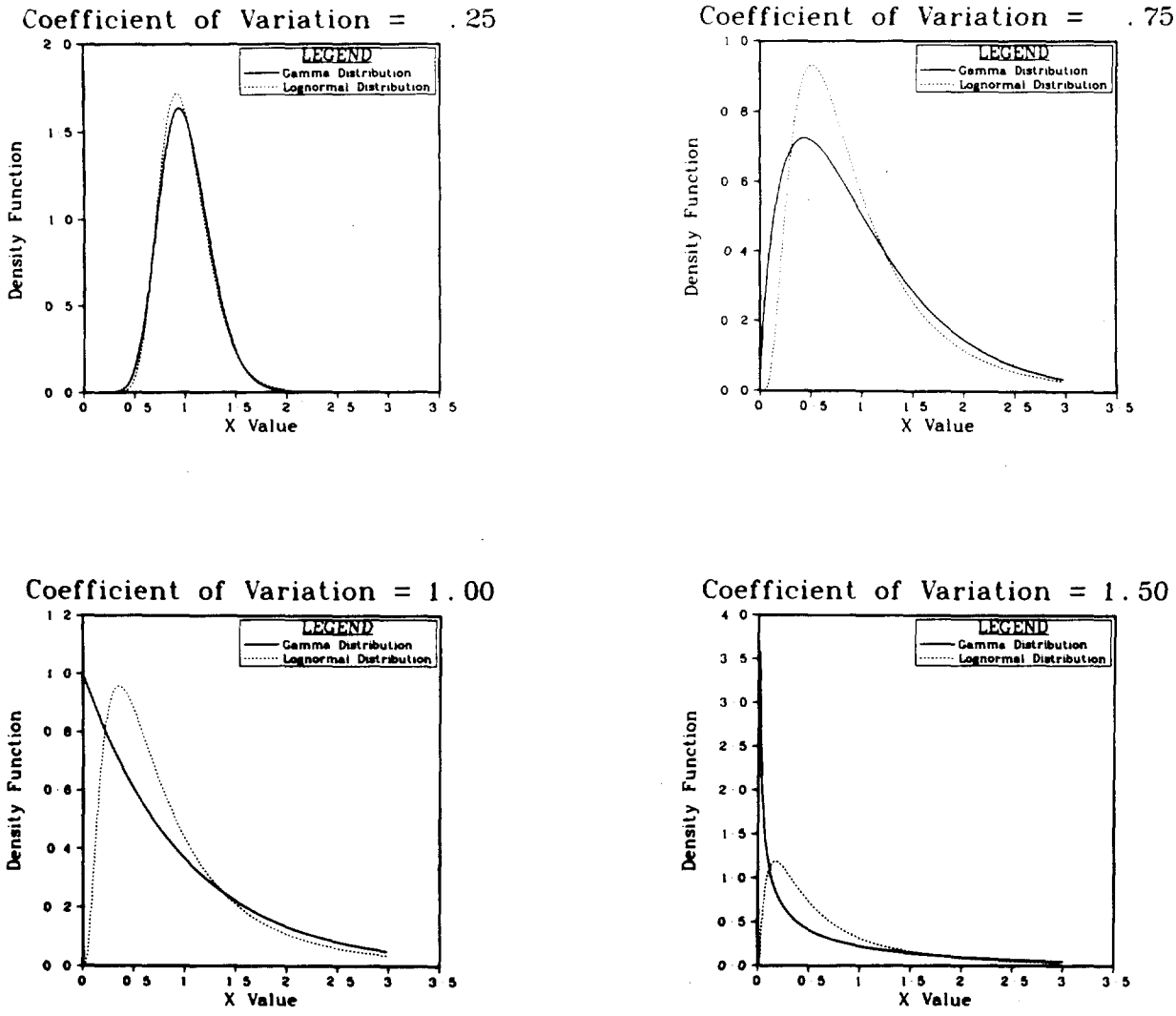

Fig. 1. Comparison of gamma and lognormal probability density functions with expected value of unity and four values of the coefficient of variation.

where μ_y and σ_y^2 are the mean and variance of $y = \ln x$, respectively. Finney (1941) derived a minimum variance unbiased estimator (MVUE) for EX because of the large bias of the maximum likelihood estimator (MLE). Finney's estimator is

$$\hat{E}(x) = \exp(\bar{y})\ g_n(s_y^2/2)$$

where $\bar{y}$ is the arithmetic mean of the log transformed x values, s_y^2 is the variance of the log transformed x values, and the function g is the infinite series

$$g_n(t) = 1 + \frac{(n-1)t}{n} + \frac{(n-1)^3 t^2}{n^2(n+1)2!} + \frac{(n-1)^5 t^3}{n^3(n+1)(n+3)3!} + \ldots$$

A finite sample confidence interval can be estimated for $\hat{E}(x)$ by Cox's direct method (Land, 1972). A confidence interval is calculated for the value $\bar{y} + 1/2\ s_y^2$ and then antiloged to achieve an interval on E(x). This interval is asymmetric, but has the desirable property that the lower confidence bound cannot be negative. Cox's direct method was shown to be easily the best of the approximate methods considered by Land and was recommended by him when dealing with large sample sizes and moderate values of s_y^2. Land's exact method is not used because of the computational difficulties involved.

Estimation of the EX for the gamma distribution is much simpler than for the lognormal distribution. The EX of the gamma distribution is the product of the parameters α and β, where the probability density function is

$$f_x(x) = \frac{1}{\Gamma(\alpha)\beta^\alpha} \exp(-x/\beta)\ x^{\alpha-1}\ dx \quad (x > 0;\ \alpha > 0,\ \beta > 0) \quad .$$

The maximum likelihood equations to estimate α and β are (Choi and Wette, 1969)

$$\Psi(\hat{\alpha}) + \log \hat{\beta} = \bar{y} \quad , \text{ and } \hat{\alpha}\ \hat{\beta} = \bar{x}$$

where $\Psi(t)$ is the psi (diagamma) function. Hence we see by the invariance property of MLE's that $\bar{x}$ is the MLE of EX for the gamma distribution. In addition, $\bar{x}$ is also an MVUE of EX. This result is known because (1) the gamma distribution is a member of the exponential family, (2) the set of minimal sufficient statistics (MSS) is

$$\left\{ \sum_{i=1}^{n} x_i \ , \ \sum_{i=1}^{n} \log x_i \right\} \ ,$$

(3) this set of MSS is complete, and (4) any function of the MSS is an MVUE if the function is unbiased. To see that $\bar{x}$ is unbiased,

$$E(\bar{X}) = E(X_1 + X_2 + \ldots + X_n)/n$$

$$= [E(x_1) + E(x_2) + \ldots + E(x_n)]/n$$

$$= (n \mu_x)/n$$

$$= \mu_x \ .$$

Hence $\bar{X}$ is an MVUE of EX. The details of this proof can be obtained in Mood *et al.* (1974). The result that $\bar{x}$ is an MVUE is particularly fortuitous as the arithmetic mean of the sample has often been used to estimate EX for real data. The usual confidence intervals for $\bar{x}$, namely

$$\bar{x} \pm t_{(n-1)} \ s_x/\sqrt{n} \ ,$$

will be used, with the Central Limit Theorem and the asymptotic normality of an MLE to justify the assumption of normality. Because of this assumption, this confidence interval may perform poorly for small sample sizes. The variance estimate thus obtained is not the same as the variance of $\bar{x}$ calculated by the maximum likelihood estimation procedure. However, the calculations are much easier to perform, and this estimator is the one commonly used in the transuranic literature. Therefore, of interest is whether confidence intervals based on this simple variance estimator are valid. Of particular concern is the validity of this approach for small sample sizes, say n = 5.

ROBUSTNESS

Both estimators described above are known to have optimal properties when used with data derived from their respective distributions. In addition, the performance of each estimator when applied to other distribution functions is of interest, i.e., how robust the estimator may be.

Neither the gamma nor lognormal distribution can be mixed with another gamma or lognormal distribution and the result still be gamma or lognormally distributed. Formally, let $f_1(x; \theta_2)$ and $f_2(x; \theta_2)$ be either gamma or lognormal probability density functions with parameter vectors θ_1 and θ_2, respectively. Then assume we sample from a population with probability p that the variate is distributed as $f_1(x; \theta_1)$. The resulting variate is distributed as

$$pf_1(x; \theta_1) + (1-p) f_2(x; \theta_2) \quad .$$

The concept of mixing two distributions can be extended farther. Suppose that the $EX = \mu_x$ of f(x) is actually drawn from a second density, $g(\mu_x)$. Then the distribution of x is

$$f_{x|\mu_x}(x|\mu_x) = \frac{f_x(x,\mu_x)}{g(\mu_x)}$$

or $$f_x(x,\mu_x) = f_{x|\mu_x}(x|\mu_x)\, g(\mu_x) \quad .$$

$f_x(x, \mu_x)$ is a family of distributions indexed by the parameter μ_x (see Mood *et al.*, 1974:122-124).

This result can be applied to transuranic research by conceptualizing the distribution of radioactivity in a fallout pattern. Suppose we stratify the fallout area into n strata, each with mean concentration EX_i, i=1, 2, ..., n. If a random sample of 1-m^2 quadrats are taken from strata i, the expected concentration will be EX_i. However, quadrats closer to ground zero would be expected to have slightly larger concentrations on the average than quadrats farther away from ground zero. However, this process is stochastic so one method of expressing this randomness is to assume the expected value of a quadrat is actually drawn from some distribution, $g(\mu_x)$.

To simulate this process, $g(\mu_x)$ was assumed to be a uniform distribution with density function

$$g(\mu_x) = \frac{1}{b-a}\, d\mu_x$$

Thus, the expected value of an observation was first drawn from a uniform distribution, and then a variate generated from a gamma or lognormal distribution with this expected value. The expected value of the resulting distribution must be evaluated to show that indeed the expected value is (a + b)/2:

$$EX = E[E(X|\mu_x)]$$

$$= E(\mu_x)$$

$$= (a + b)/2$$

Comparisons of the lognormal density function and the compound uniform-lognormal density function are made in Fig. 2. Comparisons of the gamma density function and the compound uniform-gamma density function are made in Fig. 3.

MONTE CARLO SIMULATIONS

Random normal deviates were generated by the method suggested by Bell (1968) and then transformed to a lognormal deviate by $x = \exp(y)$. Random gamma deviates with nonintegral shape parameter were generated with the method presented by Fishman (1973). Briefly, the method involves summing k (= greatest integer of α) exponential variates, $\mathcal{E}(1)$, adding to this sum a product of a beta variate distributed as $\beta e(\alpha - k, 1 - \alpha + k)$ and an exponential $\mathcal{E}(1)$, and multiplying the total by the parameter β.

Samples of size n = 5, 10, 20, 30, 50, and 100 were drawn from each of the lognormal and gamma distributions. All possible combinations of EX = 1, 5, 10, 50, and 100 and coefficient of variation of c = 0.25, 0.5, 0.75, 1.0, 1.25, 1.5, and 2.0 were used for both distributions. These combinations give a total of 210 cases per distribution. Each case was replicated 1,000 times to estimate the bias and achieved coverage (proportion of replicates in which the constructed 95% confidence interval contained the true parameter value) for the two estimators discussed above. In addition, the average length of the confidence interval for E(x) was calculated for each estimator.

Parameters were calculated from EX and c for the lognormal distribution as:

$$\sigma_y^2 = \ln (c^2+1)$$

$$\mu_y = 1/2 \ln [(EX)^2/(c^2+1)] \quad .$$

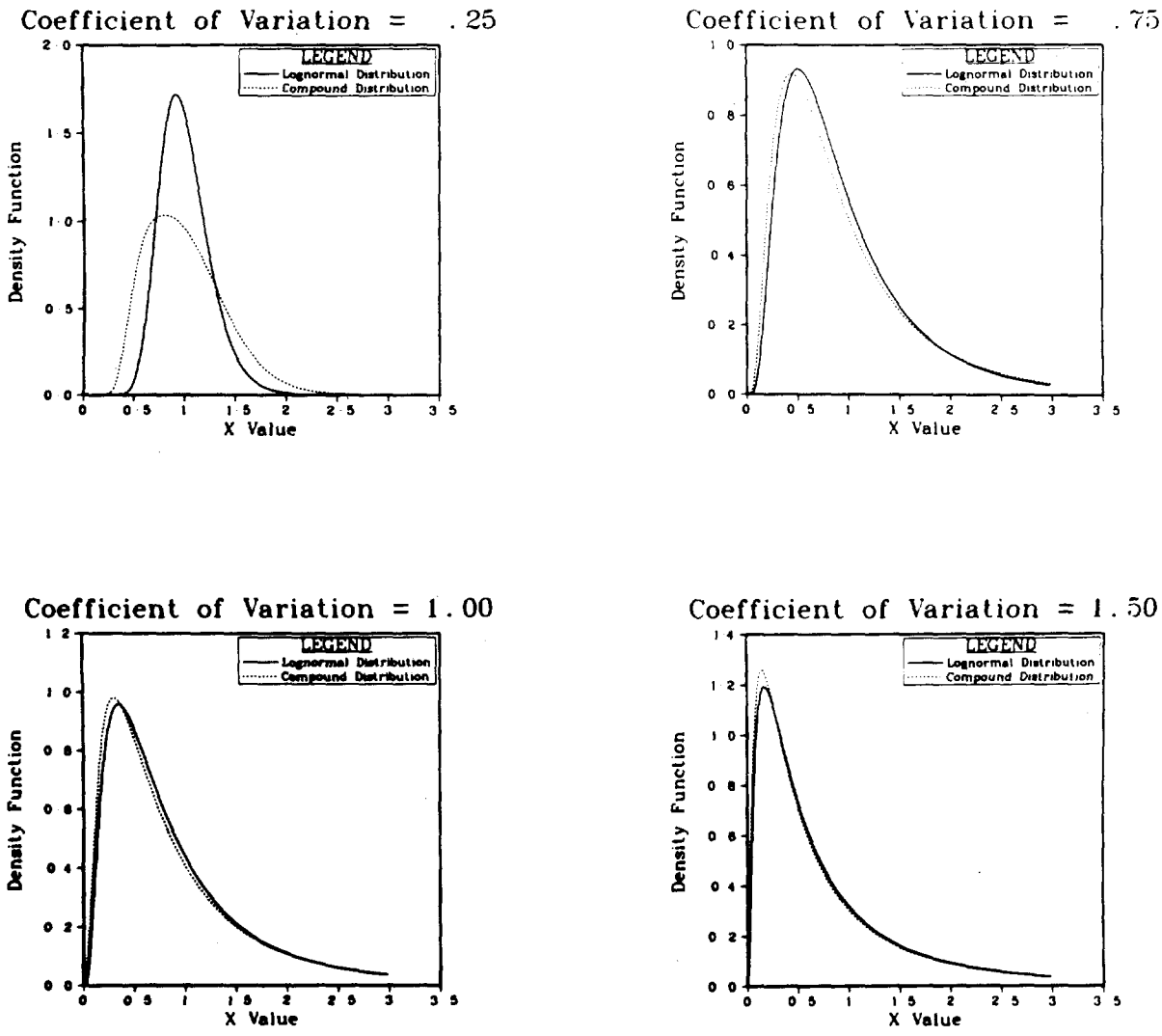

Fig. 2. Comparison of lognormal and compound uniform-lognormal probability density functions with expected value of unity and four values of the coefficient of variation.

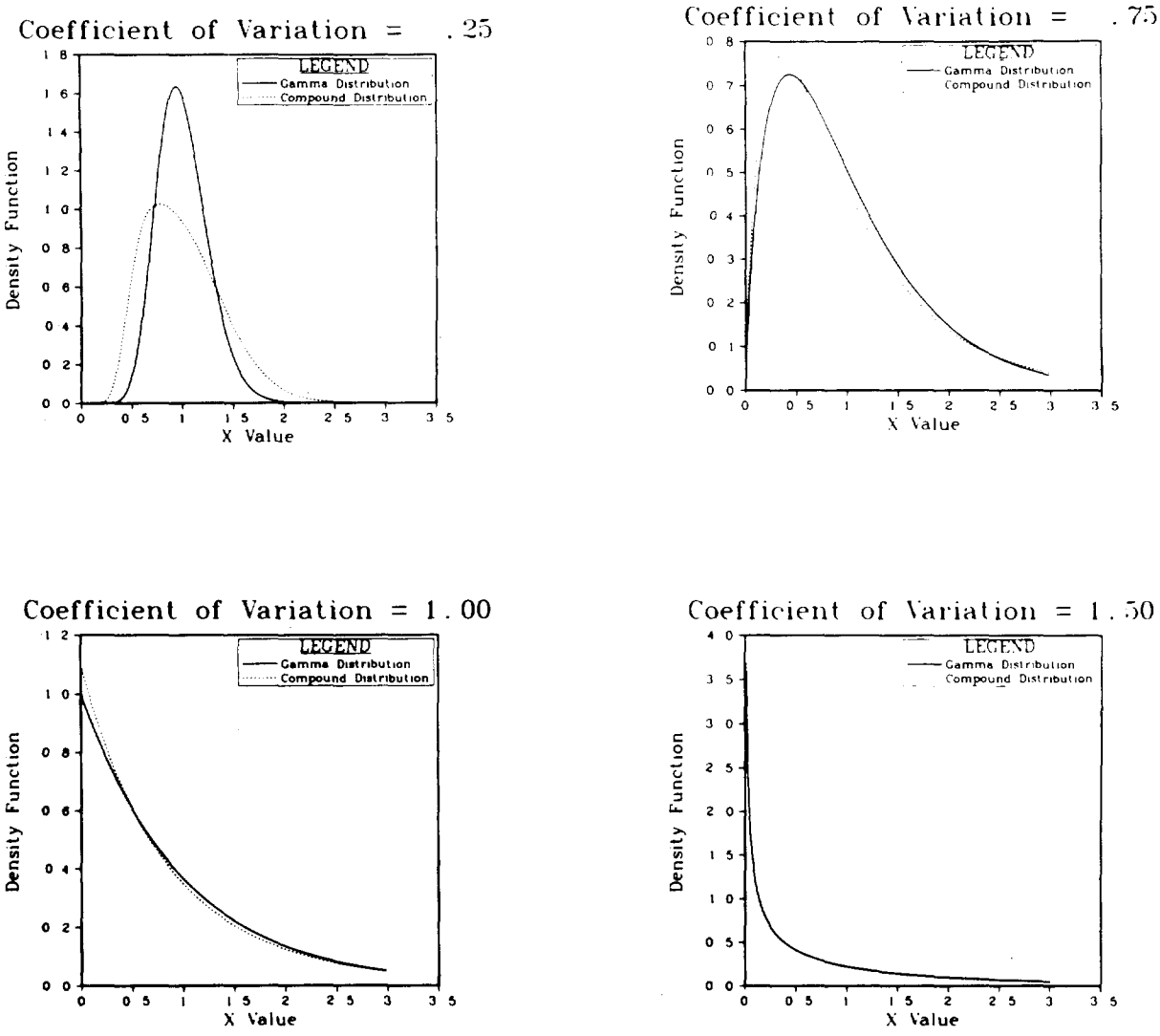

Fig. 3. Comparison of gamma and compound uniform-gamma probability density functions with expected value of unity and four values of the coefficient of variation.

Parameters were calculated from EX and c for the gamma distribution as:

$$\alpha = 1/c^2$$

$$\beta = EX\ c^2$$

In simulations where EX was selected from a uniform distribution, a and b are defined to be ±50% of the desired expected value of the distribution. For example, suppose EX is to be 10.0. Then a = (1-0.5)10 and b = (1+0.5)10, or EX is selected from the interval (5, 15). The parameter values for α, β, μ_y, and σ_y^2 were then calculated with the formulas given above to generate one realization of x.

The infinite series, $g_n(t)$, necessary to calculate $\hat{E}(x)$ assuming lognormality was evaluated to a point where the ratio of an additional term to the summation was less than 1E-7. Values of the t-statistic were obtained from tabled values.

RESULTS AND DISCUSSION

In general, the expected value of the distributions had no effect on the results. Rather, the coefficient of variation tended to explain the observed phenomena. Hence in the following sections, the statements made will apply to the range of expected values simulated. A complete listing of the simulation results is given in White (in preparation).

Gamma Estimator With Gamma Distributed Data

The arithmetic mean is an unbiased estimator for EX, and so the simulations showed. Of course, individual point estimates may vary widely. Hence, the main purpose of simulating this estimator was to check the achieved coverage against the predicted value. A gradual decline in achieved coverage was noted with an increase in the coefficient of variation (Fig. 4). However, for all cases simulated, the achieved coverage is greater than 70%. A slight decline in achieved coverage is noted also for decreasing sample sizes. This trend is more apparent for c = 2 than any other case.

Lognormal Estimator for Lognormally Distributed Data

Because this estimator is MVUE for lognormally distributed data, the chief purpose for the simulation was to check the coverage of the confidence interval. The achieved coverage is always close to the predicted 95% for n = 100. However, the achieved coverage declines with decreasing

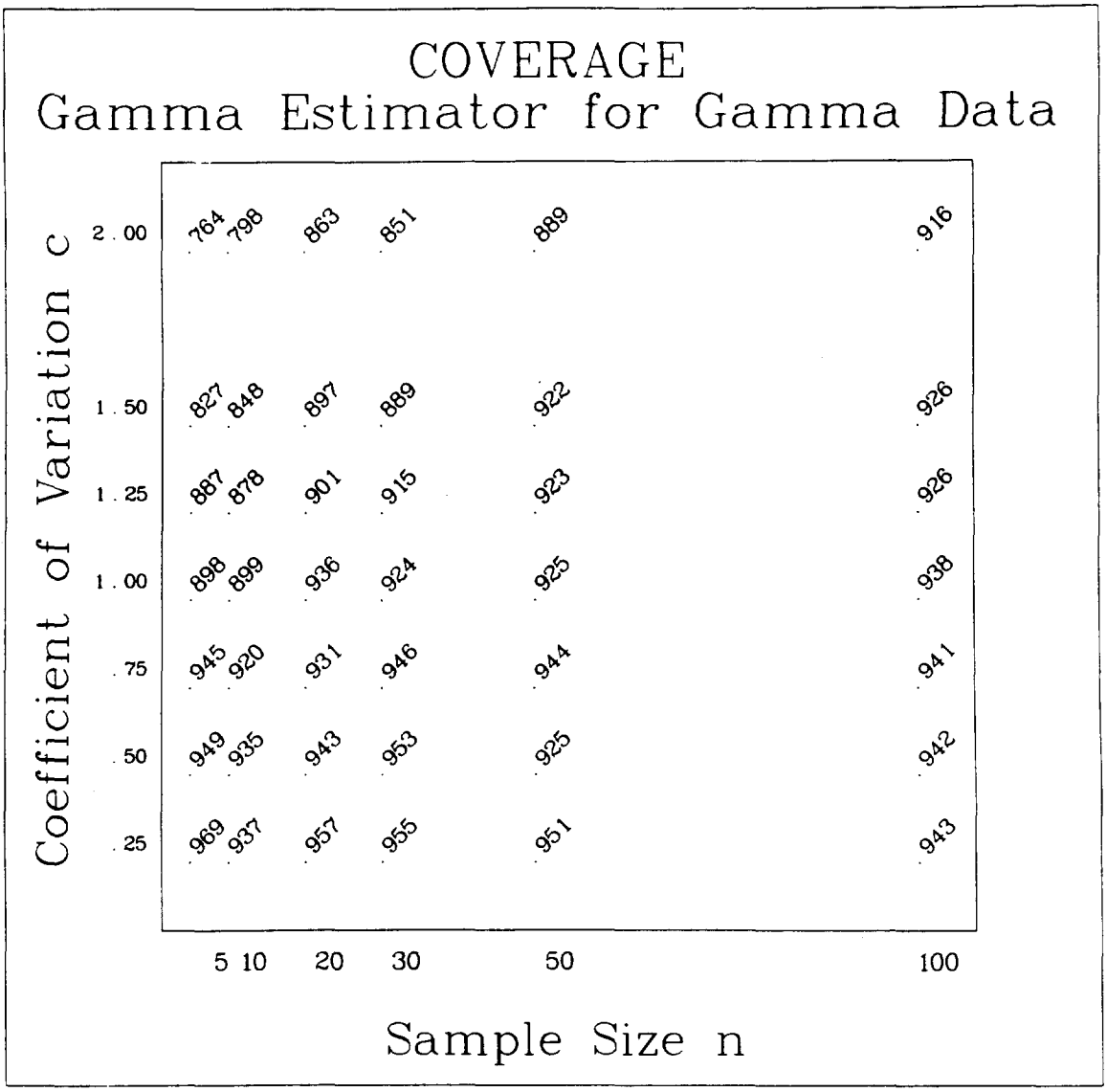

Fig. 4. Monte Carlo simulation results on confidence interval coverage of the gamma estimator (arithmetic mean) with gamma distributed data, EX=1. Values at the intersections of rows and columns are the proportion of 1000 replications where the computed confidence interval included the true expected value.

sample sizes (Fig. 5). The minimum achieved coverage is greater than 80% in all cases. These results are consistent with the findings of Land (1972).

Lognormal Estimator for Gamma Distributed Data

A major finding is that the bias of the lognormal estimator becomes large for gamma distributed data as α becomes small or c becomes large. In particular, a relative bias (100[Ave(E(x)) - EX]/EX) of about 25% is present for $\alpha = 1$ (Fig. 6). The case $\alpha = 1$ corresponds to the exponential distribution. The relative bias of the lognormal estimator becomes much worse for $\alpha < 1$. This result would be expected because the shapes of the two distributions differ greatly for $\alpha \leq 1$. However, even for $c = 0.75$ ($\alpha = 1.78$), the relative bias of the lognormal estimator for gamma distributed data is about 6%. Also, the achieved coverage of the confidence interval begins to decrease for $c = 1.0$ and $n = 100$ (Fig. 6). Coverage becomes very poor for $c > 1$.

Gamma Estimator for Lognormally Distributed Data

In contrast to the lognormal estimator for gamma distributed data, the gamma estimator for lognormal data does quite well. This estimator is unbiased, and so the simulations showed. Also, the achieved coverage of this estimator is good for small sample sizes ($n = 5$) (Fig. 7), whereas the coverage of the lognormal estimator is usually significantly less than the predicted 95% for $n = 5$. However, the average confidence interval width is usually greater for the arithmetic mean. The achieved coverage of the arithmetic mean drops as c increases, but never below 75%, even for $n = 5$ and $c = 2$. Also for $c = 0.75$, the average confidence interval length becomes about the same for the two estimators.

Robustness

The same general conclusions discussed in the preceding four sections also hold when the lognormal and gamma estimators are applied to a compound lognormal or gamma distribution with the expected value selected from a uniform distribution. The arithmetic mean still provides an unbiased estimate of EX in all cases, while the lognormal estimator provides an unbiased estimate when the variate is uniform-lognormal distributed, but not for the case when the variate is uniform-gamma distributed.

Confidence interval coverage for both estimators is always greater than 70% when there is negligible bias. Generally, the arithmetic mean had better coverage for the smaller sample sizes, while the lognormal estimator had better coverage for $n = 100$. Also, the lognormal estimator tended to have better coverage when $c \geq 1.0$. Of course, the average confidence interval width was also greater for the lognormal estimator when the coverage was larger than the gamma estimator. For the case $EX = 1.0$ and uniform-lognormal data, Fig. 8 provides the reader with some feel for the relationship between sample size c and coverage for the two estimators considered.

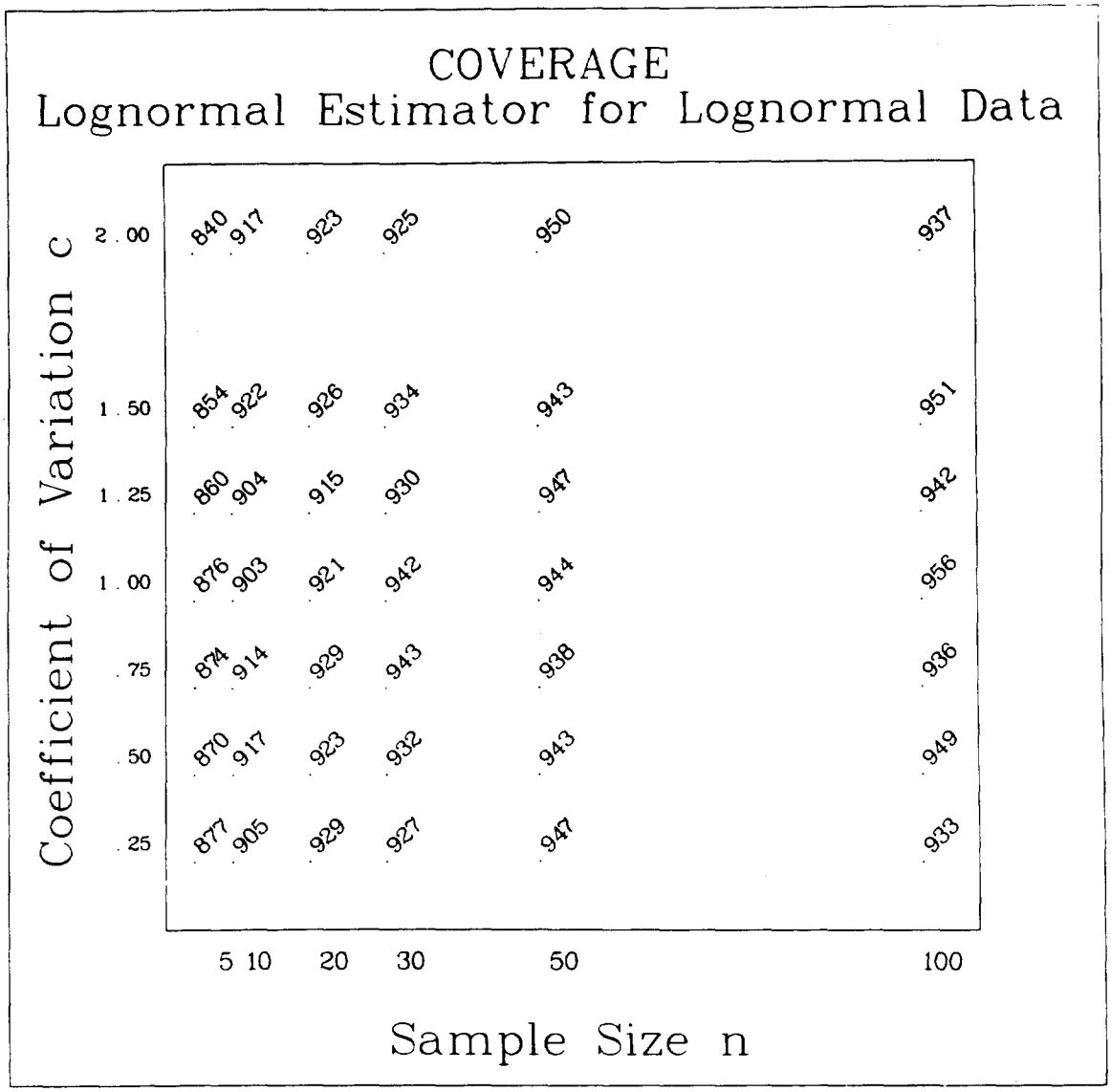

Fig. 5. Monte Carlo simulation results on confidence interval coverage of the lognormal estimator with lognormally distributed data, EX = 1. Values at the intersections of rows and columns are the proportion of 1000 replications where the computed confidence interval included the true expected value.

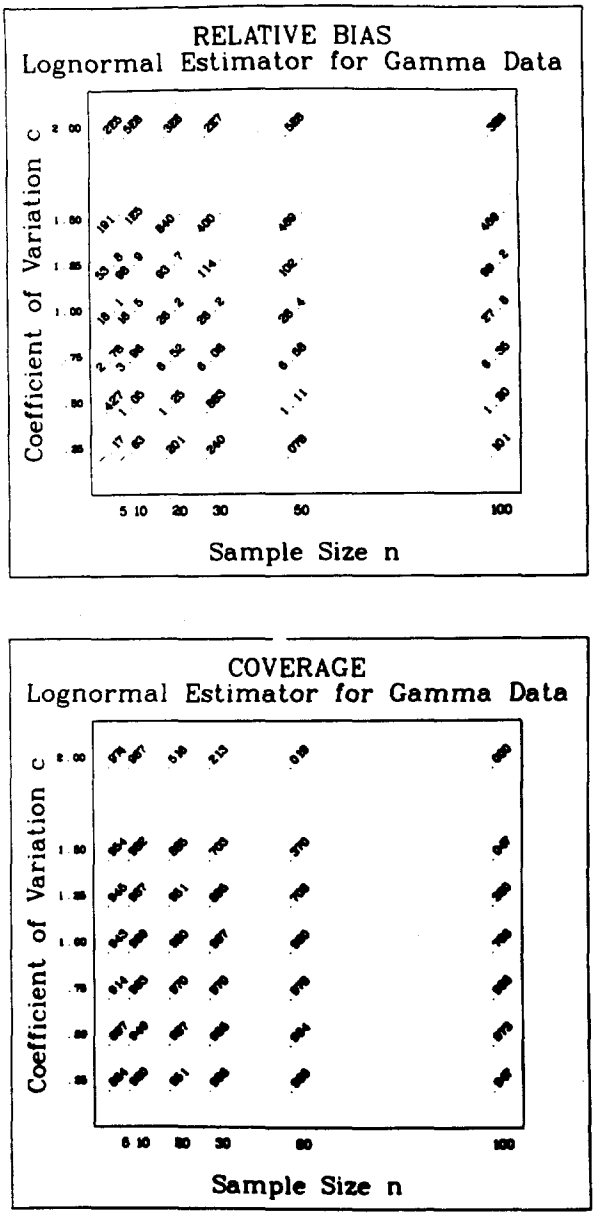

Fig. 6. Monte Carlo simulation results on bias and confidence interval coverage of the lognormal estimator with gamma distributed data, EX = 1. Values at the intersections of rows and columns are either $100[\text{Ave}(\hat{E}(x)) - EX]/EX$ (upper figure) or the proportion of 1000 replications where the computed confidence interval included the true expected value (lower figure).

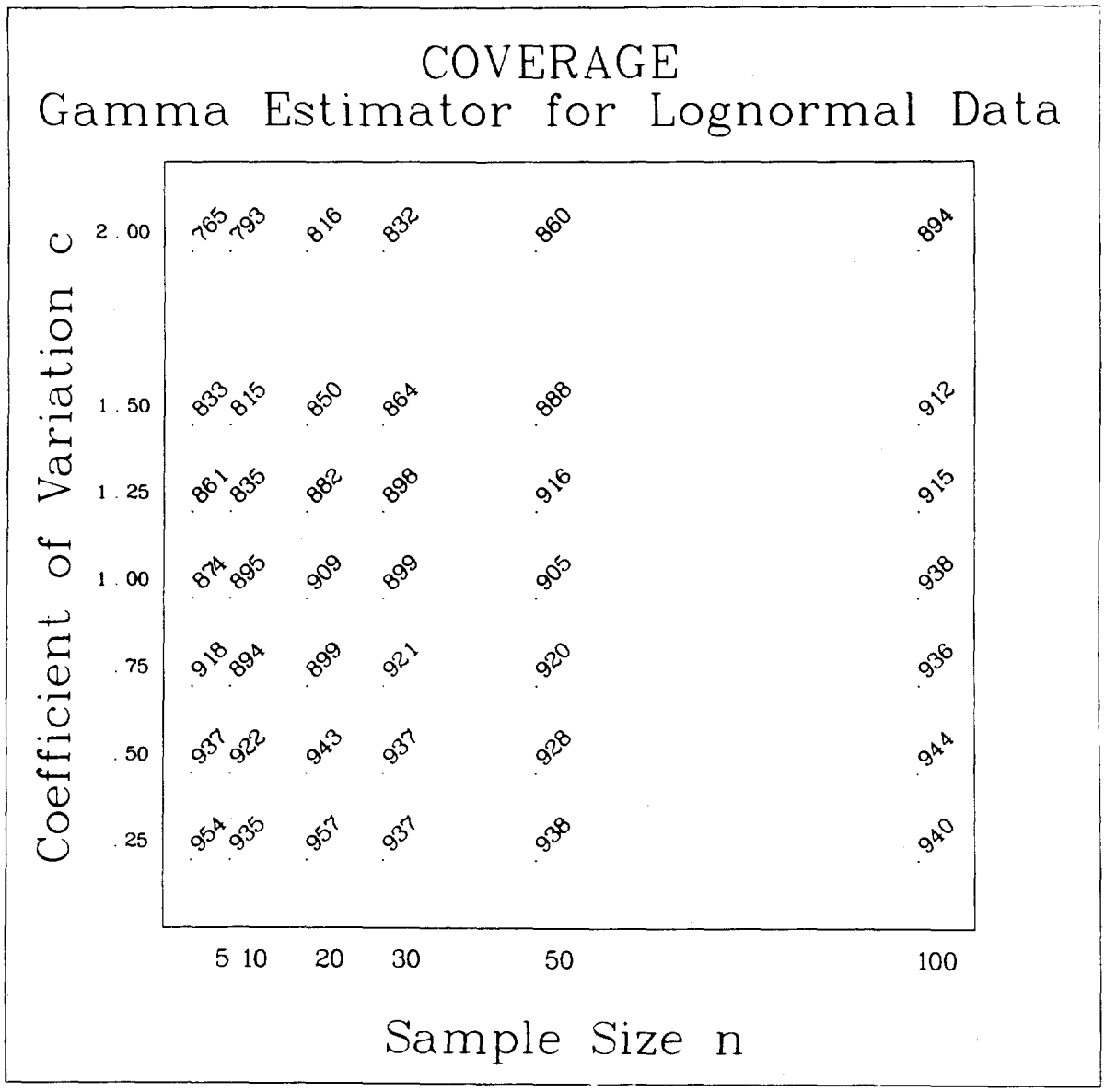

Fig. 7. Monte Carlo simulation results on confidence interval coverage of the gamma estimator (arithmetic mean) with lognormally distributed data, EX = 1. Values at the intersections of rows and columns are the proportion of 1000 replicates where the computed confidence interval included the true expected value.

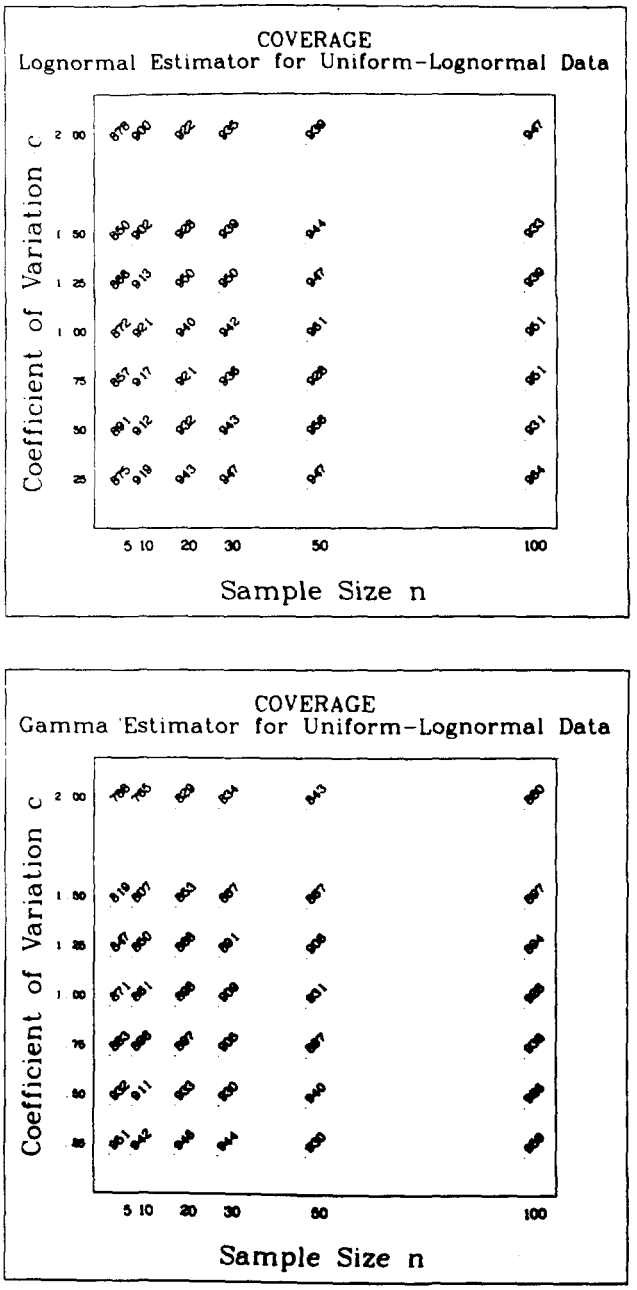

Fig. 8. Monte Carlo simulation results on confidence interval coverage of the two estimators with the uniform-lognormal compound distributions, EX = 1. Values at the intersections of rows and columns are the proportion of 1000 replications where the computed confidence interval included the true expected value.

CONCLUSIONS AND RECOMMENDATIONS

For small values of c ($c < 1$), the differences between the two estimators is relatively small. Generally, the confidence interval on the arithmetic mean provides better coverage at the expense of a wider confidence interval. For larger values of c ($1 \leq c \leq 2$), the lognormal estimator becomes very biased for gamma distributed data, and coverage tends to decline with increasing c. If no theoretical reasons are available for selecting one of the distributions simulated, then the arithmetic mean is to be preferred because it is unbiased for either of the distributions and tends to have reasonable coverage.

ACKNOWLEDGMENTS

I thank R. O. Gilbert, Battelle Pacific Northwest Laboratories, and R. J. Beckman, Los Alamos Scientific Laboratory, for reviewing drafts of this manuscript. Funding for this work was provided under Contract No. W-7405-ENG.36 between the Department of Energy and Los Alamos Scientific Laboratory.

REFERENCES

1. Aitchison, J., and J. A. C. Brown. 1976. *The Lognormal Distribution.* Cambridge Univ. Press, Cambridge.

2. Bell, J. R. 1968. "Algorithm 334 Normal Random Deviates [G5]." *Communications of the ACM* 11:498.

3. Choi, S. C., and R. Wette. 1969. "Maximum Likelihood Estimation of the Parameters of the Gamma Distribution and Their Bias." *Technometrics* 11:683-690.

4. Eberhardt, L. L., and R. O. Gilbert. 1973. "Gamma and Lognormal Distributions as Models in Studying Food-Chain Kinetics." Battelle Pacific Northwest Laboratories. BNWL-1747.

5. Eberhardt, L. L., and R. O. Gilbert. 1975. "Statistics and Sampling in Transuranic Studies." *In: Transuranic Elements in the Environment.* W. C. Hanson, Ed. U.S. Dept. of Energy. (In Preparation.)

6. Ellett, W. H., and G. L. Brownell. 1964. "The Time Analysis and Frequency Distributions of Cesium-137 Fall-Out in Muscle Samples." *In: Assessment of Radioactivity in Man.* International Atomic Energy Agency, Vienna. Vol. II. pp. 155-166.

7. Finney, D. J. 1941. "On the Distribution of a Variate Whose Logarithm is Normally Distributed." *J. Royal Statistical Society Supplement* 7:144-161.

8. Fishman, G. S. 1973. *Concepts and Methods in Discrete Event Digital Simulation.* Wiley, N.Y.

9. Forsythe, D. J., T. J. Peterle, and G. C. White. 1975. "A Preliminary Model of DDT Kinetics in an Old-Field Ecosystem." *In: Environmental Quality and Safety.* Georg Thieme, Stuttgart. Supplement Vol. III. pp. 754-759.

10. Giesy, J. P., Jr., and J. G. Weiner. 1977. "Frequency Distributions of Trace Metal Concentrations in Five Freshwater Fishes." *Trans. Am. Fish Soc.* 106:393-403.

11. Land, C. E. 1972. "An Evaluation of Approximate Confidence Interval Estimation Methods for Lognormal Means." *Technometrics* 14:145-158.

12. Link, R. F., and G. S. Koch, Jr. 1975. "Some Consequences of Applying Lognormal Theory to Pseudolognormal Distributions." *Mathematical Geology* 7:117-128.

13. Mood, A. M., F. A. Graybill, and D. C. Boes. 1974. *Introduction to the Theory of Statistics.* 3rd Ed. McGraw-Hill, N.Y.

14. Pinder, J. E., III, and M. H. Smith. 1975. "Frequency Distributions of Radiocesium Concentrations in Soil and Biota." *In: Mineral Cycling in Southeastern Ecosystems.* F. G. Howell, J. B. Gentry, and M. H. Smith (Eds.). ERDA Symposium Series. CONF-740513. pp. 107-125.

15. White, G. C. (In Preparation.) "Estimation of Expected Value and Coefficient of Variation for Lognormal and Gamma Distributions."

VARIABLE ^{241}Am CONCENTRATION IN SOIL UPTAKE AND C.R. IN BARLEY PLANTS

A. Wallace, R. T. Mueller, and E. M. Romney

Laboratory of Nuclear Medicine and Radiation Biology
University of California, Los Angeles

ABSTRACT

Barley plants (*Hordeum vulgare* L. Atlas 57) were seeded into small pots of Yolo loam soil containing different concentrations of ^{241}Am (4,000, 10,000, 20,000, and 40,000 dpm/g soil). Four successive harvests were made with the first three harvests each of one-third of the original plants, but of different ages. One set of all concentrations was without and one set with the chelator DTPA. There were four replicates. Plant uptake of ^{241}Am was related to concentration, but the C.R. decreased slightly without DTPA (about 3x) as the soil concentration was increased tenfold. With DTPA, uptake was proportional to concentration (that of concentration of DTPA supplied was constant). The effect of DTPA relative to that of no DTPA increased with increasing concentration of ^{241}Am in soil. The C.R. under these conditions was reasonably constant, but severalfold higher than without DTPA. The last harvest contained less ^{241}Am than did the first, both with and without DTPA. The value of the coefficient "Y" in the equation

$$(C_1/C_2)^Y = \text{uptake ratio}$$

was about 50% lower without DTPA compared to with DTPA. With DTPA the value of "Y" was near 1, which implies that ^{241}Am in plants was directly proportional to that in soil at all concentrations.

INTRODUCTION

The C.R. (concentration ratio) defined as the activity per weight of plant part (or any biological organism) divided by activity per weight or unit of substrate (ERDA, 1975) is the most frequently used means of

expressing the uptake of transuranium nuclides from soil. Wide ranges in C.R. values are observed (ERDA, 1975; Schulz, 1977). A series of studies has been undertaken to ascertain for a given plant species and a given soil if the C.R. is constant. It is well known that C.R. will vary with addition of chelating agents (Adriano *et al.*, 1971; Wallace, 1972a,b). The major purpose of this study was to determine how constant the C.R. would be with variation in the ^{241}Am concentration uniformly mixed in soil. One set was made without chelate and one with the chelator DTPA (diethylenetriaminepentaacetate).

MATERIALS AND METHODS

The experiment was set up with Yolo loam soil (Typic Xerorthents, fine, silty, mixed, thermic) with activity of ^{241}Am at 4,000, 10,000, 20,000, and 40,000 dpm/g soil. The activity was blended in for 1 hr with a batch mixer. There were four replications of 1,000 g each with and without DTPA, applied in solution at the rate of 100 µg/g soil. Nitrogen at the rate of 100 µg N per g soil as NH_4NO_3 was added to each pot. Soil moisture was maintained near -1/3 bar. Bush bean plants (*Phaseolus vulgaris* L. cv. Improved Tendergreen) were grown for 22 days, after which they were harvested.

After standing for two months, these pots of soil were seeded to barley (*Hordeum vulgare* L. Atlas 57). Nitrogen was then applied as above.

More DTPA was applied to the DTPA treatments (150 µg/g) one week after plants (20/pot) were seeded. One-third were harvested after another week. In 11 more days, another 1/3 were harvested and the other 1/3 after 13 more days. Then a second crop for all was harvested after 28 additional days. These were designated as harvests 1, 2, 3, and 4. All were dried, weighed, and counted for ^{241}Am by gamma well counting. The counting time was usually for 1 hr. Only the data for barley are reported in this paper. In addition to C.R. values, "Y" uptake values were computed from the formula

$$(C_1/C_2)^Y = \text{uptake ratio (Wallace, 1977).}$$

RESULTS AND DISCUSSION

The activity of ^{241}Am in plants was related to concentration in the soil (Table 1). The DTPA increased uptake manyfold and the effect was related to both concentration and time. The ratio of ^{241}Am for with DTPA ÷ without DTPA increased markedly with concentration except at the last

Table 1. Concentration of ^{241}Am in Barley Grown in Yolo Loam Soil With Different Concentrations of ^{241}Am Blended With Soil

^{241}Am Activity Level in Soil	Concentration of ^{241}Am in Barley, dpm/g Dry Weight			
	Harvest 1	Harvest 2	Harvest 3	Harvest 4
dpm/g	Without DTPA			
4,000	104	24	24	12
10,000	184	48	36	26
20,000	175	65	52	38
40,000	280	100	64	64
LSD 0.05	103	28	NS	39
	With DTPA			
4,000	638	1,483	1,370	330
10,000	1,724	3,654	2,430	764
20,000	3,043	8,600	4,770	1,310
40,000	9,700	18,840	10,860	3,194
LSD 0.05	2,008	2,159	698	838
	With DTPA/Without DTPA (ratio)			
4,000	6.1	61.8	57.1	27.5
10,000	9.4	76.1	67.5	29.4
20,000	17.4	132.3	91.7	34.5
40,000	34.6	188.4	169.7	49.9

harvest where the effect of DTPA was diminished. This was the case for both ratio and uptake. The level of chelator used was greatly in excess of that of ^{241}Am, which could account for the differences in ratio with increasing ^{241}Am concentration in soil. The same situation would occur in crop fields if DTPA were applied--its level would be in excess of that of any radionuclide.

The diminished effect of the chelator with time implied metabolism of the agent in the soil, which probably occurs, but slowly (Hale *et al.*, 1962).

The C.R. values without DTPA decreased slightly with increasing concentration (about threefold) and slightly (about fivefold) with harvest number (Table 2). Whether or not differences of this magnitude would have consequences of importance in food chain relationships is not clear at the moment. The range in ^{241}Am applied in soil was one order of magnitude. The uptake difference was less than one magnitude. The need exists for studies covering greater orders of magnitude and for greater time periods.

The C.R. did not vary much for concentration in the presence of DTPA, but this may reflect the fact that the DTPA was at the same level for all concentrations of ^{241}Am. The higher C.R. for harvest 2 than harvest 1 reflected the addition of the DTPA several days after seeding. Plants for harvest 1 were partially grown before DTPA was applied. The large decrease in C.R. for harvest 4 compared with harvest 3 reflects either metabolism of the chelator or reactions resulting in a lower degree of chelation of the ^{241}Am.

The "Y" exponent values which compare uptake at different concentrations gave different populations for with and without DTPA (Table 3). An F value which statistically compares the two groups was 21.6 and highly significant. The mean "Y" value for without DTPA was 0.53 ± 0.07 SEM and 1.05 ± 0.08 SEM with DTPA. A value of 1.0 represents uptake directly proportional to applied concentration and may indicate nonmetabolic or passive uptake. The value of 0.53 is too low to be ln2 or 0.693 which is the decay constant which enters into many reaction rates.

ACKNOWLEDGMENTS

This work was supported by Contract 60-76-103, Fin No. B2017-6 between the Nuclear Regulatory Commission and the University of California.

Table 2. Concentration Ratio (C.R.) of ^{241}Am in Barley Grown in Yolo Loam Soil With Different Concentrations of ^{241}Am Blended With Soil

^{241}Am Activity Level in Soil	Harvest 1	Harvest 2	Harvest 3	Harvest 4
dpm/g	Without DTPA			
4,000	0.023	0.006	0.006	0.0030
10,000	0.018	0.005	0.004	0.0026
20,000	0.009	0.003	0.003	0.0019
40,000	0.007	0.003	0.002	0.0016
LSD 0.05	0.007	0.002	0.002	0.0012
	With DTPA			
4,000	0.160	0.371	0.347	0.083
10,000	0.171	0.366	0.243	0.076
20,000	0.152	0.430	0.239	0.065
40,000	0.242	0.471	0.272	0.080
LSD 0.05	NS	NS	0.048	NS

Table 3. "Y" Values of ^{241}Am in Barley Grown in Yolo Loam Soil With Different Concentrations of ^{241}Am Blended With Soil

^{241}Am Activity Levels in Soil Compared	Harvest 1	Harvest 2	Harvest 3	Harvest 4
dpm/g	Without DTPA			
$\frac{10,000}{4,000}$	0.823	0.765	0.443	0.752
$\frac{20,000}{10,000}$	0.000	0.415	0.523	0.547
$\frac{40,000}{20,000}$	0.670	0.314	0.300	0.844
LSD 0.05	NS	NS	NS	NS
Mean	0.490	0.498	0.429	9.714
	With DTPA			
$\frac{10,000}{4,000}$	1.08	0.98	0.62	0.92
$\frac{20,000}{10,000}$	0.82	1.23	0.98	0.78
$\frac{40,000}{20,000}$	1.67	1.13	1.19	1.29
LSD 0.05	0.47	NS	0.30	0.43
Mean	1.19	1.11	0.93	1.00

REFERENCES

1. Adriano, D. C., M. S. Delaney, G. D. Hoyt, and D. Paine. 1971. "Availability to Plants and Soil Extraction of Americium-241 as Influenced by Chelating Agent, Lime, and Soil Type." *J. Environ. Exp. Bot.* 17:69-77.

2. ERDA. 1975. "Workshop on Environmental Research for Transuranic Elements." *Proc. Workshop Nov. 12-14, 1975*, Battelle Seattle Research Center, Seattle, WA. ERDA-76/134.

3. Hale, V. Q., A. Wallace, and N. Hemaidan. 1962. "Are Chelating Agents Metabolized in Soils and Plants?" *In: A Decade of Synthetic Chelating Agents in Inorganic Plant Nutrition*. A. Wallace (Ed. and Publisher), Los Angeles, CA. pp. 64-69.

4. Schulz, R. K. 1977. "Root Uptake of Transuranic Elements." *In: Transuranics in Natural Environments*. M. G. White and P. B. Dunaway (Eds.). USERDA Report, NVO-178. pp. 321-330.

5. Wallace, A. 1972a. "Increased Uptake of Americium-241 by Plants Caused by Chelating Agent DTPA." *Health Physics* 22:559-562.

6. Wallace, A. 1972b. "Effect of Soil pH and Chelating Agent (DTPA) on Uptake by and Distribution of Am-241 in Plant Parts of Bush Beans." *Rad. Bot.* 12:433-435.

7. Wallace, A. 1977. "Effect of Concentration on Uptake of Some Trace Metals by Plants." *Comm. Soil Sci. Plant Anal.* 8:689-691.

THE EFFECT OF FASTING ON THE TRANSIT TIME OF ^{144}CE IN THE MOUSE GUT

J. F. Weiss and H. E. Walburg

Comparative Animal Research Laboratory
Oak Ridge, Tennessee

ABSTRACT

Our work with G.I. absorption of actinide elements indicates greater absorption by fasted animals than by animals on regular diets (Weiss and Walburg, Undated). Residence time of a metallic compound in the gut may be an important factor influencing G.I. absorption. Cerium-144 (III) chloride was administered by gavage to fasted mice and to mice on regular feed. The G.I. tract was excised, cut into sections, and the activity of each section determined as a function of time after dosing. Our results indicate rapid transit of $^{144}CeCl_3$ along the empty mouse gut. One hour after dosing, about half the Ce is in the cecal contents; about 40% remains in stomach contents. Twelve hours after dosing, only about 2% remains in the cecum; by 16 hours, almost the entire dose has been cleared from the intestine. Transit times in mice with stomach and intestines containing food were 12 hours longer than in fasted mice. These results lead to the conclusion that factors other than G.I. residence time determine G.I. absorption of actinides in mice.

INTRODUCTION

G.I. uptake is influenced by several factors: gut transit time, diet, fasting, health and age of the animal, chemical form and chemistry of the dose element (Durbin, 1973), and variability among individuals of the same species. Many of these factors can combine to yield high variability in absorption data. Large absorption differences between animal species due to inherent biochemical and physiological characteristics may be obscured by this variability. In view of the need to correlate abstruse data from many laboratories and to clarify some of the biological and chemical factors influencing G.I. absorption, knowledge of gut transit time is necessary.

MATERIALS AND METHODS

Cerium-144 (III) chloride was obtained from the Oak Ridge National Laboratory in a 1 M HCl solution. The isotope as received contained no other γ-emitting impurities. Dilutions were made with distilled water to obtain a dose solution which was 0.2 M in HCl and contained 0.5 μCi/ml $^{144}CeCl_3$.

Adult male BALB/c mice 5 to 6 months old were maintained on a diet of Purina laboratory chow with water *ad libitum* throughout the course of the experiment.

Three groups of mice were used, one for each of the three fasting-feeding regimens studies. In each group, three mice were killed at 1, 2, 4, 8, 12, 16, or 24 hours after dosing. The experiment thus involved a total of 63 mice with 21 in each group. These were: I, fasted for 24 hours, dosed, fasted thereafter; II, fasted for 24 hours, dosed, fasted for 8 hours, then given feed *ad libitum*; III, fasted for 24 hours, given feed *ad libitum* for 4 hours before dosing, dosed, fasted again. The mice were dosed by gavage with 0.1 μCi of $^{144}CeCl_3$ (0.5 μCi/ml) in 0.2 ml of 0.2 M HCl solution. After dosing was completed, the mice were returned to cages which were fitted with wire mesh bottoms to inhibit ingestion of contaminated excreta. The mice were asphyxiated with CO_2, the digestive tracts excised and sectioned (Figure 1), and the sections placed into gamma counting tubes for ^{144}Ce analysis. Figures 2 and 3 show the averages for three mice expressed as percent of the administered dose. The administered dose standards and the intestinal sections were counted in equivalent volumes of water under integral counting conditions in an automatic gamma counter. The ^{144}Ce activities of the gut sections were counted in tubes that were filled to a 3-ml total volume with water to minimize the effect of changes in sample volume on the count rate of the instrument.

RESULTS

Results of the experiment are shown in Figures 2 and 3. The intestines of groups I and II were essentially clear of ^{144}Ce activity in all parts of the gut 12 hours after dosing. The group allowed to eat 4 hours before dosing and not thereafter had G.I. tracts containing food on dissection, and the ^{144}Ce activity pattern of this group of mice exhibited an anomalous rise at later hours. In addition, the gut transit time of group III was about 12 hours longer than that of groups I and II.

Results obtained in fasted mice with cerium are indicative of rapid transit of a soluble metal species along the empty gut with essentially

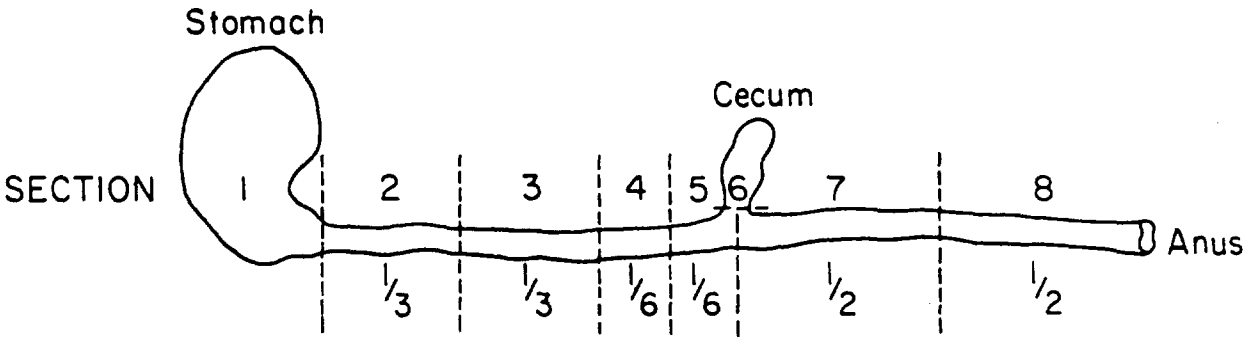

Figure 1. Schematic diagram of mouse intestine showing sections taken for analysis of ^{144}Ce content.

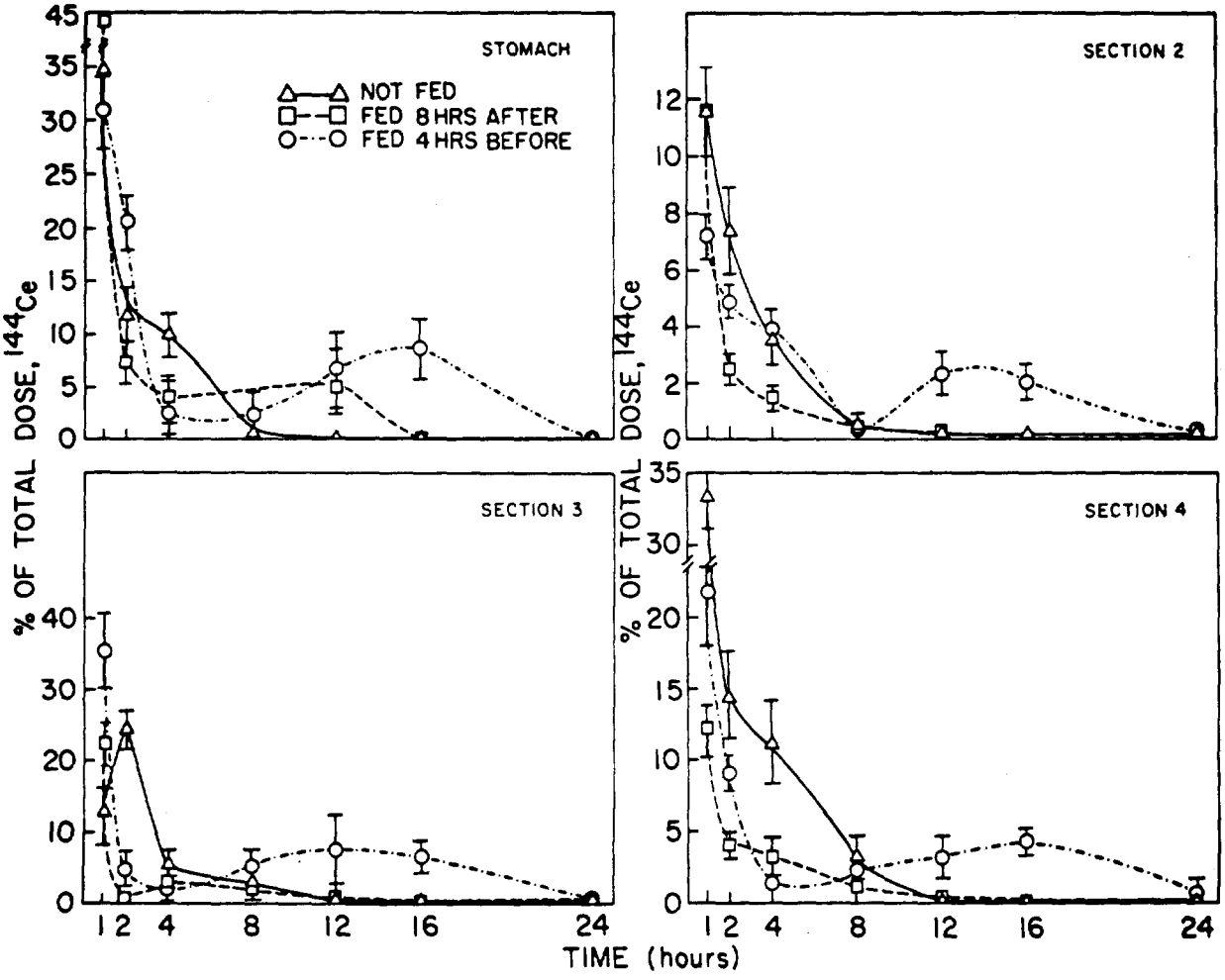

Figure 2. Percent of total ^{144}Ce activity (0.1 μCi) in the first four sections of the G.I. tract of mice on three fasting-feeding regimens as a function of time after oral dose administration. Vertical bars indicate associated standard errors.

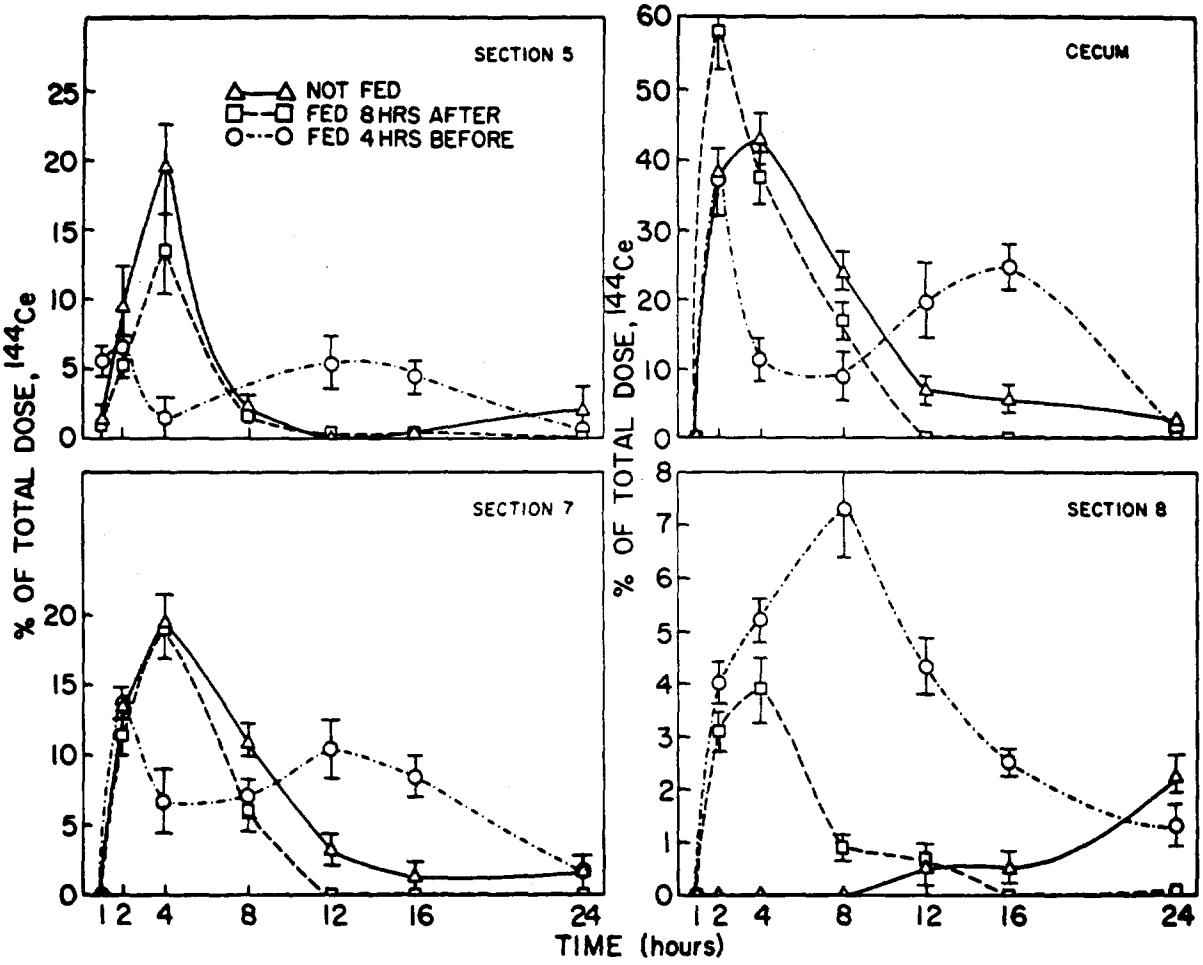

Figure 3. Percent of total ^{144}Ce activity (0.1 μCi) in the last four sections of the G.I. tract of mice on three fasting-feeding regimens as a function of time after oral dose administration. Vertical bars indicate associated standard errors.

100% clearance of radioactivity at 12 hours after dose administration. The variability observed among the data was largest in the group of mice which was allowed to eat before dosing (group III).

DISCUSSION

The results clearly indicate that the transit time of the soluble nonabsorbed marker $^{144}CeCl_3$ is much more rapid in fasted mice than in those with G.I. tracts containing food. Such a large change in transit time for an element must certainly affect its absorption. Standardization of conditions for laboratory animals with respect to fasting would help reduce the variability among data from different sources in animal experiments measuring G.I. absorption. The authors believe that the anomalous rise in measured activities in the intestines of group III at later hours is in reality visible only because of the decrease in activity immediately preceding it. This decrease we feel is due to loss of counts in the integral counting mode caused by self-absorption of the 2.99 MeV ^{144}Pr β-emission in the thicker, full gut sections as opposed to the thinner, empty gut sections of groups I and II.

Since gut transit time is a function of feeding regimen, we believe that better absorption data would be obtained using animals on regular feed. These data would then incorporate a normal gut transit time function for absorption of a substance and would be more realistic in the final analysis since adsorption or binding of the measured substances by dietary constituents is almost certainly an important factor in G.I. absorption for most heavy metallic elements.

ACKNOWLEDGMENTS

The technical assistance of Mrs. Faith Case is acknowledged. This research was supported by the Nevada Applied Ecology Group and U.S. Department of Energy Contract No. EY-76-C-05-0242 with the University of Tennessee.

REFERENCES

1. Durbin, P. W. 1973. "Metabolism and Biological Effects of the Transplutonium Elements." *In: Handbook of Experimental Pharmacology*, Vol. 36, *Uranium-Plutonium-Transuranic Elements*. H. C. Hodge, J. N. Stannard, and J. B. Hursh, Eds. New York, Springer-Verlag. pp. 739-896.

2. Weiss, J. F., and H. E. Walburg. Undated. Unpublished data.

COMPARISON OF SOIL SAMPLING TECHNIQUES AT ROCKY FLATS

D. E. Bernhardt, J. D. Bliss, and G. G. Eadie

Office of Radiation Programs
U.S. Environmental Protection Agency
Las Vegas, Nevada

ABSTRACT

In May, 1977, a cooperative plutonium soil sampling project was conducted by Rockwell International (Department of Energy contractor), Colorado Department of Health, Jefferson County Department of Health, and the U.S. Environmental Protection Agency-Office of Radiation Programs-Las Vegas. Each of the agencies collected five duplicate samples from four distinctly different pedological and morphological settings around the Rocky Flats Colorado Plant. The sampling techniques included: the Rocky Flats 0- to 5-cm depth technique (100-cm^2 area), the State of Colorado one-eighth-inch depth technique (750-cm^2 area), the Jefferson County technique (sizing of dust swept from a 4-m^2 area of the ground surface), and two EPA techniques for samples of 0- to 1-cm (450-cm^2 area) and 0- to 5-cm (500-cm^2 area) depth. A limited number of depth profile samples, down to 10 cm, were also collected by EPA.

The objectives of the project included assessing the variability and reproducibility of the techniques, comparison of the results from the various techniques, determining the applicability of the techniques to different environmental conditions, and assessing how well the techniques reflect the potential airborne hazard for resuspension of plutonium. Results of the various techniques are also to be compared to the proposed EPA guidance for transuranics in the environment (Federal Register, 42:60956, November 30, 1977), which is primarily based on activity in the surface 1 cm of soil.

This paper presents a status report of results from the EPA samples collected for this project. The emphasis is on comparing the results from 1-cm and 5-cm depth samples. The 1-cm technique samples were based on a composite of fifteen 30-cm^2 subsamples and the 5-cm technique includes a composite of five 100-cm^2 subsamples.

The preliminary results indicate that about one-third of the plutonium-239/240 activity per unit area detected in the 5-cm depth samples was accounted for in the 1-cm depth samples. A limited number of samples for the profile from 5 to 10 cm indicated about 20 percent of

the activity found in the 0- to 5-cm samples. Analysis of selected samples for cesium-137 indicated a similar vertical distribution. The cesium-137 data did not indicate the Rocky Flats oriented source distribution reflected by the plutonium-239 data.

The results (activity per unit area) for the 0- to 1-cm and 0- to 5-cm sampling techniques exhibit about the same relative uncertainty, although the trend of the data indicates that the results for the 0- to 1-cm technique are somewhat more variable than the results for the 0- to 5-cm technique. The average coefficients of variation are 42 and 30 percent, respectively.

INTRODUCTION

Investigators have applied numerous sampling techniques for plutonium in soil (reviewed by Bernhardt, 1976). The techniques are generally tailored to match the investigator's program objectives; e.g., primarily inventory or hazard assessment, which in most cases is for airborne resuspension.

The Nevada Applied Ecology Group (NAEG) techniques (Fowler *et al.*, 1976) and those described by the Nuclear Regulatory Commission Regulatory Guide 4.5 (NRC, 1974) are oriented towards inventory determination. The emphasis is to account for most of the plutonium; and a surface sample is stipulated as including the top 5 cm of soil (Bernhardt, 1976; NRC, 1974).

Since most of the plutonium is usually on the surface, the distribution of plutonium is fairly uniform at 5 cm, and small errors in the sampling depth will have a limited impact on both the mass of material sampled and total plutonium sampled. An error of plus or minus 1 cm will only affect the mass of material by about 20 percent for a 0- to 1-cm sample.

The phenomenon of resuspension has been reviewed by Oksza-Chocimowski (in press), Lem *et al.* (1977), and Anspaugh *et al.* (1975). Sampling for resuspension assessment must include the plutonium concentration in the surface layer of soil and the size distribution of the plutonium and associated soil aggregates. Particle size, which is important but difficult to realistically determine, has been studied by Bernhardt, 1976; Johnson *et al.*, 1976; Little *et al.*, 1973; Tamura, 1976, 1977. The depth involved in resuspension mechanics is not clearly known, but is dependent upon an array of soil and climatological factors and is generally believed to be within the surface 1 cm.

The proposed Environmental Protection Agency (EPA) guidance for transuranics in the environment specifies soil samples be related to the top 1 cm, and the soil fraction less than 2 mm (10-mesh sieve) in diameter

(EPA, 1977a). The technical backup for the guidance and additional consideration of the size distribution of plutonium in soil are given in EPA, 1977b.

The on-site and off-site areas of the Rocky Flats Plant contain elevated levels of plutonium from past operations (Krey and Hardy, 1970; Poet and Martell, 1974; and DOE, 1977). Several investigators and agencies have applied various soil sampling techniques in the environs of Rocky Flats. These include:

1. Krey and Hardy (1970): Collected samples for inventory determination by auger, bore, or template techniques for the 0- to 5-cm or 0- to 20-cm interval (generally a 620-cm^2 area).

2. Poet and Martell (1972): Collected samples from the top 1 cm by a spoon technique (1,000 cm^2). Also collected depth profile samples.

3. Rockwell International, contractor for the Department of Energy at Rocky Flats (1977): Collects 0- to 5-cm samples using a steel 10- by 10-cm template and scoop for removing the sample. Samples are composed of one (100 cm^2) to five aliquots.

4. Colorado Department of Health (Colorado Department of Health, 1977): Collects surface samples from top one-eighth inch (0.32 cm) using a 5- by 6-cm template and scoop designed for controlling the sampling depth. The samples are composed of 25 subsamples (750 cm^2).

5. Jefferson County Health Department (Johnson *et al.*, 1976): Collects samples by sweeping the loose material from a 2- by 2-m area. Neither the total material from the area nor the material to a fixed depth is collected. This material is then treated to disperse particle aggregates, and sized using sedimentation techniques.

Because of differences in techniques and associated results and the forthcoming proposed EPA guidance, EPA was requested to participate in a joint study with a number of the previously named investigators.

The objectives of the cooperative study were to:

1. Evaluate different soil sampling techniques to determine the best technique as related to health effects.

2. Determine the relationships between soil and air sampling techniques.

3. Determine applicability of techniques to different environmental conditions.

4. Evaluate sampling techniques as related to EPA guidelines.

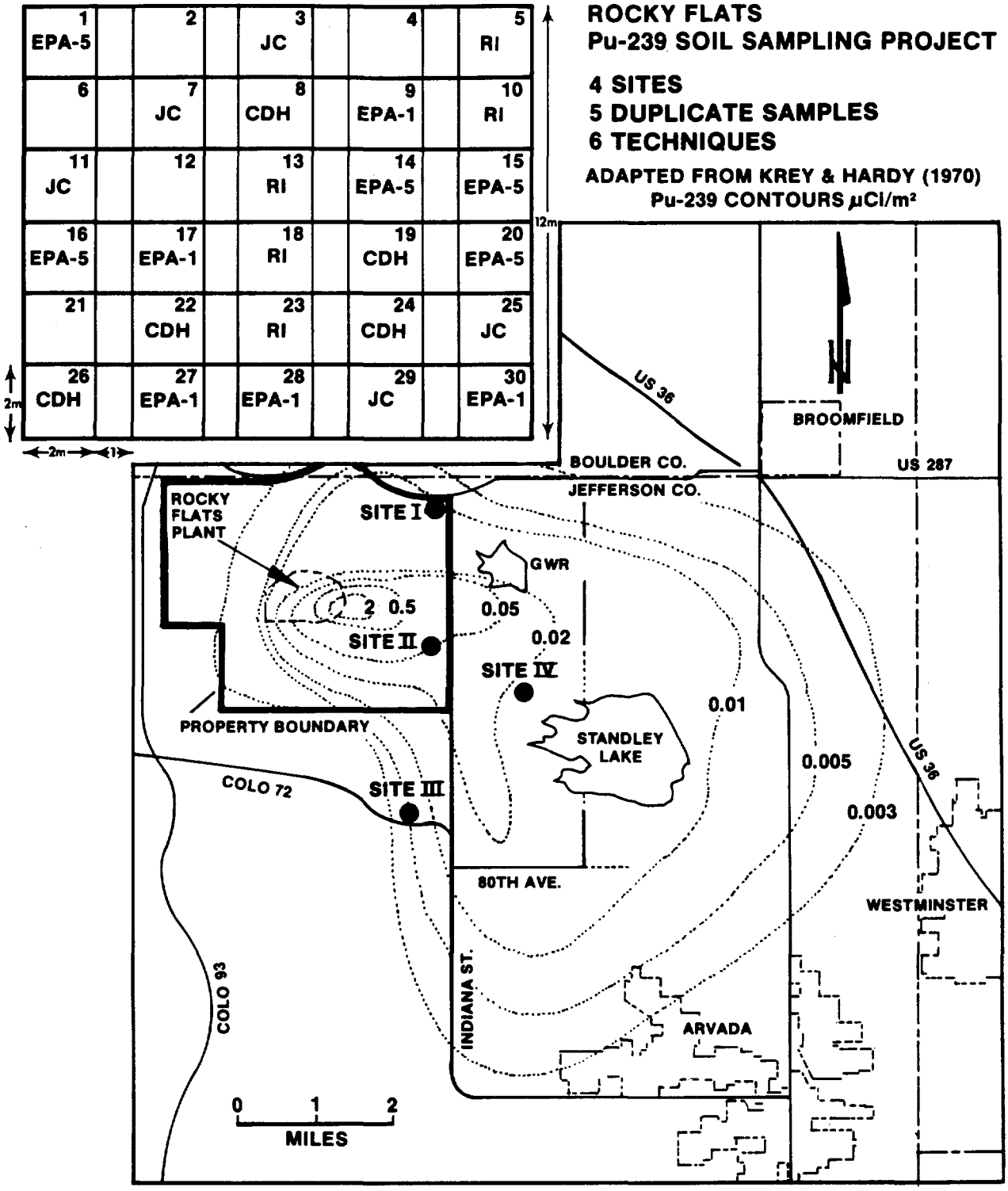
ROCKY FLATS
Pu-239 SOIL SAMPLING PROJECT
4 SITES
5 DUPLICATE SAMPLES
6 TECHNIQUES
ADAPTED FROM KREY & HARDY (1970)
Pu-239 CONTOURS μCi/m²
1 EPA-5
2
3 JC
4
5 RI
6
7 JC
8 CDH
9 EPA-1
10 RI
11 JC
12
13 RI
14 EPA-5
15 EPA-5
16 EPA-5
17 EPA-1
18 RI
19 CDH
20 EPA-5
21
22 CDH
23 RI
24 CDH
25 JC
26 CDH
27 EPA-1
28 EPA-1
29 JC
30 EPA-1
12m
2m
2m
1
US 36
BROOMFIELD
US 287
BOULDER CO.
JEFFERSON CO.
ROCKY FLATS PLANT
SITE I
GWR
2
0.5
0.05
SITE II
0.02
SITE IV
0.01
PROPERTY BOUNDARY
STANDLEY LAKE
0.005
US 36
COLO 72
SITE III
0.003
80TH AVE.
WESTMINSTER
COLO 93
INDIANA ST.
ARVADA
0
1
2
MILES

Fig. 1

Fig. 2 Sampling tool for 0- to 1-cm soil sample.

Special EPA samples included:

1. Collection of a 5- to 10-cm sample using the 10- by 10- by 5-cm-deep scoop to take a sample from the vertical wall of the hole. Since these samples were being taken only to determine the relative contamination below 5 cm for each site, five subsamples were not taken at each site.

2. Five 15-subsample top 1-cm samples were taken from Plot No. 21 of Site I (i.e., I-21). These samples were collected to obtain an indication of the variation between the results of five samples from a 2- by 2-m plot versus samples from the larger 12- by 14-m site.

3. The five 10- by 10-cm subsamples for a single 5-cm composite sample were kept separate for plots I-1 and III-14 (i.e., Site I, Plot 1, etc.). An aliquot from each of the subsamples was taken for analysis prior to compositing the subsamples and taking the primary sample aliquot. This was done to obtain information on the variability of single 10- by 10-cm subsamples versus composites based on five such samples.

SAMPLE PREPARATION AND ANALYSIS

The samples were dried (24 hours or until constant weight) in an oven at 110° C. and then mixed and broken up by autogenous milling (on rollers in a paint can without steel balls) for several hours in cans. The samples were then dry-sieved through a 10-mesh screen (2 mm). A 10-g aliquot was then taken by coning and quartering for plutonium-239 analysis. A 100-ml aliquot was taken from selected samples for cesium-137 analysis.

The samples were analyzed by the Environmental Monitoring and Support Laboratory-Las Vegas, Methods Development and Analytical Support Laboratory. All samples were analyzed for plutonium-239* by the acid dissolution technique, with plutonium separation by ion-exchange from a hydrochloric acid medium (Johns *et al.*, in press). The cesium-137 results were obtained by gamma spectroscopy on both sodium iodide and GeLi systems. Results are reported as less than an indicated value when the 2-sigma counting error was equal to or greater than the indicated value. The less-than values have been assumed to be equal to the indicated value for purposes of data evaluation.

---

*References to plutonium-239 include plutonium-240.

The results are converted from activity per gram of sample analyzed (less than 10-mesh material) to activity per unit area by multiplying by the mass of sample (less than 10 mesh) per area sampled.

The upper 5-cm samples from Site IV contained hard clods (up to about 5 cm^3) that could not be broken by autogenous milling or by hand. Based on observations of the actual presence of rocks and the amount of material that readily broke up and additional material that was broken up in a selected sample, 90 percent of the sample was assumed to be less than 10 mesh.

RESULTS AND DISCUSSION

Table 1 presents the plutonium-239 results for the top 1-cm and top 5-cm samples for the four sites. The date are given both as fCi/g of sample and nCi/m^2. The results are for the less than 10-mesh (2-mm) soil fraction. Most of the subsequent data treatment is based on the activity per unit area, thus the average, standard deviation, and coefficient of variation (C) are given for the nCi/m^2 values. The C for the activity per gram values is somewhat smaller than that for the activity per unit area. Similar data are given in Table 2 for the special samples and depth profile (5- to 10-cm) samples.

The sites were sampled and the samples prepared in order of increasing expected activity (Sites I, III, IV, and II, respectively) to minimize the hazards of cross-contamination. Appendix 1 includes a brief description of the site characteristics. The expected range of activity was 0.1 to 1 pCi/g. With the exception of two values, the sample results reflected the expected values and, recognizing the difference in sampling depths, are similar to the isopleth values given in Figure 1 (DOE, 1977, after Krey and Hardy, 1970). Krey and Hardy's values are for the total deposition down to 20 cm.

It took about the same amount of time for collecting samples by both techniques. The individual who collected the samples for the 0- to 5-cm technique had previously used the technique. All of the 0- to 5-cm samples were collected by the same person. The individual who collected most of the 0- to 1-cm samples had not previously used the technique in the field. Most of the 0- to 1-cm samples were collected by the same individual, but about 20 percent of the samples were collected by a second person.

The result for sample III-17 is grossly higher than any of the other values, and is especially higher than the other values for Site III (Tables 1 and 2). Recounting the sample confirmed the indicated value. A new aliquot of the sample is being analyzed. It is difficult to speculate how this degree of sample contamination would have occurred,

Table 1. EPA Plutonium-239 Soil Sampling Results at Rocky Flats, Colorado, Comparative Sampling for 0- to 1- and 0- to 5-cm Depth

Site	Sampling Depth (cm)	Mass/Area (g/cm^2)a	Concentration (fCi/g)b	Concentration per Unit Area: Individual Results (nCi/m^2)b	Mean (nCi/m^2)	Standard Deviation (nCi/m^2)	Coeff. of Variation C
I - 9	0 to 1	0.70	130 ± 19**	0.91			
17	"	0.84	46 ± 8	0.39			
27	"	0.59	72 ± 10	0.42			
28	"	0.57	33 ± 9	0.19			
30	"	0.66	32 ± 8	0.21	0.42	0.29	0.69
I - 1	0 to 5	4.81	14.8 ± 7*	0.71			
14	"	5.16	51 ± 9*	2.61			
15	"	4.96	40 ± 9	1.98			
16	"	4.70	29 ± 10	1.36			
20	"	5.11	23 ± 7	1.18	1.57	0.74	0.47
II - 9	0 to 1	0.43	1,500 ± 210	6.45			
17	"	0.48	950 ± 65*	4.56			
27	"	0.49	1,400 ± 96	6.86			
28	"	0.57	1,300 ± 91	7.41			
30	"	0.52	1,400 ± 110	7.28	6.51	1.15	0.18
II - 1	0 to 5	3.90	540 ± 44	21.1			
14	"	5.78	350 ± 30*	20.2**			
15	"	6.79	460 ± 37	31.2			
16	"	4.40	360 ± 30	15.8			
20	"	5.86	470 ± 41	27.5	23.2	6.14	0.26
III - 9	0 to 1	0.58	210 ± 61	1.22			
17	"	0.46	28,000 ± 6000[c]	Discounted[c] **			
27	"	0.47	120 ± 18	0.56			
28	"	0.49	170 ± 18	0.83			
30	"	0.44	130 ± 16	0.57	0.80	0.31	0.39
III - 1	0 to 5	5.03	30 ± 6	1.51			
14	"	4.64	20 ± 8*	0.93			
15	"	4.45	40 ± 7	1.78			
16	"	2.72	34 ± 8	0.93			
20	"	4.06	31 ± 7	1.26	1.28	0.37	0.29
IV - 9	0 to 1	0.34	650 ± 66	2.21			
17	"	0.31	550 ± 43**	1.71			
27	"	0.40	910 ± 62	3.64			
28	"	0.52	1,000 ± 74	5.20			
30	"	0.46	970 ± 71	4.46	3.44	1.47	0.43
IV - 1	0 to 5	3.96	302 ± 30	12.0			
14	"	5.13	250 ± 25	12.8			
15	"	6.27	240 ± 24	15.1			
16	"	4.93	360 ± 30*	17.8			
20	"	6.38	290 ± 26	18.5	15.2	2.90	0.19

a. Mass of material less than No. 10 mesh, divided by the sampled area.

b. Error term for the fCi/g values is the 2-sigma counting error term. An error term is not given for the unit area concentrations, but it would include the counting error, any error associated with the mass per area, and other errors mentioned in the text.

c. This value grossly exceeds the other 15 (this table, Table 2, and duplicates) values from this site. The value is excluded from evaluations of the data (see the text). Subsequent to the preparation of this paper, analyses of three additional aliquots of this sample indicated values of 140 fCi/g, 110 fCi/g, and 120 fCi/g, providing evidence that the value of 28,000 fCi/g was an anomaly.

* Average of two duplicates; error term is the counting error for the individual results.

** Recounted for confirmation of results.

Table 2. EPA Plutonium-239 Soil Sampling Results at Rocky Flats, Colorado, Special Samples

Site	Sampling Depth (cm)	Mass/Area (g/cm^2)a	Concentration (fCi/g)b	Concentration per Unit Area			
				Individual Results (nCi/m^2)b	Mean (nCi/m^2)	Standard Deviation (nCi/m^2)	Coeff. of Variation C
I -21-a	0 to 1	0.63	42 ± 17	0.26			
b	"	0.50	29 ± 8**	0.15			
c	"	0.55	56 ± 14	0.31			
d	"	0.60	52 ± 14	0.31			
e	"	0.56	69 ± 18	0.39	0.28	0.09	0.31
I -1-a	0 to 5	4.36	20 ± 5	0.87			
b	"	4.74	<6.9**	<0.33			
c	"	5.13	18 ± 5	0.92			
d	"	4.46	37 ± 9	1.65			
e	"	5.35	6.1 ± 4.1	0.33	0.82	0.54	0.66
III -14-a	0 to 5	6.69	<7.2**	<0.48			
b	"	2.15	32 ± 7	0.69			
c	"	5.36	13 ± 6	0.70			
d	"	5.06	22 ± 6	1.11			
e	"	3.93	12 ± 4	0.47	0.69	0.26	0.37
DEPTH PROFILE SAMPLES							
I -16	5 to 10	5.29	6 ± 5**	0.32			
-20	5 to 10	4.09	<6.1	0.25			
II	5 to 10	4.96	90 ± 12*	4.44			
III -16	5 to 10	5.24	6.1 ± 5.3**	0.32			
IV -16	5 to 10	4.14	20 ± 6	0.83			
IV Composite	5 to 10	4.35	450 ± 40[c]**	Discounted			

a. Mass of material less than No. 10 mesh, divided by the sampled area.

b. Error term for the fCi/g values is based on the 2-sigma counting error term. An error term is not given for the unit area concentrations, but it would include the counting error, any error associated with the mass per area, and other errors mentioned in the text.

c. Appears to be cross-contaminated in sampling, preparation, or analysis.

* Average of two duplicates; error term is the counting error for the individual results.

** Recounted for confirmation of results.

but it is equally difficult to justify the value as a representative or valid result. The value is easily discarded as a statistical outlier, and is thus discarded from subsequent evaluations. It is emphasized that even if it is a valid result, due to a hot particle, it does not characterize the site and it must be considered in conjunction with the other results from this site.

Sample IV composite (5-10 cm) from Table 2 also appears to be unreasonably high. The result is probably due to cross-contamination and is discounted.

Analytical Variability

As part of the analytical effort, eight samples were analyzed in duplicate. These results are given in Appendix 2. The sample activities ranged from less than 5 to 970 fCi/g. Although the difference in variability was not statistically significant, the ranges in results for the duplicates averaging greater than 100 fCi/g had less variability than samples below 100 fCi/g. The mean percent deviation between the duplicates (i.e., difference of the duplicates divided by the average of the two) was 40 percent. This is about twice the variability estimated by Krey and Hardy (1970) for results from 100-g aliquots of samples of the top 20 cm of soil. Both of these evaluations include the errors of obtaining a representative aliquot from a sample and sample analysis.

A technique for expressing the variability of results, based on duplicates, in terms of the geometric standard deviation is presented by EPA, 1977c. This technique was used to estimate the coefficient of variation based on the assumption of a normal distribution, since the data sets in this report have been evaluated based on the assumed applicability of the normal distribution (see Appendix 2). The estimated coefficient of variation for these duplicates is 29 percent.

Analysis of four duplicates for cesium-137 showed a significantly lower variability than that observed for plutonium-239. The average of the difference of the results divided by the mean was 9 percent (range of 0 to 18).

Statistical Testing

The various groups of data have been evaluated using several statistical tests. The limited amount of data minimizes the meaningfulness or power of these tests. Thus, emphasis is placed on the numerical trends of the data and the statistical tests are viewed as indicators of the uncertainties of the associated trends.

There are insufficient data points in each set to evaluate the appropriateness of any specific statistical distribution. Although environmental data are often fit to a lognormal distribution (Denham and Waite, 1975), because of the small number of data points the normal distribution has been used to characterize these data.

It is apparent, as would be expected, that the means for results for the top 1-cm samples are less than those at the respective sites for the top 5-cm samples. Thus, it was questioned whether the standard deviations would be dependent on the means. Based on graphical analysis and the Pearson product correlation coefficient (see Appendix 3), it was concluded that the means and variances were not independent. Therefore, the sample coefficient of variation (C, standard deviation divided by the mean; i.e., normalizes for differences in the means) was used for testing the variability of the techniques.

Variability of Deposition in a 2- by 2-m Plot Versus a Site

Table 3 indicates results for the top 1-cm samples for Site I and results for five samples all taken from within plot 21 of Site I (i.e., I-21). The coefficient of variation for the five samples taken from throughout the site is numerically almost twice that for the samples taken within the plot (the difference in the coefficients of variation are not significant at the 95 percent confidence level). Although this is only one point of comparison, it appears there is more variability within the 12- by 14-m site than within the 2- by 2-m plot for the 1-cm sampling depth.

Table 3. Comparison of Sampling 2- by 2-m Plot Versus 12- by 14-m Site

	Plutonium-239; Top 1-cm Depth		
Sample	Mean (fCi/m^2)	Standard Deviation (fCi/m^2)	Coefficient of Variation
Plot I-21[a]	0.28	0.09	0.31
Site I[b]	0.42	0.29	0.69

Basis (each sample composed of fifteen 30-cm^2 subsamples)

a. Average of five samples from Plot I-21 (2 by 2 m).

b. Average of five samples from five separate plots (one sample per plot) within Site I (12 by 14 m).

Compositing of Subsamples

Figure 3 presents data from the 0- to 5-cm subsamples for Sites I and III. The sample results are based on analyses of aliquots from the individual subsamples prior to compositing for the plot sample (I-1 and III-14). The C's for both groups of subsamples are about 35 percent larger (40 and 28, respectively) than the C's for the total plots (the differences are not statistically significant). It should be noted that

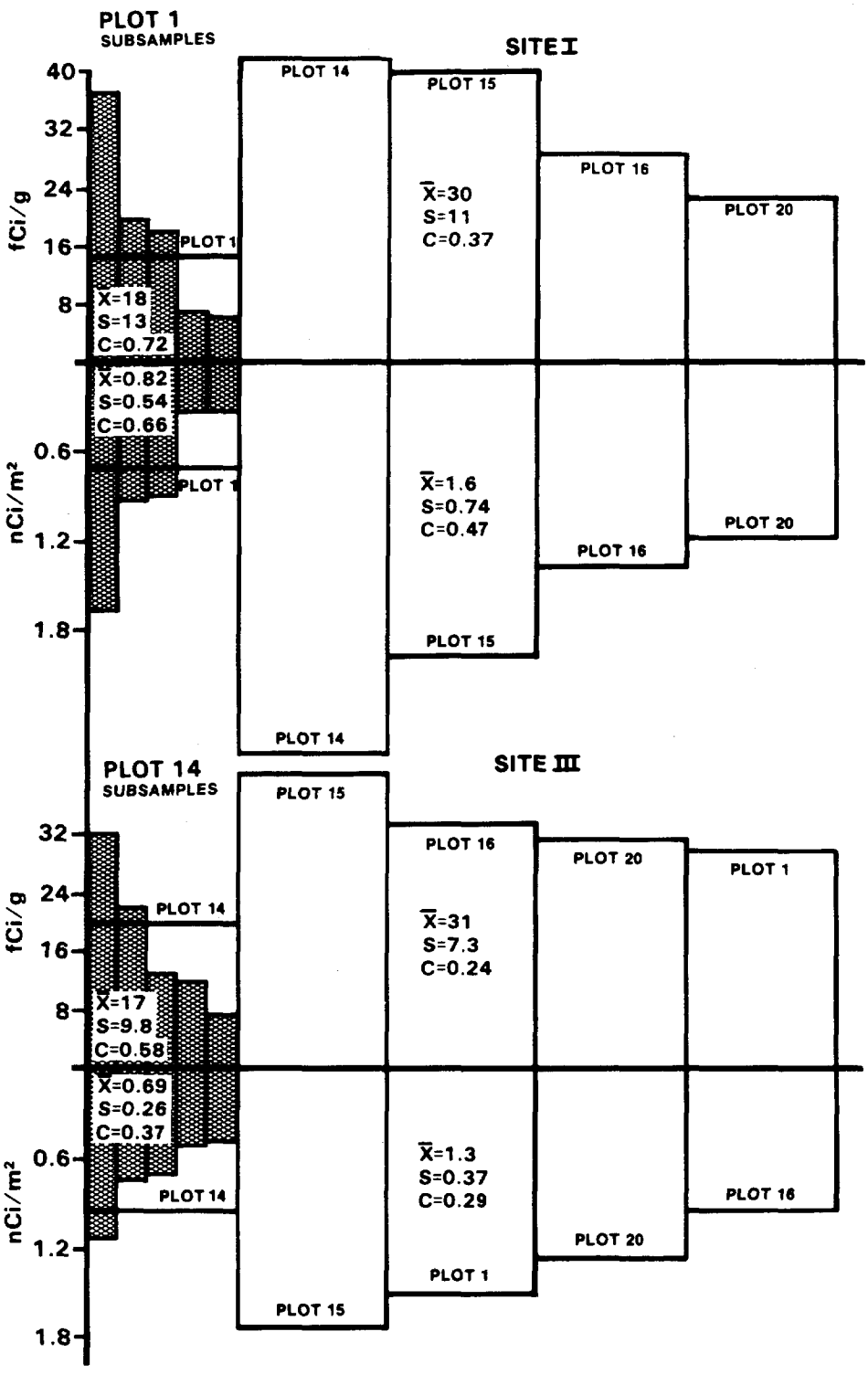

Fig. 3 Comparison of individual 100-cm^2 subsamples to five-sample composites; EPA Rocky Flats top 5-cm soil samples.

the subsample results are based on samples from a 2- by 2-m area, whereas the site results are based on samples from the 12- by 14-m site and may include the additional variability associated with coming from a larger area, as noted above. This indicates additional significance for the differences noted in the subsample and composite sample results. These results indicate the desirability of compositing samples (depending on program objectives) to decrease their variability and increase their representativeness for a given area (the parameter "s" in Figure 3 and subsequent figures stands for the sample standard deviation).

Variability of Sampling Techniques

Figure 4 gives bar graphs of the plutonium-239 activity for the 0- to 1-cm and 0- to 5-cm results for all four sites. The plutonium-239 concentrations are given for both the activity per gram and per unit area. The graphic scales are the same for both techniques at each site, but vary between sites. A horizontal bar with a vertical error bar indicates the mean and standard deviation for each sample group. In most cases, the values are uniformly distributed about the mean. A unique case is Site I for the 1-cm samples where a single high value strongly influences the mean.

Figure 5 is a bar graph of the ratios of the coefficients of variation (C) for the activity per unit area results (nCi/m^2) from the 0- to 1-cm and 0- to 5-cm sampling techniques. The bar graph shows that C for the 1-cm technique ranged from 1.3 to more than twice the C for the 0- to 5-cm technique for three of the four sites. The average C's for the 0- to 1-cm and 0- to 5-cm techniques were 0.42 and 0.30, respectively (ratio of 1.4). This indicates somewhat more uncertainty than the estimate of plus or minus 25 percent by Krey and Hardy (1970, p. 30) for samples from 0 to 20 cm.

Statistical testing for differences between the C's for the 0- to 1-cm and 0- to 5-cm results indicated a lack of general significant differences (Appendix 3). But, because of the small number of results (5 samples in each group), the test results have limited meaning.

The summaries of results in Figure 4 and especially Figure 5 indicate that the 0- to 1-cm sampling technique is somewhat more variable than the 0- to 5-cm technique. Although statistical testing of the data did not indicate this trend was statistically significant (Appendix 3), the limited amount of data results in the test giving only weak confirmation that significant differences are not present between the two techniques.

Figure 6 is a bar graph presentation of the mass of sample (that passed 10 mesh) per unit area (g/cm^2) for both techniques at all four sites. The variations include the heterogenous nature of the sampled soil; i.e., rocks and gravel, in addition to the uncertainties from sampling. The coefficients of variation (C) for the mass per unit area results are generally less than those for the activity per gram or per unit area (Figure 5). This may be interpreted as indicating that the variability

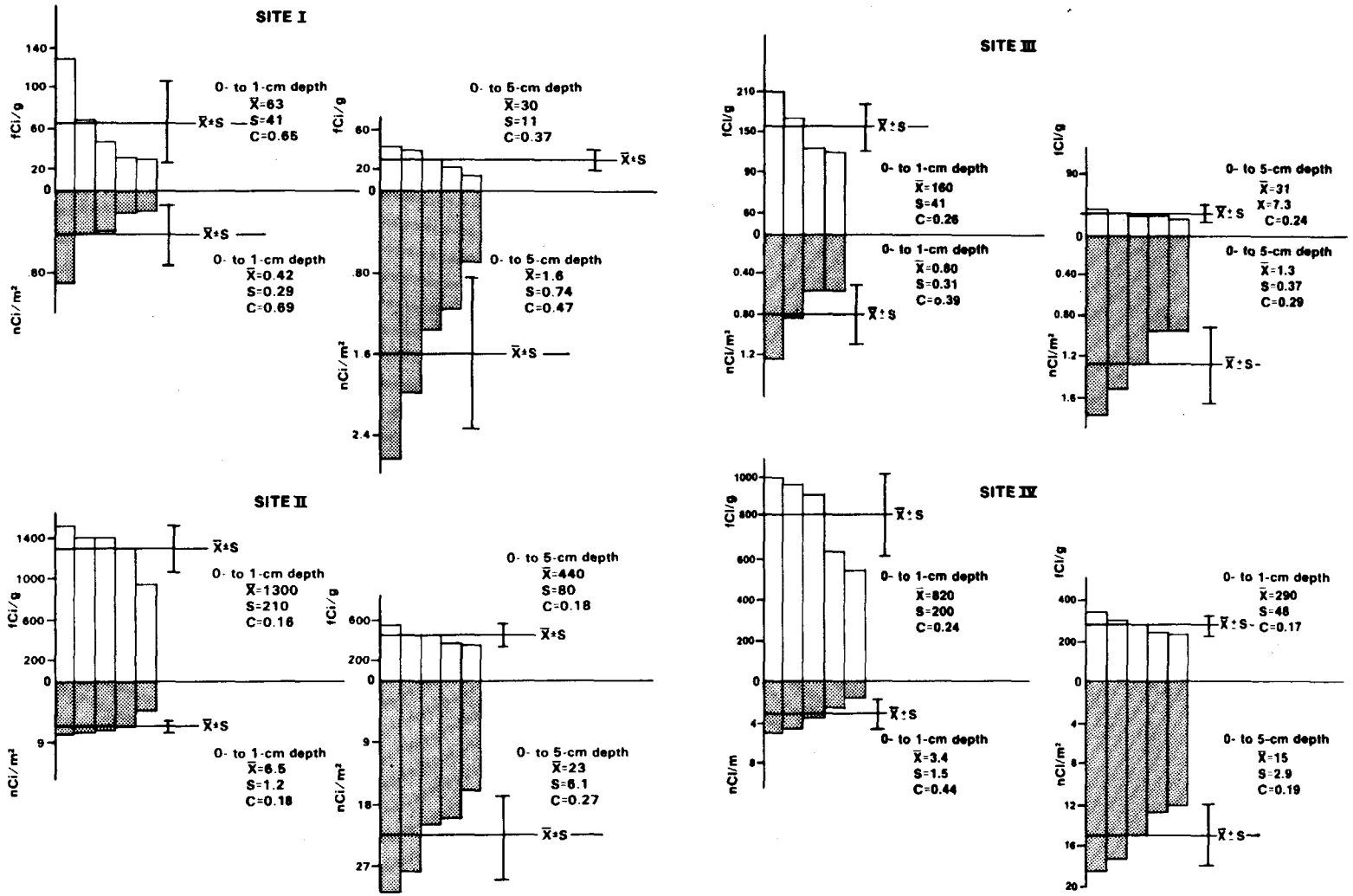

Fig. 4 Bar graph of EPA soil sampling results (Activity per gram and activity per unit area) 0- to 1-cm and 0- to 5-cm samples.

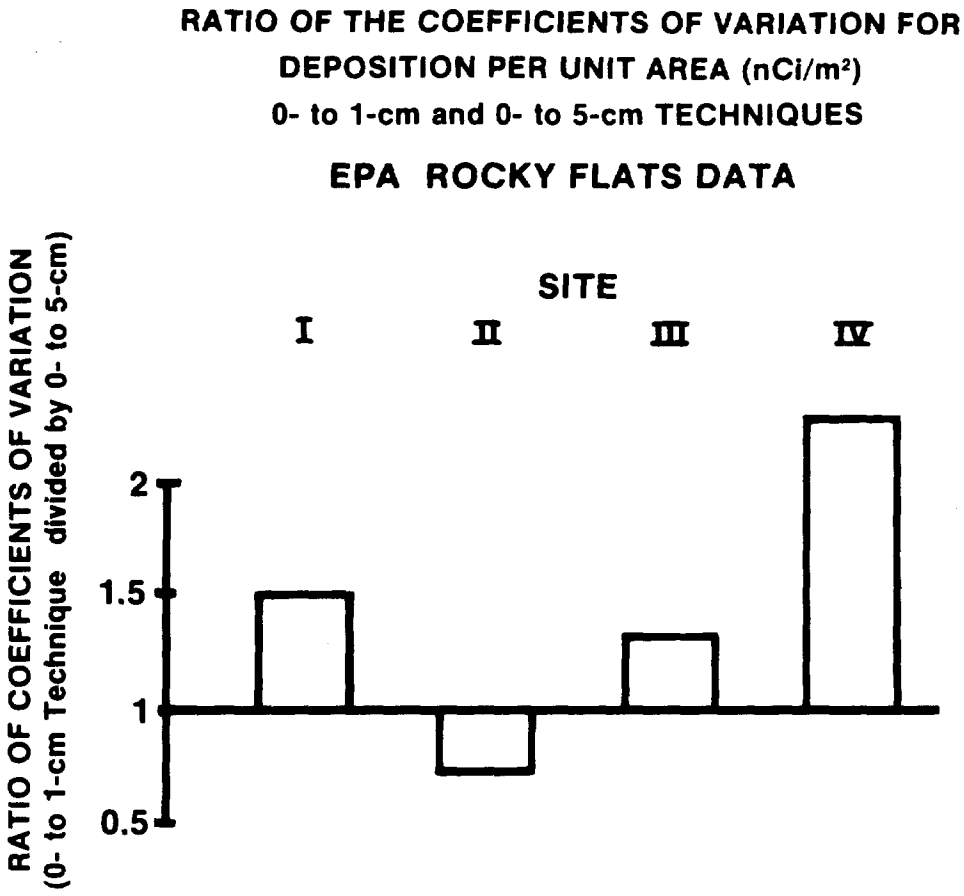

Fig. 5 Variation of 0- to 1-cm versus 0- to 5-cm soil sampling results.

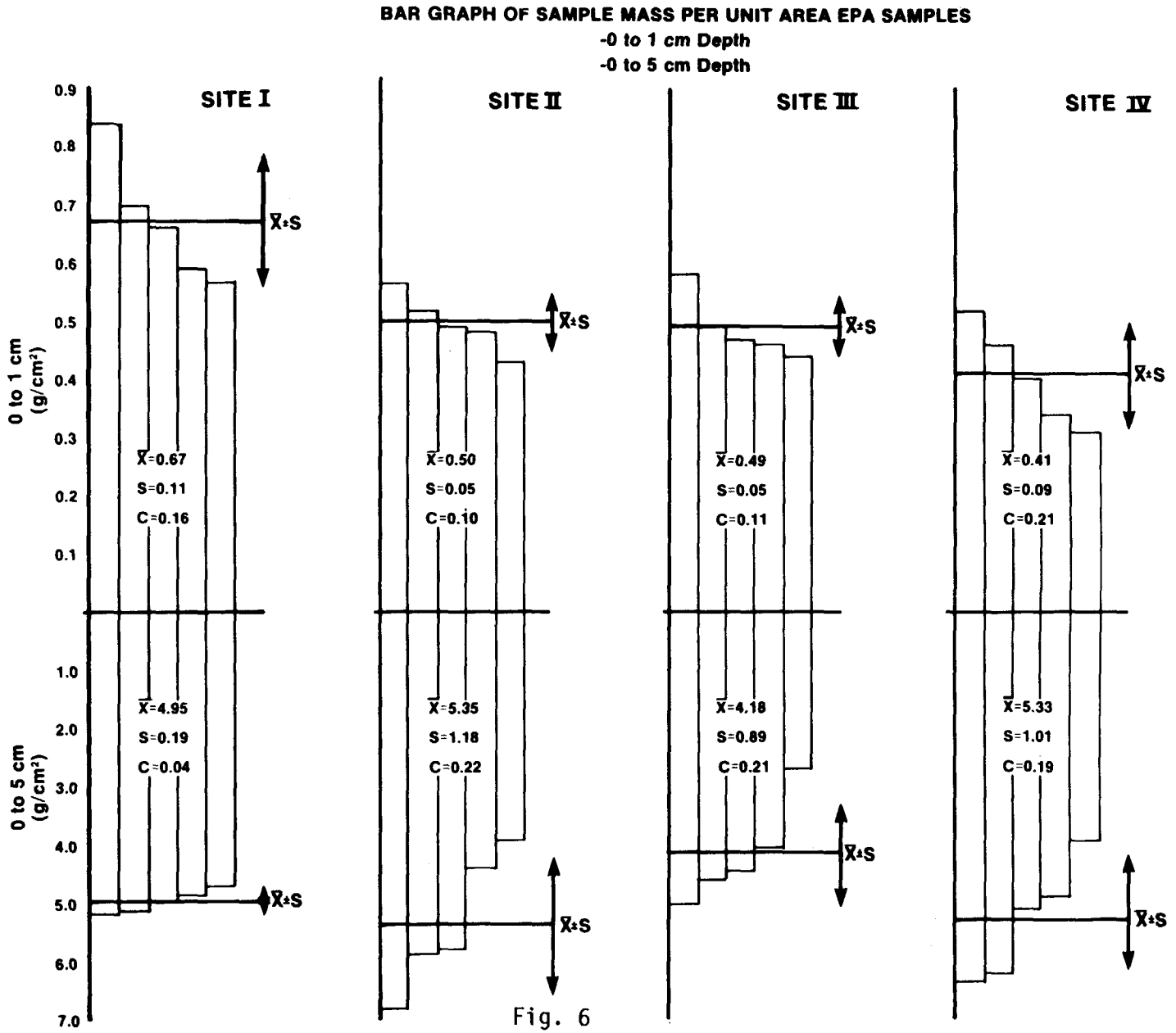
BAR GRAPH OF SAMPLE MASS PER UNIT AREA EPA SAMPLES
-0 to 1 cm Depth
-0 to 5 cm Depth
SITE I
SITE II
SITE III
SITE IV
0 to 1 cm (g/cm²)
0 to 5 cm (g/cm²)
0.9
0.8
0.7
0.6
0.5
0.4
0.3
0.2
0.1
1.0
2.0
3.0
4.0
5.0
6.0
7.0
X̄±S
X̄=0.67
S=0.11
C=0.16
X̄=4.95
S=0.19
C=0.04
X̄=0.50
S=0.05
C=0.10
X̄=5.35
S=1.18
C=0.22
X̄=0.49
S=0.05
C=0.11
X̄=4.18
S=0.89
C=0.21
X̄=0.41
S=0.09
C=0.21
X̄=5.33
S=1.01
C=0.19

Fig. 6

of plutonium in the soil (both horizontal and vertical) plus the uncertainties of aliquoting and analysis of samples contribute to the variability of results over the uncertainties of the actual sampled mass.

Except for the very low C indicated for the 0- to 5-cm technique for Site I, the C's for the 0- to 1-cm technique are essentially the same or lower than those for the 0- to 5-cm technique.

Site I was the first site sampled, and from a petrological viewpoint, an ideal site for sampling. Site III was a very rocky hillside and Site IV a dry, hard-packed, highly compacted (silt to clay valley fill) pasture. Thus, the sampling scoops for the 0- to 5-cm technique were in a bad state of disrepair prior to sampling Site II (sampling sequence I, III, IV, and II). It is noted that the variability in the upper 5-cm technique may reflect the inappropriateness of the scoop technique, which was developed for sandy desert areas, for the rocky and hard-packed loam soils around Rocky Flats. Rockwell International uses a steel 10- by 10-cm template-type device that is designed to be driven into the ground to define the sample.

A field study with the scoop technique in sandy soil indicated an uncertainty of less than 10 percent in the mass per unit area sampled (Bernhardt, 1976, p. 20). The study was based on eight depth profiles to a depth of 20 cm by two different sampling teams.

The 0- to 1-cm technique generally showed uniform variability (similar C's) at the various sites. The greatest variability was at Site IV, the hard-packed site. The ground hardness at this site was such that even the 1-cm-deep template had to be driven into the ground with a hammer. Therefore, the increased variability is not surprising.

Figure 7 illustrates the amount of plutonium-239 deposition per sampling depth denoted in this study. The results from cesium-137 are also shown for comparative purposes (the curve is given only as an approximation).

Krey and Hardy (1970, p. 22) sampled to a depth of 20 cm to assess the total plutonium inventory around Rocky Flats. They noted that as much as 60 percent of the total activity (activity per unit area) was below 5 cm. Their results from seven sites indicated that an average of 62 percent (range of 39 to 91) of the total activity fell into the top 5-cm interval. Based on three sites, 93 percent (88-98) of the activity was in the top 10-cm interval. These values indicate 67 percent of the activity in the top 10-cm interval is in the top 5-cm interval. This is somewhat lower than our average estimate of 86 percent, but the range of values overlaps.

Results from EPA samples in October, 1976 (Bernhardt *et al.*, 1977), from a hillside site about 600 m north of Site II, indicated about 44 percent of the activity from the top 5 cm was in the upper 1 cm, which is comparable to the average of 35 percent (range of 23 to 62) indicated by this study.

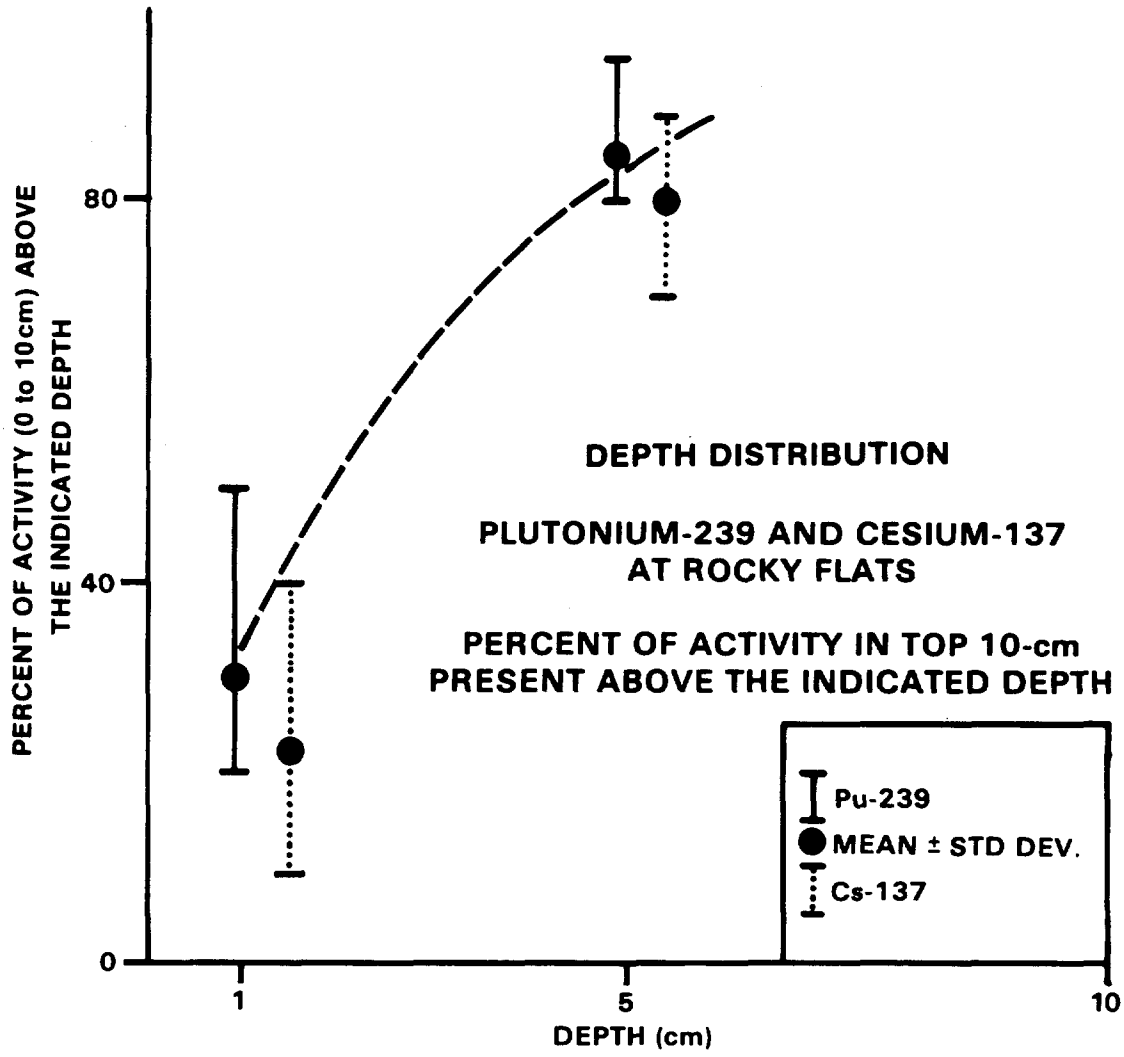
PERCENT OF ACTIVITY (0 to 10cm) ABOVE THE INDICATED DEPTH
80
40
0
1
5
10
DEPTH (cm)
DEPTH DISTRIBUTION
PLUTONIUM-239 AND CESIUM-137 AT ROCKY FLATS
PERCENT OF ACTIVITY IN TOP 10-cm PRESENT ABOVE THE INDICATED DEPTH
Pu-239
MEAN ± STD DEV.
Cs-137

Fig. 7

Poet and Martell (1974) estimated that 80 percent of the activity from the top 10 cm was in the upper 0.3 cm. An uncertainty is not associated with this statement, but it would appear to be significantly different from the results observed in the above studies.

Bernhardt (1976) summarizes values from various sites indicating the average depth distribution. These values indicate about 50 percent of the total inventory in the upper centimeter and 70 percent in the upper 5 cm. The variations on these values are about plus and minus 50 percent (numeric range) or more.

Cesium-137 results for selected samples from this study are given in Table 4. Values are given for the top 1-cm and 5-cm samples and for samples from the 5- to 10-cm depth interval. The average of the sample results for each technique and site has been used to estimate the activity in the upper 10-cm depth interval for that site (column on right). The percent distribution at various depths from this data is plotted on Figure 7. The distribution is very similar to that indicated for plutonium-239 reported by Harley (1975).

Error terms are not indicated for the accumulative cesium-137 values because some of the estimates are based on only one or two data points. The coefficients of variation (where there are several values) range from around 20 to 50 percent.

The cesium-137 data appear to be from the same population unlike the plutonium-239 data in Table 1, suggesting the absence of a significant point source (e.g., Rocky Flats) contribution.

Figure 8 is a log-probability plot of the cesium-137 data in the top 5 cm of soil. The good fit of the data to a lognormal distribution is a strong indication of the data relating to a single uniformly dispersed distribution (Denham and Waite, 1975). Hardy (1976) reports an average deposition value of 100 nCi/m^2 (surface to 15- or 30-cm sampling depth, northern Nevada and Utah). The Rocky Flats values are similar too, but appear to be somewhat lower (shallower sampling depth) than this value.

SUMMARY AND CONCLUSIONS

This is a status report of the EPA segment of a cooperative soil sampling evaluation study conducted at Rocky Flats, Colorado. The study was based on five duplicate samples by five different techniques from four sites around the Department of Energy's Rocky Flats Plant (see Figure 1). Undisturbed areas were selected for the sampling sites.

The two EPA sampling techniques discussed in this report are:

Table 4. Cesium-137 in Soil at Rocky Flats, Colorado

Site	Upper 1 cm (pCi/g)[a]	Upper 1 cm (nCi/m^2)	Upper 5 cm (pCi/g)	Upper 5 cm (nCi/m^2)	5 to 10 cm (pCi/g)	5 to 10 cm (nCi/m^2)	Cesium-137 in Upper 10 cm (nCi/m^2)
I-21-1	1.7 ± 0.12	10.7	I-1 0.73 ± 0.12*	35			
5	1.4 ± 0.13	7.8	14 1.9 ± 0.13	98			
I-9	1.7 ± 0.13*	11.9	15 1.8 ± 0.15	89			
			16 1.4 ± 0.11	66	0.31 ± 0.08	16.4	
			20 0.96 ± 0.12	49	0.11 ± 0.09	4.5	
I-Mean nCi/m		10		68		10.5	78
II-9	2.6 ± 0.16	11.2	II-1 1.1 ± 0.10	43			
17	1.9 ± 0.12	9.1	14 0.88 ± 0.09*	51			
27	1.9 ± 0.13	9.3	15 0.97 ± 0.11	66			
			16 0.95 ± 0.09	42			
			20 0.96 ± 0.11	56	0.25 ± 0.10*	13	65
II-Mean nCi/m^2		10		52			
III-9	3.7 ± 0.15	21	III-1 1.1 ± 1.0	55			
17	4.9 ± 0.17	23	14 0.50 ± 0.09*	23	0.32 ± 0.1	17	
III-Mean nCi/m^2		22		39			56
IV-9	3.0 ± 0.17	10	IV-1 1.7 ± 0.12	67	0.27 ± 0.08	11.2	
17	3.3 ± 0.28	10	14 1.2 ± 0.11	62			
28	3.3 ± 0.17	17	15 0.77 ± 0.09	48	0.16 ± 0.06	7.0	
IV-Mean nCi/m^2		13		59		9.1	68

a = Error term is 2-sigma counting error.

* = Duplicate analysis.

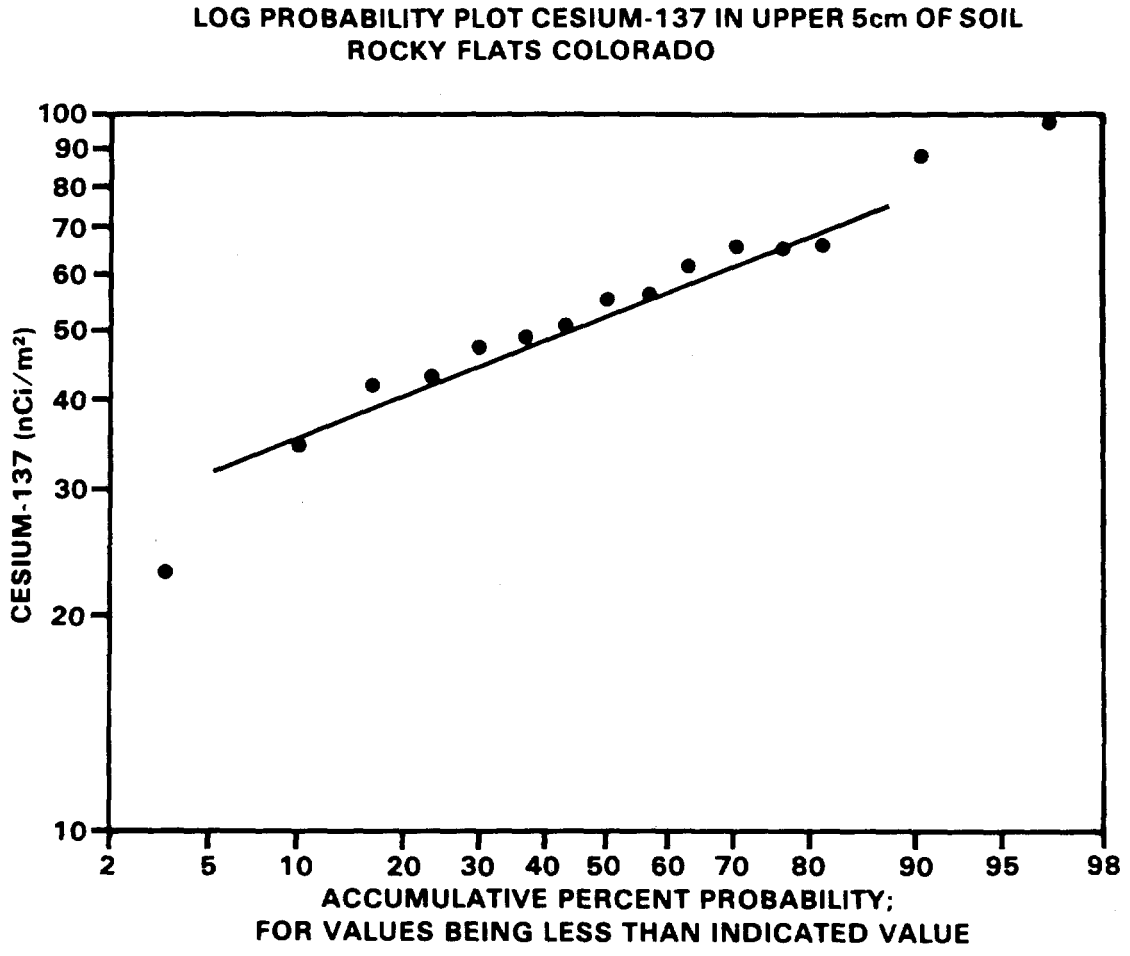
LOG PROBABILITY PLOT CESIUM-137 IN UPPER 5cm OF SOIL
ROCKY FLATS COLORADO
CESIUM-137 (nCi/m²)
100
90
80
70
60
50
40
30
20
10
2
5
10
20
30
40
50
60
70
80
90
95
98
ACCUMULATIVE PERCENT PROBABILITY;
FOR VALUES BEING LESS THAN INDICATED VALUE

Fig. 8

1. Top 1 cm of soil: Based on compositing 15 subsamples obtained using a 5- by 6-cm template (450 cm^2).

2. Top 5 cm of soil: Based on compositing five subsamples obtained using a 10- by 10-cm scoop (500 cm^2).

A limited number of 5- to 10-cm depth profile samples and individual subsamples of the 1- and 5-cm samples were also obtained and analyzed. All samples were analyzed for plutonium-239. A selected number of samples were analyzed for cesium-137 to evaluate allegations that the Rocky Flats plant was the source of localized cesium-137 contamination (Johnson, 1977).

Eight duplicate analyses were evaluated to assess the uncertainty of the sample aliquoting and analysis technique for plutonium-239.

Statistical testing and plotting of the data indicated that the variances were not independent of the means. Therefore, the coefficient of variation (C) was used, versus the variances, for testing the variations of results for the different data sets.

There were only a small number of results (generally five) in the various data groups. Thus, it is emphasized that limited significance should be placed on the test results. In general, equality was not rejected for any of the data groups; however, because of the limited amount of data, the test results give only a weak confirmation that statistical differences are not present. Although there is some uncertainty in both the direction and magnitude of indicated trends, the trends are believed to be the best observations based on the available data.

The C for five 0- to 1-cm samples collected from a 2- by 2-m plot was about one-half of that for the whole 12- by 14-m site. This trend indicates that the deposition of plutonium for the total site was more variable than that in the 2- by 2-m plot.

The C's for the activity per unit area results for the 0- to 1-cm technique are similar to but somewhat larger than for the 0- to 5-cm technique. The range of the C's for the 1-cm technique (mean of 42 percent, range of 18 to 69) overlap the C's for the 0- to 5-cm technique (mean 30 percent, range of 19 to 47).

The C's for the amount of sampled mass (less than 10-mesh) per unit area reflect smaller differences between the techniques than the activity per unit area C's. This indicates a significant fraction of the differences of the variabilities of the techniques may be due to variations in the deposition of plutonium.

There was considerable difficulty in applying the EPA 0- to 5-cm technique for the compact rocky soils around Rocky Flats. It is possible that other techniques for sampling down to 5 cm or deeper, more adaptable to the Rocky Flats type of environment, might exhibit less variability

for this area. Krey and Hardy (1970) reported about plus or minus 25 percent uncertainty.

The variability of the upper 1-cm technique (average coefficient of variation of 42 percent, range of 18 to 69) is similar to the variability indicated by duplicate sample analysis (estimated C of 29 percent, range of up to 60 percent). Thus, it appears that a significant, if not major, fraction of the variability in duplicate soil samples is related to the variability resulting from aliquoting samples for analysis and the actual variability in analysis. This is in agreement with the conclusions of Krey and Hardy (1970). Many of the lower-level activity samples (Sites I and III, Table 1) had analytical counting errors of 20 to 40 percent (2 sigma). These two sites generally had higher C's than the other sites.

The results of this project indicated about 30 percent (range of 30 to 50) of the plutonium-239 in the upper 10 cm of soil was in the upper 1 cm, with about 86 percent in the upper 5 cm. This is a somewhat higher fraction than indicated by Krey and Hardy (1970) for the Rocky Flats area, but the range of values overlaps. It does appear to be at variance with the results of Poet and Martell (1974), which indicated 80 percent of the plutonium-239 in the upper 10 cm was in the top 0.3 cm.

The activity per gram values (averaged for each site) for the 0- to 1-cm results ranged from about two to five times those for the 0- to 5-cm technique, indicating, as expected, that the activity in the surface 1 cm of soil is generally greater than that below 1 cm. Also, as expected, the activity per unit area for the 0- to 1-cm technique ranged from about 23 to 62 percent (average of 35) of that in the 0- to 5-cm samples.

From this, it is observed that 0- to 5-cm samples can be used to conservatively estimate the activity per unit area for the upper 1 cm. But, results from samples taken from a depth of less than 1 cm cannot be directly used to estimate the plutonium-239 per unit area in the surface 1 cm of soil, which is specified by the proposed EPA guidance (EPA, 1977a).

It appears there is probably some compromise in the variability of sample results associated with collecting samples related to the surface 1 cm of soil versus the top 5 cm, using the techniques applied in this study. The average C for the 1-cm technique was 40 percent greater than that for the 5-cm technique. But, given the greater applicability of plutonium results from 0- to 1-cm versus 0- to 5-cm samples for resuspension estimates, the increased uncertainty would appear to be acceptable for programs concerned with assessing potential airborne hazards. The EPA proposed transuranium guidance (EPA, 1977a) specifies the plutonium per unit area in the surface 1 cm. In summary, it is concluded that the surface 1-cm technique used in this study can be used to generally characterize an area.

Analysis of selected samples for cesium-137 indicated distribution with depth similar (slightly lower fraction near the surface) to that for plutonium-239 as reported by Harley (1975). The average concentrations in the upper 10 cm of soil for the four sites did not indicate geographical dependence such as that indicated by the plutonium-239 data.

Furthermore, all the values for the top 10-cm interval were less than the average deposition (100 nCi/m^2) reported by Hardy (1976). The 15 cesium-137 samples for the upper 5 cm give a good fit to a lognormal distribution,providing additional evidence that the cesium-137 deposition around the Rocky Flats plant fits a single distribution related to worldwide fallout.

REFERENCES

1. Anspaugh, L. R., J. H. Shinn, P. L. Phelps, and N. C. Kennedy. 1975. "Resuspension and Redistribution of Plutonium in Soils." *Health Physics* 29:571-582.

2. Bernhardt, D. E. 1976. "Evaluation of Sample Collection and Analysis Techniques for Environmental Plutonium." Environmental Protection Agency, Las Vegas, NV. Technical Note ORP/LV-76-5.

3. Bernhardt, D. E., J. D. Bliss, R. H. Johnson, Jr., and T. Reavey. 1977. "Soil Sampling and Particle Size Characterization of Plutonium With Emphasis on Resuspension." Symposium at Rocky Flats, CO. Environmental Protection Agency, Office of Radiation Programs, Las Vegas, NV.

4. Bliss, W. A. 1976. "Soil Sampling and Analytical Procedures Employed by the EPA for the NAEG." *In: Nevada Applied Ecology Group Procedures Handbook for Environmental Transuranics.* M. G. White and P. B. Dunaway (Eds.). USERDA Report, NVO-166. p. 123.

5. Colorado Department of Health. 1977. "Radioactive Soil Contamination, Cesium-137, and Plutonium in the Environment Near the Rocky Flats Nuclear Weapons Plant." Colorado Department of Health, Denver, CO.

6. Denham, D. H., and D. A. Waite. 1975. "Some Practical Applications of the Log-Normal Distribution for Interpreting Environmental Data." Battelle's Pacific Northwest Laboratories, Richland, WA. Presented at the 20th Annual Meeting of the Health Physics Society, Buffalo, NY.

7. DOE. 1977. Draft Environmental Impact Statement, Rocky Flats Plant Site, Golden, Colorado. U.S. Department of Energy. ERDA-1545-D.

8. EPA. 1977a. "Persons Exposed to Transuranic Elements in the Environment." *Federal Register* 42(230).

9. EPA. 1977b. *Proposed Guidance on Dose Limits for Persons Exposed to Transuranium Elements in the General Environment.* Environmental Protection Agency, Office of Radiation Programs, Washington, DC.

10. EPA. 1977c. *Off-Site Environmental Monitoring Report for the Nevada Test Site and Other Test Areas for Underground Nuclear Detonations.* Environmental Protection Agency, Las Vegas, NV. EMSL-LV-0539-12.

11. Fowler, E. B., R. O. Gilbert, and E. H. Essington. 1976. "Sampling of Soils for Radioactivity: Philosophy, Experience, and Results." ERDA Symposium, Richland, WA (1974), ERDA Symp. Series 38.

12. Gibbon, J. D. 1976. *Nonparametric Methods for Quantitative Analysis.* Holt, Rinehart, and Winston. pp. 123-140.

13. Hardy, E. 1976. *Plutonium in Soil Northwest of the Nevada Test Site.* HASL-306.

14. Harley, J. H. 1975. *Transuranic Elements on Land.* HASL-291.

15. Johns, F. B., P. B. Hahn, D. J. Thome, and E. W. Bretthauer (Eds.). (In Press.) "Radiochemistry Analytical Procedures for Analysis of Environmental Samples." EPA, Environmental Monitoring and Support Laboratory,Las Vegas, NV.

16. Johnson, C. 1977. "Report to the Jefferson County Board of Health: March 31, 1977." Jefferson County Health Department, Lakewood, CO.

17. Johnson, C. J., R. R. Tidball, and R. C. Severson. 1976. "Plutonium Hazard in Respirable Dust on the Surface of Soil." *Science* 193:488.

18. Koch, G. S., Jr., and R. F. Link. 1971a. *Statistical Analysis of Geological Data.* John Wiley & Sons. Vol. II. p. 438.

19. Koch, G. S., Jr., and R. F. Link. 1971b. "The Coefficient of Variation--A Guide to the Sampling of Ore Deposits." *Economic Geology* 66(2):293-301.

20. Krey, P. W., and E. P. Hardy. 1970. *Plutonium in Soil Around the Rocky Flats Plant.* HASL-235.

21. Lem, P. N., J. V. Behar, and F. N. Buck. 1977. "Resuspension of Plutonium From Contaminated Land Surfaces: Meteorological Factors." EPA-600/4-77-037.

22. Little, C. A., T. F. Windsor, J. E. Johnson, and W. F. Whicker. 1973. *Plutonium in the Terrestrial Environs of Rocky Flats.* Colorado State University. AT (11-1)-1156, COO-1156-63.

23. NRC. 1974. "Measurements of Radionuclides in the Environment, Sampling, and Analysis of Plutonium in Soil." Formerly Atomic Energy Commission, U.S. Nuclear Regulatory Commission. Regulatory Guide 4.5.

24. Oksza-Chocimowski, G. V. (In Press.) "Resuspension Models Review." Environmental Protection Agency, Office of Radiation Programs, Las Vegas, NV.

25. Poet, S. E., and E. A. Martell. 1972. "Pu-239 and Am-241 Contamination in the Denver Area." *Health Physics* 23:537-548.

26. Poet, S. E., and E. A. Martell. 1974. "Reply to Plutonium-239 Contamination in the Denver Area." *Health Physics* 26:120-122.

27. Rockwell International. 1977. *Annual Environmental Monitoring Report.* RFP-ENV-76.

28. Snedecor, G. W., and W. G. Cochran. 1967. *Statistical Method.* The Iowa State University Press, Ames, IA. 6th Ed. pp. 39-47.

29. Tamura, T. 1976. "Physical and Chemical Characteristics of Plutonium in Existing Contaminated Soils and Sediments." *In: Transuranium Nuclides in the Environment.* IAEA-SM-199/52. IAEA, Vienna. (ORNL-787.)

30. Tamura, T. 1977. "Particle Size and Plutonium Distribution in Surface Soil From Rocky Flats." *In: Transuranics in Desert Ecosystems.* M. G. White, P. B. Dunaway, and D. L. Wireman (Eds.). USDOE Report, NVO-181.

31. Wine, R. L. 1964. *Statistics for Scientists and Engineers.* Prentice-Hall. p. 671.

APPENDIX 1

MORPHOLOGICAL AND PEDOLOGICAL SKETCH OF ROCKY FLATS SAMPLING SITES
(See Figure 1 in text for locations)

Site I

The site is a flat to slightly rolling terrace surface with modest plant cover. The soil is very rocky to sandy and light in color.

Site II

The site is a gently dipping lower slope segment facing the south-southwest generally consisting of colluvium, possibly interfingering with fluvial debris from an adjacent intermittent stream. The soil is sandy to clayey, grey to brown in color, and with modest to heavy grass cover.

Site III

The site is a steeply dipping north-facing slope on colluvium with a light sandy soil and light to modest cover punctuated with cacti and yucca. The surface is interspersed with rock outcrops and there was considerable rock in the upper 5 cm of soil.

Site IV

The site is a gently undulating valley bottom made up of fluvial sediments. The soil is tightly packed, grey to brown, and predominately clayey with closely cropped vegetation. The area appeared to be frequently grazed by cattle.

APPENDIX 2

DUPLICATES

EPA (1977c) describes a technique for estimating the sampling error for individual values based on the results from duplicates. The subject technique is based on assuming the data can be fit by a lognormal distribution. Since the data treatments in this paper have been based on the assumptions of a normal distribution, this assumption will be applied here.

The variance for the individual duplicates S^2 is $(0.886R)^2$. Where R is the absolute difference between a pair of duplicates and 0.886 is a parameter for estimating the standard deviation based on the range of two values. Snedecor and Cochran (1967) note this is a statistically efficient technique for small sample sizes. The population variance for a group of variances based on duplicates is equal to the average variance. If the individual variances are not all for duplicates (e.g., triplicates and duplicates, etc.), the values have to be weighted by their respective n's.

The estimates of the respective variances are given in the column on the right in Table 2-1. The estimate of the population (average) variance is 4491 and the estimated standard deviation is 67 fCi/g. The estimated coefficient of variation is 29 percent (based on the average of the duplicates--230 fCi/g).

If the lognormal distribution had been assumed, the estimated geometric standard deviation would be 1.53.

Table 2-1. Variation of Duplicate Analysis for Pu-239

Sample Location	Depth (cm)	Pu-239 (fCi/g)	Duplicate Results (fCi/g)	Absolute Difference ÷ by Avg. %	Est. Variance (Difference of Dup. x 0.886)^2
I-16	5-10	<5	7.1 ± 4.5	35	3.46
I- 1	0-5	20 ± 6.6	9.6 ± 7.5	70	84.9
III-14	0-5	13 ± 8.1	27 ± 6.5	70	153.9
I-14	0-5	42 ± 8.8	59 ± 9.3	34	226.9
II	5-10	69 ± 9.7	110 ± 15	46	1,319
IV-16	0-5	260 ± 24	460 ± 40	56	31,400
II-14	0-5	330 ± 30	370 ± 32	11	1,256
II-17	0-1	970 ± 70	930 ± 62	4.2	1,256
Average		230		41	4,491

APPENDIX 3

ROCKY FLATS REPORT

INTRODUCTION

The following discussion presents assumptions and methodology used to evaluate the plutonium content of soil around the Rocky Flats Plant (RFP), Colorado. An important issue which this analysis hopefully will begin to define involves determining which sampling methodology has less variability. A second question is whether plot or subsample variability is of the same order as that observed over the entire sample site.

Although data for plutonium in soil have been observed to have a log-normal distribution, no transformation was made in this study. The number of samples per sample location are five or less and Denham and Waite (1975) note, for about 10 or less observations, no specific population distribution is superior. The sample sites were subdivided into sample plots which were assigned at random to collecting parties. Special collections were made on selected plots which are reflected as subsamples in subsequent discussions. For each data set, the following parameters were calculated: mean, standard deviation, variance, and coefficient of variation.

The sample design was based on four distinctly different pedological and geomorphological sites at varying distances and bearings from the RFP. Therefore, the relative contribution of RFP plutonium versus worldwide fallout is variable; and it is important, therefore, to keep inference about a specific block applicable to just that sampling block. Table 1, in the text, gives a list of plutonium results and statistics for each data set.

The two methods of soil sampling were for the upper 1-cm and 5-cm intervals. The means of the 5-cm sample results appear to be inherently larger than those for the 1-cm samples and the variances appear to be correspondingly larger as well. Before comparing variances on plutonium concentrations for the 1- and 5-cm samples, the results were pooled and a Pearson product correlation coefficient was calculated to test whether mean values and variances were independent (Koch and Link, 1971a). The coefficient computed, 0.913, was significant at the 95 percent confidence level ($t = 5.482$, $df = 6$). The dependence of the variances on the means can also be shown by a linear plot of these values. Therefore, the variances are not independent of the sample means and the direct comparison of variances is inappropriate in assessing technique variability.

In order to compensate for variance dependency on the mean between the 1-cm and 5-cm sampling procedure, the sample coefficient of variation

was used. This coefficient is simply the standard deviation divided by the mean and is particularly useful in defining the degree of spread of samples with widely different means (Wine, 1964).

Koch and Link (1971b) present a technique for comparing two coefficients of variation for data sets with large sample sizes. They suggest that the coefficient of variation is approximately normally distributed. They present a test statistic for determining whether two coefficients of variation can be considered to be drawn from populations with the same population coefficient. This same test statistic was used, but to accommodate the small sample size, the more general t distribution was used. However, inequality in sample variances causes the test statistic to no longer follow the student t distribution; therefore, the confidence level was adjusted following a procedure given in Snedecor and Cochran (1976; pp. 115-116). It is not known whether these modifications of the test are appropriate or valid. Conclusions resulting from the procedure given about should be considered to be tentative and suggestive and are certainly not definitive. The computation equation used was:

$$t' = \frac{C_1 - C_2}{\left(\frac{C_1^2 \, (1+2C_1^2) \, (df_1/N_1)}{2df_1} + \frac{C_2^2 \, (1+2C_2^2) \, (df_2/N_2)}{2df_2} \right)^{1/2}}$$

Where t' is the test statistic and the level of significance is approximated by using the t table and calculations outlined in Snedecor and Cochran (1976; pp. 115-116). C_1 and C_2 are the coefficients of variation for sample groups one and two (i.e., the top 1-cm and 5-cm sampling, respectively); df_1 and df_2 are the number of degrees of freedom associated with variance calculation for sample groups one and two; and N_1 and N_2 are the number of observations in each group. When t' exceeds the critical value, the significance between the two coefficients is denoted at some preselected confidence level and the ruling hypothesis is rejected and the alternate hypothesis is accepted.

Site I

The sampling coefficient of variation for the 1-cm samples was 0.688 as compared to 0.471 for the 5-cm samples. The ruling hypothesis is that the coefficient of variation for the 1-cm samples is the same as that for the 5-cm samples at Site I. The alternate hypothesis is that the coefficient of variation for the 1-cm samples is not the same as that for the 5-cm samples. The t' statistic for comparing these two coefficients of variation is 1.53 with four degrees of freedom. The critical value at the 95 percent confidence level is 3.18. Therefore, the ruling hypothesis is not rejected.

Site II

The sampling coefficient of variation for the 1-cm samples was 0.177 as compared to 0.265 for the 5-cm samples. The ruling hypothesis is that

the coefficient of variation for the 1-cm samples is the same as that for the 5-cm samples at Site II. The alternate hypothesis is that the coefficient of variation for the 1-cm samples is not the same as that for the 5-cm samples. The t′ statistic for comparing the two coefficients of variation is 6.21 with four degrees of freedom. The critical value at the 95 percent confidence level is 3.18. Therefore, the ruling hypothesis is rejected and the alternate hypothesis is accepted.

Site III

The sampling coefficient of variation for the 1-cm sampling was 0.390 as compared to 0.29 for the 5-cm samples. The ruling hypothesis is that the coefficient of variation for the 1-cm samples is the same as that for the 5-cm samples at Site III. The alternate hypothesis is that the coefficient of variation for the 1-cm samples is not the same as that for the 5-cm samples. The t′ statistic for comparing the two coefficients of variation is 2.33 with four degrees of freedom. The critical value at the 95 percent confidence level is 3.18. Therefore, the ruling hypothesis is not rejected.

Site IV

The sampling coefficient of variation for the 1-cm sampling was quite large, at 0.428 compared to the small value of 0.191 for 5-cm sampling. Again, the ruling hypothesis is that the coefficient of variation for the 1-cm sampling is the same as that for the 5-cm samples. The t′ statistic for comparing the two coefficients of variation is 6.71 which is larger than the critical value at the 95 percent confidence level of 3.18. Therefore, the ruling hypothesis is rejected and the alternate hypothesis that the coefficients are not equal is accepted.

SUMMARY

Assessment of the coefficients of variation of sampling depths, treating each plot independently, and using t′ seems to indicate significance in some sites, not in others. Considering the clouded validity of using t′, an alternate method of assessment of the coefficients of variation was considered.

For paired samples (in this case, the paired coefficients of variation for each site), the Wilcoxon signed rank test (Gibbons, 1976; pp. 131-137) can be helpful in defining a possible level of significance to the count of the direction of differences in paired data. In this case, the probability that only one data pair out of four pairs indicates a difference in a direction opposite of the other three (i.e., $C_5 > C_1$ (Site II) as opposite $C_1 > C_5$ (Sites I, III, and IV)) is 0.25. Even if all pairs had been in the same direction (i.e., $C_1 > C_5$ in all cases), the

probability would be 0.12 to accommodate the small sample size. In conclusion, there appears to be only weak confirmation of the ruling hypothesis (i.e., variability of 1-cm and 5-cm samples are the same). The numeric trend of the data is shown in Figure 5 of the text and discussed in the associated text.

PRELIMINARY MODEL OF PLUTONIUM TRANSPORT BY WIND AT TRINITY SITE

A. F. Gallegos

Los Alamos Scientific Laboratory
Los Alamos, New Mexico

ABSTRACT

A preliminary analysis of available data from Los Alamos Scientific Laboratory ground zero (GZ) study area at Trinity Site is discussed in an effort to develop a wind-driven plutonium transport model. The analysis reveals a dominant effect of precipitation in explaining variation in the data, although its product with normalized solar radiation pattern gives a much lower sum of squared residuals (SSR) from the regression line. The square of the average diurnal windspeed at the site was also observed to reduce the SSR further, but not to the extent expected relative to other factors. Failure to find significant plutonium concentration differences in collected dust (as a function of time and sampling height of Bagnold sampler collectors) made possible the formulation of a prediction equation for plutonium flux at GZ, using the product of the predicted dust flux at the site with the mean plutonium concentration for the dust samples analyzed.

INTRODUCTION

An objective of the Trinity Site studies is to characterize environmental transport processes governing the distribution of plutonium initially deposited as a result of fallout from the atomic bomb test in 1945 (Larson *et al.*, 1951; Hakonson and Johnson, 1974). Studies were begun on wind-driven soil transport processes using Bagnold dust samplers. This report summarizes dust flux data for ground zero (GZ) site location 1.6 km northeast of the Trinity crater along the fallout pathway, and examines the relationship between soil flux and plutonium flux, as well as other environmental parameters, using analysis of variance and regression analysis methods.

SITE CHARACTERISTICS

Trinity Site is located at the northern end of the Tularosa Basin in south-central New Mexico. The region is characterized by low annual precipitation (20-25 cm), high summer temperatures which commonly exceed 37° C. (mean annual temperature of 15° C.), and severe erosion on exposed ground surfaces. Rainfall accounts for about 90% of annual precipitation at the site, which is situated on flat relief at an elevation above mean sea level of 1,500 m. The area supports grass and shrub vegetation with a ground cover between 15-25%.

Soils at GZ are characterized as sandy loam with low soil organic carbon (about 0.5%) and a cation exchange capacity (CEC) of about 17 meg/g dry soil. The plutonium concentration ranges from about 1 pCi/g dry soil in the upper 2.5 cm soil to less than 0.01 pCi/g at lower soil depths (Nyhan *et al.*, 1976). Also, about 98% of the plutonium activity and 78% of the soil mass is associated with particles between 100-2,000 μm in diameter in the upper 2.5 cm of soil. The range in plutonium concentration for these particles is between 1-5.3 pCi/g with a coefficient of variation exceeding 1.2 (Nyhan *et al.*, 1976).

METHODS AND MATERIALS

The measurements at the site were partitioned into 30- to 40-day intervals for determination of mean diurnal temperature and windspeed, soil moisture fraction for the upper 2.5 cm of soil, total precipitation accumulation greater than 0.025 cm, and dust mass collections using the Bagnold sampler installed at the site; the latter were submitted for $^{239,240}Pu$ analysis. Windspeed and temperature measurements were made with an MRI continuous recording instrument, and precipitation was measured in 0.025-cm increments with an MRI precipitation collector. The anemometer of the MRI was placed 75 cm above the ground surface corresponding to the maximum height of the fifth collecting compartment of the Bagnold sampler. The Bagnold sampler was set to orient to windspeeds greater than 313 cm/sec (7 mph).

Because most of the MRI data has not been reduced from the charts, a representative subset was taken for preliminary analysis as it was not possible to consider the total data base at this time. Data were selected from charts beginning with the last complete day and every seventh day previous in each measurement interval. Data abstracted from the charts on the selected days were taken at 0200, 0800, 1600, and 2300 hours for windspeed and temperature measurements.

Soil moisture was measured gravimetrically at random selected locations within 50 m of the equipment installation to a depth of 2.5 cm mentioned earlier. Dust samples from the Bagnold sampler were dried at 100° C. for 24 hours prior to mechanical sieving through a sonic sifter to estimate fractions above and below 53 μm diameter.

RESULTS

The reduced data for precipitation, soil moisture, windspeed, and temperature are presented in Table 1. Bagnold data, summarized in Tables 2 and 3, were expressed as dust flux (μg/cm^2/day) and Pu concentrations (pCi/g dry dust); the values represent estimated integral averages for each time interval. Table 4 also includes the fraction of the dust particles collected with diameters greater than 53 μm to compare with soil sampling results at the site (Nyhan *et al.*, 1976). Dust flux was also estimated separately for ground creep events (C_c), saltation processes (C_s), and for total flux (C_t).

Multiple and simple linear and curvilinear regression analyses were applied to the dust flux data assuming a soil erosion relationship stating that the local wind erosion factor varies directly with the cube of the wind velocity, and inversely with the cube of the soil moisture content (Chepil and Woodruff, 1963). Additionally, the model includes an effect of air temperature near the ground on dust flux based on the relationship between heat flux from soil to air and soil moisture content via evapotranspiration (Geiger, 1965; Change *et al.*, 1965; Baver, 1964). Heat flux from soil to air was assumed to be proportional to the fourth power of the absolute temperature of air near the ground because of its relationship to soil temperature at the surface of the ground, which is so dependent.

Precipitation was assumed to affect dust flux through its effect on soil moisture status, soil crustal formation and dissolution, raindrop impact energy, and sheet water erosion in the lower collectors (Baver *et al.*, 1972).

Our initial hypothesis was that dust flux would be related to the parameters described above by a relationship of the form (Baver *et al.*, 1972; Wischmeier *et al.*, 1958):

$$C_{c,s,t} = b_1 PT^4 M^{-3} U^3 \qquad (1)$$

where

$C_{c,s,t}$ = dust flux for specified collectors (ground creep (c), saltation (s), and total (t)) μg/cm^2/day (Table 2)

b_1 = proportionality constant (regression coefficient)

Table 1. Reduced Parameters for Use in Regression Analysis

Julian Date	P	M	MA	U (C.V.)	T (C.V.)
140-172	1.118	-	-	239.4(.50)	23.61(.22)
172-194	0.914	-	-	231.9(.26)	27.67(.15)
194-221	6.630	-	-	169.0(.62)	23.85(.18)
221-264	1.980	0.0163	-	159.1(.67)	23.35(.67)
264-299	2.210	0.0397	0.0280	139.7(.75)	12.64(.28)
299-333	0.381	0.1226	0.0812	117.1(1.22)	-0.333(.63)
333-361	0.025	0.0203	0.0715	150.0(1.11)	-3.404(.36)
361-27	0.229	0.0380	0.0292	114.6(.91)	-0.6597(.40)
27-54	1.168	0.0187	0.0284	113.4(1.90)	2.847(.35)
54-83	0.025	0.0117	0.0152	251.5(.54)	9.340(.25)
83-118	2.057	0.0213	0.0165	177.7(.56)	12.35(.25)
118-151	0.4572	0.0150	0.0182	267.4(.63)	22.92(.20)
151-180	0.1524	0.0097	0.0123	245.9(.56)	26.49).16)
180-210	2.743	0.0239	0.0168	178.0(.62)	23.78).17)
210-243	2.464	0.0218	0.0229	176.3(.66)	23.88(.18)
243-273	3.150	0.0471	0.0345	172.7(.62)	21.67(.21)

P = total precipitation during time interval, cm

M = soil moisture fraction at end of time interval

MA = soil moisture fraction average between beginning and end of time interval

U(C.V.) = mean diurnal windspeed, cm/sec, during time interval. C.V. = coefficient of variation

T(C.V.) = mean diurnal air temperature, ^{o}C, for time interval 75 cm above ground with coefficient of variation, C.V.

Table 2. Dust Flux by Collecting Compartments of Bagnold Sampler ($\mu g/cm^2/day$)*

Julian Date	C_c	C_1	C_2	C_3	C_4	C_5	C_t
				C_s			
140-172	1172	1125	120.1	39.87	36.33	1.584	2495
172-194	1565	1273	304.8	58.80	47.70	1.152	3255
194-221	4170	1985	330.0	60.39	17.33	4.938	6585
221-264	1320	770.1	180.8	58.38	1.923	9.549	2341
264-299	591.6	352.8	76.92	21.79	0	0	1043
299-333	357.9	615.6	99.60	57.57	31.74	34.71	1197
333-361	2.238	7.143	0.618	0.762	0.381	0.426	11.57
361-27	23.61	12.26	2.925	3.399	0.345	8.379	49.41
27-54	299.7	255.4	86.76	62.85	39.60	42.03	786.3
54-83	73.71	94.62	26.43	26.43	9.999	10.98	235.6
83-118	579.3	404.1	94.23	29.29	15.27	14.58	1137
118-151	292.1	285.1	52.86	20.53	10.55	3.516	664.5
180-210**	3273	2312	394.2	97.77	29.78	46.26	6153
210-243	1092	582.3	126.3	37.83	13.13	14.10	1866
243-273	1142	371.4	78.48	34.83	4.302	21.25	1652

*All fluxes scaled over total collecting surface (75 cm^2).

**Determined to be outlier using method of Tietjen, 1978.

C_c, C_s, and C_t = soil creep, saltation, and total dust fluxes, respectively.

C_1, C_2,...C_5 = collecting surfaces of 15 cm^2 (1 cm wide) each; the mid-heights of these surfaces (Z) are 7.5, 22.5, 37.5, 52.5, and 67.5 cm, respectively. C_c represents a horizontal collecting surface 7 cm^2 (1 cm wide).

Table 3. Plutonium Concentrations ($^{239,240}Pu$) and Soil Size Fractions in Bagnold Samples From GZ Site

Julian Date	A	F	A	F	A	F	A	F	A	F	A	F
	C_c		1		2		3		4		5	
140-172	.0112	.9689	.1470	.9689	.1658	.9749	.0874	.9598	.1935	.9871	5.789	-
172-194	1.029	.9410	.4117	.9871	2.683	.7288	.0532	.9840	.3258	.9419	9.474	-
194-221	.3040	.9029	.3088	.9343	3.570	.9389	.0450	.9802	.1425	.7936	.5000	.8460
221-264	.9492	.7865	.7518	.7591	6.385	.7669	.0271	.5971	.8333	-	.1623	-
264-299	5.370	.6735	.1929	.3394	.6941	.4335	1.033	.5919	-	-	-	-
299-333	4.127	.9625	.8790	.9395	.3291	.9396	.5572	.8045	.7040	-	.2479	-
333-361	-	-	-	-	-	-	-	-	-	-	-	-
361-27	-	-	-	-	-	-	-	-	-	-	-	-
27-54	.8059	.9391	3.198	.9274	.0860	.8523	.0342	-	.0543	-	.6379	-
54-83	.1938	-	4.082	-	2.703	-	.1199	-	.9524	-	.8658	-
83-118	.0563	.9297	1.680	.9297	.4199	.8522	.0734	-	.1408	-	.1475	-
118-151	.8197	.9733	5.786	.9613	4.497	-	.0984	-	1.034	-	.5747	-
151-180	-	.9585	-	.9639	-	-	-	-	-	-	-	-
180-210	-	.9613	-	.9565	-	-	-	-	-	-	-	-
210-243	-	.9607	-	.9743	-	-	-	-	-	-	-	-
243-273	-	.9370	-	.8616	-	-	-	-	-	-	-	-

C_c = soil creep collecting compartment.

C_s = saltation compartments 1, 2, 3, 4, and 5.

A = $^{239,240}Pu$ activity, pCi/g dry soil.

F = fraction of dust particles greater than 53 μm.

Table 4. Predicted Plutonium ($^{239,240}Pu$) Flux at GZ Site (aCi/cm^2/day)*

Julian Date	C_1	C_2	C_3	C_4	C_5
183**	2187	192.9	62.39	29.66	17.02
208	7984	704.4	227.8	108.3	62.14
243	1657	146.2	47.26	22.47	12.89
282	803.1	70.85	22.91	10.89	6.250
316	37.09	3.272	1.058	0.503	0.289
347	0.516	0.046	0.015	0.007	0.004
12	1.729	0.153	0.049	0.023	0.013
33	56.40	4.975	1.609	0.765	0.439
69	22.73	2.005	0.648	0.308	0.177
101	1717	151.4	48.97	23.28	13.36
135	1236	109.0	35.25	16.76	9.620
166	402.9	35.54	11.49	5.464	3.135
195	3812	336.3	108.7	51.70	29.67
227	2905	256.3	82.88	39.40	22.61
258	2606	229.9	74.34	35.34	20.28

*All fluxes scaled over total collecting surface (75 cm^2).

**Represents mean Julian Date for interval in question. Collector 1 includes soil creep compartment.

P = accumulated precipitation during time interval, cm (Table 1)
T = absolute diurnal temperature, ^{o}K (Table 1)
M = mean moisture fraction in upper 2.5 cm soil (Table 1)
U = mean diurnal windspeed, cm/sec (Table 1)

or by a relationship containing some combination of these independent variables. A modified model would be possible if significant covariance existed between parameters as might be expected for those factors relating to soil moisture.

Subsequent analysis revealed that the independent variables (PT^4) provided the best fit of the data for total (C_t), saltation (C_s), and ground creep (C_c) processes. Ground creep gave the best overall fit:

$$C_c = 7.32 \times 10^{8} PT^4 \quad (r = .950,\ F = 131,\ p < 0.01) \qquad (2)$$

where

r = correlation coefficient
F = Statistic for testing significance of the regression
P = probability of obtaining a value of F this large by chance alone

A relationship of the form:

$\ln (C_c) = b_1 \ln (M) + b_2 \ln (U) + \ln (P) + 4 \ln (T)$, was fitted to obtain estimates for soil moisture and windspeed exponents for an unconstrained model fit. Only windspeed gave a significant partial regression coefficient ($b_2 \simeq 2$, $p < 0.01$), and incorporation of windspeed into the model gave:

$$C_c = 2.50 \times 10^{-12} PT^4U^2 \quad (r = .966,\ F = 200,\ p < 0.01). \qquad (3)$$

Addition of this term decreased the sum of squared residuals (SSR) from the regression line by 32%. Calculation of the percentage reduction in SSR when eq. 3 is used to replace eq. 2 was used to determine whether the former model fit the data significantly better. This is inferred by estimating the following statistic:

$F = [(SSR_2 - SSR_3)/(D_2 - D_3)] \ / \ (SSR_3/D_3)$, where

SSR_2, SSR_3 = sum of squared residuals for eq. 2, eq. 3, respectively

D_2, D_3 = degrees of freedom for eq. 2, eq. 3, respectively.

Application of this technique to the models shows that eq. 3 is a significantly better fit ($F = 6.7$, $p < 0.05$) to the data than is eq. 2. Note that eq. 3 has one degree of freedom less than eq. 2 because of the additional change in the unconstrained equation.

A regression of mean diurnal temperatures for each time interval with the normalized sinusoidal solar radiation pattern for the western hemisphere present at GZ gave the fit:

$$T = 271.9 + 14.2S_{90} \quad (4)$$
$$(r = .965,\ F = 187.7,\ p < 0.01)$$

where

T = absolute mean diurnal temperature, ^{o}K, and

S_{90} = (Sin $[2\pi\ (JD - 90)/365] + 1$), where

JD = Julian day number, 1,2,3,.....365.

The pattern yields a maximum value on a Julian day corresponding to the summer solstice in the western hemisphere. Since the pattern of absolute temperature to the fourth power also produced a similar fit ($r = .960$, $p < 0.01$) with radiation pattern, a new model for predicting dust flux was obtained by substitution of S_{90} for T^4 in eq. 2:

$$C_c = 337.5\ PS_{90} \quad (5)$$
$$(r = .970,\ F = 221,\ p < 0.01),\ \text{or to replace eq. 3:}$$

$$C_c = 1.12 \times 10^{-2} PS_{90}U^2 \quad (6)$$
$$(r = .979,\ F = 323.\ p < 0.01).$$

The windspeed term reduced the SSR by 30%, and a percentage reduction in SSR by using eq. 6 over eq. 5 was significant ($F = 6.05$, $p < 0.01$) in providing a better fit to the dust flux data. A comparison of all models (eqs. 2, 3, 5, and 6) shows declining SSRs of (2,565,603), (1,734,597), (1,579,617), and (1,103,166), respectively. Since eq. 3 fits better than eq. 2, and eq. 6 fits better than eq. 5, then eq. 6 fits significantly better than any of the other models. A plot of observed dust flux for the soil creep compartment C_c is compared with calculated values from eqs. 5, 6 is presented in Figure 1.

The explained variation in dust flux in all model equations is primarily explained by precipitation:

$$C_c = 550.8P \quad (7)$$
$$(r = .940,\ F = 107,\ p < 0.01);$$

a discussion of the possible causes for this effect is presented later in this report. Complementary equations for dust flux considering

Figure 1. Predicted and Observed Dust Flux For Soil Creep Compartment At GZ Site.

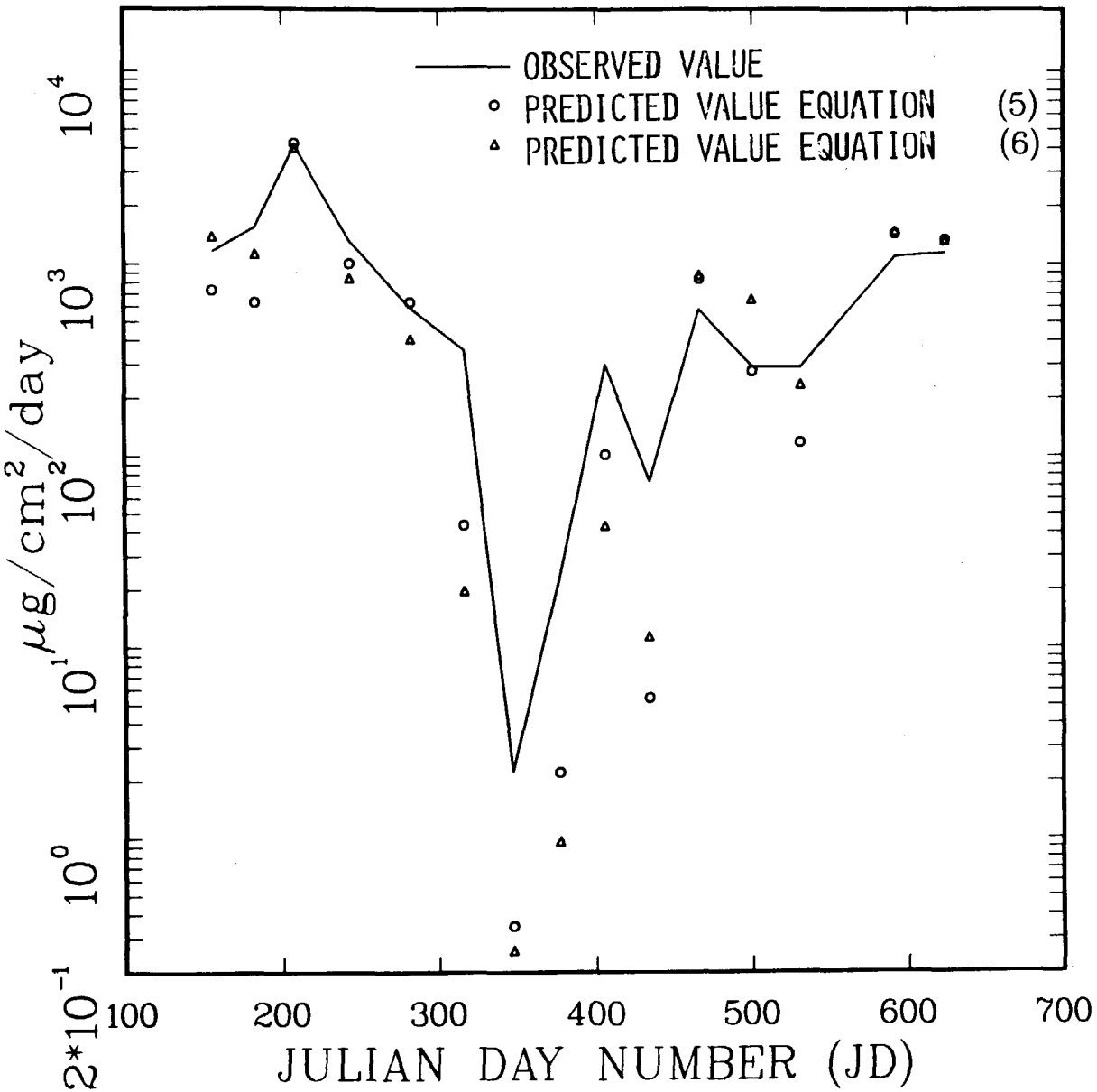

saltation events C_s, and total dust flux C_t yielded similar, but poorer fits:

$$Cs = 7.58 \times 10^{-3} PS_{90}U^2 \quad (8)$$

($r = .902$, $F = 61$, $p < 0.01$), and

$$C_t = 1.88 \times 10^{-2} PS_{90}U^2 \quad (9)$$

($r = .960$, $F = 164.1$, $p < 0.01$); where

C_s = sum of all five saltation compartment dust collections

C_t = sum of ground creep and saltation compartment collections.

The distribution of dust flux with height above the ground surface is shown in Table 2. A good fit between cumulative fractional dust flux over all time intervals, and midheight (Z) of each collector compartment of the Bagnold sampler was obtained:

$$F_t = 76.45Z^{-2.21} \quad (10)$$

($r = .999$, $F = 29117$, $p < 0.01$)

where

F_t = fraction of dust flux at height Z for saltation and soil creep processes combined

Z = midheight of collecting surface, cm.

A similar fit was obtained when saltation dust flux alone was considered:

$$F_s = 28.43Z^{-1.79} \quad (11)$$

($r = .999$, $F = 1488$, $p < 0.01$)

where

F_s = total saltation flux from all five collecting compartments.

Good fits were also obtained when collector fractions were compared:

$$C_t = 1.75C_c \quad (12)$$

($r = .992$, $F = 61.26$, $p < 0.01$),

$$C_t = 2.23C_s \quad (13)$$

($r = .987$, $F = 36$, $p < 0.01$), and

$$C_c = 1.23C_s \quad (14)$$

($r = .958$, $F = 11.2$, $p < 0.01$).

Analysis of variance was applied to the $^{239,240}Pu$ concentration and particle fractionation of dust samples in the compartments of the Bagnold sampler assuming equal variance over type and range of treatments used. The results of these analyses show that there was not a significant concentration difference ($p < 0.05$) across collector height, nor a difference in concentration across sampling intervals ($p < 0.05$). However, the particle size fractions greater than 53 μm diameter was significantly different across sampling intervals ($p < 0.05$), although not significant across collectors ($p < 0.05$). In the former comparison, only two of the particle fractions (0.7274, 0.5096) were significantly different from all other fractions, and from each other ($p < 0.05$). A mean $^{239,240}Pu$ concentration of 1.33 pCi/g dry soil was used to estimate plutonium flux using eqs. 9, 10 for any given saltation compartment:

$$C_i = 1.91 P S_{90} U^2 Z_i^{-2.21} \qquad (15)$$

where

C_i = Pu flux for ith saltation compartment, $pCi/cm^2/day$

Z_i = midheight of ith saltation compartment from ground level.

Application of this equation over all saltation compartments and time intervals is presented in Table 4. The first compartment, C_1, includes the soil creep contribution, and the plutonium concentration has a coefficient of variation of 1.5 for all determinations.

DISCUSSION

Statistical treatment of GZ data at Trinity Site indicates a number of important factors to consider when attempting to model both dust and plutonium flux at the site. It is observed that a cross-product of parameters rather than the individual ones provides better fits to observed data. Comparison of eq. 1 with those ultimately derived (eqs. 3, 5, 6) for predicting dust flux shows that accumulated precipitation, solar radiation pattern, and diurnal windspeed energy (Healy, 1974) are important interacting parameters when time intervals of about 30 days are used as sampling intervals. Since solar radiation input at the site is related to S_{90}, and also to evapotranspiration rate (Change *et al.*, 1965), it appears to be a better predictor of soil moisture status than either mean diurnal air temperature near the ground or observed soil moisture content at the beginning and end of a sampling interval. It is possible that actual measurement of solar radiation input and/or measurement of soil surface temperatures on a continuous basis would improve the fits.

Windspeed data from GZ is biased in that short-duration, relatively high windspeeds responsible for most of the resuspension of dust are obscured by more frequent and longer-duration lower windspeeds because of the long-distance integration length of the anemometer employed. Inspection of the MRI windspeed data over the intervals used did not reveal the higher-velocity gusts of wind one would expect at the site. This might explain why the prediction equation for dust flux is relatively insensitive to this parameter over long time intervals. Another explanation for low windspeed sensitivity in the prediction equation may be due to the small number of observations used in estimating diurnal windspeed averages, or that the subset used was not representative of windspeed events responsible for the bulk of particle resuspension. Future analysis of the entire data base may answer some of these questions.

The dominant effect of precipitation both individually and as part of a cross-product term in predicting dust flux (eqs. 5, 6, 7) is difficult to explain without further study. It is possible that wind-driven soil events are associated with gusts of wind that surround a precipitation event in addition to particle pickup by raindrop impaction, water erosion into the lower collectors of the Bagnold sampler, or possibly through dissolution of crustal layers that form at the site. The latter might make soil particles more resuspendable after a given rain event until the layer would reform. The breakup of crustal layers by saltation events would also be enhanced under these conditions.

Good fits for the prediction of dust flux fractions above the ground surface (eqs. 10, 11) using Bagnold sampler collections in each compartment over the entire study period, together with the good fits between soil creep and saltation events (eqs. 12, 13, 14), seemingly make possible simpler data collection schemes for predicting dust flux at GZ site. For example, one can obtain an efficient prediction equation for GZ site through the use of eqs. 5, 10, 12, which requires only that precipitation accumulation within each sampling interval be known:

$$C_i = 4.515 \times 10^4 P S_{90} Z_i^{-2.21}. \qquad (16)$$

The simplicity of this equation may be compared to eq. 15, which contained the windspeed term. However, one should use caution in attempting to generalize such a relationship unless checked at other sites with different topography, climate, and soil characteristics. Also, the substitution of solar radiation input for S_{90} would probably improve eq. 16.

The prediction of plutonium flux at GZ site was estimated using the product of the mean plutonium concentration with a dust flux predictor because analysis of variance did not show significant trends in concentration between different time intervals or with height of Bagnold sampling compartments above the ground. The fractionation of soil particles in a similar manner from ground level to 75 cm above the ground is puzzling, as is the almost constant soil fraction of particles greater than 53 μm

diameter throughout the study period. More studies are required to address these problems and to find the specific causes responsible for the large plutonium concentration variations at GZ site.

ACKNOWLEDGMENTS

The author would like to express his appreciation to E. M. Karlen, L. M. Martinez, K. V. Bostick, and T. E. Hakonson of LASL for data collection and sample processing efforts.

REFERENCES

1. Baver, L. D. 1964. "The Meteorological Approach to Irrigation Control." *Hawaiian Planters' Rec.* 54:291-298.

2. Baver, L. D., W. H. Gardner, and W. R. Gardner. 1972. *Soil Physics.* John Wiley & Sons, Inc., New York. pp. 446-451.

3. Change, Jen-hu, R. B. Campbell, H. W. Brodie, and L. D. Baver. 1965. "Evapotranspiration Research at the HSPA Experiment Station." *In:* Proc. 12th Cong. Int. Soc. Sugarcane Technologists. pp. 10-24.

4. Chepil, W. S., and N. P. Woodruff. 1963. "The Physics of Wind Erosion and Its Control." *In: Advances in Agronomy.*

5. Geiger, R. 1965. *The Climate Near the Ground.* Harvard Univ. Press, Cambridge, MA.

6. Hakonson, T. E., and L. J. Johnson. 1974. "Distribution of Environmental Plutonium in the Trinity Site Ecosystem After 27 Years." USAEC Report CONF-730907-P1. pp. 242-247.

7. Healy, J. W. 1974. "A Proposed Interim Standard for Plutonium in Soils." Los Alamos Scientific Laboratory. LA-5483-MS.

8. Larson, K. H., J. H. Olafson, J. W. Neel, W. F. Dunn, S. H. Gorden, and B. Gillooly. 1951. "The 1949 and 1950 Radiological Soil Survey of Fission Product Contamination and Some Soil-Plant Inter-Relationships of Areas in New Mexico Affected by the First Atomic Bomb Detonation." USAEC Report, UCLA-140. pp. 1-83.

9. Nyhan, J. W., F. R. Miera, Jr., and R. E. Neher. 1976. "Distribution of Plutonium in Trinity Soils After 28 Years." *J. Environmental Quality.* 5:431-437.

10. Tietjen, G. L. 1978. Personal Communication. Los Alamos Scientific Laboratory.

11. Wischmeier, W. H., D. D. Smith, and R. E. Uhland. 1958. "Evaluation of Factors in the Soil-Loss Equation." *Agr. Eng.* 39:458-462.

ENVIRONMENTAL INSTRUMENTATION FOR *IN SITU* RADIONUCLIDE ASSAY

L. E. Bruns

Rockwell Hanford Operations
Richland, Washington

ABSTRACT

To adequately characterize and note the movement of radionuclides with time in the Hanford Waste Management Complex, environmental in-field and *in situ* instruments are being developed by Rockwell Hanford Operations. The instruments should be invaluable both from a cost and adequate coverage standpoint. Several field systems have been fabricated for assaying the radionuclides using beta, gamma, neutron, alpha, and X-ray radiation. Others are in the process of being developed or in the planning stage.

INTRODUCTION

An advantage of working with radionuclides is the ability to *in situ* detect very small quantities, amounts below that which is harmful to man. For waste management of radionuclides at Hanford near Richland, Washington, public protection assurance can be enhanced today and in the future by use of environmental *in situ* instruments that can quantify very low to high levels of radionuclides rapidly and inexpensively. This presentation includes advantages of *in situ* instruments, the programs being pursued by Rockwell Hanford Operations, and future work.

Rockwell personnel proposed an environmental instrumentation program in 1973 (Bruns, 1973). This proposal included several mobile vans and other portable systems. Since 1973, temporary mobile equipment was tested and used, available instrumentation was adapted to radionuclide characterization, two van systems have been developed and fabricated, and new concepts have been devised.

ADVANTAGES OF *IN SITU* INSTRUMENTATION

Waste Management Data Base requirements that can be fulfilled by *in situ* instruments are:

- location of contaminated zones;
- measurement of types, concentrations, and amounts of radionuclides and other toxic substances;
- movement with time of toxic substances; and
- measurement of matrix parameters such as void volume, gas buildup due to radiolysis, density, porosity, moisture content, and elemental assay.

Advantages of *in situ* instruments over field sampling, laboratory sample preparation, and analyses are:

- larger "sample" size;
- sample more representative;
- improved statistics;
- cost reductions by 5-10 fold;
- results in minutes *versus* days, months;
- only method known for estimating toxic substance concentrations in heterogeneous matrices;
- better cost effective method for determining movement of toxic substances with time;
- can better detect abnormalities (e.g., smear); and
- better method for emergency situations where rapid assays are required.

ROCKWELL PROGRAM

The following instruments and what they will do constitutes Rockwell's current program.

Beta Assayer

The detector unit is a thin, massless (i.e., no attenuation correction required) gas (90 percent argon, 10 percent methane), proportional counter with multiple aluminum absorbers. On wastes aged ten years or more, laboratory tests show that both strontium-90 and cesium-137 can be assayed in the nanocurie per gram sensitivity range. The counting statistics reliability is a ±10 percent. The unit was completed and tested in the field. It is mounted on a pushcart with large balloon wheels for transport across the desert terrain. The electronics and sensing element are all on the cart, with the power system being supplied by a vehicle with a 110-volt generator.

DEV-VAN-I

This is a van housing an argon dosimeter for measurement of 50 to 1,300 milliroentgens per year, an alpha water meter for assaying below maximum permissible concentration (MPC) levels, several NaI(Tl) portable instruments, a neutron counter with directional probe and the key detector systems, a Ge(Li) collimated unit (see Figure 1), and an L-X-ray system for determining plutonium and americium at nanocurie to picocurie levels. The unit is completed and is being field tested.

DEV-VAN-II

This development van is for in-van core collimated assaying and downhole radionuclide assay. Precision draw works for depth accuracies in the centimeter range are required. A directional system allows 360° coverage using windowed Ge(Li), intrinsic germanium, neutron, and NaI(Tl) detectors. Both plume characterization and movement with time will be determined by DEV-VAN-II at the picocurie to microcurie levels. Figure 2 shows a picture of the van with a boom on the end to allow attaching tools and distance between van and wells to minimize cave-in problems, especially at burial grounds or cribs.

DEV-VAN-III

This van is in the planning stage and involves a californium-252 activation source for determining downhole plutonium and uranium, and various matrix parameters such as density, porosity, void volume, and elemental compositions.

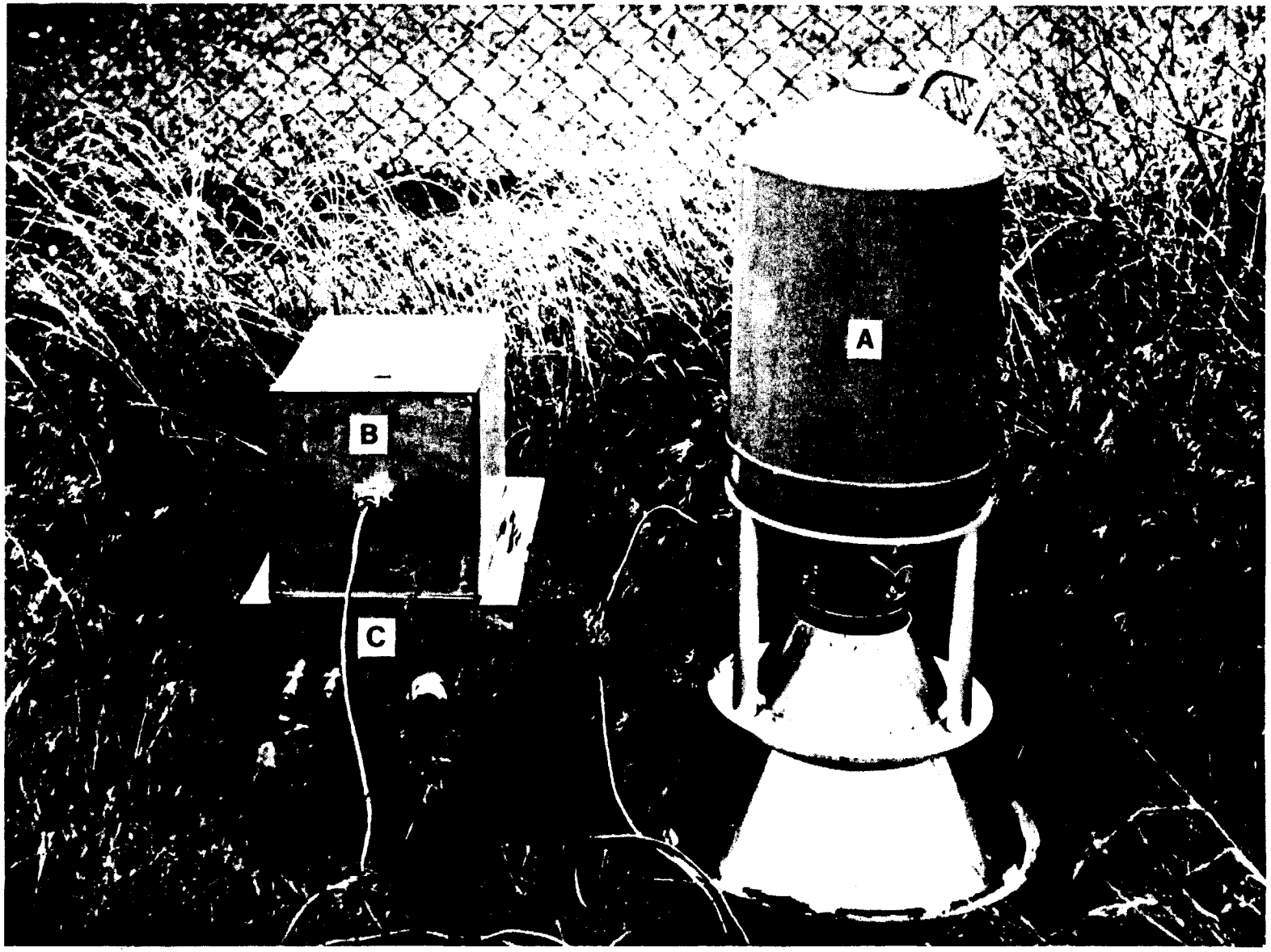

Figure 1. DEV-VAN I Ge(Li) System

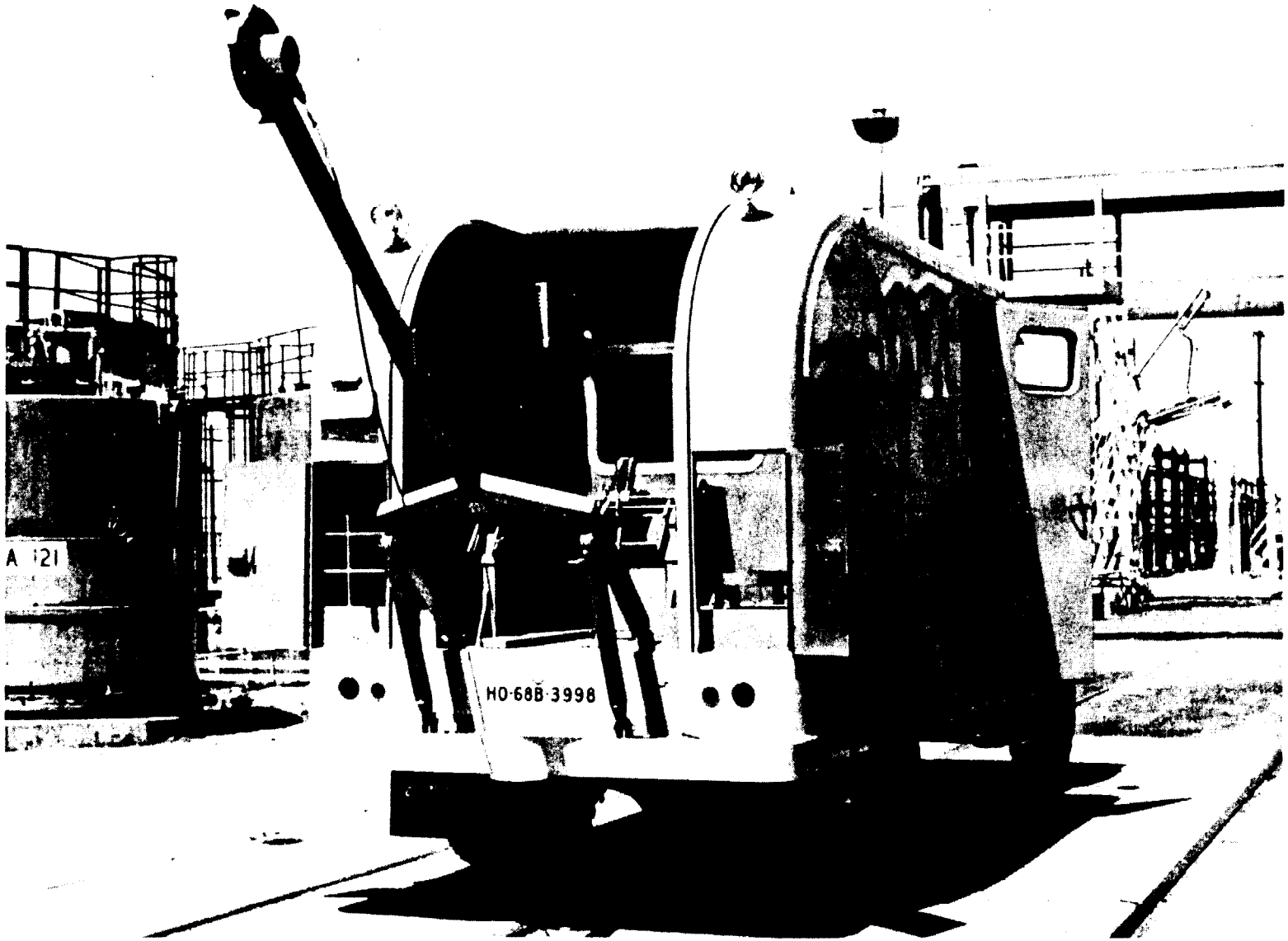

Figure 2. DEV-VAN II

Calibration Facility

To calibrate the above instruments, a calibration facility has been built which consists of a four-quadrant tank and two 4π subsurface systems (see Figure 3). All tanks are 2.4 m deep. The 3.0 m diameter, four-quadrant tank houses four different matrices: control sand, normal backfill sediments, simulated burial grounds, and salt cake. Wells are available (see Figure 3) for sources and detectors. The 4π tanks are 1.2 m in diameter. One contains a mixture of gamma emitters and control sand and the other a mixture of plutonium and sand. The Calibration Facility will be used for attenuation coefficient determinations, calibration of downhole instruments, range of interrogation determinations, effect of moisture, triangulation studies, interference studies, and special studies such as "smear" effects.

Other Systems

Other systems not included in the above are "passive" activation, void volume detectors, and measurement of nonradionuclide toxic substances. "Passive" activation is the use of metal foils downhole to determine the neutron field, and from this the plutonium plus americium can be calculated. The plutonium can then be calculated by subtracting americium as determined by gamma detectors from the total. Foils such as copper, indium, manganese, aluminum, and zinc are used. Several techniques have been explored for void volume measurements such as radar, transfer impedance, and electromagnetic wave probing. The californium-252 system will be studied for measurement of cadmium, mercury, fluoride, and other nonradionuclide toxic substances. Also, chemoluminescence, X-ray fluorescence techniques will be explored for *in situ* assay of toxic substances.

FUTURE

All systems discussed above will be updated as improved detectors, electronics, and computer components become available or are developed. New concepts will be explored, such as *in situ* measurement of cadmium, mercury, fluoride, and chloride by techniques like chemoluminescence and neutron activation. Measurement of tritium and iodine-129 will be explored using *in situ* laser techniques. Real-time gas analyzers for stack gas and resuspension assays will be studied. New uses of *in situ* instruments will be evaluated, e.g., measurement of subsurface grouting coverage by vanadium activation.

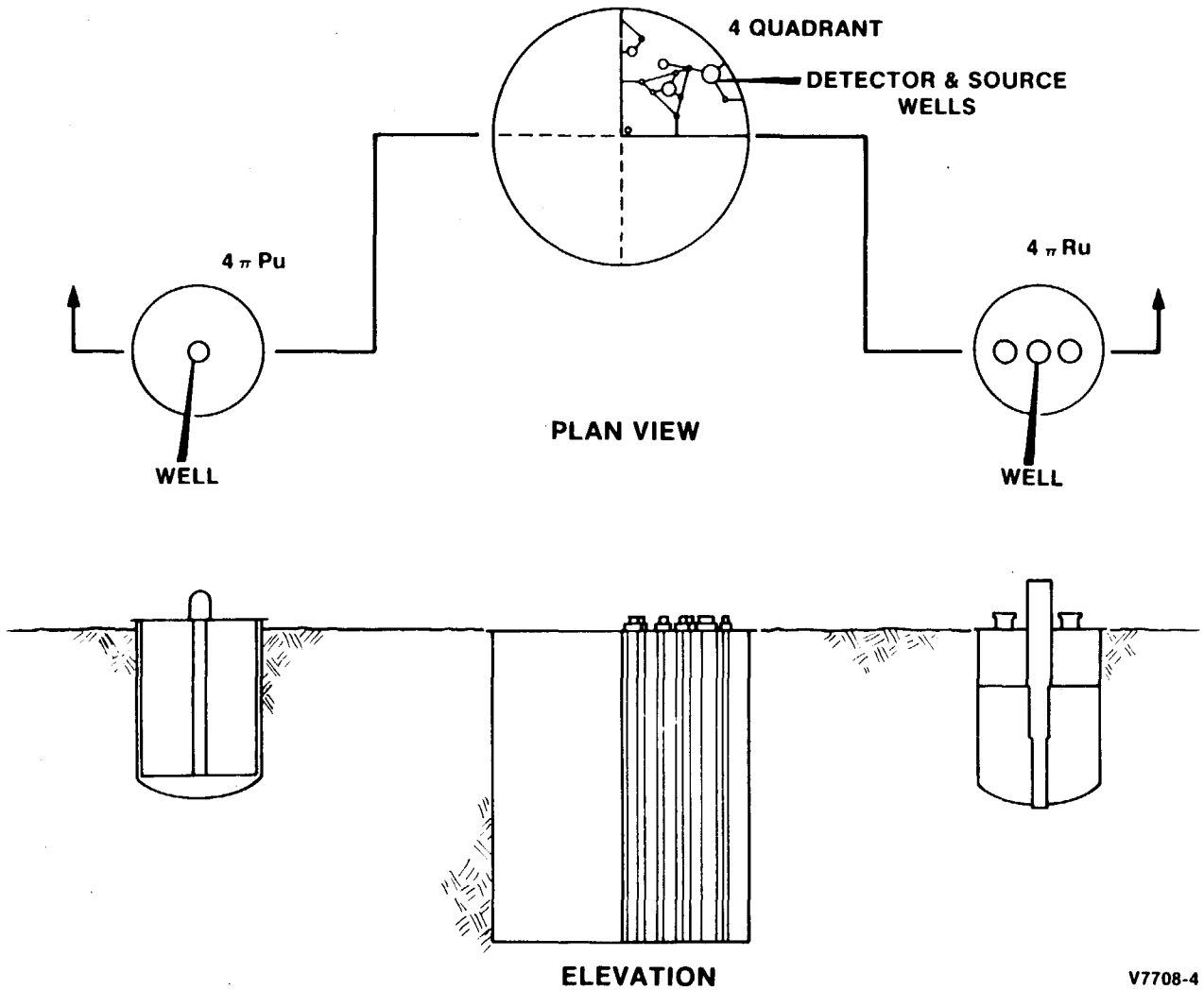

Figure 3. Calibration Facility
(Tank Arrangement)

ACKNOWLEDGMENTS

The author wishes to acknowledge Mr. W. H. Zimmer (now of ORTEC, Oak Ridge), Dr. N. D. Wogman, and Dr. R. L. Brodzinski (of Battelle Northwest Laboratory) for their assistance in technical advisement; to Dr. R. D. Fox (of Rockwell-Hanford Operations) for his assistance on editing and Ms. Trudy Jones (of Rockwell-Hanford Operations) for typing the original paper.

REFERENCE

1. Bruns, L. E. 1973. *Environmental Non-Destructive Radionuclide Assay Program.* Atlantic Richfield Hanford Company, Richland, WA. ARH-2908.

AIRBORNE PLUTONIUM-239 AND AMERICIUM-241 TRANSPORT MEASURED FROM THE 125-M HANFORD METEOROLOGICAL TOWER

G. A. Sehmel

Battelle Memorial Institute, Pacific Northwest Laboratory
Richland, Washington

ABSTRACT

Airborne plutonium-239 and americium-241 concentrations and fluxes were measured at six heights from 1.9 to 122 m on the Hanford meteorological tower. The data show plutonium-239 was transported on nonrespirable and "small" particles at all heights. Airborne americium-241 concentrations on small particles were maximum at the 91-m height.

INTRODUCTION

Studies at Rocky Flats and Hanford have shown that plutonium is resuspended. For the time periods investigated in these studies (Krey *et al.*, 1976; Sehmel, 1977a, 1977b, 1977c, 1978; Sehmel and Lloyd, 1976), airborne plutonium-239 concentrations were above fallout levels but never exceeded 2% of the maximum permissible concentration for individuals, even in an uncontrolled area. Plutonium was transported on both respirable and nonrespirable particles. In controlled areas, plutonium-239 transport occurred to at least a 30-m height. The maximum plume height was unknown and the relative transport on respirable and nonrespirable particles could only be estimated.

Americium-241 could also be resuspended from plutonium resuspension sites. Although americium-241 resuspension has been reported at low-level waste disposal areas on the Hanford area (Sehmel, 1977b, 1977c), there are few reported data showing airborne americium-241 concentrations. Nevertheless, resuspension of americium-241 could become an inhalation concern a hundred years from now after plutonium-241 has decayed to americium-241.

Simultaneous measurements of airborne plutonium-239 and americium-241 concentrations have not been reported outside of exclusion areas. Resuspension studies to date do not suggest differences in resuspension for different radionuclides, but data are limited. Simultaneous measurements of airborne concentrations of both plutonium-239 and americium-241 would indicate similarities which might be expected for different transuranics. Thus, the objectives of this study were to measure simultaneously both plutonium-239 and americium-241 airborne concentrations and fluxes on both nonrespirable and "small" particles for sampling heights up to 122 m.

SAMPLING SITE

The sampling site was at the 125 m meteorological tower located outside the exclusion area on the Hanford area. This site is approximately one km east of the 200W Separation Area fence. Air sampling equipment was located at heights of 1.9, 15, 30, 61, 91, and 122 m.

EXPERIMENTAL PROCEDURE

Air sampling was continuous for all wind speeds and directions for the time period between August 13 and November 12, 1976. Air sampling was with the impactor cowl system shown in Fig. 1 (Sehmel, 1973). The 15 cm diameter cowl inlet was continuously directed into the wind by the wind orientation tail fin. Most of the larger particles (greater than about 10- to 20-μm diameter) entering the inlet subsequently settled within the cowl body. Some larger particles were also collected inside the particle cascade impactor (Sehmel, 1973; Willeke, 1975). Interstage loss particles within the cascade impactor which are retrieved by light brushing are of nonrespirable size. It will be assumed all nonrespirable particles entering the impactor are collected as interstage loss particles. The fraction by weight and by plutonium content of these nonrespirable particles on impactor stage collection is considered to have a minimal influence on the general conclusion of this study.

Particles collected within the cowl plus impactor interstage loss particles are called "large" cowl-collected particles. Cowl-collected particles are assumed to have been collected independent of the air sampling rate.

Although the "small" impactor-collected particles are an index to the respirable airborne particle concentrations, these small particles do contain some nonrespirable particles. These small particles include all

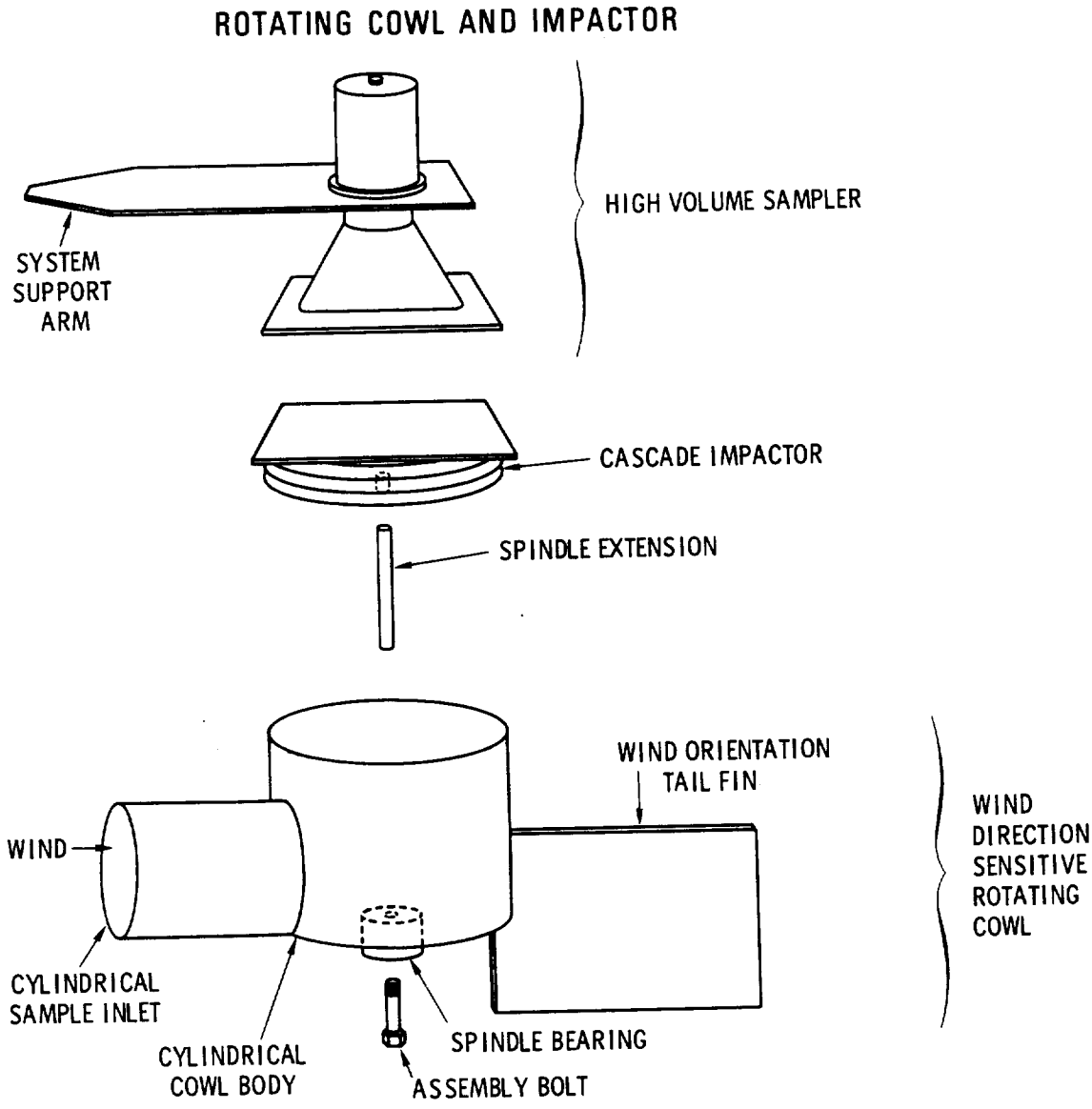
ROTATING COWL AND IMPACTOR
HIGH VOLUME SAMPLER
SYSTEM SUPPORT ARM
CASCADE IMPACTOR
SPINDLE EXTENSION
WIND ORIENTATION TAIL FIN
WIND
WIND DIRECTION SENSITIVE ROTATING COWL
CYLINDRICAL SAMPLE INLET
CYLINDRICAL COWL BODY
SPINDLE BEARING
ASSEMBLY BOLT

Figure 1

particle collection on each cascade impactor stage except for interstage loss particles. Particles were sampled at a flow rate of 0.57 m^3/min and those found on the stages were assumed to be without inertia with respect to sampling efficiency. Thus, small particles were assumed to have followed the sampled air into the cascade particle impactor. For radiochemical analysis, particles collected as interstage losses in the impactors were combined with the large cowl particles.

After sample collection, the impactor* Type "A" fiberglass stage collectors were equilibrated with laboratory humidity (approximately 50% relative humidity), weighed, and all stages and backup filter combined into one "small" particle sample. Particles collected within the cowl and interstage loss particles were brushed off for collection, weighed, and combined into one sample. These "small" and "large" particle samples were analyzed** for plutonium-239 and americium-241.

HORIZONTAL FLUX CALCULATION

Average horizontal airborne plutonium-239 and americium-241 fluxes were calculated from the collected small and large particles. Fluxes are in units of μCi/(m^2 day) for both large and small particles. Two isokinetic sampling assumptions were made for these calculations: (1) for large particles, particle inertia was assumed sufficient to cause particle collection within the cowl inlet for all wind speeds; and (2) for small particles, particles were assumed to be without inertia and followed airflow. For large particles, the flux was calculated from the μCi collected in the cowl (plus interstage impactor loss) divided by the product of cowl inlet cross-sectional area and sampling time. For small particles, the flux was calculated from the product of measured airborne concentration per unit air volume sampled in the impactor, μCi/cm^3, and average wind speed at each sampling height. The average wind speed at each height was: 1.6 m/sec at 1.9 m; 2.9 m/sec at 15 m; 3.4 m/sec at 30 m; 3.7 m/sec at 61 m; 3.8 m/sec at 91 m; and 4.0 m/sec at 122 m.

RESULTS AND DISCUSSION

Airborne plutonium-239 and americium-241 concentrations per unit air volume, concentrations per gram of airborne solid, and horizontal fluxes

---

*Andersen 2000, Inc., Model 65-100 High-Volume Sampler Head, P.O. Box 20769, AMF, Atlanta, Georgia 30302

**LFE Environmental Laboratories, Richmond, California.

were calculated. Calculated results are shown with the one-sigma radiochemical counting statistic limits around each data point. If limits are not shown, the radiochemical counting limits are within the plotting symbol.

Implications of Concentration Profiles

Airborne concentration profiles are the airborne concentrations in either $\mu Ci/cm^3$ or $\mu Ci/g$ as a function of height. In some cases, airborne concentration profiles of plutonium-239 and americium-241 can be interpreted in terms of possible resuspension sources. Concentration profiles are influenced by the extent and variation of the resuspension source, deposition between the resuspension source and sampling location, and by meteorological parameters such as wind speed and atmospheric stability. For example, the concentration profile for an infinite source would show the $\mu Ci/cm^3$ decreasing with increasing height. For an upwind source and simultaneous airborne plume depletion by deposition, the maximum airborne concentration in $\mu Ci/cm^3$ will be at some elevated height. Similarly for airborne concentration profiles in $\mu Ci/g$, the airborne concentration is influenced by sampling both the soil from the contaminant resuspension source as well as airborne soil transported from uncontaminated surfaces. An attempt will be made to interpret the experimental concentration profiles in terms of these possible sources. Each interpretation of the observed concentration profiles carries one qualification: that these average profiles are for samples collected for all wind speeds and directions. Thus, sources of airborne plutonium-239 and americium-241 cannot be identified with respect to direction from the air sampling location.

Small Particle Concentration in $\mu Ci/cm^3$

Airborne concentrations in $\mu Ci/cm^3$ for "small" particles are shown in Fig. 2. The relative plutonium-239 and americium-241 concentrations for "small" particles show distinctly different concentration profiles. The plutonium-239 airborne concentration was 1.4×10^{-17} $\mu Ci/cm^3$ (maximum) at 1.9 m and decreased with increasing height up to 91 m. From 91 m to 122 m, the plutonium-239 concentration increased. In contrast to the decrease, there was a maximum americium-241 concentration of 9.6×10^{-17} $\mu Ci/cm^3$ at a 91-m height.

It is unknown why the plutonium-239 airborne concentration in $\mu Ci/cm^3$ for "small" particles at 122 m was greater than at 91 m. The increased airborne concentration at 122 m is attributed in part to a greater plutonium-239 $\mu Ci/g$ at 122 m than at 91 m. Although the increase is unexplained, an increased concentration was also observed (Sehmel and Lloyd, 1976) at Rocky Flats for sampling heights between 10 and 30 m.

In contrast to the plutonium-239 concentration profile, the americium-241 concentration profile in $\mu Ci/cm^3$ for "small" particles suggests a surface depletion of the airborne plume. This concentration profile indicates either an upwind resuspension source or an elevated release. In any event, the americium-241 source was not determined.

AIRBORNE ^{239}Pu AND ^{241}Am CONCENTRATIONS AT THE HANFORD METEOROLOGICAL TOWER DURING AUGUST 13 TO NOVEMBER 12, 1976 (IMPACTOR STAGES PLUS BACKUP FILTER)

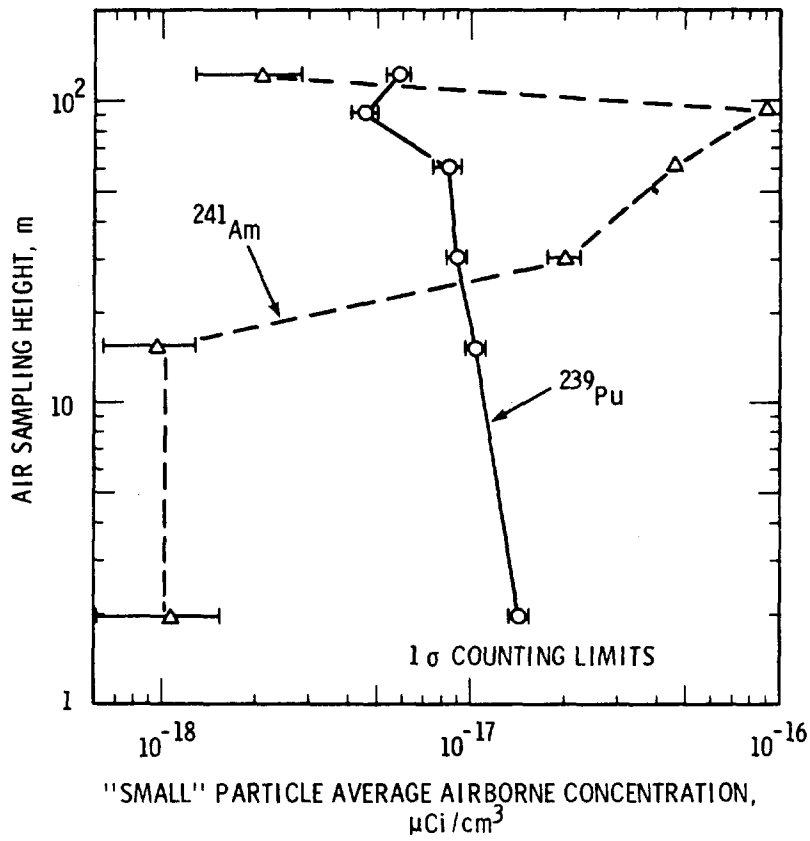

Figure 2

The maximum plutonium-239 concentration was only 0.002% of the maximum permissible airborne concentration (MPC-168hr) for an uncontrolled area (ICRP, 1959). The maximum americium-241 concentration was only 0.005% of the MPC-168hr. For a controlled area, the maximum concentrations were only 0.0002% and 0.002% of the MPC-40hr for plutonium-239 and americium-241, respectively.

Concentrations in μCi/g Airborne Soil

Plutonium-239 and americium-241 concentrations per gram airborne solids were determined for both "small" and "large" particles. Airborne concentrations in μCi/g are shown in Fig. 3 for plutonium-239. The μCi/g for small particles decreased with increasing height up to 91 m. This decrease might be explained by sampling both "more contaminated" locally resuspended particles as well as "less contaminated" soil blowing in from a greater upwind distance. In contrast, for large particles, the maximum μCi/g occurred for a sampling height of 30 to 60 m.

This "large"-particle plume concentration profile in μCi/g might be explained by assuming two possible sources of airborne particles were sampled. For one source possibility, contaminated large particles might be resuspending at a distance upwind and the airborne plume be depleted by dry deposition between the resuspension and sampling site. For the second source possibility, many "less contaminated" particles are resuspended near the sampling tower and are sampled. This less contaminated airborne soil being simultaneously sampled with soil from upwind would decrease the μCi/g.

Relationship: Plutonium-239 on Large Particles and Americium-241 on Small Particles

Airborne concentration profiles in μCi/g are shown in Fig. 4 for americium-241 collected on both "small" and "large" particles. Only two data points are shown for americium-241 transported on large particles. The maximum observed americium-241 concentration on "large" particles was 8×10^{-7} μCi/g at the lowest sampling height of 1.9 m. At the highest sampling height of 122 m, the americium-241 concentration on "large" particles had decreased over one order of magnitude to 2×10^{-8} μCi/g. At intermediate sampling heights of 15 to 91 m, americium-241 concentrations were not significantly different from zero due to the radiochemical counting statistic uncertainties.

The americium-241 μCi/g on "small" particles was minimum and constant at 1.9- and 15-m sampling heights. For greater heights, a maximum of 4×10^{-6} μCi/g was determined at a sampling height of 91 m. A possible explanation for this americium-241 on "small" particles is that resuspension occurs at a distance upwind and the airborne plume is depleted by particle dry deposition between the resuspension and sampling site. Also, many less-contaminated americium-241 small particles might be resuspended near the sampling tower and be collected in the sample. These less contaminated "small" particles would be simultaneously sampled

PLUTONIUM-239 ON AIRBORNE SOLIDS COLLECTED AT THE HANFORD METEOROLOGICAL TOWER DURING AUGUST 13 TO NOVEMBER 12, 1976

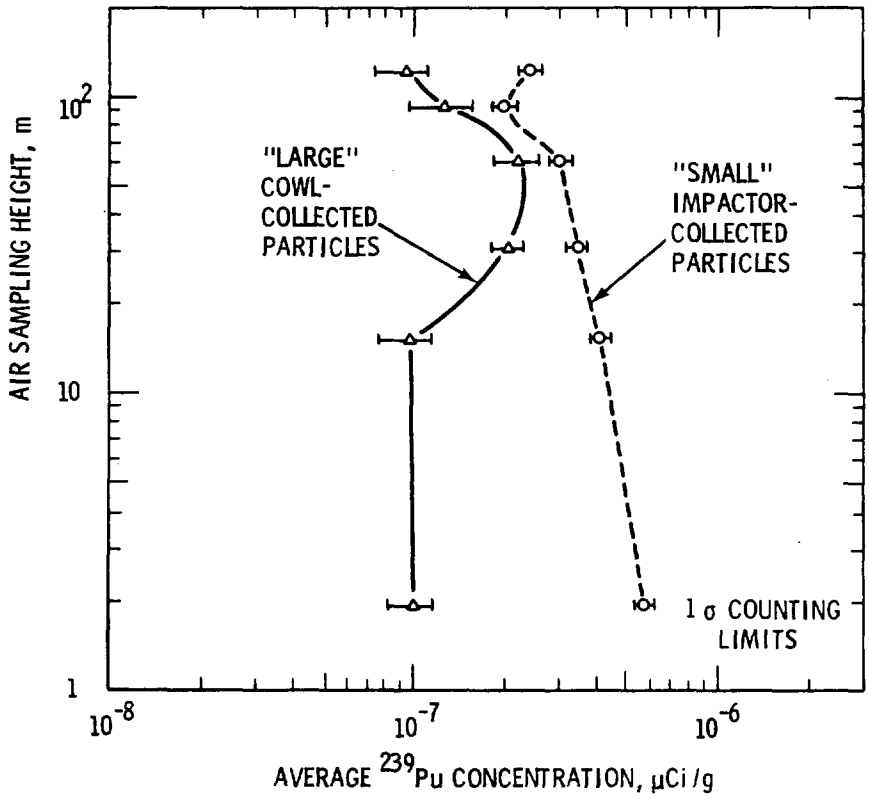

Figure 3

^{241}Am ON AIRBORNE SOLIDS COLLECTED AT THE HANFORD METEOROLOGICAL TOWER DURING AUGUST 13 TO NOVEMBER 12, 1976

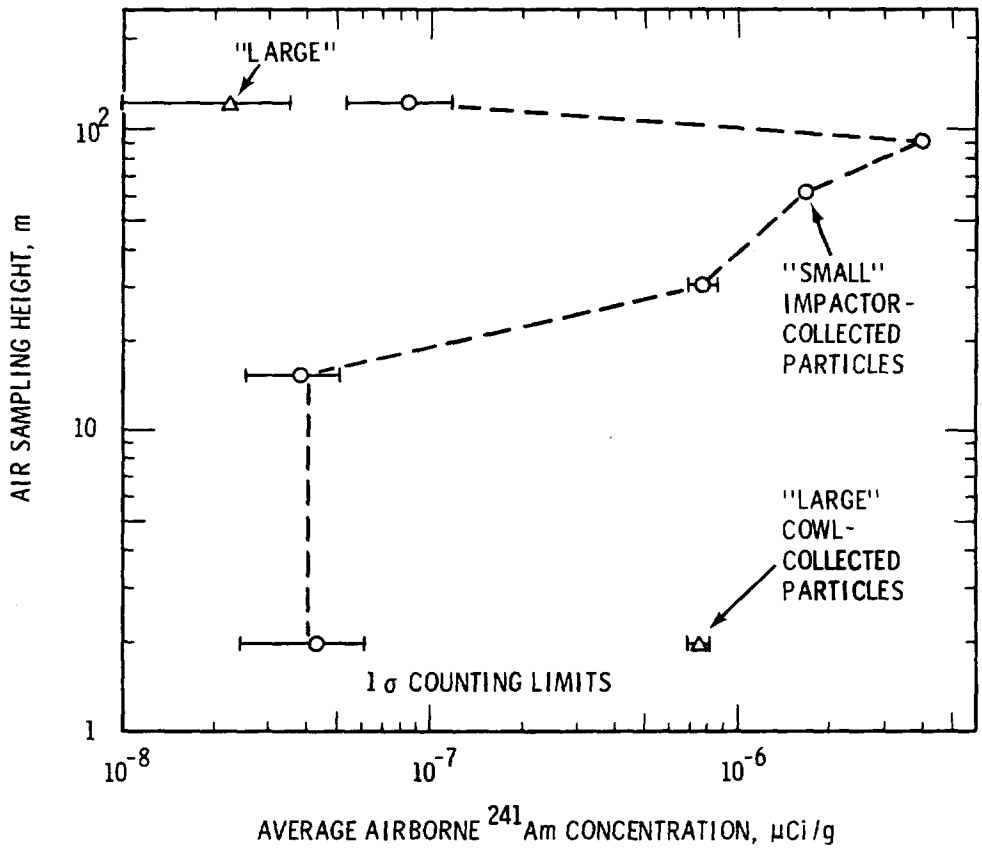

Figure 4

with "small" particles arising from upwind. Consequently, the combined sample of "small" particles would have an average μCi/g value caused by particle dilution from two sources.

In order to direct attention to a possible relationship between plutonium-239 and americium-241 resuspension, a cross comparison of data from Fig. 3 and Fig. 4 is shown in Fig. 5. In this case, the μCi/g for plutonium-239 on "large" particles is shown along with the μCi/g for americium-241 on "small" particles. In both cases, the μCi/g was constant between 1.9- and 15-m sampling heights. For greater heights, the μCi/g increased for both plutonium-239 on "large" particles and americium-241 on "small" particles. This increase was greater for americium-241 on "small" particles than for plutonium-239 on "large" particles. Nevertheless, for both plutonium-239 on "large" particles and americium-241 on "small" particles, the μCi/g decreased rapidly between sampling heights of 91 m and 122 m.

It is unknown why there appears to be a relationship between americium-241 transport on "small" particles at elevated heights as compared to plutonium-239 transport on "large" particles at elevated heights. There are at least three possible explanations for this relationship. The americium-241 and plutonium-239 were originally deposited at the resuspension source in two different size ranges. A second possibility is that plutonium-239 attaches to soil particles more readily than americium-241. The third possibility is there may be some mechanisms by which americium-241 is released from plutonium-239-241 resuspension sources.

Possibly for an aged plutonium resuspension source, sufficient daughter americium-241 has grown in by decay of plutonium-241. During decay, small americium-241 particles could be ejected from the parent plutonium. After ejection, the americium-241 small particles no longer retain their identity with the parent plutonium which may be attached to large particles. Thus, in being resuspended, americium-241 is in a small particle diameter range as compared to the parent plutonium on large particles. Additional plutonium-239 and americium-241 data concerning transport on both large and small soil particles are needed in order to clarify the physics explaining these compared observations.

Average Horizontal Fluxes

Average horizontal fluxes in μCi/(m^2 day) were calculated for both small and large particles. Average horizontal plutonium-239 fluxes are shown in Fig. 6. For large particles, the maximum flux was at a sampling height of 60 m. This maximum flux reflects, in part, the larger μCi/g at this height. The flux on small particles was less than on large particles. On the right side of the figure is shown the percent of the airborne flux on small particles. The plutonium-239 flux on small particles ranged from 32 to 46% of the total calculated flux.

Average horizontal fluxes for americium-241 are shown in Fig. 7. For transport on small particles, the flux was maximum at 5×10^{-7} μCi/(m^2

COMPARISON OF μCi/g FOR ^{239}Pu TRANSPORT ON "LARGE" PARTICLES AND ^{241}Am TRANSPORT ON "SMALL" PARTICLES COLLECTED AT THE HANFORD METEOROLOGICAL TOWER DURING AUGUST 13 TO NOVEMBER 12, 1976

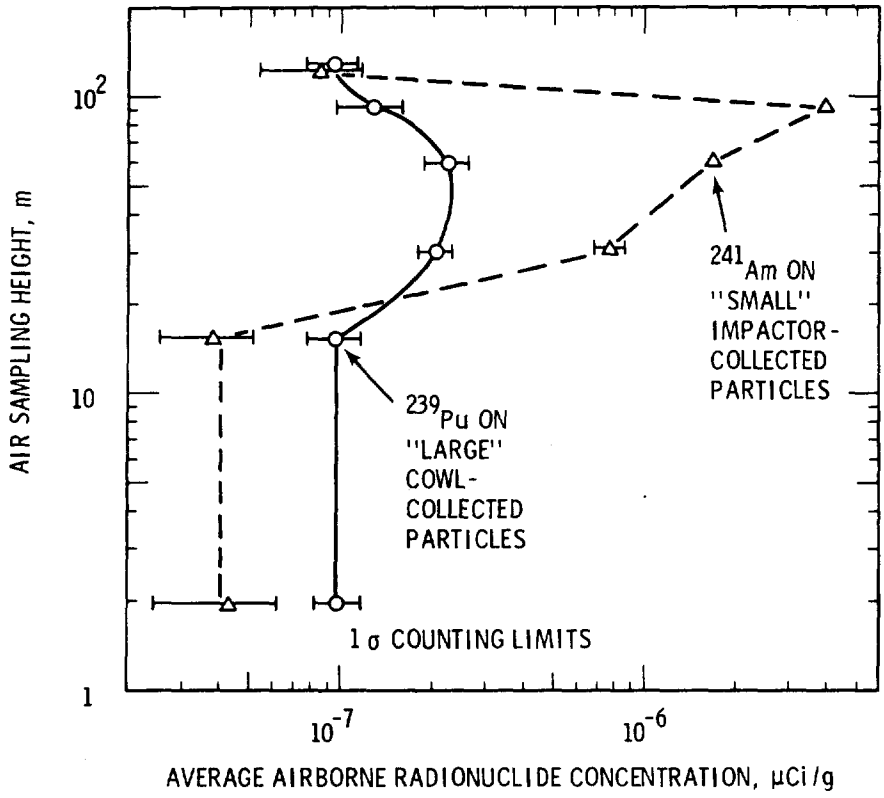

Figure 5

AIRBORNE PLUTONIUM-239 FLUXES AT THE HANFORD METEOROLOGICAL TOWER DURING AUGUST 13 TO NOVEMBER 12, 1976

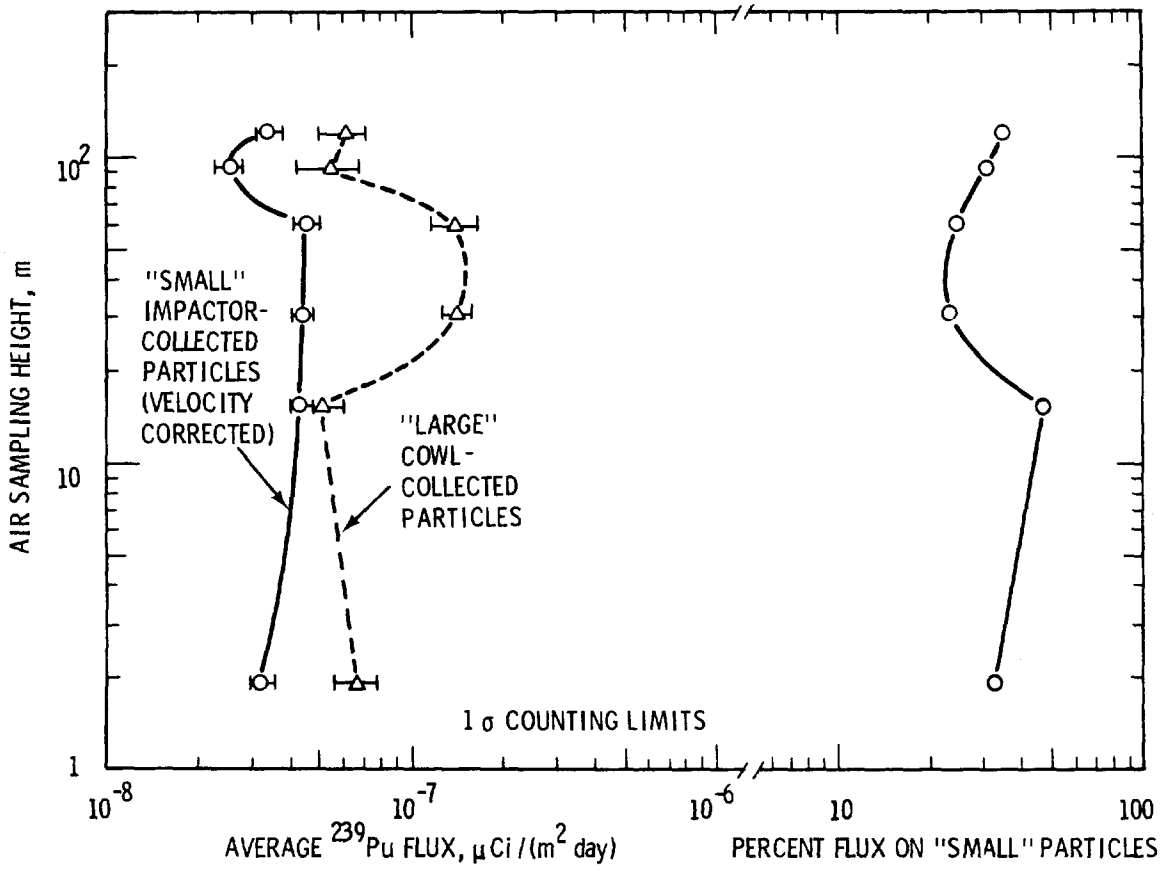

Figure 6

AIRBORNE ^{241}Am FLUXES AT THE HANFORD METEOROLOGICAL TOWER DURING AUGUST 13 TO NOVEMBER 12, 1976

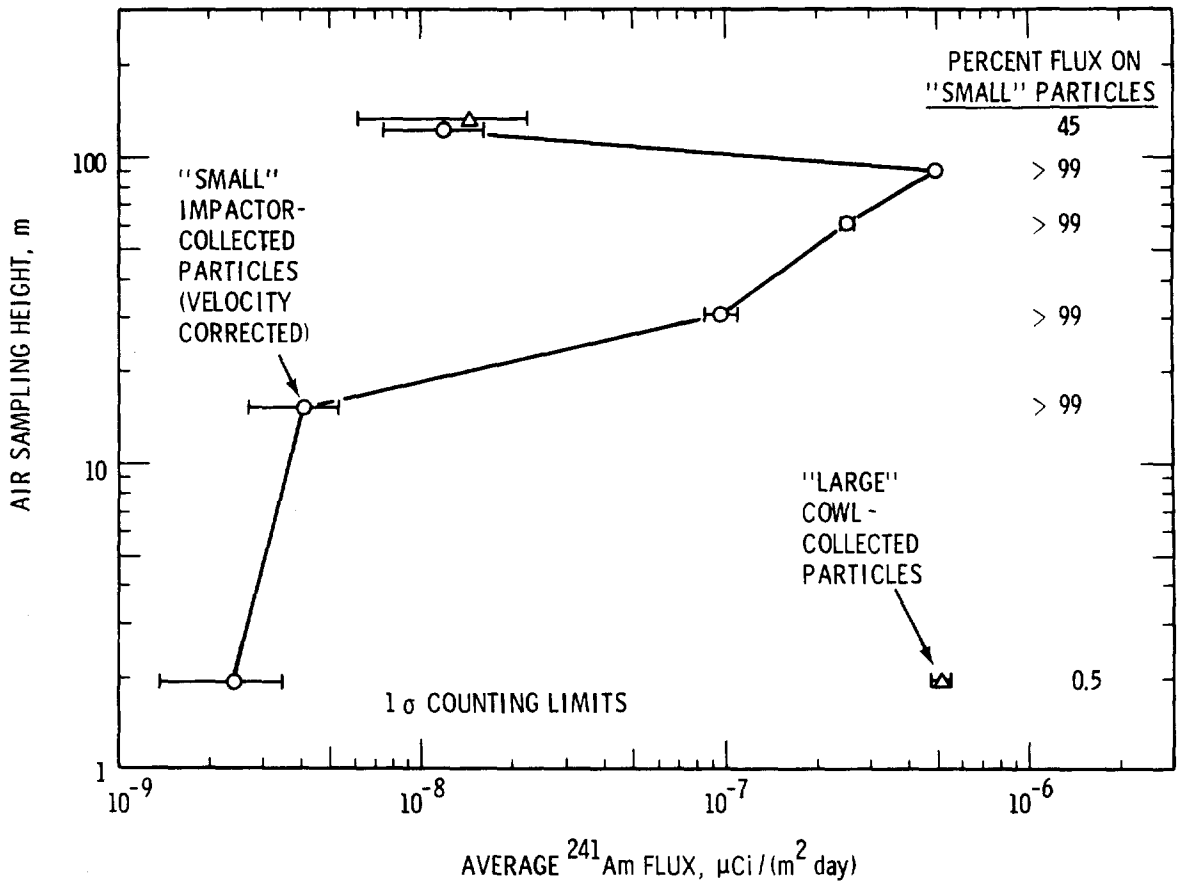

Figure 7

day) at an elevation of 91 m. The flux decreased to 1.2×10^{-8} μCi/(m^2 day) at an elevation of 122 m. At this highest sampling elevation, the flux on large particles was 1.4×10^{-8} μCi/(m^2 day). Thus, the percent of total americium-241 flux on small particles was 45% at an elevation of 122 m. This percent flux on small particles is shown on the right side of the figure. Similarly, the americium-241 flux on large particles was 5×10^{-7} μCi/(m^2 day) at a sampling height of 1.9 m. At this lowest sampling elevation, the percent of total americium-241 flux on small particles was 0.5%. Americium-241 fluxes on large particles are not shown between 1.9- and 122-m sampling height since the radiochemical results were less than radiochemical counting detection limits.

CONCLUSIONS

Both plutonium-239 and americium-241 concentrations were measured for sampling heights up to 122 m. Results are reported μCi/cm^3, μCi/g of airborne soil, and average fluxes in μCi/(m^2 day) for both large and small particles. The small particles are in the respirable diameter range. Since results were determined for heights up to 122 m, these experimental data are the first to show plutonium-239 and americium-241 concentration profiles to those heights. However, even at a sampling height of 122 m, the airborne plutonium-239 and americium-241 plumes were probably not contained.

Some correlation is suggested between americium-241 transport on small particles and plutonium-239 transport on large particles. This apparent correlation needs further validation at other sites and time periods.

Americium-241 has been studied even less than plutonium-239 resuspension. Nevertheless, americium-241 resuspension could become a potential inhalation concern of the future when americium-241 grows in as a daughter of plutonium-241 at aged plutonium resuspension sources. In addition to showing americium-241 transport by resuspension, these data also show plutonium-239 and americium-241 are transported on both small and large particles. Although transport on large particles does not present an immediate inhalation concern, transuranics transported on large particles could present a subsequent inhalation concern. After these large particles are deposited, small particles can be released from the larger host soil particles (Sehmel, 1978). If transuranics, these released small particles could then be sources for subsequent resuspension in the inhalation diameter range. Experimental data are needed to develop and validate transport models for both respirable and nonrespirable particles as well as plutonium-239 and americium-241 detachment from large particles.

ACKNOWLEDGMENT

This paper is based on work performed under U.S. Department of Energy Contract EY-76-C-06-1830.

REFERENCES

1. ICRP (International Commission on Radiological Protection). 1959. Report of Committee II on Permissible Dose for Internal Radiation. ICRP Publication 2, Recommendations of the International Commission on Radiological Protection, Pergamon Press, New York. pp. 82-83.

2. Krey, P. W., R. Knuth, T. Tamura, and L. Toonkel. 1976. "Interrelations of Surface Air Concentrations and Soil Characteristics at Rocky Flats." *In: Atmosphere-Surface Exchange of Particulate and Gaseous Pollutants*. R. J. Engelmann and G. A. Sehmel, Coordinators. CONF-740921. pp. 744-756.

3. Sehmel, G. A. 1973. "An Evaluation of a High-Volume Cascade Particle Impactor System." *In:* Proc. of the Second Joint Conference on Sensing of Environmental Pollutants. Washington, DC. Instrument Society of America, Pittsburgh, PA. pp. 109-115.

4. Sehmel, G. A. 1977a. "Airborne Plutonium Transport on Nonrespirable Particles," and "Weathering of Surfaces as Measured by Airborne Radioactive Particle Concentrations on the Hanford Reservations." *In: Atmospheric Sciences*. Battelle's Pacific Northwest Laboratory Annual Report for 1976. BNWL-2100-3. pp. 65-73, 85-88.

5. Sehmel, G. A. 1977b. "Radioactive Particle Resuspension Research Experiments on the Hanford Reservation." Battelle Pacific Northwest Laboratory Report. BNWL-2081.

6. Sehmel, G. A. 1977c. "Transuranic and Tracer Simulant Resuspension." Battelle's Pacific Northwest Laboratory Report. BNWL-SA-6236.

7. Sehmel, G. A. 1978. "Plutonium Concentrations in Airborne Soil at Rocky Flats and Hanford Determined During Resuspension Experiments." Battelle's Pacific Northwest Laboratory Report. BNWL-SA-6720.

8. Sehmel, G. A., and F. D. Lloyd. 1976. "Resuspension of Plutonium at Rocky Flats." *In: Atmosphere-Surface Exchange of Particulate and Gaseous Pollutants*. R. J. Engelmann and G. A. Sehmel, Coordinators. CONF-740921. pp. 757-779.

9. Willeke, W. 1975. "Performance of the Slotted Impactor." *Amer. Ind. Hyg. Assoc. J.* 36:683-691.

RESUSPENSION STUDIES ON FALLOUT LEVEL PLUTONIUM

N. W. Golchert and J. Sedlet

Argonne National Laboratory--Argonne, Illinois

ABSTRACT

Plutonium, uranium, and thorium concentrations in air have been measured for several years. Resuspension factors for uranium and thorium have been calculated and compared to those for plutonium. Using the uranium and thorium in air data, the contribution of plutonium in air from stratospheric fallout and from resuspended surface soil can be determined. Comparison of these data to published measurements at the GMX site is made. Plutonium in air particulates as a function of particle size was measured with an Anderson 2000 high-volume cascade impactor and is presented.

INTRODUCTION

As part of the Argonne National Laboratory (ANL) Environmental Monitoring Program, air particulate samples are collected to monitor for possible airborne releases of radionuclides. The primary interest is to measure plutonium concentrations in air because of its use at the Laboratory and the importance of public interest in this element as an environmental pollutant. Concentrations are compared to available standards of plutonium in air, DOE Manual Chapter 0524, and to the recent EPA proposed guidelines to determine compliance.

The primary source of plutonium in air at the present time is from "fallout." It is estimated that about 325 kCi of plutonium was released to the atmosphere from all the nuclear tests. Because of the monthly variations in the concentrations, it is necessary to continuously monitor. In addition, uranium and thorium concentrations are also determined and the relationship of these elements to that of plutonium provides some interesting comparisons, *i.e.*, the determination of inhalation dose.

MATERIALS AND METHODS

Particulate air samplers are run continuously at two perimeter locations and at one off-site location. Collections are made on a polystyrene filter medium. Individual samples are combined by location on a monthly basis to give a typical filtered air volume of about 25,000 m^3. Samples are ignited at 600° C. to remove organic matter and prepared for analysis by using a leach procedure employing combinations of hydrochloric, hydrofluoric, and nitric acids. A radiochemical separation procedure is used to sequentially isolate plutonium, thorium, and uranium. After separation, the fractions are electrodeposited and their isotopic composition determined by alpha spectrometry. Chemical recoveries are monitored by added known amounts of plutonium-242, thorium-234, and uranium-232 prior to ignition.

The monthly amount of plutonium deposited on the surface from the air is also determined by the above method. Wet and dry deposited material is collected in a container of known area and the residue analyzed for plutonium.

Surface soil of known area is analyzed for plutonium, uranium, and thorium. After drying, grinding, and mixing, an aliquot of soil is analyzed by a leach method similar to that used above for the air-filter residues.

RESULTS AND DISCUSSION

The concentration of plutonium-239,240 in air at ANL (Sedlet *et al.*, 1973, 1974, 1975; Golchert *et al.*, 1976, 1977) for the last five years is depicted in Figure 1. The fluctuations are primarily due to recent atmospheric nuclear tests conducted by the People's Republic of China. The approximate dates of these tests are indicated by arrows at the bottom of the figures. The concentrations in air of other fission products for which measurements were made, *i.e.*, strontium-89, strontium-90, *etc.*, show a similar distribution. Measurements of this type for this period and earlier have been made by the Environmental Measurements Laboratory (EML) (Hardy, 1978), formerly HASL, at various locations.

The monthly variations exhibit the expected maximum in the spring and the magnitude of the peak is determined by the quantity and yield of atmospheric testing the previous year. Another way of looking at this type of information is to examine ground deposition of plutonium-239,240 for the same period. This is illustrated in Figure 2. This data was generated by analyzing the contents of a known area sample collector for plutonium and expressing the results in terms of deposition (pCi/m^2).

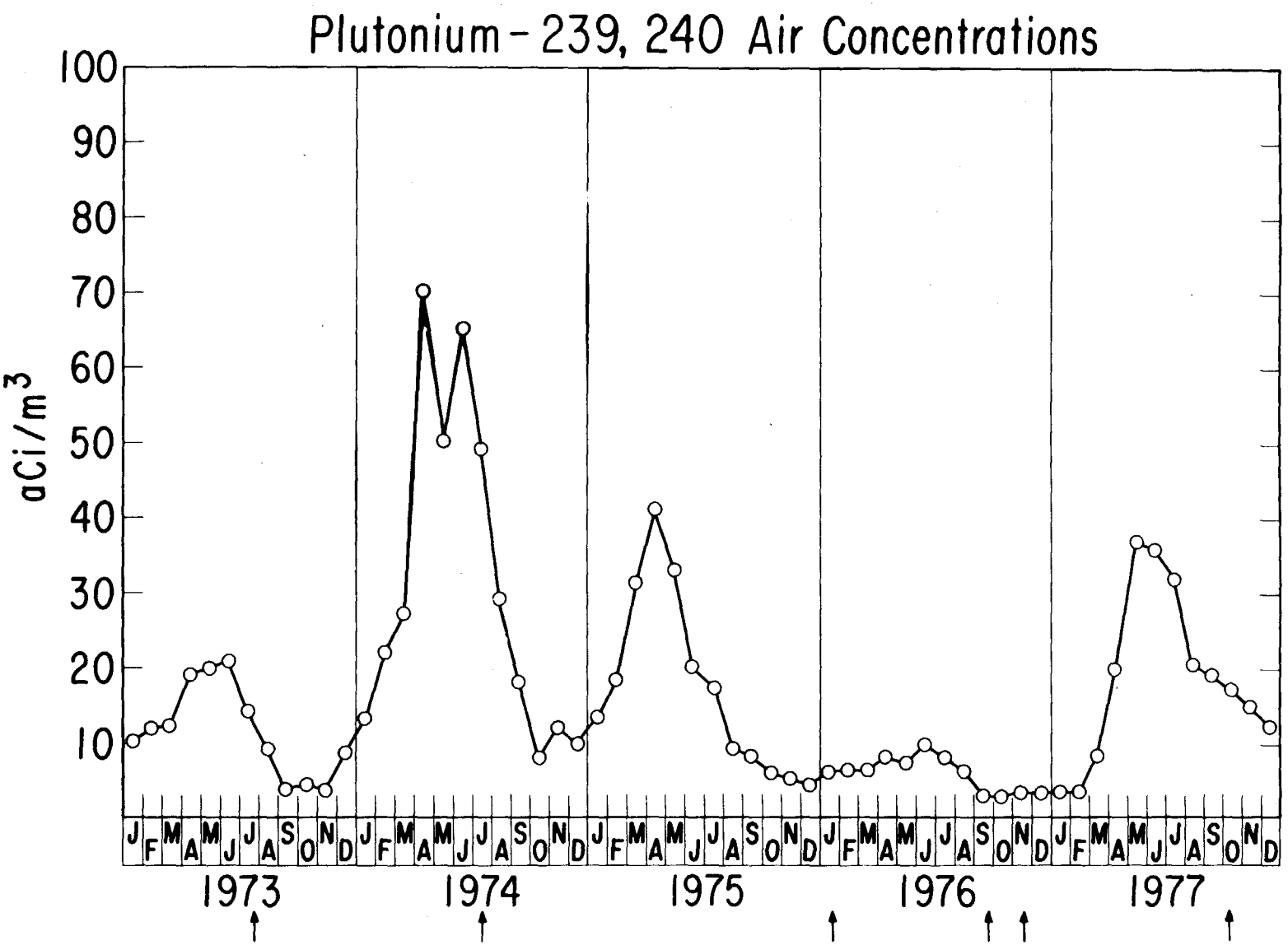
Plutonium - 239, 240 Air Concentrations
100
90
80
70
60
50
40
30
20
10
aCi/m3
J F M A M J J A S O N D J F M A M J J A S O N D J F M A M J J A S O N D J F M A M J J A S O N D J F M A M J J A S O N D
1973
1974
1975
1976
1977

Figure 1.

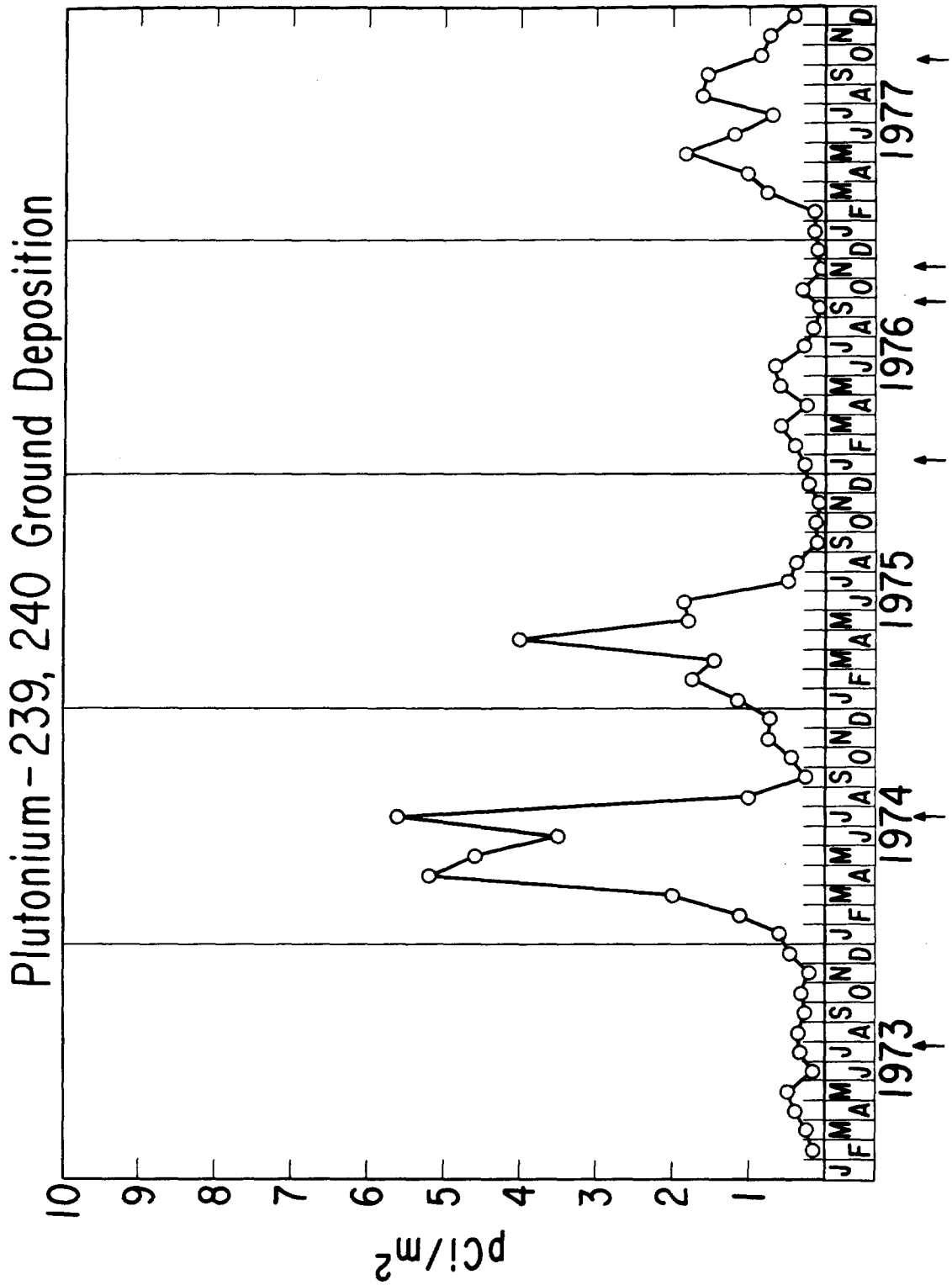
Plutonium-239, 240 Ground Deposition
pCi/m²
10
9
8
7
6
5
4
3
2
1
J F M A M J J A S O N D J F M A M J J A S O N D J F M A M J J A S O N D J F M A M J J A S O N D
1973
1974
1975
1976
1977

Figure 2.

The monthly variations in plutonium air concentrations in Figure 1 and plutonium deposition in Figure 2 are very similar. The total plutonium-239,240 deposited on the ground from all atmospheric tests to date is about 2.2 nCi/m^2 for the area near Argonne (Hardy *et al.*, 1973). Therefore, the plutonium-239,240 added to what was already on the ground was 0.2% in 1973, 1.2% in 1974, 0.6% in 1975, 0.2% in 1976, and 0.5% in 1977. This information is useful to those individuals who are studying the dynamics of plutonium in lakes and oceans.

In addition to plutonium, thorium and uranium concentrations in air have been determined for all three thorium isotopes and for total uranium at the three sampling locations. The uranium results are expressed as total uranium to allow comparison over the five-year period even though isotopic uranium results are available for the last two years. Results are similar at each location, and two of the distributions are presented here for illustrative purposes. Figure 3 is for thorium-232 and Figure 4 is for uranium at the same location. When the concentrations are expressed in units of aCi/m^3 for the five-year time period, the uranium and thorium are similar but do not show the same type of distribution as the plutonium, with its characteristic maximum in spring attributed to fallout. If the thorium and uranium concentrations are recalculated in terms of activity per gram of material collected on the paper, a lognormal plot of this data results in a straight-line fit. These are illustrated in Figure 5 for thorium-232 and Figure 6 for uranium. This implies a single source of particulate matter in air. A lognormal plot of the plutonium in air concentrations also results in a straight-line best fit, but the source of the plutonium is different. In addition, the specific activity of the material in air for thorium and uranium is related to the specific activity of thorium and uranium in soil. It appears that the amounts of thorium and uranium in an air sample are proportional to the mass of material collected on the filter paper, and the bulk of these elements in the air is due to resuspended soil.

Accepting this premise, the relative amount of plutonium in air as a result of resuspended soil can be calculated. With the presently deposited plutonium in soil at 2.2 nCi/m^2, the measured surface plutonium-239,240 concentration is about 25 fCi/g. Knowing the weight of residue material in each sample, the contribution from plutonium in soil can be determined. For example, in Figure 1, the 1976 plutonium-239,240 in air due to soil ranged from 6% in August to 22% in November of the total plutonium in the samples. The relative amount depends on the contribution from stratospheric fallout and mass of material.

Resuspension factors (RF) for thorium-228, thorium-230, thorium-232, uranium, and plutonium-239,240 were calculated and are presented in Table 1. The thorium and uranium air concentrations are the five-year averages of those displayed earlier. The plutonium-239,240 is the five-year average concentration of the plutonium in air due to resuspended soil calculated with the above procedure. All measurements are from the same air sampling location. The amount of each nuclide in terms of ground deposition was obtained by a radiochemical determination of each

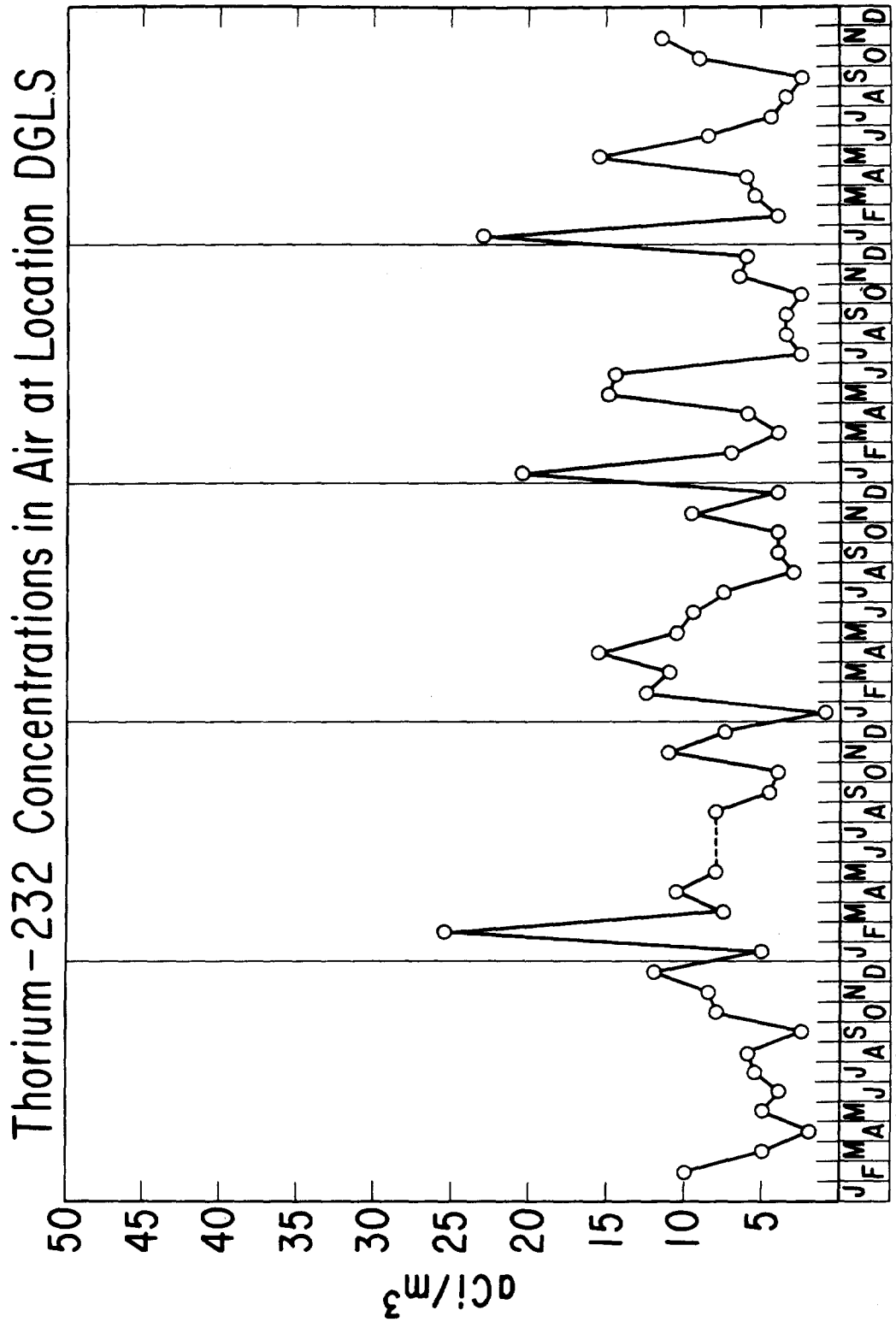
Thorium-232 Concentrations in Air at Location DGLS
pCi/m³
50
45
40
35
30
25
20
15
10
5
J F M A M J J A S O N D J F M A M J J A S O N D J F M A M J J A S O N D J F M A M J J A S O N D
1973
1974
1975
1976
1977

Figure 3.

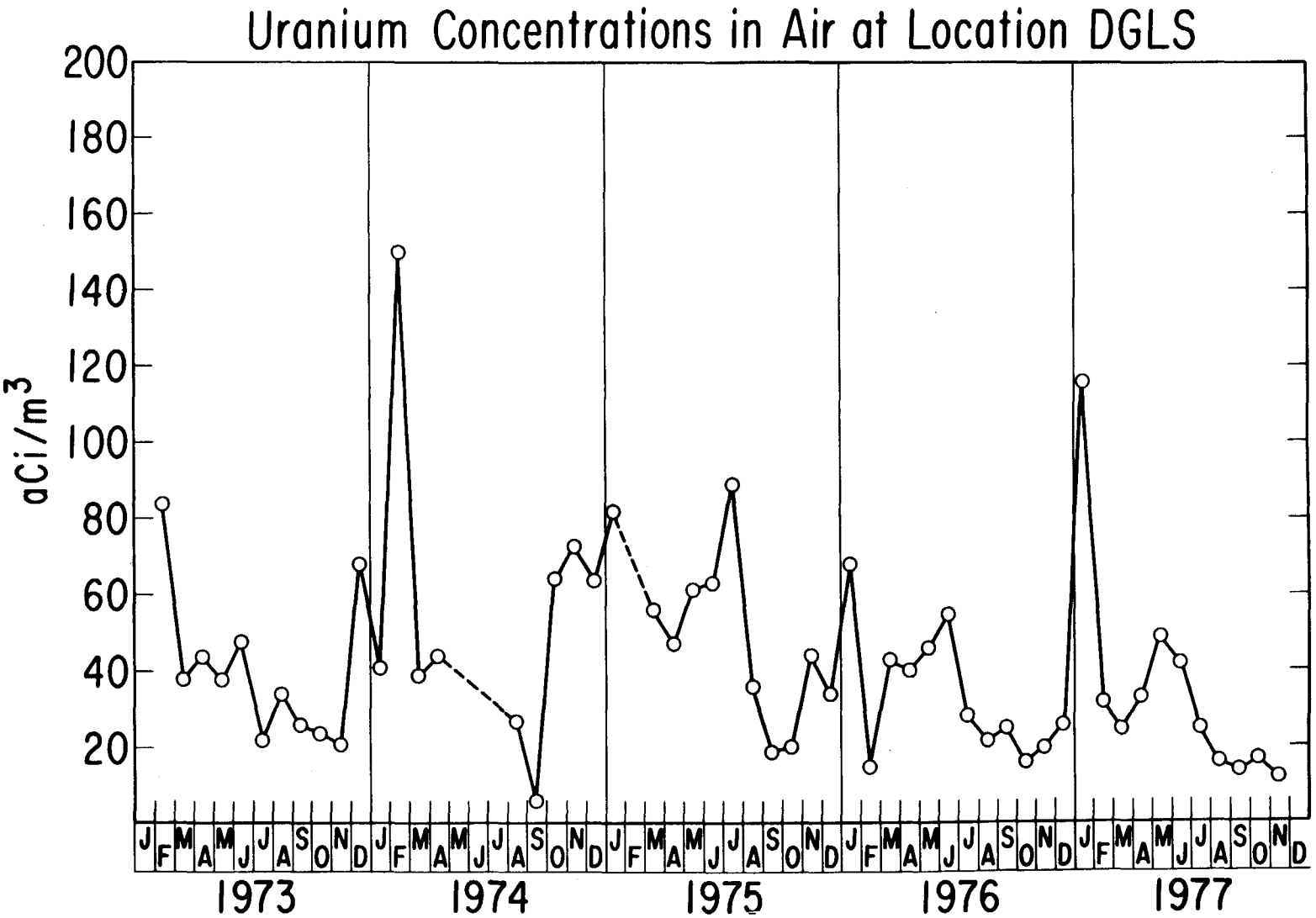
Uranium Concentrations in Air at Location DGLS
200
180
160
140
120
100
80
60
40
20
aCi/m3
J F M A M J J A S O N D J F M A M J J A S O N D J F M A M J J A S O N D J F M A M J J A S O N D J F M A M J J A S O N D
1973
1974
1975
1976
1977

Figure 4.

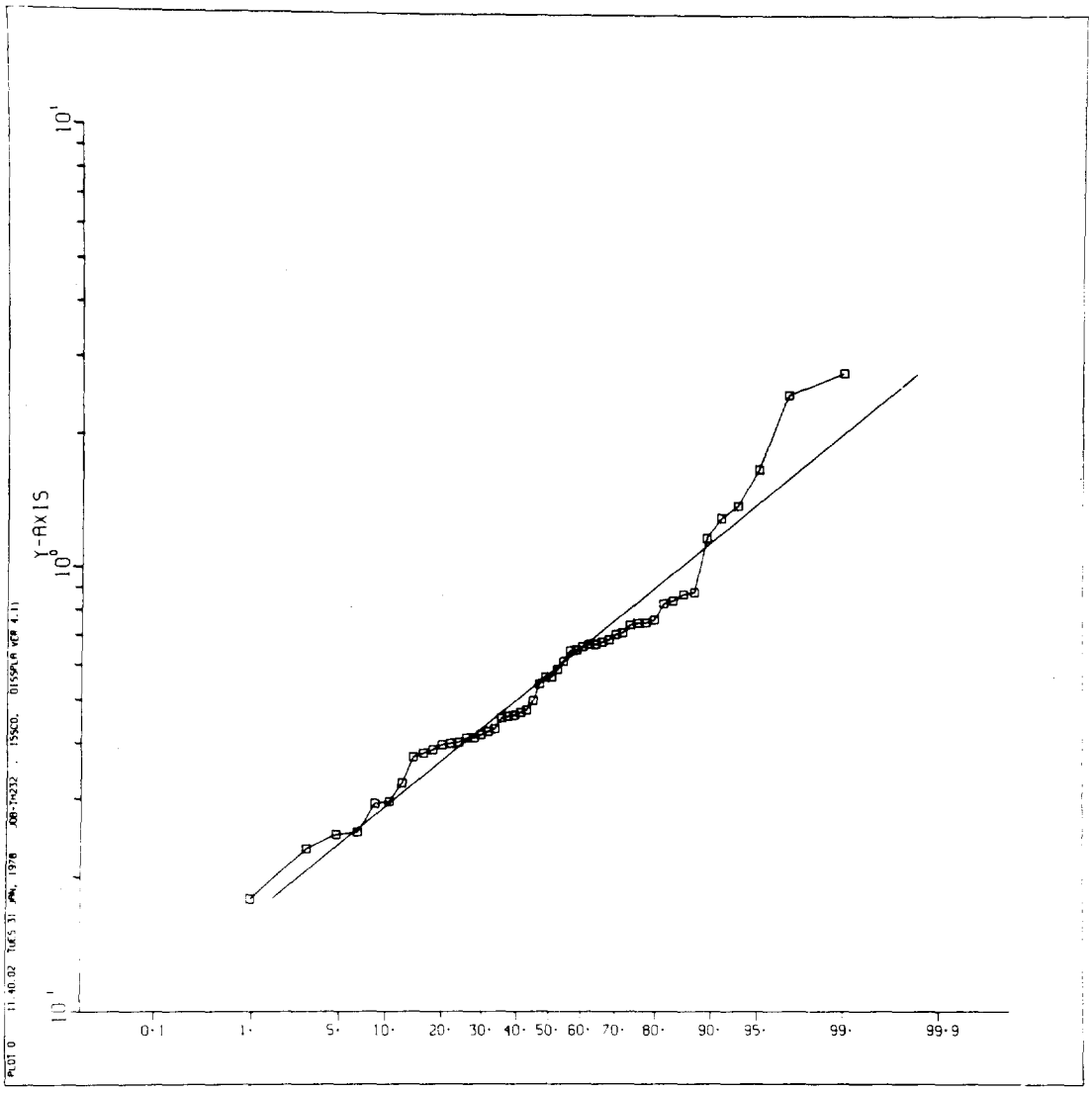

Figure 5. Log-Normal Plot of Th-232 Air Concentrations

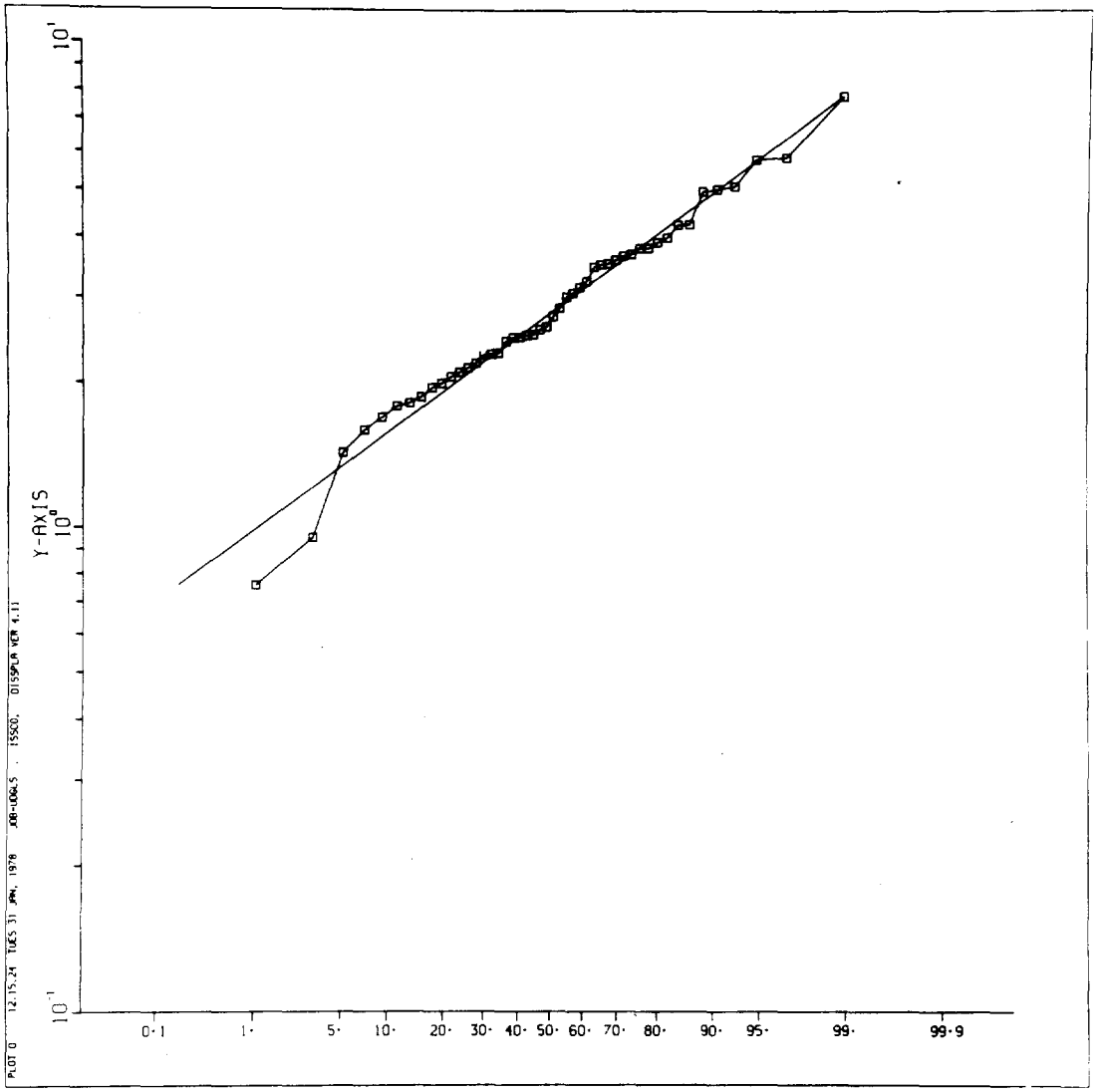

Figure 6. Log-Normal Plot of U Air Concentrations

Table 1. Resuspension Factors

Nuclide	Air Concentration (aCi/m^3)	Ground Deposition (nCi/m^2)	RF (M^{-1})
Thorium-228	8.6	17	5.1×10^{-10}
Thorium-230	14.7	28	5.3×10^{-10}
Thorium-232	8.2	15	5.5×10^{-10}
Uranium	41.9	68	6.1×10^{-10}
Plutonium-239,240	0.7	1	7×10^{-10}

and the results expressed per area with the assumption that the top one cm is available for resuspension.

The agreement appears to be quite good between all the measurements. It is generally accepted that freshly deposited material will produce air concentrations of resuspended materials that decrease with time. This decrease has a half-time of about 35 to 70 days and is presumably caused by the migration of the initially surface-deposited material into the soil. The resuspension factor should eventually reach a steady-state condition when the source has "aged" sufficiently. Calculations by Anspaugh *et al.* (1974) of 20-year-old plutonium at the Nevada Test Site give a resuspension factor of 3×10^{-10}/m and 2×10^{-9}/m. The thorium and uranium should represent the ultimate aged source and their resuspension factors, the equilibrium condition. If it is assumed that most of the fallout plutonium was deposited in the early 1960's, the agreement between the plutonium, uranium, and thorium indicates that in 15 years the plutonium has reached an aged condition. The data in Table 1, therefore, represents resuspension factors based on long-term averages of many measurements.

In order to examine the particle size distribution of fallout plutonium, samples were collected using an Anderson 2000 high-volume cascade impactor. The sampler was operated at 20 cfm and the effective cutoff diameters were assumed to be those quoted by the manufacturer. The sampling height was at one meter. The impactor was run from July 5, 1977, to August 2, 1977, and gave a total air volume of 22,800 m^3. Each stage was weighed and radiochemically analyzed. The results for particulate concentration, plutonium-239,240 air concentration, and plutonium-239,240 concentration per gram of suspended material for each stage is collected in Table 2.

The general trend of the fallout plutonium is that the concentration increases with decreasing particle size. About 67% of fallout plutonium has a particle size of less than 1.1 μm AMAD, whereas Myers *et al.* (1975) found only 50% of the soil resuspended by rototilling a sludge-contaminated field to be in this fraction. For comparison, data is included from the GMX site (Anspaugh and Phelps, 1976) and is for high-volume cascade impactor #4. No similar trend in the GMX data exists. About 20% of the resuspended plutonium at GMX would be expected to undergo pulmonary deposition, based upon the ICRP Task Group of Lung Dynamics model (Morrow, 1966), as opposed to 28% of the fallout plutonium. This compares to 25% measured by Volchok and Knuth (1972) at Rocky Flats. In either the fallout or GMX case, there is no obvious correlation of specific activity with particle size.

Thorium and uranium chemical analyses were also performed on the filter papers from the Anderson 2000 Impactor. The thorium results were unusable primarily because of the high thorium blank from the paper. Each paper had about 0.5 pCi of thorium. The uranium results are presented in Table 3. The concentrations per volume of air decrease regularly with

Table 2. Fallout Plutonium-239,240 Particle Size Distribution

Particle Range (μm)	Weight (g)	Particulate Concentration ($\mu g/m^3$)	Plutonium-239,240 Concentration (aCi/m^3)	Plutonium-239,240 Concentration (pCi/g) Fallout	GMX
> 7	0.440	19.3	0.97 (2%)	0.049	768
3.3-7	0.169	7.4	1.2 (3%)	0.16	399
2.0-3.3	0.097	4.3	3.0 (8%)	0.70	900
1.1-2.0	0.102	4.5	7.6 (20%)	1.66	862
< 1.1	0.445	19.5	25.9 (67%)	1.30	336
Total	1.253	55.0	38.7		

Table 3. Uranium Concentrations on Each Stage of the Cascade Impactor

Particle Range (μm)	Weight (g)	Particulate Concentration (μg/m^3)	Concentration (aCi/m^3) ^{234}U	^{235}U	^{238}U	Concentration (pCi/g) ^{234}U	^{235}U	^{238}U
> 7	0.440	19.3	30	1.6	29	1.55	0.083	1.50
3.3-7	0.169	7.4	18	0.6	18	2.43	0.081	2.43
2.0-3.3	0.097	4.3	16	<0.5	16	3.76	<0.2	3.76
1.1-2.0	0.102	4.5	12	<0.5	11	2.68	<0.2	2.46
< 1.1	0.445	19.5	4.5	<0.5	3.5	0.23	<0.1	0.18

decreasing particle size, the opposite of the plutonium case. The concentration per gram of residue trend is different than fallout plutonium, but shows some similarity to the GMX plutonium.

REFERENCES

1. Anspaugh, L. R., and P. L. Phelps. 1976. "Results and Data Analysis: Resuspension Element Status Report." *In: Nevada Applied Ecology Group Procedures Handbook for Environmental Transuranics*. M. G. White and P. B. Dunaway (Eds.). USERDA Report NVO-166. p. 359.

2. Anspaugh, L. R., P. L. Phelps, N. C. Kennedy, H. G. Booth, R. W. Goluba, J. M. Reichman, and J. S. Koval. 1974. *The Dynamics of Plutonium in Desert Environments*. P. B. Dunaway and M. G. White (Eds.). USAEC Report NVO-142. p. 221.

3. Golchert, N. W., T. L. Duffy, and J. Sedlet. 1976. *Environmental Monitoring at Argonne National Laboratory*. Annual Report for 1975. USERDA Report ANL-76-29.

4. Golchert, N. W., T. L. Duffy, and J. Sedlet. 1977. *Environmental Monitoring at Argonne National Laboratory*. Annual Report for 1976. USERDA Report ANL-77-13.

5. Hardy, E. P., Jr. 1978. *Environmental Measurements Laboratory Environmental Quarterly (Appendix)*. USDOE Report EML-334.

6. Hardy, E. P., Jr.; P. W. Krey; and H. L. Volchok. 1973. "Global Inventory and Distribution of Fallout Plutonium." *Nature* 241:444.

7. Morrow, P. E., Chairman, Task Group on Lung Dynamics. 1966. "Deposition and Retention Models for Internal Dosimetry of the Human Respiratory Tract." *Health Physics* 12:173.

8. Myers, D. S., W. J. Silver, D. G. Coles, K. C. Lamson, D. R. McIntyre, and B. Mendoza. 1976. "Evaluation of the Use of Sludge-Contaminated Plutonium as a Soil Conditioner for Food Crops." *In: Transuranium Nuclides in the Environment*. IAEA, Vienna.

9. Sedlet, J., N. W. Golchert, and T. L. Duffy. 1973. *Environmental Monitoring at Argonne National Laboratory*. Annual Report for 1972. USAEC Report ANL-8007.

10. Sedlet, J., N. W. Golchert, and T. L. Duffy. 1974. *Environmental Monitoring at Argonne National Laboratory*. Annual Report for 1973. USAEC Report ANL-8078.

11. Sedlet, J., N. W. Golchert, and T. L. Duffy. 1975. *Environmental Monitoring at Argonne National Laboratory*. Annual Report for 1974. USERDA Report ANL-75-18.

12. Volchok, H. L., and R. H. Knuth. 1972. "The Respirable Fraction of Plutonium at Rocky Flats." *Health Physics* 23:395.

SUMMARIZATION

SUMMARIZATION

M. G. White and P. B. Dunaway

In March, 1978, the Nevada Applied Ecology Group held the annual plutonium information conference in San Diego, California. Papers presented at the meeting included summary reports of projects, progress reports of current work, and a number of papers contributed by organizations other than NAEG. A brief summarization of the conference follows.

Following completion of scheduled studies in safety-shot areas, Nevada Applied Ecology Group studies began in 1977 in the nuclear sites at the Nevada Test Site (NTS). Ecological studies concerning small mammals were reported by Bradley and Moor of the University of Nevada, Las Vegas. In evaluation of initial species inventory of the native vertebrate biota and estimates of population numbers, it was found that rodents generally were more numerous in the intensive study nuclear site studied than in Areas 5, 11, and 13 intensive study sites of NAEG. Comparative data were presented in their report from the safety-shot site investigations. Certain analyses of samples and further evaluation of data were postponed due to cutback in NAEG funding levels.

In addition to the NTS off-site monitoring function performed by the Environmental Protection Agency for the Department of Energy, the EPA's Bioenvironmental Research Program conducts large animal studies for the NAEG. A summary of the efforts of the Environmental Monitoring and Support Laboratory-Las Vegas in the activities of NAEG was prepared by Bretthauer. Reports of several NAEG/EPA studies were in preparation for publication in 1978. Those referred to in Bretthauer's summary include, "Comparison of Pu-238 and Pu-239 Metabolism in Dairy Cows," "Metabolism of Am-241 in Dairy Animals," "Area 13 *In Vitro* Study," "Area 13 Microorganism Population Survey," "Sterile *vs* Non-Sterile Soil Pu Solubility," "Pu-238/Pu-239 *In Vitro* Study," "Soil Profiles of Pu-Contaminated Areas of the NTS," and "Am-241 *In Vitro* Study."

Metabolism of Americium-241 in dairy animals was the subject of the EPA report presented by Sutton. He and co-workers Patzer, Mullen, Hahn, and Potter conducted experiments utilizing groups of cows and goats in order to investigate oral and intravenous uptake of Am-241. Their results indicated that the largest fraction of the administered dose to the cow was retained in bone, followed by liver and kidney. In the case of the goat, retention of americium was greatest in the liver. Comparisons of Am-241 and Pu-238 metabolism in dairy cows was discussed. Among other information offered, Sutton *et al.* stated that 24-hour collections of urine and milk contained noticeably higher nuclide concentrations when

the animals were injected with americium, as opposed to plutonium; nuclide retention in the liver was also greater for animals that had received americium; a marked similarity existed in the nuclide deposition pattern following ingestion of either Am-241 chloride or citrate-buffered Pu-238 nitrate. (Editor's note: The acknowledgments paragraph of Sutton's report includes several additional EPA personnel who have assisted in NAEG large animal studies, performed at the NTS experimental farm. Their assistance in these studies has been greatly appreciated by the NAEG/Department of Energy.)

Americium-241 studies were also reported by J. Barth, EPA. The alimentary solubility and behavior of Am-241 were investigated in an artificial rumen and simulated bovine gastrointestinal fluids. Barth stated that the data indicate that Am-241 administered as Am-241 nitrate solution remains soluble in ruminant digestive fluids to considerable degree. In most digestive stages, the solubility of Pu-238 was greater than that of Am-241, when both were in nitrate solution. Barth discussed the results with those of an EPA Am-241 metabolism study with dairy cows in order to predict tissue retention and milk secretion of field-deposited Am-241 ingested by cattle grazing in Area 13 of the Nevada Test Site.

Data was presented by Smith, EPA, concerning the NAEG long-term grazing study with a reproducing beef herd on a plutonium-contaminated intensive study site in Area 13, NTS. Food habit analyses were discussed with implications for relationships between actinide concentrations in the ingesta and *Eurotia lanata* content. Other interesting information reported by Smith related to the Pu-239 concentrations in bone, lung, and liver collected from wildlife with free access to and from the plutonium-contaminated study site. Concentrations in bone, lung, and liver ranged from 1 percent to 10 percent of those in the cattle confined to the intensive study site. A brief summary of the long-term study concluded Smith's report.

Au and Beckert, EPA, presented results of a study to determine whether plutonium associated with fungal tissue could be taken up by a successive generation, or whether it becomes immobilized after metabolism by the fungus. Their results indicated that such transfer is possible to the spores of new growth, using *Aspergillus n.* A summary was also included concerning the previous NAEG microorganism studies of plutonium transport in the NTS environment.

Plant uptake of Pu and Am through roots was investigated further by Romney, Wallace, and Kinnear, UCLA, using NTS soils. Their evaluation of recent results indicated that vegetation-to-soil concentration ratios (C.R.) varied from 10^{-5} to 10^{-3} for $^{239,240}Pu$, and from 10^{-4} to 10^{-1} for ^{241}Am, depending on the type soil and agricultural amendments applied; that generally Am was taken up by plants at a faster rate than Pu; that DTPA chelate increased root uptake of both Pu and Am when added with nitrogen, organic matter, or sulfur amendments; C.R. values were lower for fruit than for vegetative parts of soybeans; Am was slightly more available for transport from shoots to fruits of soybeans than Pu.

Wallace and Romney discussed the need to retain certain of the NAEG safety-shot intensive study sites for further ecological investigations not yet addressed by the NAEG. Their contributions through the years of NAEG research have been thorough and excellent. Their suggestions concerning questions yet unanswered and mechanisms not investigated are very timely. NAEG research funding has recently been reduced, and it is important that such information be recorded for future use. Many of the suggested projects are concerned with cleanup or decontamination of the safety shot study areas.

Factors in ionic diffusion from soil to plant roots was one of several aspects of an approach to studying radionuclide uptake by plants at NTS reported by Baker, Pillay, Rose, and Ciolkosz of Penn State. They have begun an investigation into soil mineralogy and soil chemistry experimentation which may be required for management systems to minimize the movement of transuranics in the environment to man.

Rhoads, EG&G, Goleta, presented an interesting discussion of supportive evidence for probable radiation damage to both annual and perennial vegetation from the Sedan cratering event of 1962. In his report, he examines data from Baneberry, Small Boy, and Sedan in light of extensive recent investigations into Baneberry fallout radiation effects at NTS, reported in NAEG publications.

Uncontaminated soil profiles from Area 18, NTS, were established as microcosms in environmental chambers at Battelle's Columbus Laboratory. Ausmus and Dodson reported the use of CO_2 efflux as the parameter monitored to establish parameter behavior in the soils from the various sites. $CdCl_2$ was administered to the soils in order to measure the effects of stress on such a desert ecosystem. Follow-on investigations will explore the effects of certain transuranics on ecosystem processes and feasibility of decontamination or stabilization techniques to be tested in the laboratory prior to field trials.

Essington, Los Alamos Scientific Laboratory, reported on the status of LASL participation in NAEG soil studies. His outstanding paper in this document includes a survey of soils studies conducted by LASL for the NAEG, current data evaluation concerning vertical movement of transuranics in desert soil profiles, and discussion of distribution of uranium in blow-sand mounds in NAEG safety-shot sites. Recommendations for further studies concerning redistribution of radionuclides at NTS are also offered by Essington.

A summary report on NAEG plutonium-soil association research in the safety-shot areas of NTS was given by Tamura, Oak Ridge National Laboratory. In addition, he discussed initiation of cleanup trials at NTS while the studies in nuclear event areas are progressing. His consideration of soil-related problems in clean-up trials included possible soil activity levels above which cleanup should be planned and how the levels would perhaps be defined as lower limits. Other considerations mentioned were hot particles, gravel cover (protective blanket), stabilization of

surface to minimize erosion, wet sieving, and other means to effect safe personnel operations as well as efficient collection of contaminated materials. Tamura has provided leadership in many of the NAEG soils studies.

Leavitt, EPA (EMSL-Las Vegas), in his report at San Diego, described the soil surveys accomplished for the NAEG. His slides demonstrated the various soil types at NTS and the methods used to determine soil characteristics for classification. His paper in this document includes a summary of the dominant factors of the areas surveyed for NAEG, both in narrative form and as a table. Leavitt's results indicate that a large portion of the land surveyed for NAEG is of a soil type that is potentially good winter range for cattle.

Reports from the Nevada Applied Ecology Group service and support contractors included presentations from Reynolds Electrical & Engineering Co. (REECo) concerning on-NTS activities for NAEG during 1977. Brady, Rakow, and Rosenberry discussed logistics of the collection, preparation, and shipment of NAEG soil, vegetation, and animal samples. NAEG activities in the safety-shot intensive study sites at NTS and Tonopah Test Range, as well as nuclear site study areas, are supported by REECo personnel. A glance at the report will give the reader only a glimpse of the high quality, on-schedule, dependable assistance NAEG has had from the REECo people assigned to our activities year after year of NTS field investigations.

Wireman of REECo prepared a comprehensive summary of REECo participation in NAEG studies, 1972 through 1977. Included in this important report is information related to NAEG methodology and sample/data status. Of special significance is a discussion of chronological sequence of the execution of a typical NAEG intensive study at NTS. (Editor's note: Wireman not only assisted in developing many of the NAEG standard methods for sampling, but in recent years was assigned as NAEG/REECo Coordinator in the DOE-Las Vegas complex.)

REECo data processing support of the NAEG for 1977 was the subject of Zellers', REECo, presentation. Details, problems, and some solutions of NAEG data documentation were included. The complex environmental data base of NAEG is a very workable system utilized by the NAEG investigators, management, and analysis personnel.

Versatility, ease of access, and early reporting of information are the major assets of the Nevada Applied Ecology Information Center data base, Oak Ridge National Laboratory. Pfuderer reported on the scope and history of the NAEIC which produced the excellent bibliographic volumes of the Environmental Aspects of the Transuranics. Under the former guidance of Oens, ORNL, and more recently, Pfuderer, the Ecological Sciences Information Center of ORNL has developed and produced effective information transfer on plutonium in the environment, as well as other transuranics. Many users other than NAEG investigators have benefited from the documentation of information provided by the NAEIC.

One of the most important aspects of any research project is the analysis of samples. LFE Environmental Analysis Laboratories pioneered much of the methodology for analytical procedures for transuranics. Wessman, Leventhal, and Melgard discussed the LFE support to NAEG as well as other NTS environmental samples which have been processed by their laboratory.

Wessman and Benz, LFE, presented a paper regarding the problems of analysis of natural and artificial isotopes of uranium. As the presence of natural uranium isotopes in environmental samples is a general problem, the reader is referred to their solution for accurate analysis of such samples, obtained by balancing sample and tracer activity levels and determining correction factors.

Sequential separation of ^{90}Sr, ^{239}Pu, and ^{231}Am is a procedure discussed by Lee and Straight of REECo. The separation and purification of ^{90}Sr requires a highly sensitive chemical procedure. The basic work for the REECo procedure was done by Sill, DOE, Idaho Operations, and extended by T. D. Filer, Los Alamos Scientific Laboratory.

The estimation of spatial pattern or geographical distribution of environmental contaminants is a problem in many environmental sampling programs. In NAEG studies, the concentration in surface soil distribution of plutonium around ground zero at Area 13 needed to be estimated in order to predict the potential hazard to man from this contamination in a safety-shot area. Gilbert of Battelle Pacific Northwest Laboratory discussed the use of an iterative procedure for estimating grid values (to arrive at the total estimated inventory) at regular intervals on a grid covering the study site using data collected at varying locations over the area. Plots of sample data on estimated contour maps suggest locations where more data should be collected.

Delfiner, Centre de Geostatistique in Ecole des Mines de Paris, and Gilbert, Battelle's Pacific Northwest Laboratory, completed a joint study of NAEG Area 13 soils data on plutonium. Estimates of average ^{239,240} concentrations in surface soil (0-5 cm) were obtained using kriging technique. These then were compared with NAEG observed plutonium data, in order to calculate possible correction factors to provide even more accurate plutonium inventory estimates than are presently available. The necessity for careful planning of field sampling studies in order for kriging or any statistical technique to give reasonable estimates of inventory and spatial distribution of plutonium and other radionuclides is also discussed.

Gilbert and Eberhardt, PNL, presented a summary of PNL's statistical design and analysis activities for the NAEG since 1971 and a report on the current status of their work. A list of references is included on statistical topics of interest to environmental studies planning groups such as the NAEG.

For future planning purposes, Gilbert and Eberhardt included the following items in their summary:

1. Pu and Am concentrations on over 500 new soil and vegetation samples from safety-shot sites are essentially ready for statistical analysis to update estimates of Pu spatial pattern and inventory. These data are in the NAEG data bank and also on computer cards at Battelle-Northwest.

2. 320 soil samples have been collected at the grid intersections in Figure 5 at NS-201, but have not been shipped to analytical laboratories for radionuclide analyses. If these data are obtained, they would be useful for estimating spatial pattern and inventory of radionuclides at NS-201.

3. Plans are ready for Phase 1 sampling to begin at several nuclear sites, including NS-200 discussed in this paper and NS's-202 and 203 as discussed by Essington (1978).

4. Design plans for additional studies at Clean Slate 2 in anticipation of a possible cleanup effort at that site have been submitted to the NAEG. Samples of the type specified in recent EPA guidelines should be collected for evaluation of their applicability to NTS and TTR sites.

5. Statistical analyses for the estimation of Pu inventory in blow-sand mounds at Area 13 and Clean Slate 3 are completed (Gilbert and Essington, 1977). Particle size and spatial distribution aspects of Pu and Am are suggested as future blow-sand mound studies.

6. FIDLER and other mobile field detectors should continue to be evaluated for their applicability to field studies. Special studies aimed at calibrating more closely these instrument readings to Pu concentrations in field samples are encouraged.

Gilbert and Eberhardt's analyses have been invaluable to the synthesis of environmental NAEG data.

A study of variability of data with aliquot size was accomplished and reported by Doctor and Gilbert of PNL. These results indicate a linear relationship between aliquot variability (standard deviation) and aliquot size (both in logarithmic scale) over the range of aliquot sizes studied (standard deviation decreasing with aliquot size). In other words, substantial reduction in variability occurs between aliquots from the same sample if 50-gram rather than 1- or 10-gram aliquots are used for analysis.

The effect of variations in source term and parameter values on estimates of radiation dose to man are examined by Bloom and Martin, Battelle's Columbus Laboratories. The variations in source terms and parameters are many, due to uncertainties in sampling, measuring, and interpretation

of plutonium levels in field and laboratory investigations. Soil concentration is the most significant source term, subject to wide variation. Mass loading factor for air and parameters of the lung model used for radiation dose estimates also affect the sensitivity of estimates of radiation dose to man. Bloom and Martin report their analysis of the effects of variations in these important factors. Results indicated that none of the variations examined were surprising except, perhaps, for the large range that occurred due to variations in the parameters of the lung model. The largest variations were due to translocation class, a parameter which could cause a factor of 600-700 variation in dose rate to lungs in respirable size range particles; rate for bone parameter caused less than a factor of 4 variation with particle size, where translocation class caused less than a factor of 60 variation. These wide ranges of values need further exploration in attempts to move narrowly defined bioenvironmental differences and impacts on modeling efforts.

Martin and Bloom, BCL, also conducted additional simulation modeling studies for the NAEG grazing cattle plutonium ingestion investigation. Martin and Bloom concluded that the grazing, soil, and plant studies conducted in Area 13, NTS, were apparently well designed; that a repetition of the study would probably yield results similar to those already obtained; that given an adequate sampling design, reasonably accurate estimates of plutonium ingestion rates by grazing cattle can be obtained in spite of the extreme variability of contributing factors; and that given site-specific input parameters, the simulation model provides estimates of plutonium ingestion rates which are as accurate as those obtained from long-term grazing studies relying on fistulated steers. It is suggested that the model can be applied to other contaminated areas at or near NTS, but the results of such applications are uncertain unless supported by valid estimates of soil ingestion rates and the digestibility of vegetation available to grazing cattle at a specific site.

The results of observations by Nathans, LFE Environmental Analysis Laboratories, are reported on shape, density, color, and specific activity of radioactive particles in "close-in" fallout. Data on particles from cratering events and from surface and near-surface bursts are evaluated and classified by Nathans as part of a characterization of fallout particles containing transuranic elements and present in the soil of NTS.

Nathans and Francisco, LFE, presented plutonium-bearing particle isolation methods and some observations with regard to particles isolated at LFE for the Nevada Applied Ecology Group. Certain characteristics of the particles after isolation are listed to indicate similarity and variation in NTS samples undergoing analysis.

In environmental studies, development and application of techniques are very important to increase understanding of results of sampling programs and to assist in cutting down analytical costs.

In the contributed papers session, Wong, Noshkin, and Jokela of Lawrence Livermore Laboratory demonstrated that data obtained through use of the MICE samples (Mn O_2 Impregnated Cartridge Extraction) can be compared in certain respects with a radiochemical coprecipitation method for the radiochemical separation of transuranic elements. The sampler was developed by Wong to preconcentrate in the field (Enewetak) low-level plutonium and other radionuclides from fresh and salt waters, with subsequent plutonium analysis of the Mn O_2 cartridges. A schematic for the collection of water samples is included in their report.

Alpha autoradiography accomplished by Buddemeier, Bierman, and Gatrousis, Lawrence Livermore Laboratory, with Kodak LR-115, Type II cellulose nitrate alpha track detection film was studied to determine usefulness of the film in environmental plutonium soil sample analysis. Results indicated that alpha track detectors could be useful in analysis of amounts and distributions of activity in small samples such as aerosol filters, specific soil or sediment size fractions, and certain biological subsamples; for screening samples for limitation of numbers of radiochemical analyses; and for research into the statistical basis for environmental sampling design.

White of Los Alamos Scientific Laboratory discussed the statistical estimation of expected values of environmental pollutants with lognormal and gamma distributions. Tests conducted indicated that the arithmetic mean provides an unbiased estimate of expected value, and that the achieved coverage of the confidence interval is greater than 75 percent for coefficients of variation less than two.

Using barley plants, Wallace, Mueller, and Romney of UCLA investigated whether varying americium-241 concentrations in yolo loam soil would cause variance in the uptake and concentration in the plant, and what effect the addition of chelate would have on any such variance. Results indicated that ^{241}Am in plants was directly proportional to that in soil at all concentrations with DTPA. The uptake of americium from soil decreased slightly (about three times) without DTPA as the soil concentration of ^{241}Am was increased tenfold.

G.I. absorption of actinide elements is greater in fasted animals than in those on regular diets, according to Weiss and Walburg of the Comparative Animal Research Laboratory, University of Tennessee. Cerium-144 (III) chloride was given to fasted and nonfasting mice in efforts to evaluate differences reported in animal experiments measuring G.I. absorption. Weiss and Walburg recommend that better absorption data would be obtained using animals on regular feed and a more normal gut transit time for absorption and complexing of most heavy metallic elements.

Bernhardt, Bliss, and Eadie, EPA (Office of Radiation Programs), Las Vegas, reported on results of EPA samples taken in a project conducted by Rockwell International; Colorado Department of Health; Jefferson County (Colo.) Department of Health; and the EPA. The samples were

taken around the Rocky Flats, Colorado Plant. EPA samples discussed in the report were those from 1-cm and 5-cm depth, together with some EPA soil profile sample data. The project was undertaken in an attempt to resolve differences in reported data due to soil sampling techniques employed by those agencies/institutions participating in the project. A discussion is included concerning Cs-137 in soil, with data tables for Cs-137 and Pu-239.

Golchert and Sedlet of Argonne National Laboratory presented a discussion of resuspension studies on fallout-level plutonium. Measurements of plutonium concentrations in air calculated at Argonne are compared with data from GMX-5, Nevada Test Site. An Anderson 2000 Impactor was used to collect particles for analysis for comparison of particle size with concentration (distribution) of plutonium. Table I of their paper includes resuspension factors calculated for thorium-228, thorium-230, thorium-232, uranium, and plutonium-239,240 used in their comparisons.

In efforts to characterize environmental transport of plutonium deposited by the Trinity event, a preliminary model for wind movement was discussed by Gallegos, Los Alamos Scientific Laboratory. His paper summarizes dust flux data for a Trinity ground zero site location near the crater along the fallout pathway and examines the relationship between soil and plutonium flux, using analysis of variance and regression analysis methods.

Environmental in-field and *in situ* instruments are being developed by Rockwell-Hanford Operations and were reported by Bruns. The systems are designed for use in areas of waste management of radioactive materials. Following migration of radionuclides, identification of contaminated regions, measurement of void volumes (such as potential cave-ins where old waste material was buried and have decayed or disintegrated and may collapse), gas buildup due to radiolysis, density, porosity, moisture content, elemental assay, and down hole radionuclide assay are a few of the uses of the Rockwell instrumentation systems in *in situ* situations.

Sehmel, Battelle Pacific Northwest Laboratory, discussed measurements of airborne plutonium-239 and americium-241 transport, data obtained from the 125 M Hanford meteorological tower. The experiment was conducted to obtain a better understanding of possible differences in resuspension for the two different nuclides. After measurements of both nonrespirable and small particles at six heights from the meteorological tower, results indicated that plutonium-239 was transported on nonrespirable and "small" particles at all heights. Concentrations of americium-241 on small particles were maximum at the 91-m height. An apparent correlation was indicated between transport of americium-241 on small particles and plutonium-239 transport on large particles.

AUTHORS AND PARTICIPANTS
(AUTHORS IN ITALICS)

Alexander, C. A., BCL, Columbus, OH
Anspaugh, L. R., LLL, Livermore, CA
Arthur, W. J., DOE/ID, Idaho Falls, ID
Au, F. H. F., EMSL/EPA, Las Vegas, NV
Auer, C. H. V., REECo, Las Vegas, NV
Ausmus, B. S., BCL, Columbus, OH
Baker, D. E., Penn. State Univ., University Park, PA
Barth, J., EMSL/EPA, Las Vegas, NV
Bean, E. W., DOE/RF, Golden, CO
Beckert, W. F., EMSL/EPA, Las Vegas, NV
Benz, M., LFE-EAL, Richmond, CA
Bernhardt, D. E., ORP/EPA, Las Vegas, NV
Berry, H. A., REECo, Mercury, NV
Best, T. L., East. NM Univ., Portales, NM
Biermann, A. H., LLL, Livermore, CA
Bliss, J. D., ORP/EPA, Las Vegas, NV
Bliss, W. A., EMSL/EPA, Las Vegas, NV
Bloom, S. G., BCL, Columbus, OH
Bradley, W. G., UNLV, Las Vegas, NV
Brady, D. N., REECo, Mercury, NV
Bretthauer, E. W., EMSL/EPA, Las Vegas, NV
Bruns, L. E., Rockwell Hanford Co., Richland, WA
Buddemeier, R. W., Univ. of Hawaii, Honolulu, HI
Childers, R. E., S.W. Research Institute, Houston, TX
Ciolkosz, E. J., Penn. State Univ., University Park, PA
Cleveland, J. M., USGS, Lakewood, CO
Comar, C. L., EPRI, Palo Alto, CA
Corley, J. P., BNWL, Richland, WA
Couch, R. F., MCL, McClellan AFB, CA
Cushman, M. E., San Diego State Univ., San Diego, CA
Dean, P. N., LLL, Livermore, CA
Delfiner, P., Fontainbleau, France
Doctor, P. G., BNWL, Richland, WA
Dodson, G., BCL, Columbus, OH
Dunaway, P. B., DOE/NV, Las Vegas, NV
Eadie, G. G., ORP/EPA, Las Vegas, NV
Eberhardt, L. L., BNWL, Richland, WA
Efurd, D. W., MCL, McClellan AFB, CA
Essington, E. H., LASL, Los Alamos, NM
Facer, G. C., DMA, DOE/HQ, Washington, DC
Ficke, R., San Diego State Univ., San Diego, CA
Fowler, E. B., LASL, Los Alamos, NM
Francisco, E., LFE-EAL, Richmond, CA
Gallegos, A. F., LASL, Los Alamos, NM
Gatrousis, C., LLL, Livermore, CA
Gilbert, R. O., BNWL, Richland, WA
Golchert, N. W., Argonne National Lab., Argonne, IL

Graham, B., San Diego State Univ., San Diego, CA
Hahn, P. B., EMSL/EPA, Las Vegas, NV
Helm, K., San Diego State Univ., San Diego, CA
Homan, D. N., LLL, Livermore, CA
Horton, J. H., DuPont, SRL, Aiken, SC
Howard, W. A., DOE/NV, Las Vegas, NV
Hurley, J. D., Rockwell International, Golden, CO
Jakubowski, F. M., EMSL/EPA, Las Vegas, NV
Jokela, T. A., LLL, Livermore, CA
Jordan, H. S., LASL, Los Alamos, NM
Kasper, R. B., Rockwell Hanford Co., Richland, WA
Kennedy, N. C., WSNSO (NOAA), Las Vegas, NV
Kinnear, J. E., UCLA, Los Angeles, CA
Kirby, J. A., LLL, Livermore, CA
Leavitt, V. D., EMSL/EPA, Las Vegas, NV
Lee, K. D., REECo, Mercury, NV
Leventhal, L., LFE-EAL, Richmond, CA
Mansfield, G. San Diego State Univ., San Diego, CA
Martin, W. E., BCL, Columbus, OH
McMurray, B. J., BNWL, Richland, WA
Means, J., BCL, Columbus, OH
Melgard, R. N., LFE-EAL, Richmond, CA
Merritt, M. L., Sandia, Albuquerque, NM
Moor, K. S., UNLV, Las Vegas, NV
Morris, W. B., DOE/NV, Las Vegas, NV
Mueller, R. T., UCLA, Los Angeles, CA
Mullen, A. A., EMSL/EPA, Las Vegas, NV
Nathans, M. W., LFE-EAL, Richmond, CA
Nervik, W. E., LLL, Livermore, CA
Nishita, H., UCLA, Los Angeles, CA
Noshkin, V. E., LLL, Livermore, CA
Park, J. F., BNWL, Richland, WA
Patzer, R. G., EMSL/EPA, Las Vegas, NV
Payne, J. G., EMSL/EPA, Las Vegas, NV
Pfuderer, H. A., ORNL, Oak Ridge, TN
Phelps, P. L., LLL, Livermore, CA
Pillay, K. K. S., Penn. State Univ., University Park, PA
Polzer, W. L., LASL, Los Alamos, NM
Potter, G. D., EMSL/EPA, Las Vegas, NV
Rakow, L. M., REECo, Mercury, NV
Rees, T. F., USGS, Lakewood, CO
Rhoads, W. A., EG&G, S-B, Goleta, CA
Romney, E. M., UCLA, Los Angeles, CA
Rose, A. W., Penn. State Univ., University Park, PA
Rosenberry, C. E., REECo, Mercury, NV
Sanchez, E. A., Eberline, Albuquerque, NM
Santolucito, J. A., EMSL/EPA, Las Vegas, NV
Schmitt, M., DOE/NV, Las Vegas, NV
Schulz, R. K., UCB, Berkeley, CA

Sedlet, J., Argonne National Lab., Argonne, IL
Sehmel, G. A., BNWL, Richland, WA
Shinn, J. H., LLL, Livermore, CA
Skolil, L. L., San Diego State Univ., San Diego, CA
Smith, D. D., EMSL/EPA, Las Vegas, NV
Smith, M. H., SREL, Aiken, SC
Smith, P. B., EPA, Denver, CO
Stannard, J. N., San Diego, CA
Steinkruger, F. J., LASL, Los Alamos, NM
Stevens, J. F., KAPL, Schenectady, NY
Straight, R. J., REECo, Mercury, NV
Sutton, W. W., EMSL/EPA, Las Vegas, NV
Swanberg, F., USNRC, Washington, DC
Szalinski, P. A., San Diego, State Univ., San Diego, CA
Tamura, T., ORNL, Oak Ridge, TN
Teasdale, C., San Diego State Univ., San Diego, CA
Till, H., EPRI, Palo Alto, CA
Ushino, T., San Diego State Univ., San Diego, CA
Walburg, H. E., UT-CARL, Oak Ridge, TN
Wallace, A., UCLA, Los Angeles, CA
Watson, E. C., BNWL, Richland, WA
Weiss, J. F., UT-CARL, Oak Ridge, TN
Wessman, R. A., LFE-EAL, Richmond, CA
White, G. C., LASL, Los Alamos, NM
White, J. H., LLL, Livermore, CA
White, M. G., DOE/NV, Las Vegas, NV
Wireman, D. L., REECo, Mercury, NV
Wong, K. M., LLL, Livermore, CA
Wu, S-J., San Diego State Univ., San Diego, CA
Zellers, K. W., REECo, Las Vegas, NV

DISTRIBUTION LIST
NVO-192

UC-11--Standard Distribution--256

Special Distribution:

D. C. Sewell, Asst. Sec., DP, DOE/HQ, Washington, DC
R. C. Clusen, Asst. Sec., EV, DOE/HQ, Washington, DC
Gen. J. K. Bratton, MA, DOE/HQ, Washington, DC
G. C. Facer, MA, DOE/HQ, Washington, DC (2)
J. M. Deutch, Act. Assist. Sec., ET, DOE/HQ, Washington, DC
W. J. McCool, Act. Dir., OS, DOE/HQ, Washington, DC
W. E. Mott, Act. Dir., ECT, DOE/HQ, Washington, DC
W. W. Burr, DBER, DOE/HQ, Washington, DC
R. J. Engelman, DBER, DOE/HQ, Washington, DC
R. Franklin, DBER, DOE/HQ, Washington, DC
Arthur Schoen, DOES, DOE/HQ, Washington, DC
J. H. Kane, DBER, DOE/HQ, Washington, DC
R. L. Watters, DBER, DOE/HQ, Washington, DC
J. Olson, DBER, DOE/HQ, Washington, DC
W. S. Osburn, Jr., DBER, DOE/HQ, Washington, DC
J. A. Harris, OPA, USNRC, Washington, DC
G. W. Cunningham, WPR, DOE/HQ, Washington, DC
R. E. Allen, DOES, DOE/HQ, Washington, DC
J. N. Stannard, San Diego, CA
W. J. Bair, Battelle Northwest Labs., Richland, WA
R. C. Thompson, Battelle Northwest Labs., Richland, WA
J. H. Harley, EML/DOE, New York, NY
J. W. Healy, LASL, Los Alamos, NM
T. T. Mercer, Univ. of Rochester, Rochester, NY
C. L. Comar, EPRI, Palo Alto, CA
R. E. Luna, SL, Albuquerque, NM
F. W. Whicker, CSU, Fort Collins, CO
W. T. Carnall, ANL, Argonne, IL
J. Swinebroad, DBER, DOE/HQ, Washington, DC
L. J. Deal, DOES, DOE/HQ, Washington, DC
T. F. McCraw, DOES, DOE/HQ, Washington, DC
A. F. Kluk, ECT, DOE/HQ, Washington, DC
J. J. Davis, USNRC, Silver Spring, MD
H. S. Jordan, LASL, Los Alamos, NM
J. E. Dummer, LASL, Los Alamos, NM
P. L. Phelps, LLL, Livermore, CA
W. E. Nervik, LLL, Livermore, CA
M. L. Merritt, SL, Albuquerque, NM
W. A. Myers, DIA/USAF, Washington, DC
M. E. Gates, DOE/NV, Las Vegas, NV
P. B. Dunaway, BSD, DOE/NV, Las Vegas, NV (30)
M. G. White, BSD, DOE/NV, Las Vegas, NV (30)

W. Howard, BSD, DOE/NV, Las Vegas, NV
H. A. Pfuderer, ORNL, Oak Ridge, TN
T. Tamura, ORNL, Oak Ridge, TN
Nancy Vaughan, ORNL, Oak Ridge, TN (2)
E. H. Essington, LASL, Los Alamos, NM
F. H. F. Au, EMSL/EPA, Las Vegas, NV
J. Barth, EMSL/EPA, Las Vegas, NV
W. A. Bliss, EMSL/EPA, Las Vegas, NV
E. W. Bretthauer, EMSL/EPA, Las Vegas, NV
W. F. Beckert, EMSL/EPA, Las Vegas, NV
F. M. Jakubowski, EG&G Idaho, Inc., Idaho Falls, ID
V. D. Leavitt, EMSL/EPA, Las Vegas, NV
A. A. Mullen, EMSL/EPA, Las Vegas, NV
R. G. Patzer, EMSL/EPA, Las Vegas, NV
G. D. Potter, EMSL/EPA, Las Vegas, NV
D. D. Smith, EMSL/EPA, Las Vegas, NV
G. B. Morgan, EMSL/EPA, Las Vegas, NV
R. E. Stanley, EMSL/EPA, Las Vegas, NV
P. B. Hahn, EMSL/EPA, Las Vegas, NV
W. W. Sutton, EMSL/EPA, Las Vegas, NV
S. G. Bloom, BCL, Columbus, OH
W. E. Martin, BCL, Columbus, OH
R. O. Gilbert, Battelle Northwest Labs., Richland, WA
P. G. Doctor, Battelle Northwest Labs., Richland, WA
L. L. Eberhardt, Battelle Northwest Labs., Richland, WA
Leon Leventhal, LFE-EAL, Richmond, CA
R. N. Melgard, LFE-EAL, Richmond, CA
M. W. Nathans, LFE-EAL, Richmond, CA
A. J. Soinski, State Energy Commission, Sacramento, CA
R. A. Wessman, LFE-EAL, Richmond, CA
L. R. Anspaugh, LLL, Livermore, CA
J. A. Kirby, LLL, Livermore, CA
J. H. Shinn, LLL, Livermore, CA
J. E. Kinnear, UCLA, Los Angeles, CA
E. M. Romney, UCLA, Los Angeles, CA
H. Nishita, UCLA, Los Angeles, CA
A. Wallace, UCLA, Los Angeles, CA
A. E. Bicker, REECo, Mercury, NV
D. N. Brady, REECo, Mercury, NV
D. E. Engstrom, REECo, Mercury, NV
E. L. Hensley, REECo, Mercury, NV
L. M. Rakow, REECo, Mercury, NV
C. H. V. Auer, REECo, Las Vegas, NV
K. W. Zellers, REECo, Las Vegas, NV
C. E. Rosenberry, Jr., REECo, Mercury, NV
E. R. Sorom, REECo, Mercury, NV
R. J. Straight, REECo, Mercury, NV
B. P. Smith, REECo, Mercury, NV
A. W. Western, REECo, Mercury, NV
D. L. Wireman, REECo, Las Vegas, NV
H. D. Cunningham, REECo, Las Vegas, NV

K. D. Lee, REECo, Mercury, NV
W. A. Rhoads, EG&G, S-B, Goleta, CA
E. L. Geiger, EIC, Santa Fe, NM
E. A. Sanchez, EIC, Albuquerque, NM
J. M. Elliott, MCL, McClellan AFB, CA
D. W. Efurd, MCL, McClellan AFB, CA
R. F. Couch, MCL, McClellan AFB, CA
N. C. Kennedy, WSNSO (NOAA), Las Vegas, NV
W. G. Bradley, UNLV, Las Vegas, NV
K. S. Moor, UNLV, Las Vegas, NV
E. D. Campbell, BSD, DOE/NV, Las Vegas, NV
G. L. Merrill, Vallecitos, GE, Pleasanton, CA
H. N. Friesen, DRI, Las Vegas, NV
M. G. Barnes, DRI, Las Vegas, NV
L. J. Johnson, LASL, Los Alamos, NM
D. E. Bernhardt, EMSL/EPA, Las Vegas, NV
B. S. Ausmus, BCL, Columbus, OH
G. B. Wiersma, EMSL/EPA, Las Vegas, NV
C. S. Fore, ORNL, Oak Ridge, TN
D. N. Homan, LLL, Livermore, CA
J. C. McFarlane, EMSL/EPA, Las Vegas, NV
J. W. Mullins, EMSL/EPA, Las Vegas, NV
D. E. Baker, Penn. State Univ., University Park, PA
E. J. Ciolkosz, Penn. State Univ., University Park, PA
W. F. Witzig, Penn. State Univ., University Park, PA
K. K. S. Pillay, Penn. State Univ., University Park, PA
A. W. Rose, Penn. State Univ., University Park, PA
D. A. Brown, Univ. of Arkansas, Fayetteville, AR
L. Dietz, Knolls Atomic, Schenectady, NY
T. W. Buttery, DPR, DOE/HQ, Washington, DC
C. A. Alexander, BCL, Columbus, OH
J. O. Duguid, BCL, Columbus, OH
D. T. Schueler, DOE/ALO, Albuquerque, NM
P. J. Mudra, DOE/NV, Las Vegas, NV
Chief, NOB/DNA, DOE/NV, Las Vegas, NV
W. J. Tipton, EG&G, Las Vegas, NV
M. Schmitt, DOE/NV, Las Vegas, NV
J. R. Roeder, DOE/ALO, Albuquerque, NM
W. B. Johnston, DOE/ALO, Albuquerque, NM
J. F. Burke, DOE/ALO, Albuquerque, NM
O. D. Markham, DOE/ID, Idaho Falls, ID
C. W. Sill, DOE/ID, Idaho Falls, ID
E. W. Bean, DOE/RF, Golden, CO
G. N. Huffman, DOE/RF, Golden, CO
W. S. Twenhofel, USGS, Denver, CO
R. W. Hoff, LLL, Livermore, CA
V. E. Noshkin, LLL, Livermore, CA
W. L. Robison, LLL, Livermore, CA
D. L. Ermak, LLL, Livermore, CA
C. R. Richmond, ORNL, Oak Ridge, TN
R. G. Thomas, LASL, Los Alamos NM

W. C. Hanson, Battelle Northwest Labs., Richland, WA
A. F. Gallegos, LASL, Los Alamos, NM
D. C. Hoffman, LASL, Los Alamos, NM
T. E. Hakonson, LASL, Los Alamos, NM
E. B. Fowler, LASL, Los Alamos, NM
Auda Morrow, UCLA/CETO, Mercury, NV (2)
B. G. Maza, UCLA/CETO, Mercury, NV
P. A. Medica, UCLA/CETO, Mercury, NV
P. T. Tueller, UNR, Reno, NV
J. P. Corley, Battelle Northwest Labs., Richland, WA
M. A. Thompson, Stearns-Roger, Inc., Denver, CO
J. A. Hayden, Rockwell International, Golden, CO
J. M. Cleveland, USGS, Lakewood, CO
O. G. Raabe, UCD, Davis, CA
S. I. Auerbach, ORNL, Oak Ridge, TN
R. C. Dahlman, DBER, DOE/HQ, Washington, DC
W. R. Hansen, LASL, Los Alamos, NM
I. Aoki, DOS, DOE/ID, Idaho Falls, ID
R. K. Schulz, UCB, Berkeley, CA
K. R. Price, Battelle Northwest Labs., Richland, WA
L. E. Bruns, Rockwell Hanford Co., Richland, WA
R. L. Douglas, ORP/EPA, Las Vegas, NV
R. R. Kinnison, EMSL/EPA, Las Vegas, NV
J. J. Lorenz, EMSL/EPA, Las Vegas, NV
J. G. Payne, Jr., EMSL/EPA, Las Vegas, NV
K. W. Brown, EMSL/EPA, Las Vegas, NV
D. W. Hendricks, ORP/EPA, Las Vegas, NV
C. F. Costa, EMSL/EPA, Las Vegas, NV
V. E. Andrews, EMSL/EPA, Las Vegas, NV
P. B. Smith, ORP, EPA, Denver, CO
L. Fraley, Colo. State Univ., Fort Collins, CO
H. A. Kornberg, Elec. Power Res. Inst., Palo Alto, CA
L. K. Bustad, Washington State Univ., Pullman, WA
R. K. Mullen, USNRC, Washington, DC
E. T. Bramlitt, DNA, Kirtland AFB, NM
D. C. Durrill, Westinghouse, E-MAD, Jackass Flats, NV
M. E. Joyner, Westinghouse, E-MAD, Jackass Flats, NV
M. H. Smith, SREL, Aiken, SC
H. E. Walburg, CARL, Oak Ridge, TN
M. Goldman, UCD, Davis, CA
T. P. O'Farrell, Boulder City, NV
Mary Meadows, DBER, DOE/HQ, Washington, DC
B. W. Wachholz, DBER, DOE/HQ, Washington, DC
C. W. Pelzer, OPA, DOE/HQ, Washington, DC
W. O. Forster, DBER, DOE/HQ, Washington, DC
K. R. Baker, DOES, DOE/HQ, Washington, DC
J. R. Maher, DTO, DOE/HQ, Germantown, MD
G. H. Daly, DNFC&P, Environment & Safety, DOE/HQ, Washington, DC
D. R. Elle, DOE/RO, Richland, WA
W. E. Lotz, DBER, DOE/HQ, Washington, DC
G. Burley, ORP, EPA, Washington, DC

M. A. Parsont, USNRC, Washington, DC
P. O. Strom, NRC, Idaho Falls, ID
J. W. King, OPA, DOE/HQ, Washington, DC
E. P. Hardy, DOE/EML, New York, NY
P. W. Krey, DOE/EML, New York, NY
Y. C. Ng, LLL, Livermore, CA
M. E. Mount, LLL, Livermore, CA
K. M. Wong, LLL, Livermore, CA
E. A. Bondietti, ORNL, Oak Ridge, TN
G. E. Cosgrove, S. D. Zoo. Soc., San Diego, CA
D. A. Cataldo, Battelle Northwest Labs., Richland, WA
J. F. Cline, Battelle Northwest Labs., Richland, WA
R. G. Schreckhise, Battelle Northwest Labs., Richland, WA
G. A. Sehmel, Battelle Northwest Labs., Richland, WA
S. M. Price, Rockwell Hanford Co., Richland, WA
V. T. Bowen, Woods Hole Oceanographic Inst., Woods Hole, MA
A. L. Boni, SRL, DuPont, Aiken, SC
J. C. Corey, SRL, DuPont, Aiken, SC
S. M. Fried, Argonne National Lab., Argonne, IL
J. C. Cobb, Univ. of Colorado, Denver, CO
R. W. Engelhart, NUS Corp., Rockville, MD
T. R. Folsom, Scripps Oceanographic Institute, La Jolla, CA
D. C. Adriano, SREL, Aiken, SC
K. W. McLeod, SREL, Aiken, SC
M. W. Carter, Georgia Tech., Atlanta, GA
A. A. Moghissi, Georgia Tech., Atlanta, GA
G. W. Phillips, Naval Research Lab., Washington, DC
J. E. Pinder, SREL, Aiken, SC
R. G. Post, Univ. of Arizona, Tucson, AZ
M. W. Tiernan, DOE, Richland, WA
A. D. Volk, Rockwell Int., Golden, CO
R. D. Woods, NASA-AMES Res. Center, Moffett Field, CA
S. R. Wright, DOE/SRO, Aiken, SC
Sidney Langer, General Atomic Co., San Diego, CA
Walter Meyer, Univ. of Missouri, Columbia, MO
J. R. Burdick, SAMSO/MNBS, Norton AFB, San Bernardino, CA
Nevada State Library, Documents Section, Carson City, NV (2)
R. H. Johnston, DOE/NV, Las Vegas, NV
A. T. Vollmer, UCLA/CETO, Mercury, NV
J. A. Merrill, Battelle Northwest Labs., Richland, WA
D. K. Halford, DOE/ID, Idaho Falls, ID
C. Gatrousis, LLL, Livermore, CA
L. Hopkins, Monsanto-Mound Lab., Miamisburg, OH
J. A. Santolucito, EMSL/EPA, Las Vegas, NV
M. J. Feldman, ORNL, Oak Ridge, TN
G. M. Lodde, Army Environ. Hygiene Agency, Aberdeen Proving Ground, MD
R. H. Wilson, Univ. of Rochester, Rochester, NY
C. D. W. Thornton, P&A, DOE/HQ, Washington, DC
C. S. Abrams, Argonne National Lab., Idaho Falls, ID
J. P. Brannen, SL, Albuquerque, NM
D. Cohen, Argonne National Lab., Argonne, IL

P. Delfiner, Fontainebleau, France
M. R. Dolenc, EG&G, Idaho Falls, ID
A. J. Francis, Brookhaven National Lab., Upton, NY
H. Hawthorne, GE-Tempo, Santa Barbara, CA
G. W. Huckabay, LLL, Livermore, CA
P. K. Kuroda, Univ. of Arkansas, Fayetteville, AR
W. D. McCormack, Battelle Northwest Labs., Richland, WA
J. R. Naidu, Brookhaven National Lab., Upton, NY
J. D. Navratil, Rockwell International, Golden, CO
M. Ruggien, UCB, Berkeley, CA
R. C. Smith, Westinghouse Hanford, Richland, WA
L. F. Soholt, DRI, Boulder City, NV
J. K. Soldat, Battelle Northwest Labs., Richland, WA
F. Swanberg, USNRC, Washington, DC
R. J. Teunis, Argonne National Lab., Argonne, IL
W. J. Thomas, Jr., Battelle Northwest Labs., Richland, WA
H. Till, EPRI, Palo Alto, CA
E. C. Watson, Battelle Northwest Labs., Richland, WA
M. Werkema, Rockwell International, Golden, CO
C. E. Williams, DOE/ID, Idaho Falls, ID
Seymour Schwiller, House Armed Services Committee, Washington, DC
Library of Congress, Documents Section, Washington, DC
W. J. Arthur, DOE/ID, Idaho Falls, ID
H. A. Berry, REECo, Mercury, NV
T. L. Best, East NM Univ., Portales, NM
A. H. Bierman, LLL, Livermore, CA
J. D. Bliss, EMSL/EPA, Las Vegas, NV
R. W. Buddemeier, Univ., of Hawaii, Honolulu, HI
R. E. Childers, S.W. Research Institute, Houston, TX
M. E. Cushman, San Diego State Univ., San Diego, CA
P. N. Dean, LLL, Livermore, CA
G. J. Dodson, ORNL, Oak Ridge, TN
R. Ficke, San Diego State Univ., San Diego, CA
E. Francisco, LFE-EAL, Richmond, CA
N. W. Golchert, Argonne National Lab., Argonne, IL
B. Graham, San Diego State Univ., San Diego, CA
K. Helm, San Diego State Univ., San Diego, CA
J. H. Horton, DuPont, SRL, Aiken, SC
J. D. Hurley, Rockwell International, Golden, CO
T. A. Jokela, LLL, Livermore, CA
R. B. Kasper, Rockwell Hanford Co., Richland, WA
G. G. Eadie, EMSL/EPA, Las Vegas, NV
G. Mansfield, San Diego State Univ., San Diego, CA
B. J. McMurray, Battelle Northwest Labs., Richland, WA
J. Means, BCL, Columbus, OH
W. B. Morris, DOE/NV, Las Vegas, NV
R. T. Mueller, UCLA, Los Angeles, CA
J. F. Park, Battelle Northwest Labs., Richland, WA
W. L. Polzer, LASL, Los Alamos, NM
T. F. Rees, USGS, Lakewood, CO
J. Sedlet, Argonne National Lab., Argonne, IL

L. L. Skolil, San Diego State Univ., San Diego, CA
F. J. Steinkruger, LASL, Los Alamos, NM
J. F. Stevens, KAPL, Schenectady, NY
P. A. Zalinski, San Diego State Univ., San Diego, CA
C. Teasdale, San Diego State Univ., San Diego, CA
T. Ushino, San Diego State Univ., San Diego, CA
J. F. Weiss, CARL, Oak Ridge, TN
G. C. White, LASL, Los Alamos, NM
J. H. White, LLL, Livermore, CA
S-J. Wu, San Diego State Univ., San Diego, CA
M. Benz, LFE-EAL, Richmond, CA

OTHER NAEG PUBLICATIONS

Publications of the Nevada Applied Ecology Group, DOE/NV, available through the National Technical Information Services, NTIS.

U.S. Department of Commerce
5285 Port Royal Road
Springfield, Virginia 22161

U.S. AEC Report, NVO-142, THE DYNAMICS OF PLUTONIUM IN DESERT ENVIRONMENTS, P. B. Dunaway and M. G. White, Eds., 1974.

U.S. ERDA Report, NVO-153, THE RADIOECOLOGY OF PLUTONIUM AND OTHER TRANSURANICS IN DESERT ENVIRONMENTS, M. G. White and P. B. Dunaway, Eds., 1975.

U.S. ERDA Report, NVO-159, STUDIES OF ENVIRONMENTAL PLUTONIUM AND OTHER TRANSURANICS IN DESERT ECOSYSTEMS, M. G. White and P. B. Dunaway, Eds., 1976.

U.S. ERDA Report, NVO-166 (2 Vols.), NEVADA APPLIED ECOLOGY GROUP PROCEDURES HANDBOOK FOR ENVIRONMENTAL TRANSURANICS, M. G. White and P. B. Dunaway, Eds., 1976.

U.S. ERDA Report, NVO-171, ENVIRONMENTAL PLUTONIUM ON THE NEVADA TEST SITE AND ENVIRONS, M. G. White, P. B. Dunaway, and W. A. Howard, Eds., 1977.

U.S. ERDA Report, NVO-178, TRANSURANICS IN NATURAL ENVIRONMENTS, M. G. White and P. B. Dunaway, Eds., 1977.

U.S. DOE Report, NVO-181, TRANSURANICS IN DESERT ECOSYSTEMS, M. G. White, P. B. Dunaway, and D. L. Wireman, Eds., 1977.